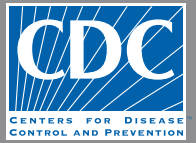


EMERGING INFECTIOUS DISEASES[®]



Fungal Infections

September 2019



Helen Beatrice Potter (1866–1943), *Agaricus augustus* (c. 1892–1895). Watercolor on paper, 9 in × 7 in/23 cm × 18 cm, Perth Museum & Art Gallery, Perth & Kinross Council, Scotland.

EMERGING INFECTIOUS DISEASES®

EDITOR-IN-CHIEF

D. Peter Drotman

ASSOCIATE EDITORS

Paul M. Arguin, Atlanta, Georgia, USA
 Charles Ben Beard, Fort Collins, Colorado, USA
 Ermias Belay, Atlanta, Georgia, USA
 David M. Bell, Atlanta, Georgia, USA
 Sharon Bloom, Atlanta, Georgia, USA
 Richard Bradbury, Bratislava, Slovakia
 Mary Brandt, Atlanta, Georgia, USA
 Corrie Brown, Athens, Georgia, USA
 Charles H. Calisher, Fort Collins, Colorado, USA
 Benjamin J. Cowling, Hong Kong, China
 Michel Drancourt, Marseille, France
 Paul V. Effler, Perth, Australia
 Anthony Fiore, Atlanta, Georgia, USA
 David O. Freedman, Birmingham, Alabama, USA
 Peter Gerner-Smidt, Atlanta, Georgia, USA
 Stephen Hadler, Atlanta, Georgia, USA
 Matthew J. Kuehnert, Edison, New Jersey, USA
 Nina Marano, Atlanta, Georgia, USA
 Martin I. Meltzer, Atlanta, Georgia, USA
 David Morens, Bethesda, Maryland, USA
 J. Glenn Morris, Jr., Gainesville, Florida, USA
 Patrice Nordmann, Fribourg, Switzerland
 Johann D.D. Pitout, Calgary, Alberta, Canada
 Ann Powers, Fort Collins, Colorado, USA
 Didier Raoult, Marseille, France
 Pierre E. Rollin, Atlanta, Georgia, USA
 David H. Walker, Galveston, Texas, USA
 J. Todd Weber, Atlanta, Georgia, USA
 J. Scott Weese, Guelph, Ontario, Canada

Managing Editor

Byron Breedlove, Atlanta, Georgia, USA

Copy Editors

Kristina Clark, Dana Dolan, Karen Foster,
 Thomas Gryczan, Amy Guinn, Michelle Moran, Shannon O'Connor,
 Jude Rutledge, P. Lynne Stockton, Deborah Wenger

Production

Thomas Eheman, William Hale, Barbara Segal,
 Reginald Tucker

Journal Administrator

Susan Richardson

Editorial Assistants

Kelly Crosby, Kristine Phillips

Communications/Social Media

Sarah Logan Gregory,
 Tony Pearson-Clarke, Deanna Altomara (intern)

Founding Editor

Joseph E. McDade, Rome, Georgia, USA

EDITORIAL BOARD

Barry J. Beaty, Fort Collins, Colorado, USA
 Martin J. Blaser, New York, New York, USA
 Christopher Braden, Atlanta, Georgia, USA
 Arturo Casadevall, New York, New York, USA
 Kenneth G. Castro, Atlanta, Georgia, USA
 Vincent Deubel, Shanghai, China
 Christian Drosten, Charité Berlin, Germany
 Isaac Chun-Hai Fung, Statesboro, Georgia, USA
 Kathleen Gensheimer, College Park, Maryland, USA
 Rachel Gorwitz, Atlanta, Georgia, USA
 Duane J. Gubler, Singapore
 Richard L. Guerrant, Charlottesville, Virginia, USA
 Scott Halstead, Arlington, Virginia, USA
 David L. Heymann, London, UK
 Keith Klugman, Seattle, Washington, USA
 Takeshi Kurata, Tokyo, Japan
 S.K. Lam, Kuala Lumpur, Malaysia
 Stuart Levy, Boston, Massachusetts, USA
 John S. Mackenzie, Perth, Australia
 John E. McGowan, Jr., Atlanta, Georgia, USA
 Jennifer H. McQuiston, Atlanta, Georgia, USA
 Tom Marrie, Halifax, Nova Scotia, Canada
 Nkuchia M. M'ikanatha, Harrisburg, Pennsylvania, USA
 Frederick A. Murphy, Bethesda, Maryland, USA
 Barbara E. Murray, Houston, Texas, USA
 Stephen M. Ostroff, Silver Spring, Maryland, USA
 Mario Raviglione, Milan, Italy, and Geneva, Switzerland
 David Relman, Palo Alto, California, USA
 Guenael R. Rodier, Saône-et-Loire, France
 Connie Schmaljohn, Frederick, Maryland, USA
 Tom Schwan, Hamilton, Montana, USA
 Frederic E. Shaw, Atlanta, Georgia, USA
 Rosemary Soave, New York, New York, USA
 P. Frederick Sparling, Chapel Hill, North Carolina, USA
 Robert Swanepoel, Pretoria, South Africa
 David E. Swayne, Athens, Georgia, USA
 Phillip Tarr, St. Louis, Missouri, USA
 Duc Vugia, Richmond, California, USA
 Mary E. Wilson, Cambridge, Massachusetts, USA

Emerging Infectious Diseases is published monthly by the Centers for Disease Control and Prevention, 1600 Clifton Rd NE, Mailstop H16-2, Atlanta, GA 30329-4027, USA. Telephone 404-639-1960, fax 404-639-1954, email eideditor@cdc.gov.

The conclusions, findings, and opinions expressed by authors contributing to this journal do not necessarily reflect the official position of the U.S. Department of Health and Human Services, the Public Health Service, the Centers for Disease Control and Prevention, or the authors' affiliated institutions. Use of trade names is for identification only and does not imply endorsement by any of the groups named above.

All material published in Emerging Infectious Diseases is in the public domain and may be used and reprinted without special permission; proper citation, however, is required.

Use of trade names is for identification only and does not imply endorsement by the Public Health Service or by the U.S. Department of Health and Human Services.

EMERGING INFECTIOUS DISEASES is a registered service mark of the U.S. Department of Health & Human Services (HHS).

∞ Emerging Infectious Diseases is printed on acid-free paper that meets the requirements of ANSI/NISO Z39.48-1992 (Permanence of Paper)

EMERGING INFECTIOUS DISEASES®

Fungal Infections

September 2019



On the Cover

Helen Beatrix Potter (1866–1943), *Agaricus augustus* (c. 1892–1895). Watercolor on paper, 9 in × 7 in/ 23 cm × 18 cm, Perth Museum & Art Gallery, Perth & Kinross Council, Scotland.

About the Cover p. 1786

Clinical Characteristics and Treatment Outcomes for Patients Infected with *Mycobacterium haemophilum*
P. Nookeu et al. **1648**

Research

***Theileria orientalis* Ikeda Genotype in Cattle, Virginia, USA**
V.J. Oakes et al. **1653**

Genetic Characterization and Enhanced Surveillance of Ceftriaxone-Resistant *Neisseria gonorrhoeae* Strain, Alberta, Canada, 2018
B.M. Berenger et al. **1660**

Clonality of Fluconazole-Nonsusceptible *Candida tropicalis* Bloodstream Infections, Taiwan, 2011–2017
P.-Y. Chen et al. **1668**


Related material available online:
 http://wwwnc.cdc.gov/eid/article/25/9/19-0520_article

Association of Enterovirus D68 with Acute Flaccid Myelitis, Philadelphia, Pennsylvania, USA, 2009–2018
P. Uprety et al. **1676**

Related material available online:
 http://wwwnc.cdc.gov/eid/article/25/9/19-0468_article

Synopses

Genotyping Approach for Potential Common Source of *Enterocytozoon bieneusi* Infection in Hematology Unit
G. Desoubieux et al. **1625**

Related material available online:
 http://wwwnc.cdc.gov/eid/article/25/9/19-0311_article

Epidemiology of Carbapenemase-Producing *Klebsiella pneumoniae* in a Hospital, Portugal
M. Aires-de-Sousa et al. **1632**

Medscape
EDUCATION
ACTIVITY

Classification of Trauma-Associated Invasive Fungal Infections to Support Wound Treatment Decisions

The proposed classification, based on diagnostic certainty, provides a framework for determining initial empiric and subsequent targeted therapy.

A. Ganesan et al. **1639**

Medscape
EDUCATION
ACTIVITY

Risk for *Clostridioides difficile* Infection among Older Adults with Cancer

Incidence was higher for patients with cancer, independent of prior healthcare-associated exposure.
M. Kamboj et al. **1683**

EMERGING INFECTIOUS DISEASES®

September 2019

Whole-Genome Sequencing of *Salmonella* Mississippi and Typhimurium Definitive Type 160, Australia and New Zealand

L. Ford et al. 1690



Related material available online:
http://wwwnc.cdc.gov/eid/article/25/9/18-1811_article

Epidemiologic Shift in Candidemia Driven by *Candida auris*, South Africa, 2016–2017

E. van Schalkwyk et al. 1698

Effect of Pneumococcal Conjugate Vaccines on Pneumococcal Meningitis, England and Wales, July 1, 2000–June 30, 2016

G. Oligbu et al. 1708

Dispatches

Rickettsia japonica Infections in Humans, Xinyang, China, 2014–2017

H. Li et al. 1719



Related material available online:
http://wwwnc.cdc.gov/eid/article/25/9/17-1421_article

Climate Classification System–Based Determination of Temperate Climate Detection of *Cryptococcus gattii* sensu lato

E.S. Acheson et al. 1723



Related material available online:
http://wwwnc.cdc.gov/eid/article/25/9/18-1884_article

Cluster of Nasal Rhinosporidiosis, Eastern Province, Rwanda

A.I. Izimukwiye et al. 1727

Use of Human Intestinal Enteroids to Detect Human Norovirus Infectivity

M.C.-W. Chan et al. 1730

Vaccine Effectiveness against DS-1–Like Rotavirus Strains in Infants with Acute Gastroenteritis, Malawi, 2013–2015

K.C. Jere et al. 1734

Rodent Host Abundance and Climate Variability as Predictors of Tickborne Disease Risk 1 Year in Advance

E. Tkadlec et al. 1738



Related material available online:
http://wwwnc.cdc.gov/eid/article/25/9/19-0684_article

Delays in Coccidioidomycosis Diagnosis and Relationship to Healthcare Utilization, Phoenix, Arizona, USA

R. Ginn et al. 1742



Related material available online:
http://wwwnc.cdc.gov/eid/article/25/9/19-0019_article

Delays in Coccidioidomycosis Diagnosis and Associated Healthcare Utilization, Tucson, Arizona, USA

F.M. Donovan et al. 1745



Related material available online:
http://wwwnc.cdc.gov/eid/article/25/9/19-0023_article

Research Letters

Soft Tissue Infection with *Diaporthe phaseolorum* in Heart Transplant Recipient with End-Stage Renal Failure

J.C. Howard et al. 1748

Disseminated Emergomycosis in a Person with HIV Infection, Uganda

I. Rooms et al. 1750



Related material available online:
http://wwwnc.cdc.gov/eid/article/25/9/18-1234_article

Bourbon Virus in Wild and Domestic Animals, Missouri, USA, 2012–2013

K.C. Jackson et al. 1752



Related material available online:
http://wwwnc.cdc.gov/eid/article/25/9/18-1902_article

Fatal Case of Lassa Fever, Bangolo District, Côte d'Ivoire, 2015

M. Mateo et al. 1753



Household Transmission of Human Adenovirus Type 55 in Case of Fatal Acute Respiratory Disease

S. Jing et al. **1756**



Related material available online:
http://wwwnc.cdc.gov/eid/article/25/9/18-1937_article

Worldwide Reduction in MERS Cases and Deaths since 2016

C.A. Donnelly et al. **1758**



Related material available online:
http://wwwnc.cdc.gov/eid/article/25/9/19-0143_article

Limited Scope of Shorter Drug Regimen for MDR TB Caused by High Resistance to Fluoroquinolone

P.K. Singh, A. Jain **1760**

***Candida auris* in Germany and Previous Exposure to Foreign Healthcare**

A. Hamprecht et al. **1763**



Related material available online:
http://wwwnc.cdc.gov/eid/article/25/9/19-0262_article

Characterization of Clinical Isolates of *Talaromyces marneffi* and Related Species, California, USA

L. Li et al. **1765**



Related material available online:
http://wwwnc.cdc.gov/eid/article/25/9/19-0380_article

***Parathyridaria percutanea* and Subcutaneous Phaeohyphomycosis**

S.M. Rudramurthy et al. **1768**



Related material available online:
http://wwwnc.cdc.gov/eid/article/25/9/19-0383_article

Disease Exposure and Antifungal Bacteria on the Skin of Invasive Cane Toads, Australia

C.L. Weitzman et al. **1770**



Related material available online:
http://wwwnc.cdc.gov/eid/article/25/9/19-0386_article

Case of *Plasmodium knowlesi* Malaria in Poland Linked to Travel in Southeast Asia

S.P. Nowak et al. **1772**



Related material available online:
http://wwwnc.cdc.gov/eid/article/25/9/19-0445_article

Bombali Virus in *Mops condylurus* Bats, Guinea

L.S. Karan et al. **1774**



Related material available online:
http://wwwnc.cdc.gov/eid/article/25/9/19-0581_article

Blastomycosis Misdiagnosed as Tuberculosis, India

A. Kumar et al. **1776**

Invasive Fungal Disease, Isavuconazole Treatment Failure, and Death in Acute Myeloid Leukemia Patients

A.-P. Bellanger et al. **1778**

Potential Fifth Clade of *Candida auris*, Iran, 2018

N.A. Chow et al. **1780**



Related material available online:
http://wwwnc.cdc.gov/eid/article/25/9/19-0686_article

Dengue Virus Type 1 Infection in Traveler Returning from Tanzania to Japan, 2019

K. Okada et al. **1782**



Related material available online:
http://wwwnc.cdc.gov/eid/article/25/9/19-0814_article

Books and Media

Infections of Leisure, Fifth Edition

K. Fullerton **1785**

About the Cover

Beatrix Potter, Author, Naturalist, Mycologist

B. Breedlove **1786**

Etymologia

Sporothrix schenckii

F.P. Sellera, C.E. Larsson **1631**

Online Report

Decision Tool for Herpes B Virus Antiviral Prophylaxis after Macaque-Related Injuries in Research Laboratory Workers

S. Barkata et al.

https://wwwnc.cdc.gov/eid/article/25/9/19-0045_article

Subscribe online

Get the content you want delivered to your inbox

- Ahead of print articles
- Continuing Medical Education
- Online reports
- Podcasts
- Spotlight articles
- Table of Contents

Online subscription: wwwnc.cdc.gov/eid/subscribe/htm

World Rabies Day is September 28

Every nine minutes, someone dies from this deadly, yet preventable disease.

Join the fight to end human deaths from canine rabies by 2030.

Vaccinate your dog against rabies.

A close-up photograph of a person's hands drawing a purple liquid vaccine from a small vial into a syringe. The person is wearing a black bracelet. The background is a blurred outdoor setting with a blue tarp and a person's head in profile.

The Rabies Crisis by the Numbers

40%

40% of the people
bitten by dogs
globally are
children.

150

Rabies occurs
in more than 150
countries.

70%

Vaccinating just
70% of dogs will
protect humans
in at-risk areas.

Globally, more than 95% of human rabies deaths occur after bites from rabid dogs. Most of these cases are in sub-Saharan Africa and Asia. CDC, in collaboration with the Global Alliance for Rabies Control and Mission Rabies, is helping countries around the world tackle rabies through education and mass dog rabies vaccination campaigns. To learn more, go to www.cdc.gov/rabies.

Genotyping Approach for Potential Common Source of *Enterocytozoon bieneusi* Infection in Hematology Unit

Guillaume Desoubeaux, Céline Nourrisson, Maxime Moniot, Marie-Alix De Kyvon, Virginie Bonnin, Marjan Ertault De La Bretonnière, Virginie Morange, Éric Bailly, Adrien Lemaigen, Florent Morio, Philippe Poirier

Microsporidiosis is a fungal infection that generally causes digestive disorders, especially in immunocompromised hosts. Over a 4-day period in January 2018, 3 patients with hematologic malignancies who were admitted to the hematology unit of a hospital in France received diagnoses of *Enterocytozoon bieneusi* microsporidiosis. This unusually high incidence was investigated by sequence analysis at the internal transcribed spacer rDNA locus and then by 3 microsatellites and 1 minisatellite for multilocus genotyping. The 3 isolates had many sequence similarities and belonged to a new genotype closely related to genotype C. In addition, multilocus genotyping showed high genetic distances with all the other strains collected from epidemiologically unrelated persons; none of these strains belonged to the new genotype. These data confirm the epidemiologic link among the 3 patients and support a common source of infection.

Microsporidia are spore-forming eukaryotic and opportunistic intracellular pathogens related to fungi (1,2). Microsporidiosis usually occurs in the form of isolated cases in immunocompromised patients, including HIV-infected persons and solid-organ transplant recipients (1) but can also arise in travelers and is common in children in developing countries. Infection causes digestive disorders, including diarrhea (1,3). Microsporidia are orally transmitted by interindividual contacts and likely less frequently transmitted by foodborne or waterborne spores from excreta of a

wide range of host species (1,4). At least 16 microsporidian species have been described in humans, but *Enterocytozoon bieneusi* is the most common (5). However, little is known about the actual epidemiology of *E. bieneusi* microsporidiosis, and there is a need for a better understanding of its pathophysiology and parasitic cycle (3,5). Unfortunately, epidemiologic studies are complicated because *E. bieneusi* infection has a low incidence rate worldwide (6), and its microbiological diagnosis is difficult and likely often overlooked (7). In addition, the species is not easy to cultivate in vitro in routine practice. Investigations can be carried out directly only from infected biologic samples, which usually use DNA from fecal specimens (1,3,7).

More than 250 genotypes of *E. bieneusi* have been identified on the basis of their internal transcribed spacer (ITS) region (8,9). Depending on the ITS genotypes, zoonotic or host-adapted groups have been identified within species. Phylogenetic studies were able to distinguish ≥ 10 groups; most ITS genotypes belonged to group 1, which contains genotypes found in both humans and animals, including cats, pigs, and cattle (2). However, ITS sequencing has certain limitations because the same ITS genotype can be isolated from different host species and from different regions. This possible strain diversity within 1 ITS genotype cannot be addressed by a single sequence-based genotyping technique (10).

In human and animal medicine, several molecular techniques have been developed to investigate the epidemiology of transmissible agents (11–15), such as multilocus sequence typing (MLST) analysis or mini/microsatellite length polymorphism using short tandem-repeat markers. A MLST method was developed in 2011 to discriminate among *E. bieneusi* isolates (16). Four loci were analyzed with 1 minisatellite (MS4) and 3 microsatellites (MS1, MS3, and MS7). The combination of these 4 markers with the ITS genotype allows for the determination of multilocus

Author affiliations: Université de Tours, Tours, France (G. Desoubeaux); CHU Bretonneau, Tours (G. Desoubeaux, M.-A. De Kyvon, M. Ertault De La Bretonnière, V. Morange, É. Bailly, A. Lemaigen); Université Clermont-Auvergne, Aubière, France (C. Nourrisson, M. Moniot, V. Bonnin, P. Poirier); CHU Gabriel-Montpied, Clermont-Ferrand, France (C. Nourrisson, M. Moniot, P. Poirier); CHU Hôtel Dieu, Nantes, France (F. Morio); Université de Nantes, Nantes (F. Morio)

DOI: <https://doi.org/10.3201/eid2509.190311>

genotypes (MLGs). MLG analyses are useful to discriminate between isolates derived from various hosts (17) and to detect mixed infections (18).

To assess epidemiologic links among 3 cases of *E. bienersi* infections occurring concomitantly in a single hematology unit in a hospital in France, we used the MLG analysis method. The results showed the utility of this approach in the investigation of a cluster of cases.

Materials and Methods

Ethics

The study patients gave informed consent for the use of their samples in the research project. All their personal data were anonymous. We received approval from the ethics committee of the University Hospital of Tours (Center 1, Espace de Réflexion Éthique, Région Centre-Val de Loire, France). The study registration number 2015_003 was issued by the National Commission for Information Technology and Individual Freedom (Commission Nationale de l'Informatique et des Libertés) on January 10, 2015. We performed the study in accordance with the Code of Ethics of the World Medical Association (Declaration of Helsinki) and complied with BRISQ guidelines (19). We received technical and financial support from the French Microsporidiosis Network, assisted by the Clinical Research and Innovation Department (DRCI) of the University Hospital of Clermont-Ferrand (Center 2) and the French National Reference Center for Cryptosporidiosis.

Context of the Study

Center 1 is a university hospital in France that contains 2,008 inpatient beds and comprises 3 main sites spread over a distance of a few kilometers. The hematology unit is located in the Center for Adult Medicine (Tours, France; latitude 47.3900474, longitude 0.6889268). Systematic surveillance and exhaustive registration of all cases of microsporidiosis began in the hospital in January 2011. During January 2011–January 2018, there were 33,769 inpatient admissions. Only 2 cases of *E. bienersi* were diagnosed in the hematology unit and the oncology department in patients admitted in 2017; these cases occurred at different times. In contrast, 3 patients with hematologic malignancies, designated M01-05 to M01-07, received diagnoses of *E. bienersi* microsporidiosis during a 4-day period, January 12–16, 2018.

Biologic Procedures for Routine Diagnosis of *E. bienersi* Infection

All diarrheic fecal specimens and feces obtained from high-risk patients, including HIV-positive persons, solid-organ/bone-marrow transplant recipients, and patients with cancer or autoimmune diseases (1,20), were systematically

screened for microsporidia in the parasitology–mycology laboratory of center 1. The first-line diagnostic procedure used a real-time qualitative PCR (qPCR) that targets the 18S rRNA gene of *E. bienersi*. We performed genomic DNA extraction with the QIAmp DNA Stool Mini Kit (QIAGEN, <https://www.qiagen.com>), according to the manufacturer's instructions. We stored DNA extracts at -20°C until subsequent analysis. We completed amplification with Eb and Eb5 oligonucleotide primers at a final concentration of $0.5\ \mu\text{mol/L}$ and detected the 180-bp product using the specific fluorescent TaqMan probe EbS2 in the LightCycler 480 II apparatus (Roche, <https://www.roche.com>) as described previously (7,21). We set the positive cutoff value of qPCR at ≤ 39 quantitative cycles (Cq) and tested each clinical sample in duplicate. We assessed inhibition with a positive exogenous internal control (Universal Inhibition Control Cy5; Diagenode, <https://www.diagenode.com>). We confirmed all samples with positive qPCR results using microscopy with specific staining of microsporidia spores by the Uvitex 2B brightener (Ciba-Geigy, <https://www.novartis.com>) according to van Gool's method (22) (Appendix Figure 1, <http://wwwnc.cdc.gov/EID/article/25/9/19-0311-App1.pdf>).

Study Population and Biologic Samples

In this study, we included all patients from center 1 who were found to be positive for *E. bienersi* detection during January 2011–December 2018; they were considered a priori to be epidemiologically unrelated to the 3 cluster cases (M01-05 to M01-07). We included 8 supplementary control cases in the study: 4 were provided by a second university hospital, center 2 (Clermont-Ferrand, France; latitude 45.759549, longitude 3.089723), and the remaining 4 by another university hospital, center 3 (Nantes, France; latitude 47.2121974, longitude -1.554346).

Genotyping of Clinical *E. bienersi* Strains

Genotype Identification by Sequence Typing of ITS rDNA Region

We amplified the DNA extract in a $25\text{-}\mu\text{L}$ final volume and sequenced it for the ITS rDNA region. For patients with multiple positive samples, we tested only the first sample by genotyping. We used the MSP3 and MSP4B primers (23). ITS PCR products were purified and nucleotide sequencing performed on both strands by Eurofins Laboratories (<https://www.eurofins.com>). We compared the 243-bp sequences obtained with all *E. bienersi* sequences available from the National Center for Biotechnology Information using the BLAST algorithm (<http://blast.ncbi.nlm.nih.gov/Blast.cgi>). We performed the evolutionary analysis of *E. bienersi* ITS genotypes with MEGA version 7.0.26 (<https://www.megasoftware.net>)

(24) and aligned all genotypes with 40 *E. bienersi* ITS genotype sequences from GenBank(9).

Minisatellite and Microsatellite Polymorphism Genotyping

We studied the genetic diversity of the clinical strains of *Enterocytozoon bienersi* further by analyzing 1 minisatellite (MS4) and 3 microsatellites (MS1, MS3, and MS7), as previously described (16). We defined sequence types by comparing MS sequences. We then performed multilocus analysis by combining ITS sequences with the 4 MS markers to define MLGs. We used the Clustal Omega algorithm (<https://www.ebi.ac.uk/Tools/msa/clustalo>) for sequence alignment and examined the relationship between MLGs by a median-joining network analysis using Network version 5.0.1.1 and Network Publisher version 2.1.1.2 software (<http://www.fluxus-engineering.com>). To confirm the clustering of cases, we also performed an evolutionary analysis of combined nucleotide sequences by the maximum likelihood method based on the Tamura 3-parameter model in MEGA version 7.0.26. We uploaded all sequences to GenBank (accession numbers in Appendix Table).

Transmission Map

We studied patient movements within center 1 and to identify possible sites where the 3 cluster cases with *E. bienersi* microsporidiosis (M01-05 to M01-07) may have come into contact. To do so, we extracted dates of outpatient visits and hospitalizations retrospectively from the medical records (Dossier Patient Partagé, Cerner SAS, Paris-La Défense, France).

Results

Description of Cluster Cases

During January 1–December 31, 2018, we found 44 fecal samples obtained from 25 patients at center 1 positive for *E. bienersi* (overall prevalence 0.53% of fecal samples; Figure 1; Appendix Figure 1). The cohort of microsporidiosis cases included HIV-infected persons; solid-organ transplant recipients; and patients with hematologic malignancies, autoimmune diseases, or cirrhosis (Appendix Table). The yearly frequency of diagnosis of *E. bienersi* infection varied randomly during the study period (Figure 1). The 3

cluster cases of *E. bienersi* microsporidiosis (M01-05 to M01-07) were diagnosed in the same hematology department over a 4-day period, January 12–16, 2018. All 3 patients had been admitted to the hospital for symptoms of diarrhea, deterioration of their general health status, or both. No individual risk behaviors, including swimming in wild rivers, consumption of nonpotable water, or close contact with animals, were identified in these patients. They resided in towns that were geographically located at distances 28.7–104.0 km apart.

Full details of all their medical consultations and hospital admissions were available and in-hospital movements collected (Figure 2). Only 1 period for possible direct patient-to-patient contact was determined: December 26–28, 2017, in the hematology inpatient department. The patients were placed in neighboring rooms 15 and 17 days before the first sample was found positive for *E. bienersi*, the only period of concomitant hospitalization. However, during January 11–12, 2018, patients M01-06 and M01-07 spent time in 3 different but closely located hospital wards: in the short-stay oncology unit (M01-06) and in the hematology inpatient department and the oncology outpatient unit (M01-07). These 3 clinical units are in the same hospital building on the same floor and share the same food and water supplies and some common healthcare staff.

ITS Genotyping of Clinical *E. bienersi* Strains

We included 33 cases in our study; 25 from center 1, 4 from center 2, and 4 from center 3 were successfully genotyped. The remaining 8 cases were unavailable for genotyping (Figure 1). On the basis of ITS rDNA sequencing, we determined that the 3 *E. bienersi* strains from cluster cases belonged to a new genotype, closely related to genotype C (referred to hereafter as C-like01; Appendix Figure 2). We identified 2 other new genotypes in the center 1 cohort: C-like04, which was closely related to genotype C (synonym genotype II), and IV-like01, closely related to genotype IV (synonym genotype K) (Appendix Figure 2). C-like01 and C-like04 genotypes differed from genotype C by 1 single-nucleotide polymorphism (SNP), at positions 83 (G→A) for the C-like01 genotype and 236 (G→A) for the C-like04 genotype. The IV-like01 genotype also differed from the IV genotype by 1 SNP (G→A) at position 236 (Appendix Figure 3). Other genotypes identified in our study



Figure 1. Incident number and ITS rDNA region genotypes of *Enterocytozoon bienersi* infection cases (n = 25) in center 1 university hospital, France, January 1, 2011–December 31, 2018. ITS, internal transcribed spacer.

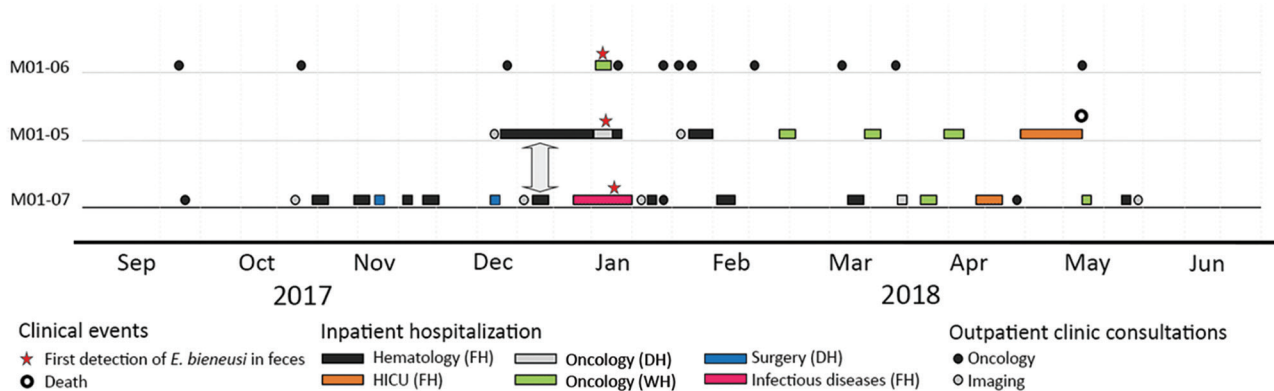


Figure 2. Hospitalization mapping for 3 patients with concomitant *Enterocytozoon bieneusi* microsporidiosis in the hematology unit of Center 1 university hospital, France. On the x-axis, dates (month-year) range from 5 months before to 5 months after the outbreak; on the y-axis, anonymous patient codes are given. The vertical arrow indicates the period December 26–28, 2017, when 2 patients, M01-05 and M01-07, were concomitantly housed in the same clinical department (FH in the hematology unit). DH, day hospitalization; FH, full hospitalization; HICU, hematology intensive care unit; WH, week hospitalization.

(Appendix Table) belonged to genotypes C (n = 13), IV (n = 3), and S9 (n = 2).

MLG Analyses

We performed MLG analyses using the combination of ITS with MS1, MS3, MS4, and MS7 loci. In 3 of the 25 isolates (M01-18, M01-77, and M01-79), ≥1 MS markers could not be successfully amplified (Appendix Table). Amplification efficiency was 96.0% for MS1, 92.0% for MS3 and MS7, and 88.0% for MS4. Sequence analysis of each MS marker showed a high diversity of sequence types (STs). The MS3 marker was the least variable marker, with only 5 different STs, followed by MS7 (8 STs) and MS4 (12 STs); MS1 was the most polymorphic, with 16 different STs (Appendix Table). Combination of ITS with MS markers for the 22 complete isolates (isolates for which all MS markers were successfully sequenced) resulted in 20 different MLGs (Appendix Table). Network analysis confirmed that the 3 isolates from the cluster cases in the hematology unit were very similar (Figure 3). M01-06 and M01-07 were 100% identical among the 1,904 nt positions analyzed. M01-05 differed slightly from MS7 at 1 tandem repeat. Overall, phylogenetic analyses confirmed the close relationship among the 3 isolates (Appendix Figure 4).

The MLG results, together with the short period between the occurrence of the 3 cluster cases and the association of the new C-like01 genotype with the cluster cases, provided evidence that the isolates were epidemiologically related. In addition, the MLG analyses showed a high heterogeneity among isolates belonging to the same ITS genotype. Only M01-06/M01-07 (C-like01 ITS genotype) from cluster cases and M01-67/M01-68 (C-like04 ITS genotype) were 100% identical to each other. M01-67 and M01-68 were isolated from 2 patients in center 1 during a 7-day

period in 2017. M01-67 was isolated from a 61-year-old woman admitted to the department of internal medicine with rheumatoid purpura, and M01-68 was isolated from a 70-year-old woman with hepatocellular carcinoma who died after a hospital stay of 15 days in the hepatology department. The C-like04 genotype had also been identified 2 years previously in a patient (M01-72) from center 1. However, this isolate was clearly different from the others (Figure 3).

Discussion

The infection rate of intestinal microsporidiosis remains elevated in children in developing countries (1). The incidence among the HIV-positive population has been greatly reduced as a result of highly active antiretroviral therapy

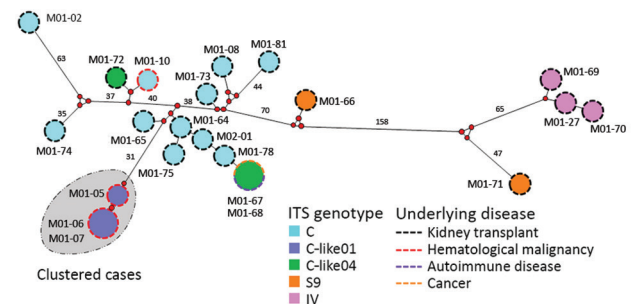


Figure 3. Median-joining analysis of the multilocus sequence typing (MLST) data for 22 *Enterocytozoon bieneusi* isolates from 3 different hospital centers in France, determined by using Network version 5.0.1.1 and Network Publisher version 2.1.1.2 software (<http://www.fluxus-engineering.com>). Circles are proportional to the frequency of each genotype (a total of 20 multilocus genotypes were obtained based on segregating sites). Pairwise differences >25 single-nucleotide polymorphisms (SNPs) are shown close to branches, which were shortened for better presentation. Gray shading indicates isolates from the cluster investigated in this study. ITS, internal transcribed spacer.

and subsequent immunity restoration (1). In addition to sporadic cases in travelers, infections in new populations of immunocompromised patients exposed to the disease are now emerging; these populations include solid-organ transplant recipients and patients who have cancer and hematologic malignancies. In our study, 1 of 25 patients from center 1 was HIV positive, and 15 of 25 were solid-organ transplant recipients (20,25). A recent monocentric study in a hospital in France estimated the overall prevalence of microsporidia spores in fecal samples over a 2-year period at 1.1% (26).

To study the epidemiology of pathogens and specifically to address outbreaks (27), sequence typing has long been considered to be the standard for most infectious diseases (11–14). Many previous studies focused on *E. bienersi* were restricted to an overall determination of its genotype and investigated only nucleotide sequences of the ITS rDNA region (28,29). In 2011, Feng et al. reported a MLST-based method for *E. bienersi* genotyping (16). This powerful tool has been widely used in animals and humans to decipher genetic diversity within the *E. bienersi* species (10). We applied this method to an outbreak investigation. The MLST method generated a great length of microsporidian DNA containing highly variable regions ranging from 1,856 to 2,160 bp. Thus, the discriminatory power between *E. bienersi* strains was much stronger by this technique than with ITS genotyping alone.

Using the MLST genotyping method, we defined the *E. bienersi* strains isolated from the 3 patients admitted to the hematology unit as a new genotype (C-like01); these strains were closely clustered. This finding supported the conclusion that these patients shared the same strain, likely from a common source of contamination that remains undetermined (18). In our study, hospitalization mapping of the patients' movements supported the hypothesis of nosocomial acquisition. Because this was a retrospective investigation, we were unable to evaluate the safety of the food and beverages that were provided to the patients in the hospital during the weeks before the report of the outbreak (30).

Reports of community-acquired foodborne or waterborne microsporidiosis outbreaks are rare. The recent literature includes the massive epidemic in Lyon, France, with an attack rate of 1.0% in HIV-positive patients each month during the summer of 1995 (31). At that time, molecular tools were not available to investigate the epidemiologic links between microsporidian strains. In 2009, a probable outbreak in a hotel in Sweden involving 135 persons with an attack rate of 30.0% was associated with cucumber consumption (32). In that study, the authors stated that 6 *E. bienersi* strains were identified as genotype C, but no detailed genotyping was performed to investigate the genetic relationships among the isolates. The authors reported the

incubation period of *E. bienersi* infection in this outbreak ranged from 0 to 21 days.

In our study, 2 of the 3 cluster case patients were hospitalized ≥ 15 days before their first symptoms, which is compatible with nosocomial acquisition. The remaining patient was admitted to the short-stay oncology unit for 2 days when microsporidiosis occurred, but he also visited the hospital every month for regular medical consultations. We cannot exclude the possibility that the transmission of *E. bienersi* involved asymptomatic persons, such as transiently colonized nurses and doctors or other patients as direct person-to-person contacts (33). However, few studies have been able to provide molecular evidence that colonized persons can serve as direct infectious sources (3,12). Comprehensive demonstration of transmission is hampered (34) because the time lapse for spore excretion in the feces and the minimal infective inoculum are unknown. Indirect transmission is also a possibility because the spores have protective walls formed of proteins and chitin that would allow them to persist in the environment for at least several weeks (3).

With respect to these findings, it is difficult to define a robust method to prevent *E. bienersi* infection in patients at risk. Recent data support the inclusion of microsporidia on the National Institutes of Health/Centers for Disease Control and Prevention biodefense category B list of pathogens of concern for waterborne and foodborne transmission. Unfortunately, official guidelines are scarce, especially regarding persons with hematologic malignancies. In HIV-positive patients with T-cell lymphocyte CD4+ count < 200 cells/ μL , the Centers for Disease Control and Prevention strongly recommends reducing environmental exposure by avoiding untreated water sources (level of evidence: AIII) (35). Regardless of the context, we suggest that standard hygiene precautions be used, including decontamination of the hands with an alcohol-based rub. In addition, wearing personal protective equipment when in close contact with infected patients should be standard practice, as should thorough cleaning of environmental surfaces.

In conclusion, our study presents a report of 3 cluster cases of microsporidiosis in a hospital and provides strong epidemiologic and molecular evidence of a common source of contamination. We also demonstrate the high genetic diversity of *Enterocytozoon bienersi*. Our findings suggest that the MLG approach will further extend our knowledge about the epidemiology of microsporidiosis and that incidence of nosocomial contamination may be more common than previously recognized.

Acknowledgments

We thank the French Microsporidiosis Network and the French National Reference Center of cryptosporidiosis for their support. We are also grateful to Ophélie Derouard, Béatrice Champion-

Yzon, and Lucie Schwaar for their technical help in handling the *E. bienersi* strains and to Valentin Travia for his protocol describing the qPCR method. We further thank Jeffrey Watts for advice on the English version of the manuscript and Carolyn Cray for editing the final submitted version.

This work was supported by the Direction de la Recherche Clinique et de l'Innovation of the University Hospital of Clermont-Ferrand, France, and by internal laboratory funding.

About the Author

Prof. Desoubeaux is a parasitologist and mycologist working in the University Hospital of Tours, France. His primary research interest is in epidemiological investigations of fungal diseases.

References

- Didier ES, Weiss LM. Microsporidiosis: current status. *Curr Opin Infect Dis.* 2006;19:485–92. <https://doi.org/10.1097/01.qco.0000244055.46382.23>
- Mathis A, Weber R, Deplazes P. Zoonotic potential of the microsporidia. *Clin Microbiol Rev.* 2005;18:423–45. <https://doi.org/10.1128/CMR.18.3.423-445.2005>
- Anane S, Attouchi H. Microsporidiosis: epidemiology, clinical data and therapy. *Gastroenterol Clin Biol.* 2010;34:450–64. <https://doi.org/10.1016/j.gcb.2010.07.003>
- Wasson K, Peper RL. Mammalian microsporidiosis. *Vet Pathol.* 2000;37:113–28. <https://doi.org/10.1354/vp.37-2-113>
- Stentiford GD, Becnel J, Weiss LM, Keeling PJ, Didier ES, Williams BP, et al. Microsporidia—emergent pathogens in the global food chain. *Trends Parasitol.* 2016;32:336–48. <https://doi.org/10.1016/j.pt.2015.12.004>
- Yakoob J, Abbas Z, Beg MA, Jafri W, Naz S, Khalid A, et al. Microsporidial infections due to *Encephalitozoon intestinalis* in non-HIV-infected patients with chronic diarrhoea. *Epidemiol Infect.* 2012;140:1773–9. <https://doi.org/10.1017/S0950268811002639>
- Desoubeaux G, Caumont C, Passot C, Dartigeas C, Bailly E, Chandener J, et al. Two cases of opportunistic parasite infections in patients receiving alemtuzumab. *J Clin Pathol.* 2012;65:92–5. <https://doi.org/10.1136/jclinpath-2011-200403>
- Santín M, Calero-Bernal R, Carmena D, Mateo M, Balseiro A, Barral M, et al. Molecular characterization of *Enterocytozoon bienersi* in wild carnivores in Spain. *J Eukaryot Microbiol.* 2018;65:468–74. <https://doi.org/10.1111/jeu.12492>
- Santín M, Fayer R. *Enterocytozoon bienersi* genotype nomenclature based on the internal transcribed spacer sequence: a consensus. *J Eukaryot Microbiol.* 2009;56:34–8. <https://doi.org/10.1111/j.1550-7408.2008.00380.x>
- Li W, Xiao L. Multilocus sequence typing and population genetic analysis of *Enterocytozoon bienersi*: host specificity and its impacts on public health. *Front Genet.* 2019;10:307. <https://doi.org/10.3389/fgene.2019.00307>
- Desoubeaux G, Debourogne A, Wiederhold NP, Zaffino M, Sutton D, Burns RE, et al. Multi-locus sequence typing provides epidemiological insights for diseased sharks infected with fungi belonging to the *Fusarium solani* species complex. *Med Mycol.* 2018;56:591–601. <https://doi.org/10.1093/mmy/56/3/591>
- Le Gal S, Damiani C, Rouillé A, Grall A, Tréguer L, Virmaux M, et al. A cluster of *Pneumocystis* infections among renal transplant recipients: molecular evidence of colonized patients as potential infectious sources of *Pneumocystis jirovecii*. *Clin Infect Dis.* 2012;54:e62–71. <https://doi.org/10.1093/cid/cir996>
- Maitte C, Leterrier M, Le Pape P, Miegerville M, Morio F. Multilocus sequence typing of *Pneumocystis jirovecii* from clinical samples: how many and which loci should be used? *J Clin Microbiol.* 2013;51:2843–9. <https://doi.org/10.1128/JCM.01073-13>
- Desoubeaux G, Dominique M, Morio F, Thepault R-A, Franck-Martel C, Tellier A-C, et al. Epidemiological outbreaks of *Pneumocystis jirovecii* pneumonia are not limited to kidney transplant recipients: genotyping confirms common source of transmission in a liver transplantation unit. *J Clin Microbiol.* 2016;54:1314–20. <https://doi.org/10.1128/JCM.00133-16>
- Hadrich I, Neji S, Drira I, Trabelsi H, Mahfoud N, Ranque S, et al. Microsatellite typing of *Aspergillus flavus* in patients with various clinical presentations of aspergillosis. *Med Mycol.* 2013;51:586–91. <https://doi.org/10.3109/13693786.2012.761359>
- Feng Y, Li N, Dearen T, Lobo ML, Matos O, Cama V, et al. Development of a multilocus sequence typing tool for high-resolution genotyping of *Enterocytozoon bienersi*. *Appl Environ Microbiol.* 2011;77:4822–8. <https://doi.org/10.1128/AEM.02803-10>
- Li W, Wan Q, Yu Q, Yang Y, Tao W, Jiang Y, et al. Genetic variation of mini- and microsatellites and a clonal structure in *Enterocytozoon bienersi* population in foxes and raccoon dogs and population differentiation of the parasite between fur animals and humans. *Parasitol Res.* 2016;115:2899–904. <https://doi.org/10.1007/s00436-016-5069-3>
- Widmer G, Dilo J, Tumwine JK, Tzipori S, Akiyoshi DE. Frequent occurrence of mixed *Enterocytozoon bienersi* infections in humans. *Appl Environ Microbiol.* 2013;79:5357–62. <https://doi.org/10.1128/AEM.01260-13>
- Moore HM, Kelly AB, Jewell SD, McShane LM, Clark DP, Greenspan R, et al. Biospecimen reporting for improved study quality (BRISQ). *Cancer Cytopathol.* 2011;119:92–102. <https://doi.org/10.1002/cncy.20147>
- Didier ES, Weiss LM. Microsporidiosis: not just in AIDS patients. *Curr Opin Infect Dis.* 2011;24:490–5. <https://doi.org/10.1097/QCO.0b013e32834aa152>
- Lejeune A, Espern A, Phung DC, Nguyen TC, Miegerville M. Presentation of the first *Enterocytozoon bienersi* intestinal microsporidia case in an HIV patient, Hanoi, Vietnam [in French]. *Med Mal Infect.* 2005;35:425–6. <https://doi.org/10.1016/j.medmal.2005.06.003>
- van Gool T, Dankert J. Human microsporidiosis: clinical, diagnostic and therapeutic aspects of an increasing infection. *Clin Microbiol Infect.* 1995;1:75–85. <https://doi.org/10.1111/j.1469-0691.1995.tb00450.x>
- Katzwinkel-Wladarsch S, Lieb M, Heise W, Löscher T, Rinder H. Direct amplification and species determination of microsporidian DNA from stool specimens. *Trop Med Int Health.* 1996;1:373–8. <https://doi.org/10.1046/j.1365-3156.1996.d01-51.x>
- Tamura K, Stecher G, Peterson D, Filipiński A, Kumar S. MEGA6: Molecular Evolutionary Genetics Analysis version 6.0. *Mol Biol Evol.* 2013;30:2725–9. <https://doi.org/10.1093/molbev/mst197>
- Galván AL, Martín Sánchez AM, Pérez Valentín MA, Henriques-Gil N, Izquierdo F, Fenoy S, et al. First cases of microsporidiosis in transplant recipients in Spain and review of the literature. *J Clin Microbiol.* 2011;49:1301–6. <https://doi.org/10.1128/JCM.01833-10>
- Greigert V, Pfaff AW, Abou-Bacar A, Candolfi E, Brunet J. Intestinal microsporidiosis in Strasbourg from 2014 to 2016: emergence of an *Enterocytozoon bienersi* genotype of Asian origin. *Emerg Microbes Infect.* 2018;7:1–7. <https://doi.org/10.1038/s41426-018-0099-9>
- van Diepeningen AD, Feng P, Ahmed S, Sudhadham M, Bunyaratavej S, de Hoog GS. Spectrum of *Fusarium* infections in

- tropical dermatology evidenced by multilocus sequencing typing diagnostics. *Mycoses*. 2015;58:48–57. <https://doi.org/10.1111/myc.12273>
28. Pomares C, Santin M, Miegerville M, Espem A, Albano L, Marty P, et al. A new and highly divergent *Enterocytozoon bieneusi* genotype isolated from a renal transplant recipient. *J Clin Microbiol*. 2012;50:2176–8. <https://doi.org/10.1128/JCM.06791-11>
 29. Zhang X, Wang Z, Su Y, Liang X, Sun X, Peng S, et al. Identification and genotyping of *Enterocytozoon bieneusi* in China. *J Clin Microbiol*. 2011;49:2006–8. <https://doi.org/10.1128/JCM.00372-11>
 30. Ben Ayed L, Yang W, Widmer G, Cama V, Ortega Y, Xiao L. Survey and genetic characterization of wastewater in Tunisia for *Cryptosporidium* spp., *Giardia duodenalis*, *Enterocytozoon bieneusi*, *Cyclospora cayatanensis* and *Eimeria* spp. *J Water Health*. 2012;10:431–44. <https://doi.org/10.2166/wh.2012.204>
 31. Cotte L, Rabodonirina M, Chapuis F, Bailly F, Bissuel F, Raynal C, et al. Waterborne outbreak of intestinal microsporidiosis in persons with and without human immunodeficiency virus infection. *J Infect Dis*. 1999;180:2003–8. <https://doi.org/10.1086/315112>
 32. Decraene V, Lebbad M, Botero-Kleiven S, Gustavsson A-M, Löfdahl M. First reported foodborne outbreak associated with microsporidia, Sweden, October 2009. *Epidemiol Infect*. 2012;140:519–27. <https://doi.org/10.1017/S095026881100077X>
 33. Scaglia M, Gatti S, Sacchi L, Corona S, Chichino G, Bernuzzi AM, et al. Asymptomatic respiratory tract microsporidiosis due to *Encephalitozoon hellem* in three patients with AIDS. *Clin Infect Dis*. 1998;26:174–6. <https://doi.org/10.1086/516264>
 34. Choukri F, Menotti J, Sarfati C, Lucet J-C, Nevez G, Garin YJF, et al. Quantification and spread of *Pneumocystis jirovecii* in the surrounding air of patients with *Pneumocystis pneumonia*. *Clin Infect Dis*. 2010;51:259–65. <https://doi.org/10.1086/653933>
 35. Kaplan JE, Benson C, Holmes KK, Brooks JT, Pau A, Masur H, et al. Guidelines for prevention and treatment of opportunistic infections in HIV-infected adults and adolescents: recommendations from CDC, the National Institutes of Health, and the HIV Medicine Association of the Infectious Diseases Society of America. *MMWR Recomm Rep*. 2009;58:1–207.

Address for correspondence: Philippe Poirier, CHU Gabriel-Montpied, Laboratoire de Parasitologie-Mycologie, 58 Rue Montalembert, 63000 Clermont-Ferrand, France; email: ppoirier@chu-clermontferrand.fr

etymologia

Sporothrix [spor'o-thriks] *schenckii*

Fábio P. Sellera, Carlos E. Larsson

From the Greek *sporotrich* and later from the Latin *spor-* (spore) + *thrix* (hair), *Sporothrix schenckii* was named as a tribute to Benjamin Schenck, a medical student at the Johns Hopkins Hospital, who first isolated the fungus from a patient who had lesions on the right hand and arm in 1896. This fungus was erroneously assigned to the genus *Sporotrichum* until 1962, when it was reclassified as *Sporothrix*.

S. schenckii is a saprophyte and pathogenic fungus that is responsible for sporotrichosis that is endemic mostly to tropical and subtropical regions. Sporotrichosis (also known as “rose gardener’s disease”) was related primarily to agricultural workers who had cuts or abrasions in the skin, and later to scratches and bites from companion and wild animals. Currently, it is recognized that *S. schenckii* is a species complex that includes *S. brasiliensis*, *S. globosa*, *S. mexicana*, *S. luriei*, and *S. schenckii sensu stricto*.



Petri dish culture of a colony of the fungus *Sporothrix schenckii* strain M-36-53. This fungus is the cause of sporotrichosis. Centers for Disease Control and Prevention, Dr. Lucille K. Georg, 1964

Author affiliation: Universidade de São Paulo, São Paulo, Brazil

Sources

1. Barros MB, de Almeida Paes R, Schubach AO. *Sporothrix schenckii* and sporotrichosis. *Clin Microbiol Rev*. 2011;24:633–54. <http://dx.doi.org/10.1128/CMR.00007-11>
2. Gold JA, Derado G, Mody RK, Benedict K. Sporotrichosis-associated hospitalizations, United States, 2000–2013. *Emerg Infect Dis*. 2016;22:1817–20. <http://dx.doi.org/10.3201/eid2210.160671>
3. Marimon R, Cano J, Gené J, Sutton DA, Kawasaki M, Guarro J. *Sporothrix brasiliensis*, *S. globosa*, and *S. mexicana*, three new *Sporothrix* species of clinical interest. *J Clin Microbiol*. 2007;45:3198–206. <https://doi.org/10.1128/JCM.00808-07>
4. Schenck BR. On refractory subcutaneous abscess caused by a fungus possibly related to the Sporotricha. *Bull Johns Hopkins Hosp*. 1898;9:286–90.
5. Schubach A, Schubach TM, Barros MB, Wanke B. Cat-transmitted sporotrichosis, Rio de Janeiro, Brazil. *Emerg Infect Dis*. 2005;11:1952–4. <http://dx.doi.org/10.3201/eid1112.040891>

Address for correspondence: Fábio P. Sellera, Department of Internal Medicine, School of Veterinary Medicine and Animal Science, Universidade de São Paulo, São Paulo, SP 05508-270, Brazil; email: fsellera@usp.br

DOI: <https://doi.org/10.3201/eid2509.ET2509>

Epidemiology of Carbapenemase-Producing *Klebsiella pneumoniae* in a Hospital, Portugal

Marta Aires-de-Sousa, José Manuel Ortiz de la Rosa, Maria Luísa Gonçalves, Ana Luísa Pereira, Patrice Nordmann, Laurent Poirel

We aimed to provide updated epidemiologic data on carbapenem-resistant *Klebsiella pneumoniae* in Portugal by characterizing all isolates (N = 46) recovered during 2013–2018 in a 123-bed hospital in Lisbon. We identified *bla*_{KPC-3} (n = 36), *bla*_{OXA-181} (n = 9), and *bla*_{GES-5} (n = 8) carbapenemase genes and observed co-occurrence of *bla*_{KPC-3} and *bla*_{GES-5} in 7 isolates. A single GES-5–producing isolate co-produced the extended-spectrum β-lactamase BEL-1; both corresponding genes were co-located on the same ColE1-like plasmid. The *bla*_{OXA-181} gene was always located on an IncX3 plasmid, whereas *bla*_{KPC-3} was carried on IncN, IncFII, IncFIB, and IncFIIA plasmid types. The 46 isolates were distributed into 13 pulsotypes and 9 sequence types. All isolates remained susceptible to ceftazidime/avibactam, but some exhibited reduced antimicrobial susceptibility (MIC = 3 mg/L).

Klebsiella pneumoniae is a major cause of hospital-acquired infections, mainly responsible for urinary, respiratory, and bloodstream infections, as well as infections in intensive care unit (ICU) patients. The emergence of antimicrobial resistance, in particular the rise of carbapenem-resistant isolates, is a serious concern for the management of infections caused by *K. pneumoniae* because treatment alternatives are limited. Therefore, carbapenem-resistant *K. pneumoniae* are ranked among the recently published World Health Organization list of antibiotic-resistant “priority/critical” pathogens, for which research and development of new antibiotics is required (1).

Author affiliations: Escola Superior de Saúde da Cruz Vermelha Portuguesa, Lisbon, Portugal (M. Aires-de-Sousa); Instituto de Tecnologia Química e Biológica António Xavier, Universidade Nova de Lisboa, Oeiras, Portugal (M. Aires-de-Sousa); Université de Fribourg, Fribourg, Switzerland (M. Aires-de-Sousa, J.M. Ortiz de la Rosa, P. Nordmann, L. Poirel); Hospital SAMS, Lisbon (M.L. Gonçalves, A.L. Pereira); Swiss National Reference Center for Emerging Antibiotic Resistance, Fribourg (P. Nordmann, L. Poirel); University of Lausanne, Lausanne, Switzerland (P. Nordmann); University Hospital Centre, Lausanne (P. Nordmann)

DOI: <https://doi.org/10.3201/eid2509.190656>

Carbapenem resistance in *K. pneumoniae* arises from 2 main mechanisms: permeability defects combined with overexpression of a β-lactamase with weak carbapenemase activity (mostly CTX-M or AmpC cephalosporinases) and the acquisition of carbapenemases (2). Carbapenemase enzymes belong to 3 different Ambler classes (3). Class A includes the KPC-type enzyme, which has been extensively reported in *K. pneumoniae*; to date, although >20 different KPC variants have been described, KPC-2 and KPC-3 remain the most common types (4). In addition, a few studies reported the carbapenemase GES-5 (a point mutant derivative of the extended-spectrum β-lactamase [ESBL] GES-1) in *K. pneumoniae* (5). Class B includes the metallo-β-lactamases, which are mainly NDM-, VIM-, and IMP-type enzymes, and class D includes OXA-48–like β-lactamases.

The first clinical carbapenemase-producing *K. pneumoniae* in Portugal was isolated at a Lisbon hospital in 2009 (6). Since then, only sporadic infection isolates and single hospital cases have been reported (7,8), as well as a single outbreak of KPC-3–producing *K. pneumoniae* in 2013 (9). Surprisingly, no other carbapenemase type, such as OXA-48 and derivatives that are widespread in other countries in Europe (8), has been identified in *K. pneumoniae* in Portugal so far. A survey of *Enterobacteriaceae* collected in 13 hospitals in Portugal confirmed a low prevalence of carbapenemase producers in the country until 2013 (35/2105 [1.7%]) and a predominance of *K. pneumoniae* KPC-3 producers (10). However, in 2017, according to the annual report of the European Centre for Disease Prevention and Control on antimicrobial resistance in Europe, 8.6% of *K. pneumoniae* causing invasive infections in Portugal were resistant to carbapenems (11). That report also showed that Portugal faced an annual increasing trend of carbapenem resistance among *K. pneumoniae* since 2014 (1.8% in 2014, 3.4% in 2015, 5.2% in 2016, and 8.6% in 2017), exceeding the overall prevalence for Europe (7.2%). Nevertheless, data on the molecular epidemiology of nosocomial carbapenemase-producing *K. pneumoniae* in Portugal are still limited, and the existing studies include isolates

recovered until 2014 only (10,12,13). Therefore, the aim of our study was to provide updated epidemiologic data on contemporary carbapenemase-producing *K. pneumoniae* in an acute-care facility hospital in Portugal by characterizing a collection of nonrepetitive isolates recovered during a 6-year period (2013–2018).

Materials and Methods

Bacterial Isolates

Carbapenemase-producing *K. pneumoniae* isolates (N = 46) recovered during 2013 (n = 1), 2014 (n = 1), 2016 (n = 9), 2017 (n = 12), and 2018 (n = 23) in a 123-bed hospital (SAMS Hospital) in Lisbon, Portugal, were used for our study. All isolates were from single patients and recovered from colonization and infection sites: rectal swabs (n = 20), urine (n = 15), sputum (n = 4), blood (n = 4), and other sites (n = 3). The isolates were obtained from 22 inpatients (ICU, n = 7; medicine ward, n = 11; surgery ward, n = 3; other, n = 1) and 24 outpatients (emergency department, n = 21; ambulatory consultation, n = 3).

Susceptibility Testing

We performed antimicrobial susceptibility testing by using the disk diffusion method on Mueller-Hinton agar plates (Bio-Rad, <http://www.bio-rad.com>) for amoxicillin, amoxicillin/clavulanic acid, ticarcillin, ticarcillin/clavulanic acid, piperacillin, piperacillin/tazobactam, temocillin, ceftazidime, cefotaxime, cefoxitin, aztreonam, imipenem, ertapenem, meropenem, gentamicin, amikacin, ciprofloxacin, tigecycline, trimethoprim-sulfamethoxazole (SXT), and fosfomycin, following EUCAST recommendations (<http://www.eucast.org>). We determined MICs for imipenem, ertapenem, meropenem, and ceftazidime/avibactam by Etest (bioMérieux, <http://www.biomerieux.com>). Interpretation of MICs and zone diameters followed EUCAST breakpoint tables (http://www.eucast.org/fileadmin/src/media/PDFs/EUCAST_files/Breakpoint_tables/v_9.0_Breakpoint_Tables.pdf).

We assessed selection of carbapenemase producers by using the Rapidec Carba NP test (bioMérieux) (14). In addition, we evaluated colistin susceptibility by using the Rapid Polymyxin NP test (ELITechGroup Microbiology, <http://www.elitechgroup.com>) (15).

Molecular Analysis

We identified carbapenemases (16) and ESBL genes (17) and detected the *mcr*-type colistin-resistance gene (18) by using PCR amplification, followed by sequencing of the amplicons. We used standard PCR conditions to amplify the β -lactamase gene *bla*_{CMY}, encoding plasmid-mediated cephalosporinases (19), and the *qnrS* quinolone resistance gene (20). We detected the *bla*_{OXA-9} gene encoding a narrow-

spectrum class D β -lactamase by using PCR amplification with primers OXA-9 FW 5'-ATGAAGGATACCTTGATGAAAA-3' and OXA-9 RW 5'-TCATTGTTACCCATCAACACG-3'.

We evaluated the clonal relationship of the isolates by pulsed-field gel electrophoresis (PFGE), as described previously (21). We performed multilocus sequence typing (MLST) for a representative strain of each PFGE type and assigned sequence types (STs) by using the MLST database for *K. pneumoniae* (<http://bigsd.bpasteur.fr/klebsiella/klebsiella.html>).

Conjugation Experiments and Plasmid Analysis

We performed mating-out assays by using the azide-resistant *Escherichia coli* J53 as the recipient. We separately inoculated donors carrying *E. coli* J53 and *bla*_{KPC-3} or *bla*_{OXA-181} overnight into LB broth (5 mL) and incubated, then subsequently mixed samples at a ratio of 10:1 (donor:recipient) for 5 h. We deposited 100 μ L of this mix onto 22- μ m filters and incubated overnight at 37°C on LB agar plates. After the incubation, we resuspended filters in 0.85% NaCl, then plated 100 μ L of this mixture onto LB agar plates supplemented with ticarcillin (100 μ g/mL) and azide (100 μ g/mL). We performed susceptibility testing for all *E. coli* transconjugants and assessed positivity for *bla*_{KPC-3} or *bla*_{OXA-181} by using PCR.

We classified plasmids according to their incompatibility group by using the PCR-based replicon typing method as described previously (22). We characterized the plasmid carrying *bla*_{BEL-1} and *bla*_{GES-5} genes by using primers for ColE1-like plasmids, as previously described (23).

Results

Among the 46 carbapenemase-producing isolates, the most common carbapenemase identified was KPC-3 (n = 36 [78%]), followed by OXA-181 (n = 9 [20%]) and GES-5 (n = 8 [17%]) (Table). Seven isolates co-harbored >1 carbapenemase gene (*bla*_{KPC-3} and *bla*_{GES-5}). The *bla*_{OXA-9} gene encoding a narrow-spectrum class D β -lactamase was identified in 31 isolates, all of which were KPC-3 producers. A single GES-5-producing isolate co-produced the ESBL BEL-1.

Mating-out assays followed by PCR-based replicon typing revealed that the *bla*_{OXA-181} gene was always located onto an IncX3 plasmid, whereas the *bla*_{KPC-3} gene was carried onto IncN, IncFII, IncFIB, and IncFIIA plasmid types. The genes *bla*_{GES-5} and *bla*_{BEL-1} were co-located on the same ColE1-like plasmid.

Antimicrobial susceptibility testing showed that 13 (28%) of the 46 carbapenemase producers were susceptible to imipenem (MIC \leq 0.5 mg/L) and 10 (22%) isolates were susceptible to meropenem (MIC \leq 1 mg/L). Eight (17%) isolates were susceptible to both carbapenems, and all except 1 were OXA-181 producers (p<0.001). The

SYNOPSIS

Table. Characteristics of 46 carbapenemase-producing *Klebsiella pneumoniae* isolates collected in a hospital in Portugal, 2013–2018*

PFGE type	ST	Isolation year†	No. isolates	Resistance determinants‡	Plasmid type§	MIC for ceftazidime/avibactam, mg/L	Nonsusceptible phenotype¶
A	147	2016 (6) 2018 (1)	7 (15%)	<i>bla</i>_{KPC-3}, <i>bla</i>_{GES-5}, <i>bla</i>_{OXA-9}, <i>qnrS</i>	IncFII/ColE1 IncN/ColE1	1.5–3	PPT, TCC, AMC, CZD, CTX, FOX, ATM, IMP, ETP, MEM, GMI (6), AKN (6), CIP, TIG (1), SXT
B	147	2016 (2) 2017 (2) 2018 (2)	6 (13%)	<i>bla</i>_{KPC-3}, <i>bla</i>_{OXA-9}, <i>qnrS</i>	IncFII	1–2	PPT, TCC, AMC, CZD, CTX, FOX, ATM, IMP, ETP, MEM, GMI, AKN, CIP, TIG, SXT
C	231	2014 (1) 2017 (1) 2018 (1)	3	<i>bla</i>_{KPC-3}, <i>qnrS</i> <i>bla</i>_{KPC-3}, <i>bla</i>_{OXA-9}, <i>qnrS</i> <i>bla</i>_{KPC-3}, <i>bla</i>_{OXA-9}, <i>qnrS</i>	IncFII	1.5	PPT, TCC, AMC, CZD, CTX, FOX, ATM, IMP (2), ETP, MEM, GMI (2), AKN (2), CIP, TIG (1), SXT
D	13	2017 (2) 2018 (5)	7 (15%)	<i>bla</i>_{KPC-3}, <i>bla</i>_{OXA-9}, <i>qnrS</i> <i>bla</i>_{KPC-3}, <i>bla</i>_{OXA-9} (3), <i>qnrS</i>	IncFIB	0.75–2	PPT, TCC, AMC, CZD, CTX, FOX, ATM, IMP (4), ETP, MEM, GMI (5), AKN (4), CIP (2), TIG (1), FOS (1), SXT
E	147	2017 (2) 2018 (1)	3	<i>bla</i>_{KPC-3}, <i>bla</i>_{OXA-9} (1), <i>qnrS</i> <i>bla</i>_{KPC-3}, <i>bla</i>_{OXA-9}, <i>qnrS</i>	IncFIIA	0.75–1.5	PPT, TCC, AMC, CZD, CTX, FOX, ATM, IMP, ETP, MEM, GMI (1), AKN (1), CIP, TIG (1), SXT (2)
F	960	2013	1	<i>bla</i>_{KPC-3}, <i>qnrS</i>	IncN	2	PPT, TCC, AMC, CZD, CTX, FOX, ATM, IMP, ETP, MEM, SXT
G	348	2017 (1) 2018 (6)	7 (15%)	<i>bla</i>_{KPC-3}, <i>bla</i>_{OXA-9}, <i>qnrS</i> <i>bla</i>_{KPC-3}, <i>bla</i>_{OXA-9} (5), <i>qnrS</i>	IncFII	0.5–2	PPT, TCC, AMC, CZD, CTX, FOX, ATM, IMP (6), ETP, MEM, GMI (6), AKN (5), CIP (6), TIG (2), FOS (1), SXT (6), COL (1)
H	45	2017	1	<i>bla</i>_{KPC-3}, <i>bla</i>_{OXA-9}, <i>qnrS</i>	IncFII	0.75	PPT, TCC, AMC, CZD, CTX, FOX, ATM, IMP, ETP, CIP, SXT
I	35	2018	1	<i>bla</i>_{KPC-3}, <i>bla</i>_{OXA-9}, <i>qnrS</i>	IncN	0.75	PPT, TCC, AMC, CZD, CTX, FOX, ATM, IMP, ETP, MEM, GMI, AKN, CIP, SXT
J	17	2016 (1) 2017 (1) 2018 (4)	6 (13%)	<i>bla</i>_{OXA-181}, <i>qnrS</i>	IncX3	0.125–0.25	PPT, TCC, AMC, CZD, CTX, FOX (5), ATM, IMP (3), ETP, GMI (5), AKN (3), CIP, SXT
L	17	2017	1	<i>bla</i>_{OXA-181}, <i>qnrS</i>	IncX3	0.25	PPT, TCC, AMC, CZD, CTX, ATM, ETP, GMI, CIP, SXT
M	35	2017 (1) 2018 (1)	2	<i>bla</i>_{OXA-181}, <i>qnrS</i>	IncX3	0.25	PPT, TCC, AMC, CZD, CTX, FOX, ATM, ETP, GMI, CIP, SXT PPT, TCC, AMC, CZD, CTX, ATM, ETP, CIP, SXT
N	29	2018	1	<i>bla</i>_{GES-5}, <i>bla</i>_{BEL-1}, <i>qnrS</i>	ColE	0.5	PPT, TCC, AMC, CZD, FOX, FOS

*AKN, amikacin; AMC, amoxicillin/clavulanic acid; ATM, aztreonam; CIP, ciprofloxacin; COL, colistin; CTX, cefotaxime; CZD, ceftazidime; ETP, ertapenem; FOS, fosfomicin; FOX, ceftazidime; GMI, gentamicin; IMP, imipenem; MEM, meropenem; PFGE, pulsed-field gel electrophoresis; PPT, piperacillin/tazobactam; ST, sequence type (determined by multilocus sequence typing); SXT, trimethoprim/sulfamethoxazole; TCC, ticarcillin/clavulanic acid; TIG, tigecycline.

†Periods for which the clonal type is clearly predominant shown in bold. Numbers in parentheses indicate number of isolates recovered for each year listed.

‡Carbapenemase genes are shown in bold. Numbers in parentheses indicate the number of isolates that carry the resistance gene, if not all.

§Type of the plasmid carrying the carbapenemase gene.

¶Numbers in parentheses indicate number of isolates that are nonsusceptible to the antimicrobial agent, if not all.

remaining isolate harbored *bla*_{GES-5} and *bla*_{BEL-1} and was also susceptible to ertapenem (MIC 0.25 mg/L). This isolate was the only isolate showing susceptibility to aztreonam. Despite the low MICs for carbapenems, all isolates grew on the chromID CARBA SMART agar (bioMérieux); the OXA-181 producers grew on the OXA side, whereas the GES-5/BEL-1 producer grew on the CARBA side, as did all KPC producers.

A substantial proportion of isolates showed reduced susceptibility to SXT (93%), ciprofloxacin (85%), gentamicin (76%), and amikacin (63%). In addition, nonsusceptibility to tigecycline was found in 28% of the isolates, resistance to fosfomicin in 3 isolates, and resistance to colistin in 1 isolate (i.e., negative for *mcr*-type genes). All isolates remained susceptible to ceftazidime/avibactam (MIC values ranging from 0.125 to 3 mg/L), although some exhibited

reduced susceptibility (resistance breakpoint >8 mg/L). Isolates co-possessing bla_{KPC-3} and bla_{GES-5} genes showed higher MICs for ceftazidime/avibactam (≥ 1.5 mg/L [$p = 0.014$]), whereas isolates producing carbapenemase OXA-181 had lower values (≤ 0.25 mg/L [$p < 0.001$]).

The plasmid-mediated quinolone resistance gene $qnrS$ was present in all isolates. No isolates carried the β -lactamase gene bla_{CMY} .

PFGE analysis distributed the 46 isolates into 13 pulsed types (Table). PFGE type A included the 7 isolates co-producing KPC-3 and GES-5 carbapenemases. The 29 isolates producing KPC-3 alone belonged to 8 different PFGE types: B ($n = 6$), C ($n = 3$), D ($n = 7$), E ($n = 3$), F ($n = 1$), G ($n = 7$), H ($n = 1$), and I ($n = 1$). PFGE types J ($n = 6$), L ($n = 1$), and M ($n = 2$) included the 9 isolates that were positive for $bla_{OXA-181}$, and the 1 isolate co-producing GES-5 and BEL-1 belonged to PFGE type N.

By using MLST, we found that the 13 PFGE types corresponded to 9 STs (Table). These STs were ST147 ($n = 16$ [35%]), ST13 ($n = 7$ [15%]), ST17 ($n = 7$ [15%]), ST348 ($n = 7$ [15%]), ST231 ($n = 3$ [7%]), ST35 ($n = 3$ [7%]), ST29 ($n = 1$), ST45 ($n = 1$), and ST960 ($n = 1$).

Analyzing the different clonal types over time (Figure), we observed that clone F-ST960 (KPC-3), recovered in 2013 in a single isolate, was no longer detected in the following years. Clone A-ST147 (KPC-3/GES-5), which was 1 of the 2 major clones found in our study, was clearly predominant in 2016 (6/7 isolates) but became a sporadic clone in 2018 (1 isolate). Conversely, clone G-ST348 (KPC-3), which emerged as a single isolate in 2017, became the major clone in 2018; this clone and clone D-ST13 are currently the predominant KPC-3 clones in the hospital. The first OXA-181 isolate was detected in 2016 (clone J-ST17), and although the 9 isolates producing this enzyme were distributed into 3 clones, J-ST17 became the predominant OXA-181 clone in 2018. The diversity of clones among carbapenemase producers increased over time together with the increase of isolates, especially in 2017 (9 clones among 12 isolates) (Figure).

Discussion

Our epidemiologic study describes the evolution of carbapenem-resistant *K. pneumoniae* over time in a hospital in Portugal, including contemporary isolates recovered after 2014. We report an increasing rate of carbapenemase producers in this hospital since 2016, which is consistent with the rise of carbapenem-resistant isolates in the country as reported by the European Centre for Disease Prevention and Control (11).

We found a clear predominance (78%) of *K. pneumoniae* KPC-3 producers, as observed in previous studies describing isolates in Portugal until 2014 (10,24,25). The KPC-3 producers belonged to a high diversity of clones ($n = 9$), and the bla_{KPC-3} gene was carried onto 4 plasmid

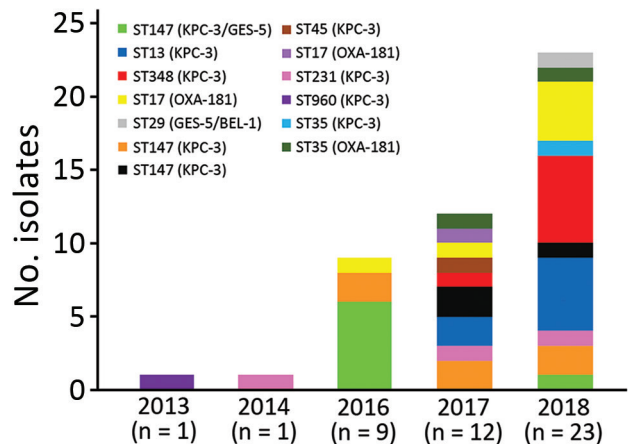


Figure. Evolution of clonal types of carbapenem-producing *Klebsiella pneumoniae* in a hospital in Portugal, 2013–2018. ST, sequence type.

types (IncN, IncFII, IncFIB, and IncFIIA). Therefore, the increasing number of KPC-3-producing isolates in this hospital might result mainly from recurrent introductions of those strains rather than the dissemination of specific plasmids or particular clones. ST147 was the predominant background type identified, either producing KPC-3 or OXA-181, which correlates with previous findings showing that this ST (belonging to clonal complex 258, as commonly found with KPC-2 or KPC-3 producers worldwide) was mainly associated with the spread of KPC-3-producing *K. pneumoniae* in the community in North Portugal (25).

Furthermore, most KPC-3-producing isolates ($n = 31$ [86%]) also carried the narrow-spectrum class D β -lactamase bla_{OXA-9} . This association has been previously described in an *Enterobacter cloacae* strain from a patient in France who was transferred from a hospital in the United States (26) and also among *K. pneumoniae* isolates from Italy (27). The co-production of OXA-9 contributes to the high-level resistance observed for amoxicillin/clavulanic acid because KPC-3 activity remains partially antagonized by clavulanate.

We have shown that OXA-181 producers have emerged among clinical isolates in Portugal and have been appearing at an increasing rate over time in this hospital. This carbapenemase, which is emerging worldwide, was found in isolates recovered since 2016, and its prevalence among carbapenemases is on the rise, which is a worrying and unexplained phenomenon. We recently described the massive occurrence of *K. pneumoniae* isolates carrying the $bla_{OXA-181}$ gene located onto an IncX3 plasmid in Angola (21,28) and also some isolates in São Tomé and Príncipe (29). The genetic backgrounds of those OXA-181-producing *K. pneumoniae* were different, with no ST17 detected, in contrast to our findings in this study; nevertheless, the identification of a very similar plasmid carrying $bla_{OXA-181}$ likely suggests a wide plasmid dissemination as a source of carbapenemase gene

acquisition. The frequent exchange of populations between these 2 countries, which are former colonies of Portugal, and Portugal itself could have driven the intercontinental spread of carbapenemase producers. Some recent studies have underscored the emergence of OXA-181 carbapenemase mediated by acquisition of similar IncX3-type plasmids, such as in China or South Africa (30,31), suggesting that spread of this carbapenem-resistance trait could be linked in large part to a wide plasmid diffusion.

Our data indicate the emergence and spread of *K. pneumoniae* isolates co-producing KPC-3 and GES-5. GES-5 has been found previously in Portugal in a *K. pneumoniae* environmental isolate (32) and in a single clinical strain (24) but never in combination with KPC. The fact that isolates co-possessing *bla*_{KPC-3} and *bla*_{GES-5} showed higher MICs to ceftazidime/avibactam is of concern.

β -lactamase GES-5 has been reported in *K. pneumoniae*, mainly among sporadic isolates with origins in Asia, namely from a patient from France who had been hospitalized in Bangkok, Thailand (33), in 1 isolate from China (34), and in 1 isolate from South Korea (35). A single study reported the spread of *K. pneumoniae* GES-5-producing isolates recovered during 2012–2013 in South Africa that carried *bla*_{GES-5} in an IncQ plasmid (36).

Our study identified 1 isolate co-producing GES-5 and the ESBL BEL-1. The 2 corresponding genes were embedded in the same class 1 integron structure, as first and second gene cassette positions, respectively (data not shown). The occurrence of the *bla*_{BEL-1} gene in an enterobacterial isolate is noteworthy because this gene has been identified mainly in *Pseudomonas aeruginosa*. Likewise, *bla*_{GES-5} is commonly identified in *P. aeruginosa*. Therefore, our finding suggests that this ColE1 plasmid bearing these 2 uncommon broad-spectrum β -lactamases might originate from *P. aeruginosa*. This isolate co-producing GES-5 and the ESBL BEL-1 showed only decreased susceptibility to imipenem, meropenem, and ertapenem. A similar isolate carrying both enzymes, also showing only decreased susceptibility to all carbapenems, was recovered in 2009 from an ICU patient in Portugal (23).

We detected several OXA-181 producers that remained susceptible to imipenem and meropenem. This phenomenon has been reported previously (37) and has contributed substantially to the misrecognition of such carbapenemase producers and therefore to their silent spread. Nevertheless, we must underscore that all isolates from our collection could be detected by using available commercial selective media, such as the chromID CARBA SMART agar (bioMérieux).

The high rate ($n = 12$ [26%]) of carbapenem producers in our study being pandrug-resistant (i.e., having resistance to fluoroquinolones, aminoglycosides, tigecycline, and SXT) is of concern. The high rate of fluoroquinolone resistance was partly related to the occurrence of the *qnrS* gene. We have

highlighted its endemic spread because it was identified in all of the carbapenemase-producing isolates identified, regardless of their clonal background and type of carbapenemase produced. Moreover, some isolates exhibited a worrying decreased susceptibility to ceftazidime/avibactam (MIC 3 mg/L; resistance breakpoint >8 mg/L), likely suggesting that some isolates actually started developing reduced susceptibility to that drug combination and moving toward resistance. Selection of KPC-producing *K. pneumoniae* exhibiting resistance to ceftazidime/avibactam has been observed recently in Italy, where KPC is endemic. This resistance occurred in particular through substitutions in the KPC enzyme, leading to increased hydrolysis of ceftazidime and decreased affinity to avibactam (38). In our study, we did not observe selection of KPC-3 variants; therefore, the reduced susceptibility probably is mainly related to the co-production of GES-5, permeability defects, or both. Nevertheless, all isolates remained susceptible to the combination ceftazidime/avibactam, independently of the clonal type and the carbapenemase produced (whether KPC-3, OXA-181, or GES-5). In addition, fosfomycin and polymyxins are still therapeutic alternatives because very few isolates exhibited resistance to these antimicrobial agents (3 to fosfomycin and 1 to polymyxins).

Our study has some limitations, given that we included isolates from a single hospital. However, this private hospital receives patients transferred from several public hospitals in Lisbon and its surroundings and therefore might reflect at least the global situation in this capital city of Portugal, which includes approximately one third of the national population. This phenomenon is evident in the diversity of enzymes, plasmids, and clonal backgrounds identified in our study.

In summary, KPC-3 was the most common carbapenemase identified in *K. pneumoniae* isolated at the SAMS Hospital in Lisbon, Portugal, followed by OXA-181, which emerged in 2016 and appears to be on the rise. In addition, a large proportion of isolates are pandrug-resistant, drastically diminishing the options for treatment. Finally, considering the increasing identification of carbapenemase-producing *K. pneumoniae* in this hospital, systematic carriage screening at hospital admission, additional surveillance studies, and early detection of such isolates are required to limit their further spread. These measures would help mitigate the spread of these isolates in Portugal and avert the endemic levels that have been observed in other countries in Europe.

Acknowledgments

We are grateful to Faustino Ferreira and Ana Bela Correia for providing us the local authorizations to perform this study.

This work was partly supported by the University of Fribourg; the Swiss National Science Foundation (project nos. FNS-31003A_163432 and FNS-407240_177381); INSERM (Paris, France);

Fundação para a Ciência e a Tecnologia (project no. PTDC/DTP-EPI/0842/2014) (Portugal); and Programa Operacional Competitividade e Internacionalização (project no. LISBOA-01-0145-FEDER-007660 [Microbiologia Molecular, Estrutural e Celular] funded by FEDER funds through COMPETE2020).

About the Author

Dr. Aires-de-Sousa is a professor at Escola Superior de Saúde da Cruz Vermelha Portuguesa, Lisbon, Portugal. Her research interests include the molecular epidemiology of antimicrobial-resistant bacteria.

References

- Taconelli A, Magrini N. Global priority list of antibiotic-resistant bacteria to guide research, discovery, and development of new antibiotics. Geneva: World Health Organization; 2017.
- Pitout JD, Nordmann P, Poirel L. Carbapenemase-producing *Klebsiella pneumoniae*, a key pathogen set for global nosocomial dominance. *Antimicrob Agents Chemother*. 2015;59:5873–84. <http://dx.doi.org/10.1128/AAC.01019-15>
- Queenan AM, Bush K. Carbapenemases: the versatile beta-lactamases. *Clin Microbiol Rev*. 2007;20:440–58. <http://dx.doi.org/10.1128/CMR.00001-07>
- Munoz-Price LS, Poirel L, Bonomo RA, Schwaber MJ, Daikos GL, Cormican M, et al. Clinical epidemiology of the global expansion of *Klebsiella pneumoniae* carbapenemases. *Lancet Infect Dis*. 2013;13:785–96. [http://dx.doi.org/10.1016/S1473-3099\(13\)70190-7](http://dx.doi.org/10.1016/S1473-3099(13)70190-7)
- Poirel L, Carrër A, Pitout JD, Nordmann P. Integron mobilization unit as a source of mobility of antibiotic resistance genes. *Antimicrob Agents Chemother*. 2009;53:2492–8. <http://dx.doi.org/10.1128/AAC.00033-09>
- Machado P, Silva A, Lito L, Melo-Cristino J, Duarte A. Emergence of *Klebsiella pneumoniae* ST11-producing KPC-3 carbapenemase at a Lisbon hospital. *Clin Microbiol Infect*. 2010;16(Suppl 2):S28.
- Albiger B, Glasner C, Struelens MJ, Grundmann H, Monnet DL; European Survey of Carbapenemase-Producing Enterobacteriaceae (EuSCAPE) Working Group. Carbapenemase-producing *Enterobacteriaceae* in Europe: assessment by national experts from 38 countries, May 2015. *Euro Surveill*. 2015;20:30062. <http://dx.doi.org/10.2807/1560-7917.ES.2015.20.45.30062>
- Grundmann H, Glasner C, Albiger B, Aanensen DM, Tomlinson CT, Andrasević AT, et al.; European Survey of Carbapenemase-Producing Enterobacteriaceae (EuSCAPE) Working Group. Occurrence of carbapenemase-producing *Klebsiella pneumoniae* and *Escherichia coli* in the European survey of carbapenemase-producing *Enterobacteriaceae* (EuSCAPE): a prospective, multinational study. *Lancet Infect Dis*. 2017;17:153–63. [http://dx.doi.org/10.1016/S1473-3099\(16\)30257-2](http://dx.doi.org/10.1016/S1473-3099(16)30257-2)
- Vubil D, Figueiredo R, Reis T, Canha C, Boaventura L, DA Silva GJ. Outbreak of KPC-3-producing ST15 and ST348 *Klebsiella pneumoniae* in a Portuguese hospital. *Epidemiol Infect*. 2017;145:595–9. <http://dx.doi.org/10.1017/S0950268816002442>
- Manageiro V, Ferreira E, Almeida J, Barbosa S, Simões C, Bonomo RA, et al.; Antibiotic Resistance Surveillance Program in Portugal (ARSIP). Predominance of KPC-3 in a survey for carbapenemase-producing *Enterobacteriaceae* in Portugal. *Antimicrob Agents Chemother*. 2015;59:3588–92. <http://dx.doi.org/10.1128/AAC.05065-14>
- European Centre for Disease Prevention and Control. Surveillance of antimicrobial resistance in Europe—annual report of the European Antimicrobial Resistance Surveillance Network (EARS-Net) 2017 [cited 2019 Apr 10]. <https://ecdc.europa.eu/sites/portal/files/documents/EARS-Net-report-2017-update-jan-2019.pdf>
- Pires D, Zagalo A, Santos C, Cota de Medeiros F, Duarte A, Lito L, et al. Evolving epidemiology of carbapenemase-producing Enterobacteriaceae in Portugal: 2012 retrospective cohort at a tertiary hospital in Lisbon. *J Hosp Infect*. 2016;92:82–5. <http://dx.doi.org/10.1016/j.jhin.2015.11.006>
- Caneiras C, Lito L, Mayoralas-Alises S, Diaz-Lobato S, Melo-Cristino J, Duarte A. Virulence and resistance determinants of *Klebsiella pneumoniae* isolated from a Portuguese tertiary university hospital centre over a 31-year period. *Enferm Infect Microbiol Clin*. 2019;37:387–93. <http://dx.doi.org/10.1016/j.eimc.2018.11.001>
- Poirel L, Nordmann P. Rapidec Carba NP test for rapid detection of carbapenemase producers. *J Clin Microbiol*. 2015;53:3003–8. <http://dx.doi.org/10.1128/JCM.00977-15>
- Jayol A, Kieffer N, Poirel L, Guérin F, Güneser D, Cattoir V, et al. Evaluation of the Rapid Polymyxin NP test and its industrial version for the detection of polymyxin-resistant Enterobacteriaceae. *Diagn Microbiol Infect Dis*. 2018;92:90–4. <http://dx.doi.org/10.1016/j.diagmicrobio.2018.05.006>
- Poirel L, Walsh TR, Cuvillier V, Nordmann P. Multiplex PCR for detection of acquired carbapenemase genes. *Diagn Microbiol Infect Dis*. 2011;70:119–23. <http://dx.doi.org/10.1016/j.diagmicrobio.2010.12.002>
- Ortiz de la Rosa JM, Nordmann P, Poirel L. ESBLs and resistance to ceftazidime/avibactam and ceftolozane/tazobactam combinations in *Escherichia coli* and *Pseudomonas aeruginosa*. *J Antimicrob Chemother*. 2019;74:1934–9. <http://dx.doi.org/10.1093/jac/dkz149>
- Lescat M, Poirel L, Nordmann P. Rapid multiplex polymerase chain reaction for detection of *mcr-1* to *mcr-5* genes. *Diagn Microbiol Infect Dis*. 2018;92:267–9. <http://dx.doi.org/10.1016/j.diagmicrobio.2018.04.010>
- Philippon A, Arlet G, Jacoby GA. Plasmid-determined AmpC-type beta-lactamases. *Antimicrob Agents Chemother*. 2002;46:1–11. <http://dx.doi.org/10.1128/AAC.46.1.1-11.2002>
- Cattoir V, Poirel L, Rotimi V, Soussy CJ, Nordmann P. Multiplex PCR for detection of plasmid-mediated quinolone resistance *qnr* genes in ESBL-producing enterobacterial isolates. *J Antimicrob Chemother*. 2007;60:394–7. <http://dx.doi.org/10.1093/jac/dkm204>
- Kieffer N, Nordmann P, Aires-de-Sousa M, Poirel L. High prevalence of carbapenemase-producing *Enterobacteriaceae* among hospitalized children in Luanda, Angola. *Antimicrob Agents Chemother*. 2016;60:6189–92. <http://dx.doi.org/10.1128/AAC.01201-16>
- Carattoli A, Bertini A, Villa L, Falbo V, Hopkins KL, Threlfall EJ. Identification of plasmids by PCR-based replicon typing. *J Microbiol Methods*. 2005;63:219–28. <http://dx.doi.org/10.1016/j.jmimet.2005.03.018>
- Papagiannitsis CC, Dolejska M, Izdebski R, Dobiasova H, Studentova V, Esteves FJ, et al. Characterization of pKP-M1144, a novel ColE1-like plasmid encoding IMP-8, GES-5, and BEL-1 beta-lactamases, from a *Klebsiella pneumoniae* sequence type 252 isolate. *Antimicrob Agents Chemother*. 2015;59:5065–8. <http://dx.doi.org/10.1128/AAC.00937-15>
- Manageiro V, Romão R, Moura IB, Sampaio DA, Vieira L, Ferreira E, et al.; Network EuSCAPE-Portugal. Network EuSCAPE-Portugal. Molecular epidemiology and risk factors of carbapenemase-producing *Enterobacteriaceae* isolates in Portuguese hospitals: results from European survey on carbapenemase-producing *Enterobacteriaceae* (EuSCAPE). *Front Microbiol*. 2018;9:2834. <http://dx.doi.org/10.3389/fmicb.2018.02834>
- Rodrigues C, Bavlović J, Machado E, Amorim J, Peixe L, Novais Â. KPC-3-producing *Klebsiella pneumoniae* in Portugal linked to previously circulating non-CG258 lineages and uncommon genetic platforms (Tn4401d-IncFIA and Tn4401d-IncN). *Front Microbiol*. 2016;7:1000. <http://dx.doi.org/10.3389/fmicb.2016.01000>

26. Dortet L, Radu I, Gautier V, Blot F, Chachaty E, Arlet G. Intercontinental travels of patients and dissemination of plasmid-mediated carbapenemase KPC-3 associated with OXA-9 and TEM-1. *J Antimicrob Chemother.* 2008;61:455–7. <http://dx.doi.org/10.1093/jac/dkm455>
27. Kocsis E, Lo Cascio G, Piccoli M, Cornaglia G, Mazzariol A. KPC-3 carbapenemase harbored in FIIk plasmid from *Klebsiella pneumoniae* ST512 and *Escherichia coli* ST43 in the same patient. *Microb Drug Resist.* 2014;20:377–82. <http://dx.doi.org/10.1089/mdr.2013.0152>
28. Poirel L, Goutines J, Aires-de-Sousa M, Nordmann P. High rate of association of 16S rRNA methylases and carbapenemases in *Enterobacteriaceae* recovered from hospitalized children in Angola. *Antimicrob Agents Chemother.* 2018;62:e00021–18. <http://dx.doi.org/10.1128/AAC.00021-18>
29. Poirel L, Aires-de-Sousa M, Kudyba P, Kieffer N, Nordmann P. Screening and characterization of multidrug-resistant Gram-negative bacteria from a remote African area, São Tomé and Príncipe. *Antimicrob Agents Chemother.* 2018;62:e01021–18. <http://dx.doi.org/10.1128/AAC.01021-18>
30. Liu Y, Feng Y, Wu W, Xie Y, Wang X, Zhang X, et al. First report of OXA-181-producing *Escherichia coli* in China and characterization of the isolate using whole-genome sequencing. *Antimicrob Agents Chemother.* 2015;59:5022–5. <http://dx.doi.org/10.1128/AAC.00442-15>
31. Lowe M, Kock MM, Coetzee J, Hoosien E, Peirano G, Strydom KA, et al. *Klebsiella pneumoniae* ST307 with bla_{OXA-181}. South Africa, 2014–2016. *Emerg Infect Dis.* 2019;25:739–47. <http://dx.doi.org/10.3201/eid2504.181482>
32. Manageiro V, Ferreira E, Caniça M, Manaia CM. GES-5 among the β-lactamases detected in ubiquitous bacteria isolated from aquatic environment samples. *FEMS Microbiol Lett.* 2014;351:64–9. <http://dx.doi.org/10.1111/1574-6968.12340>
33. Bonnin RA, Jousset AB, Urvoy N, Gauthier L, Tlili L, Creton E, et al. Detection of GES-5 carbapenemase in *Klebsiella pneumoniae*, a newcomer in France. *Antimicrob Agents Chemother.* 2017;61:e02263–16. <http://dx.doi.org/10.1128/AAC.02263-16>
34. Chen DQ, Wu AW, Yang L, Su DH, Lin YP, Hu YW, et al. Emergence and plasmid analysis of *Klebsiella pneumoniae* KP01 carrying bla_{GES-5} from Guangzhou, China. *Antimicrob Agents Chemother.* 2016;60:6362–4. <http://dx.doi.org/10.1128/AAC.00764-16>
35. Yoon EJ, Yang JW, Kim JO, Lee H, Lee KJ, Jeong SH. Carbapenemase-producing *Enterobacteriaceae* in South Korea: a report from the National Laboratory Surveillance System. *Future Microbiol.* 2018;13:771–83. <http://dx.doi.org/10.2217/fmb-2018-0022>
36. Pedersen T, Sekyere JO, Govinden U, Moodley K, Sivertsen A, Samuelsen Ø, et al. Spread of plasmid-encoded NDM-1 and GES-5 carbapenemases among extensively drug-resistant and pandrug-resistant clinical *Enterobacteriaceae* in Durban, South Africa. *Antimicrob Agents Chemother.* 2018;62:e02178–17. <http://dx.doi.org/10.1128/AAC.02178-17>
37. Potron A, Poirel L, Rondinaud E, Nordmann P. Intercontinental spread of OXA-48 beta-lactamase-producing *Enterobacteriaceae* over a 11-year period, 2001 to 2011. *Euro Surveill.* 2013;18:20549. <http://dx.doi.org/10.2807/1560-7917.ES2013.18.31.20549>
38. Gaibani P, Campoli C, Lewis RE, Volpe SL, Scaltriti E, Giannella M, et al. In vivo evolution of resistant subpopulations of KPC-producing *Klebsiella pneumoniae* during ceftazidime/avibactam treatment. *J Antimicrob Chemother.* 2018;73:1525–9. <http://dx.doi.org/10.1093/jac/dky082>

Address for correspondence: Laurent Poirel, Medical and Molecular Microbiology Unit, Faculty of Science and Medicine, University of Fribourg, Chemin du Musée 18, CH-1700 Fribourg, Switzerland; email: laurent.poirel@unifr.ch



**EMERGING
INFECTIOUS DISEASES®**

March 2018

Mycobacteria

- Coccidioidomycosis Outbreaks, United States and Worldwide, 1940–2015
- Multistate Epidemiology of Histoplasmosis, United States, 2011–2014
- Epidemiology of Recurrent Hand, Foot and Mouth Disease, China, 2008–2015
- Capsule Typing of *Haemophilus influenzae* by Matrix-Assisted Laser Desorption/Ionization Time-of-Flight Mass Spectrometry
- Emergence of *Streptococcus pneumoniae* Serotype 12F after Sequential Introduction of 7- and 13-Valent Vaccines, Israel
- Major Threat to Malaria Control Programs by *Plasmodium falciparum* Lacking Histidine-Rich Protein 2, Eritrea
- Use of Influenza Risk Assessment Tool for Prepandemic Preparedness
- Use of Verbal Autopsy to Determine Underlying Cause of Death during Treatment of Multidrug-Resistant Tuberculosis, India
- Increasing Prevalence of Nontuberculous Mycobacteria in Respiratory Specimens from US-Affiliated Pacific Island Jurisdictions
- Use of Genome Sequencing to Define Institutional Influenza Outbreaks, Toronto, Ontario, Canada, 2014–15
- Influenza Vaccination and Incident Tuberculosis among Elderly Persons, Taiwan
- Epidemiology and Molecular Identification and Characterization of *Mycoplasma pneumoniae*, South Africa, 2012–2015
- Prospective Observational Study of Incidence and Preventable Burden of Childhood Tuberculosis, Kenya
- Acquired Resistance to Antituberculosis Drugs in England, Wales, and Northern Ireland, 2000–2015
- Characteristics Associated with Negative Interferon-γ Release Assay Results in Culture-Confirmed Tuberculosis Patients, Texas, USA, 2013–2015

To revisit the March 2018 issue, go to:
[https://wwwnc.cdc.gov/eid/articles/
issue/24/3/table-of-contents](https://wwwnc.cdc.gov/eid/articles/issue/24/3/table-of-contents)

Classification of Trauma-Associated Invasive Fungal Infections to Support Wound Treatment Decisions

Anuradha Ganesan, Faraz Shaikh, William Bradley, Dana M. Blyth, Denise Bennett, Joseph L. Petfield, M. Leigh Carson, Justin M. Wells, David R. Tribble; Infectious Disease Clinical Research Program Trauma Infectious Disease Outcomes Study Group

Medscape **ACTIVITY** EDUCATION

In support of improving patient care, this activity has been planned and implemented by Medscape, LLC and Emerging Infectious Diseases. Medscape, LLC is jointly accredited by the Accreditation Council for Continuing Medical Education (ACCME), the Accreditation Council for Pharmacy Education (ACPE), and the American Nurses Credentialing Center (ANCC), to provide continuing education for the healthcare team.

Medscape, LLC designates this Journal-based CME activity for a maximum of 1.00 **AMA PRA Category 1 Credit(s)**[™]. Physicians should claim only the credit commensurate with the extent of their participation in the activity.

Successful completion of this CME activity, which includes participation in the evaluation component, enables the participant to earn up to 1.0 MOC points in the American Board of Internal Medicine's (ABIM) Maintenance of Certification (MOC) program. Participants will earn MOC points equivalent to the amount of CME credits claimed for the activity. It is the CME activity provider's responsibility to submit participant completion information to ACCME for the purpose of granting ABIM MOC credit.

All other clinicians completing this activity will be issued a certificate of participation. To participate in this journal CME activity: (1) review the learning objectives and author disclosures; (2) study the education content; (3) take the post-test with a 75% minimum passing score and complete the evaluation at <http://www.medscape.org/journal/eid>; and (4) view/print certificate. For CME questions, see page 1789.

Release date: August 21, 2019; Expiration date: August 21, 2020

Learning Objectives

Upon completion of this activity, participants will be able to:

- Distinguish a classification system for fungal wound infections
- Assess clinical variables associated with invasive fungal wound infections
- Evaluate the microbiology of fungal wound infections
- Analyze the outcomes of fungal wound infections of variable severity

CME Editor

P. Lynne Stockton Taylor, VMD, MS, ELS(D), Technical Writer/Editor, Emerging Infectious Diseases. *Disclosure: P. Lynne Stockton Taylor, VMD, MS, ELS(D), has disclosed no relevant financial relationships.*

CME Author

Charles P. Vega, MD, Clinical Professor, Health Sciences, Department of Family Medicine, University of California, Irvine School of Medicine, Irvine, California. *Disclosure: Charles P. Vega, MD, FAAFP, has disclosed the following relevant financial relationships: served as an advisor or consultant for Genentech, Inc.; GlaxoSmithKline; Johnson & Johnson Pharmaceutical Research & Development, L.L.C.; served as a speaker or a member of a speakers bureau for Shire.*

Authors

Disclosures: Anuradha Ganesan, MBBS, MPH; Faraz Shaikh, MS; William P. Bradley, MS; Dana Blyth, MD; Denise L. Bennett, MS; Joseph L. Petfield, MD; Leigh Carson, MS; Justin M. Wells, MD; and David Tribble, MD, DrPH, have disclosed no relevant financial relationships.

Author affiliations: The Henry M. Jackson Foundation for the Advancement of Military Medicine, Inc., Bethesda, Maryland, USA (A. Ganesan, F. Shaikh, W. Bradley, D. Bennett, M.L. Carson); Uniformed Services University of the Health Sciences, Bethesda (A. Ganesan, F. Shaikh, W. Bradley, D. Bennett, M.L. Carson, D.R. Tribble); Walter Reed National Military

Medical Center, Bethesda (A. Ganesan, J.M. Wells); Brooke Army Medical Center, San Antonio, Texas, USA (W. Bradley, D.M. Blyth); Landstuhl Regional Medical Center, Landstuhl, Germany (J.L. Petfield)

DOI: <https://doi.org/10.3201/eid2509.190168>

To evaluate a classification system to support clinical decisions for treatment of contaminated deep wounds at risk for an invasive fungal infection (IFI), we studied 246 US service members (413 wounds) injured in Afghanistan (2009–2014) who had laboratory evidence of fungal infection. A total of 143 wounds with persistent necrosis and laboratory evidence were classified as IFI; 120 wounds not meeting IFI criteria were classified as high suspicion (patients had localized infection signs/symptoms and had received antifungal medication for ≥ 10 days), and 150 were classified as low suspicion (failed to meet these criteria). IFI patients received more blood than other patients and had more severe injuries than patients in the low-suspicion group. Fungi of the order Mucorales were more frequently isolated from IFI (39%) and high-suspicion (21%) wounds than from low-suspicion (9%) wounds. Wounds that did not require immediate antifungal therapy lacked necrosis and localized signs/symptoms of infection and contained fungi from orders other than Mucorales.

Cutaneous invasive fungal infections (IFI) occur in deep tissue wounds contaminated by environmental debris; such wounds are caused by agricultural accidents, tornadoes, and blast trauma (1–7). Among severely injured trauma patients (military and civilian), IFIs have emerged as a serious complication (2,4,6,7). Specifically, coinciding with the surge of service members into Afghanistan and the rising frequency of blast injuries, IFIs have emerged as serious complications of blast trauma sustained by soldiers while on foot patrol. The first reported cases were among UK military personnel injured while in Helmand Province, Afghanistan (8), followed by 37 cases among US military personnel (1). Common characteristics among these IFI patients were battlefield blast injuries sustained while on foot patrol, extensive wounds or amputation sites heavily contaminated with debris, and receipt of large-volume blood transfusions (>8 units of blood) within 24 hours of injury (1,8). These infections were associated with substantial morbidity (e.g., surgical amputations and hemipelvectomies) and considerable death rates, especially before the syndrome was recognized (1,3,9). Given the progressive nature and substantial morbidity associated with such infections, patients at risk for IFI needed to be identified and given early treatment with aggressive surgical debridement and systemic antifungal therapy. Defining what constitutes a wound suspected of having an IFI is also critical, and clinicians were advised to use hallmark wound necrosis and preliminary risk factors to establish an IFI diagnosis as early as possible (10).

For the initial IFI cases in the United States, the median time from injury to IFI diagnosis was 10 days. In 2011, in an effort to hasten IFI diagnoses, a performance improvement measure that involved early tissue sampling of wounds (usually after 1 debridement) from those at high

risk for IFI was introduced at the Landstuhl Regional Medical Center in Germany (LRMC) (11). After the introduction of this diagnostic approach, it became clear that fungal contamination of battlefield blast wounds was common (12,13); therefore, it is necessary to differentiate wounds contaminated by fungi from those that are truly infected. Furthermore, the inability to easily discriminate between infected and colonized wounds (based on injury and patient demographic characteristics) led to wide practice variations. In this study, we examined the epidemiology of IFIs among US military personnel injured in Afghanistan. We also assessed the discriminatory capacity of clinical and pathologic/microbiological criteria for stratifying patients into risk groups that would enable treatment and resource prioritization and reduce practice variations.

Methods

Study Population

Data were collected as part of the Department of Defense, Department of Veterans Affairs, multicenter Trauma Infectious Disease Outcomes Study, an observational study of infectious complications among wounded military personnel (14). Eligible patients were US service members who had sustained traumatic wounds while on the battlefield in Afghanistan during June 1, 2009–December 31, 2014, and who had been evacuated to LRMC before transfer to a participating military hospital in the United States: Walter Reed National Military Medical Center (Bethesda, MD; National Naval Medical Center and Walter Reed Army Medical Center before September 2011) and Brooke Army Medical Center (San Antonio, TX). The study was approved by the institutional review board of the Uniformed Services University of the Health Sciences.

We obtained information about patient demographics, injury characteristics, trauma and clinical history, and surgical management history from the US Department of Defense Trauma Registry (15) and clinical laboratory results, infectious outcomes, culture and histopathology, and antifungal treatment from the Trauma Infectious Disease Outcomes Study infectious disease module (14). To assess patients, we used the Injury Severity Score (ISS) (16) and Sequential Organ Failure Assessment (SOFA) score (17). The ISS is an anatomic scoring system used for patients with multiple injuries. Each injury is evaluated and assigned an Abbreviated Injury Scale code, which is an anatomic consensus-based global score. The injuries are divided into 6 body regions, and the 3 most severely injured body region scores are squared and added to produce a composite score. An ISS score of 0–9 is classified as minor, 10–15 as moderate, 16–25 as severe, and ≥ 26 as critical.

Case Definitions

We examined patients with laboratory evidence of infection with a filamentous fungus (positive histopathologic findings, positive fungal culture, or both). We modified case definitions from the 2008 European Organization for Research and Treatment of Cancer/Invasive Fungal Infections Cooperative Group and the National Institute of Allergy and Infectious Diseases Mycoses Study Group (EORTC/MSG) Consensus Group for use with trauma patients (3,18). After patients were admitted to LRMC, wounds with persistent necrosis and presence of filamentous fungus (after ≥ 2 surgical debridements) were classified as IFI (Table 1). IFI wounds were further categorized according to histopathologic findings as proven (with angioinvasion), probable (fungal hypha tissue invasion but without angioinvasion), or possible (positive cultures and negative histopathologic findings).

Wounds not meeting criteria for IFI were classified as being of high or low suspicion for IFI. We modified National Healthcare Safety Network (NHSN) definitions for skin and soft tissue infections (SSTI) and used them to differentiate between high-suspicion and low-suspicion wounds. The NHSN definition of SSTI relies on the presence of localized signs and symptoms (e.g., pain, tenderness, swelling, erythema, heat) without another recognized cause (19). A deep SSTI met NHSN criteria and included wounds that spontaneously dehisced and those requiring surgical intervention. Wounds that met criteria for a deep SSTI that the treating physician attributed to a fungus and that were treated with antifungal medications for ≥ 10 days were classified as high-suspicion wounds. Patients who had died or undergone a definitive amputation (proximal to the infected wound) within 10 days of initiation of antifungal medication were also included because both events could lead to withdrawal of antifungal medication. The low-suspicion group included wounds that met deep SSTI criteria but were attributed by the treating physician to bacteria, wounds that failed to meet

deep SSTI criteria, and deep SSTIs for which the patient received antifungal medication for < 10 days.

Statistical Considerations

Because multiple traumatic injuries were frequent, patients often had multiple wounds with laboratory evidence of a fungus. We evaluated wound characteristics (e.g., culture findings) and patient-level characteristics (e.g., injury severity). Patients with 2 wounds that met different classifications were classified according to the highest level (e.g., if 1 wound met IFI criteria and the other was of low suspicion, the patient was classified as having an IFI). We performed a restricted analysis for patients with wounds that met criteria for a single classification.

Fungal culture results were categorized into 4 main groups: all fungi belonging to the order Mucorales (with/without fungi of other genera), fungi of the genus *Aspergillus* (with/without other fungi), fungi of genus *Fusarium* (with/without other fungi), and all other fungi. Polymicrobial wounds may be counted under multiple fungal groups (e.g., order Mucorales plus *Aspergillus* spp.). Data from patients who had undergone multiple debridements and multiple specimen collections were pooled for the wound site.

We compared categorical variables by using the Fisher exact and χ^2 tests. We compared overall continuous variable distributions by using the Kruskal-Wallis test and performed statistical analyses in SAS version 9.3 (<https://www.sas.com>). We defined significance as $p < 0.05$.

Results

Study Population

Of the 1,932 patients evaluated at the participating hospitals, 720 (37%) had penetrating wounds and operative cultures/histopathology findings submitted for evaluation. Of these, 246 (34%) had ≥ 1 wound with laboratory evidence of fungal infection (Figure 1). All patients were young

Table 1. Definitions for the classification of evidence for fungal infections*

Term	Definition†
Persistent necrosis‡	Presence of necrosis after ≥ 2 surgical debridements
Persistent laboratory evidence of fungal infection‡	Presence of positive histopathology and/or culture after ≥ 2 surgical debridements
Wounds meeting criteria for IFI	Includes wounds with persistent necrosis and persistent laboratory evidence of fungal infection
Wounds highly suspicious for fungal infection (high-suspicion wounds)	Includes wounds that did not meet the criteria for an IFI but produced signs and symptoms suggestive of a deep SSTI ascribed to a fungus (based on the use of antifungals for ≥ 10 d and a physician report). Wounds that did not meet criteria for an IFI but required a proximal amputation were included, irrespective of the duration of antifungal use.
Wounds with low suspicion for fungal infection (low-suspicion wounds)	Includes wounds that did not meet the criteria for an IFI and did not meet the criteria for a deep SSTI. This category also includes wounds that produced signs and symptoms of a deep SSTI attributed to bacteria (based on physician report or the use of antifungals for < 10 d) but with laboratory evidence of fungus (i.e., positive fungal cultures, histopathologic findings, or both).

*IFI, invasive fungal infection; SSTI, skin and soft tissue infection.

†Centers for Disease Control and Prevention National Healthcare Safety Network criteria for deep SSTIs were adapted for this definition (19).

‡Excludes any additional debridement that was performed in the battlefield hospitals in Afghanistan.

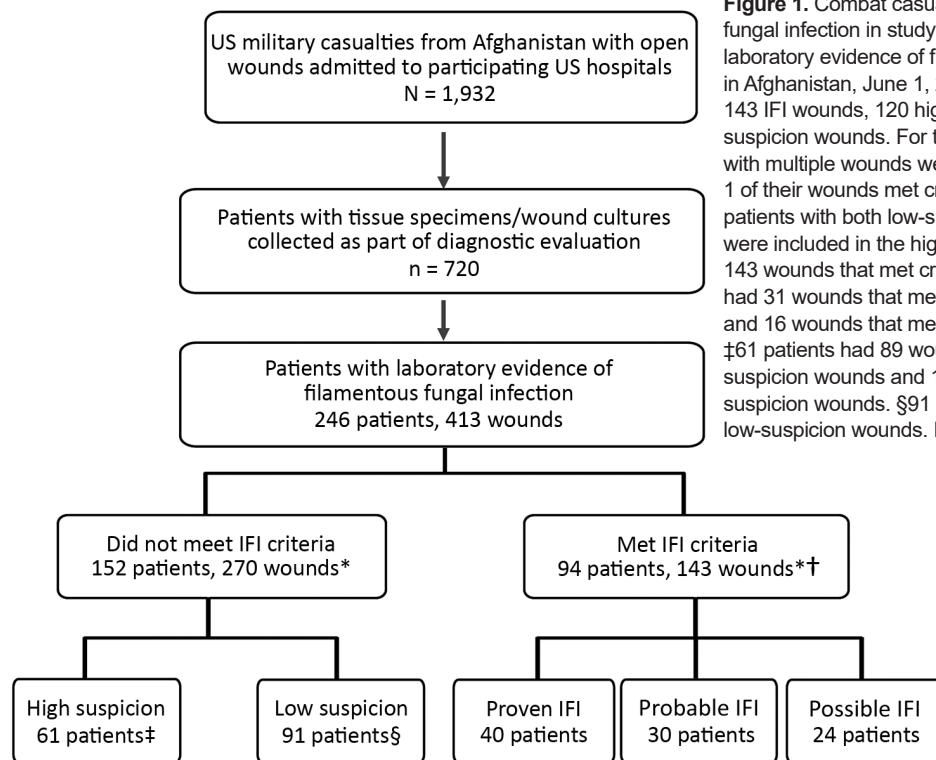


Figure 1. Combat casualties with laboratory evidence of fungal infection in study of US military patients who had laboratory evidence of fungal infection after battlefield trauma in Afghanistan, June 1, 2009–December 31, 2014. *Total of 143 IFI wounds, 120 high-suspicion wounds, and 150 low-suspicion wounds. For the person-level analysis, patients with multiple wounds were included in the IFI group even if 1 of their wounds met criteria other than for an IFI; similarly, patients with both low-suspicion and high-suspicion wounds were included in the high-suspicion group. †94 patients had 143 wounds that met criteria for an IFI; these same patients had 31 wounds that met criteria for high-suspicion wounds and 16 wounds that met criteria for low-suspicion wounds. ‡61 patients had 89 wounds that met criteria for high-suspicion wounds and 14 wounds that met criteria for low-suspicion wounds. §91 patients had 120 wounds classified as low-suspicion wounds. IFI, invasive fungal infection.

men; median age at injury was 24 years (interquartile range [IQR] 21–27 years). Nearly all patients had been injured by a blast (98%) while on foot patrol (95%).

The 246 patients had 413 wounds with laboratory evidence of a filamentous fungus. Of these, 143 wounds (94 patients) met the criteria for an IFI (Figure 1). The remaining 270 wounds did not meet IFI criteria, either because they appeared no longer suspicious for infection (i.e., no ongoing necrosis after ≥ 2 debridements; 167 wounds) or because laboratory evidence of fungal infection was evident early (i.e., at or before the first or second debridement) but not in subsequent samples (103 wounds). Of the 270 non-IFI wounds, 194 met criteria for deep SSTI; 120 of those were treated with directed antifungal therapy and were classified as high-suspicion wounds (107 with ≥ 10 days of antifungal therapy and 13 with < 10 days of antifungal therapy but the patient had undergone a proximal amputation or died). Of the 150 low-suspicion wounds, 76 did not meet criteria for deep SSTI and 74 met the criteria for deep SSTI but were treated with either directed antibiotic therapy (36 wounds) or antifungal therapy for < 10 days (38 wounds). Most wounds classified as low suspicion had only positive culture results (125 [83.3%] wounds), and none showed angioinvasion histopathologically.

Proven, Probable, and Possible IFI

Patients with proven, probable, and possible IFIs had been critically injured, and most had an ISS of ≥ 26 : 98% in the

proven group, 90% probable, and 88% possible (Table 2). SOFA scores at admission to US hospitals were lower among those in the possible IFI group ($p = 0.007$). Otherwise, no clinically relevant distinguishing differences were found among the IFI classification groups. Patients with IFI classified as proven or probable had received antifungal therapy longer than those with possible IFI ($p < 0.001$; Table 2).

IFI, High-Suspicion, and Low-Suspicion Wounds

Patient demographics and mechanisms of injury were similar among those with IFI, high-suspicion, or low-suspicion wounds. Injury severity was high overall (median ISS 34, IQR 30–45). Thus, a large proportion of patients with wounds classified in all 3 groups had undergone amputations (68% for IFI, 79% for high suspicion, 80% for low suspicion; Table 3).

IFI and High-Suspicion Wounds

For patients with IFI and high-suspicion wounds, ISSs were similar (median 40 vs. 38; $p = 0.262$; Table 3). Compared with patients with high-suspicion wounds, IFI patients had higher SOFA scores at admission to LPMC (median 11 vs. 8; $p = 0.028$) and US hospitals (median 7 vs. 4; $p = 0.022$) and received more blood transfusions within 24 hours of injury (median 31 vs. 21; $p = 0.003$). Patients with wounds classified as IFI also received antifungal therapy longer than patients with high-suspicion

Table 2. Characteristics of US military patients with IFI after battlefield trauma in Afghanistan, June 1, 2009–December 31, 2014*

Characteristic	IFI			p value
	Proven, n = 40	Probable, n = 30	Possible, n = 24	
Blast injury	40 (100)	29 (96.7)	23 (95.8)	0.327
Injured while on foot patrol†	29 (100)	26 (96.3)	18 (85.7)	0.062
Injury severity score				
Median (IQR)	42 (33–57)	40 (33–50)	35 (30–44)	0.127
≥26/critical	39 (97.5)	27 (90.0)	21 (87.5)	0.279
Blood units received 24 h after injury‡				
Median (IQR)	31 (23–43)	34 (23–47)	27 (17–37)	0.276
10–20 units	6 (15.0)	4 (13.3)	8 (34.8)	0.121
>20 units	33 (82.5)	24 (80.0)	14 (60.9)	0.074
Traumatic amputation§	30 (75.0)	20 (66.7)	14 (58.3)	0.376
SOFA score, median (IQR)				
Germany	11 (8–15)	10.5 (7–12)	11 (5–12)	0.413
US hospital	9 (5–13)	7.5 (1–11)	4.5 (1–7.5)	0.007
Duration of antifungal use, median (IQR)	36 (23–49)	24 (18–36)	16 (0–24)	<0.001
Outcome				
Surgical amputations¶	27 (67.5)	13 (43.3)	10 (41.7)	0.057
Death	7 (17.5)	1 (3.3)	0	0.030

*Values are no. (%) except as indicated. IFI, invasive fungal wound infections; IQR, interquartile range; SOFA, sequential organ failure assessment.
†Status of whether patient was on foot patrol or in a vehicle is missing for 17 IFI patients (11 Proven, 3 Probable, and 3 Possible). Percentages and p-values based on total minus missing.
‡Blood information is missing for 1 patient with a possible IFI. Percentages and p-values based on total minus missing.
§Includes amputations that occurred before admission to a US hospital.
¶Defined as amputations that occurred after admission to a US hospital.

wounds (median 25 vs. 21; $p = 0.006$). Although blood urea nitrogen levels differed significantly between the groups, the levels were not clinically meaningful (data not shown). When analysis was restricted to the 56 patients whose wounds only met IFI criteria or the 50 patients whose wounds only met high-suspicion criteria, IFI patients were more likely to have received >20 units of blood within 24 hours (70% vs. 58%; $p = 0.016$).

IFI and Low-Suspicion Wounds

The median ISS was higher among patients with IFI wounds than among those with low-suspicion wounds (40 vs. 33; $p < 0.001$; Table 3). Compared with patients with low-suspicion wounds, patients with IFI wounds had higher SOFA scores at admission to LRMC (11 vs. 6; $p < 0.001$) and to US hospitals (7 vs. 1; $p < 0.001$) and received more blood transfusions within 24 hours of injury (median 31

Table 3. Characteristics of US military patients with laboratory evidence of invasive fungal infection of wound sustained on battlefield, Afghanistan, June 1, 2009–December 31, 2014*

Characteristic	IFI, n = 94	High suspicion, n = 61	p value†	Low suspicion, n = 91	p value‡
Blast injury	92 (97.9)	61 (100)	0.520	89 (97.8)	1.000
Injured while on foot patrol§	73 (94.8)	51 (94.4)	1.000	80 (95.2)	1.000
Injury severity score					
Median (IQR)	40 (33–50)	38 (30–45)	0.262	33 (27–42)	<0.001
≥26/critical	87 (92.6)	52 (85.3)	0.144	75 (82.4)	0.037
Blood units received 24 h after injury, median (IQR)¶	31 (21–43)	21 (15–32)	0.003	17 (12–24)	<0.001
10–20	18 (19.4)	25 (41.0)	0.003	42 (48.3)	<0.001
>20	71 (76.3)	31 (50.8)	0.002	30 (34.5)	<0.001
Traumatic amputation#	64 (68.1)	48 (78.7)	0.150	73 (80.2)	0.060
SOFA score, median (IQR)					
Germany	11 (7–13)	8 (4–13)	0.028	6 (2–9)	<0.001
US hospital	7 (2–11)	4 (1–8)	0.022	1 (0–6)	<0.001
Duration of antifungal use, median (IQR)	24 (14–43)	21 (14–27)	0.006	0	NA
Outcome					
Surgical amputation**	50 (53.2)	26 (42.6)	0.199	24 (26.4)	<0.001
Death	8 (8.5)	1 (1.6)	0.090	0	0.007

*Values are no. (%) except as indicated. Patients with >1 wound with differing classifications are classified at the highest level. One patient with a wound classified as high suspicion died within 24 h of collection of sample providing laboratory evidence of fungal infection, precluding classification as having an IFI. IFI, invasive fungal wound infection; IQR, interquartile range; SOFA, sequential organ failure assessment.

†Compares characteristics between those having an IFI and those having a high-suspicion wound.

‡Compares characteristics between those having an IFI and those having a low-suspicion wound.

§Information about whether patient was on foot patrol or in a vehicle is missing for 17 IFI patients, 7 patients with high-suspicion wounds, and 7 patients with low-suspicion wounds. Percentages and p-values based on total minus missing.

¶Information missing for 1 patient with an IFI and 4 patients with low-suspicion wounds. Percentages and p-values based on total minus missing.

#Includes amputations that occurred before admission to a US hospital.

**Defined as amputation that occurred after admission to a US hospital.

vs. 17; $p < 0.001$). Blood urea nitrogen levels, liver function test results, and leukocyte counts were also higher among those in the IFI group (data not shown). Patients classified as having IFI also received antifungal therapy longer than those with low-suspicion wounds (median 25 vs. 0; $p = 0.006$). When analysis was restricted to patients whose wounds only met IFI criteria (56) or patients whose wounds only low-suspicion criteria (91), statistical differences were similar to those of the full population.

Wound Microbiology

Among 413 wounds with documented laboratory evidence of fungal infection, fungal cultures had been submitted for 97% and culture results were negative for 11% (Figure 2; Table 4). Fungi of the order Mucorales were more likely to be isolated from IFI wounds (39%) than from high-suspicion (22%) and low-suspicion (9%) wounds ($p < 0.05$; Table 4). Fungi of the order Mucorales were isolated from over half (52.6%) of IFI wounds with documented angioinvasion (proven IFI), 31.3% of probable IFI wounds, and 26.3% of possible IFI wounds ($p = 0.016$). In contrast, a higher proportion of low-suspicion (46%) and high-suspicion (23%) than IFI (13%) wounds grew other fungi ($p < 0.05$). Fungi belonging to the genus *Fusarium* were more commonly isolated from IFI wounds than from low-suspicion wounds (17% vs. 4%; $p < 0.001$). Between high-suspicion and low-suspicion wounds, the proportions of growth of fungi of the order Mucorales ($p = 0.003$), *Fusarium* spp. ($p = 0.001$), and other fungi ($p < 0.001$) differed significantly.

Bacterial cultures collected within 14 days of injury were assessed for 378 (92%) of wounds; only 1% were negative for bacteria (Table 4). Most frequently isolated were *Enterococcus* spp. (38%) and *Escherichia coli* (17%); not

commonly isolated was *Staphylococcus aureus* (0.5%). The bacteria isolated differed among the 3 groups of wounds. *Acinetobacter baumannii* was more frequently isolated from patients in the IFI group (22%) than from patients in the other 2 groups (9% with high-suspicion wounds [$p = 0.006$] and 5% with low-suspicion wounds [$p < 0.001$]). In addition, the proportion of multidrug-resistant organisms isolated was higher among patients with IFI (37%) than among those with low-suspicion (17%) wounds ($p < 0.001$).

Outcomes

The proportion of deaths or surgical amputations did not differ significantly between patients in the IFI and high-suspicion groups. A higher proportion of patients in the IFI group required a surgical amputation (53% vs. 26%; $p < 0.001$) or died (9% vs. 0; $p = 0.007$) than did patients in the low-suspicion group (Table 3). The number of debridements in the first 4 weeks after injury was similar for patients with IFI wounds (median 10, IQR 7–11) and high-suspicion wounds (median 9, IQR 7–11; $p = 0.034$); however, patients with low-suspicion wounds underwent fewer debridements (median 7; IQR 5–9; $p < 0.001$) than patients with IFI wounds. In addition, 70 (49%) of 143 IFI wounds required that the patient undergo surgical amputations compared with 48 (40%) of 120 high-suspicion wounds ($p = 0.146$) and 45 (30%) of 150 low-suspicion wounds ($p = 0.001$).

Discussion

As part of our comprehensive evaluation of IFIs among US military personnel wounded in Afghanistan, we propose definitions for the risk stratification of wounds with laboratory evidence of fungal infection (i.e., positive culture results, histopathologic results, or both). Using our definitions, wounds can be grouped into 3 relatively homogeneous groups with different probabilities of IFI: wounds with IFI, those at high suspicion for IFI, and those at low suspicion for IFI. The categorization of wounds into risk groups is designed to provide a framework to help with clinical decision making and reduce practice variations and to provide definitions that could be used to group wounds for clinical and epidemiologic research.

We had previously proposed a modification of the EORTC/MSG criteria (18) to provide a better disease definition and classification for trauma-related IFI. Using this definition, wounds with necrosis present after ≥ 2 debridements and laboratory evidence of filamentous fungi at any time (either early or late) were classified as IFI (1,3). We had previously considered this classification sufficient for IFI wounds in the military setting and for clinical care (1,3). However, a comprehensive review of all cases suggested that the previously proposed criteria failed to sufficiently account for temporal aspects relevant to fungal contamination of wounds and necrosis associated with trauma.

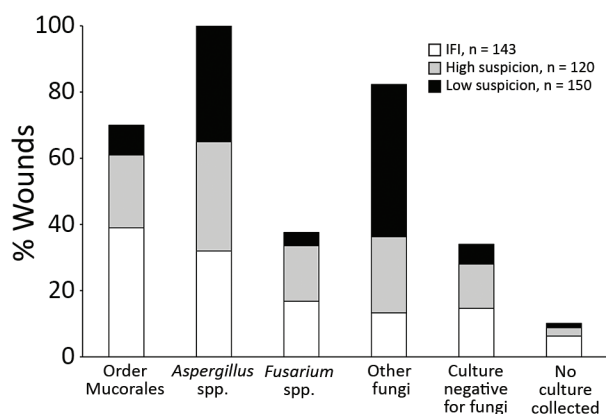


Figure 2. Wound culture mycology distribution, by wound classification, in study of US military patients who had laboratory evidence of fungal infection after battlefield trauma in Afghanistan, June 1, 2009–December 31, 2014. Because wound infections were polymicrobial, organisms are not mutually exclusive for a classification type. IFI, invasive fungal infection; other fungi, filamentous fungi other than order *Mucorales*, *Aspergillus* spp., and *Fusarium* spp.

Table 4. Microbiological findings for US military patients who had battlefield trauma wounds with invasive fungal infections and laboratory evidence of fungal infection, June 1, 2009–December 31, 2014*

Culture findings	IFI wounds, n = 143	High-suspicion wound, n = 120	p value†	Low-suspicion wound, n = 150	p value‡
Fungal cultures not sent	9 (6.3)	3 (2.5)	0.235	2 (1.3)	0.032
Fungal growth§					
None	21 (14.7)	16 (13.5)	0.774	9 (6.0)	0.014
1 fungus	55 (38.5)	50 (41.7)	0.597	91 (60.7)	<0.001
≥1 fungi	58 (40.6)	51 (42.5)	0.751	48 (32.0)	0.128
≥1 fungi plus bacteria¶	82 (57.3)	80 (66.7)	0.121	83 (55.3)	0.729
Order Mucorales	55 (38.5)	26 (21.7)	0.003	13 (8.7)	<0.001
<i>Aspergillus</i> spp.	45 (31.5)	39 (32.5)	0.858	55 (36.7)	0.348
<i>Fusarium</i> spp.	24 (16.8)	20 (16.7)	0.980	6 (4.0)	<0.001
Other filamentous fungi#	19 (13.3)	27 (22.7)	0.046	69 (45.7)	<0.001
Bacterial growth§					
None	3 (2.1)	1 (0.8)	0.628	3 (2.0)	≈1.00
<i>Staphylococcus aureus</i> **	0	0	NA	2 (1.3)	0.499
<i>Enterococcus</i> spp.	53 (37.1)	51 (42.5)	0.369	42 (28.0)	0.098
<i>E. faecalis</i>	5 (3.5)	5 (4.2)	0.777	8 (5.3)	0.445
<i>E. faecium</i>	41 (28.7)	42 (35.0)	0.271	31 (20.7)	0.111
<i>Escherichia coli</i>	22 (15.4)	20 (16.7)	0.777	23 (15.3)	0.990
<i>Pseudomonas</i> spp.	21 (14.7)	23 (19.2)	0.332	16 (10.7)	0.301
<i>P. aeruginosa</i>	16 (11.2)	14 (11.7)	0.903	11 (7.3)	0.254
<i>Acinetobacter baumannii</i>	29 (20.3)	11 (9.2)	0.012	6 (4.0)	<0.001
Other gram-negative bacilli	30 (21.0)	29 (24.2)	0.537	21 (14.0)	0.115
ESKAPE pathogen††	49 (34.3)	50 (41.7)	0.217	44 (29.3)	0.365
Multidrug resistant†††	53 (37.1)	34 (28.3)	0.134	26 (17.3)	<0.001

*Values are no. (%) except as indicated. IFI, invasive fungal infection; NA, not applicable.

†Compares characteristics between IFI and high-suspicion wounds.

‡Compares characteristics between IFI and low-suspicion wounds.

§Because of polymicrobial wounds, organisms are not mutually exclusive and will add to more than the total. Bacterial cultures were restricted to those collected within 14 d of injury.

¶Category of ≥1 fungi plus bacteria is not mutually exclusive from fungal cultures with 1 fungus or ≥1 fungi.

#Includes *Acrophialophora* spp., *Alternaria* spp., *Bipolaris* spp., *Scedosporium* spp., and *Trichoderma*.

**Includes methicillin-resistant and methicillin-susceptible *S. aureus*.

††ESKAPE pathogens are *Enterococcus faecium*, *Staphylococcus aureus*, *Klebsiella pneumoniae*, *Acinetobacter baumannii*, *Pseudomonas aeruginosa*, and *Enterobacter* spp.

†††Multidrug resistant is defined as resistance to ≥3 of 4 antibiotic classes or production of extended-spectrum β-lactamase or carbapenemases.

In this iteration, to account for the temporality of events, we propose a definition that requires ongoing necrosis and persistence of laboratory evidence of fungus after ≥2 debridements to define IFI. Furthermore, we categorize wounds into 3 categories of varying risk, whereas the previous definition defined only IFIs. The prior definition was based on review of 37 initial cases, whereas this definition is comprehensive and includes data from 246 patients. Were we to apply the current criteria to 77 previously identified cases (3), one third of them would no longer be classified as IFI (25% would be reclassified as high suspicion and 10% as low suspicion; data not shown).

According to our schema, IFI case-patients accounted for ≈5% (range 2.7%–6.6% annually) of all admissions for battlefield trauma during 2009–2014; however, it should be noted that specimens were not consistently collected for histopathologic examination until late 2010. Of 94 IFI patients, 8 (9%) died and about half underwent surgical amputations. Two thirds of wounds with laboratory evidence of fungal infection did not meet our definition of IFI. Specifically, one third of wounds were classified as low suspicion, and patients with these wounds generally had very severe injuries; however, by the time of admission to a US hospital, they were not critically ill, as

evidenced by a median SOFA score of 1, and they were less likely to undergo subsequent surgical amputation. Laboratory evidence for these patients was often based on isolation of fungi (83%) with negative histopathologic findings. These patients were also less likely to receive antifungal medications (only 15%) and to receive them for a shorter duration (median 6.5 days for patients with low-suspicion wounds who received antifungal medications). Among this group, approximately half of the wounds had no evidence of deep SSTI, which confirms that isolation of fungus from a wound, even in critically injured patients with blast injuries sustained on foot patrol, is not enough evidence to suggest an IFI (13).

Given the substantial morbidity associated with IFI, in February 2011, a hospital-based clinical practice guideline was implemented at LRMC to enable earlier IFI diagnosis and initiation of antifungal therapy with the goal of improving clinical outcomes. Per the guideline, based on previously identified independent risk factors, specimens for histopathologic examination and fungal/bacterial cultures were systematically collected from at-risk patients after the first wound debridement (11). Although this risk-based sampling strategy successfully resulted in earlier IFI diagnosis (average 4 vs. 9 days before implementation

of the guideline), it also resulted in practice variation and use of antifungal medications for patients with low risk for wound progression to IFI (11). Our study suggests that approximately one third of patients for whom tissue was submitted had laboratory evidence of a fungus. Therefore, it became essential to objectively discriminate between wounds that require intensified surgical management and initiation of antifungal medications and wounds that can be closely followed up without substantial interventions (13). Because this patient group was composed primarily of men critically injured in a blast while on foot patrol and who received massive blood transfusions, all risk factors for IFI (demographic characteristics and injury patterns), although useful for identifying those at risk for an IFI (5), do not discriminate among those who need intensified surgical management and antifungal medications and those for whom antifungal medications can be withheld. Similarly, laboratory parameters differed significantly but are not clinically meaningful. Thus, we examined and used wound characteristics (i.e., persistence of necrosis, local signs and symptoms of a deep SSTI) in our classification. Empiric use of antifungal medications was common in this population (received by 63%); similarly, isolation of bacteria was very common (98% of cultures). Hence, to try and delineate between bacterial and fungal wound infections, we incorporated the prolonged use of antifungal medications (≥ 10 days) in our classification schema. Although this measure is based on the provider's judgment, we believe that the focus on local signs and symptoms of a wound, along with wound mycology, can be used for clinical decision making; however, our classification needs to be validated prospectively in other civilian and military trauma settings, outside of the Afghanistan theater, and ideally prospectively.

On the basis of IFI risk factors, a tool to support clinical treatment decisions near the point of injury and after admission to military hospitals has been developed (20). Data from our analysis may be used to further refine that clinical tool. The Joint Trauma System provides evidence-based recommendations for trauma care for the military. The Joint Trauma System has developed a Clinical Practice Guideline for management of IFI in wounded persons (21), and data from this analysis have been briefed to the Joint Trauma System leadership for potential refining of the IFI guidelines to enable wider dissemination throughout the military care community.

Clinical mycology, although not used in our classification schema, is another feature for distinguishing wounds. Fungi of the order Mucorales (39%) predominated in IFI wounds, and other fungi were more frequent in low-suspicion wounds (46%). The negative effect that fungi associated with IFIs have on wound healing has been previously demonstrated; fungi from the order Mucorales are associated with a statistically significant longer time to wound closure

(12). Thus, when ongoing necrosis, persistence of laboratory evidence of fungus, and objective evidence of deep SSTI are lacking, antifungal medications can be withheld if the patient is closely followed. In particular, antifungal medications may be withheld when high-risk features such as growth of order Mucorales fungi or angioinvasion are lacking.

In conclusion, we found that blast-associated injuries were common in this population of US service members and resulted in multiple heterogeneous wounds with evidence of fungal infection. Focusing on the wound characteristics (e.g., absence of ongoing necrosis and persistence of fungi), especially in the absence of objective signs of deep SSTIs, identifies wounds at low risk for IFI. When close clinical follow-up can be ensured, these wounds can be monitored without the immediate use of antifungal therapy. The characteristics of the fungi isolated also seem to stratify wound risk; isolation of fungi of the order Mucorales is associated with wounds with IFI or highly suspicious of IFI. Our proposed definitions help divide wounds into 3 groups based on the certainty of diagnosis, providing a framework to support clinical decision making, both initial empiric and subsequent targeted antifungal therapy, and reductions in practice variations.

Acknowledgments

We are indebted to the Infectious Disease Clinical Research Program Trauma Infectious Disease Outcomes Study team of clinical coordinators, microbiology technicians, data managers, clinical site managers, and administrative support personnel for the tireless hours they spent to ensure the success of this project. Specifically, we thank Laveta Stewart, Dan Lu, Marcia Goodrich, Brian Johnson, Teresa Merritt, Nicole Flores, and Virginia Hawthorne for their work.

This work (IDCRP-024) was conducted by the Infectious Disease Clinical Research Program, a US Department of Defense program executed through the Uniformed Services University of the Health Sciences, Department of Preventive Medicine and Biostatistics through a cooperative agreement with The Henry M. Jackson Foundation for the Advancement of Military Medicine, Inc. This project has been funded by the National Institute of Allergy and Infectious Diseases, National Institute of Health, under Inter-Agency Agreement Y1-AI-5072, the Department of the Navy under the Wounded, Ill and Injured Program, and the Defense Medical Research and Development Program.

The views expressed are those of the authors and do not reflect the official views of the Uniformed Services University of the Health Sciences; the Henry M. Jackson Foundation for the Advancement of Military Medicine, Inc.; the National Institutes of Health or the Department of Health and Human Services; Brooke Army Medical Center; Walter Reed National Military Medical Center; Landstuhl Regional Medical Center; the US Army Medical Department; the US Army Office of the Surgeon

General; the Department of Defense; or the Departments of the Army, Navy, or Air Force. Mention of trade names, commercial products, or organization does not imply endorsement by the US government.

About the Author

Dr. Ganesan is an infectious disease specialist at Walter Reed National Military Medical Center and a research principal investigator with the Infectious Disease Clinical Research Program. Her research interests include invasive fungal wound infections and molecular diagnostics.

References

- Warkentien T, Rodriguez C, Lloyd B, Wells J, Weintrob A, Dunne JR, et al.; Infectious Disease Clinical Research Program Trauma Infectious Disease Outcomes Study Group. Invasive mold infections following combat-related injuries. *Clin Infect Dis*. 2012;55:1441–9. <http://dx.doi.org/10.1093/cid/cis749>
- Tribble DR, Rodriguez CJ. Combat-related invasive fungal wound infections. *Curr Fungal Infect Rep*. 2014;8:277–86. <http://dx.doi.org/10.1007/s12281-014-0205-y>
- Weintrob AC, Weisbrod AB, Dunne JR, Rodriguez CJ, Malone D, Lloyd BA, et al.; Infectious Disease Clinical Research Program Trauma Infectious Disease Outcomes Study Group. Combat trauma-associated invasive fungal wound infections: epidemiology and clinical classification. *Epidemiol Infect*. 2015;143:214–24. <http://dx.doi.org/10.1017/S095026881400051X>
- Neblett Fanfair R, Benedict K, Bos J, Bennett SD, Lo Y-C, Adebajo T, et al. Necrotizing cutaneous mucormycosis after a tornado in Joplin, Missouri, in 2011. *N Engl J Med*. 2012;367:2214–25. <http://dx.doi.org/10.1056/NEJMoa1204781>
- Rodriguez CJ, Weintrob AC, Shah J, Malone D, Dunne JR, Weisbrod AB, et al.; Infectious Disease Clinical Research Program Trauma Infectious Disease Outcomes Study Group. Risk factors associated with invasive fungal infections in combat trauma. *Surg Infect (Larchmt)*. 2014;15:521–6. <http://dx.doi.org/10.1089/sur.2013.123>
- Vitrat-Hincky V, Lebeau B, Bozonnet E, Falcon D, Pradel P, Faure O, et al. Severe filamentous fungal infections after widespread tissue damage due to traumatic injury: six cases and review of the literature. *Scand J Infect Dis*. 2009;41:491–500. <http://dx.doi.org/10.1080/00365540902856537>
- Kronen R, Liang SY, Bochicchio G, Bochicchio K, Powderly WG, Spec A. Invasive fungal infections secondary to traumatic injury. *Int J Infect Dis*. 2017;62:102–11. <http://dx.doi.org/10.1016/j.ijid.2017.07.002>
- Evriviades D, Jeffery S, Cubison T, Lawton G, Gill M, Mortiboy D. Shaping the military wound: issues surrounding the reconstruction of injured servicemen at the Royal Centre for Defence Medicine. *Philos Trans R Soc Lond B Biol Sci*. 2011;366:219–30. <http://dx.doi.org/10.1098/rstb.2010.0237>
- Lewandowski LR, Weintrob AC, Tribble DR, Rodriguez CJ, Petfield J, Lloyd BA, et al.; Infectious Disease Clinical Research Program Trauma Infectious Disease Outcomes Study Group. Early complications and outcomes in combat injury related invasive fungal wound infections: a case-control analysis. *J Orthop Trauma*. 2016;30:e93–9. <http://dx.doi.org/10.1097/BOT.0000000000000447>
- Rodriguez CJ, Tribble DR, Malone DL, Murray CK, Jessie EM, Khan M, et al. Treatment of suspected invasive fungal infection in war wounds. *Mil Med*. 2018;183(suppl_2):142–6. <http://dx.doi.org/10.1093/milmed/usy079>
- Lloyd B, Weintrob AC, Rodriguez C, Dunne JR, Weisbrod AB, Hinkle M, et al.; Infectious Disease Clinical Research Program Trauma Infectious Disease Outcomes Study Group. Effect of early screening for invasive fungal infections in U.S. service members with explosive blast injuries. *Surg Infect (Larchmt)*. 2014;15:619–26. <http://dx.doi.org/10.1089/sur.2012.245>
- Warkentien TE, Shaikh F, Weintrob AC, Rodriguez CJ, Murray CK, Lloyd BA, et al.; Infectious Disease Clinical Research Program Trauma Infectious Disease Outcomes Study Group. Impact of Mucorales and other invasive molds on clinical outcomes of polymicrobial traumatic wound infections. *J Clin Microbiol*. 2015;53:2262–70. <http://dx.doi.org/10.1128/JCM.00835-15>
- Rodriguez C, Weintrob AC, Dunne JR, Weisbrod AB, Lloyd B, Warkentien T, et al.; the Infectious Disease Clinical Research Program Trauma Infectious Disease Outcomes Study Investigative Team. Clinical relevance of mold culture positivity with and without recurrent wound necrosis following combat-related injuries. *J Trauma Acute Care Surg*. 2014;77:769–73. <http://dx.doi.org/10.1097/TA.0000000000000438>
- Tribble DR, Conger NG, Fraser S, Gleeson TD, Wilkins K, Antonille T, et al. Infection-associated clinical outcomes in hospitalized medical evacuees after traumatic injury: trauma infectious disease outcome study. *J Trauma*. 2011;71(Suppl):S33–42. <http://dx.doi.org/10.1097/TA.0b013e318221162e>
- Eastridge BJ, Jenkins D, Flaherty S, Schiller H, Holcomb JB. Trauma system development in a theater of war: experiences from Operation Iraqi Freedom and Operation Enduring Freedom. *J Trauma*. 2006;61:1366–73. <http://dx.doi.org/10.1097/01.ta.0000245894.78941.90>
- Linn S. The injury severity score—importance and uses. *Ann Epidemiol*. 1995;5:440–6. [http://dx.doi.org/10.1016/1047-2797\(95\)00059-3](http://dx.doi.org/10.1016/1047-2797(95)00059-3)
- Antonelli M, Moreno R, Vincent JL, Sprung CL, Mendoça A, Passariello M, et al. Application of SOFA score to trauma patients. Sequential Organ Failure Assessment. *Intensive Care Med*. 1999;25:389–94. <http://dx.doi.org/10.1007/s001340050863>
- De Pauw B, Walsh TJ, Donnelly JP, Stevens DA, Edwards JE, Calandra T, et al.; European Organization for Research and Treatment of Cancer/Invasive Fungal Infections Cooperative Group; National Institute of Allergy and Infectious Diseases Mycoses Study Group (EORTC/MSG) Consensus Group. Revised definitions of invasive fungal disease from the European Organization for Research and Treatment of Cancer/Invasive Fungal Infections Cooperative Group and the National Institute of Allergy and Infectious Diseases Mycoses Study Group (EORTC/MSG) Consensus Group. *Clin Infect Dis*. 2008;46:1813–21. <http://dx.doi.org/10.1086/588660>
- Centers for Disease Control and Prevention. CDC/NHSN surveillance definitions for specific types of infections [cited 2019 Jan 2]. http://www.cdc.gov/nhsn/pdfs/pscmanual/17pscnoinfdef_current.pdf
- Potter BK, Forsberg JA, Silvius E, Wagner M, Khatri V, Schobel SA, et al. Combat-related invasive fungal infections: development of a clinically applicable clinical decision support system for early risk stratification. *Mil Med*. 2019;184:e235–42. <http://dx.doi.org/10.1093/milmed/usy182>
- Rodriguez CJ, Tribble DR, Murray CK, Jessie EM, Fleming ME, Potter BK, et al. Invasive fungal infection in war wounds (CPG: 28). 2016. Joint Trauma System [cited 2019 Jan 2]. [https://jts.amedd.army.mil/assets/docs/cpgs/JTS_Clinical_Practice_Guidelines_\(CPGs\)/Invasive_Fungal_Infection_04_Aug_2016_ID28.pdf](https://jts.amedd.army.mil/assets/docs/cpgs/JTS_Clinical_Practice_Guidelines_(CPGs)/Invasive_Fungal_Infection_04_Aug_2016_ID28.pdf)

Address for correspondence: Anuradha Ganesan, Walter Reed National Military Medical Center, 8901 Wisconsin Ave, Bethesda, MD 20889, USA; email: anuradha.ganesan.ctr@mail.mil

Clinical Characteristics and Treatment Outcomes for Patients Infected with *Mycobacterium haemophilum*

Pornboonya Nookeu, Nasikarn Angkasekwinae, Suporn Foongladda, Pakpoom Phoompson

Mycobacterium haemophilum is a nontuberculous mycobacterium that can infect immunocompromised patients. Because of special conditions required for its culture, this bacterium is rarely reported and there are scarce data for long-term outcomes. We conducted a retrospective study at Siriraj Hospital, Bangkok, Thailand, during January 2012–September 2017. We studied 21 patients for which HIV infection was the most common concurrent condition. The most common organ involvement was skin and soft tissue (60%). Combination therapy with macrolides and fluoroquinolones resulted in a 60% cure rate for cutaneous infection; adding rifampin as a third drug for more severe cases resulted in modest (66%) cure rate. Efficacy of medical therapy in cutaneous, musculoskeletal, and ocular diseases was 80%, 50%, and 50%, respectively. All patients with central nervous system involvement showed treatment failures. Infections with *M. haemophilum* in HIV-infected patients were more likely to have central nervous system involvement and tended to have disseminated infections and less favorable outcomes.

Mycobacterium haemophilum is a nontuberculous mycobacterium that causes localized and disseminated infections in immunocompromised patients and rarely in immunocompetent patients (1). It is a slow-growing, aerobic, fastidious mycobacterium that requires heme-supplemented culture medium and low temperatures of 30°C–32°C for optimal growth (2). Because of the special conditions required for culture, it is frequently not isolated because of use of inappropriate techniques, and thus is rarely reported in the medical literature.

The most common clinical manifestation of infection in adult patients is cutaneous disease (3,4), either localized or as part of disseminated disease that occurs mainly in severely immunocompromised patients, such as those infected with HIV, those with autoimmune disease, or

those who have undergone solid organ or stem cell transplantation (5–10). Thus, infection with *M. haemophilum* should be suspected in immunocompromised patients who have unexplained skin lesions and are smear positive for acid-fast bacilli, but show negative results for routine mycobacterial culture.

There is no current standardized guideline for optimal management of patients infected with *M. haemophilum*. Furthermore, the long-term outcome of this infection has not been well documented. The purpose of this study was to determine clinical characteristics, treatment, and long-term outcomes for infections with *M. haemophilum*.

Methods

We conducted a retrospective cohort study at Siriraj Hospital, the largest academic hospital in Bangkok, Thailand, during January 2012–September 2017. We identified all patients who were given a diagnosis of *M. haemophilum* infection by culture or molecular methods. Specimens of all types underwent smear microscopic analysis by using auramine–rhodamine staining and mycobacterial culture by using Lowenstein-Jensen solid medium and liquid medium containing mycobacteria growth indicator. All specimens were incubated at 35°C, and those from skin, bone, and joint were also incubated at 30°C. We performed species identification by using the INNO-LiPA Mycobacteria Version 2 Assay (Innogenetics [now Fujiregio], <https://www.fujirebio-europe.com>). We reviewed baseline demographics, clinical characteristics, microbiological data, antimicrobial and surgical treatment, and clinical outcome. All patients were followed up for ≥1 year after diagnosis. This study was approved by the institutional review board committee at Siriraj Hospital (Chart of Accounts no. Si 630/2017).

Results

A total of 21 patients were included in this study; 67% were women (median age 53 years, range 25–73 years). All 21

Author affiliation: Faculty of Medicine, Siriraj Hospital, Bangkok, Thailand

DOI: <https://doi.org/10.3201/eid2509.190430>

patients were immunocompromised. The most common concurrent condition was HIV infection (8 patients, 38%), followed by systemic lupus erythematosus (5 patients, 23.8%), γ -interferon autoantibody (2 patients, 9.5%), kidney transplantation (2 patients, 9.5%), diabetes mellitus (2 patients, 9.5%), ankylosing spondylitis (1 patient), and nephrotic syndrome (1 patient).

All HIV-infected patients except 1 had CD4 cell counts <200 cells/mm³. Among non-HIV-infected patients, those with systemic lupus erythematosus, kidney transplantation, and nephrotic syndrome received corticosteroids or other immunosuppressive agents.

The most common organ involved was skin and soft tissue (13 patients), followed by bone and joint (3 patients), central nervous system (CNS) (3 patients), eye (2 patients), and lymph nodes (1 patient). Two patients (1 with CNS involvement [no. 1] and 1 with bone and joint infection [no. 14]) had concomitant mycobacteremia. The most common cutaneous manifestation was an erythematous nodule that commonly occurred on the extensor surface of elbows, legs, and the auricular area (Figure 1). Of 7 skin biopsy specimens, granulomatous inflammation was the most common pathologic finding. Three patients who had CNS involvement had advanced HIV disease and CD4 cell counts <50 cells/mm³. We obtained computed tomography (CT) and

magnetic resonance imaging findings for 3 patients with CNS involvement (Figure 2).

We did not perform antimicrobial drug susceptibility testing on any bacterial isolate because of a failure of growth in solid medium. A total of 20/21 patients were treated with a combination of antimycobacterial agents. For 19 patients whose outcomes were available, 11 patients were cured, 1 patient improved with ongoing antimicrobial drug treatment, 3 patients required surgical excision after failure of medical therapy, 3 patients had a relapse of their infection after treatment discontinuation, and 1 patient died from disseminated disease after 1 month of therapy (Table).

The success rate of medical therapy for cutaneous infection was 80%. However, this rate was lower (50%) for bone, joint, and ocular infections. All patients with CNS diseases and involvement showed treatment failures.

The most commonly used regimen included a combination of macrolides and fluoroquinolones (3 patients, 14.3%) or these combined regimens with rifampin (9 patients, 42.9%). Combination therapy with macrolides and fluoroquinolones resulted in a success rate of 60% for treatment of cutaneous infection. Use of rifampin as the third drug for more severe cases also resulted in a modest (66%) success rate. Sulfamethoxazole/trimethoprim, doxycycline, and cycloserine were also replaced with rifampin,

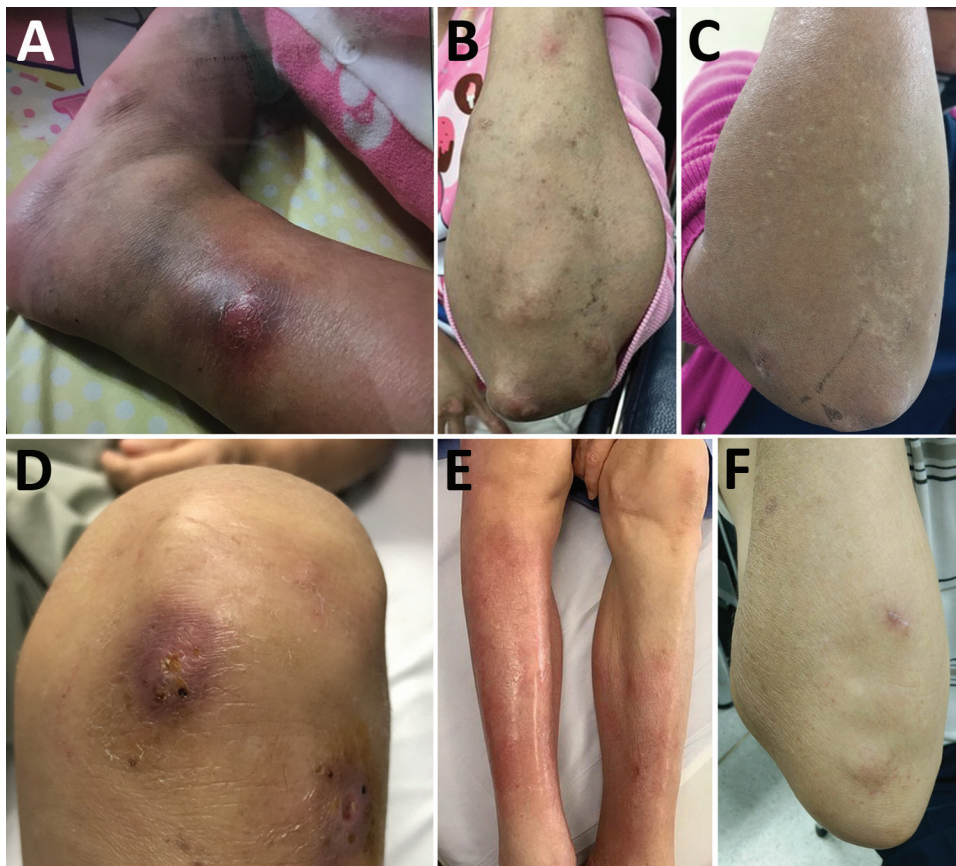
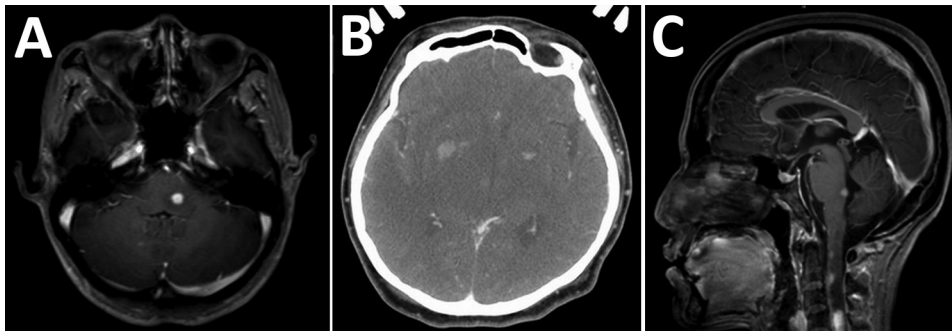


Figure 1. Cutaneous manifestation in non-HIV-infected patients infected with *Mycobacterium haemophilum*, Bangkok, Thailand. A) Patient 9, B) patient 11, C) patient 12, D) patient 16, E) patient 17, F) patient 21.

Figure 2. Imaging of brain and spine of 3 patients infected with *Mycobacterium haemophilum* who had involvement of the central nervous system, Bangkok, Thailand. A) Patient 1, axial T1-weighted magnetic resonance imaging scan with gadolinium showing enhanced nodule at left dorsal pons. B) Patient 2, axial contrast-enhanced computed tomography scan showing hypodensity lesions in both thalami and nodular enhancement at the bilateral basal ganglia. C) Patient 3, sagittal T1-weighted magnetic resonance imaging scan with gadolinium showing multiple enhancing nodules at dorsal pons and upper cervical cord.



which showed clinically successful results. For 11 patients in whom antimicrobial drugs could be discontinued, the median duration of treatment was 12 months (range 3–12 months for skin and soft tissue infections, 6 months for bone and joint infections, and 12 months for lymphadenitis and eye infections).

The patient who died of disseminated *M. haemophilum* infection was a 25-year-old man who was given a new diagnosis of infection with HIV and had a CD4 cell count of 17 cells/mm³. He had diplopia for 1 month and a low-grade fever. Physical examination showed multiple left-sided cranial nerve palsies (V [trigeminal], VI [abducens], and VII [facial]), and lower motor neuron lesions. Magnetic resonance imaging of the brain showed multiple, abnormal, high-signal-intensity lesions on T2-weighted imaging with gadolinium, as well as nodular enhancement of the left dorsal pons, right ventral pons, mid pons, left cerebellar peduncle, and medulla (Figure 2, panel A). Examination of cerebrospinal fluid showed standard results; hemoculture grew *M. haemophilum*. He was given levofloxacin, azithromycin, and ethambutol. However, his clinical condition deteriorated rapidly. Right hemiparesis then developed and he became stuporous. He died from acute respiratory failure secondary to aspiration pneumonia.

When we compared HIV-infected and non-HIV-infected patients, HIV-infected patients were younger (median age 36 years vs. 57 years; $p = 0.017$), more likely to have disseminated infection (37.5% vs. 15.4%; $p = 0.325$), more likely to have CNS involvement (37.5% vs. 0%; $p = 0.042$), and more likely to have a less favorable prognosis (50% vs. 77%; $p = 0.38$).

Discussion

We report 21 cases of *M. haemophilum* infection over a 6-year period at the largest academic hospital in Thailand. *M. haemophilum* commonly causes infection in immunocompromised persons. Advanced HIV infection remains the most common immunocompromised condition associated with this infection, as reported (1,3). Approximately

60% of patients have skin and soft tissue involvement, and the most commonly involved areas are the extensor surfaces of the extremities and auricular regions, which could be explained by the predilection of the organism for body areas with lower temperatures.

Although CNS infection with *M. haemophilum* is extremely rare and only a few case-patients have been reported (11–13), we identified CNS involvement in 3 of 21 case-patients in our study. All had advanced HIV disease: 2 patients had multiple brain abscesses, which was similar to those previously described, and 1 patient had myelitis. A total of 2 of 3 previous case reports of CNS involvement in patients with *M. haemophilum* infection were from Thailand and in HIV-infected patients (11,12), whereas the 2 largest case series (23 and 15 cases) reported from the United States found no cases of CNS involvement (3,4). Further study is needed to determine whether genetic or environmental factors will influence clinical manifestations of *M. haemophilum* infection.

Treatment with a combination of fluoroquinolones, rifampin, and macrolides is suggested for treating *M. haemophilum* infection (14). However, our study demonstrated that 2 antimycobacterial agents (macrolides and fluoroquinolones) were successfully used for patients with isolated cutaneous diseases. Conversely, surgical resection might be needed for some case-patients, such as those who showed treatment failure or those in which there was CNS involvement. Because of poor penetration of the CNS by these antimicrobial agents, patients who had mycobacterial infections with CNS involvement are often associated with poorer outcomes (15,16). Two previous case reports of persons with CNS disease were successfully treated with surgical excision in combination with antimicrobial drugs, although there were residual neurologic deficits (11,13). Another study reported a case-patient who did not respond to medical therapy alone and subsequently died (12).

Treatment for *M. haemophilum* infection should last ≈3–12 months and should be tailored on the basis of severity of disease and immunocompromised conditions. Isolated

cutaneous disease usually responds well to shorter duration of therapy (3–6 months), and CNS infections, bone and joint infections, and disseminated disease usually require longer therapy (12 months) (1). Relapse cases have been rarely reported (17), and accounted for just 4% in the largest case series (1). However, our study showed a higher

Table. Clinical characteristics and treatment for 21 patients infected with *Mycobacterium haemophilum*, Bangkok, Thailand*

Patient no.	Age, y/sex	Disease or condition, CD4 cell count/mm ³	Clinical manifestation	Site of positive culture	Surgical treatment	Drug treatment	Treatment duration, mo†	Outcome
1	25/F	AIDS, 17	Brain abscesses, septicemia	Blood	None	AZM, LVX, EMB	1	Died
2	35/F	AIDS, 12	Brain abscesses	Brain tissue	None	NA	NA	Lost to follow-up
3	35/F	AIDS, 40	Myelitis	Spinal cord tissue	None	INH, RIF, PZA, EMB, CLR, AMK	2	Treatment failure
4	29/M	AIDS, 14	Skin nodule (left popliteal fossa)	Skin	None	AZM, LVX, RIF	NA	Lost to follow-up
5	52/M	AIDS, 6	Plague (right hand)	Skin	None	CLR, CIP, RIF	6	Cured
6	46/F	AIDS, 190	Chronic ulcer (left foot)	Pus	None	MFX	3	Cured
7	36/F	AIDS, 12	Auricular abscess	Pus	None	AZM, LVX, RIF	12	Cured
8	53/F	HIV+, 657	Preauricular abscess	Pus	I and D	CLR, CIP	12	Cured
9	25/F	SLE	Chronic wound and osteomyelitis (right ankle), olecranon bursitis	Bone	Debridement	IMI, AMK; then AZM, CIP, RIF	6 (1.5/4.5)	Relapsed
10	39/F	SLE	Tenosynovitis (right index finger)	Pus	Debridement	AMK; then CLR, LVX	6 (2/4)	Cured
11	57/F	SLE	Skin nodules (both elbows)	Skin	None	CLR, CIP, RIF	6	Cured
12	47/F	SLE, dermatomyositis	Skin nodules (both elbows)	Skin	None	IMI, AMK; then AZM, CIP, RIF	6 (0.5/5.5)	Cured
13	39/F	SLE, DM	Skin abscess (right ankle)	Pus	I and D	AMK; then CLR, LVX, DCS	12 (2/10)	Cured
14	69/M	IFN- γ autoantibody	Septicemia, spondylodiscitis	Blood	None	CLR, LVX, RIF	24	Relapsed
15	73/F	IFN- γ autoantibody	Lymphadenitis (right cervical node)	Lymph node	None	IMI, CLR; then CLR, CIP, SXT	12	Cured
16	60/F	Kidney transplant	Skin nodules (both arms/legs), septic arthritis (right ankle)	Pus	Debridement	AMK, CLR, LVX, LZD; then MFX, AZM, RIF, LZD	11 (1/10)	Improved
17	58/F	Kidney transplant	Plague (both legs)	Skin	None	IMI, AMK, CLR; then AZM, LVX, RIF	12 (1/11)	Relapsed
18	65/F	DM, A1C 6.7%	Scleritis and keratitis	Sclera	Enucleation	IMI, CLR, LVX, RIF, LZD	4	Treatment failure
19	65/M	DM, A1C 13.3%	Endophthalmitis	Vitreous fluid	None	IMI, AMK, LVX; then AZM, RIF, DOX	12 (0.5/11.5)	Cured
20	53/M	Ankylosing spondylitis	Skin nodules (right elbow)	Skin	Surgical excision	CLR, LVX	6	Treatment failure
21	48/M	Nephrotic syndrome	Skin nodules (right elbow)	Skin	None	CLR, CIP, RIF	12	Cured

*AMK, amikacin; AZM, azithromycin; A1C, hemoglobin A1C; CIP, ciprofloxacin; CLR, clarithromycin; DCS, D-cycloserine; DM, diabetes mellitus; DOX, doxycycline; EMB, ethambutol; I and D, incision and drainage; IFN- γ , interferon- γ ; IMI, imipenem; INH, isoniazid; LVX, levofloxacin; LZD, linezolid; MFX, moxifloxacin; NA, not available; PZA, pyrazinamide; RIF, rifampin; SLE, systemic lupus erythematosus; SXT, sulfamethoxazole/trimethoprim; +, positive. †Values in parentheses are durations for each drug group.

relapse rate (14%); therefore, we suggest that careful monitoring after discontinuation of treatment is warranted.

One limitation of our study was that no antimicrobial susceptibility testing was available because all culture-positive cases were detected in liquid medium. However, no data support the correlation of in vitro susceptibility testing and treatment response for this type of infection.

M. haemophilum infections should be suspected in immunocompromised patients who have unexplained cutaneous lesions, especially at auricular or extensor surfaces of extremities, who are smear positive for acid-fast bacilli, but show negative results for routine mycobacterial culture. Combination antimycobacterial therapy should be given for ≥ 3 months and extended to 12 months depending on the site of isolation. CNS involvement might occur more commonly than previously believed and is associated with worse outcome. Relapses are not uncommon; therefore, clinical monitoring after discontinuation of treatment is warranted.

Acknowledgments

We thank all medical staff and laboratory technicians who were involved in the study and those who cared for the patients.

About the Author

Dr. Nooku is a physician in the Faculty of Medicine, Siriraj Hospital, Mahidol University, Bangkok, Thailand. Her primary research interest is nontuberculous mycobacteria.

References

1. Lindeboom JA, Bruijnesteijn van Coppenraet LE, van Soolingen D, Prins JM, Kuijper EJ. Clinical manifestations, diagnosis, and treatment of *Mycobacterium haemophilum* infections. *Clin Microbiol Rev*. 2011;24:701–17. <http://dx.doi.org/10.1128/CMR.00020-11>
2. Dawson DJ, Jennis F. Mycobacteria with a growth requirement for ferric ammonium citrate, identified as *Mycobacterium haemophilum*. *J Clin Microbiol*. 1980;11:190–2.
3. Shah MK, Sebti A, Kiehn TE, Massarella SA, Sepkowitz KA. *Mycobacterium haemophilum* in immunocompromised patients. *Clin Infect Dis*. 2001;33:330–7. <http://dx.doi.org/10.1086/321894>
4. Tyner HL, Wilson JW. Fifteen-year clinical experience with *Mycobacterium haemophilum* at the Mayo Clinic: a case series. *J Clin Tuberc Other Mycobact Dis*. 2017;8:26–32. <http://dx.doi.org/10.1016/j.jctube.2017.06.002>
5. Kelley CF, Armstrong WS, Eaton ME. Disseminated *Mycobacterium haemophilum* infection. *Lancet Infect Dis*. 2011;11:571–8. [http://dx.doi.org/10.1016/S1473-3099\(11\)70029-9](http://dx.doi.org/10.1016/S1473-3099(11)70029-9)
6. Brix SR, Iking-Konert C, Stahl RA, Wenzel U. Disseminated *Mycobacterium haemophilum* infection in a renal transplant recipient. *BMJ Case Rep*. 2016;2016:pii:bcr2016216042.
7. Jacobs SE, Zhong E, Hartono C, Satlin MJ, Magro CM, Jenkins SG, et al. The brief case: disseminated *Mycobacterium haemophilum* infection in a kidney transplant recipient. *J Clin Microbiol*. 2017;56:e00561–17.
8. Otome O, O'Reilly M, Lim L. Disseminated *Mycobacterium haemophilum* skeletal disease in a patient with interferon-gamma deficiency. *Intern Med J*. 2015;45:1073–6. <http://dx.doi.org/10.1111/imj.12875>
9. Brissot E, Gomez A, Aline-Fardin A, Lalande V, Lapusan S, Isnard F, et al. Report of disseminated *Mycobacterium haemophilum* infection after double cord blood allo-SCT. *Bone Marrow Transplant*. 2014;49:1347–8. <http://dx.doi.org/10.1038/bmt.2014.144>
10. Collin CS, Terrell C, Mueller P. Disseminated *Mycobacterium haemophilum* infection in a 72-year-old patient with rheumatoid arthritis on infliximab. *BMJ Case Rep*. 2013;2013:pii:bcr2012008034.
11. Phowthongkum P, Puengchitprapai A, Udomsantisook N, Tumwasorn S, Suankratay C. Spindle cell pseudotumor of the brain associated with *Mycobacterium haemophilum* and *Mycobacterium simiae* mixed infection in a patient with AIDS: the first case report. *Int J Infect Dis*. 2008;12:421–4. <http://dx.doi.org/10.1016/j.ijid.2007.11.010>
12. Buppajarntham A, Apisarnthanarak A, Rutjanawech S, Khawcharoenporn T. Central nervous system infection due to *Mycobacterium haemophilum* in a patient with acquired immunodeficiency syndrome. *Int J STD AIDS*. 2015;26:288–90. <http://dx.doi.org/10.1177/0956462414535750>
13. Barr LK, Sharer LR, Khadka Kunwar E, Kapila R, Zaki SR, Drew CP, et al. Intraventricular granulomatous mass associated with *Mycobacterium haemophilum*: a rare central nervous system manifestation in a patient with human immunodeficiency virus infection. *J Clin Neurosci*. 2015;22:1057–60. <http://dx.doi.org/10.1016/j.jocn.2014.11.036>
14. Medical Section of the American Lung Association. Diagnosis and treatment of disease caused by nontuberculous mycobacteria. This official statement of the American Thoracic Society was approved by the Board of Directors, March 1997. *Am J Respir Crit Care Med*. 1997;156:S1–25.
15. Jacob CN, Henein SS, Heurich AE, Kamholz S. Nontuberculous mycobacterial infection of the central nervous system in patients with AIDS. *South Med J*. 1993;86:638–40. <http://dx.doi.org/10.1097/00007611-199306000-00009>
16. Lee MR, Cheng A, Lee YC, Yang CY, Lai CC, Huang YT, et al. CNS infections caused by *Mycobacterium abscessus* complex: clinical features and antimicrobial susceptibilities of isolates. *J Antimicrob Chemother*. 2012;67:222–5. <http://dx.doi.org/10.1093/jac/dkr420>
17. Ducharlet K, Murphy C, Tan SJ, Dwyer KM, Goodman D, Aboltins C, et al. Recurrent *Mycobacterium haemophilum* in a renal transplant recipient. *Nephrology (Carlton)*. 2014;19(Suppl 1):14–7. <http://dx.doi.org/10.1111/nep.12193>

Address for correspondence: Pakpoom Phoompoung, Faculty of Medicine, Siriraj Hospital, Mahidol University, 2 Wang Lang Rd, Siriraj, Bangkok Noi, Bangkok 10700, Thailand; email: benefat@hotmail.com

Theileria orientalis Ikeda Genotype in Cattle, Virginia, USA

Vanessa J. Oakes, Michael J. Yabsley, Diana Schwartz, Tanya LeRoith, Carolyn Bissett, Charles Broaddus, Jack L. Schlater, S. Michelle Todd, Katie M. Boes, Meghan Brookhart, Kevin K. Lahmers

Theileria orientalis Ikeda genotype is a parasite that causes a disease in cattle that results in major economic issues in Asia, New Zealand, and Australia. The parasite is transmitted by *Haemaphysalis longicornis* ticks, which have recently been reported in numerous states throughout the eastern United States. Concurrently, cattle in Virginia showed clinical signs consistent with a hemoprotozoan infection. We used amplicons specific for the major piroplasm surface protein and small subunit rDNA of piroplasms to test blood samples from the cattle by PCR. Bidirectional Sanger sequencing showed sequences with 100% identity with *T. orientalis* Ikeda genotype 2 sequences. We detected the parasite in 3 unrelated herds and from various animals sampled at 2 time points. Although other benign *T. orientalis* genotypes are endemic to the United States, detection of *T. orientalis* Ikeda genotype might represent a risk for the cattle industry in Virginia.

Theileria orientalis is an emerging parasitic pathogen of cattle that was originally identified in the Eastern Hemisphere (1). The taxonomy of this group is evolving (2–4); taxonomic classification relies on sequencing of 2 major genes: the small ribosomal subunit (SSU) and the major piroplasm surface protein (MPSP). Use of the names of *T. orientalis* genotypes Ikeda, Chitose, and Buffeli is embedded in the clinical literature; these designations are used throughout this article. A genotype scheme proposed in 2014 classifies *T. orientalis* into 11 genotypes according to variability in the MPSP gene (4); *T. orientalis* genotype Ikeda correlates with genotype 2 (3,5).

Consistent with other members of the genus, *T. orientalis* is a tickborne hemoprotozoan with a life cycle

that affects erythrocytes and leukocytes and contributes to chronic anemia, ill-thrift, and persistent subclinical infections. However, it has not been associated with the lymphoproliferative disease seen with *T. parva* and *T. annulata* (1). *Haemaphysalis* spp. ticks are the primary biological vector of *T. orientalis* (6) and are believed to be essential for completion of the *T. orientalis* life cycle (7), although there is limited evidence suggesting that transmission might occur through flies, lice, or vaccine needles (1).

In Asia, New Zealand, and Australia, theileriosis caused by *T. orientalis* is an economically serious disease manifested primarily by loss of revenue from deaths or illness in beef and dairy cattle (1,8–10). Of increasing concern is the Ikeda genotype of *T. orientalis*, which has been implicated as the etiologic agent of infectious bovine anemia (11,12). In Asia, Australia, and New Zealand, the primary tick vector for the *T. orientalis* Ikeda genotype is *Haemaphysalis longicornis*, which is also known as the Asian longhorned or bush tick.

The Asian longhorned tick was first detected in the United States in August 2017 and has subsequently been detected in New Jersey (13), New York, North Carolina, Virginia, West Virginia, Pennsylvania, Maryland, Connecticut, and Arkansas (14,15). However, examination of archived tick samples has identified *H. longicornis* ticks in the United States since 2010 (14). Because of the wide host range of this tick, its bisexual nature, and its ability to reproduce parthenogenetically (16), concern is increasing that there are established populations in the mid-Atlantic states.

In September 2017, a beef cattle herd in Virginia was given a diagnosis of anemia and suspected anaplasmosis. Blood samples were negative for *Anaplasma marginale* ticks by PCR, but blood smears showed numerous pleomorphic piroplasms. We report identification and characterization of *T. orientalis* Ikeda genotype 2 from an index farm, in adjacent herds, and 2 other counties in Virginia. Although other genotypes of *T. orientalis* are present in the United States (17–19), the Ikeda genotype in particular has not been identified in North America and represents an emerging infectious disease with potential for major animal

Author affiliations: Virginia–Maryland College of Veterinary Medicine, Blacksburg, Virginia, USA (V.J. Oakes, T. LeRoith, S.M. Todd, K.M. Boes, M. Brookhart, K.K. Lahmers); University of Georgia, Athens, Georgia, USA (M.J. Yabsley); Kansas State University, Manhattan, Kansas, USA (D. Schwartz); Virginia Department of Agriculture and Consumer Services, Richmond, Virginia, USA (C. Bissett, C. Broaddus); US Department of Agriculture, Ames, Iowa, USA (J.L. Schlater)

DOI: <https://doi.org/10.3201/eid2509.190088>

health and economic impacts, especially because a competent vector has been identified in this region and in 2 of the 3 farms described in this report.

Materials and Methods

Animals

All cattle were client-owned animals. In August 2017, seven cattle from a herd in Albemarle County, Virginia, died after showing adverse clinical signs, including weakness and malaise. Affected cattle included bulls, cows, and steers ranging in age from 3 months to 13 years. All animals were born and raised on a farm. In September 2017, an additional cow from the index farm was examined for weakness, icterus, and anemia (packed cell volume [PCV] 12.0%). Blood from this animal was collected and submitted to the Kansas State Veterinary Diagnostic Laboratory (Manhattan, KS, USA). Blood smear analysis showed evidence of a hemoprotozoal infection (Figure 1). Molecular testing of this sample resulted in a diagnosis of infection with *T. orientalis*, which prompted quarantine of the affected farm and further investigation.

A foreign animal disease investigation was instituted during December 2017, and blood was collected from the index cow and 5 additional, randomly sampled cattle from the herd. We collected blood by jugular vein venipuncture from each animal in 10-mL BD Vacutainer plastic red-top tubes containing no anticoagulant and in 10-mL BD Vacutainer plastic purple-top tubes containing EDTA

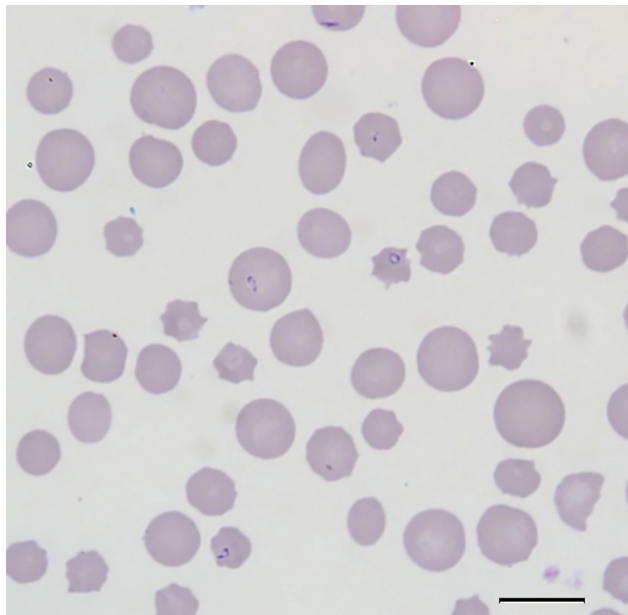


Figure 1. Blood smear of an animal from a farm in Albemarle County, Virginia, USA, that was infected with *Theileria orientalis* Ikeda genotype. There is evidence of a regenerative response to anemia (anisocytosis and polychromasia) and intracellular piroplasms within erythrocytes. Scale bar indicates 10 μm .

anticoagulant (both from Becton, Dickinson and Company, <https://www.bd.com>) as part of a routine diagnostic investigation for suspected anaplasmosis or as part of a random sampling effort.

DNA Extraction and PCR Testing

We extracted DNA from EDTA anticoagulant blood by using the DNeasy Blood and Tissue Kit (QIAGEN, <https://www.qiagen.com>) according to the nonnucleated blood protocol. We performed the final elution stage by using 50 μL of nuclease-free water and incubating the spin column membrane for 1 min at room temperature. This step was repeated to yield a final elution volume of 100 L.

We performed amplification for the MPSP by using 10.5 μL of DNA in a 25- μL reaction volume containing primers MPSP forward (5'-CTTTGCCTAGGATACTTCCT-3') and MPSP reverse (5'-ACGGCAAGTGGTGAGAACT-3') as described (11,20). Each amplification had a final reaction primer concentration of 0.4 $\mu\text{mol/L}$.

We performed amplification for the internal segment of the SSU by using 10 μL of DNA in a 25- μL reaction volume containing primers SSU internal forward (5'-ATTG-GAGGGCAAGTCTGGTG-3') and SSU internal reverse (5'-CTCTCGGCCAAGGATAAACTCG-3') as described (11,20) and identical PCR protocols as we described previously. We also used a Biometra TProfessional Thermocycler (AnalytikJena AG, <https://www.analytik-jena.com>).

We visualized amplicons by electrophoresis on a 1.0% agarose gel containing ethidium bromide and Tris-borate-EDTA buffer and examined amplicons by using UV transillumination. Amplicons with sizes of 700–800 bp were submitted to the Virginia Biocomplexity Institute (Blacksburg, VA, USA) for bidirectional Sanger sequencing.

Anaplasmosis Testing

Animals sampled as part of a foreign animal disease investigation were tested for *Anaplasma*, *Babesia*, and *Leptospira* spp. at the National Veterinary Services Laboratories (NVSL; Ames, IA, USA). The other animals involved in this study were tested for *Anaplasma marginale* by using a quantitative PCR used and validated by the Virginia Tech Animal Laboratory Services (ViTALS, Blacksburg, VA, USA) diagnostic laboratory (21) (Table).

For the samples tested by ViTALS, we extracted DNA from blood by using the protocol we described previously. DNA samples were diluted 1:10 with nuclease-free water. Amplifications were performed by using AM-For 16S forward primer (5'-TTGGCAAGGCAGCAGCTT-3') and AM-Rev 16S reverse primer (5'-TTCCGCGAGCATGTGCAT-3') at a concentration of 0.6 $\mu\text{mol/L}$ each, and AM-Pb probe (5'-6-FAM/TCGGTCTAACATCTCCAGGCTTTCAT/3BHQ_1-3') at a concentration of 0.2 $\mu\text{mol/L}$. Reactions were performed in an ABI 7500 Fast thermocycler

Table. Diagnostic testing results for *Theileria orientalis* Ikeda genotype in cattle, Virginia, USA*

Animal ID	Icterus/PCV/parasitemia	<i>Anaplasma</i> tick	Origin	Date
I1	Yes /12.0%/6%	Negative (NVSL)	Albemarle (Index farm)	Sep 2017, Dec 2017
I2	No	Negative (NVSL)	Albemarle (Index farm)	Dec 2017, May 2018
I3	No	Negative (NVSL)	Albemarle (Index farm)	Dec 2017, May 2018
I4	No	Negative (ViTALS)	Albemarle (Index farm)	Jul 2018
I5	No	Negative (ViTALS)	Albemarle (Index farm)	Jul 2018
A11	No	Negative (ViTALS)	Albemarle	Aug 2018
A12	Yes/10.0%/NA	Negative (ViTALS)	Albemarle	Oct 2018
P1	Yes/14.4%/16.4%	Positive (ViTALS)	Pulaski	Oct 2018
A1	No	Negative (ViTALS)	Augusta	Oct 2018
A2	No	Negative (ViTALS)	Augusta	Oct 2018

*ID, identification; PCV, packed cell volume; NA, not available; NVSL, National Veterinary Services Laboratories; ViTALS, Virginia Tech Animal Laboratory Services.

(Thermo Fisher Scientific, <https://www.thermofisher.com>) as described (21).

Sequence Analysis

We examined Sanger sequences of SSU and MPSP amplicons for quality and integrity and generated a consensus sequence by using Geneious Prime R11 (Biomatters, <https://www.geneious.com>). For paired samples of insufficient quality to form a consensus sequence, the highest quality sequence of the 2 sequences was used. We then aligned consensus sequence extractions with sequences of 3 *T. orientalis* Ikeda genotypes (GenBank accession nos. AB581627, AP011946, and D11046) by using Geneious Prime.

Phylogenetic Analysis

To examine the phylogenetic relationship of the cattle parasite in Virginia with other *Theileria* species, including the 3 genotypes of *T. orientalis*, we constructed a neighbor-joining tree by using a Tamura–Nei genetic distance model with 100 replications. We used the phylogenetic tree for the MPSP gene to best illustrate the relatedness of the samples from cattle in Virginia to the described *T. orientalis* genotypes (4). Phylogenetic analysis for the SSU gene included the *T. orientalis* Chitose genotype (GenBank accession no. AB520954), 2 *T. orientalis* Buffeli genotypes (accession nos. AB520955–6), 2 *T. orientalis* Ikeda genotypes (accession nos. AB520957–8), and *T. annulata* (accession no. AY524666) and *T. parva* (accession no. AF013418) as outgroups.

Results

Animals

Serologic analysis performed at NVSL for the 6 cattle tested showed negative results for *Anaplasma*, *Babesia*, and *Leptospira* species; all 6 animals were infected with piroplasmid hemoparasites on the basis of blood smear review. Subsequent blood samples were collected during May 2018 from 7 animals within the index herd. Two of these animals previously had intracellular piroplasms; 5 of these animals

were sampled randomly. Multiple cattle were infested with ticks, which were morphologically identified as *H. longicornis* by NVSL (14). In July 2018, blood samples were collected from 21 cattle representing animals from the index herd and others owned by the same producer on other farms in the county. Before the day of collection, there had been no contact among cattle from different herds. The 21 samples collected represented blood from 20 previously unsampled animals (sampled randomly) and 1 from a calf that had been piroplasm positive during May 2018.

A random sample from a livestock auction from a cow in Albemarle County was submitted during August 2018 (A11). Four additional samples were submitted from animals in Augusta (A1, A2), Pulaski (P1), and Albemarle (A12) Counties during October 2018. These animals were unrelated to the cattle at the index farm and had no contact with each other. Of these 5 samples, 3 samples were random samples from a livestock auction (A1, A2, A11), and 2 samples were submitted for evaluation of clinical disease (P1, A12). All animals, except P1, were negative for *Anaplasma marginale*. On the basis of a blood smear, P1 had 16% of its erythrocytes parasitized by piroplasms (Table). In addition, this animal had a marked macrocytic, hypochromic, regenerative anemia, hyperbilirubinemia, and icteric plasma consistent with hemolytic anemia (PCV 14.4% [reference range 24.0%–46.0%]; mean corpuscular volume 94.4 fL [reference range 40.0 fL–60.0 fL]; mean corpuscular hemoglobin concentration 27.3 g/dL [reference range 30.0 g/dL–36.0 g/dL]; reticulocytes 194,400/μL [reference range not established]; and total bilirubin 4.1 mg/dL [reference range 0.1 mg/dL–0.6 mg/dL]). Blood smear analysis revealed a 16% parasitemia. P1 died shortly after the blood draw; another animal on the farm had icterus and died 3 days earlier. A12 had a PCV of 10.0% and showed signs of icterus and lethargy.

Blood Smears

The blood smear examinations for the cow that became ill during September 2017 showed evidence of a regenerative response to anemia (anisocytosis, polychromasia, basophilic stippling) and numerous oval, racquet, signet ring, and

linear piroplasms within erythrocytes (Figure 1). During May 2018, blood smear analysis on 7 additional, randomly sampled animals did not show piroplasms. Two of these samples were from animals that had blood collected and analyzed by NVSL during December 2017; both of these animals were positive for piroplasms in blood smears at that time.

PCR

Molecular testing of the initial blood sample from the cow that became ill during September 2017 (I1) resulted in a diagnosis of infection with *T. orientalis*. This finding, which, in conjunction with the severity of the clinical signs in this animal and death of previous animals on the premises, led to further investigation of the genotype of the organism and quarantine of the affected farm.

Five of the 6 blood samples taken from cattle during December 2017 were positive by MPSP or SSU assays. Six of 7 cattle from the index herd sampled during May 2018 were positive by MPSP and SSU assays. Of the additional 21 samples collected during July 2018 from the index herd and adjacent properties, only samples from 3 animals were negative by MPSP and SSU assays. Three cattle from Augusta and Pulaski Counties (A1, A2, P1) and 2 cattle from an unrelated herd in Albemarle County (A11, A12) were positive by MPSP and SSU assays. A total of 34 sequences were available for analysis, representing 31 unique animals from multiple farms across southwestern Virginia.

Two cattle (I2 and I3) were positive by MPSP and SSU assays during December 2017, and remained positive by these assays during May 2018. One animal was positive by MPSP and SSU assays during May 2018, and remained positive for both assays during July 2018. The presence of positive samples at a sampling interval of 1–5 months suggests a chronic or persistent component of the infection.

Sequence and Phylogenetic Analysis

All 34 MPSP gene (719 bp) sequences from cattle from multiple farms in all 3 counties in Virginia sampled were identical to each other and to *T. orientalis* Ikeda and

genotype 2 sequences from GenBank (Figure 2). MPSP sequences of animals I2 and I3 sampled during December 2017 and May 2018 were identical.

On the basis of MPSP gene sequence phylogeny reported by Sivakumar et al. (4), all clinical samples clustered together, along with *T. orientalis* Ikeda and genotype 2 sequences retrieved from GenBank (Figure 3). The next closest related branch was composed of the cluster of *T. orientalis* genotype 7. Outgroups composed of *T. annulata* and *T. parva* clustered appropriately. On the basis of SSU gene sequence phylogeny (4,22) all clinical samples clustered together, along with *T. orientalis* Ikeda genotype sequences from GenBank (Figure 4).

Discussion

Genotypes of *Theileria orientalis* are native to the United States, but are of the Buffeli genotype and are typically nonpathogenic (17–19). *T. orientalis* Ikeda/genotype 2, a novel, virulent genotype, has not been previously identified in North America. Although the vector of *T. orientalis* among cattle in Virginia is unknown, *H. longicornis* ticks are a major vector in New Zealand, Australia, and Asia (1). The recent identification of this tick in the United States and clinical signs of anemia in an *Anaplasma*-negative herd of cattle infested by *H. longicornis* ticks prompted further investigation into the genotype of *T. orientalis* detected in the cattle sampled.

MPSP is an antigenic marker of *Theileria* spp., and is used to genotype the 11 *Theileria* groups (4,5). The sequences analyzed in this study are phylogenetically consistent with genotype 2, equivalent to the Ikeda genotype. Because the samples examined in this study represent individual cattle from geographically distant herds, there is concern that *T. orientalis* Ikeda/genotype 2 could be widespread in the region. This concern is especially potent given the presence of a known vector, *H. longicornis* ticks, within the region simultaneously (14). No ticks from the region have been tested for *T. orientalis*. Thus, further work is needed to better understand transmission of *T. orientalis* Ikeda by *H. longicornis* ticks or other tick species in Virginia.



Figure 2. DNA sequences from 10 cattle from a farm in Albemarle County, Virginia, USA, infected with *Theileria orientalis* Ikeda genotype 2 aligned with 3 GenBank sequences of *T. orientalis* genotype 2 for the major piroplasm surface protein. Alignment shows 100% consensus. Samples represent cattle from 6 different herds, and 2 samples were obtained at 2 time points. Nucleotides at the top indicate the consensus sequence. The GenBank sequence THEPMiPI is RNA with uracil substituted for thymine. A color version of this figure is available online (<http://wwwnc.cdc.gov/EID/article/25/9/19-0088-F2.htm>).

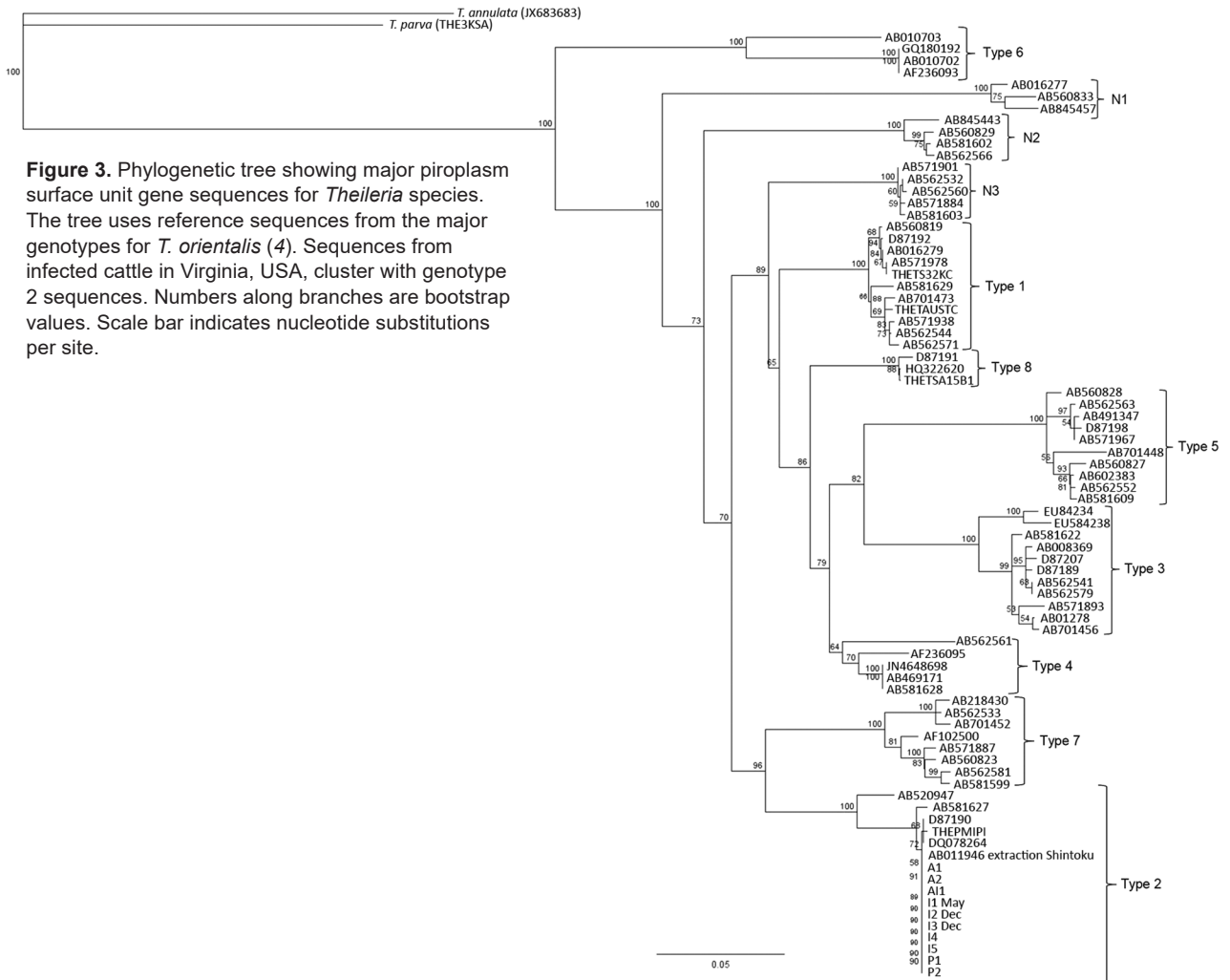


Figure 3. Phylogenetic tree showing major piroplasm surface unit gene sequences for *Theileria* species. The tree uses reference sequences from the major genotypes for *T. orientalis* (4). Sequences from infected cattle in Virginia, USA, cluster with genotype 2 sequences. Numbers along branches are bootstrap values. Scale bar indicates nucleotide substitutions per site.

The presence of *T. orientalis* Ikeda/genotype 2 in Augusta County is of particular concern because this county has the second largest number of cattle in Virginia (23). Rockingham County, which produces most of the cattle in Virginia, is adjacent to Augusta and Albemarle Counties. Future studies are needed to determine the presence of *H. longicornis* ticks and *T. orientalis* Ikeda/genotype 2 in this area, but disease transmission to and within this area is of concern to cattle producers in Virginia. In countries in which *T. orientalis* Ikeda is established, the parasite contributes to economic losses through chronically ill animals. During 2010 in Australia, losses caused by *T. orientalis* Ikeda were estimated to be Aus ≈\$20 million (5,10). In New Zealand, the cost of 1 outbreak on a large dairy farm was estimated to be ≈1 million New Zealand dollars (5).

In this initial study of cattle in the United States, some of the animals that were positive for *T. orientalis* Ikeda by PCR remained positive 5 months later, suggesting a chronic state, although the animals that had initially exhibited

clinical signs were no longer clinically ill during the spring and summer months. In New Zealand, disease caused by *T. orientalis* demonstrates seasonal pathogenicity, and anemia is more pronounced during autumn and winter months (12). Whether this trend is the case in Virginia will require future exploration. These cattle were also initially suspected to have anaplasmosis and had additional testing not been conducted, the detection of this pathogenic *Theileria* species might not have occurred. This study highlights the need for more surveillance and appropriate characterization of any parasites detected.

The source and timing of introduction of *T. orientalis* Ikeda/genotype 2 into the United States is unclear. One potential mechanism of introduction is through subclinically infected live cattle imported from disease-endemic regions. Approximately 200 live Wagyu cattle were imported from Japan during 1993–1997 before a ban on exports of Wagyu cattle by Japan in 1997 (24). Some of these same cattle were exported to Australia. It is possible that this or other

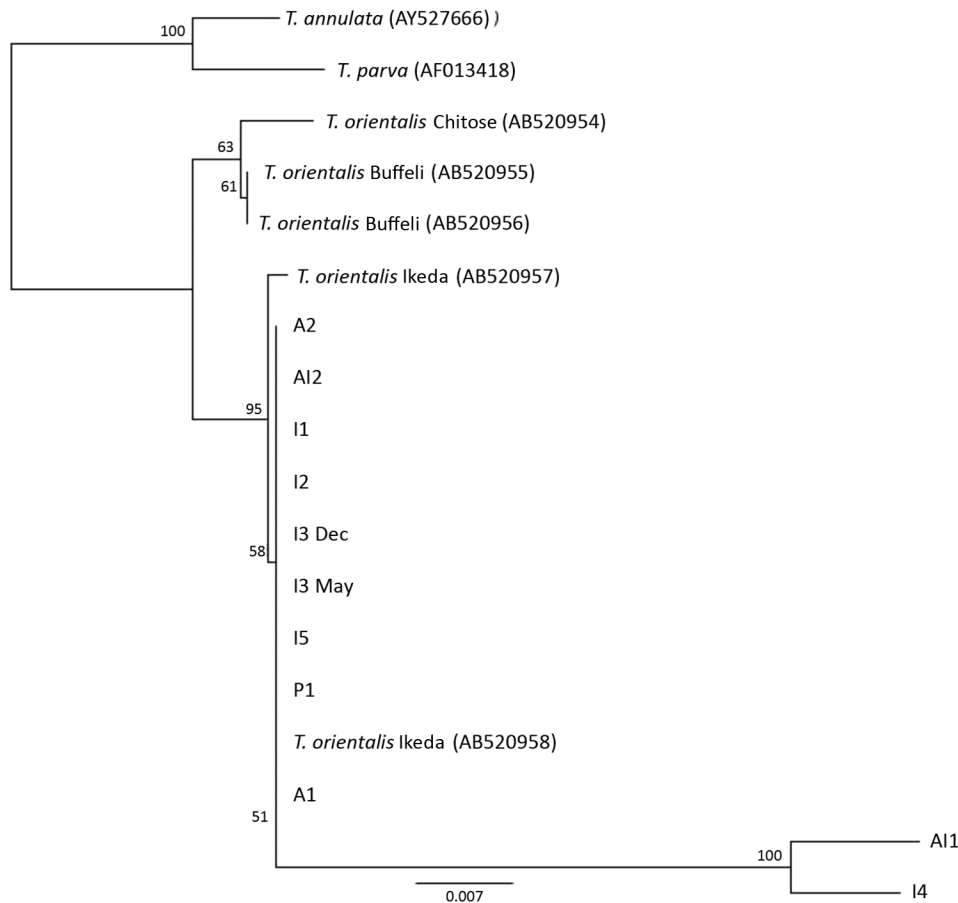


Figure 4. Phylogenetic tree showing small subunit rDNA gene sequences for *Theileria* species. Representative samples from cattle in 6 herds in Virginia, USA, cluster with the reference sequences for the Ikeda genotype. The next most closely related branch is composed of *T. orientalis* Chitose genotype and then *T. orientalis* Buffeli genotype. The outgroup is composed of a single reference sequence each for *T. parva* and *T. annulata*. Small subunit rDNA sequences for I4 and AI1 were of low quality (6.4% and 3.9%, respectively). Numbers along branches are bootstrap values. Scale bar indicates nucleotide substitutions per site.

similar live cattle trade introduced this genotype to the United States. Another possibility is transstadial transmission of *H. longicornis* ticks accidentally brought into the United States on other animals in shipments. Other genotypes of *T. orientalis* have been identified in the United States (14,17,18), suggesting that there were previous introductions. Regardless, now that both the tick and the hemoprotezoan are established in this region, *H. longicornis* ticks will probably play a role in continued transmission of the parasite, and *Theileria*-associated bovine infectious anemia will likely continue to occur within the area. A study modeling the most likely suitable habitats of the Asian longhorned tick throughout North America predicts that the tick will thrive along the eastern United States seaboard from Maine to North Carolina, along the western United States seaboard from Washington to northern California, and from northern Louisiana northward into Wisconsin and Ohio (25). With such a broad range, we predict *T. orientalis* Ikeda will become established in multiple states throughout the country.

Acknowledgments

We thank the farmers, producers, and veterinarians who have dedicated their time and effort to this study, often at

their own inconvenience; in particular, Bruce Bowman, Brendan Martin, and Melinda McCall, who actively pursued this investigation.

About the Author

Dr. Oakes is a third-year resident in veterinary anatomic pathology and a second-year PhD student at the Virginia–Maryland College of Veterinary Medicine. Her research interests include infectious disease (particularly zoonoses), molecular diagnostics, and bioinformatics.

References

1. Watts JG, Playford MC, Hickey KL. *Theileria orientalis*: a review. *N Z Vet J*. 2016;64:3–9. <https://doi.org/10.1080/00480169.2015.1064792>
2. Gubbels MJ, Hong Y, van der Weide M, Qi B, Nijman IJ, Guangyuan L, et al. Molecular characterisation of the *Theileria buffeli/orientalis* group. *Int J Parasitol*. 2000;30:943–52. [https://doi.org/10.1016/S0020-7519\(00\)00074-6](https://doi.org/10.1016/S0020-7519(00)00074-6)
3. Bogema DR, Micalef ML, Liu M, Padula MP, Djordjevic SP, Darling AE, et al. Analysis of *Theileria orientalis* draft genome sequences reveals potential species-level divergence of the Ikeda, Chitose and Buffeli genotypes. *BMC Genomics*. 2018;19:298. <https://doi.org/10.1186/s12864-018-4701-2>

4. Sivakumar T, Hayashida K, Sugimoto C, Yokoyama N. Evolution and genetic diversity of *Theileria*. *Infect Genet Evol*. 2014;27:250–63. <https://doi.org/10.1016/j.meegid.2014.07.013>
5. Yam J, Bogema DR, Jenkins C. Oriental theileriosis. *Ticks and Tick-Borne Pathogens*. 2018;1–31 [cited 2019 Jun 3]. <https://www.intechopen.com/books/ticks-and-tick-borne-pathogens/oriental-theileriosis>
6. Heath A. Biology, ecology and distribution of the tick, *Haemaphysalis longicornis* Neumann (Acari: Ixodidae) in New Zealand. *N Z Vet J*. 2016;64:10–20. <https://doi.org/10.1080/00480169.2015.1035769>
7. McFadden AM, Vink D, Pulford DJ, Lawrence K, Gias E, Heath AC, et al. Monitoring an epidemic of *Theileria*-associated bovine anaemia (Ikeda) in cattle herds in New Zealand. *Prev Vet Med*. 2016;125:31–7. <https://doi.org/10.1016/j.prevetmed.2015.11.005>
8. Jenkins C. Bovine theileriosis: Molecular diagnosis and strain analyses. Meat and Livestock Australia Limited; 2017 Mar 16;1–111 [cited 2019 Jun 5]. <https://www.mla.com.au/research-and-development/search-rd-reports/final-report-details/Animal-Health-and-Biosecurity/Bovine-theileriosis-Molecular-diagnosis-and-strain-analyses/3252>
9. Theileria Working Group. *Theileria* veterinary handbook 2; 2015. Wellington (New Zealand): Ministry for Primary Industries; 2015. p. 1–32 [cited 2019 Jun 3]. <https://www.mpi.govt.nz/dmsdocument/9518-theileria-veterinary-handbook-2-august-2015>
10. Lawrence KE, Lawrence BL, Kickson RE, Hewitt CA, Gedye K, Fermin LM, et al. Associations between *Theileria orientalis* Ikeda type infection and the growth rates and haematocrit of suckled beef calves in the North Island of New Zealand. *N Z Vet J*. 2018;67:66–73. <https://doi.org/10.1080/00480169.2018.1547227>
11. Kamau J, de Vos AJ, Playford M, Salim B, Kinyanjui P, Sugimoto C. Emergence of new types of *Theileria orientalis* in Australian cattle and possible cause of theileriosis outbreaks. *Parasit Vectors*. 2011;4:22. <https://doi.org/10.1186/1756-3305-4-22>
12. Lawrence KE, Sanson RL, McFadden AMJ, Pulford DJ, Pomroy WE. The effect of month, farm type and latitude on the level of anaemia associated with *Theileria orientalis* Ikeda type infection in New Zealand cattle naturally infected at pasture. *Res Vet Sci*. 2018;117:233–8. <https://doi.org/10.1016/j.rvsc.2017.12.021>
13. Rainey T, Occi JL, Robbins RG, Egizi A. Discovery of *Haemaphysalis longicornis* (Ixodida: Ixodidae) parasitizing a sheep in New Jersey, United States. *J Med Entomol*. 2018;55:757–9. <https://doi.org/10.1093/jme/tjy006>
14. Animal Plant and Health Inspection Service. Longhorned tick: information for livestock and pet owners. USDA. 2019 May [cited 2019 Jun 3]. https://www.aphis.usda.gov/publications/animal_health/fs-longhorned-tick.pdf
15. Beard CB, Occi J, Bonilla DL, Egizi AM, Fonseca DM, Mertins JW, et al. Multistate infestation with the exotic disease-vector tick *Haemaphysalis longicornis*—United States, August 2017–September 2018. *MMWR Morb Mortal Wkly Rep*. 2018;67:1310–3. <https://doi.org/10.15585/mmwr.mm6747a3>
16. Chen Z, Yang X, Bu F, Yang X, Liu J. Morphological, biological and molecular characteristics of bisexual and parthenogenetic *Haemaphysalis longicornis*. *Vet Parasitol*. 2012;189:344–52. <https://doi.org/10.1016/j.vetpar.2012.04.021>
17. Cossio-Bayugar R, Pillars R, Schlater J, Holman PJ. *Theileria buffeli* infection of a Michigan cow confirmed by small subunit ribosomal RNA gene analysis. *Vet Parasitol*. 2002;105:105–10. [https://doi.org/10.1016/S0304-4017\(02\)00003-1](https://doi.org/10.1016/S0304-4017(02)00003-1)
18. Stockham SL, Kjemtrup AM, Conrad PA, Schmidt DA, Scott MA, Robinson TW, et al. Theileriosis in a Missouri beef herd caused by *Theileria buffeli*: case report, herd investigation, ultrastructure, phylogenetic analysis, and experimental transmission. *Vet Pathol*. 2000;37:11–21. <https://doi.org/10.1354/vp.37-1-11>
19. Kubota S, Sugimoto C, Kakuda T, Onuma M. Analysis of immunodominant piroplasm surface antigen alleles in mixed populations of *Theileria sergenti* and *T. buffeli*. *Int J Parasitol*. 1996;26:741–7. [https://doi.org/10.1016/0020-7519\(96\)00047-1](https://doi.org/10.1016/0020-7519(96)00047-1)
20. Kamau J, Salim B, Yokoyama N, Kinyanjui P, Sugimoto C. Rapid discrimination and quantification of *Theileria orientalis* types using ribosomal DNA internal transcribed spacers. *Infect Genet Evol*. 2011;11:407–14. <https://doi.org/10.1016/j.meegid.2010.11.016>
21. Carelli G, Decaro N, Lorusso A, Elia G, Lorusso E, Mari V, et al. Detection and quantification of *Anaplasma marginale* DNA in blood samples of cattle by real-time PCR. *Vet Microbiol*. 2007;124:107–14. <https://doi.org/10.1016/j.vetmic.2007.03.022>
22. Kakuda T, Shiki M, Kubota S, Sugimoto C, Brown WC, Kosum C, et al. Phylogeny of benign *Theileria* species from cattle in Thailand, China and the U.S.A. based on the major piroplasm surface protein and small subunit ribosomal RNA genes. *Int J Parasitol*. 1998;28:1261–7. [https://doi.org/10.1016/S0020-7519\(98\)00113-1](https://doi.org/10.1016/S0020-7519(98)00113-1)
23. USDA National Agriculture Statistics Service. Cattle county estimates—January 1, 2017 [cited 2019 Mar 24]. https://www.nass.usda.gov/Statistics_by_State/Virginia/Publications/County_Estimates/Cattle17_VA.pdf
24. Wagyu International. History of Wagyu exports from Japan; 2013 [cited 2010 Mar 25]. http://www.wagyuinternational.com/global_USA.php
25. Rochlin I. Modeling the Asian longhorned tick (Acari: Ixodidae) suitable habitat in North America. *J Med Entomol*. 2019;56:384–91. <https://doi.org/10.1093/jme/tjy210>

Address for correspondence: Kevin K. Lahmers, Department of Biomedical Sciences and Pathobiology, Virginia–Maryland College of Veterinary Medicine, 205 Duck Pond Dr, Blacksburg, VA 24060, USA; email: klahmers@vt.edu

Genetic Characterization and Enhanced Surveillance of Ceftriaxone-Resistant *Neisseria gonorrhoeae* Strain, Alberta, Canada, 2018

Byron M. Berenger, Walter Demczuk, Jennifer Gratrix, Kanti Pabbaraju, Petra Smyczek, Irene Martin

In July 2018, a case of *Neisseria gonorrhoeae* associated with ceftriaxone treatment failure was identified in Alberta, Canada. We identified the isolate and nucleic acid amplification testing (NAAT) specimen as the ceftriaxone-resistant strain multilocus sequence type 1903/NG-MAST 3435/NG-STAR 233, originally identified in Japan (FC428), with the same *penA* 60.001 mosaic allele and genetic resistance determinants. Core single-nucleotide variant (SNV) analysis identified 13 SNVs between this isolate and FC428. Culture-independent surveillance by PCR for the A311V mutation in the *penA* allele and *N. gonorrhoeae* multiantigen sequence typing directly from NAAT transport media positive for *N. gonorrhoeae* by NAAT did not detect spread of the strain. We identified multiple sequence types not previously detected in Alberta by routine surveillance. This case demonstrates the benefit of using culture-independent methods to enhance detection, public health investigations, and surveillance to address this global threat.

As incidence of *Neisseria gonorrhoeae* infection increases worldwide (1–3), sporadic cases of the ceftriaxone-resistant multilocus sequence type (MLST) 1903 (original isolate FC428 identified in Japan) continue to be detected (4). The emergence of extended-spectrum cephalosporin-resistant (ESCR) strains threatens the ability to treat and control the increasing number of *N. gonorrhoeae* infections.

Nucleic acid amplification tests (NAAT) are the preferred method used for diagnosis of *N. gonorrhoeae* infection because they have advantages over culture-based methods, such as enhanced sensitivity (5) and rapid

turnaround time, and they can be automated. Because of the widespread use of NAAT, culture has been typically restricted to specific screening programs (e.g., sexually transmitted infection [STI] clinics), in cases of treatment failure, or for high-risk patients (6). In 2016 in Canada, ≈80% of the reported *N. gonorrhoeae* cases were diagnosed using NAAT (7). Historically, genomic typing and susceptibility testing required bacterial culture. Although culture is still the standard to determine antimicrobial susceptibilities, sequence typing can be performed independently from culture directly from NAAT transport media (8). Palmer et al. (9) have shown that antimicrobial resistance in *N. gonorrhoeae* is usually uniform within a given sequence type and the susceptibility pattern can be predicted for sequence types with known phenotypic susceptibilities. Genetic antimicrobial resistance markers can also be detected directly from specimens collected in NAAT transport media, including the *penA* (penicillin-binding protein 2) 60.001 allele associated with ESCR in MLST1903 (10).

In January 2017, a ceftriaxone-resistant *N. gonorrhoeae* strain (MIC 1 mg/L) was identified in Quebec (11), isolated from a 23-year-old woman whose partner had reported sexual contact during travel to China and Thailand during fall 2016. She was successfully treated with combination therapy of cefixime (800 mg orally) and azithromycin (1 g orally), followed by azithromycin (2 g orally) 13 days later.

In July 2018, a second case of ceftriaxone-resistant *N. gonorrhoeae* infection causing urethritis was detected in Canada in the province of Alberta; the male patient probably acquired it through an anonymous sexual encounter in Alberta with a visitor from Taiwan or mainland China (12). Current *N. gonorrhoeae* culture protocols only capture a small portion of the *N. gonorrhoeae*-infected population and, as with the Alberta case, there can be a delay of

Author affiliations: University of Calgary, Calgary, Alberta, Canada (B. Berenger); Alberta Public Laboratories, Calgary (B. Berenger, K. Pabbaraju); Public Health Agency of Canada, Winnipeg, Manitoba, Canada (W. Demczuk, I. Martin); Alberta Health Services, Edmonton, Alberta (J. Gratrix, P. Smyczek)

DOI: <https://doi.org/10.3201/eid2509.190407>

months from initial sexual encounter to NAAT diagnosis and the determination of ESCR by culture. In the Alberta case, the infection probably occurred sometime during December 2017–February 2018; no sexual encounters were reported afterward. The *N. gonorrhoeae* infection was diagnosed by NAAT on a urethral swab in May; the patient was treated with ceftriaxone (250 mg intramuscularly) and azithromycin (1 g orally). His urethritis recurred; he tested positive by NAAT again on a urethral swab and urine in June and was referred to the STI clinic. He sought care at the clinic in July and the initial treatment of ceftriaxone and azithromycin was repeated. Upon notification of the ESCR urethral-swab isolate, STI services treated him with gentamicin (240 mg intramuscularly) and azithromycin (2 g orally). Urethral swab culture and urine NAAT taken 4 weeks later tested negative.

This study had 2 aims. The first was to describe the microbiological investigation into this case at the local, provincial, and national levels using phenotypic antimicrobial susceptibility testing and nucleic acid–based antibiotic susceptibility determination, as well as genetic typing of the June 2018 NAAT specimen and the July 2018 Alberta isolate (designated 51742). Because anonymous sexual encounters made traditional contact investigation impossible and diagnosis was delayed, it was possible that this ceftriaxone-resistant strain had spread within Alberta. The second aim was to determine any further dissemination of the strain by expanding sequence typing and testing for the same *penA* allele using NAAT transport media specimens from clients tested in the same geographic area shortly after the case was detected.

Methods

Detection of *N. gonorrhoeae* and Phenotypic Antimicrobial Susceptibility Determination

NAAT-based diagnosis of *N. gonorrhoeae* infection was performed using the Aptima Combo 2 nucleic acid amplification test kit (Hologic Inc., <https://www.hologic.com>) for *N. gonorrhoeae* and *Chlamydia trachomatis* at Calgary Laboratory Services, Calgary, Alberta. The province of Alberta (population 4.25 million) is divided into 5 health zones (North, Edmonton, Central, Calgary, and South); Calgary Laboratory Services performs all NAAT for *N. gonorrhoeae* and *C. trachomatis* for the Calgary Zone (population 1.6 million) and South Zone (population 0.3 million) (13).

N. gonorrhoeae was cultured at the Alberta Provincial Laboratory for Public Health (ProvLab) from a specimen planted onto Thayer-Martin agar with antibiotics at the time of collection at the Calgary STI clinic. Agar plates were prepared in-house with GC agar base (BD Difco;

Becton-Dickinson, <https://www.bd.com>). Susceptibility testing was conducted in accordance with Clinical and Laboratory Standards Institute (CLSI) M100 guidelines (14). Antimicrobial susceptibility was tested by gradient diffusion at ProvLab using Etest (BioMérieux, <https://www.biomerieux.com>), except for ertapenem, which was tested with Liofilchem (<https://www.liofilchem.com>) at the National Microbiology Laboratory (NML), Public Health Agency of Canada. Agar dilution was performed at the NML in accordance with CLSI M100 (14) for azithromycin, cefixime, ceftriaxone, erythromycin, penicillin, spectinomycin, tetracycline (Sigma-Aldrich, <https://www.sigmaaldrich.com>), ciprofloxacin (Bayer Healthcare, <https://www.bayer.com>), ertapenem (Sequoia Research, www.seqchem.com), and gentamicin (MP Biomedical, <https://www.mpbio.com>). Ertapenem gradient diffusion and agar dilution were done using growth supplement without cysteine. We analyzed β -lactamase production using nitrocefin (Oxoid Canada, <http://www.oxoid.com>).

MIC interpretations were based on CLSI M100 2019 guidelines (15) except for erythromycin (resistant ≥ 2 mg/L) (16), ertapenem (nonsusceptible ≥ 0.064 mg/L) (17), and gentamicin (resistant ≥ 32 mg/L) (18,19). *N. gonorrhoeae* reference cultures used as controls were ATCC49226, WHO-F, WHO-G, WHO-K, and WHO-P/WHO-U.

Whole-Genome Sequencing of *N. gonorrhoeae* Isolate

Genomic analyses were conducted at the NML as previously described (4). *N. gonorrhoeae* culture was extracted by standard protocols using Lucigen MasterPure Complete DNA and RNA Extraction Kit (Mandel Scientific, <http://www.mandel.ca>). Multiplexed libraries were created with Nextera XT specimen preparation kits (Illumina, <https://www.illumina.com>). Paired-end, 300-bp indexed reads generated on the Illumina MiSeq platform yielded 567,231 reads/genome and average genome coverage of 84 \times . Reads were merged using FLASH (20) and assembled with SPAdes (21), yielding an average contig length of 7,081 bp; the average N50 contig length was 39,185 bp. We submitted raw whole-genome sequence (WGS) read data to the National Center for Biotechnology Information under BioProject no. PRJNA526031. We created a core single-nucleotide variation (SNV) phylogeny by mapping reads to FA1090 (GenBank accession no. NC_002946.2) using a custom Galaxy SNVPhyl workflow (22). We used a meta-alignment of informative core SNV positions to create a maximum-likelihood phylogenetic tree for the strains 51742, A7536, A7846, FC428, FC460, and 47707, as well as the ceftriaxone-resistant strains that the World Health Organization named as a reference panel: H041 (WHO-X), F89 (WHO-Y), and A8806 (WHO-Z) (23). We excluded variant calls within potential problematic regions,

including repetitive regions, using MUMmer version 3.23 (<http://mummer.sourceforge.net>) with a minimum length of repeat region set to 150 and the minimum percent identity of repeat region set to 90%. We removed highly recombinant regions with >2 SNVs per 500 nt from the analysis (20). The percentage of valid and included positions in the core genome was 97.3%; 571 sites were used to generate the phylogeny. We generated the phylogenetic tree using FigTree version 1.4 (<http://tree.bio.ed.ac.uk/software/figtree>) (Figure).

We determined DNA sequences for *N. gonorrhoeae* multiantigen sequence typing (NG-MAST) (24), multilocus sequence typing (25), and *N. gonorrhoeae* sequence typing for antimicrobial resistance (NG-STAR) (26) in silico from WGS data and allocated sequence types using NG-MAST (<http://www.ng-mast.net>), *Neisseria* multilocus sequence typing (<http://pubmlst.org/neisseria>), and NG-STAR (<https://ngstar.canada.ca>) schemes. We determined NG-MAST of the Alberta isolate at ProvLab in accordance with Allen et al. (27).

Genotyping of NAAT Specimen Collected from the Case with Treatment Failure

We referred the NAAT specimen collected in June 2018 to the NML, where DNA extraction, preparation, real-time PCR, NG-MAST, and analysis of results were performed as previously described (28,29). The NG-MAST protocol was performed with the following modifications: a nested PCR for both *porB* and *tbpB*, with *porB* using primers porF1 (5'-CAATGAAAAAATCCCTGATTG-3') and porR1 (TTTGAGATTAGAATTTGTGG) for the first step and primers porF2 (CTGATTGCCCTGACTTTGGCAG) and porR2 (AGAAGTGCCTTTGGAGAAGTCG) for the second step; and nested PCR for *tbpB* using primers tbpBF1 (AGGAATTGGTTTTCCGCTTT) and tbpBR1 (CG-GTTTTCGCCATACCTTTA) for the first step, and *tbpB* primers by Martin et al. (24) for the second step. We evaluated SNV targets associated with ceftriaxone-resistant *penA* mutation (A311V), cephalosporin-decreased susceptibility (*ponA* L421P, *mtrR* 35delA, *porB* G120/A121, and *penA* mosaic allele), ciprofloxacin resistance (*gyrA* S91,

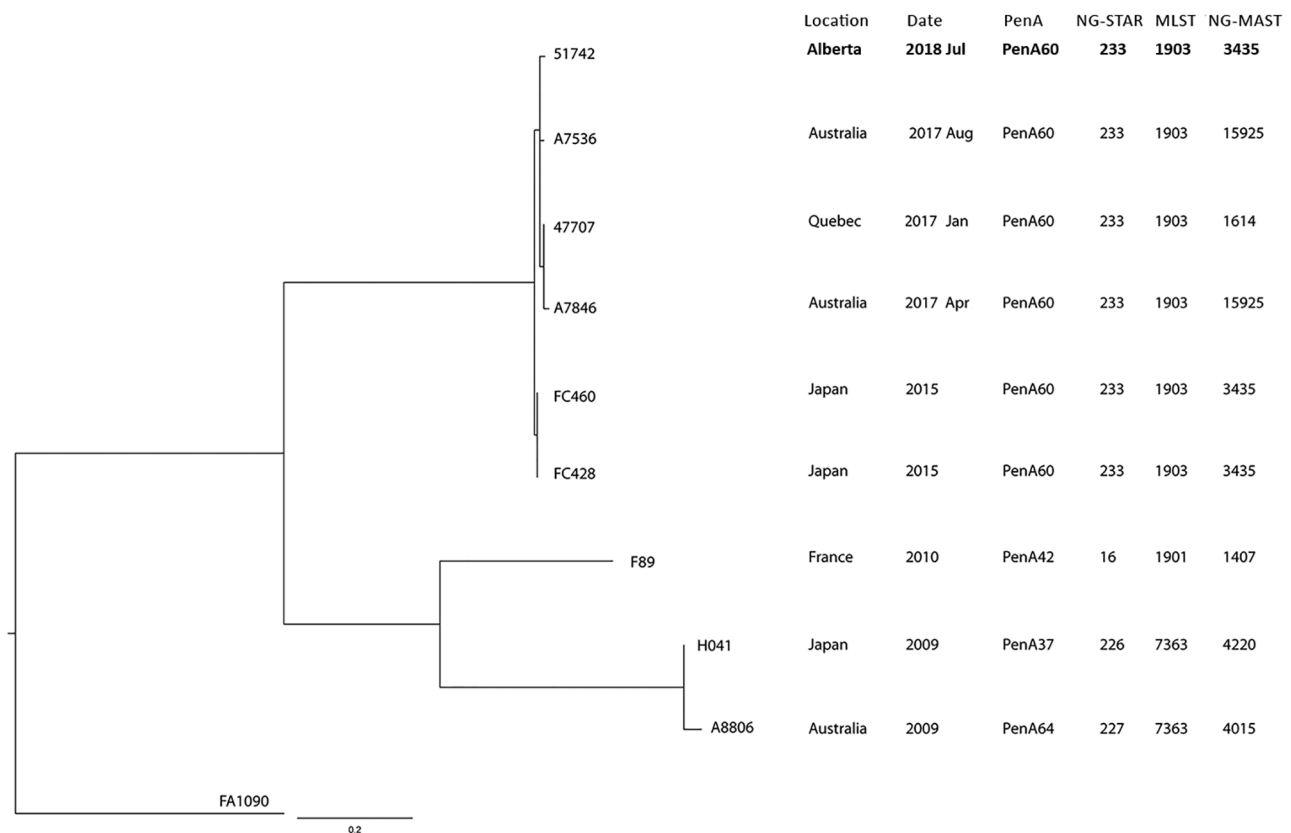


Figure. Core single-nucleotide variant (SNV) phylogenetic tree of ceftriaxone-resistant *Neisseria gonorrhoeae* identified from enhanced surveillance in Alberta, Canada (bold), and reference isolates. The maximum-likelihood phylogenetic tree is rooted on the reference genome of *N. gonorrhoeae* FA1090 (GenBank accession no. NC_002946.2). Scale bar represents the estimated evolutionary divergence between isolates on the basis of average genetic distance between strains (estimated number of substitutions in the sample/total number of high-quality SNVs). Strains F89 (WHO-Y), A8806 (WHO-Z), and H041 (WHO-X), A7536, 47707, A7846, FC460, and FC428 are previously reported ceftriaxone-resistant reference strains (4). MLST, multilocus sequence typing; NG-MAST, *N. gonorrhoeae* multiantigen sequence typing; NG-STAR, *N. gonorrhoeae* sequence typing for antimicrobial resistance.

D95, and *parC* D86/S87/S88), and azithromycin resistance (23S rRNA A2059G, C2611T) (10,28,29).

Enhanced Surveillance of Additional NAAT Specimens

In Alberta, routine *N. gonorrhoeae* antimicrobial resistance surveillance involves sequence typing of all resistant and susceptible isolates cultured within the first 15 days of each month, collected primarily from the 3 provincial STI clinics located in Calgary (population 1.24 million), Edmonton (population 0.93 million), and Fort McMurray (population 66,653) (30). Because of increased rates of gonorrhea and nonavailability of cultures, all NAAT specimens from the North Zone (population 0.48 million) are typed by NG-MAST sequence typing. For further information refer to the publication by Gratrix et al. (31) and the Alberta Health Zone map (13).

We conducted NG-MAST sequence typing and testing for the *penA* A311V mutation as above from remnant clinical NAAT specimens collected during August 1–September 15, 2018, from the Calgary and South Zones in southern Alberta by the NML. Specimens collected before these dates were not tested; they were discarded in accordance with routine laboratory protocols.

Results

Antimicrobial susceptibility by gradient diffusion at ProvLab detected an isolate resistant to ceftriaxone, cefixime, and penicillin, which was confirmed by agar dilution at the NML (Table 1). Overall, we found categorical agreement between the 2 methods, except for tetracycline, which was intermediate by gradient diffusion but resistant by agar dilution. Gentamicin was not tested by Etest due to unacceptable MIC essential agreement (<90%) compared to the

agar dilution reference method (T.C. Dingle and P. Naidu, Alberta Public Laboratories, pers. comm., email, 2019 Mar 11), but the isolate was susceptible by agar dilution. Genetic resistance marker testing correlated with susceptibility phenotypes (Table 1). No specific genetic determinants of ertapenem susceptibility or nonsusceptibility have been established, but there may be overlap with mechanisms of resistance for other β -lactams (32). The isolate tested negative for β -lactamase production.

Within 2 days of the isolate being identified as ESCR, sequencing of *porB* and *thpB* at the ProvLab revealed that the isolate was NG-MAST 3435, the same sequence type as the FC428 isolate from Japan isolated in 2015 (33). The isolate also had the same *penA* mutations as FC 428 (A311V and T483S), providing genetic confirmation of the phenotypic resistance results. Sequence typing at NML confirmed the findings at the ProvLab and further characterized the isolate as MLST1903, NG-STAR 233, and *penA* mosaic 60.001, which were the same as other ESCR MLST1903 (4). WGS revealed that the isolate had ≤ 13 SNV differences from other ESCR MLST1903 isolates (Figure). The isolate was most closely related to A7536 from Australia (7 SNV) and distantly related (about 300 SNV) to other ceftriaxone-resistant isolates (France 2010 F89, Australia 2009 A8806, and Japan 2009 H041) (Figure).

In addition to the *penA* mutations, resistance determinants found in other ESCR MLST1903 isolates and ESCR MLST1901, including a –35A deletion in the *mtrR* promoter, the *porB* mutations G120K and A121D, *ponA* L421P, *gyrA* S91F, *gyrA* D95A, and *parC* S87R, were also found in the Alberta isolate (4,34,35). We detected these resistant determinants, along with *penA* A311V, by direct testing of the Alberta June 2018 NAAT specimen.

Table 1. Phenotypic and genetic antibiotic susceptibility testing for ceftriaxone-resistant *Neisseria gonorrhoeae* isolate, Alberta, Canada, 2018*

Antimicrobial drug	Etest MIC, $\mu\text{g}/\text{mL}$	Agar dilution, $\mu\text{g}/\text{mL}$	Interpretation	Genetic markers/mutations identified in genome: result
Ceftriaxone	0.5–1	0.5	R	<i>penA</i> : mosaic 60.001, A311V, T483S; <i>mtrR</i> promoter: –35A deletion; <i>mtrR</i> : wild types for A39 and G45; <i>porB</i> : G120K, A121D; <i>porB</i> structure: <i>porB</i> 1b; <i>ponA</i> : L421P
Cefixime	2	2	R	
Penicillin	4	2	R	
Ertapenem	0.064	0.125	NS	
Azithromycin	0.5–1	0.25	S	23S rRNA A2059G and C2611T: absent; <i>ermB</i> : negative; <i>ermC</i> : negative; <i>mtrR</i> promoter: –35A deletion; <i>mtrR</i> : wild types for A39 and G45
Ciprofloxacin	≥ 32	32	R	<i>gyrA</i> : S91F and D95A; <i>parC</i> : D86, S87R, and wild type S88
Tetracycline	1	2	R†	<i>rpsJ</i> : <i>rpsJ</i> _3 (V57M); <i>tetM</i> : negative; <i>mtrR</i> promoter: –35A deletion; <i>mtrR</i> : wild types for A39 and G45
Gentamicin	ND	8	S	Genetic resistance determinants not determined
Spectinomycin	ND	16	S	
Moxifloxacin	4	ND	NA	

*Interpretations based on agar dilution. NA, breakpoint not available; ND, not done; NS, nonsusceptible; R, resistant; S, susceptible.

†Tetracycline resistance would be intermediate on the basis of Etest MIC.

Of the 3,677 NAAT specimens tested from Calgary and South Zones during August 1–September 15, 2018, a total of 254 (from 215 cases) were positive for *N. gonorrhoeae* and 232 (from 194 cases) could be located for sequence typing (by NG-MAST) and screening for the *penA* A311V mutation. Of the 232 positive specimens, 95 (41.0%) were collected from urine, 57 (24.6%) from the pharynx, 32 (13.7%) from the vagina, 29 (12.5%) from the rectum, 11 (4.7%) from the cervix, and 8 (3.5%) from the urethra. All specimens tested negative for the *penA* A311V mutation. We were able to determine the ST from 173 specimens (74.6% of specimens) each representing 1 case (89% of cases): 90 urine, 28 vaginal, 24 rectal, 14 pharyngeal, 9 cervical, and 8 urethral specimens. Of the 232 positive specimens, 59 (25.4%) were nontypeable because of either poor sequence quality or no amplicon for one or both targets; 8 had a *porB* sequence only and 38 *tbpB* only. Among the 173 specimens sequence typed, we detected 53 different NG-MAST; the most prevalent STs (>10 specimens) were ST8890 (34; 19.7%), ST5441 (17; 9.8%), and ST16065 (12; 6.9%) (Table 2). We did not detect

NG-MAST-3435 in these specimens or in any other specimen or isolate typed as a part of routine testing in Alberta as of June 30, 2019. We did not have culture data available for 30 sequence types (56.6%) to predict susceptibility.

The enhanced surveillance during August 1–September 15, 2018, resulted in successful sequence typing of 89% of 215 cases in the Calgary and South Zones and 42.5% of 703 cases in all Alberta health zones. In comparison, the sequence typing success rate for December 1, 2017–July 31, 2018, was 18.5% (139/748) of *N. gonorrhoeae* infection cases in Calgary and South Zones and 18.5% (566/2,807) of cases in all of Alberta.

Of the 194 cases included in the enhanced surveillance specimens, 22 (11.3%) also had a culture-positive isolate with a sequence type identified through routine surveillance. In 11/22 cases, the ST from the NAAT matched the isolate. In 10 of 26 NAAT specimens from the 22 cases with an isolate available, the NAAT ST was nontypeable, and in 1 case, the ST isolate and NAAT (both collected on the same day from the same pharynx sample) differed by 1 nucleotide, indicating that the infecting strain had mutated.

Table 2. Test results and antimicrobial resistance pattern predictions of sequence types identified from enhanced surveillance of *Neisseria gonorrhoeae* samples, Alberta, Canada*

Sequence type by NG-MAST	No. specimens (% of all specimens), n = 232†	No. cases, n = 194†	Antimicrobial resistance pattern prediction‡	No. specimens with specified AMR/no. cultures identified with ST§
Nontypeable	59 (25.4)	35	NA	
ST8890	34 (14.7)	33	TetR	43/45
ST5441	17 (7.3)	17	Susceptible	66/79
ST16065	12 (5.2)	9	CipR/TetR	63/63
ST14788	7 (3.0)	6	Susceptible	21/26
ST5985	7 (3.0)	7	TRNG	649/730
ST11086	6 (2.6)	5	CipR/EryR/PenR/TetR	30/30
ST12302	6 (2.6)	6	CipR/EryR/TetR/often AziR	1,198/1,211 (CipR/EryR/TetR); 687/1,211 (are also AziR)
ST4637	6 (2.6)	5	Susceptible	17/20
ST8288	6 (2.6)	6	Penicillinase-producing/CipR	12/14
ST1387§	4 (1.7)	4	No culture available	0
ST16288	4 (1.7)	4	CipR/EryR	26/26
ST16972	4 (1.7)	4	Susceptible	4/5
ST17029	4 (1.7)	4	No culture available	0
ST18135	4 (1.7)	2	No culture available	0
ST4186	4 (1.7)	4	Susceptible	4/4
ST11461	3 (1.3)	3	TRNG	161/166
ST13489	3 (1.3)	3	Susceptible	1/1
ST16211	3 (1.3)	2	EryR/TetR	2/2
ST14698	2 (0.86)	2	AziR/CipR/EryR/TetR	142/208
ST16825§	2 (0.86)	1	No culture available	0
ST18126§	2 (0.86)	2	No culture available	0
ST18154	2 (0.86)	2	No culture available	0

**N. gonorrhoeae* infection was diagnosed by the Aptima Combo 2 nucleic acid amplification test kit (Hologic Inc., <https://www.hologic.com>). AziR, azithromycin resistant; CipR, ciprofloxacin resistant; EryR, erythromycin resistant; NG-MAST, *N. gonorrhoeae* multiantigen sequence typing; ST, sequence type; TetR, tetracycline-resistant; TRNG, TetR *N. gonorrhoeae* (high-level plasmid mediated).

†Sequence types detected in only 1 specimen and resistance patterns (if known) are as follows and represent individual cases unless noted as an additional site: ST10451 (PenR/CipR/EryR/TetR); ST11691 (CipR/EryR/TetR and half are AziR); ST11933 (susceptible or TetR); ST-16161 (TetR); ST16595 (TRNG); ST18146; ST18156; ST3935 (EryR/TetR, sometimes PenR); ST9120. Sequence types detected in only 1 specimen that had not previously been detected in Alberta are ST14797; ST17196; ST18057; ST18134; ST18136; ST18137; ST18138; ST18155 (additional site); ST18157; ST18158; ST18159; ST18160; ST18161; ST18162; ST18340 (additional site); ST18341; ST18342; ST18343; ST18344; ST18345 (additional site); ST5308 (XDR: AzR/CeDS/CipR/PenR/TetR/EryR); ST6339.

‡Based on data from the Canadian national gonococcal collection, which included 7,498 gonococcal cultures with sequence typing and phenotypic susceptibility results collected during 2016–2018.

§Sequence type had not been previously detected in Alberta.

Twenty-three cases had multiple sites of infection, and 6 of these had distinct strains at each site, determined by either different STs ($n = 3$) or *porB* ($n = 2$) or *tbpB* ($n = 1$) alleles. We found no evidence of mixed infections at the same site.

The additional surveillance of NAAT specimens in the Calgary and South Zones for 1.5 months identified 26 new NG-MAST for Alberta. Most of these new ST ($n = 24$, 92.3%) represented individual cases. ST1387 was new to Alberta with 4 cases and ST18126 with 2 cases (Table 2).

Discussion

Continued detection and control of ESCR globally requires rapid detection of cases, coordinated public health interventions, and enhanced surveillance for antimicrobial resistance. Critical to the detection and prevention of further cases from the laboratory standpoint is the maintenance of culture and susceptibility testing along with rapid molecular confirmation of resistance and determination of sequence type. Because diagnosis of *N. gonorrhoeae* infections by NAAT is far more widespread than by culture, NAAT specimens can be used to detect ESCR in the population by culture-independent methods. The detection of the second case of ceftriaxone resistance in Canada highlights the use of these methods to facilitate public health investigation in a timely manner. Our findings show that current surveillance activities fail to conduct sequence typing in 80% of cases. Laboratory detection must, of course, be accompanied by appropriate clinical case management and public health follow-up, including partner notification and test of cure for treatment of drug-resistant or treatment failure cases.

In the Alberta ESCR case, we could not exclude the possibility of further spread of the ESCR because of the patient's anonymous sexual encounters and the long delay in diagnosis. Alberta and other provinces in Canada currently rely on susceptibility testing in select populations (e.g., STI clinic patients) to detect *N. gonorrhoeae* resistance. This surveillance covers only 22% of the cases in Alberta (31); alternative approaches to susceptibility testing, such as screening for resistance markers and typing of NAAT specimens, are required for greater representation of the population.

Upon sequence typing specimens for 6 weeks after detection of the ESCR case, we found 26 STs that were previously not detected in Alberta. Although no ceftriaxone-resistant specimens were detected, 1 was identified as NG-MAST-5308, which had not been previously detected in Alberta and has been associated with multidrug resistance and decreased susceptibility to cephalosporins (I. Martin, unpub. data). ST5308 has been circulating in a neighboring province and, upon further investigation, we found that the case-patient was a resident of that province.

In line with World Health Organization recommendations (36), our study supported the value of enhanced culture-independent surveillance of NAAT specimens after detection of an ESCR isolate by sequence typing and PCR for resistance markers such as *penA* mutations. In our study, the ad hoc rapid population surveillance indicated that the strain was not circulating in our population by increasing the percentage of *N. gonorrhoeae* cases sequence typed in the Calgary and South Zones from 18.5% to 89%. The appropriate follow-up period for enhanced surveillance should take into account local baseline surveillance practices and the risk of transmission into the local population. Our risk assessment took into account the clinical and sexual history, number of sexual encounters, location of the sexual encounters, ability to reach case-contacts, and resource availability to run culture-independent surveillance. In our study, the risk for transmission was determined to be low based on the patient's sexual history, and we chose not to do any further enhanced surveillance.

Sequence typing and NAAT-based detection of genetic resistance determinants can act as a surrogate for culture (8,9); however, there are limitations. First, the susceptibility pattern of the sequence type needs to be known (only 44% were in our study), and the correlation between sequence type and susceptibility pattern needs to be well documented. The detection of genetic resistance markers by molecular techniques can also be challenging when multiple resistance markers can contribute to a single phenotype or the markers are unknown (as is the case with ertapenem [32]). Fortunately, in the case of NG-MAST 3435, the specific *penA* allele is known and the method for nucleic acid-based detection of this allele has been published (10). Advances in streamlining the methods for sequence typing and resistance marker detection from NAAT specimens are also needed because the current methods are labor intensive and costly. Of note, performing nucleic acid-based surveillance requires the availability of specimens. In our case, the laboratory stored positive specimens routinely for 1 month after collection, but upon detection of the ESCR case, this time was changed to 2 months. Longer storage times of positive samples would improve surveillance of NAAT specimens collected before an ESCR isolate is detected by culture. We were also able to get specimens easily, because CT/GC NAAT is centralized to 1 site in southern Alberta.

Additional phenotypic susceptibility testing of our isolate was challenging within the province because agar dilution was not available and published evaluations comparing the accuracy of gradient diffusion methods for alternate antibiotics, especially aminoglycosides, are lacking. In the absence of accurate susceptibility testing for gentamicin, STI services treated the Alberta case empirically based on Canada's STI guidelines. The previously unreported MIC of the Quebec 2017 isolate (47707) was determined by

agar dilution at NML to be 0.125 µg/mL; our results would indicate that NG-MAST 3435/MLST1903 isolates should be considered nonsusceptible to ertapenem. Ertapenem has also been used as a treatment option for an ESCR case in the United Kingdom (37), but most ESCR publications have not reported the MICs for ertapenem, other than the United Kingdom case (0.032 µg/mL; susceptible) (37) and a case in France (0.004 µg/mL; susceptible) for which only Etest results were reported (34). We recommend that future descriptions of ESCR include MICs for all antimicrobial drugs that are considered treatment options by both gradient diffusion and agar dilution.

To curtail the international spread of ESCR strains, proactive surveillance by molecular techniques may be necessary to detect cases, especially where culture is not available. Jurisdictions should also consider increasing the number of cases for which culture is available. Once a case is found, rapid molecular confirmation of ESCR strains to determine the possible origin and confirm the phenotypic results is imperative to aid public health authorities. Consideration of optimal surveillance strategies needs to be part of a global effort that encompasses continued international surveillance; open and complete data sharing; and enhancement of laboratory, treatment, and public health support to resource-limited areas of the world.

Acknowledgments

We thank all those who were involved in testing and identification of the isolate, including ProvLab and the NML laboratory staff, Prenilla Naidu, and Tanis Dingle. We thank Julie Carson, Jacqueline Lardeur, Barbara Violante, and other laboratory staff at Calgary Laboratory Services (now Alberta Public Laboratories) for identifying and arranging referral of NAAT specimens, and Calgary STI Clinic staff for the management of the case and case information.

This study was funded by internal Public Health Agency of Canada and Alberta ProvLab funds.

About the Author

Dr. Berenger is a physician with a specialization in medical microbiology who is a clinical assistant professor with the University of Calgary and consults for Alberta Public Laboratories microbiology services, including the ProvLab. His research interests include diagnostic microbiology relevant to public health.

References

- Centers for Disease Control and Prevention. Sexually transmitted disease surveillance 2017. Atlanta: The Centers; 2018.
- Choudhri Y, Miller J, Sandhu J, Leon A, Aho J. Gonorrhoea in Canada, 2010–2015. *Can Commun Dis Rep*. 2018;44:37–42. <https://doi.org/10.14745/ccdr.v44i02a01>
- European Centre for Disease Prevention and Control. Control. ECDC Annual epidemiological report for 2016. Stockholm: The Centre; 2018.
- Lahra MM, Martin I, Demczuk W, Jennison AV, Lee K-I, Nakayama S-I, et al. Cooperative recognition of internationally disseminated ceftriaxone-resistant *Neisseria gonorrhoeae* strain. *Emerg Infect Dis*. 2018;24:148. <https://doi.org/10.3201/eid2404.171873>
- Papp J, Schachter J, Gaydos C, Van Der Pol B. Recommendations for the laboratory-based detection of *Chlamydia trachomatis* and *Neisseria gonorrhoeae*—2014. *MMWR Recomm Rep* 2014;63(RR-02):1–19.
- Public Health Agency of Canada. Canadian guidelines on sexually transmitted infections. 2018 [cited 2019 Jul 3]. <https://www.canada.ca/en/public-health/services/infectious-diseases/sexual-health-sexually-transmitted-infections/canadian-guidelines.html>
- Martin I, Sawatzky P, Allen V, Lefebvre B, Hoang L, Naidu P, et al. Multidrug-resistant and extensively drug-resistant *Neisseria gonorrhoeae* in Canada, 2012–2016. *Can Commun Dis Rep*. 2019;45:45–53. <https://doi.org/10.14745/ccdr.v45i23a01>
- Peterson SW, Martin I, Demczuk W, Hoang L, Wylie J, Lefebvre B, et al. A comparison of real-time polymerase chain reaction assays for the detection of antimicrobial resistance markers and sequence typing from clinical nucleic acid amplification test samples and matched *Neisseria gonorrhoeae* culture. *Sex Transm Dis*. 2018;45:92–5. <https://doi.org/10.1097/OLQ.0000000000000707>
- Palmer HM, Young H, Graham C, Dave J. Prediction of antibiotic resistance using *Neisseria gonorrhoeae* multi-antigen sequence typing. *Sex Transm Infect*. 2008;84:280–4. <https://doi.org/10.1136/sti.2008.029694>
- Whiley DM, Mhango L, Jennison AV, Nimmo G, Lahra MM. Direct detection of *penA* gene associated with ceftriaxone-resistant *Neisseria gonorrhoeae* FC428 strain by using PCR. *Emerg Infect Dis*. 2018;24:1573–5. <https://doi.org/10.3201/eid2408.180295>
- Lefebvre B, Martin I, Demczuk W, Deshaies L, Michaud S, Labbé A-C, et al. Ceftriaxone-resistant *Neisseria gonorrhoeae*, Canada, 2017. *Emerg Infect Dis*. 2018;24:381–3. <https://doi.org/10.3201/eid2402.171756>
- Smyczek P, Berenger BM, Chu A. A case of an emerging international strain of multi-drug resistant *Neisseria gonorrhoeae* infection in a male with urethral discharge. *Can Fam Physician*. In press 2019.
- Alberta Health Services. AHS map and zone overview. 2017 [cited 2019 Feb 19]. <https://www.albertahealthservices.ca/assets/about/publications/ahs-ar-2017/zones.html>
- Clinical Laboratory Standards Institute (CLSI). Performance standards for antimicrobial susceptibility testing; twenty-eighth informational supplement. Wayne (PA): The Institute; 2018.
- Clinical Laboratory Standards Institute (CLSI). Performance standards for antimicrobial susceptibility testing; twenty-ninth informational supplement. Wayne (PA): The Institute; 2019.
- Ehret JM, Nims LJ, Judson FN. A clinical isolate of *Neisseria gonorrhoeae* with in vitro resistance to erythromycin and decreased susceptibility to azithromycin. *Sex Transm Dis*. 1996;23:270–2. <https://doi.org/10.1097/00007435-199607000-00004>
- Unemo M, Fasth O, Fredlund H, Limnios A, Tapsall J. Phenotypic and genetic characterization of the 2008 WHO *Neisseria gonorrhoeae* reference strain panel intended for global quality assurance and quality control of gonococcal antimicrobial resistance surveillance for public health purposes. *J Antimicrob Chemother*. 2009;63:1142–51. <https://doi.org/10.1093/jac/dkp098>
- Brown LB, Krysiak R, Kamanga G, Mapanje C, Kanyamula H, Banda B, et al. *Neisseria gonorrhoeae* antimicrobial susceptibility in Lilongwe, Malawi, 2007. *Sex Transm Dis*. 2010;37:169–72. <https://doi.org/10.1097/OLQ.0b013e3181bf575c>

19. Daly CC, Hoffman I, Hobbs M, Maida M, Zimba D, Davis R, et al. Development of an antimicrobial susceptibility surveillance system for *Neisseria gonorrhoeae* in Malawi: comparison of methods. *J Clin Microbiol*. 1997;35:2985–8.
20. Magoč T, Salzberg SL. FLASH: fast length adjustment of short reads to improve genome assemblies. *Bioinformatics*. 2011;27:2957–63. <https://doi.org/10.1093/bioinformatics/btr507>
21. Bankevich A, Nurk S, Antipov D, Gurevich AA, Dvorkin M, Kulikov AS, et al. SPAdes: a new genome assembly algorithm and its applications to single-cell sequencing. *J Comput Biol*. 2012;19:455–77. <https://doi.org/10.1089/cmb.2012.0021>
22. Petkau A, Mabon P, Sieffert C, Knox NC, Cabral J, Iskander M, et al. SNVPhyl: a single nucleotide variant phylogenomics pipeline for microbial genomic epidemiology. *Microb Genom*. 2017;3:e000116. <https://doi.org/10.1099/mgen.0.000116>
23. Unemo M, Golparian D, Sánchez-Busó L, Grad Y, Jacobsson S, Ohnishi M, et al. The novel 2016 WHO *Neisseria gonorrhoeae* reference strains for global quality assurance of laboratory investigations: phenotypic, genetic, and reference genome characterization. *J Antimicrob Chemother*. 2016;71:3096–108. <https://doi.org/10.1093/jac/dkw288>
24. Martin IMC, Ison CA, Aanensen DM, Fenton KA, Spratt BG. Rapid sequence-based identification of gonococcal transmission clusters in a large metropolitan area. *J Infect Dis*. 2004;189:1497–505. <https://doi.org/10.1086/383047>
25. Jolley KA, Maiden MCJ. BIGSdb: Scalable analysis of bacterial genome variation at the population level. *BMC Bioinformatics*. 2010;11:595. <https://doi.org/10.1186/1471-2105-11-595>
26. Demczuk W, Sidhu S, Unemo M, Whiley DM, Allen VG, Dillon JR, et al. *Neisseria gonorrhoeae* sequence typing for antimicrobial resistance, a novel antimicrobial resistance multilocus typing scheme for tracking global dissemination of *N. gonorrhoeae* strains. *J Clin Microbiol*. 2017;55:1454–68.
27. Allen VG, Farrell DJ, Rebbapragada A, Tan J, Tijet N, Perusini SJ, et al. Molecular analysis of antimicrobial resistance mechanisms in *Neisseria gonorrhoeae* isolates from Ontario, Canada. *Antimicrob Agents Chemother*. 2011;55:703–12. <https://doi.org/10.1128/AAC.00788-10>
28. Trembizki E, Buckley C, Donovan B, Chen M, Guy R, Kaldor J, et al. Direct real-time PCR-based detection of *Neisseria gonorrhoeae* 23S rRNA mutations associated with azithromycin resistance. *J Antimicrob Chemother*. 2015;70:3244–9.
29. Peterson SW, Martin I, Demczuk W, Bharat A, Hoang L, Wylie J, et al. Molecular assay for detection of genetic markers associated with decreased susceptibility to cephalosporins in *Neisseria gonorrhoeae*. Ledeboer NA, editor. *J Clin Microbiol*. 2015;53:2042–8.
30. Canada S. Census profile, 2016 census. Ottawa, ON, Canada. November 29, 2017 [cited 2019 Jul 12]. <https://www12.statcan.gc.ca/census-recensement/2016/dp-pd/prof/index.cfm>
31. Gratrix J, Kamruzzaman A, Martin I, Smyczek P, Read R, Bertholet L, et al. Surveillance for antimicrobial resistance in gonorrhoea: the Alberta model, 2012–2016. *Antibiotics (Basel)*. 2018;7:63. <https://doi.org/10.3390/antibiotics7030063>
32. Unemo M, Golparian D, Limnios A, Whiley D, Ohnishi M, Lahra MM, et al. In vitro activity of ertapenem versus ceftriaxone against *Neisseria gonorrhoeae* isolates with highly diverse ceftriaxone MIC values and effects of ceftriaxone resistance determinants: ertapenem for treatment of gonorrhoea? *Antimicrob Agents Chemother*. 2012;56:3603–9. <https://doi.org/10.1128/AAC.00326-12>
33. Nakayama S, Shimuta K, Furubayashi K, Kawahata T, Unemo M, Ohnishi M. New ceftriaxone- and multidrug-resistant *Neisseria gonorrhoeae* strain with a novel mosaic *penA* gene isolated in Japan. *Antimicrob Agents Chemother*. 2016;60:4339–41. <https://doi.org/10.1128/AAC.00504-16>
34. Poncin T, Fouere S, Braille A, Camelena F, Agsous M, Bebear C, et al. Multidrug-resistant *Neisseria gonorrhoeae* failing treatment with ceftriaxone and doxycycline in France, November 2017. *Euro Surveill*. 2018;23:e1002344. <https://doi.org/10.2807/1560-7917.ES.2018.23.21.1800264>
35. Chen S-C, Yin Y-P, Chen X-S. Cephalosporin-resistant *Neisseria gonorrhoeae* clone, China. *Emerg Infect Dis*. 2018;24:804–6. <https://doi.org/10.3201/eid2404.171817>
36. World Health Organization. Global action plan to control the spread and impact of antimicrobial resistance in *Neisseria gonorrhoeae*. 2012 [cited 2019 Jul 3]. www.who.int/reproductivehealth/publications/rtis/9789241503501
37. Eyre DW, Sanderson ND, Lord E, Regisford-Reimmer N, Chau K, Barker L, et al. Gonorrhoea treatment failure caused by a *Neisseria gonorrhoeae* strain with combined ceftriaxone and high-level azithromycin resistance, England, February 2018. *Euro Surveill*. 2018;23:364. <https://doi.org/10.2807/1560-7917.ES.2018.23.27.1800323>

Address for correspondence: Byron M. Berenger, Alberta ProvLab, 3030 Hospital Dr NW, Calgary, Alberta T2N 4W4, Canada; email: byron.berenger@albertapubliclabs.ca

Clonality of Fluconazole-Nonsusceptible *Candida tropicalis* in Bloodstream Infections, Taiwan, 2011–2017

Pao-Yu Chen, Yu-Chung Chuang, Un-In Wu, Hsin-Yun Sun, Jann-Tay Wang, Wang-Huei Sheng, Hsiu-Jung Lo, Hurng-Yi Wang, Yee-Chun Chen, Shan-Chwen Chang

Candida tropicalis is the leading cause of non-*C. albicans* candidemia in tropical Asia and Latin America. We evaluated isolates from 344 patients with an initial episode of *C. tropicalis* candidemia. We found that 58 (16.9%) patients were infected by fluconazole-nonsusceptible (FNS) *C. tropicalis* with cross resistance to itraconazole, voriconazole, and posaconazole; 55.2% (32/58) of patients were azole-naïve. Multilocus sequence typing analysis revealed FNS isolates were genetically closely related, but we did not see time- or place-clustering. Among the diploid sequence types (DSTs), we noted DST225, which has been reported from fruit in Taiwan and hospitals in Beijing, China, as well as DST376 and DST505–7, which also were reported from hospitals in Shanghai, China. Our findings suggest cross-boundary expansion of FNS *C. tropicalis* and highlight the importance of active surveillance of clinical isolates to detect dissemination of this pathogen and explore potential sources in the community.

Candida species are the leading fungal pathogens causing severe healthcare-associated infections in immunocompromised patients globally (1). *C. tropicalis* is among the top 4 *Candida* species responsible for candidemia worldwide and is the most common cause of invasive candidiasis in tropical Asia and in Latin America (2–5).

C. tropicalis and *C. albicans* are ascomycetous diploid yeasts, closely related among pathogenic *Candida* species, and belong in a single *Candida* clade characterized by the unique translation of CUG codons as serine rather than leucine (6,7). These pathogens initially were considered to be susceptible to azoles (8–12) with the same clinical

breakpoints (13,14). The widespread use of azoles during the past 2 decades coincided with a decrease in incidence of *C. tropicalis* and *C. albicans* infections, which was coupled with an increase in infections caused by *C. glabrata* and other less susceptible and azole-resistant *Candida* species (12,15,16). Azole-resistant, less susceptible *C. tropicalis* has emerged worldwide, particularly in the Asia Pacific region (5,16–21). A multicenter study conducted in this region found that the 90% (MIC₉₀) of fluconazole for *C. tropicalis* increased to 32 µg/mL, the same as the MIC₉₀ of *C. glabrata* and much higher than the MIC₉₀ of *C. albicans*, 0.064 µg/mL (19).

Some studies of the genetic relationship of clinical fluconazole-nonsusceptible (FNS) *C. tropicalis* isolates have reported clonal diversity (22–24), whereas others have demonstrated clonal clusters (20,25,26). Among these studies, few examined the association between genetic relatedness of FNS *C. tropicalis* and clinical characteristics and outcomes of the infected patients (23,27). We conducted a study of 334 patients with *C. tropicalis* bloodstream infections (BSIs) in Taiwan to examine these relationships in greater detail. We determined the genetic relationships of fluconazole-susceptible (FS) and FNS *C. tropicalis* isolates from blood cultures; compared the relationship of isolates according to time, place, and person; and analyzed the clinical characteristics and outcomes of the patients according to susceptibility to fluconazole and genetic relationship. We further explored the potential emergence and spread of FNS *C. tropicalis* globally.

Methods

Study Designs, Setting, and Patients

We conducted a 7-year prospective observational study of adult patients with *C. tropicalis* BSIs admitted to the National Taiwan University Hospital (NTUH; Taipei, Taiwan) during March 1, 2011–December 31, 2017. NTUH is a 2,300-bed teaching hospital that provides both primary and

Author affiliations: National Taiwan University Hospital, Taipei, Taiwan (P.-Y. Chen, Y.-C. Chuang, U.-I. Wu, H.-Y. Sun, J.-T. Wang, W.-H. Sheng, Y.-C. Chen, S.-C. Chang); National Taiwan University College of Medicine, Taipei (P.-Y. Chen, H.-Y. Wang, Y.-C. Chen, S.-C. Chang); National Health Research Institutes, Miaoli, Taiwan (J.-T. Wang, H.-J. Lo, Y.-C. Chen)

DOI: <https://doi.org/10.3201/eid2509.190520>

tertiary care. We obtained patient data from the clinical records, including demographics, underlying disease, severity of illness, initial and follow-up blood cultures, focus of infection, antifungal therapy, presence of indwelling catheters, and fatality. We followed patients until discharge or death. This study was approved by the Research and Ethics Committees of NTUH (approval nos. NTUH-201103121RB and NTUH-201502034RIND).

Patients with candidemia were treated according to the guidelines of the Infectious Diseases Society of Taiwan (28). Central venous catheters were removed when feasible. Antifungal susceptibility tests were performed at physicians' request. Systemic antifungal agents included fluconazole, voriconazole, posaconazole, caspofungin, micafungin, anidulafungin, amphotericin B deoxycholate, liposomal amphotericin B, and flucytosine. We defined antifungal exposure as receipt of ≥ 1 antifungal agent within 6 months of onset of *C. tropicalis* BSI. We defined breakthrough *C. tropicalis* BSI as a positive blood culture for *C. tropicalis* in patients receiving an antifungal agent for ≥ 2 days.

Microbiology

We prospectively collected all *C. tropicalis* blood isolates from the hospital clinical microbiology laboratory. We reconfirmed the species identity by using CHROMagar Candida medium (Becton Dickinson, <https://www.bd.com>) and the Vitek 2 yeast identification system (bioMérieux, <https://www.biomerieux.com>). We performed DNA sequencing by using the internal transcribed spacer regions of the ribosomal 18S rRNA gene for *Candida* species, as described previously (29).

Antifungal Susceptibility Testing

We determined the MIC of the first *Candida* blood isolate from each patient by using the microdilution colorimetric Sensititre YeastOne YO-09 panel (ThermoFisher Scientific, <https://www.thermofisher.com>), in accordance with the manufacturer's instructions. We interpreted MICs according to clinical breakpoints proposed by the Clinical and Laboratory Standards Institute (CLSI) for antifungal agents (14); for posaconazole, we used breakpoints proposed by the European Committee on Antimicrobial Susceptibility Testing (EUCAST) (13). We defined FS as MIC of ≤ 2 $\mu\text{g}/\text{mL}$; susceptible-dose-dependent as MIC of 4 $\mu\text{g}/\text{mL}$; and resistant as MIC of ≥ 8 $\mu\text{g}/\text{mL}$. We further categorized FNS as susceptible-dose-dependent or resistant. We used epidemiologic cutoff values proposed by CLSI to categorize antifungal agents without established clinical breakpoints as wild type or non-wild type (9,30). We used *C. albicans* (ATCC 90028), *C. parapsilosis* (ATCC 22019), and *C. krusei* (ATCC 6258) as reference strains for quality control. We defined multidrug-resistant (MDR) *C. tropicalis* as nonsusceptible to ≥ 1 agent in ≥ 2 antifungal classes (31).

DNA Extraction, PCR Amplification, and Sequencing

We extracted whole-genome DNA of *C. tropicalis* isolates in Sabouraud dextrose agar pure colonies by using Quick-DNA Fungal/Bacterial DNA MiniPrep Kit (Zymo Research, <https://www.zymoresearch.com>) according to manufacturer's protocol. We measured DNA concentrations by using NanoDrop 2000 (ThermoFisher Scientific, <https://www.thermofisher.com>). We stored DNA extracts at -20°C before conducting amplification in a reaction volume of 20 μL , consisting of 2 μL of DNA, 1 μL each of forward and reverse primers (50 mmol/L), 10 μL KAPA HotStart ReadyMix (KAPA Biosystems, <https://www.kapabiosystems.com>), and 6 μL of water. We performed PCR amplification by the following methods: 95°C for 3 min; 30 cycles of 95°C for 30 sec, 60°C for 30 sec, and 72°C for 30 sec; 72°C for 3 min; and a final hold at 4°C .

Multilocus Sequence Typing

We typed all FNS isolates and randomly selected FS isolates to type at a ratio of 1:2 a multilocus sequence typing (MLST) scheme previously described by Tavanti et al (32). In brief, we used sequences of the oligonucleotide primers for PCR amplification of 6 gene fragments, *ICL1*, *MDR1*, *SAPT2*, *SAPT4*, *XYR1*, and *ZWF1a*. We purified the PCR amplification products and sequenced both strands of the fragments by using an Applied Biosystems PRISM 3730 DNA Analyzer (ThermoFisher Scientific, <https://www.thermofisher.com>). We defined nucleotide sequences by alignment of forward and reverse sequences by using BioNumerics version 6.6 (Applied Maths, <http://www.applied-maths.com>) and confirmed polymorphic sites by visual examination of the chromatograms. We defined heterozygosity as the presence of 2 coincident peaks in both the forward and reverse sequence chromatograms. We defined the results by using heterozygous data (K, M, R, S, W, and Y) from the International Union of Pure and Applied Chemistry (<https://iupac.org>) nomenclature.

To assign allele numbers and diploid sequence types (DSTs), we compared our sequences with *C. tropicalis* available in the central MLST database (<https://pubmlst.org/ctropicalis>) and assigned new allele numbers as needed. We used a combination of the results from the 6 gene fragments that yielded unique DSTs to quantify the similarities and putative genetic relationships between *C. tropicalis* isolates.

Phylogenetic Analysis

We conducted phylogenetic analysis by the UPGMA and applied minimum spanning tree algorithms based on p-distance by using BioNumerics version 6.6 to concatenated sequence data of 165 *C. tropicalis* isolates in this cohort.

Only 55 FNS isolates were typable. We determined the value of the cluster nodes by bootstrapping with 1,000 randomizations and used eBURST V3 (Imperial College London, UK; <http://eburst.mlst.net>) to determine putative relationships between strains. When 5 of the 6 alleles were identical between a pair, we considered the strains related and placed them into clonal complexes (CCs) (32). We predicted the putative founding DST of each CC by using the eBURST algorithm, where possible.

We downloaded 185 FNS *C. tropicalis* isolates from the MLST database and included these for phylogenetic analyses to elucidate the global clonal spread of these fungi. We also reviewed the MLST database and the literature to identify the year, country, and city from which these isolates were reported or detected.

Data Analysis

We expressed continuous variables as medians and interquartile ranges, and categorical variables as absolute frequencies and percentages. To compare clinical and microbiological factors between FS and FNS groups, we analyzed continuous data with the Mann-Whitney U test. We compared categorical data using χ^2 or Fisher exact test. For 3 groups categorized by CCs and FS, we performed post hoc analysis using the Mann-Whitney U test or Fisher exact test with a Bonferroni-adjusted α for pairwise comparisons if the result of the initial test was statistically significant. We examined time trends of the rates by logistic regression analysis. To analyze the predictors of FNS *C. tropicalis* BSIs, we subsequently entered all variables with $p < 0.20$ in univariate analysis and probable biologic meaning into the multivariate analysis. We developed multivariate models by using a stepwise method, with minimization of the Akaike information criterion, then considered variables statistically significant only when $p \leq 0.05$ and included these in the final model. We performed analyses with Stata version 14 (StataCorp LLC, <https://www.stata.com>) software and considered 2-sided p values < 0.05 statistically significant.

Results

C. tropicalis Susceptibility

We compiled in vitro susceptibility profiles to 9 antifungal drugs for 344 initial *C. tropicalis* blood isolates (Table 1). We found 58 (16.9%) isolates that were either FS (48/344, 14.0%) or susceptible-dose-dependent (10/344, 2.9%). We noted some differences in susceptibility to other azoles. Two isolates were resistant to 3 echinocandins, and all were susceptible to amphotericin B. Overall, only 1 isolate was categorized as MDR to all tested azoles and echinocandins.

We also compiled annual FNS rates for all *C. tropicalis* isolates during 2011–2017 (Figure 1, panel A). Of

note, the rate of resistance to fluconazole increased from 6.7% in 2011 to 19.3% in 2017 ($p = 0.07$ for the trend). The distribution of fluconazole MICs was bimodal. The highest peak ranged from 0.5 to 2 $\mu\text{g/mL}$, with a smaller peak at 128–512 $\mu\text{g/mL}$ (Figure 1, panel B).

Phylogenetic Analysis of the *C. tropicalis* Blood Isolates

The UPGMA dendrogram for 55 FNS and 110 FS isolates (Appendix Figure 1 (<http://www.nce.cdc.gov/EID/article/25/9/19-0520-App1.pdf>)) showed that the 165 isolates belonged to 16 groups defined by similarities of $\geq 80\%$ and consisting of 87 DSTs. eBURST analysis revealed 78 DSTs grouped into 24 CCs; 9 DSTs were classified as singletons (Appendix Figure 1, Appendix Table 1). The CCs determined by eBURST were concordant to groups defined by UPGMA, except for some minor CCs and singletons that were grouped with other major CCs by UPGMA. CC3 was most common (40/165, 24.2%), correlating with UPGMA group 9 with 85.2% similarity; isolates were assigned to 12 DSTs, including DST225 ($n = 9$) as the putative founder based on eBURST algorithm. CC2 was the second most common, correlating with UPGMA group 4; these 33 isolates were assigned to 13 DSTs, with DST140 ($n = 14$) as the putative founder. CC4, UPGMA group 7, included 22 isolates assigned to 12 DSTs, with DST139 ($n = 7$) as the putative founder.

CC3 had an FNS rate of 90.0% (36/40) compared with variable rates for the other CCs; 65.5% (36/55) of the FNS isolates from this study belonged to CC3, including DST225 ($n = 9$), DST375 ($n = 1$), DST376 ($n = 6$), DST505 ($n = 1$), DST506 ($n = 6$), DST507 ($n = 10$), DST753 ($n = 1$), DST754 ($n = 1$), and DST838 ($n = 1$). A minor cluster of FNS isolates belonged to CC11, including DST508 ($n = 3$) and DST752 ($n = 1$). The remaining 18 FNS isolates were scattered among 11 different CCs or singletons. We found similar genetic relationships with other azoles, but no correlation of genetically similar isolates with time or place, or clustering of the cases in the hospital (Appendix Figure 1).

Genetic Relationships of FNS *C. tropicalis*

We further evaluated the genetic relationships of 165 *C. tropicalis* blood isolates from our cohort with 185 FNS strains available in the MLST database. The minimum spanning tree of the 350 isolates is composed largely of CC3, CC10, and CC11 with high FNS rates (Figure 2) that share 78.0% similarity on the basis of the UPGMA algorithm (Appendix Figure 2).

We also summarized the year of isolation, country and city of origin, and clinical or environmental sites of *C. tropicalis* CC3, CC10, and CC11, all of which were reported from countries in Asia, most after 2011 (Appendix Table 2). CC3 again formed the largest cluster;

Table 1. Comparison of antifungal susceptibility distribution of 344 *Candida tropicalis* blood isolates, Taiwan, 2011–2017*

Antifungal agents	Total, n = 344	Fluconazole-susceptible isolates, n = 286	Fluconazole-nonsusceptible isolates		
			Total,† n = 58	Clonal complex 3,‡ n = 36	Other clonal complexes,‡ n = 19
Fluconazole					
MIC ₅₀	1	1	216	256	8
MIC ₉₀	32	2	512	512	128
Range	0.06–512	0.06–2	4–512	32–512	4–512
NS rates, no. (%)	58 (16.9)	0	58 (100)§	36 (100)	19 (100)
Itraconazole					
MIC ₅₀	0.25	0.25	0.5	0.5	0.06
MIC ₉₀	0.5	0.25	1	1	1
Range	0.06–32	0.03–0.5	0.06–32	0.25–1	0.06–32
NWT rates, no. (%)	20 (5.8)	0	20 (34.5)§	18 (50)	2 (10.5)
Posaconazole					
MIC ₅₀	0.25	0.25	0.5	0.5	0.5
MIC ₉₀	0.5	0.5	1	1	1
Range	0.06–16	0.004–0.5	0.06–16	0.25–2	0.06–16
NS rates, no. (%)	285 (82.9)	228 (79.7)	57 (98.3)§	36 (100)	18 (94.7)
Voriconazole					
MIC ₅₀	0.12	0.12	4	8	0.5
MIC ₉₀	2	0.12	16	16	4
Range	0.004–16	0.004–0.25	0.25–16	1–16	0.25–16
NS rates, no. (%)	75 (21.8)	17 (5.9)	58 (100)§	36 (100)	19 (100)
Anidulafungin					
MIC ₅₀	0.06	0.06	0.12	0.12	0.06
MIC ₉₀	0.12	0.12	0.12	0.12	0.12
Range	0.008–1	0.008–0.5	0.008–1	0.008–1	0.008–0.25
NS rates¶, no. (%)	2 (0.6)	1 (0.4)	1 (1.7)	1 (2.8)	0
Caspofungin					
MIC ₅₀	0.06	0.06	0.06	0.06	0.06
MIC ₉₀	0.12	0.12	0.25	0.25	0.25
Range	0.015–8	0.015–2	0.015–8	0.015–8	0.015–0.25
NS rates¶, no. (%)	3 (0.9)	2 (0.7)	1 (1.7)	1 (2.8)	0
Micafungin					
MIC ₅₀	0.03	0.03	0.03	0.03	0.03
MIC ₉₀	0.03	0.03	0.03	0.03	0.03
Range	0.015–2	0.004–1	0.015–2	0.015–2	0.015–0.03
NS rates¶, no. (%)	2 (0.6)	1 (0.4)	1 (1.7)	1 (2.8)	0
Amphotericin					
MIC ₅₀	1	1	1	1	1
MIC ₉₀	1	1	1	1	1
Range	0.25–1	0.25–1	0.25–1	0.50–1	0.25–1
NWT rates, no. (%)	0	0	0	0	0
Flucytosine					
MIC ₅₀	0.03	0.03	0.03	0.03	0.03
MIC ₉₀	0.06	0.06	0.12	0.03	0.50
Range	0.03–64	0.03–64	0.03–32	0.03–0.03	0.03–32
NWT rates, no. (%)	4 (1.2)	3 (1.0)	1 (1.7)	0	1 (5.3)

*MICs and ranges are reported in µg/mL. NS, nonsusceptible; NWT, non-wild-type.

†Of 58 fluconazole-nonsusceptible isolates, only 55 isolates were typable with subsequent assignment of clonal complex.

‡Details of CCs and corresponding MIC data are available in Appendix Table 1 (<https://wwwnc.cdc.gov/EID/article/25/9/19-0520-App1.pdf>).

§Comparison of antifungal NS rates between FS isolates (n = 256) and FNS isolates (n = 58) by χ^2 tests, $p \leq 0.001$.

¶The susceptibility discrepancy among 3 echinocandins may be attributed to significant variability in caspofungin susceptibility testing, which resulted in false resistance reporting.

22 DSTs, including DST225, were isolated from the environment and hospitals in Taiwan. DST225 also was isolated in hospitals in Beijing, China. DST375 and DST505–7 were isolated in hospitals in Shanghai, China. CC10 was the second largest cluster with 12 DSTs reported from Singapore and Nanchang, China, but we did not find these in our study. CC11 with 5 DSTs was reported from Singapore and China (Beijing, Shanghai, and Nanchang). DST508 was isolated in the current study in Taiwan and Beijing.

Clinical Characteristics and Outcomes of Patients with *C. tropicalis* BSIs

Of the 58 patients in this study with FNS isolates, 32 (55.2%) had no previous antifungal exposure (Table 2, Appendix Table 3). Nevertheless, multivariate logistic regression analysis revealed that antifungal drug exposure was associated with FNS infection (odds ratio [OR] 5.64, 95% CI 2.94–10.81; $p < 0.001$). Another risk factor for FNS infection was moderate to severe liver disease (adjusted OR 3.13, 95% CI 1.06–9.24; $p = 0.04$). We saw no statistically significant difference in

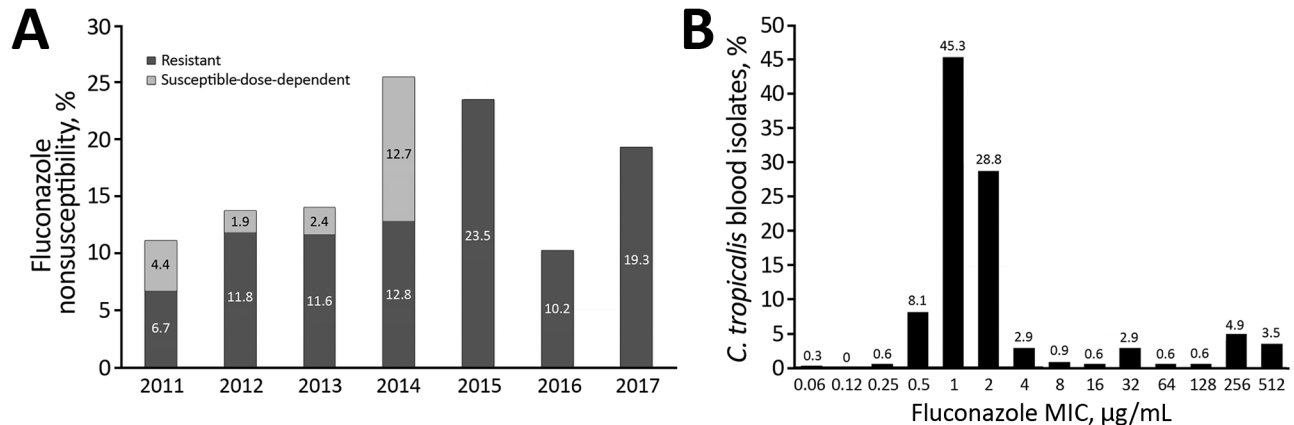


Figure 1. Fluconazole nonsusceptibility of *Candida tropicalis* blood isolates, Taiwan, 2011–2017. A) Proportions of fluconazole nonsusceptibility among 344 *C. tropicalis* blood isolates by year. B) Distributions of fluconazole MICs among *C. tropicalis* blood isolates.

deaths or persistent candidemia between patients according to the degree of fluconazole susceptibility of their isolates.

We divided the 165 initial blood isolates with known DSTs into 3 groups, FNS CC3, FNS other CCs, and FS isolates (Appendix Table 4). Patients infected with FNS CC3 were more likely to have neutropenia, previous steroid use, and chemotherapy by Fisher exact test with a Bonferroni adjustment; two thirds previously were exposed to antifungal

drugs. We saw no statistically significant difference in outcome among patients from the 3 groups.

Discussion

In our 7-year observational study in Taiwan, we found an increasing trend over time in the emergence of fluconazole-resistant *C. tropicalis* isolates in blood. Over time, fluconazole susceptible-dose-dependent *C. tropicalis* strains were replaced

Figure 2. Minimum spanning tree of 350 *C. tropicalis* isolates from multilocus sequence typing (MLST) data. A) Minimum spanning tree of 165 *C. tropicalis* blood isolates from this study's cohort (Taiwan, 2011–2017) and 185 isolates with fluconazole nonsusceptibility from the central *C. tropicalis* MLST global database (<https://pubmlst.org/ctropicalis>). Each circle corresponds to a diploid sequence type (DST). The size of the circle indicates the number of the isolates belonging to a specific DST and classified as fluconazole resistant (red), susceptible-dose-dependent (yellow), or susceptible (white). Lines between circles indicate the similarity between profiles: bold lines indicate 5 of 6 alleles are identical, solid lines indicate 4 alleles are identical, and dotted lines indicate ≤ 3 alleles are similar. Shaded areas indicate groups of target clonal complexes (CCs). B) Enlarged area of CC10 and CC11 (purple shading). C) Enlarged area of fluconazole-nonsusceptible CC3 (green shading). D) Enlarged area of fluconazole-susceptible CC3 (pink shading).

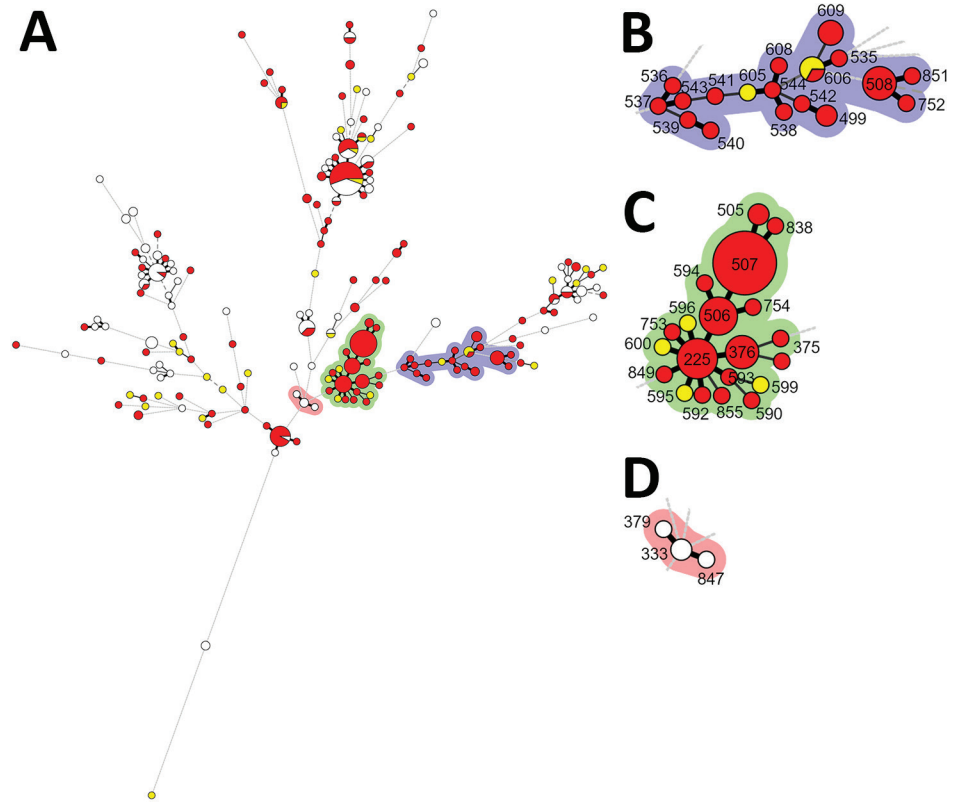


Table 2. Comparisons of clinical and microbiological characteristics between fluconazole-susceptible and fluconazole-nonsusceptible *Candida tropicalis* bloodstream infections, Taiwan, 2011–2017*

Characteristic	Total, n = 344	With FS <i>C. tropicalis</i> BSIs, n = 286	With FNS <i>C. tropicalis</i> BSIs, n = 58	p value
Demographics				
Age, y, median (IQR)	62.8 (53.2–73.5)	62.4 (53.0–74.3)	63.4 (55.2–72.1)	0.85
Sex, no. (%)				0.54
M	201 (58.4)	165 (57.7)	36 (62.1)	
F	143 (41.6)	121 (42.3)	22 (37.9)	
Disease severity				
ICU onset, no. (%)	105 (30.7)	85 (29.9)	20 (34.5)	0.49
APACHE II score, median (IQR)	20.0 (15.0–26.0)	20.0 (15.0–26.0)	19.0 (15.5–26.0)	0.85
Healthcare factors, no. (%)†				
Solid organ transplant	4 (1.2)	3 (1.1)	1 (1.8)	0.52
Hematopoietic stem cell transplant	10 (2.9)	9 (3.2)	1 (1.8)	0.99
Major surgery	40 (11.6)	34 (11.9)	6 (10.3)	0.99
Parenteral hyperalimentation	189 (59.4)	155 (54.2)	34 (58.6)	0.54
Steroid use	170 (49.4)	133 (46.5)	37 (63.8)	0.02
Chemotherapy	153 (44.5)	123 (43.0)	30 (51.7)	0.22
Neutropenia	91 (26.8)	69 (24.5)	22 (38.6)	0.03
Mechanical ventilator	101 (29.4)	84 (29.4)	17 (29.3)	0.99
Indwelling urinary catheter	138 (40.1)	110 (38.5)	28 (48.3)	0.16
Central venous catheter	286 (83.1)	238 (83.2)	48 (82.8)	0.93
Antifungal exposure	60 (17.4)	34 (11.9)	26 (44.8)	<0.001
Antibiotics exposure	300 (87.7)	248 (87.3)	52 (89.7)	0.62
Therapeutic intervention, no. (%)‡				
Early appropriate antifungal agents	261 (75.9)	243 (85.0)	18 (31.0)	<0.001
Fluconazole as the first antifungal agent	221 (64.2)	185 (64.7)	36 (62.1)	0.71
Early removal of central venous catheter	162/286 (56.6)	131/238 (55.0)	31/48 (64.6)	0.22
Clinical outcomes, no. (%)§				
Death				
7 d	73 (21.2)	60 (21.0)	13 (22.4)	0.81
14 d	117 (34.0)	99 (34.6)	18 (31.0)	0.60
28 d	167 (48.6)	141 (49.3)	26 (44.8)	0.53
In hospital	226 (65.7)	187 (65.4)	39 (67.2)	0.79
Persistence, no. (%)§	81 (27.7)	65 (26.6)	16 (33.3)	0.34

*Additional information on patient conditions and microbiological data can be found in Appendix Table 3 (<https://wwwnc.cdc.gov/EID/article/25/9/19-0520-App1.pdf>). APACHE, Acute Physiology and Chronic Health Evaluation; BSIs, bloodstream infections; FNS, fluconazole nonsusceptible; FS, fluconazole susceptible; ICU, intensive care unit; IQR, interquartile range.

†Major surgery refers to cardiovascular or abdominal surgery. Classes of antifungal exposure to azole or echinocandin, 31/3 in FS group vs. 24/2 in FNS group; of note, 14 (24.1%) patients in the FNS group experienced breakthrough bloodstream infections, compared with 18 (6.3%) patients in the FS group ($p < 0.001$).

‡Early adequate antifungal agents refers to administration of the recommended dose of an intravenous antifungal agent within 48 h after first positive blood culture collection for a susceptible *Candida* isolate, according to the Clinical and Laboratory Standards Institute (CLSI) species-specific breakpoints (14). Early removal of central venous catheters is defined as removal of all similar devices, including tunneled and peripherally inserted central catheters, within 48 h after obtaining the first positive blood culture.

§Persistence is defined as >5 days of blood cultures positive for the same *Candida* species.

by fully resistant strains. Many of the FNS isolate strains were genetically closely related to each other and to strains from the environment and other hospitals in Taiwan and other countries in Asia. We found a 6-fold increase in the risk for FNS *C. tropicalis* infection in patients with prior exposure to antifungal drugs, but half of the FNS isolates we obtained were from azole-naïve patients. We saw no statistically significant relationship of the cases to time and place and no clustering.

The drive of antifungal resistance is most commonly attributed to antifungal selection pressure, especially in human use (23). Our finding of an increased risk for *C. tropicalis* BSIs in patients who received antifungal drugs in the preceding 6 months supports this scenario. Furthermore, our study showed a high rate (14/26, 53.8%) of breakthrough BSIs (receipt of antifungal drugs ≥ 2 days before BSI onset) among FNS isolates from patients with antifungal exposure. These breakthrough isolates showed

higher fluconazole MIC₅₀ (256 $\mu\text{g}/\text{mL}$) than isolates with only prior exposure to antifungal agents (32 $\mu\text{g}/\text{mL}$). This result reflected higher antifungal selection pressure during current antifungal use than with previous use only.

Alternatively, azole resistance in human fungal pathogens might develop through exposure to azole fungicides in the environment. Our nationwide environmental surveillance and multicenter clinical study is concordant with global concerns that azole resistance in *A. fumigatus* human isolates, at least in part, resulted from resistant strains in the environment and the use of azole fungicides in agricultures (33,34). According to that study, annual consumption of 5 fungicide azoles in Taiwan increased 4-fold during 2003–2016, indicating long-existing high fungicide burdens in the environment in Taiwan during our study period (34).

Meanwhile, nationwide environmental surveys in Taiwan isolated *C. tropicalis* DST225 from fruit (35) and

from patients in different hospitals enrolled in the Taiwan Surveillance of Antimicrobial Resistance of Yeasts (35). DST225 isolates in that investigation showed cross resistance to fluconazole and triadimenol, an azole fungicide (35). Given that DST225 and genetically related DSTs were identified in clinical isolates obtained from azole-naïve patients in our study and in a report from China (27), along with high fungicide burden in Asia (36), we suggest that patients could acquire FNS *C. tropicalis* from the environment in the community. FNS *C. tropicalis* without time- and place-clustering in this study further excludes the potential for cross-transmission in hospitals.

We propose the multifocal emergence of genetically related FNS *C. tropicalis* strains in Taiwan and other countries in Asia (25–27) is a result of the selective pressure of intense use of azole antifungal agents in humans and agriculture (34–36). Furthermore, human use promotes the selection of resistant strains in patients already colonized from environmental sources by susceptible-dose-dependent or resistant genotypes of *C. tropicalis*. It is unclear whether these strains arise independently or are spread by extensive trade of agricultural products among these countries.

In our study, FNS isolates were not associated with worse clinical and microbiological outcomes. This finding was concordant with prior studies demonstrating no good correlations between outcomes of patients with *Candida* BSIs and fluconazole MIC or pharmacodynamics parameters, such as the area under the concentration-time curve to MIC ratio (11,18,37).

The strength of this study is that it used a large cohort of *C. tropicalis* blood isolates collected over a 7-year period and integrated with the *C. tropicalis* MLST central database and other published data through literature review and to infer the genetic relationships of FNS *C. tropicalis* globally (Appendix Table 2). However, this study has several limitations. It was conducted in a single hospital in Taiwan, and one should be cautious in making generalizations because differences in nosocomial spread might occur in other institutions. We likely underestimate the proportion of FNS *C. tropicalis* in this cohort because the study focused on isolates from blood and was limited to the first episode of *C. tropicalis* BSI from each patient. Furthermore, we did not define the mechanisms for development of resistance, which were previously examined in China and Singapore. Other studies have shown that *ERG11* mutations combined with or without *MDR1* overexpression produce high-level resistance to fluconazole and other azoles in *C. tropicalis* isolates belonging to CC3, CC10, and CC11, consisting of DST225 and genetically related DSTs (26,27).

In conclusion, FNS *C. tropicalis* clones appear to have emerged in part due to use of azole antifungal agents in agriculture, with cross-country expansion fostered by

therapeutic use in hospitals. The concept that FNS *C. tropicalis* was acquired outside the hospital is supported by the lack of evidence of nosocomial spread. These findings emphasize the importance of active surveillance of FNS *C. tropicalis* in agriculture, hospitals, and the community.

Acknowledgments

We thank Calvin M. Kunin for his critical review and suggestions for the manuscript. We also thank Li-Fang Chen and Ching-Tzu Dai for laboratory support and Yi-Hsin Liu for collection of clinical data.

This study was supported by the Ministry of Science and Technology (grant nos. 102-2314-B-002-158-MY3, 104-2314-B-002-241, 107-2314-B-002-181) and the Ministry of Health and Welfare, Taiwan (grant nos. 107-TDU-B-211-123002, 106-TDU-B-211-113002). The funding source played no role in study design and conduct, data collection, analysis or interpretation, writing of the manuscript, or the decision to submit it for publication.

About the Author

Dr. Pao-Yu Chen is an infectious disease physician at National Taiwan University Hospital. His main research interests include molecular epidemiology and mechanisms of antimicrobial resistance in human pathogens, with a focus on fungi.

References

1. Brown GD, Denning DW, Gow NA, Levitz SM, Netea MG, White TC. Hidden killers: human fungal infections. *Sci Transl Med*. 2012;4:165rv13. <https://doi.org/10.1126/scitranslmed.3004404>
2. Chen PY, Chuang YC, Wang JT, Sheng WH, Yu CJ, Chu CC, et al. Comparison of epidemiology and treatment outcome of patients with candidemia at a teaching hospital in Northern Taiwan, in 2002 and 2010. *J Microbiol Immunol Infect*. 2014;47:95–103. <https://doi.org/10.1016/j.jmii.2012.08.025>
3. Tan BH, Chakrabarti A, Li RY, Patel AK, Watcharananan SP, Liu Z, et al.; Asia Fungal Working Group (AFWG). Incidence and species distribution of candidaemia in Asia: a laboratory-based surveillance study. *Clin Microbiol Infect*. 2015;21:946–53. <https://doi.org/10.1016/j.cmi.2015.06.010>
4. Colombo AL, Júnior JNA, Guinea J. Emerging multidrug-resistant *Candida* species. *Curr Opin Infect Dis*. 2017;30:528–38. <https://doi.org/10.1097/QCO.0000000000000411>
5. Wu PF, Liu WL, Hsieh MH, Hii IM, Lee YL, Lin YT, et al. Epidemiology and antifungal susceptibility of candidemia isolates of non-albicans *Candida* species from cancer patients. *Emerg Microbes Infect*. 2017;6:1–7. <https://doi.org/10.1038/emi.2017.74>
6. Butler G, Rasmussen MD, Lin MF, Santos MA, Sakthikumar S, Munro CA, et al. Evolution of pathogenicity and sexual reproduction in eight *Candida* genomes. *Nature*. 2009;459:657–62. <https://doi.org/10.1038/nature08064>
7. Jensen RH. Resistance in human pathogenic yeasts and filamentous fungi: prevalence, underlying molecular mechanisms and link to the use of antifungals in humans and the environment. *Dan Med J*. 2016;63:B5288.
8. Chen YC, Chang SC, Luh KT, Hsieh WC. Stable susceptibility of *Candida* blood isolates to fluconazole despite increasing use during the past 10 years. *J Antimicrob Chemother*. 2003;52:71–7. <https://doi.org/10.1093/jac/dkg275>

9. Pfaller MA, Diekema DJ. Progress in antifungal susceptibility testing of *Candida* spp. by use of Clinical and Laboratory Standards Institute broth microdilution methods, 2010 to 2012. *J Clin Microbiol*. 2012;50:2846–56. <https://doi.org/10.1128/JCM.00937-12>
10. da Matta DA, Souza ACR, Colombo AL. Revisiting species distribution and antifungal susceptibility of *Candida* bloodstream isolates from Latin American medical centers. *J Fungi (Basel)*. 2017;3:E24. <https://doi.org/10.3390/jof3020024>
11. Fernández-Ruiz M, Guinea J, Lora-Pablos D, Zaragoza Ó, Puig-Asensio M, Almirante B, et al.; CANDIPOP Project; GEIH-GEMICOMED (SEIMC) and REIPI. Impact of fluconazole susceptibility on the outcome of patients with candidemia: data from a population-based surveillance. *Clin Microbiol Infect*. 2017;23:672.e1–11. <https://doi.org/10.1016/j.cmi.2017.01.014>
12. Astvad KMT, Johansen HK, Røder BL, Rosenvinge FS, Knudsen JD, Lemming L, et al. Update from a 12-year nationwide fungemia surveillance: increasing intrinsic and acquired resistance causes concern. *J Clin Microbiol*. 2018;56:e01564–17.
13. European Committee on Antimicrobial Susceptibility Testing Antifungal Agents. Breakpoint tables for interpretation of MICs, version 9.0 [cited 2019 May 14]. <http://www.eucast.org/astoffungi/clinicalbreakpointsforantifungals>
14. Clinical and Laboratory Standards Institute. Reference method for broth dilution antifungal susceptibility testing of yeasts: 4th informational supplement (M27–S4). Wayne (PA): The Institute; 2012.
15. Pfaller MA, Diekema DJ. Epidemiology of invasive candidiasis: a persistent public health problem. *Clin Microbiol Rev*. 2007;20:133–63. <https://doi.org/10.1128/CMR.00029-06>
16. Teo JQ, Candra SR, Lee SJ, Chia SY, Leck H, Tan AL, et al. Candidemia in a major regional tertiary referral hospital—epidemiology, practice patterns and outcomes. *Antimicrob Resist Infect Control*. 2017;6:27. <https://doi.org/10.1186/s13756-017-0184-1>
17. Huang YT, Liu CY, Liao CH, Chung KP, Sheng WH, Hsueh PR. Antifungal susceptibilities of *Candida* isolates causing bloodstream infections at a medical center in Taiwan, 2009–2010. *Antimicrob Agents Chemother*. 2014;58:3814–9. <https://doi.org/10.1128/AAC.01035-13>
18. Fernández-Ruiz M, Puig-Asensio M, Guinea J, Almirante B, Padilla B, Almela M, et al.; CANDIPOP Project; GEIH-GEMICOMED (SEIMC); REIPI. *Candida tropicalis* bloodstream infection: incidence, risk factors and outcome in a population-based surveillance. *J Infect*. 2015;71:385–94. <https://doi.org/10.1016/j.jinf.2015.05.009>
19. Tan TY, Hsu LY, Alejandria MM, Chaiwarith R, Chinniah T, Chayakulkeeree M, et al. Antifungal susceptibility of invasive *Candida* bloodstream isolates from the Asia-Pacific region. *Med Mycol*. 2016;54:471–7. <https://doi.org/10.1093/mmy/myv114>
20. Fan X, Xiao M, Liao K, Kudinha T, Wang H, Zhang L, et al. Notable increasing trend in azole non-susceptible *Candida tropicalis* causing invasive candidiasis in China (August 2009 to July 2014): molecular epidemiology and clinical azole consumption. *Front Microbiol*. 2017;8:464. <https://doi.org/10.3389/fmicb.2017.00464>
21. Morris AJ, Rogers K, McKinney WP, Roberts SA, Freeman JT. Antifungal susceptibility testing results of New Zealand yeast isolates, 2001–2015: impact of recent CLSI breakpoints and epidemiological cut-off values for *Candida* and other yeast species. *J Glob Antimicrob Resist*. 2018;14:72–7. <https://doi.org/10.1016/j.jgar.2018.02.014>
22. Magri MM, Gomes-Gouvêa MS, de Freitas VL, Motta AL, Moretti ML, Shikanai-Yasuda MA. Multilocus sequence typing of *Candida tropicalis* shows the presence of different clonal clusters and fluconazole susceptibility profiles in sequential isolates from candidemia patients in Sao Paulo, Brazil. *J Clin Microbiol*. 2013;51:268–77. <https://doi.org/10.1128/JCM.02366-12>
23. Choi MJ, Won EJ, Shin JH, Kim SH, Lee WG, Kim MN, et al. Resistance mechanisms and clinical features of fluconazole-nonsusceptible *Candida tropicalis* isolates compared with fluconazole-less-susceptible isolates. *Antimicrob Agents Chemother*. 2016;60:3653–61. PubMed <https://doi.org/10.1128/AAC.02652-15>
24. Wu JY, Guo H, Wang HM, Yi GH, Zhou LM, He XW, et al. Multilocus sequence analyses reveal extensive diversity and multiple origins of fluconazole resistance in *Candida tropicalis* from tropical China. *Sci Rep*. 2017;7:42537. <https://doi.org/10.1038/srep42537>
25. Wang Y, Shi C, Liu JY, Li WJ, Zhao Y, Xiang MJ. Multilocus sequence typing of *Candida tropicalis* shows clonal cluster enrichment in azole-resistant isolates from patients in Shanghai, China. *Infect Genet Evol*. 2016;44:418–24. <https://doi.org/10.1016/j.meegid.2016.07.026>
26. Chew KL, Cheng JWS, Jureen R, Lin RTP, Teo JWP. *ERG11* mutations are associated with high-level azole resistance in clinical *Candida tropicalis* isolates, a Singapore study. *Mycoscience*. 2017;58:111–5. <https://doi.org/10.1016/j.myc.2016.11.001>
27. Jin L, Cao Z, Wang Q, Wang Y, Wang X, Chen H, et al. *MDR1* overexpression combined with *ERG11* mutations induce high-level fluconazole resistance in *Candida tropicalis* clinical isolates. *BMC Infect Dis*. 2018;18:162. <https://doi.org/10.1186/s12879-018-3082-0>
28. Kung HC, Huang PY, Chen WT, Ko BS, Chen YC, Chang SC, et al.; Infectious Diseases Society of Taiwan; Medical Foundation in Memory of Dr. Deh-Lin Cheng; Foundation of Professor Wei-Chuan Hsieh for Infectious Diseases Research and Education; CY Lee's Research Foundation for Pediatric Infectious Diseases and Vaccines. 2016 guidelines for the use of antifungal agents in patients with invasive fungal diseases in Taiwan. *J Microbiol Immunol Infect*. 2018;51:1–17. <https://doi.org/10.1016/j.jmii.2017.07.006>
29. Lin KY, Chen PY, Chuang YC, Wang JT, Sun HY, Sheng WH, et al. Effectiveness of echinocandins versus fluconazole for treatment of persistent candidemia: a time-dependent analysis. *J Infect*. 2018;77:242–8. <https://doi.org/10.1016/j.jinf.2018.05.011>
30. Clinical and Laboratory Standards Institute. Epidemiological cutoff values for antifungal susceptibility testing. 2nd ed. Supplement M59. Wayne (PA): The Institute; 2018.
31. Arendrup MC, Patterson TF. Multidrug-Resistant *Candida*: Epidemiology, Molecular Mechanisms, and Treatment. *J Infect Dis*. 2017;216(suppl_3):S445–51. <https://doi.org/10.1093/infdis/jix131>
32. Tavanti A, Davidson AD, Johnson EM, Maiden MC, Shaw DJ, Gow NA, et al. Multilocus sequence typing for differentiation of strains of *Candida tropicalis*. *J Clin Microbiol*. 2005;43:5593–600. <https://doi.org/10.1128/JCM.43.11.5593-5600.2005>
33. Wu CJ, Wang HC, Lee JC, Lo HJ, Dai CT, Chou PH, et al. Azole-resistant *Aspergillus fumigatus* isolates carrying TR₂/L98H mutations in Taiwan. *Mycoses*. 2015;58:544–9. <https://doi.org/10.1111/myc.12354>
34. Wang HC, Huang JC, Lin YH, Chen YH, Hsieh MI, Choi PC, et al. Prevalence, mechanisms and genetic relatedness of the human pathogenic fungus *Aspergillus fumigatus* exhibiting resistance to medical azoles in the environment of Taiwan. *Environ Microbiol*. 2018;20:270–80. <https://doi.org/10.1111/1462-2920.13988>
35. Lo HJ, Tsai SH, Chu WL, Chen YZ, Zhou ZL, Chen HF, et al. Fruits as the vehicle of drug resistant pathogenic yeasts. *J Infect*. 2017;75:254–62. <https://doi.org/10.1016/j.jinf.2017.06.005>
36. Stensvold CR, Jørgensen LN, Arendrup MC. Azole-resistant invasive aspergillosis: relationship to agriculture. *Curr Fungal Infect Rep*. 2012;6:178–91. <https://doi.org/10.1007/s12281-012-0097-7>
37. Brosh-Nissimov T, Ben-Ami R. Differential association of fluconazole dose and dose/MIC ratio with mortality in patients with *Candida albicans* and non-albicans bloodstream infection. *Clin Microbiol Infect*. 2015;21:1011–7. <https://doi.org/10.1016/j.cmi.2015.07.005>

Address for correspondence: Yee-Chun Chen, National Taiwan University Hospital, Department of Internal Medicine, No. 7 Chung-Shan South Road, Taipei 100, Taiwan; email: yeechunchen@gmail.com

Association of Enterovirus D68 with Acute Flaccid Myelitis, Philadelphia, Pennsylvania, USA, 2009–2018

Priyanka Uprety, Darcy Curtis, Michael Elkan, Jeffrey Fink, Ramakrishnan Rajagopalan, Chunyu Zhao, Kyle Bittinger, Stephanie Mitchell, Erlinda R. Ulloa, Sarah Hopkins, Erin H. Graf

Acute flaccid myelitis (AFM) is a polio-like disease that results in paralysis in previously healthy persons. Although the definitive cause of AFM remains unconfirmed, enterovirus D68 (EV-D68) is suspected based on 2014 data demonstrating an increase in AFM cases concomitant with an EV-D68 outbreak. We examined the prevalence in children and the molecular evolution of EV-D68 for 2009–2018 in Philadelphia, Pennsylvania, USA. We detected widespread EV-D68 circulation in 2009, rare detections in 2010 and 2011, and then biennial circulation, only in even years, during 2012–2018. Prevalence of EV-D68 significantly correlated with AFM cases during this period. Finally, whole-genome sequencing revealed early detection of the B1 clade in 2009 and continued evolution of the B3 clade from 2016 to 2018. These data reinforce the need to improve surveillance programs for nonpolio enterovirus to identify possible AFM triggers and predict disease prevalence to better prepare for future outbreaks.

A large outbreak of enterovirus D68 (EV-D68) in children in the United States caught national attention during late summer and fall of 2014. That outbreak was characterized by severe lower respiratory tract disease resulting in respiratory failure in many cases (1); a paralytic condition occurred in a smaller subset of children (2). Previous reports of invasive EV-D68 disease had been described across the globe (3,4), but the magnitude of this 2014 outbreak with regard to childhood illness was unprecedented. The Centers for Disease Control and Prevention (CDC) called for national heightened awareness, particularly for rapid onset of a traumatic limb weakness along with radiologic evidence

of gray matter lesions, coined acute flaccid myelitis (AFM) (2,5–7). A second period of EV-D68 circulation, again associated with severe respiratory disease, was described during late summer and fall of 2016, although 2 studies suggest lower levels of circulation during that period than in 2014 (8,9). Despite a documented spike in AFM in US children during the fall of 2016 and 2018 (10), EV-D68 surveillance data from this time are limited (11,12). In addition, little is known about the circulation of EV-D68 and association with AFM before 2014.

Although the definitive cause of AFM remains unknown, growing evidence (13,14) supports the association between EV-D68 and AFM. Epidemiologists have found that similar temporal associations between the 2014 EV-D68 outbreak and AFM cases also occurred in other countries (14). Hixon et al. found that paralysis could be elicited in mice infected with EV-D68 strains from the 2014 outbreak (15). As in children with AFM, these EV-D68–infected mice had a loss of motor neurons in the anterior horns of spinal cord segments corresponding to paralyzed limbs. Last, virus isolated from spinal cords of infected mice transmitted disease when injected into naive mice (15).

Despite the mounting evidence (13,14), the association between EV-D68 and AFM remains controversial. The detection of EV-D68 primarily in respiratory specimens with a concomitant lack of regular detection in cerebrospinal fluid (CSF) (7,16) continues to cast doubt, even though other neurotropic viruses (such as polioviruses) have similar detection patterns (14).

What remains to be shown for EV-D68 is whether its genome has changed over time to enable increased neurotropism. Since the first description of the nonneuroinvasive EV-D68 prototype in 1962, different genetic clades associated with neuroinvasion have been identified (15). Whole-genome sequencing (WGS) of the 2014 epidemic strains (dominated by clade B1) demonstrated a possible

Author affiliations: Children's Hospital of Philadelphia, Philadelphia, Pennsylvania, USA (P. Uprety, D. Curtis, M. Elkan, J. Fink, R. Rajagopalan, C. Zhao, K. Bittinger, E.R. Ulloa, S. Hopkins, E.H. Graf); University of Pennsylvania, Philadelphia (P. Uprety, K. Bittinger, S. Mitchell, E.R. Ulloa, S. Hopkins, E.H. Graf)

DOI: <https://doi.org/10.3201/eid2509.190468>

association between specific polymorphisms in EV-D68 and their overlap with other neurotropic and AFM-causing enteroviruses, such as poliovirus or enteroviruses D70 and A71 (16). These data suggest that the EV-D68 genome has changed over time to enable neurotropism or possibly increased virulence resulting in more widespread disease. Given that most studies have been based on partial instead of WGS, we also might be underestimating the number of clinically important genetic mutations in EV-D68 that drive increased infections with poor patient outcomes. Recognizing that longitudinal analyses of viral patterns and the molecular evolution of EV-D68 by WGS are sparse, we investigated the prevalence of EV-D68 in children in the Children's Hospital of Philadelphia (CHOP; Philadelphia, PA, USA) during 2009–2018 in relationship to AFM cases. We also investigated the phylogenetic relationships and genotypic features through WGS during this period to shed light on relevant mutations from year to year.

Materials and Methods

Specimen Selection

Nasopharyngeal aspirate samples that tested positive for rhinovirus/enterovirus (RV/EV) by laboratory-developed real-time reverse transcription PCR (rRT-PCR) through routine clinical diagnostic testing at CHOP were included in this study. Specimens have been archived and stored in multiple aliquots at -80°C since 2009. Based on data from prior publications (8,9), we selected a subset (every 5th specimen) of RV/EV-positive samples from August 1 through November 30 of 2009–2018 for subsequent testing for EV-D68. In total, we tested 1,433 specimens across the 10-year period for EV-D68. We further subjected a smaller subset of those positive for EV-D68 (26 samples) and residual EV-D68-positive cases of AFM (4 samples) to shotgun metagenomic RNA sequencing. In addition to these specimens, we also tested residual RV/EV-positive nasopharyngeal aspirates from 12 children confirmed to have AFM for EV-D68 by rRT-PCR. Detailed methods are provided in the Appendix (<https://wwwnc.cdc.gov/EID/article/25/9/19-0468-App1.pdf>). The Institutional Review Board of CHOP approved this study (IRB 16-012987).

AFM Cases

We retrospectively identified AFM cases from 2009 to initiation of CDC surveillance in 2014 through a search of International Classification of Diseases, 9th Revision, diagnosis codes in CHOP's electronic health record system and a text search of spinal magnetic resonance imaging (MRI) reports (M.M. Cortese, CDC, pers. comm. 2019 Jan 14). A neurologist reviewed MRI images and clinical information to identify cases meeting the 2014 CDC criteria for confirmed AFM. We identified cases from 2014

on prospectively. AFM cases were considered confirmed if they met the CDC criteria of illness with the acute onset of flaccid limb weakness and MRI demonstrating lesions restricted to the gray matter of the spinal cord that span ≥ 1 vertebral segments.

Statistical Analyses

All statistical analyses were performed in GraphPad Prism version 7.0 (GraphPad Software, San Diego, CA, USA). These analyses comprised Spearman correlation and linear regression analyses.

Results

Prevalence of EV-D68 and Association with AFM

We tested 1,433 respiratory specimens that were PCR-positive for RV/EV from August 1 through November 30 of 2009–2018 for EV-D68 by rRT-PCR. EV-D68 was detected in all years except 2013, 2015, and 2017 (Figure 1). Detections in 2010 and 2011 were rare—3 samples were positive in 2010 and 1 in 2011—and $<4\%$ of all RV/EV-positive samples tested those years were typed as EV-D68 (Figure 1, panel A). In contrast, $>10\%$ of RV/EV-positive specimens typed as EV-D68 in 2009, 2012, 2014, 2016, and 2018. The highest percentage occurred in 2016, when 27% of RV/EV-positive specimens (30/112 RV/EV-positive samples tested) were typed as EV-D68. In addition, we observed a 19% (35/180 RV/EV-positive samples tested) prevalence of EV-D68 in 2009 and an 11% (12/107 RV/EV-positive samples tested) prevalence of EV-D68 in 2012. The circulation appears to follow a biennial pattern from 2012 to 2018; however, a 2-year gap occurred in widespread circulation during 2009–2012, breaking this every-other-year cycle.

AFM cases from CHOP identified during the same 10-year period showed a similar biennial pattern of presence/absence during 2012–2018 (Figure 1, panel A); the highest number were identified in 2016. Two AFM cases were identified in 2009 when EV-D68 circulation was high and 1 in 2010 when circulation was low among the study population, and no cases were identified in 2011. Because the association between EV-D68 and AFM and subsequent importance of respiratory specimen collection were not recognized until late 2014, respiratory samples were not routinely collected for investigation of AFM at CHOP before 2016. During 2009–2018, a total of 20 AFM cases were identified. For 17 of these, respiratory specimens were collected at the time the child was brought to the hospital for care, and 14 (82%) of respiratory specimens tested positive for RV/EV (Figure 1, panel A). Twelve RV/EV-positive respiratory specimens taken from children in whom AFM was diagnosed had a residual sample for retrospective EV-D68 testing. Ten (83%) of these tested positive for

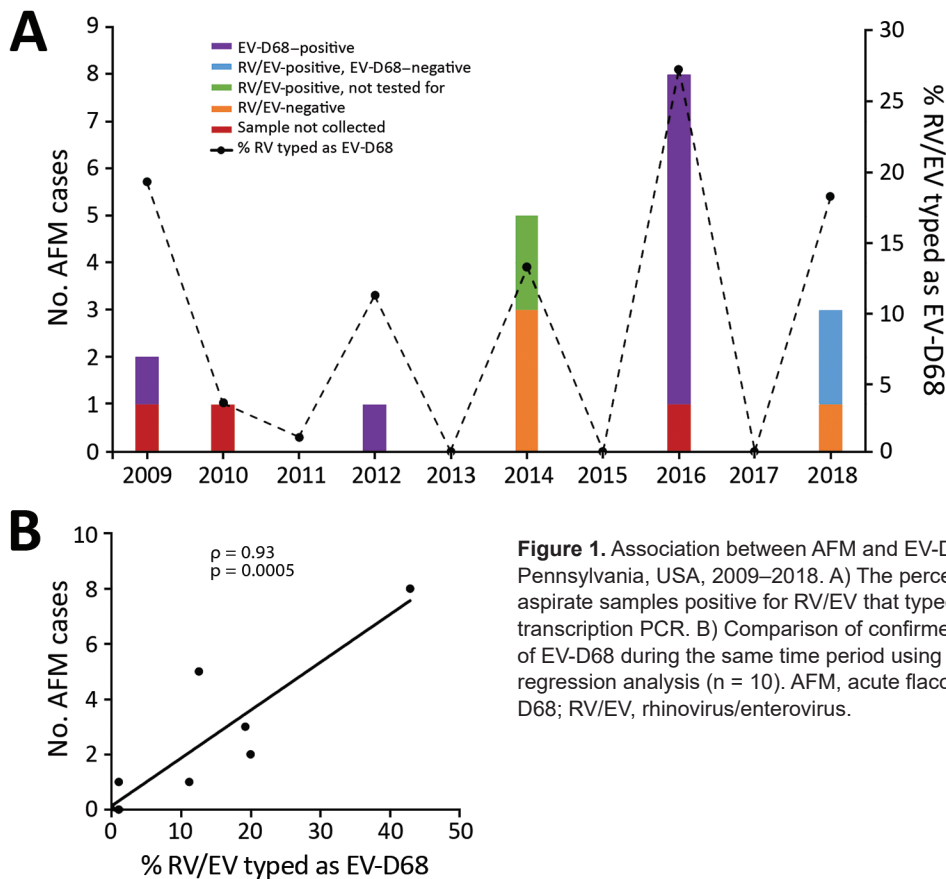


Figure 1. Association between AFM and EV-D68 prevalence, Philadelphia, Pennsylvania, USA, 2009–2018. A) The percentage of nasopharyngeal aspirate samples positive for RV/EV that typed as EV-D68 by real-time reverse transcription PCR. B) Comparison of confirmed AFM cases with the prevalence of EV-D68 during the same time period using Spearman correlation ρ and linear regression analysis ($n = 10$). AFM, acute flaccid myelitis; EV-D68, enterovirus D68; RV/EV, rhinovirus/enterovirus.

EV-D68, including 7 from 2016 (Figure 1, panel A). One of the children who tested positive, from 2009, had a respiratory sample collected that tested positive for RV/EV, but a residual sample was not available for retrospective analysis. However, a specimen collected 21 days later that also tested positive for RV/EV was available for retrospective EV-D68 typing. This sample was positive for RV/EV at a crossing cycle threshold (C_t) of 42 and typed as EV-D68 at a C_t of 38. The specimen collected when care was sought had a C_t of 22 for RV/EV, suggesting the sample from 21 days later was not a new infection. The remaining 10 AFM children who were not tested for EV-D68, or were negative, had either no infectious etiology identified (7 cases), an RV/EV detected that was not typed (2 cases), or a non-D68 enterovirus identified (1 case).

The high prevalence of EV-D68 in 2016 coincided with a high number of confirmed AFM cases at CHOP and led us to question whether the association could be investigated further back. We compared the number of AFM cases identified from August through November during 2009–2018 with the percentage of RV/EV-positive respiratory samples that typed as EV-D68 during the same period. We found a significant positive linear correlation between these 2 values over the decade sampled (Spearman ρ 0.93;

$p = 0.0005$; Figure 1, panel B). This finding suggests a strong association between circulation of EV-D68 and increases in AFM in children at CHOP.

Phylogenetic Analysis of EV-D68 WGS

To determine which clades were circulating in CHOP, we performed metagenomic sequencing on a subset of EV-D68-positive specimens collected during 2009–2018 from children without AFM (26 specimens) and from children with AFM (4 cases) for whom a residual sample was available. We were able to assemble complete polyprotein sequences from 28 of the 30 samples; 1 sample from 2009 and 1 from 2018 did not have sufficient EV-D68 genome coverage and were excluded from the analysis.

Phylogenetic analysis showed that EV-D68 from the study population in 2009 belonged to clade A (2 samples) and clade C (4 samples); 1 sample belonged to clade B1 (Figure 2, no. 13785). The clade B1 sample from 2009 showed 99.8% pairwise identity with a clade B1 sample from 2012 (Figure 2, no. 10549). By 2012, clade B1 was more common (3 samples); 1 sample belonged to clade A. As expected in 2014, all samples clustered in clade B1 but at a distinctly different lineage from the 2012 viruses identified from the study population (Figure 2). The 2016

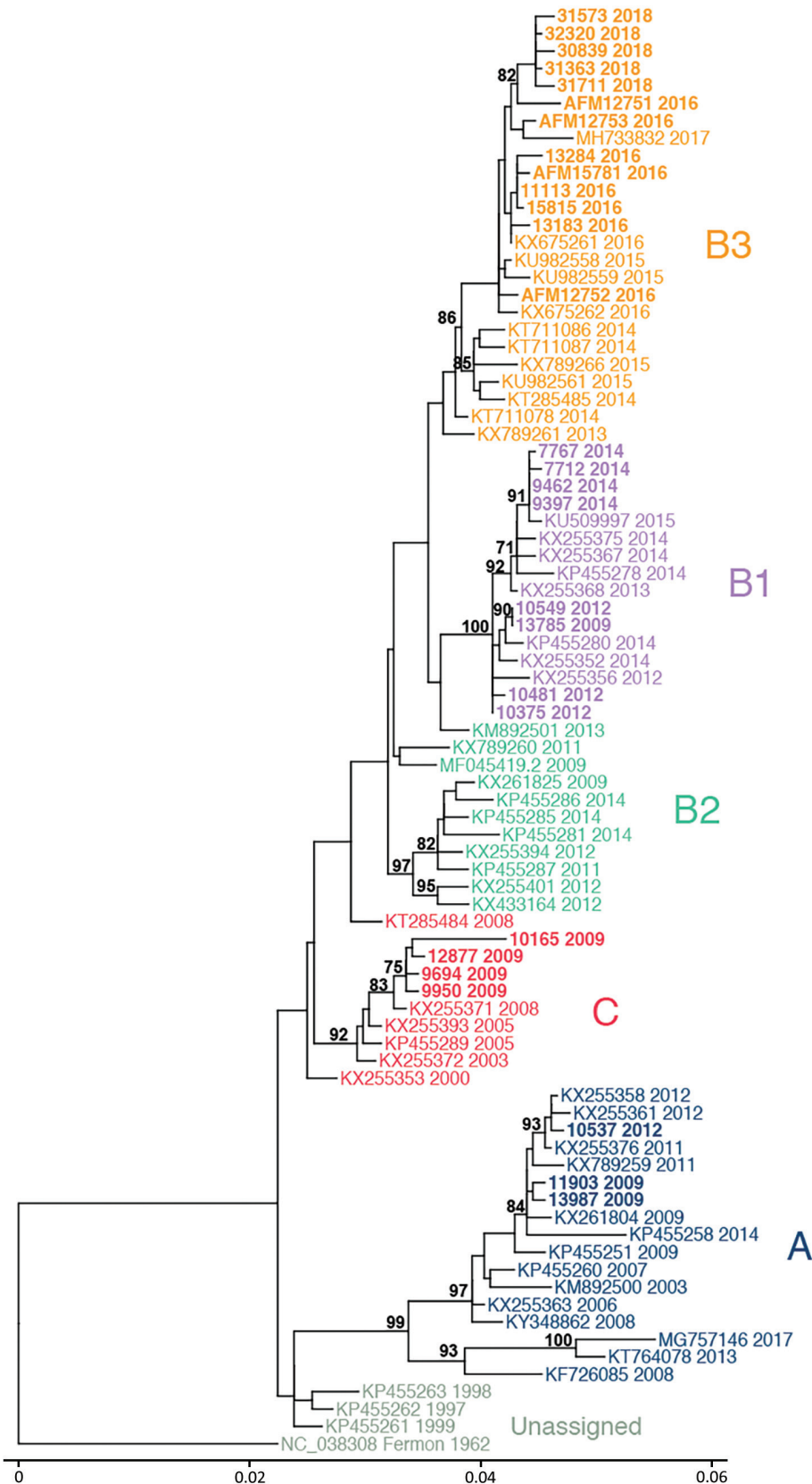


Figure 2. Phylogenetic relationships between Philadelphia whole enterovirus D68 (EV-D68) genomes, including AFM cases, Philadelphia, Pennsylvania, USA, 2009–2018. EV-D68 polyprotein sequences from GenBank (n = 55) and this study (n = 28) were used to build a maximum-likelihood tree. EV-D68 clades, defined in prior publications, are indicated. Sequences from this study are indicated in bold, and AFM cases are indicated with that prefix. AFM, acute flaccid myelitis. Scale bar indicates nucleotide substitutions per site.

samples clustered in clade B3, consistent with previous observations (17). AFM cases were interspersed with non-AFM cases from the same period. Phylogenetic analysis indicates that the 2016 clade B3 virus emerged from a common ancestor shared between the 2012 and 2014 clade B1 viruses and did not evolve directly from a previously circulating virus. In 2018, the samples continued to cluster in the B3 clade but formed a lineage distinct from the 2016 samples.

Protein and Nucleotide Changes in the EV-D68 Genome Circulating in Philadelphia during 2009–2018

We compared amino acid (aa) substitutions across the entire 2,190-aa polyprotein among the 28 whole EV-D68 genome sequences from our study. We observed 46 aa substitutions when we compared sequences across all years (Appendix Figure, panel A), many of which were previously described when comparing 2014 clade B1 and 2016 clade B3 viruses circulating in New York state (Appendix Table 1) (17). Not surprisingly, most of these (25 aa substitutions) were present in the viral capsid proteins, which are the primary focus of host immune responses but are also responsible for receptor binding and cell tropism (18). Only 2 aa substitutions, both in the viral protein (VP) 1 protein, were different for most viruses circulating in Philadelphia in 2016 and 2018. All other amino acid positions are largely conserved between 2016 and 2018 viruses. In a prior publication, 6 aa residues were implicated for possible neurotropism because of conservation between other neurotropic enteroviruses with different identities from nonneurotropic enteroviruses as well as rhinoviruses (16). These 6 residues (Appendix Table 1) were present in circulating 2014 viruses in our study. However, in 2016 and 2018, including the 4 AFM cases from CHOP that we were able to subject to WGS from 2016, the aa in these 6 positions were the same as the dominant sequence in 2009. We did not identify any conserved aa substitutions between sequences from the 2016 AFM cases that were not also conserved in other 2016 sequences from the CHOP population.

To investigate differences that might explain changes in neurotropism, we compared aa substitutions between the nonneurotropic Fermon strain and the CHOP sequences. We found 37 aa substitutions between the prototype Fermon strain and all circulating strains in Philadelphia during 2009–2018 (Appendix Table 1; Appendix Figure 1, panel A, bottom row). Twenty-six (70%) of these substitutions were present in the structural region of the polyprotein, VP4–VP1. To further investigate the potential significance of these 37 substitutions, we analyzed the changes through scoring as described by Grantham (19). A substitution at position 1641, different from the 1962 strain but conserved among all strains circulating in Philadelphia during 2009–2018, appears to have the highest deleterious effect on the

virus (Appendix Figure 1, panel B). This change, from cysteine to tyrosine, falls in the 3C viral protease that is responsible for cleaving the viral polyprotein. Other mutations with high scores include positions 379, 391, and 849, which correspond to the VP3 (379 and 391) and VP1 (849) capsid regions, respectively.

Like the structural proteins, the 5' untranslated region of enteroviruses is also implicated in cell tropism and neuropathogenesis because of differences in translational efficiency (20). We saw little diversity in this region between years with 8 single-nucleotide polymorphisms between years and 1 nt (620) that was deleted in all 2018 sequences but was not in prior years (Appendix Table 2). A previously identified deletion that has been described in sequences from the United Kingdom and Japan (21) was also observed in all 2014–2018 sequences and was found in 4 of 7 sequences from 2009 and in 3 of 4 from 2012. As with the amino acid comparisons, we found no genetic changes in the 5' untranslated region of all 4 AFM cases that were not also conserved in other non-AFM sequences from the same year. We identified 2 differences between the prototype 1962 Fermon strain and all EV-D68 in our study. A single deletion at nt 29 was observed in the Fermon strain, as well as a large deletion from nt 682–704 (Appendix Table 2) that previously was described in the same study from the United Kingdom and Japan (21).

Discussion

In this 10-year longitudinal study, we showed that EV-D68 circulated in a biennial pattern among children at a hospital in Philadelphia, and circulation was widespread in even years, except for a peak in 2009 and largely absent circulation in 2010–2011. AFM cases peaked during the same years in the study population, and prevalence of EV-D68 correlated significantly with the number of AFM cases during the past decade. Half of the AFM cases were associated with EV-D68 through retrospective detection in archived respiratory samples, including a case from 2009 that would be the second earliest detection of an association between EV-D68 and AFM (22). For 10 EV-D68-positive cases, no other infectious etiology was identified despite extensive testing.

Genomic analysis revealed an interesting evolutionary pattern of EV-D68 in the CHOP population. As we reported in this study, clades A and C dominated in 2009. However, we also identified a single specimen with clade B1 sequence, which slightly predates modeled estimates (16). The evolution of lineages within a clade during 2012–2014 and again during 2016–2018 sharply contrasted with the introduction of the new B3 clade from 2014 through 2016. The 2016 clade B3 virus emerged from a common ancestor of the 2012–2014 clade B1 viruses rather than directly evolving from them. It is possible this happened over time from a minor population in Philadelphia. However, it is

more likely that a new EV-D68 was introduced from a location outside the region, given that the B3 clade had been reported in 2015 (23), predating the 2016 CHOP outbreak. This finding has important implications about immunity within Philadelphia because we might expect another clade to emerge in 2020 based on this pattern.

US and worldwide circulation patterns of EV-D68 remain unclear. Like other enteroviruses, EV-D68 appears to skip some years in certain locations, although the years skipped are not universal across continents, even in the same hemisphere. For example, despite a high prevalence of EV-D68 even among adults in Europe in 2010 (3,4,21,24) and in Thailand in 2010 and 2011 (25), it was nearly quiescent in the United States during that time. Surveillance data from CDC indicate EV-D68 was the most commonly detected enterovirus in 2009, with less frequent detection in 2011 and almost complete absence in 2010 and 2012 (26). The peaks in 2012, 2014, and 2018 were consistent with reports from other US pediatric institutions (11,12). However, the increase we found in 2016, while consistent with reports from the Netherlands (27), was greater than that reported in 2 other studies of US children (8,9). Taken together, these data suggest that local pockets of transmission can occur, leading to bias in surveillance programs that rely on passive reporting or submission of specimens.

Despite mounting data, EV-D68–associated AFM remains controversial given that EV-D68 is rarely isolated from CSF. Only a handful of cases have identified EV-D68 in the central nervous system, including 1 postmortem detection (13,22). In our study, we focused on respiratory specimens because the respiratory tract is the most common site of EV-D68 replication. Consistent with other studies (16), enterovirus was not detected by standard-of-care PCR in the CSF in the cohort of EV-D68–positive children with AFM at CHOP. That being said, the cases of AFM positive for EV-D68 we describe had no other infectious etiology identified despite extensive testing.

Our study had several limitations, including small sample size and failure to detect an infectious etiology in 9 AFM cases. Of these 9 children, 7 had no positive infectious testing (although 3 did not have a respiratory specimen collected/tested) and 2 had a respiratory specimen positive for RV/EV, but the type was not identified. It remains possible that these children were sampled too late, because earlier respiratory sampling (≤ 1 week from symptom onset) is associated with higher detection rates of EV-D68 (7).

Our study has several other important limitations. Archived specimens were tested after storage in -80°C for up to almost a decade. Although it is unlikely that viral RNA degraded during this time because these samples were not thawed before use for this study, it remains possible that EV-D68 detection rates could have been higher in prospectively tested specimens. With the exception of AFM

samples, there was selection bias to sequence specimens with higher viral titers ensuring genome coverage. As a result, the clades observed might be misrepresentations for each year. Although samples with weaker viral titers are unlikely to track with specific clades, it is possible. Finally, all of the samples in this study were collected from a tertiary-care hospital serving a limited catchment area of 1 state, making it difficult to extrapolate EV-D68 circulation patterns and strain diversity over broader geographic regions of the United States.

The data presented here strengthen the association between EV-D68 infection and AFM. They also support the need for continued surveillance for EV-D68 in the United States and worldwide as the virus continues to circulate perhaps biennially, with unique prevalence in geographic pockets. Genomic analysis, particularly WGS, is also critical to clarify transmission, clade changes, and subsequent implications for immunity. WGS is also important for the association of specific genomic changes with the ability of the virus to cause AFM, requiring experimental analysis of mutations analogous to the extensive work done in poliovirus and enterovirus 71. Overall, these data reinforce the need to improve EV-D68 surveillance programs as a means of identifying possible AFM triggers that may lead to therapeutic interventions for this severe condition.

Acknowledgments

We acknowledge members of CHOP's Infectious Disease Diagnostics Laboratory (and former Virology Laboratory) for archiving, retrieving, and extracting specimens.

About the Author

Dr. Uprety is a clinical microbiology postdoctoral fellow at the Perelman School of Medicine, University of Pennsylvania, and CHOP. Her primary research interests include applications of clinical metagenomics and molecular epidemiology.

References

1. Midgley CM, Jackson MA, Selvarangan R, Turabelidze G, Obringer E, Johnson D, et al. Severe respiratory illness associated with enterovirus D68—Missouri and Illinois, 2014. *MMWR Morb Mortal Wkly Rep.* 2014;63:798–9.
2. Pastula DM, Aliabadi N, Haynes AK, Messacar K, Schreiner T, Maloney J, et al.; Centers for Disease Control and Prevention (CDC). Acute neurologic illness of unknown etiology in children—Colorado, August–September 2014. *MMWR Morb Mortal Wkly Rep.* 2014;63:901–2.
3. Tokarz R, Firth C, Madhi SA, Howie SR, Wu W, Sall AA, et al. Worldwide emergence of multiple clades of enterovirus 68. *J Gen Virol.* 2012;93:1952–8. <http://dx.doi.org/10.1099/vir.0.043935-0>
4. Rahamat-Langendoen J, Riezebos-Brilman A, Borger R, van der Heide R, Brandenburg A, Schölvinc E, et al. Upsurge of human enterovirus 68 infections in patients with severe respiratory tract infections. *J Clin Virol.* 2011;52:103–6. <http://dx.doi.org/10.1016/j.jcv.2011.06.019>

5. Aliabadi N, Messacar K, Pastula DM, Robinson CC, Leshem E, Sejvar JJ, et al. Enterovirus D68 infection in children with acute flaccid myelitis, Colorado, USA, 2014. *Emerg Infect Dis.* 2016;22:1387–94. <http://dx.doi.org/10.3201/eid2208.151949>
6. Messacar K, Schreiner TL, Maloney JA, Wallace A, Ludke J, Oberste MS, et al. A cluster of acute flaccid paralysis and cranial nerve dysfunction temporally associated with an outbreak of enterovirus D68 in children in Colorado, USA. *Lancet.* 2015; 385:1662–71. [http://dx.doi.org/10.1016/S0140-6736\(14\)62457-0](http://dx.doi.org/10.1016/S0140-6736(14)62457-0)
7. Sejvar JJ, Lopez AS, Cortese MM, Leshem E, Pastula DM, Miller L, et al. Acute flaccid myelitis in the United States, August–December 2014: results of nationwide surveillance. *Clin Infect Dis.* 2016;63:737–45. <http://dx.doi.org/10.1093/cid/ciw372>
8. Srinivasan M, Niesen A, Storch GA. Enterovirus D68 surveillance, St. Louis, Missouri, USA, 2016. *Emerg Infect Dis.* 2018;24:2115–7. <http://dx.doi.org/10.3201/eid2411.180397>
9. Messacar K, Robinson CC, Pretty K, Yuan J, Dominguez SR. Surveillance for enterovirus D68 in Colorado children reveals continued circulation. *J Clin Virol.* 2017;92:39–41. <http://dx.doi.org/10.1016/j.jcv.2017.05.009>
10. McKay SL, Lee AD, Lopez AS, Nix WA, Dooling KL, Keaton AA, et al. Increase in acute flaccid myelitis—United States, 2018. *MMWR Morb Mortal Wkly Rep.* 2018;67:1273–5. <http://dx.doi.org/10.15585/mmwr.mm6745e1>
11. Kujawski SA, Midgley CM, Rha B, Lively JY, Nix WA, Curns AT, et al. Enterovirus D68-associated acute respiratory illness—New Vaccine Surveillance Network, United States, July–October, 2017 and 2018. *MMWR Morb Mortal Wkly Rep.* 2019;68:277–80. <http://dx.doi.org/10.15585/mmwr.mm6812a1>
12. Messacar K, Pretty K, Reno S, Dominguez SR. Continued biennial circulation of enterovirus D68 in Colorado. *J Clin Virol.* 2019;113:24–6. <http://dx.doi.org/10.1016/j.jcv.2019.01.008>
13. Messacar K, Asturias EJ, Hixon AM, Van Leer-Buter C, Niesters HGM, Tyler KL, et al. Enterovirus D68 and acute flaccid myelitis—evaluating the evidence for causality. *Lancet Infect Dis.* 2018;18:e239–47. [http://dx.doi.org/10.1016/S1473-3099\(18\)30094-X](http://dx.doi.org/10.1016/S1473-3099(18)30094-X)
14. Dyda A, Stelzer-Braid S, Adam D, Chughtai AA, MacIntyre CR. The association between acute flaccid myelitis (AFM) and enterovirus D68 (EV-D68)—what is the evidence for causation? *Euro Surveill.* 2018;23:23. <http://dx.doi.org/10.2807/1560-7917.ES.2018.23.3.17-00310>
15. Hixon AM, Yu G, Leser JS, Yagi S, Clarke P, Chiu CY, et al. A mouse model of paralytic myelitis caused by enterovirus D68. *PLoS Pathog.* 2017;13:e1006199. <http://dx.doi.org/10.1371/journal.ppat.1006199>
16. Greninger AL, Naccache SN, Messacar K, Clayton A, Yu G, Somasekar S, et al. A novel outbreak enterovirus D68 strain associated with acute flaccid myelitis cases in the USA (2012–14): a retrospective cohort study. *Lancet Infect Dis.* 2015;15:671–82. [http://dx.doi.org/10.1016/S1473-3099\(15\)70093-9](http://dx.doi.org/10.1016/S1473-3099(15)70093-9)
17. Wang G, Zhuge J, Huang W, Nolan SM, Gilrane VL, Yin C, et al. Enterovirus D68 subclade B3 strain circulating and causing an outbreak in the United States in 2016. *Sci Rep.* 2017;7:1242. <http://dx.doi.org/10.1038/s41598-017-01349-4>
18. Yuan J, Shen L, Wu J, Zou X, Gu J, Chen J, et al. Enterovirus A71 proteins: structure and function. *Front Microbiol.* 2018;9:286. <http://dx.doi.org/10.3389/fmicb.2018.00286>
19. Grantham R. Amino acid difference formula to help explain protein evolution. *Science.* 1974;185:862–4. <http://dx.doi.org/10.1126/science.185.4154.862>
20. McGoldrick A, Macadam AJ, Dunn G, Rowe A, Burlison J, Minor PD, et al. Role of mutations G-480 and C-6203 in the attenuation phenotype of Sabin type 1 poliovirus. *J Virol.* 1995;69:7601–5.
21. Lauinger IL, Bible JM, Halligan EP, Aarons EJ, MacMahon E, Tong CY. Lineages, sub-lineages and variants of enterovirus 68 in recent outbreaks. *PLoS One.* 2012;7:e36005. <http://dx.doi.org/10.1371/journal.pone.0036005>
22. Kreuter JD, Barnes A, McCarthy JE, Schwartzman JD, Oberste MS, Rhodes CH, et al. A fatal central nervous system enterovirus 68 infection. *Arch Pathol Lab Med.* 2011;135:793–6.
23. Kaida A, Iritani N, Yamamoto SP, Kanbayashi D, Hirai Y, Togawa M, et al. Distinct genetic clades of enterovirus D68 detected in 2010, 2013, and 2015 in Osaka City, Japan. *PLoS One.* 2017;12:e0184335. <http://dx.doi.org/10.1371/journal.pone.0184335>
24. Holm-Hansen CC, Midgley SE, Fischer TK. Global emergence of enterovirus D68: a systematic review. *Lancet Infect Dis.* 2016; 16:e64–75. [http://dx.doi.org/10.1016/S1473-3099\(15\)00543-5](http://dx.doi.org/10.1016/S1473-3099(15)00543-5)
25. Linsuwanon P, Puenpa J, Suwannakam K, Auksornkitti V, Vichiwattana P, Korkong S, et al. Molecular epidemiology and evolution of human enterovirus serotype 68 in Thailand, 2006–2011. *PLoS One.* 2012;7:e35190. <http://dx.doi.org/10.1371/journal.pone.0035190>
26. Abedi GR, Watson JT, Pham H, Nix WA, Oberste MS, Gerber SI. Enterovirus and human parechovirus surveillance—United States, 2009–2013. *MMWR Morb Mortal Wkly Rep.* 2015;64:940–3. <http://dx.doi.org/10.15585/mmwr.mm6434a3>
27. Knoester M, Schölvinck EH, Poelman R, Smit S, Vermont CL, Niesters HG, et al. Upsurge of enterovirus D68, the Netherlands, 2016. *Emerg Infect Dis.* 2017;23:140–3. <http://dx.doi.org/10.3201/eid2301.161313>

Address for correspondence: Erin H. Graf, Children’s Hospital of Philadelphia, 3401 Civic Center Blvd, Philadelphia, PA 19104, USA; email: grafe@email.chop.edu

Risk for *Clostridioides difficile* Infection among Older Adults with Cancer

Mini Kamboj, Renee L. Gennarelli, Jennifer Brite, Kent Sepkowitz, Allison Lipitz-Snyderman

Medscape **ACTIVITY** EDUCATION

In support of improving patient care, this activity has been planned and implemented by Medscape, LLC and Emerging Infectious Diseases. Medscape, LLC is jointly accredited by the Accreditation Council for Continuing Medical Education (ACCME), the Accreditation Council for Pharmacy Education (ACPE), and the American Nurses Credentialing Center (ANCC), to provide continuing education for the healthcare team.

Medscape, LLC designates this Journal-based CME activity for a maximum of 1.00 **AMA PRA Category 1 Credit(s)**[™]. Physicians should claim only the credit commensurate with the extent of their participation in the activity.

Successful completion of this CME activity, which includes participation in the evaluation component, enables the participant to earn up to 1.0 MOC points in the American Board of Internal Medicine's (ABIM) Maintenance of Certification (MOC) program. Participants will earn MOC points equivalent to the amount of CME credits claimed for the activity. It is the CME activity provider's responsibility to submit participant completion information to ACCME for the purpose of granting ABIM MOC credit.

All other clinicians completing this activity will be issued a certificate of participation. To participate in this journal CME activity: (1) review the learning objectives and author disclosures; (2) study the education content; (3) take the post-test with a 75% minimum passing score and complete the evaluation at <http://www.medscape.org/journal/eid>; and (4) view/print certificate. For CME questions, see page 1790.

Release date: August 21, 2019; Expiration date: August 21, 2020

Learning Objectives

Upon completion of this activity, participants will be able to:

- Describe findings of factors affecting risk for *Clostridioides difficile* infection (CDI) in older adults, according to a retrospective cohort study analysis using population-based SEER-Medicare data for 2011
- Determine findings of factors affecting risk for CDI in older adults, according to a nested case-control study analysis using population-based SEER-Medicare data for 2011
- Identify clinical implications of risk factors for CDI in older adults, according to a retrospective cohort study with a nested case-control analysis using population-based SEER-Medicare data for 2011

CME Editor

P. Lynne Stockton Taylor, VMD, MS, ELS(D), Technical Writer/Editor, Emerging Infectious Diseases. *Disclosure: P. Lynne Stockton Taylor, VMD, MS, ELS(D), has disclosed no relevant financial relationships.*

CME Author

Laurie Barclay, MD, freelance writer and reviewer, Medscape, LLC. *Disclosure: Laurie Barclay, MD, has disclosed no relevant financial relationships.*

Authors

Disclosure: Mini Kamboj, MD; Renee Lynn Gennarelli, MS; Jennifer Brite, DrPH; Kent Sepkowitz, MD; and Allison Lipitz-Snyderman, PhD, have disclosed no relevant financial relationships.

Author affiliations: Memorial Sloan Kettering Cancer Center, New York, New York, USA (M. Kamboj, R.L. Gennarelli, J. Brite, K. Sepkowitz, A. Lipitz-Snyderman); Weill Cornell Medical College, New York (M. Kamboj, K. Sepkowitz)

DOI: <https://doi.org/10.3201/eid2509.181142>

To assess whether risk for *Clostridioides difficile* infection (CDI) is higher among older adults with cancer, we conducted a retrospective cohort study with a nested case-control analysis using population-based Surveillance, Epidemiology, and End Results-Medicare linked data for 2011. Among 93,566 Medicare beneficiaries, incident CDI and odds for

acquiring CDI were higher among patients with than without cancer. Specifically, risk was significantly higher for those who had liquid tumors and higher for those who had recently diagnosed solid tumors and distant metastasis. These findings were independent of prior healthcare-associated exposure. This population-based assessment can be used to identify targets for prevention of CDI.

Healthcare-associated infections are common and often preventable infections that lead to high morbidity and mortality rates (1). The bacterium *Clostridioides difficile* (formerly *Clostridium difficile*) causes inflammation of the colon, which commonly causes diarrhea. In the United States, *C. difficile* infection (CDI) is the leading cause of healthcare-associated infections (2).

Among the general population, the risk for CDI among older adults (≥ 65 years of age) is up to 26 times greater than that among younger adults (2). The effects of this infection are also worse for older persons. In 2015, CDI ranked as the 18th leading cause of death for persons ≥ 65 years of age (3). Although persons in this age group accounted for only 48% of CDI cases, they accounted for $\approx 87\%$ of deaths from CDI (3,4).

For older adults, the risk for CDI may be amplified even further by cancer or its treatment. Common factors that influence risk for CDI in general are advanced age, diminished humoral immune response, healthcare-associated exposures, and extended receipt of antimicrobial drugs, all of which are widely prevalent aspects of oncologic and supportive care (5). In addition, exposure to certain cytotoxic chemotherapeutic drugs has been postulated to induce a loss of resistance to colonization with *C. difficile*, although the mechanisms are unclear (6,7). Yet, the complex relationship between cancer in older adults and CDI remains weakly characterized at the population level (8,9).

Our objective with this study was to determine whether the risk for CDI is higher among older adults with cancer than among older adults without cancer. A population-level assessment of cancer-specific incidence of CDI among older adults would not only increase our knowledge of the disease epidemiology in this specialized population but could also guide primary prevention strategies, focusing on those at greatest risk for development of this complication.

Methods

Study Design

This study was considered exempt research by the institutional review board of Memorial Sloan Kettering Cancer Center (New York, New York, USA). Use of Surveillance, Epidemiology, and End Results (SEER)–Medicare data for this study was approved by the National Cancer Institute (Bethesda, MD, USA).

We conducted a retrospective cohort study with a nested case–control analysis and used population-based SEER–Medicare–linked data to assess CDI occurrence in 2011. The National Cancer Institute–sponsored SEER program includes regions that cover $\approx 28\%$ of the US population. SEER registries include information about cancer site, initial treatments, and active follow-up for death. The SEER–Medicare dataset links cancer registry files with Medicare enrollment information and claims for Medicare beneficiaries with a diagnosis of cancer. Compared with the US older adult population, the SEER–Medicare cohort has a similar age and sex distribution, slightly higher proportion of patients residing in urban and high-income areas, and smaller proportion of nonwhite persons (10). We used the random 5% sample of Medicare beneficiaries who reside in SEER regions to identify non–cancer patients.

Study Participants

We included Medicare beneficiaries with and without a cancer diagnosis. For beneficiaries with cancer, we included those with solid (breast, colon, lung, prostate, and head and neck cancers) and liquid (lymphoma, myeloma, leukemia) tumors diagnosed during 2006–2010. We required that participants had been ≥ 66 years of age at the time of diagnosis to allow for 1 year of claims to assess prior healthcare use and CDI diagnoses. For inclusion in the non–cancer patient sample, we required that Medicare beneficiaries had been ≥ 66 years of age at the start of 2011 with no history of cancer.

All patients included in the cohort had to have been hospitalized ≥ 1 time in 2011. We excluded those for whom Medicare Parts A and B coverage during 2010–2011 was incomplete and those who had a diagnosis of CDI in 2010 (the year before our study year).

Variables

CDI diagnoses were based on code 008.45 of the International Classification of Diseases, 9th Revision, on an inpatient claim. Because of a lack of dates for diagnosis codes on inpatient claims, the admission date of the first claim with a CDI diagnosis was used as the CDI date. We examined the following patient characteristics: age, sex, race, geographic region, urban/rural location, hospitalizations from the prior year (within 12 months before the index date), and stays in a skilled nursing facility from the prior year (within 12 months before the index date). Cancer status was categorized as cancer versus no cancer, as solid versus liquid tumors, and by individual disease types. For cancer patients, stage at diagnosis was categorized according to the SEER historic staging variable: in situ, local/regional, or distant or unknown.

Cohort Analysis

We determined CDI incidence in 2011 for hospitalized patients with and without cancer. Incidence was reported

as the percentage of the cohort in whom CDI developed during the study period. We also examined the overall proportion of patients with CDI and CDI incidence by patient characteristics.

Nested Case–Control Analysis

We included all patients with a diagnosis of CDI in 2011 in the nested case–control analysis; the index date was defined as the date of first CDI diagnosis in 2011. We randomly selected 5 control participants for each case-patient, matched by age (± 1 year) at study start date (January 1, 2011) and sex. The index date for each control was the date of CDI for the matched case-patient. Each matched control must have had follow-up through at least the case-patient's index date with no occurrence of CDI from study start date through index date. Case-patients could not be their own controls, but a case-patient was eligible to be a control for another case-patient if the criteria were met.

We compared the cancer status and other characteristics of the case-patients and controls. We used conditional logistic regression models for individually matched case-patients and controls to obtain the odds of CDI among those with a cancer diagnosis. We calculated adjusted and unadjusted odds ratios (ORs) for CDI by tumor type, stage at diagnosis, and year of diagnosis; the reference group was non-cancer patients. The stage-specific model was run for solid tumors with the following 3 SEER categories: in situ, locoregional, or distant versus no cancer (reference group). Odds of CDI for patients with liquid tumors were not reported because liquid tumors are staged as distant disease. Odds of CDI occurrence were also calculated by prior hospitalizations and prior stays at a skilled nursing facility. All conditional logistic regression models included as covariates patient race, geographic region, urban/rural location, cancer status, prior hospitalizations, and prior stays at a skilled nursing facility. For the case–control analysis, we used stays within 12 months before a patient's index date to define prior hospitalizations and prior skilled nursing facility stays.

To examine associations among cancer patients who were likely to actively receive treatment, we also repeated the analysis for patients whose cancer was diagnosed during 2009–2010 only and those without a cancer diagnosis. We used the same method to obtain new matched case-patients and controls for this analysis. We considered $p < 0.05$ to be statistically significant. All analyses were conducted by using SAS version 9.4 (SAS Institute Inc., <https://www.sas.com>).

Results

Cohort Analysis

For the 93,566 beneficiaries in the study cohort, 2.6% had CDI during the study period. In unadjusted analyses, a

higher proportion of patients with cancer had CDI (2.8%) than did patients without cancer (2.4%). The proportion with CDI was higher among female patients and patients living in the Northeast and metropolitan areas. When we analyzed by 5-year age intervals, we found an incremental increase in CDI risk, from 1.9% among patients 66–69 years of age to 2.9% among patients ≥ 85 years of age (Table 1).

Nested Case–Control Analysis

For the 2,421 case-patients with CDI, we identified 12,105 matched controls. A higher proportion of case-patients (54%) than controls (49%) had cancer. The distribution of race was similar among case-patients and controls, but distribution by geography differed slightly. Higher proportions of case-patients than controls had been hospitalized multiple times before or had stayed in a skilled nursing facility (Table 2).

The odds of CDI developing were higher among cancer patients than non-cancer patients (adjusted OR 1.15, 95% CI 1.04–1.26; $p = 0.005$). When cancer was subdivided into solid and liquid tumor types, having a solid tumor was not significantly associated with an increased risk for CDI compared with having no cancer diagnosis (adjusted OR 1.05, 95% CI 0.95–1.16); an underlying diagnosis of a liquid tumor was significantly associated with increased risk for CDI compared with no cancer diagnosis (adjusted OR 1.74, 95% CI 1.48–2.06; $p < 0.001$). When we restricted the analysis to only patients who had received a cancer diagnosis within the past 2 years or no cancer diagnosis at

Table 1. *Clostridioides difficile* infection, by cohort characteristics, in study of risk among older adults with cancer, United States

Characteristic	Total no.	% Patients with <i>C. difficile</i> infection
Total	93,566	2.6
Cancer status		
Cancer	47,323	2.8
No cancer	46,243	2.4
Age, y		
66–69	12,001	1.9
70–74	20,691	2.4
75–79	20,155	2.6
80–84	18,651	2.8
≥ 85	22,068	2.9
Sex		
M	42,330	2.4
F	51,236	2.8
Race		
White	77,831	2.6
Black	8,885	2.6
Other/unknown	6,850	2.2
Urban/rural		
Metropolitan	76,808	2.8
Not metropolitan	16,703	1.8
US region		
West	36,726	2.5
Midwest	12,086	3.0
South	24,980	2.0
Northeast	19,774	3.3

Table 2. Characteristics of case-patients and controls in study of *Clostridioides difficile* infection in older adults with cancer, United States

Characteristic	% Total case-patients, n = 2,421	% Total controls, n = 12,105
Cancer diagnosis		
No cancer	46	51
Solid tumor	43	43
Liquid tumor	12	7
Age, y*		
66–69	10	10
70–74	20	21
75–79	21	21
80–84	22	22
≥85	27	27
Sex*		
M	41	41
F	59	59
Race		
White	84	83
Black	10	9
Other/unknown	6	7
Urban/rural		
Metropolitan	87	83
Not metropolitan	13	17
US region		
West	38	40
Midwest	15	13
South	20	26
Northeast	27	21
Prior hospitalizations†		
0	20	37
1	18	32
2	19	16
3	12	6
4	10	4
>5	22	5
Prior skilled nursing facility stay†		
No	56	83
Yes	44	18

*Case-patients with *Clostridioides difficile* infection were matched to controls without *C. difficile* infection, by age and sex.

†Stays within 12 mo before a patient's index date were used to define prior hospitalizations and prior skilled nursing facility stays.

all, we found that both solid and liquid tumor types were significantly associated with increased odds of CDI compared with no cancer diagnosis (Tables 3, 4). Regardless of a cancer diagnosis, ≥2 prior hospitalizations or a prior stay at a skilled nursing facility were each associated with increased odds of CDI occurrence (Table 3).

Findings from our adjusted stage-specific model demonstrated that the odds of CDI were higher for patients with a solid tumor than for those with no cancer (Figure). Odds of CDI were also higher for patients with solid cancer at an unknown stage at diagnosis, although this finding probably depends on the constructs of the historic staging variable in SEER. Odds of CDI did not differ significantly for cancer patients with in situ or local/regionalized solid tumors at diagnosis, compared with non-cancer patients.

Discussion

The main findings of our study, derived from a population-based cohort of Medicare beneficiaries >65 years of age, indicate that the risk for CDI is greater for older adults undergoing treatment for cancer than for age-matched controls. We show that much of this excess risk is associated with the type of underlying cancer and advanced disease and remains independent of prior health-care-associated exposure from inpatient and skilled nursing facility stays. Risk was highest for patients with hematologic malignancies. In comparison, for solid tumor patients, odds of developing CDI were higher only for those with a recent cancer diagnosis and those with distant metastasis at diagnosis.

Our findings collectively expand knowledge of how cancer diagnosis affects CDI-associated illness among older adults. Reports of CDI in the absence of exposure to antimicrobial drugs has been well described for patients receiving cytotoxic chemotherapy (11), plausibly related to

Table 3. Odds ratios of infection occurrence, nested case-control analysis in study of *Clostridioides difficile* infection in older adults with cancer

Characteristic	Primary analysis: cancer patients and non-cancer patients*			
	Unadjusted OR (95% CI)	p value	Adjusted OR (95% CI)†	p value
Tumor type				
None	1.00		1.00	
Solid	1.13 (1.03–1.24)	0.01	1.05 (0.95–1.16)	0.32
Liquid	1.94 (1.67–2.26)	<0.001	1.74 (1.48–2.06)	<0.001
Prior hospitalizations				
0	1.00		1.00	
1	1.11 (0.96–1.28)	0.15	1.07 (0.93–1.23)	0.37
2	2.33 (2.02–2.69)	<0.001	1.83 (1.56–2.14)	<0.001
3	3.55 (2.99–4.20)	<0.001	2.68 (2.22–3.23)	<0.001
4	4.93 (4.09–5.96)	<0.001	3.49 (2.81–4.31)	<0.001
≥5	8.63 (7.39–10.09)	<0.001	5.76 (4.74–6.99)	<0.001
Prior skilled nursing facility stay				
No	1.00		1.00	
Yes	3.93 (3.56–4.33)	<0.001	1.59 (1.39–1.82)	<0.001

*For cancer patients, diagnosis was made during 2006–2010. OR, odds ratio.

†Adjusted odds of *C. difficile* infection based on conditional logistic regression model. Adjusted for age, sex, race, geographic region, urban/rural location, prior hospitalizations, and prior skilled nursing facility stays. Separate models were conducted for all patients with a cancer diagnosed 2006–2010 and noncancer patients, and for recently diagnosed cancer patients (diagnosis 2009–2010) and non-cancer patients.

Table 4. Adjusted odds ratios of *Clostridioides difficile* infection occurrence, nested case-control analysis

Characteristic	Subanalysis: recently diagnosed cancer patients and non-cancer patients*			
	Unadjusted OR (95% CI)	p value	Adjusted OR (95% CI)†	p value
Tumor type				
None	1.00		1.00	
Solid	1.36 (1.22–1.53)	0.01	1.24 (1.10–1.40)	<0.001
Liquid	2.22 (1.83–2.69)	<0.001	1.84 (1.49–2.26)	<0.001
Prior hospitalizations				
0	1.00		1.00	
1	1.13 (0.96–1.33)	0.13	1.07 (0.91–1.26)	0.40
2	2.28 (1.94–2.68)	<0.001	1.73 (1.44–2.08)	<0.001
3	3.17 (2.60–3.86)	<0.001	2.32 (1.86–2.88)	<0.001
4	4.31 (3.48–5.33)	<0.001	2.92 (2.29–3.72)	<0.001
≥5	8.34 (7.00–9.94)	<0.001	5.25 (4.21–6.55)	<0.001
Prior skilled nursing facility stay				
No	1.00		1.00	
Yes	3.80 (3.40–4.24)	<0.001	1.64 (1.41–1.92)	<0.001

*For cancer patients, diagnosis was made during 2009–2010. OR, odds ratio.

†Adjusted odds of CDI based on conditional logistic regression model. Adjusted for age, sex, race, geographic region, urban/rural location, prior hospitalizations, and prior skilled nursing facility stays. Separate models were conducted with all patients with a cancer diagnosis during 2006–2010 and noncancer patients, and for recently diagnosed cancer patients (those diagnosed 2009–2010) and noncancer patients.

intestinal dysbiosis caused by these agents. In our study, the occurrence of CDI seemed to be influenced by active oncologic therapy among patients with solid tumors, as suggested by the heightened risk at the time of new diagnosis, when the intensity of treatment is expected to be greater. Similarly, the CDI risk for patients with solid tumors was also higher for those with distant site metastases at the time of diagnosis, underscoring the complexities in management of advanced cancers. We cannot determine from this study whether these associations are driven by type of cancer treatment, excessive use of antimicrobial drugs, or a consequence of immunologic and microbial perturbation associated with cancer treatment in persons of advanced age.

We were unable to quantify antecedent exposure to antimicrobial drugs, a major driver of CDI (12–15); the coexistence of several confounding factors makes this distinction particularly challenging. When we made risk adjustments for race, geographic region, type of healthcare facility, and number of prior healthcare facility stays, the odds of CDI in patients with liquid tumors were significantly higher. Similar to previous studies of non-cancer populations, we found an incremental increase in CDI risk with number of hospitalizations; risk for those with >3 hospital stays was 3-fold higher (12,16).

Symptoms of primary and recurrent CDI can be particularly debilitating in persons with advanced age and

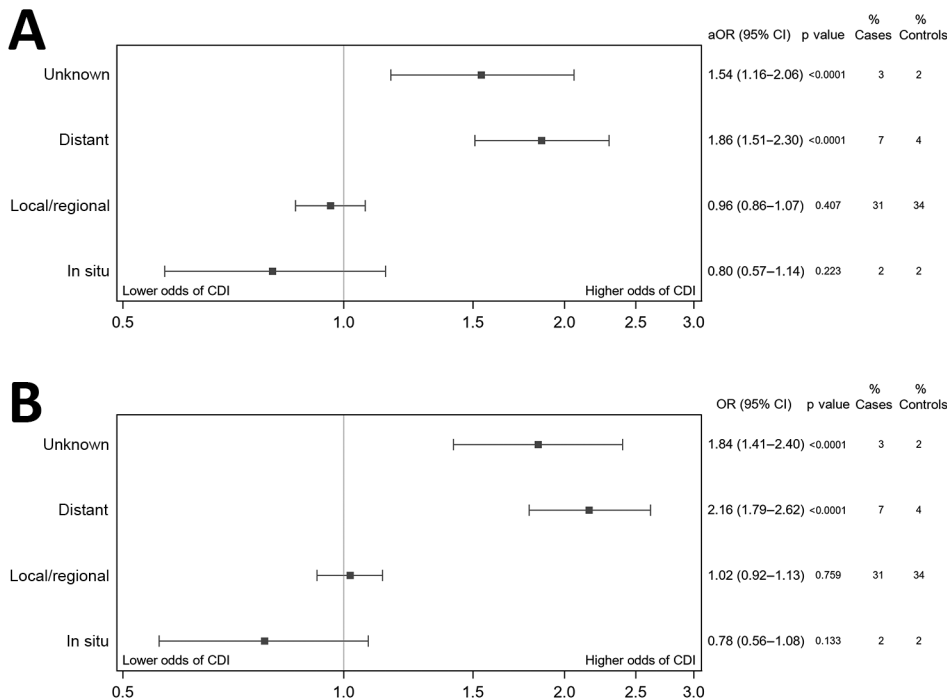


Figure. Adjusted (A) and unadjusted (B) odds of CDI for cancer patients with solid tumor compared with non-cancer patients. Stage is based on Surveillance, Epidemiology, and End Results historic staging variable. aOR estimates were generated from a logistic regression model adjusted for age, sex, race geographic region, urban/rural location, prior hospitalization, and prior skilled nursing stay. Non-cancer patients serve as the reference group, indicated by the reference line at 1.0. Error bars indicate 95% CIs. aOR, adjusted odds ratio; CDI, *Clostridioides difficile* infection; OR, odds ratio.

are frequently associated with postinfectious irritable bowel syndrome (5). In patients receiving concomitant cancer therapy, CDI symptoms are often indistinguishable from the gastrointestinal side effects of chemotherapy, radiation, and newer immunotherapies (17). For these complex reasons, CDI during cancer treatment can lead to delays in future chemotherapy or radiation cycles and have been shown to negatively affect eligibility for curative treatment options (18). In addition, the estimated surplus healthcare-associated costs of primary CDI in patients with advanced age is estimated to be around US \$37,000 and for patients with immunocompromising conditions US \$16,000, almost 2-fold higher than costs of CDI for patients without immunocompromising conditions (19). The wide-ranging effects of CDI in this population warrants assessment of primary prevention strategies (20–22). Our study defines the subset of older adults with cancer who would probably benefit the most from such therapies to minimize the vulnerability to CDI during cancer treatment.

The strength of our study is that it provides population-based quantitative estimates of the differential effects of CDI among older adults with and without cancer. Despite the many advantages of the SEER-Medicare dataset, our study has limitations: we were able to measure CDI-related disease burden only in the hospital setting, and community-acquired (or community-onset) cases were not included unless they resulted in a hospitalization. Although we excluded patients who received a CDI diagnosis in 2010, case-patients do not necessarily represent those with primary infections. We used only the first Medicare claim with a CDI diagnosis; outpatient diagnoses would be missed and recurrent disease could potentially be represented as incident CDI. In addition, we did not measure relapsing CDI.

In summary, the burden of CDI among older adults is greater among those with underlying cancer. Regardless of prior healthcare-associated exposure, risk for CDI was highest for patients with hematologic malignancy and those with recent diagnosis of solid tumor or distant metastatic disease at diagnosis. These findings can be used to guide CDI prevention strategies.

Funding for this study was provided by the National Institutes of Health, National Cancer Institute Cancer Center Support Grant P30 (CA008748).

About the Author

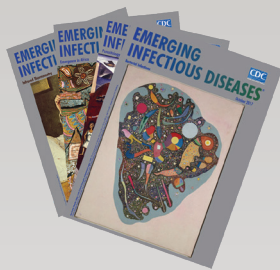
Dr. Kamboj is an infectious disease physician and hospital epidemiologist at Memorial Sloan Kettering Cancer Center in New York, NY. Her research interests include the epidemiology of healthcare-associated infections in patients undergoing cancer treatment.

References

- Magill SS, Edwards JR, Bamberg W, Beldavs ZG, Dumyati G, Kainer MA, et al.; Emerging Infections Program Healthcare-Associated Infections and Antimicrobial Use Prevalence Survey Team. Multistate point-prevalence survey of health care-associated infections. *N Engl J Med*. 2014;370:1198–208. <https://doi.org/10.1056/NEJMoa1306801>
- Lessa FC, Mu Y, Bamberg WM, Beldavs ZG, Dumyati GK, Dunn JR, et al. Burden of *Clostridium difficile* infection in the United States. *N Engl J Med*. 2015;372:825–34. <https://doi.org/10.1056/NEJMoa1408913>
- Murphy SL, Xu J, Kochanek KD, Curtin SC, Arias E. Deaths: final data for 2015. *Natl Vital Stat Rep*. 2017;66:1–75.
- Centers for Disease Control and Prevention. 2015 Annual Report for the Emerging Infections Program for *Clostridium difficile* Infection [cited 2018 Jun 18]. <https://www.cdc.gov/hai/eip/Annual-CDI-Report-2015.html>
- Neemann K, Freifeld A. *Clostridium difficile*-associated diarrhea in the oncology patient. *J Oncol Pract*. 2017;13:25–30. <https://doi.org/10.1200/JOP.2016.018614>
- Anand A, Glatt AE. *Clostridium difficile* infection associated with antineoplastic chemotherapy: a review. *Clin Infect Dis*. 1993;17:109–13. <https://doi.org/10.1093/clinids/17.1.109>
- Loo VG, Bourgault AM, Poirier L, Lamothe F, Michaud S, Turgeon N, et al. Host and pathogen factors for *Clostridium difficile* infection and colonization. *N Engl J Med*. 2011;365:1693–703. <https://doi.org/10.1056/NEJMoa1012413>
- Chopra T, Alangaden GJ, Chandrasekar P. *Clostridium difficile* infection in cancer patients and hematopoietic stem cell transplant recipients. *Expert Rev Anti Infect Ther*. 2010;8:1113–9. <https://doi.org/10.1586/eri.10.95>
- Kamboj M, Son C, Cantu S, Chemaly RF, Dickman J, Dubberke E, et al. Hospital-onset *Clostridium difficile* infection rates in persons with cancer or hematopoietic stem cell transplant: a C3IC network report. *Infect Control Hosp Epidemiol*. 2012;33:1162–5. <https://doi.org/10.1086/668023>
- Warren JL, Klabunde CN, Schrag D, Bach PB, Riley GF. Overview of the SEER-Medicare data: content, research applications, and generalizability to the United States elderly population. *Med Care*. 2002;40(Suppl):IV-3–18. <https://doi.org/10.1097/00005650-200208001-00002>
- Kamthan AG, Bruckner HW, Hirschman SZ, Agus SG. *Clostridium difficile* diarrhea induced by cancer chemotherapy. *Arch Intern Med*. 1992;152:1715–7. <https://doi.org/10.1001/archinte.1992.00400200139025>
- Cohen SH, Gerding DN, Johnson S, Kelly CP, Loo VG, McDonald LC, et al.; Society for Healthcare Epidemiology of America; Infectious Diseases Society of America. Clinical practice guidelines for *Clostridium difficile* infection in adults: 2010 update by the Society for Healthcare Epidemiology of America (SHEA) and the Infectious Diseases Society of America (IDSA). *Infect Control Hosp Epidemiol*. 2010;31:431–55. <https://doi.org/10.1086/651706>
- McFarland LV, Clarridge JE, Beneda HW, Raugi GJ. Fluoroquinolone use and risk factors for *Clostridium difficile*-associated disease within a Veterans Administration health care system. *Clin Infect Dis*. 2007;45:1141–51. <https://doi.org/10.1086/522187>
- Nelson DE, Auerbach SB, Baltch AL, Desjardin E, Beck-Sague C, Rheel C, et al. Epidemic *Clostridium difficile*-associated diarrhea: role of second- and third-generation cephalosporins. *Infect Control Hosp Epidemiol*. 1994;15:88–94. <https://doi.org/10.2307/30145537>
- Stevens V, Dumyati G, Fine LS, Fisher SG, van Wijngaarden E. Cumulative antibiotic exposures over time and the risk of *Clostridium difficile* infection. *Clin Infect Dis*. 2011;53:42–8. <https://doi.org/10.1093/cid/cir301>

16. Tabak YP, Johannes RS, Sun X, Nunez CM, McDonald LC. Predicting the risk for hospital-onset *Clostridium difficile* infection (HO-CDI) at the time of inpatient admission: HO-CDI risk score. *Infect Control Hosp Epidemiol*. 2015;36:695–701. <https://doi.org/10.1017/ice.2015.37>
17. Kamboj M, Brite J, Aslam A, Kennington J, Babady NE, Calfee D, et al. Artificial differences in *Clostridium difficile* infection rates associated with disparity in testing. *Emerg Infect Dis*. 2018;24:584–7. <https://doi.org/10.3201/eid2403.170961>
18. Hautmann MG, Hipp M, Kölbl O. *Clostridium difficile*-associated diarrhea in radiooncology: an underestimated problem for the feasibility of the radiooncological treatment? *Radiat Oncol*. 2011;6:89. <https://doi.org/10.1186/1748-717X-6-89>
19. Zhang D, Prabhu VS, Marcella SW. Attributable healthcare resource utilization and costs for patients with primary and recurrent *Clostridium difficile* infection in the United States. *Clin Infect Dis*. 2018;66:1326–32. <https://doi.org/10.1093/cid/cix1021>
20. Wilcox MH, Gerding DN, Poxton IR, Kelly C, Nathan R, Birch T, et al.; MODIFY I and MODIFY II Investigators. Bezlotoxumab for prevention of recurrent *Clostridium difficile* infection. *N Engl J Med*. 2017;376:305–17. <https://doi.org/10.1056/NEJMoa1602615>
21. Lewis BB, Pamer EG. Microbiota-based therapies for *Clostridium difficile* and antibiotic-resistant enteric infections. *Annu Rev Microbiol*. 2017;71:157–78. <https://doi.org/10.1146/annurev-micro-090816-093549>
22. Martin J, Wilcox M. New and emerging therapies for *Clostridium difficile* infection. *Curr Opin Infect Dis*. 2016;29:546–54. <https://doi.org/10.1097/QCO.0000000000000320>

Address for correspondence: Mini Kamboj, Memorial Sloane Kettering Cancer Center, 1275 York Ave, New York, NY 10065, USA; email: kamboj@mskcc.org



EMERGING
INFECTIOUS DISEASES®

October 2017

Bacterial Infections

- Fatal Rocky Mountain Spotted Fever along the United States–Mexico Border, 2013–2016
- Surveillance of Extrapulmonary Nontuberculous Mycobacteria Infections, Oregon, USA, 2007–2012
- Investigation of Outbreaks of *Salmonella enterica* Serovar Typhimurium and Its Monophasic Variants Using Whole-Genome Sequencing, Denmark
- Enteric Infections Circulating during Hajj Seasons, 2011–2013
- Economic Assessment of Waterborne Outbreak of Cryptosporidiosis
- Antimicrobial Drug Prescription and *Neisseria gonorrhoeae* Susceptibility, United States, 2005–2013
- Poliovirus Excretion in Children with Primary Immunodeficiency Disorders, India
- Disease Burden of *Clostridium difficile* Infections in Adults, Hong Kong, China, 2006–2014
- Molecular Tracing to Find Source of Protracted Invasive Listeriosis Outbreak, Southern Germany, 2012–2016
- Dengue Virus 1 Outbreak in Buenos Aires, Argentina, 2016
- Mild Illness during Outbreak of Shiga Toxin–Producing *Escherichia coli* O157 Infections Associated with Agricultural Show, Australia
- Enterovirus D68–Associated Acute Flaccid Myelitis in Immunocompromised Woman, Italy
- Diagnosis of Fatal Human Case of St. Louis Encephalitis Virus Infection by Metagenomic Sequencing, California, 2016
- Usutu Virus RNA in Mosquitoes, Israel, 2014–2015
- Macrolide-Resistant *Mycoplasma pneumoniae* Infection, Japan, 2008–2015
- Epidemiology of Reemerging Scarlet Fever, Hong Kong, 2005–2015
- Off-Label Use of Bedaquiline in Children and Adolescents with Multidrug-Resistant Tuberculosis
- Monitoring Avian Influenza Viruses from Chicken Carcasses Sold at Markets, China, 2016
- Bedaquiline and Delamanid Combination Treatment of 5 Patients with Pulmonary Extensively Drug-Resistant Tuberculosis
- Hantavirus Pulmonary Syndrome Caused by Maripa Virus in French Guiana, 2008–2016
- Bedaquiline and Linezolid for Extensively Drug-Resistant Tuberculosis in Pregnant Woman
- Carbapenemase VCC-1–Producing *Vibrio cholerae* in Coastal Waters of Germany
- Autochthonous Transmission of East/Central/South African Genotype Chikungunya Virus, Brazil
- Fluoroquinolone-Resistant *Alcaligenes faecalis* Related to Chronic Suppurative Otitis Media, Angola

To revisit the October 2017 issue, go to:

<https://wwwnc.cdc.gov/eid/articles/issue/23/10/table-of-contents>

Whole-Genome Sequencing of *Salmonella* Mississippi and Typhimurium Definitive Type 160, Australia and New Zealand

Laura Ford, Danielle Ingle, Kathryn Glass, Mark Veitch, Deborah A. Williamson, Michelle Harlock, Joy Gregory, Russell Stafford, Nigel French, Samuel Bloomfield, Zoe Grange, Mary Lou Conway, Martyn D. Kirk

We used phylogenomic and risk factor data on isolates of *Salmonella enterica* serovars Mississippi and Typhimurium definitive type 160 (DT160) collected from human, animal, and environmental sources to elucidate their epidemiology and disease reservoirs in Australia and New Zealand. Sequence data suggested wild birds as a likely reservoir for DT160; animal and environmental sources varied more for *Salmonella* Mississippi than for *Salmonella* Typhimurium. Australia and New Zealand isolates sat in distinct clades for both serovars; the median single-nucleotide polymorphism distance for DT160 was 29 (range 8–66) and for *Salmonella* Mississippi, 619 (range 565–737). Phylogenomic data identified plausible sources of human infection from wildlife and environmental reservoirs and provided evidence supporting New Zealand-acquired DT160 in a group of travelers returning to Australia. Wider use of real-time whole-genome sequencing in new locations and for other serovars may identify sources and routes of transmission, thereby aiding prevention and control.

Nontyphoidal *Salmonella enterica* subsp. *enterica* causes substantial illness and death throughout the world (1,2). In Australia, rates of notified infection are

higher than in other high-income countries (3). Preventing infection by understanding sources and routes of transmission and controlling outbreaks rapidly is key to reducing the rate of salmonellosis in Australia. Whole-genome sequencing (WGS) is increasingly being used as a tool to help with prevention and control by investigating the relationship between isolates, sources of infection, and routes of transmission (4). Evidence shows that WGS is useful in foodborne nontyphoidal *S. enterica* outbreak detection and control (5–7).

On mainland Australia (Figure 1), *Salmonella* Typhimurium is the most commonly notified nontyphoidal *S. enterica* serovar. In contrast, *Salmonella* Mississippi is the most commonly notified nontyphoidal *S. enterica* serovar infecting residents of the island state of Tasmania, where 2.1% of the population of Australia resides (3,8). Most persons with *Salmonella* Mississippi who are residents of mainland Australia have traveled to Tasmania or one of several Pacific Islands to which *Salmonella* Mississippi was endemic during their exposure period (9,10). In Tasmania, *Salmonella* Mississippi has been isolated from wildlife, and some evidence indicates that human infections might result from environmental transmission more frequently than from foodborne transmission (9,11). A case-control study in Tasmania during 2001–2002 found that case-patients were more likely than controls to have had indirect contact with native birds, consumed untreated drinking water, and traveled within the state (9), although the sources of infection and vehicles of transmission are still largely unknown.

Salmonella Typhimurium definitive type 160 (DT160) has more recently emerged in Tasmania, while remaining rare in the rest of the country. In 2008, ten years after its emergence in humans in New Zealand, the first locally acquired case of DT160 was reported in Tasmania; unusual sparrow (*Passer domesticus*) deaths were observed in the same area in 2009, consistent with sparrow deaths in New

Author affiliations: The Australian National University, Acton, Australian Capital Territory, Australia (L. Ford, D. Ingle, K. Glass, M.D. Kirk); The University of Melbourne at the Peter Doherty Institute for Infection and Immunity, Melbourne, Victoria, Australia (D. Ingle, D.A. Williamson); Department of Health, Hobart, Tasmania, Australia (M. Veitch, M. Harlock); Victorian Department of Health and Human Services, Melbourne (J. Gregory); Queensland Department of Health, Brisbane, Queensland, Australia (R. Stafford); New Zealand Food Safety Science and Research Centre, Manawatu-Wanganui, New Zealand (N. French); Massey University, Manawatu-Wanganui (N. French); Quadram Institute, Norwich, UK (S. Bloomfield); University of California–Davis, Davis, California, USA (Z. Grange); Department of Primary Industries, Parks, Water and Environment, Hobart (M.L. Conway)

DOI: <https://doi.org/10.3201/eid2509.181811>

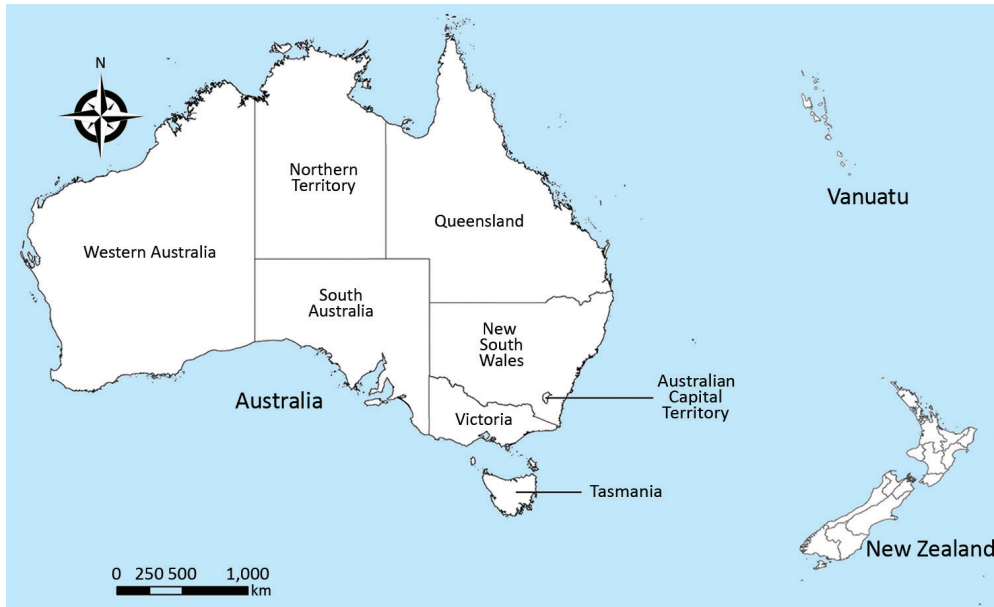


Figure 1. Relative locations of Australia, New Zealand, and Vanuatu.

Zealand in 2000 (12–15). Since then, DT160 has affected ≈ 50 Tasmania residents and $\approx 3,000$ New Zealand residents and has been associated with wild bird deaths in both countries (16–18). Although a case–control study conducted in 2001 in New Zealand suggested that handling of dead wild birds, contact with persons with diarrheal illness, and ingestion of fast food were associated with illness (12), the relationship between the Tasmania and New Zealand DT160 infections and the relationship between animal and human isolates in Tasmania is unknown. Accordingly, we aimed to use these 2 nontyphoidal *S. enterica* serovars as case studies to investigate how epidemiologic and genomic data can be integrated to better understand the geographic niche and transmission pathways of these organisms to subsequently improve prevention and control strategies.

Methods

Ethics Considerations and Data Sources

The Australian National University Human Research Ethics Committee (2016/269) granted ethics approval for this project. We used data from the Australian National Notifiable Diseases Surveillance System (18) and the New Zealand Enteric Reference Laboratory (19) to examine trends in *Salmonella* Mississippi and DT160 in Australia and New Zealand. Population denominator data were obtained from the Australian Bureau of Statistics (8) and Statistics New Zealand (20). We used postcode of residence to determine Australian state or territory. Travel information was not available, so postcode might not represent place of acquisition for all notifications.

We collated epidemiologic data obtained through enhanced surveillance of cases of *Salmonella* Mississippi and

DT160 that were notified to the Department of Health and Human Services in Tasmania, the Department of Health and Human Services in Victoria, and Queensland Health. Case-patients were interviewed at the time of notification using a standardized questionnaire, and this information was collected under each jurisdiction's public health legislation. For human isolates for which sequence data were available, we obtained the following case data fields from these questionnaires: type of case (sporadic, household, cluster, outbreak); hospitalization (yes/no); symptoms; travel; close contact with farm animals, native animals, birds, or pets (yes/no and type); lives on a rural property (yes/no); bushwalking or camping (yes/no); water source (public, private, or bottled); gardening (yes/no); swimming (yes/no); other risk factors (free text). Data on risk factors were collected for the week before illness onset.

Isolate Selection

For *Salmonella* Mississippi, we selected 34 human isolates from Tasmania residents and 28 human isolates from residents of other states and territories in Australia that were referred for characterization to the Microbiological Diagnostic Unit Public Health Laboratory (MDU PHL) in Melbourne during January 1, 2011–December 31, 2015, for WGS (Appendix, <https://wwwnc.cdc.gov/EID/article/25/9/18-1811-App1.pdf>). We also selected all viable isolates with a recorded source from 42 animal sources and 18 environmental sources in the MDU PHL collection with an isolation date from January 1, 2000, through December 31, 2016; these isolates were all from Tasmania. For DT160, all viable isolates held in the MDU PHL collection at the beginning of 2016 were included in genomic analysis.

Sequencing and Bioinformatics

MDU PHL performed DNA extraction and WGS for the Australia isolates. Sequence libraries were prepared using NexteraXT and sequenced on the Illumina NextSeq500 platform (Illumina, <https://www.illumina.com>) with 150 bp paired-end reads. Reads are available from the National Center for Biotechnology Information Sequence Read Archive (PRJNA319593). *Salmonella* Typhimurium L2 (accession no. NC003197 [https://www.ncbi.nlm.nih.gov/nucleotide/NC_003197.2]) was used as a reference for DT160, and because complete genomes were not publicly available, we used a local reference (AUSMDU00020775) for *Salmonella* Mississippi by assembling 1 of the isolates in this analysis (Appendix). We included 10 publicly available draft assemblies from 2011 through 2013 from New Zealand and the United States (Appendix) in the *Salmonella* Mississippi analysis (21,22) and 106 publicly available DT160 genomes from 1992 through 2012 from humans, wild birds, poultry, and bovine sources in New Zealand in the DT160 analysis (16).

Salmonella Mississippi and DT160 genomes were analyzed separately using Nullarbor version 2 (<https://github.com/tseemann/nullarbor>). Short-read data of the isolates were mapped to the reference using Snippy version 4.0-dev2 (<https://github.com/tseemann/snippy>). The 10 publicly available *Salmonella* Mississippi draft assemblies were also mapped to the *Salmonella* Mississippi reference using Snippy, with the `-ctgs` parameter that enables mapping of assembly contigs to a reference. A core genome alignment was produced using Snippy-core (v4.0-dev 2), and the resulting full alignment was then filtered for recombination using Gubbins (23) using the weighted Robinson-Foulds method to estimate convergence with an initial 10 iterations. The resulting recombination-filtered core genome alignment of 8,573 bases for *Salmonella* Mississippi and 2,203 bases for DT160 was then passed to RAxML version 8.2.11 (24) to infer maximum-likelihood (ML) phylogenetic trees, using the generalized time-reversible model with a γ -distribution to model site-specific rate variation and ascertain bias correction. For each analysis, we used

3 independent runs with 1,000 bootstrap pseudoreplicates to assess branch support, with the phylogenetic trees with the highest support across the 3 runs used as the final tree for each analysis. The pairwise single-nucleotide polymorphism (SNP) distances between isolates were calculated from the recombination-filtered core genome alignment using *afa-pairwise.pl* within Nullarbor. De novo genome assemblies were generated using SPAdes version 3.12.0 (25), and the presence of known antimicrobial resistance genes was investigated using ABRicate (<https://github.com/tseemann/abricate>) in conjunction with the genome assemblies and the National Center for Biotechnology Information antimicrobial resistance database with a minimum coverage of 90% and minimum identity of 90%.

Data Analysis

We collated epidemiologic and SNP data in Microsoft Excel 2013 (<https://www.microsoft.com>) and performed descriptive analyses in Stata SE 14 (<https://www.stata.com>). We used sequence data to explore hypotheses about the epidemiologic relatedness of isolates. We compared risk factors between DT160 and *Salmonella* Mississippi cases using a 2-sample test of proportions. Based on SNPs between isolates of each serovar with known epidemiologic links (household or epidemiologic cluster), we considered isolates within 8 SNPs of each other for DT160 and 10 SNPs of each other for *Salmonella* Mississippi a putative phylogenetic cluster for further investigation.

Results

Salmonella Mississippi

During January 1, 2000–December 31, 2016, the median annual notification rate of *Salmonella* Mississippi in Tasmania was 15 cases (range 12–24 cases) per 100,000 population, compared with a notification rate of 0.11 cases (range 0.007–0.16 cases) per 100,000 population on mainland Australia and 0.3 cases (range 0.16–0.47 cases) per 100,000 population in New Zealand (Figure 2). In Australia,

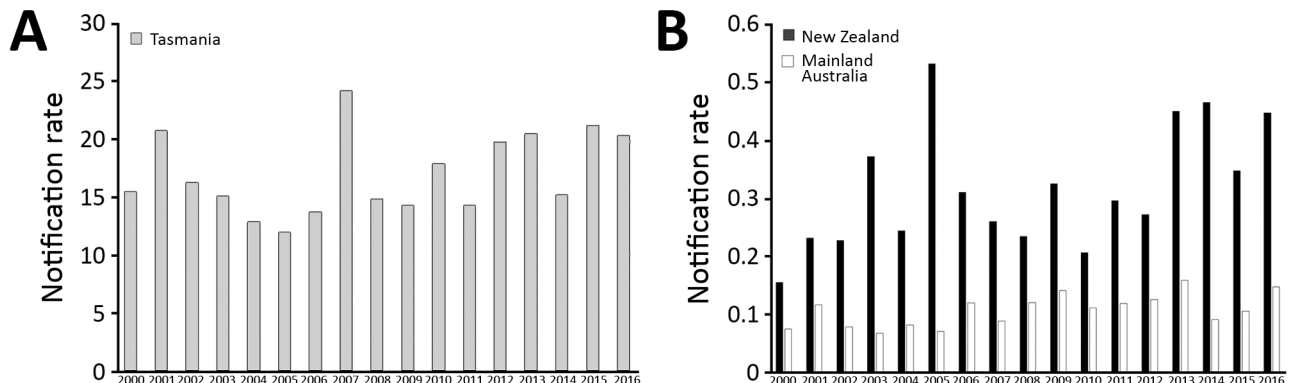


Figure 2. Notification rates for *Salmonella enterica* serovar Mississippi, Tasmania (A) and mainland Australia and New Zealand (B), 2000–2016. Rates are per 100,000 population.

934 (50.5%) of 1,851 notifications occurred in female patients. Children 0–4 years of age were the most frequently notified age group (458 [24.7%]). Notification rates were higher in warmer months, similar to those for other non-Typhimurium serovars (26).

For sequenced *Salmonella* Mississippi isolates, the ML tree showed that the isolates from Vanuatu, United States, and New Zealand were distinctly different from the Australia isolates (Figure 3); median SNP distance was 619 (range 565–737) between Australia and New Zealand isolates (Appendix Figure 1) and 1,625 (range 963–1,923) between Australia and Vanuatu or US isolates. An isolate from a 17-week-old mainland Australia resident with no history of overseas travel grouped on the phylogenetic tree with the isolates acquired in Vanuatu. Within the large Australia group, the 114 isolates were diverse; median SNP distance was 169 (range 3–649). Of these Australia isolates, 24 (21.1%) of 114 were within 10 SNPs of another isolate and grouped into 8 phylogenetic clusters. The Australia human isolates grouped with Australia animal and environmental isolates over several years. We observed considerable genetic diversity between isolates from various animal sources. For example, isolates from wombats were a median of 87 (range 44–97) SNPs apart, and isolates from bovines were a median of 140 (range 10–201) SNPs apart. We did not detect any antimicrobial resistance genes in these

isolates, except for 1 human isolate from Tasmania that had the *bla*_{TEM-1} gene, which mediates resistance to ampicillin.

Travel data were available for 51 (82%) of 62 of case-patients in Australia residents for which an isolate was sequenced. Of these, 6 (12%) reported international travel to Vanuatu and 19 (37%) reported domestic travel during their incubation period; 8 traveled from mainland states to Tasmania, 9 traveled within Tasmania, 1 traveled from Queensland to South Australia, and 1 traveled from Victoria to Queensland. Three Tasmania isolates investigated as an epidemiologic cluster clustered genetically and temporally with an isolate from Victoria, for which no epidemiologic data were available. Although 2 other phylogenetic clusters included >1 human isolate, epidemiologic data were limited for these cases, and the infections were not clustered in time. Although not statistically significant, among case-patients who resided in or were known to have acquired infection in Tasmania and answered risk factor questions about exposures, a higher proportion of *Salmonella* Mississippi than DT160 case-patients reported drinking water from an untreated raw water source (i.e., tank, spring, or bore) (61% vs. 40%; $p = 0.1$) and camping (8% vs. 0%; $p = 0.07$) (Appendix Table 4). A similar proportion of DT160 and *Salmonella* Mississippi cases reported bushwalking (8% vs. 7.5%; $p = 0.94$), gardening (16% vs. 22%; $p = 0.56$), and swimming (16% vs. 18%; $p = 0.84$)

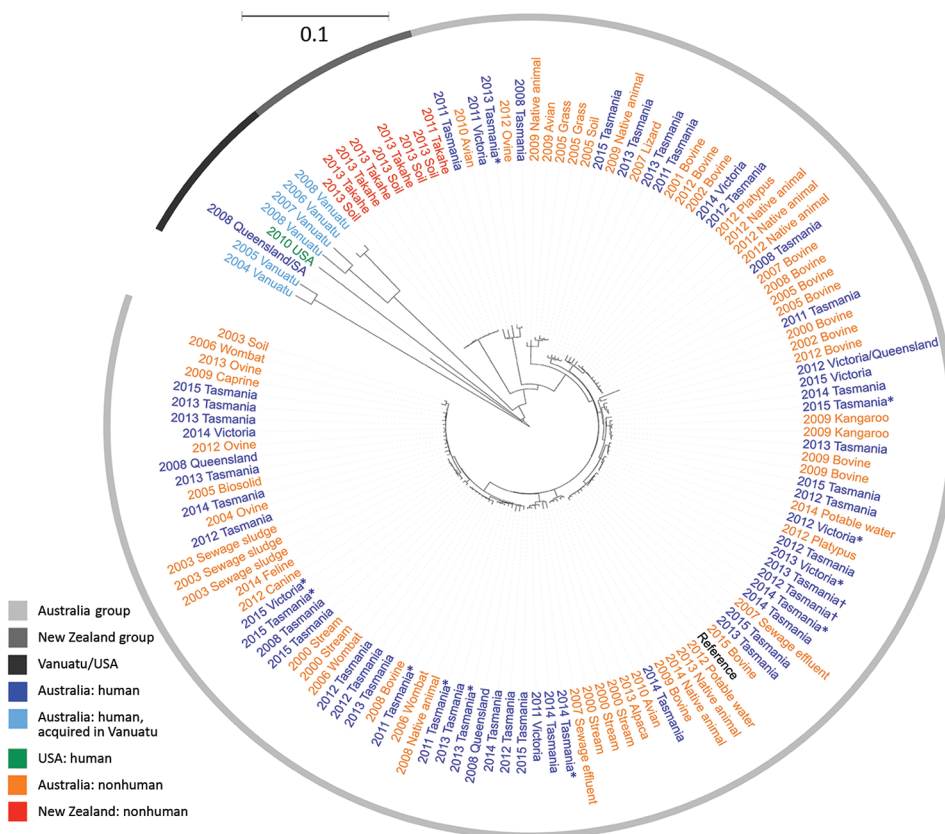


Figure 3. Maximum-likelihood phylogeny of 132 sequenced *Salmonella enterica* serovar Mississippi isolates from Australia and New Zealand and reference isolates, inferred from 8,573 core single-nucleotide polymorphisms. Nodes are labeled with isolation year, isolate source if nonhuman (all from Tasmania), and Australia state of acquisition or residence if human. Tree visualized with iTOL (<https://itol.embl.de>) and midpoint rooted. Scale bar indicates nucleotide substitutions per site. *State of residence was used instead of state of acquisition because no travel data were available. †Investigated as part of an epidemiologic cluster. A color version of this figure is available online (<http://wwwnc.cdc.gov/EID/article/25/9/18-1811-F3.htm>).

exposures. Of the 13 case-patients who resided in or acquired their infection in an Australia state other than Tasmania, 4 (31%) reported eating oysters during the exposure period, including 2 cases in a phylogenetic cluster; however, not all case-patients were asked specifically about oysters.

Salmonella Typhimurium DT160

A total of 61 DT160 cases in Australia residents were notified during 1999–2014. The 12 infections reported in Australia residents before 2008 were believed to be acquired overseas, including cases on an Australia–New Zealand cruise in 2003. Most Australia DT160 notifications had a postcode of residence in Tasmania, where the median annual rate per 100,000 population of DT160 in the 9 years from 1999 to 2007 was 0 cases and in the 7 years from 2008 to 2014 was 1.2, peaking at 2.8 in 2009, when 14 cases occurred. In New Zealand, the median annual rate per 100,000 population of DT160 in the 9 years from 1999 to 2007 was 6, peaking at 20.4 in 2001, when 791 cases occurred. In the 7 years from 2008 to 2014, the median annual rate was 1.6 per 100,000 population (Figure 4). Of all 61 Australia notifications during 1999–2014, a total of 34 (56%) occurred in females, and children aged 0–4 years were the most frequently notified age group (14 [23%]). Because of the small number of cases, we found no clear seasonal pattern.

Of Australia isolates, we sequenced 62 human and 30 animal isolates (20 from sparrows). The ML tree of Australia and New Zealand isolates showed 2 distinct groups; 1 comprised isolates from humans and animals in Australia, and 1 comprised humans and animals from New Zealand and the 7 Australia residents who had reported travel to New Zealand (Figure 5). The median pairwise SNP difference between the Australia and New Zealand groups was 29 (range 8–66), and the median pairwise SNP difference within each group was 21 (Australia, range 2–56; New Zealand, range 0–55) (Appendix Figure 4). Within the Australia group, 45 (53%) of 85 isolates were within

8 SNPs of another isolate, and the isolates grouped into 8 phylogenetic clusters. Of these 8 phylogenetic clusters, 3 contained >2 isolates; isolates from humans and birds over several years clustered. No known antimicrobial resistance genes were detected among any of the isolates.

Epidemiologic risk factor data were available for 55 (90%) of the 61 DT160 cases in Australia residents from the 62 sequenced human isolates (1 person contributed 2 isolates, 13 days and 7 SNPs apart). Of these 55 persons, 7 (12%) of 59 acquired their infection in New Zealand, 6 in 2003 on an Australia–New Zealand cruise, and 1 in 2009. All others were residents of, or had traveled to, Tasmania, except for 1 case-patient, who was a resident of New South Wales and had no reported travel outside the state. Two separate household clusters were investigated in 2012 and were phylogenetically clustered. In 2015, five isolates were investigated as part of an epidemiologic cluster; however, no epidemiologic link was found, and they were subsequently found not to be phylogenetically clustered (median SNPs 25.5, range 9–33). A higher proportion of DT160 case-patients than *Salmonella* Mississippi case-patients reported direct contact with wild or domestic animals (88% vs. 68%; $p = 0.04$) (Appendix Table 4).

Discussion

Phylogenomics plays a valuable role in identifying plausible sources of *Salmonella* infection from wildlife and environmental reservoirs. For both serovars considered in this article, the integration of clinical and genomic data enhanced existing evidence on source reservoirs by showing that human and animal or environmental isolates were genetically interspersed. Phylogenomic analysis revealed genetic diversity and persistence of *Salmonella* Mississippi strains in the environment and animals, suggesting it is endemic with a broad range of host reservoirs in Tasmania that is persisting over time. As in other countries (16,27–29), genomic analysis provided evidence that wild birds are a source of human infection with DT160. No characterized antimicrobial resistance genes were detected in any of

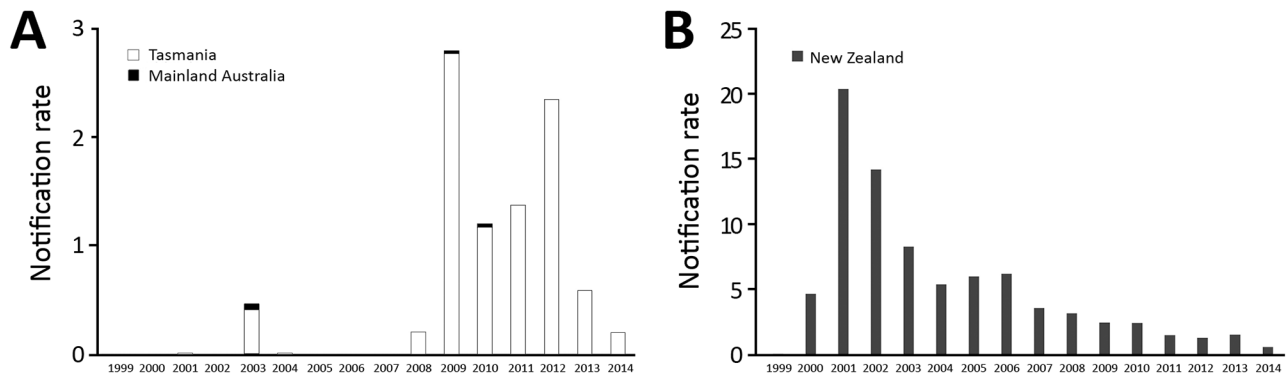


Figure 4. *Salmonella enterica* serovar Typhimurium definitive type 160 notification rate, Tasmania and mainland Australia (A) and New Zealand (B), 1999–2014. Rates are per 100,000 population.

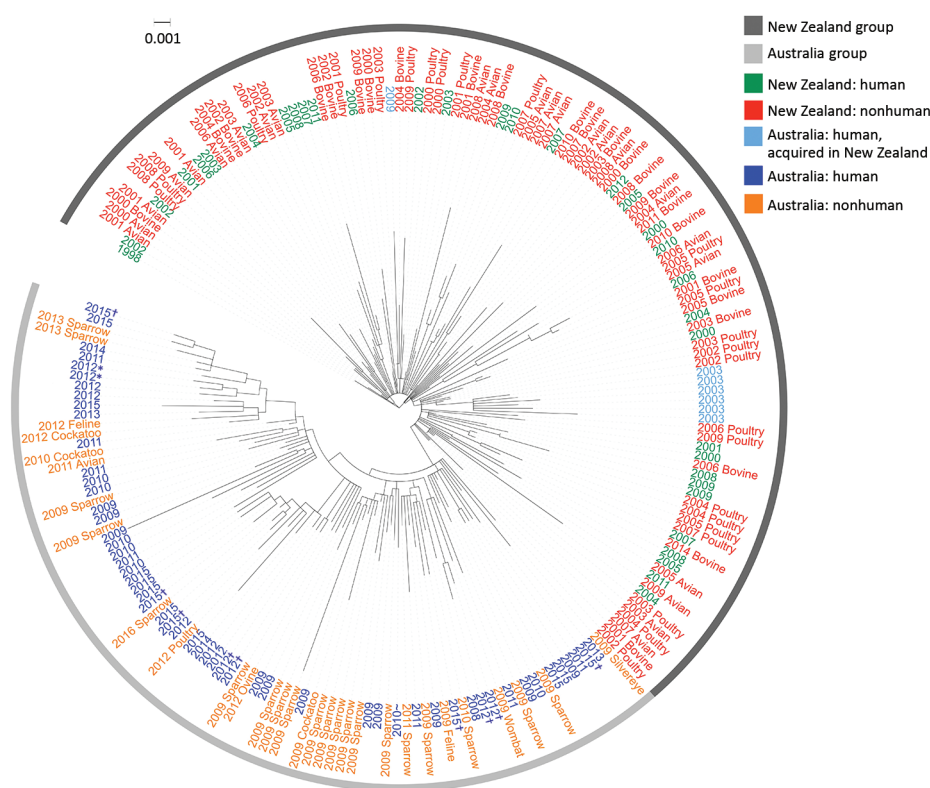


Figure 5. Maximum-likelihood phylogeny of 198 sequenced *Salmonella enterica* serovar Typhimurium definitive type 160 isolates from Australia and New Zealand and reference isolates, inferred from 2,203 core single-nucleotide polymorphisms, Australia and New Zealand. Nodes are labeled with isolate type and isolation year. All Australian isolates are from Tasmania unless specified otherwise. Figure created with iTOL (<https://itol.embl.de>). Scale bar indicates nucleotide substitutions per site. *Specimens from the same person. †Investigated as part of an epidemiologic cluster. ‡Acquired in New South Wales. A color version of this figure is available online (<http://wwwnc.cdc.gov/EID/article/25/9/18-1811-F5.htm>).

the DT160 draft genome sequences, suggesting low or no antimicrobial resistance, consistent with other *Salmonella* strains found in wild birds (30,31).

In contrast to *Salmonella* Mississippi, *Salmonella* Typhimurium DT160 isolates from Australia and New Zealand were similar, suggesting possible recent trans-Tasmania transmission of DT160 through wildlife, as well as its potential to spread from Tasmania to the Australia mainland. Further, the inferred population structure of these Australia strains provided evidence for this hypothesis of import and subsequent microevolution within the Australia strains. In New Zealand, DT160 has been transmitted between multiple hosts, and humans have been infected from multiple sources (16). Other *Salmonella* serovars with wild bird reservoirs have been transmitted to cattle, pigs, sheep, and poultry (32). The incidence of human infection in Australia most likely would increase if DT160 were to become established in local animal food sources.

Epidemiologic evidence that 88% of DT160 case-patients had direct animal contact and the close genetic relatedness between Australia human and animal isolates suggest that DT160 in Tasmania is predominantly a locally acquired zoonotic infection. Control measures should therefore focus on promoting hand hygiene after contact with wild birds and other animals, keeping food preparation and eating areas free from birds, treating drinking water that is accessible to birds and other animals, and

appropriately cleaning and maintaining birdfeeders (32,33). In addition to monitoring the effect of such measures, continued isolation, identification, and WGS of DT160 isolates from humans, animals, and the environment could be used to monitor emergence in other settings that pose particular risks to the food supply and provide early warning of the need for specific control measures.

Risk factors for *Salmonella* Mississippi are less evident, although the proportion of case-patients who reported drinking water from a private source (61%) was similar to that of an Australia case-control study of *Salmonella* Mississippi (63% of case-patients vs. 23% of controls reported drinking any untreated water; adjusted odds ratio 6.13, 95% CI 3.19–11.76) (9). The range of animal and environmental sources and the high genetic diversity make identifying control strategies difficult. Because genomic analyses of WGS data have detected clusters when epidemiologic links are obscured (7), prospective WGS of case isolates and integration of WGS data from human, animal, and environmental isolates could help to identify putative clusters for targeted epidemiologic investigation. Source attribution studies might enable quantification of the contribution of raw water as a vehicle for *Salmonella* Mississippi infection in Tasmania.

One limitation of this study is that our sampling frame for sequencing and analysis might not have produced a representative sample of all infections; however, we tried to maximize variability of sources and isolation dates.

Although epidemiologic risk factor data were incomplete for sequenced human cases, sufficient data were available for us to generate hypotheses that could be further investigated. Our case–case method is not as robust as a case–control study with a neutral control group, but we believe it is a reasonable point of comparison, emphasizing the difference in risk between these 2 serovars. Some more recent Australia DT160 notifications might not have been captured by the national notification system because phage typing for *Salmonella* Typhimurium is being phased out across Australia. However, we believe this omission would be a small number because phage typing continued in most of the country until 2016 (M. Valcanis, MDU PHL, pers. comm., 2018 Oct 10). Without phage typing, and as the use of WGS for *Salmonella* surveillance becomes more routine, it will be difficult to compare new isolates with historically phage-typed isolates that have not been sequenced.

We used SNP thresholds based on known epidemiologic clusters to define putative phylogenetic clusters and to examine epidemiologic risk factors. Because SNPs depend on the reference genome and the isolates in the analysis, SNP thresholds for cluster analysis are likely to differ according to context. Local references were unavailable for both serovars in this study. We assembled a reference for *Salmonella* Mississippi using an isolate in this study, and the *Salmonella* Typhimurium isolate used was a median of 899 (range 883–921) SNPs from the DT160 isolates in our study. A closer reference for DT160 might have provided higher resolution of the relatedness of isolates. Few international *Salmonella* Mississippi genomes were publicly available. Therefore, the relationship we found between Australia and New Zealand isolates might not be representative of all *Salmonella* Mississippi isolates in these 2 countries. Although beyond the scope of this study, identifying the most recent common ancestor using Bayesian phylogeographic analyses would improve our understanding of endemic strains such as *Salmonella* Mississippi and the translocation of emerging strains such as DT160.

Wildlife can contribute to substantial rates of endemic and epidemic infection from *Salmonella*. For these 2 *Salmonella* serovars with wild animal and environmental reservoirs in Australia and New Zealand, WGS combined with epidemiologic risk factor data provided some evidence for prevention and control efforts demonstrating the potential benefits of using WGS for prospective *Salmonella* surveillance. Real-time sequencing of these strains could help monitor emergence and identify clusters, enabling epidemiologists to more accurately identify common risk factors and aid in source attribution. Local references, publicly available international genomes, phylogeographic analyses, additional tools to define a WGS cluster, and source-assigned case–control studies would improve our understanding of the epidemiology of these 2 *Salmonella* serovars in this region.

Acknowledgments

We thank Kinley Wangdi for his assistance in generating the map in Figure 1. We also thank Anastasia Stylianopoulos, Marion Easton, Timothy Sloan-Gardner, and Robert Bell for their assistance in collecting case epidemiologic data. Finally, we thank John Bates, Mary Valcanis, Anders Gonçalves da Silva, Dieter Bulach, and Siobhan St. George for their assistance with sequence data and related metadata.

L.F. is supported by an Australian Government Research Training Program Scholarship. M.D.K. is supported by a National Health & Medical Research Council fellowship (APP1145997). D.A.W. is supported by a National Health & Medical Research Council fellowship (APP1123854).

About the Author

Ms. Ford is a PhD candidate in the Infectious Disease, Epidemiology, and Modelling group at the National Centre for Epidemiology and Population Health at the Australian National University. Her research interests include foodborne diseases and the application of sequencing for public health surveillance.

References

1. Majowicz SE, Musto J, Scallan E, Angulo FJ, Kirk M, O'Brien SJ, et al.; International Collaboration on Enteric Disease 'Burden of Illness' Studies. The global burden of nontyphoidal *Salmonella* gastroenteritis. *Clin Infect Dis*. 2010;50:882–9. <https://doi.org/10.1086/650733>
2. Havelaar AH, Kirk MD, Torgerson PR, Gibb HJ, Hald T, Lake RJ, et al.; World Health Organization Foodborne Disease Burden Epidemiology Reference Group. World Health Organization global estimates and regional comparisons of the burden of foodborne disease in 2010. *PLoS Med*. 2015;12:e1001923. <https://doi.org/10.1371/journal.pmed.1001923>
3. Ford L, Glass K, Veitch M, Wardell R, Polkinghorne B, Dobbins T, et al. Increasing incidence of *Salmonella* in Australia, 2000–2013. *PLoS One*. 2016;11:e0163989. <https://doi.org/10.1371/journal.pone.0163989>
4. Deng X, den Bakker HC, Hendriksen RS. Genomic epidemiology: whole-genome-sequencing-powered surveillance and outbreak investigation of foodborne bacterial pathogens. *Annu Rev Food Sci Technol*. 2016;7:353–74. <https://doi.org/10.1146/annurev-food-041715-033259>
5. Simon S, Trost E, Bender J, Fuchs S, Malorny B, Rabsch W, et al. Evaluation of WGS based approaches for investigating a food-borne outbreak caused by *Salmonella enterica* serovar Derby in Germany. *Food Microbiol*. 2018;71:46–54. <https://doi.org/10.1016/j.fm.2017.08.017>
6. Leekitcharoenphon P, Nielsen EM, Kaas RS, Lund O, Aarestrup FM. Evaluation of whole genome sequencing for outbreak detection of *Salmonella enterica*. *PLoS One*. 2014;9:e87991. <https://doi.org/10.1371/journal.pone.0087991>
7. Waldram A, Dolan G, Ashton PM, Jenkins C, Dallman TJ. Epidemiological analysis of *Salmonella* clusters identified by whole genome sequencing, England and Wales 2014. *Food Microbiol*. 2018;71:39–45. <https://doi.org/10.1016/j.fm.2017.02.012>
8. Australian Bureau of Statistics. 3101.0 Australian demographic statistics, Sep 2017. Table 4. Estimated resident population, states and territories (number) [dataset]. 2018 Mar 22 [cited

- 2018 Mar 28]. <http://www.abs.gov.au/AUSSTATS/abs@.nsf/DetailsPage/3101.0Sep%202017?OpenDocument>
9. Ashbolt R, Kirk MD. *Salmonella* Mississippi infections in Tasmania: the role of native Australian animals and untreated drinking water. *Epidemiol Infect.* 2006;134:1257–65. <https://doi.org/10.1017/S0950268806006224>
 10. OzFoodNet Working Group. Monitoring the incidence and causes of diseases potentially transmitted by food in Australia: annual report of the OzFoodNet Network, 2009. *Commun Dis Intell Q Rep.* 2010;34:396–426.
 11. Hall GV, D'Souza RM, Kirk MD. Foodborne disease in the new millennium: out of the frying pan and into the fire? *Med J Aust.* 2002;177:614–8.
 12. Thornley CN, Simmons GC, Callaghan ML, Nicol CM, Baker MG, Gilmore KS, et al. First incursion of *Salmonella enterica* serotype typhimurium DT160 into New Zealand. *Emerg Infect Dis.* 2003;9:493–5. <https://doi.org/10.3201/eid0904.020439>
 13. Alley MR, Connolly JH, Fenwick SG, Mackereth GF, Leyland MJ, Rogers LE, et al. An epidemic of salmonellosis caused by *Salmonella* Typhimurium DT160 in wild birds and humans in New Zealand. *N Z Vet J.* 2002;50:170–6. <https://doi.org/10.1080/00480169.2002.36306>
 14. Wildlife Health Australia. WHA Fact sheet: *Salmonella* Typhimurium DT160 in house sparrows [cited 2018 Mar 28]. <https://wildlifehealthaustralia.com.au/Portals/0/Documents/FactSheets/Avian/Salmonella%20Typhimurium%20DT160%20in%20House%20Sparrows%20in%20Australia.pdf>
 15. Grillo T. Australian Wildlife Health Network. Animal Health Surveillance Quarterly Report. 2009;14(3):6–8 [cited 2018 Mar 29]. <http://www.sciquest.org.nz/elibrary/edition/5546>
 16. Bloomfield SJ, Benschop J, Biggs PJ, Marshall JC, Hayman DTS, Carter PE, et al. Genomic analysis of *Salmonella enterica* serovar Typhimurium DT160 associated with a 14-year outbreak, New Zealand, 1998–2012. *Emerg Infect Dis.* 2017;23:906–13. <https://doi.org/10.3201/eid2306.161934>
 17. Grillo T, Post L. Australian Wildlife Health Network. Animal Health Surveillance Quarterly Report. 2010;14(4):6–8 [cited 2018 Mar 29]. <http://www.sciquest.org.nz/elibrary/edition/5545>
 18. Australian Government Department of Health. National Notifiable Diseases Surveillance System. 2018 [cited 2018 Aug 6]. <http://www9.health.gov.au/cda/source/cda-index.cfm>
 19. New Zealand Ministry of Health. Enteric Reference Laboratory. Human *Salmonella* isolates. 2018 [cited 2018 Apr 20]. https://surv.esr.cri.nz/enteric_reference/human_salmonella.php
 20. Statistics New Zealand Infoshare. Estimated resident population by age and sex (1991+) (Annual-Jun). 2018 [cited 2018 Jun 26]. <http://archive.stats.govt.nz/infoshare/?url=/infoshare/ViewTable.aspx&pxID=d25f4bca-d895-4ef4-8cf5-c6368155c39e>
 21. Grange ZL, Biggs PJ, Rose SP, Gartrell BD, Nelson NJ, French NP. Genomic epidemiology and management of *Salmonella* in island ecosystems used for takahe conservation. *Microb Ecol.* 2017;74:735–44. <https://doi.org/10.1007/s00248-017-0959-1>
 22. Gupta R, Schmidtke A, Sabol A, Castillo D, Ribot E, Trees E. *Salmonella enterica* subsp. *enterica* serovar Mississippi str. 2010K–1406, whole genome shotgun sequencing project. Accession ALPQ000000001: GenBank; 2012 [cited 2018 Apr 23]. <https://www.ncbi.nlm.nih.gov/nuccore/ALPQ000000001>
 23. Croucher NJ, Page AJ, Connor TR, Delaney AJ, Keane JA, Bentley SD, et al. Rapid phylogenetic analysis of large samples of recombinant bacterial whole genome sequences using Gubbins. *Nucleic Acids Res.* 2015;43:e15. <https://doi.org/10.1093/nar/gku1196>
 24. Stamatakis A. RAxML version 8: a tool for phylogenetic analysis and post-analysis of large phylogenies. *Bioinformatics.* 2014;30:1312–3. <https://doi.org/10.1093/bioinformatics/btu033>
 25. Bankevich A, Nurk S, Antipov D, Gurevich AA, Dvorkin M, Kulikov AS, et al. SPAdes: a new genome assembly algorithm and its applications to single-cell sequencing. *J Comput Biol.* 2012;19:455–77. <https://doi.org/10.1089/cmb.2012.0021>
 26. Fearnley EJ, Lal A, Bates J, Stafford R, Kirk MD, Glass K. *Salmonella* source attribution in a subtropical state of Australia: capturing environmental reservoirs of infection. *Epidemiol Infect.* 2018;146:1903–8. <https://doi.org/10.1017/S0950268818002224>
 27. Piccirillo A, Mazzariol S, Caliarì D, Menandro ML. *Salmonella* Typhimurium phage type DT160 infection in two Moluccan cockatoos (*Cacatua moluccensis*): clinical presentation and pathology. *Avian Dis.* 2010;54:131–5. <https://doi.org/10.1637/8969-062509-Case.1>
 28. Tizard IR, Fish NA, Harneson J. Free flying sparrows as carriers of salmonellosis. *Can Vet J.* 1979;20:143–4.
 29. Lawson B, Howard T, Kirkwood JK, Macgregor SK, Perkins M, Robinson RA, et al. Epidemiology of salmonellosis in garden birds in England and Wales, 1993 to 2003. *EcoHealth.* 2010;7:294–306. <https://doi.org/10.1007/s10393-010-0349-3>
 30. Hughes LA, Shopland S, Wigley P, Bradon H, Leatherbarrow AH, Williams NJ, et al. Characterisation of *Salmonella enterica* serotype Typhimurium isolates from wild birds in northern England from 2005–2006. *BMC Vet Res.* 2008;4:4. <https://doi.org/10.1186/1746-6148-4-4>
 31. Afema JA, Sischo WM. *Salmonella* in wild birds utilizing protected and human impacted habitats, Uganda. *EcoHealth.* 2016; 13:558–69. <https://doi.org/10.1007/s10393-016-1149-1>
 32. Tizard I. Salmonellosis in wild birds. *Seminars in Avian and Exotic Pet Medicine.* 2004;13:50–66.
 33. Friend M. Salmonellosis. In: Friend M, Franson J, editors. Field manual of wildlife diseases. General field procedures and diseases of birds. Washington (DC): US Geological Survey, US Department of the Interior; 1999. p. 99–110.

Address for correspondence: Martyn D. Kirk, National Centre for Epidemiology and Population Health, Research School of Population Health, The Australian National University, Canberra, Australian Capital Territory, 2601 Australia; email: martyn.kirk@anu.edu.au

Epidemiologic Shift in Candidemia Driven by *Candida auris*, South Africa, 2016–2017¹

Erika van Schalkwyk,² Ruth S. Mpembe, Juno Thomas, Liliwe Shuping, Husna Ismail, Warren Lowman, Alan S. Karstaedt, Vindana Chibabhai, Jeannette Wadula, Theunis Avenant, Angeliki Messina, Chetna N. Govind, Krishnee Moodley, Halima Dawood, Praksha Ramjathan, Nelesh P. Govender,² for GERMS-SA

Candida auris is an invasive healthcare-associated fungal pathogen. Cases of candidemia, defined as illness in patients with *Candida* cultured from blood, were detected through national laboratory-based surveillance in South Africa during 2016–2017. We identified viable isolates by using mass spectrometry and sequencing. Among 6,669 cases (5,876 with species identification) from 269 hospitals, 794 (14%) were caused by *C. auris*. The incidence risk for all candidemia at 133 hospitals was 83.8 (95% CI 81.2–86.4) cases/100,000 admissions. Prior systemic antifungal drug therapy was associated with a 40% increased adjusted odds of *C. auris* fungemia compared with bloodstream infection caused by other *Candida* species (adjusted odds ratio 1.4 [95% CI 0.8–2.3]). The crude in-hospital case-fatality ratio did not differ between *Candida* species and was 45% for *C. auris* candidemia, compared with 43% for non-*C. auris* candidemia. *C. auris* has caused a major epidemiologic shift in candidemia in South Africa.

Since 2009, when the first case of *Candida auris* infection was identified in South Africa, the number of laboratory-confirmed cases has increased exponentially (1).

Author affiliations: National Institute for Communicable Diseases, Johannesburg, South Africa (E. van Schalkwyk, R.S. Mpembe, J. Thomas, L. Shuping, H. Ismail, N.P. Govender); Vermaak & Partners–Pathcare Pathologists, Johannesburg (W. Lowman); Wits Donald Gordon Medical Centre, Johannesburg (W. Lowman); University of the Witwatersrand, Johannesburg (W. Lowman, A.S. Karstaedt, V. Chibabhai, J. Wadula, A. Messina, N.P. Govender); University of Pretoria and Kalafong Provincial Tertiary Hospital, Pretoria, South Africa (T. Avenant); Netcare Hospitals Ltd, Johannesburg (A. Messina); Lancet Laboratories, Durban, South Africa (C.N. Govind, K. Moodley); University of KwaZulu-Natal, Durban (C.N. Govind, H. Dawood, P. Ramjathan); Grey’s Hospital, Pietermaritzburg, South Africa (H. Dawood); National Health Laboratory Service, Johannesburg (V. Chibabhai, J. Wadula, P. Ramjathan)

DOI: <https://doi.org/10.3201/eid2509.190040>

This multidrug-resistant fungal pathogen emerged worldwide, appearing almost simultaneously on 6 continents, causing invasive disease and protracted healthcare-associated outbreaks (2–5). The reported crude case-fatality ratio among patients with invasive *C. auris* infections is high, although the attributable mortality rate has not been determined (3,6). *C. auris* persists on surfaces, is transmitted among patients in the healthcare environment, forms biofilms, and resists routinely used environmental cleaning agents (7–10). *Candida* spp. are a common cause of bloodstream infections and were responsible for 13% (95% CI 6%–26%) of healthcare-associated bloodstream infections according to a 2015 US point-prevalence survey (11). *C. parapsilosis* was the dominant species causing candidemia according to a national survey in South Africa conducted during 2009–2010 (12). Patients at risk for candidemia in general are the critically ill (especially premature neonates) and those with serious underlying illnesses (e.g., diabetes mellitus and hematologic malignancies), prior or prolonged exposure to broad-spectrum antimicrobial drugs, and invasive medical and surgical interventions (13). Previously described characteristics associated with candidemia among adults in South Africa included abdominal surgery, trauma, diabetes mellitus, cancer, and HIV infection (14). *C. auris* is thought to occupy a similar niche in the healthcare environment as *C. parapsilosis* because both organisms colonize human skin and adhere to healthcare surfaces and devices. Clinical risk factors for *C. auris* infection would be expected to be similar to those for *C. parapsilosis* infection, but these factors are largely reported from several small case series. Risk factors for *C. auris* candidemia (compared with other species) among patients admitted to 27 intensive care

¹Preliminary results from this study were presented at the Federation of Infectious Diseases Societies of Southern Africa (FIDSSA) conference (oral abstract no. 8,382), November 9–11 2017, Cape Town, South Africa.

²These authors contributed equally to this article.

units in India included underlying respiratory disease, vascular surgery, having a urinary catheter in situ, prior antifungal drug exposure, and a low APACHE II score at admission (6). In South Africa, most reported cases of *C. auris* colonization or invasive disease occurred in older patients (median age 60 years) (1) (R.E. Magobo, National Institute for Communicable Diseases [NICD], South Africa, pers. comm., 2019 Jul 1). To inform infection prevention and empiric antifungal treatment strategies, we used national surveillance data for South Africa to estimate the total incidence risk for candidemia and the proportion of candidemia cases caused by *C. auris* and to determine factors associated with *C. auris* candidemia compared with other *Candida* species,

Materials and Methods

Surveillance for Candidemia

From January 1, 2016, through December 31, 2017, we conducted active national laboratory-based surveillance for candidemia by using the NICD GERMS-SA surveillance platform. We requested that *Candida* species from any episode of bloodstream infection, with an accompanying laboratory report (including basic patient demographic data), be submitted from all clinical microbiology laboratories within the National Health Laboratory Service (NHLS), a national public-sector laboratory network, and from all pathology laboratory practices in the private sector. We have previously described the methods used by private and NHLS laboratories for species identification (1). Isolates were sent to the NICD's Mycology Reference Laboratory for confirmation of identification and antifungal drug susceptibility testing. In addition, surveillance officers (nurses or pharmacists) collected basic clinical and demographic data on standardized electronic case report forms at 22 public-sector and 3 private-sector enhanced surveillance sites, all of which were large acute-care hospitals. We did not collect sufficient data to define severity of illness scores (e.g., APACHE II or McCabe scores). We conducted retrospective audits to ensure complete case ascertainment.

We extracted line list data from the laboratory information systems of NHLS and private laboratories, compared those data with reported cases, deduplicated the data (by using patient name, surname, date of birth, hospital number, and specimen collection date), and added missing cases to the surveillance database. For cases detected by audit, we recorded the *Candida* species identification reported by the reporting laboratory. In 2013, the estimated number of beds in private-sector hospitals nationwide was 34,572, of which 45% were located in Gauteng Province, the most economically active and densely populated province of South Africa (15).

Case Definitions

We defined a case of candidemia as illness in any patient at a healthcare facility in South Africa who had *Candida* species isolated from a blood culture specimen processed by an NHLS or private-sector diagnostic laboratory. We defined a confirmed case of *C. auris* candidemia as illness in a patient with an isolate confirmed as *C. auris* at NICD, regardless of the referring laboratory's initial identification. We also included probable cases for which the referring laboratory identified *C. auris* or *Candida haemulonii* but a viable isolate was not available for confirmation at NICD. Multiple *Candida* isolates cultured within 30 days of the first positive blood culture specimen were included in a single case. We classified cases of candidemia into 2 groups on the basis of NICD identification (or the referring laboratory's identification if a viable isolate was not available): *C. auris* and non-*C. auris* candidemia.

Reference Laboratory Methods

Isolates were submitted to NICD on Dorset transport medium (Diagnostic Media Products, <http://www.nhls.ac.za>). For viable isolates, species-level identification was confirmed by using matrix-assisted laser desorption/ionization time-of-flight (MALDI-TOF) mass spectrometry (Bruker Corporation, <https://www.bruker.com>). We amplified and sequenced the internal transcribed spacer or D1/D2 region of the ribosomal gene for isolates when MALDI-TOF mass spectrometry did not yield a score ≥ 2 .

Statistical Analyses

We calculated the overall incidence risk for candidemia for hospitals for which admissions data were available, stratified by healthcare sector, by dividing the total number of new cases of candidemia by the total number of hospital admissions (i.e., number of persons at risk) in each sector for the 2-year period. We also calculated healthcare facility incidence risk per hospital when admission denominator data were available. We obtained admissions data by directly approaching private hospital groups and through the GERMS-SA surveillance platform for public-sector hospitals. We used ArcGIS mapping software (<https://www.esri.com>) to plot the location and number of *C. auris* candidemia cases at hospitals in Gauteng Province and used inverse distance-weighted interpolation to map hotspot hospitals, which we defined as those with >10 reported cases of *C. auris* candidemia during the 2-year period.

We hypothesized a priori that systemic azole exposure was associated with candidemia caused by *C. auris* rather than other *Candida* species. Distinguishing cases of *C. auris* candidemia from those caused by other species is important to physicians choosing an empiric antifungal treatment regimen for suspected candidemia and to infection prevention and control practitioners for rapid identification

of cases requiring contact precautions. We used multivariable logistic regression to assess this association among patients admitted to 25 enhanced surveillance sites.

We compared proportions between groups by using a χ^2 or Fisher exact test. We compared medians by using a Wilcoxon rank-sum test.

Ethics

NICD obtained annual approval for GERMS-SA laboratory-based surveillance from the human research ethics committees of several universities in South Africa. Patients from whom surveillance data were collected prospectively through interview provided written informed consent.

Results

During the 2-year surveillance period, 6,669 cases of candidemia (6,629 first and 40 recurrent episodes) were detected across South Africa at 103 public-sector and 166 private-sector hospitals (2,529 cases [38%] in the public sector, 4,140 cases [62%] in the private sector). Of the 6,669 cases, viable isolates were identified to species level at NICD for 3,020 (45%) cases. Species identification was available for a further 2,856 cases (2,842 from private laboratories, 14 from NHLS laboratories). Among 5,876 cases with a species-level identification, 794 (14%) were caused by *C. auris* and 5,082 (86%) by other *Candida* species (Figure

1). The most common *Candida* species in the non-*C. auris* group were *C. parapsilosis* (2,600 [44%]), *C. albicans* (1,353 [23%]), *C. glabrata* (598 [10%]), *C. tropicalis* (140 [2%]), and *C. krusei* (98 [2%]). Twenty-nine cases had a mixed episode of candidemia caused by *C. auris* and another *Candida* species (mostly *C. parapsilosis* [21 cases]).

The total incidence risk for candidemia (expressed as cases/100,000 hospital admissions) at 115 private-sector and 18 public-sector hospitals with available admissions data was 71.2 (95% CI 68.6–73.8) in the private sector and 149.5 (95% CI 141.1–158.1) in the public sector, for a total of 83.8 (95% CI 81.2–86.4) (Table 1). Incidence risk for *C. auris* was 13.6 (95% CI 12.4–14.8) in the private sector, compared with 6.9 (95% CI 5.2–9.0) in the public sector; incidence risk ratio was 1.96 (95% CI 1.4–2.6). Individual healthcare facility incidence risk ranged from 2.6 to 375 for *C. parapsilosis*, 1.3 to 221 for *C. albicans*, 0.9 to 154 for *C. auris*, and 1.7 to 107 for *C. glabrata*.

We received 4,236 isolates from 70 NHLS laboratories and 4 amalgamated private-sector pathology practices, and we identified an additional 3,307 cases (with 3,373 corresponding isolates) by retrospective audits. Of the 400 confirmed viable *C. auris* isolates received, 258 (65%) had an initial identification of *C. auris*.

Among 435 patients with *C. auris* candidemia for whom data were available (including 9 patients with probable

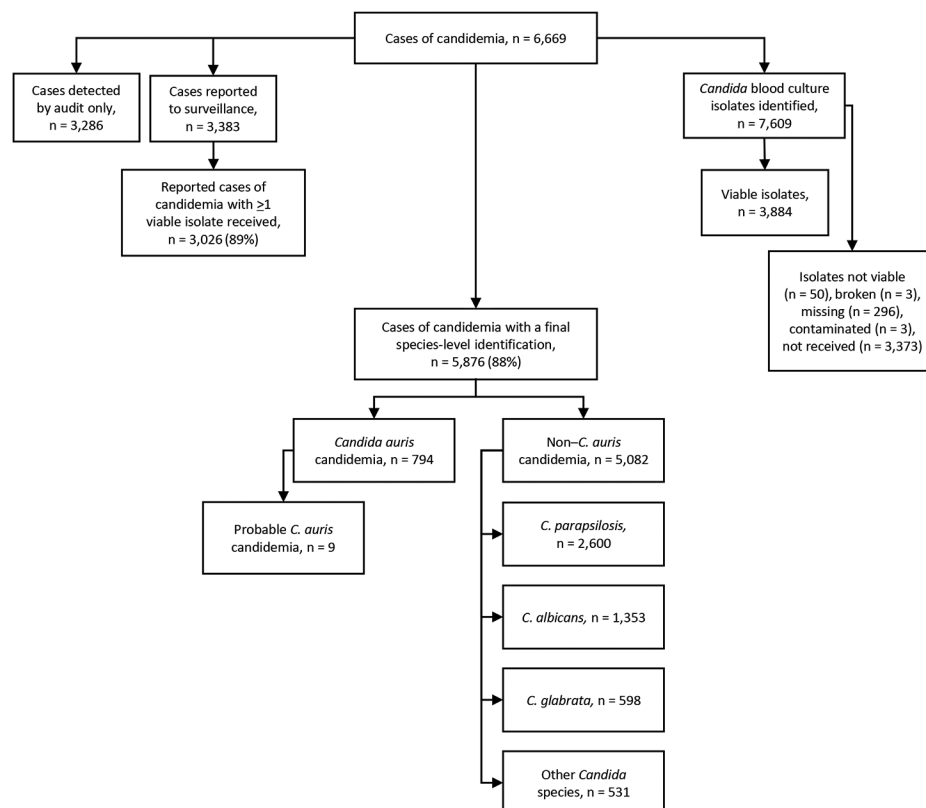


Figure 1. Flowchart showing numbers of candidemia cases detected by national surveillance and *Candida* species identified, South Africa, 2016–2017.

Table 1. Incidence risk for candidemia at a limited number of public- and private-sector hospitals with available admissions data, by *Candida* species and healthcare sector, South Africa, 2016–2017*

<i>Candida</i> species	No. cases at 133 hospitals	Total incidence risk† (95% CI)	Incidence risk at 18 public-sector hospitals† (95% CI)	Incidence risk at 115 private-sector hospitals† (95% CI)	Incidence risk ratio, private sector:public sector (95% CI)
<i>C. parapsilosis</i>	1,657	32.98 (31.3–34.6)	27.98 (24.4–31.9)	33.94 (32.2–35.8)	1.21 (1.0–1.4)
<i>C. albicans</i>	735	14.63 (13.5–15.8)	34.55 (30.6–38.9)	10.82 (9.5–11.9)	0.31 (0.2–0.4)
<i>C. auris</i>	628	12.50 (11.5–13.6)	6.93 (5.2–9.0)	13.57 (12.4–14.8)	1.96 (1.4–2.6)
<i>C. glabrata</i>	352	7.01 (6.2–7.8)	12.13 (9.8–14.8)	6.02 (5.31–6.9)	0.50 (0.3–0.7)
Other	308	6.13 (5.4–6.9)	13.25 (10.8–16.1)	4.77 (4.1–5.5)	0.36 (0.2–0.5)
Total‡	4,209	83.78 (81.2–86.4)	149.46 (141.1–158.1)	71.20 (68.6–73.8)	0.48 (0.4–0.6)

*Admissions data were available for 115 private-sector hospitals (4,216,306 admissions) and 18 public-sector hospitals (807,600 admissions).

†No. cases/100,000 hospital admissions.

‡A total of 529 candidemia cases had no *Candida* species identified, and incidence risk for these are not displayed in the table. However, these case numbers are included in the total number of candidemia cases and total incidence risk calculations.

C. auris infection), the median age was 54 years (interquartile range [IQR] 34–67 years), compared with a median of 27 years (IQR 0–57 years) among 4,050 patients with non-*C. auris* candidemia ($p < 0.001$) (Table 2; Figure 2). Neonates comprised the largest proportion of patients with non-*C. auris* candidemia (1,015/4,050; 25%), whereas only 20 cases (5%) in the *C. auris* group were in neonates (Table 2). Of patients with *C. auris*, 61% (284/463) were male; 54% (1,729/3,216) were male in the non-*C. auris* group.

Most (86%, 680/794) cases of *C. auris* candidemia were from hospitals in Gauteng Province and 88% (695/794) from private-sector facilities, compared with 60% (3,549/5,875) in Gauteng Province and 59% (3,445/5,875) from private-sector facilities among non-*C. auris* cases. Cases of *C. auris* candidemia were diagnosed at 14 public-sector and 67 private-sector hospitals (Figure 3), most of which are located in Gauteng Province (Figure 4). Among these, 25 hospitals had >10 cases of *C. auris* candidemia during the 2-year period (meeting our definition of hotspot hospitals); the largest absolute number of cases was reported from a large private hospital and another large academic teaching hospital. However, incidence risk for *C. auris* candidemia was highest in a smaller private-sector hospital (13 cases/8,431 admissions [154 cases/100,000 admissions]). Of the 20 hospitals with the highest incidence, 19 were private-sector facilities. Several small outbreaks occurred at these hotspot hospitals, but in different wards within each hospital (data not shown).

We collected clinical data for 2,067 patients at enhanced surveillance sites, including 535 patients whose isolates were not identified at the species level. Most patients with *C. auris* bloodstream infections had received prior (≤ 14 days before diagnosis) systemic antimicrobial drug therapy (77/94 [82%]), and 30/95 (32%) had received prior systemic antifungal drug therapy. Of the 30 patients with prior antifungal therapy, 16 had received azoles, 7 had received amphotericin B, and 13 had received echinocandins. Among 105 patients with *C. auris* candidemia for whom clinical data were available, the median length

of hospitalization before onset of candidemia was 28 days (IQR 15–46 days), compared with 12 days (IQR 5–23 days) among 1,852 patients with non-*C. auris* candidemia ($p < 0.001$). Approximately one third (32/105 [31%]) of patients with *C. auris* candidemia spent >6 weeks in hospital before the first positive blood culture was obtained. Seventy-seven (74%) patients with *C. auris* infection had been hospitalized in the past year, and 110 (88%) patients were admitted to an intensive care unit at some point during their current hospital stay. Eleven (26%) of 43 patients with *C. auris* candidemia were HIV-seropositive, similar to patients infected with other *Candida* species (251/972; 26%). The crude in-hospital case-fatality ratio did not differ between *Candida* species and was 45% for *C. auris* candidemia, compared with 43% for non-*C. auris* candidemia ($p = 0.6$) (*C. albicans*, 50%; *C. parapsilosis*, 32%; *C. glabrata*, 51%) (Table 2).

Prior systemic antifungal drug therapy was associated with 40% increased adjusted odds of *C. auris* fungemia; nevertheless, an effect ranging from a 20% decrease to a 2.5-fold increase is also consistent with our data (adjusted odds ratio [aOR] 1.4 [95% CI 0.8–2.3]). A central venous catheter in situ also independently increased the odds of *C. auris* infection 2-fold (aOR 1.8 [95% CI 1.05–3.01]). Admission to a private-sector facility increased the odds of *C. auris* candidemia 3-fold (aOR 2.7 [95% CI 1.5–4.7]). Older patients (aOR 1.01 [95% CI 1.01–1.03] for every year) with longer hospitalization before the first positive blood culture (aOR 1.01 [95% CI 1.01–1.02] for every day admitted) were more likely to have *C. auris* fungemia.

To understand whether inherent differences between healthcare sectors influenced risk factors, we stratified *C. auris* data by healthcare sector (Table 3). In the public sector, prior antifungal drug therapy (especially azole therapy) was associated with 2-fold increased odds of *C. auris* bloodstream infection (aOR 2.0 [95% CI 1.0–3.9]; $p = 0.04$) after adjustment for patient age, sex, length of hospital stay, previous hospitalization, and presence of a central venous catheter in situ.

Table 2. Demographic and clinical characteristics of 6,669 patients with candidemia caused by *Candida auris* compared with other *Candida* species, South Africa, 2016–2017*

Characteristics	All candidemia	<i>C. auris</i>	Non- <i>C. auris</i>	<i>C. parapsilosis</i>	<i>C. albicans</i>	<i>C. glabrata</i>
No. case-patients	6,669	794	5,875	2,600	1,353	598
Systemic antifungal drug therapy ≤14 d before positive culture†	317/1,829 (17.3)	30/95 (31.6)	287/1,734 (16.6)	108/477 (22.6)	36/441 (8.2)	11/166 (6.6)
Azole	219/317 (69.1)	16/30 (53.3)	203/287 (70.7)	72/108 (66.7)	30/36 (83.3)	9/11 (81.8)
Polyene/amphotericin B	38/317 (12)	7/30 (23.3)	31/287 (10.8)	12/108 (11.1)	5/36 (13.9)	0/11 (0)
Echinocandin	79/317 (24.9)	13/30 (43.3)	66/287 (23)	27/108 (25)	2/36 (5.6)	2/11 (18.2)
Age, y, median (IQR)	32 (0–58)	54 (34–67)	27 (0–57)	24 (0–58)	24 (0–56)	54 (32–67)
Sex						
Men and boys	2,013/3,679 (54.7)	284/463 (61.3)	1,729/3,216 (53.8)	806/1,474 (54.7)	533/978 (54.5)	232/444 (52.3)
Women and girls	1,666/3,679 (45.3)	179/463 (38.7)	1,487/3,216 (46.2)	668/1,474 (45.3)	445/978 (45.5)	212/444 (47.7)
Length of hospital stay, d median (IQR)	32 (16–54)	55 (32–81)	31 (15–52)	40 (25–59)	24 (12–43)	22 (9–41)
Length of stay until first positive blood culture, d, median (IQR)	13 (5–24)	28 (15–46)	12 (5–23)	16 (10–27)	10 (3–19)	6 (1–16)
Province						
Gauteng	4,229/6,669 (63.4)	680/794 (85.6)	3,549/5,875 (60.4)	1,651/2,600 (63.5)	736/1,353 (54.4)	323/598 (54)
Other	2,440/6,669 (36.6)	114/794 (14.4)	2,326/5,875 (39.6)	949/2,600 (36.5)	617/1,353 (45.6)	275/598 (46)
Healthcare sector						
Public	2,529/6,669 (37.9)	99/794 (12.5)	2,430/5,875 (41.4)	599/2,600 (23)	673/1,353 (49.7)	248/598 (41.5)
Private	4,140/6,669 (62.1)	695/794 (87.5)	3,445/5,875 (58.6)	2,001/2,600 (77)	680/1,353 (50.3)	350/598 (58.5)
Hospital admission in past 12 mo	1,428/1,967 (72.6)	77/104 (74)	1,351/1,863 (72.5)	378/529 (71.5)	341/486 (70.2)	126/174 (72.4)
Intensive care unit admission	1,579/2,167 (72.9)	110/125 (88)	1,469/2,042 (71.9)	502/606 (82.8)	377/539 (69.9)	133/190 (70)
Mechanical ventilation	611/1,818 (33.6)	44/91 (48.4)	567/1,727 (32.8)	175/476 (36.8)	129/440 (29.3)	57/165 (34.6)
Central venous catheter in situ	1,031/1,817 (56.7)	69/92 (75)	962/1,725 (55.8)	289/479 (60.3)	229/443 (51.7)	89/165 (53.9)
Systemic antimicrobial drug therapy in 14 d before positive culture	1,292/1,830 (70.6)	77/94 (81.9)	1,215/1,736 (70)	349/481 (72.6)	284/441 (64.4)	105/164 (64.0)
Crude in-hospital case-fatality ratio	8,39/1,966 (42.7)	46/102 (45.1)	793/1,864 (42.5)	166/516 (32.2)	247/492 (50.2)	91/179 (50.8)

*Values are no. (%) except as indicated. The 3 most common *Candida* species in the non-*C. auris* group (*C. parapsilosis*, *C. albicans*, and *C. glabrata*) are shown separately for comparison. For the purpose of this analysis, cases of candidemia with no final species identification were included in the non-*C. auris* group. IQR, interquartile range.

†Patients could have received >1 class of antifungal drug therapy.

Discussion

In conducting this comprehensive national survey, we found that *C. auris* caused >10% of all cases of candidemia in South Africa and was the third most common *Candida* species. The incidence of *C. auris* candidemia was highest in private-sector hospitals in Gauteng Province. The crude in-hospital case-fatality ratio did not differ between *Candida* species. Prior systemic antifungal drug therapy was associated with increased adjusted odds of *C. auris* fungemia compared with candidemia caused by other species, and this effect was stronger in public-sector hospitals.

C. auris has rapidly emerged as a major cause of candidemia in South Africa, surpassing the number of cases caused by *C. glabrata*, *C. tropicalis*, and *C. krusei* over the past 7 years. A clear shift has occurred in the epidemiology observed from a previous national survey during 2009–

2010 and a recent dramatic increase in the number of cases of *C. auris* invasive infection and colonization nationwide (1,12). We speculate that delayed clinician and laboratory awareness might have led to undetected transmission of the pathogen early in the epidemic (16).

The incidence of *C. auris* candidemia was highest in hospitals in Gauteng Province and is partly attributable to ongoing and recurrent clusters in these hospitals during the surveillance period. We speculate that the epidemic in South Africa might be centered in this area because of a combination of complex and interdependent health-care system and behavioral factors, including a highly concentrated and mobile patient population; a large number of referrals and admission of patients with clinically complex cases to hospitals in the region; indiscriminate use of antimicrobial agents, including azoles and

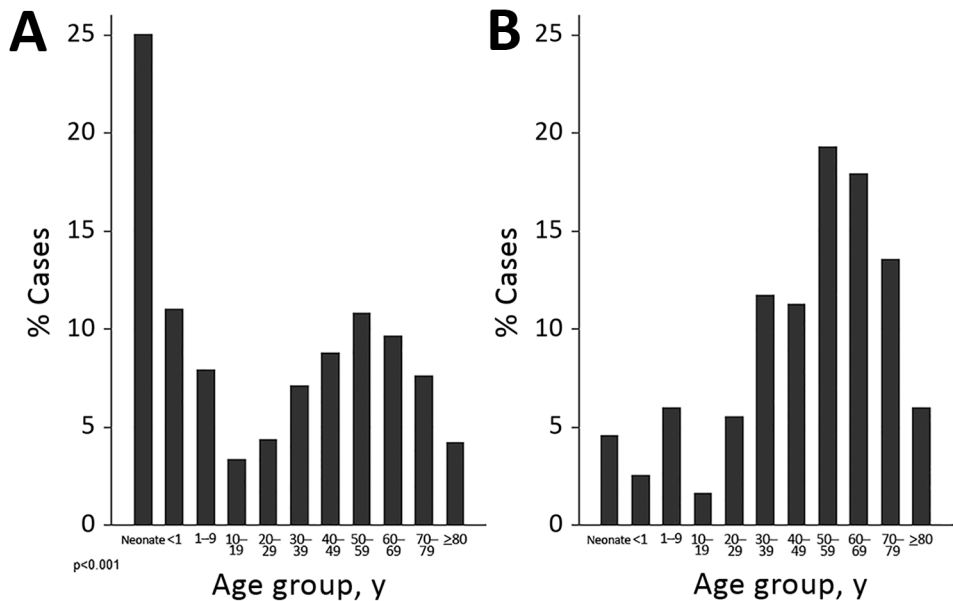
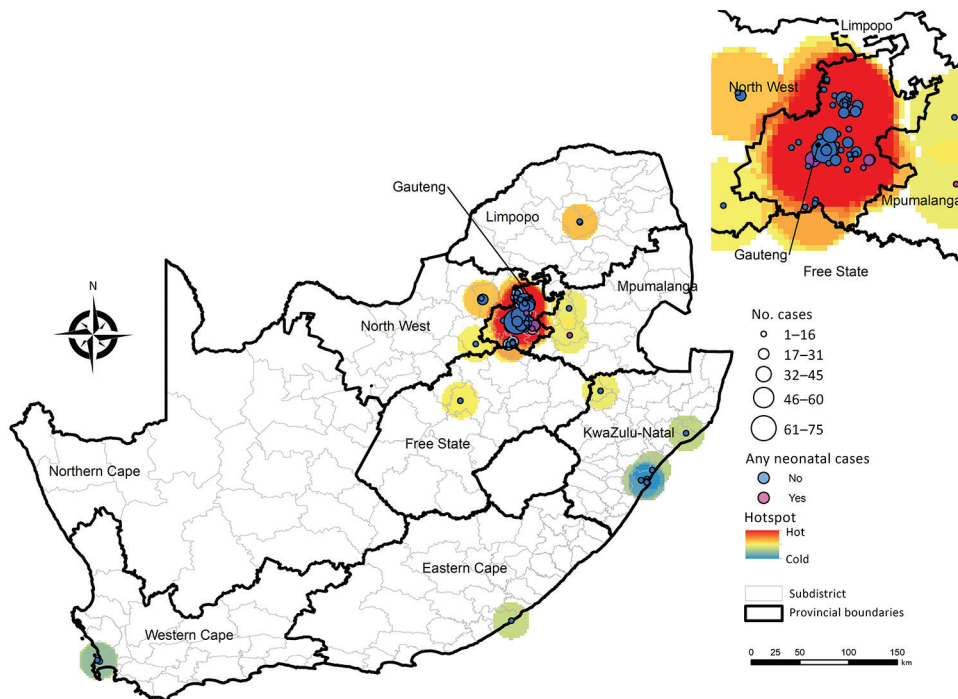


Figure 2. Age distribution of case-patients with candidemia caused by *Candida auris* compared with other *Candida* species, South Africa, 2016–2017. A) *C. auris* patient median age was 54 years (interquartile range 34–67 years); B) other *Candida* species patient median age was 27 years (interquartile range 0–57 years).

echinocandins; and suboptimal infection prevention and control practices. In addition, international travel to and from Gauteng Province might also play a role, as suggested by recent case reports and outbreaks in other continents caused by the South Africa clade of *C. auris* (5,17–20). In the United States, 90% of clinical cases of *C. auris* occurred in the New York metropolitan area, and most patients had lengthy hospitalizations in facilities that had capacity for highly skilled nursing and mechanical ventilation (21), suggesting that a large susceptible population of severely ill patients within a facility might provide a starting

point for an outbreak that is then amplified by transmission. Individual hospital outbreaks seemed to overlap in Gauteng Province, suggesting that interfacility and intersectoral transmission of infections might have occurred; however, we have not yet established epidemiologic links among cases from different facilities. Whole-genome sequencing to establish molecular links is under way to more clearly characterize the epidemiology of *C. auris* candidemia in South Africa.

Prior systemic antifungal drug use was associated with *C. auris* candidemia, particularly in public-sector



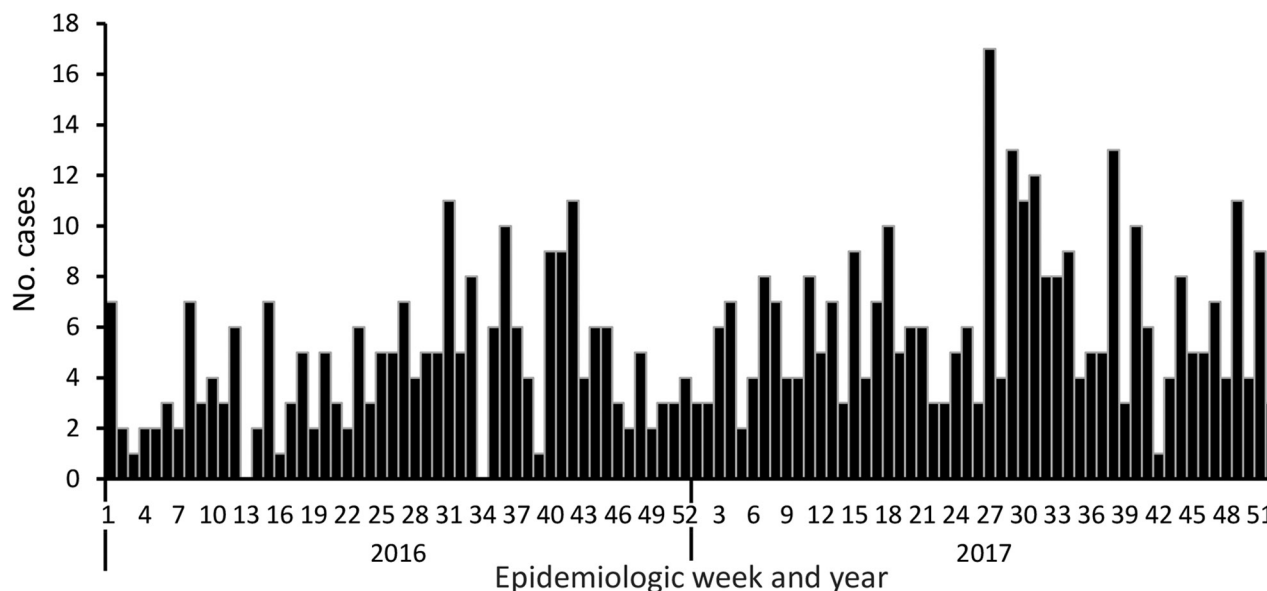


Figure 4. Cases of *Candida auris* candidemia (N = 557), by epidemiologic week, Gauteng Province, South Africa, 2016–2017. Date of blood culture collection was missing for 123 cases.

hospitals. This finding is consistent with data from similar studies and is probably related to selective pressure by azoles (6). Almost all tested *C. auris* isolates from South Africa are resistant to fluconazole (2) (T.G. Maphanga, NICD, pers. comm., 2018 Jul 27). Fluconazole is commonly used as a first-line treatment option, especially in public-sector hospitals, where access to echinocandin antifungal drugs is currently limited. The forthcoming 2019 guidelines for treatment of *C. auris* in South Africa recommend echinocandins as a first-line treatment for candidemia

and amphotericin B deoxycholate if echinocandins are unavailable (22). In contrast to other *Candida* species, such as *C. parapsilosis*, for which a substantial proportion of infections occur among the neonatal population, *C. auris* occurs among older adults (12). In South Africa, an outbreak among 6 neonates in a neonatal unit has been documented (23), and several other small outbreaks have occurred (N.P. Govender, unpub. data). To date, no neonatal cases have been reported from the United States or Europe, although India, Colombia, and Venezuela have reported cases (4–6,19,24,25). Whether this phenomenon

Table 3. Demographic and clinical characteristics of patients with *Candida auris* candidemia, by healthcare sector, South Africa, 2016–2017*

Characteristic	Public-sector hospitals, n = 99	Private-sector hospitals, n = 695	p value†
Age, y, median (IQR)	27 (2–42)	58 (44–70)	<0.001
Sex			0.64
Men and boys	63/99 (64)	221/364 (61)	NA
Women and girls	36/99 (36)	143/364 (39)	NA
Length of hospital stay, d, median (IQR)	49 (30–72)	68 (40–140)	0.03
Length of stay to first positive blood culture, d, median (IQR)	26 (13–42)	35 (16–58)	0.21
Hospital admission in past 12 mo	37/62 (60)	40/42 (95)	<0.001
Intensive care unit admission	54/68 (79.4)	56/57 (98.3)	0.001
Mechanical ventilation	21/52 (40)	23/39 (59)	0.09
Central venous catheter in situ	40/54 (74)	29/38 (76)	1.0
Total parenteral nutrition	22/52 (42)	15/38 (39)	0.83
Systemic antimicrobial drug therapy ≤14 d before positive culture	36/52 (69)	41/42 (98)	<0.001
Systemic antifungal drug therapy ≤14 d before positive culture‡	14/53 (26)	16/42 (38)	0.27
Azole	12/14 (85.7)	4/16 (25)	0.001
Polyene/amphotericin B	4/14 (28.6)	3/16 (18.8)	0.68
Echinocandin	0/14 (0)	13/16 (81.3)	<0.001
Crude in-hospital mortality ratio	22/59 (37)	24/43 (56)	0.07

*Values are no. (%) except as indicated. Age data were available for 435 patients, and data on sex were available for 428 patients. For the rest of the variables, data were available for only a small proportion of patients from enhanced surveillance sites (total, N = 110; public sector, n = 67; private sector, n = 43). IQR, interquartile range; NA, not applicable.

†Proportions were compared by using a χ^2 or Fisher exact test; medians were compared by using the Wilcoxon rank-sum test.

‡Patients could have received >1 class of antifungal drug therapy.

is attributable to inherent factors of the pathogen, environmental factors in neonatal units, or chance is still unclear. Nevertheless, we should be proactive to not let *C. auris* establish a foothold in neonatal units in developing countries as *C. parapsilosis* has done (12,26).

In the unique healthcare environment of South Africa, patients admitted to private-sector facilities were more likely to have *C. auris* candidemia. We hypothesize that this might be attributable to early undetected outbreaks in this sector, inherent differences in the patient populations admitted, or structural differences in the 2 healthcare sectors; more patients with *C. auris* candidemia at private-sector facilities were mechanically ventilated, had prior hospitalization, and had prior systemic antimicrobial drug therapy. Antimicrobial drug prescription behavior and differences in antimicrobial drug stewardship practices, including easier access to a broader range of antifungal drugs, might also play a role. Last, ongoing outbreaks at a few facilities might drive the higher case numbers in the private healthcare sector. The presence of a central venous catheter is a well-established risk factor for bloodstream infections (27). It is not surprising that central venous catheters were associated with *C. auris* candidemia because the pathogen has been shown to form biofilms and adhere to polymeric surfaces (8,10).

To address the continued transmission of *C. auris* in health facilities in South Africa, *C. auris* has been identified as a priority pathogen for surveillance to monitor emergence of antifungal drug resistance from all infection sites. We have also adapted published laboratory methods for rapid identification of *C. auris* colonization in the context of outbreak investigations (28). Local studies are also being planned to investigate the efficacy of novel antifungal agents (29).

This study had several limitations. We analyzed data for laboratory-confirmed candidemia only and did not include patients with other invasive *Candida* infections, culture-negative sepsis, or colonization, which might underestimate the extent of the problem in South Africa. However, 18%–22% of reported cases of *C. auris* infection in Europe and South Africa are bloodstream infections, and 58% of clinical isolates in the United States are from blood (1,19,30). In addition, 77% of cases of *C. auris* infection reported in the international literature are cases of candidemia; therefore, our study provides a plausible representation of the epidemiology of *C. auris*, albeit just the proverbial tip of the iceberg (3). The determination of incidence risk was based on data from a limited number of hospitals with admissions data available, mostly from the private sector. Therefore, we might have underestimated the incidence risk in the public sector. The reference laboratory confirmed the species identification of bloodstream isolates from only 45% of all detected cases of candidemia.

Most cases without a reference laboratory species identification (70%) were from the private sector and had been detected retrospectively through audits. However, we believe that these national surveillance data still provide an accurate representation of the actual distribution of *C. auris* candidemia cases across sectors because most private laboratories used MALDI-TOF mass spectrometry methods to confirm *Candida* species identification. For cases at enhanced surveillance sites, we were limited to the availability of secondary data collected through an established surveillance program; we were unable to assess the duration of exposure to certain factors, such as parenteral nutrition and type of prior antimicrobial drug exposure. In addition, the linking of audit cases to reported cases was limited by demographic data available; therefore, we might have included duplicate cases in our analysis. Misclassification error might have occurred, given that a proportion of isolates did not have a species-level identification.

C. auris was the third most common cause of candidemia in South Africa and caused 14% of all cases during 2016–2017. Ongoing and recurrent micro-outbreaks might have driven the larger epidemic centered in Gauteng Province. Individual patient and healthcare risk factors should be considered when managing patients with suspected candidemia. The use of molecular epidemiology is needed to further characterize outbreaks in South Africa and better understand transmission dynamics of this emerging pathogen.

Acknowledgments

We are grateful to Jimmy Khosa for designing the maps included in this paper. We acknowledge Briette du Toit, Angeliki Messina, Hleziphi Mahlangu, and Joy Cleghorn for providing denominator data for the major private-sector hospital groups. We also acknowledge the following contributors to the GERMS-SA candidemia surveillance programme for participating in surveillance and sending *Candida* isolates to the National Institute for Communicable Diseases: John Black, Shareef Abrahams, Vanessa Pearce, Anwar Hoosen, Vicky Kleinhans, Masego Moncho, Alan Karstaedt, Caroline Maluleka, Charl Verwey, Charles Feldman, David Moore, Gary Reubenson, Khine Swe Swe Han, Jeannette Wadula, Jeremy Nel, Kathy Lindeque, Maphoshane Nchabeleng, Nazlee Samodien, Nicolette du Plessis, Nontombi Mbelle, Nontuthuko Maningi, Norma Bosman, Ranmini Kularatne, Sharona Seetharam, Teena Thomas, Theunis Avenant, Trusha Nana, Vindana Chibabhai, Adhil Maharj, Asmeeta Burra, Fathima Naby, Halima Dawood, Jade Mogamberry, Koleka Mlisana, Lisha Sookan, Praksha Ramjathan, Prasha Mahabeer, Romola Naidoo, Sumayya Haffejee, Yacoob Coovadia Khine Swe Swe Han, Nomonde Dlamini, Surendra Sirkar, Ken Hamese, Ngoaka Sibiyi, Ruth Lekalakala, Greta Hoyland, Jacob Lebudi, Pieter Jooste, Ebrahim Variava, Erna du Plessis, Andrew Whitelaw,

Kessendri Reddy, Mark Nicol, Preneshni Naicker, Colleen Bamford, Adrian Brink, Ebrahim Hoosien, Elizabeth Prentice, Inge Zietsman, Maria Botha, Peter Smith, Terry Marshall, Xoliswa Poswa, Chetna Govind, Juanita Smit, Keshree Pillay, Sharona Seetharam, Suzy Budavari, Victoria Howell, Carel Haumann, Catherine Samuel, Marthinus Senekal, Andries Dreyer, Khatija Ahmed, Louis Marcus, Warren Lowman, Angeliki Messina, Dena van den Bergh, and Karin Swart. We also acknowledge our NICD GERMS-SA colleagues: Ananta Nanoo, Andries Dreyer, Anne von Gottberg, Anthony Smith, Arvinda Sooka, Cecilia Miller, Charlotte Sriruttan, Cheryl Cohen, Chikwe Ihekweazu, Claire von Mollendorf, Desiree du Plessis, Erika van Schalkwyk, Farzana Ismail, Frans Radebe, Genevieve Ntshoe, Gillian Hunt, Hlengani Mathema, Husna Ismail, Jacqueline Weyer, Jackie Kleynhans, Jenny Rossouw, John Freaan, Joy Ebonwu, Judith Mwansa-Kambafwile, Karen Keddy, Kerrigan McCarthy, Liliwe Shuping, Linda de Gouveia, Linda Erasmus, Lucille Blumberg, Marshagne Smith, Martha Makgoba, Motshabi Modise, Nazir Ismail, Nelesh Govender, Neo Legare, Nicola Page, Ntsieni Ramalwa, Nuraan Paulse, Phumeza Vazi, Olga Perovic, Penny Crowther-Gibson, Portia Mutevedzi, Riyadh Manesen, Ranmini Kularatne, Ruth Mpmembe, Sarona Lengana, Shabir Madhi, Shaheed Vally Omar, Sibongile Walaza, Sonwabo Lindani, Sunnieboy Njikhoh, Susan Meiring, Thejane Motladiile, Tiisetso Lebaka, Vanessa Quan, and Verushka Chetty. Finally, we acknowledge persons from the Centre for Healthcare-Associated Infections, Antimicrobial Resistance, and Mycoses at NICD: Serisha Naicker, Tsidiso Maphanga, Mabatho Mhlanga, Thokozile Gloria Zulu, Ernest Tsotetsi, Phelly Matlapeng, Sipiwe Kutta, Lerato Qoza, Sydney Mogokotleng, Mbali Dube, and Amanda Shilubane.

This work was supported in its entirety by NICD, a division of NHLS, in Johannesburg, South Africa.

About the Author

Dr. van Schalkwyk is a medical epidemiologist at the National Institute for Communicable Diseases, South Africa. Her research interests include mycoses, healthcare-associated infections, and antimicrobial resistance.

References

- Govender NP, Magobo RE, Mpmembe R, Mhlanga M, Matlapeng P, Corcoran C, et al. *Candida auris* in South Africa, 2012–2016. *Emerg Infect Dis*. 2018;24:2036–40. <http://dx.doi.org/10.3201/eid2411.180368>
- Lockhart SR, Etienne KA, Vallabhaneni S, Farooqi J, Chowdhary A, Govender NP, et al. Simultaneous emergence of multidrug-resistant *Candida auris* on 3 continents confirmed by whole-genome sequencing and epidemiological analyses. *Clin Infect Dis*. 2017;64:134–40. <http://dx.doi.org/10.1093/cid/ciw691>
- Jeffery-Smith A, Taori SK, Schelenz S, Jeffery K, Johnson EM, Borman A, et al.; *Candida auris* Incident Management Team. *Candida auris* Incident Management Team. *Candida auris*: a review of the literature. *Clin Microbiol Rev*. 2017;31:e00029–17. <http://dx.doi.org/10.1128/CMR.00029-17>
- Schelenz S, Hagen F, Rhodes JL, Abdolrasouli A, Chowdhary A, Hall A, et al. First hospital outbreak of the globally emerging *Candida auris* in a European hospital. *Antimicrob Resist Infect Control*. 2016;5:35. <http://dx.doi.org/10.1186/s13756-016-0132-5>
- Ruiz-Gaitán A, Moret AM, Tasiias-Pitarch M, Aleixandre-López AI, Martínez-Morel H, Calabuig E, et al. An outbreak due to *Candida auris* with prolonged colonisation and candidaemia in a tertiary care European hospital. *Mycoses*. 2018;61:498–505. <http://dx.doi.org/10.1111/myc.12781>
- Rudramurthy SM, Chakrabarti A, Paul RA, Sood P, Kaur H, Capoor MR, et al. *Candida auris* candidaemia in Indian ICUs: analysis of risk factors. *J Antimicrob Chemother*. 2017;72:1794–801. <http://dx.doi.org/10.1093/jac/dkx034>
- Ku TSN, Walraven CJ, Lee SA. *Candida auris*: disinfectants and implications for infection control. *Front Microbiol*. 2018;9:726. <http://dx.doi.org/10.3389/fmicb.2018.00726>
- Welsh RM, Bentz ML, Shams A, Houston H, Lyons A, Rose LJ, et al. Survival, persistence, and isolation of the emerging multidrug-resistant pathogenic yeast *Candida auris* on a plastic health care surface. *J Clin Microbiol*. 2017;55:2996–3005. <http://dx.doi.org/10.1128/JCM.00921-17>
- Piedrahita CT, Cadnum JL, Jencson AL, Shaikh AA, Ghannoum MA, Donskey CJ. Environmental surfaces in health-care facilities are a potential source for transmission of *Candida auris* and other *Candida* species. *Infect Control Hosp Epidemiol*. 2017;38:1107–9. <http://dx.doi.org/10.1017/ice.2017.127>
- Sherry L, Ramage G, Kean R, Borman A, Johnson EM, Richardson MD, et al. Biofilm-forming capability of highly virulent, multidrug-resistant *Candida auris*. *Emerg Infect Dis*. 2017;23:328–31. <http://dx.doi.org/10.3201/eid2302.161320>
- Magill SS, O’Leary E, Janelle SJ, Thompson DL, Dumyati G, Nadle J, et al.; Emerging Infections Program Hospital Prevalence Survey Team. Changes in prevalence of health care-associated infections in U.S. hospitals. *N Engl J Med*. 2018;379:1732–44. <http://dx.doi.org/10.1056/NEJMoa1801550>
- Govender NP, Patel J, Magobo RE, Naicker S, Wadula J, Whitelaw A, et al.; TRAC-South Africa group. Emergence of azole-resistant *Candida parapsilosis* causing bloodstream infection: results from laboratory-based sentinel surveillance in South Africa. *J Antimicrob Chemother*. 2016;71:1994–2004. <http://dx.doi.org/10.1093/jac/dkw091>
- Cornely OA, Bassetti M, Calandra T, Garbino J, Kullberg BJ, Lortholary O, et al.; ESCMID Fungal Infection Study Group. ESCMID guideline for the diagnosis and management of *Candida* diseases 2012: non-neutropenic adult patients. *Clin Microbiol Infect*. 2012;18(Suppl 7):19–37. <http://dx.doi.org/10.1111/1469-0691.12039>
- Kreusch A, Karstaedt AS. Candidemia among adults in Soweto, South Africa, 1990–2007. *Int J Infect Dis*. 2013;17:e621–3. <http://dx.doi.org/10.1016/j.ijid.2013.02.010>
- Econex. The South African private healthcare sector: role and contribution to the economy [cited 2019 Jan 9]. https://econex.co.za/wp-content/uploads/2016/09/Econex_private_health_sector_study_12122013-1.pdf
- Magobo RE, Corcoran C, Seetharam S, Govender NP. *Candida auris*-associated candidemia, South Africa. *Emerg Infect Dis*. 2014;20:1250–1. <http://dx.doi.org/10.3201/eid2007.131765>
- Eyre DW, Sheppard AE, Madder H, Moir I, Moroney R, Quan TP, et al. A *Candida auris* outbreak and its control in an intensive care setting. *N Engl J Med*. 2018;379:1322–31. <http://dx.doi.org/10.1056/NEJMoa1714373>
- Belkin A, Gazit Z, Keller N, Ben-Ami R, Wieder-Finesod A, Novikov A, et al. *Candida auris* infection leading to nosocomial

- transmission, Israel, 2017. *Emerg Infect Dis.* 2018;24:801–4. <http://dx.doi.org/10.3201/eid2404.171715>
19. Chow NA, Gade L, Tsay SV, Forsberg K, Greenko JA, Southwick KL, et al.; US *Candida auris* Investigation Team. Multiple introductions and subsequent transmission of multidrug-resistant *Candida auris* in the USA: a molecular epidemiological survey. *Lancet Infect Dis.* 2018;18:1377–84. [http://dx.doi.org/10.1016/S1473-3099\(18\)30597-8](http://dx.doi.org/10.1016/S1473-3099(18)30597-8)
 20. Heath CH, Dyer JR, Pang S, Coombs GW, Gardam DJ. *Candida auris* sternal osteomyelitis in a man from Kenya visiting Australia, 2015. *Emerg Infect Dis.* 2019;25:192–4. <http://dx.doi.org/10.3201/eid2501.181321>
 21. Tsay S, Welsh RM, Adams EH, Chow NA, Gade L, Berkow EL, et al. Ongoing transmission of *Candida auris* in health care facilities—United States, June 2016–May 2017. *MMWR Morb Mortal Wkly Rep.* 2017;66:514–5. <http://dx.doi.org/10.15585/mmwr.mm6619a7>
 22. Govender NP, Avenant T, Brink A, Chibabhai V, Cleghorn J, du Toit B, et al. FIDSSA guideline: recommendations for detection, management and prevention of healthcare-associated *Candida auris* colonisation and disease in South Africa S. *Afr J Infect Dis.* 2019. In press.
 23. Moema I, Ismail H, van Schalkwyk E, Shuping L, Govender NP. Outbreak of culture-confirmed *Candida auris* bloodstream infection in the neonatal unit of a public-sector hospital, South Africa, July through September 2017. In: Abstracts of the 67th Annual Epidemic Intelligence Service Conference; Atlanta; 2018 April 16–19 [cited 2018 Sep 28]. <https://www.cdc.gov/eis/downloads/eis-conference-2018-508.pdf>
 24. Escandón P, Cáceres DH, Espinosa-Bode A, Rivera S, Armstrong P, Vallabhaneni S, et al. Surveillance for *Candida auris*—Colombia, September 2016–May 2017. *MMWR Morb Mortal Wkly Rep.* 2018;67:459–60. <http://dx.doi.org/10.15585/mmwr.mm6715a6>
 25. Calvo B, Melo AS, Perozo-Mena A, Hernandez M, Francisco EC, Hagen F, et al. First report of *Candida auris* in America: Clinical and microbiological aspects of 18 episodes of candidemia. *J Infect.* 2016;73:369–74. <http://dx.doi.org/10.1016/j.jinf.2016.07.008>
 26. Pammi M, Holland L, Butler G, Gacser A, Bliss JM. *Candida parapsilosis* is a significant neonatal pathogen: a systematic review and meta-analysis. *Pediatr Infect Dis J.* 2013;32:e206–16. <http://dx.doi.org/10.1097/INF.0b013e3182863a1c>
 27. Crnich CJ, Maki DG. The role of intravascular devices in sepsis. *Curr Infect Dis Rep.* 2001;3:496–506. <http://dx.doi.org/10.1007/s11908-001-0086-4>
 28. Sexton DJ, Kordalewska M, Bentz ML, Welsh RM, Perlin DS, Litvintseva AP. Direct detection of emergent fungal pathogen *Candida auris* in clinical skin swabs by SYBR green-based quantitative PCR assay. *J Clin Microbiol.* 2018;56:e01337–18. <http://dx.doi.org/10.1128/JCM.01337-18>
 29. Berkow EL, Lockhart SR. Activity of novel antifungal compound APX001A against a large collection of *Candida auris*. *J Antimicrob Chemother.* 2018;73:3060–2. <http://dx.doi.org/10.1093/jac/dky302>
 30. Kohlenberg A, Struelens MJ, Monnet DL, Plachouras D; The *Candida Auris* Survey Collaborative Group. *Candida auris*: epidemiological situation, laboratory capacity and preparedness in European Union and European Economic Area countries, 2013 to 2017. *Euro Surveill.* 2018;23:23. <http://dx.doi.org/10.2807/1560-7917.ES.2018.23.13.18-00136>

Address for correspondence: Nelesh P. Govender, National Institute for Communicable Diseases, 1 Modderfontein Rd, Sandringham, Johannesburg, 2131, South Africa; email: neleshg@nicd.ac.za

EID podcast

Developing Biological Reference Materials to Prepare for Epidemics



Having standard biological reference materials, such as antigens and antibodies, is crucial for developing comparable research across international institutions. However, the process of developing a standard can be long and difficult.

In this EID podcast, Dr. Tommy Rampling, a clinician and academic fellow at the Hospital for Tropical Diseases and University College in London, explains the intricacies behind the development and distribution of biological reference materials.

Visit our website to listen:
<https://go.usa.gov/xyfJX>

**EMERGING
 INFECTIOUS DISEASES®**

Effect of Pneumococcal Conjugate Vaccines on Pneumococcal Meningitis, England and Wales, July 1, 2000–June 30, 2016

Godwin Oligbu, Sarah Collins, Abdelmajid Djennad, Carmen L. Sheppard, Norman K. Fry, Nick J. Andrews, Ray Borrow, Mary E. Ramsay, Shamez N. Ladhani

We describe the effects of the 7-valent (PCV7) and 13-valent (PCV13) pneumococcal conjugate vaccines on pneumococcal meningitis in England and Wales during July 1, 2000–June 30, 2016. Overall, 84,473 laboratory-confirmed invasive pneumococcal disease cases, including 4,160 (4.9%) cases with meningitis, occurred. PCV7 implementation in 2006 did not lower overall pneumococcal meningitis incidence because of replacement with non-PCV7-type meningitis incidence. Replacement with PCV13 in 2010, however, led to a 48% reduction in pneumococcal meningitis incidence by 2015–16. The overall case-fatality rate was 17.5%: 10.7% among patients <5 years of age, 17.3% among patients 5–64 years of age, and 31.9% among patients ≥65 years of age. Serotype 8 was associated with increased odds of death (adjusted odds ratio 2.9, 95% CI 1.8–4.7). In England and Wales, an effect on pneumococcal meningitis was observed only after PCV13 implementation. Further studies are needed to assess pneumococcal meningitis caused by the replacing serotypes.

Streptococcus pneumoniae is a major cause of bacterial meningitis across all age groups in the United Kingdom and worldwide (1,2); the case-fatality rate (CFR) ranges from 10% to 40% (2–4). Survivors of pneumococcal meningitis are more likely than survivors of other types of bacterial meningitis to have neurologic and other serious long-term sequelae (5,6); a meta-analysis indicated that 32% of pneumococcal meningitis patients experienced sequelae (7). The pathophysiologic mechanisms leading to neurologic damage in patients with bacterial meningitis are

complex and multifaceted, involving the secretion of potent bacterial toxins and excessive host immune responses against the invading pneumococci in the cerebrospinal fluid (8,9).

Before the introduction of the 7-valent pneumococcal conjugate vaccine (PCV7), ≈500 confirmed pneumococcal meningitis cases occurred annually in England and Wales (2). The serotypes covered by PCV7 were responsible for 57% of all pneumococcal meningitis cases and 72% of cases in children <2 years of age; the CFR increased with age, from 5% in children to 30% in older adults (10).

In September 2006, the United Kingdom introduced PCV7 into the childhood immunization program; children were scheduled to receive the vaccine at 2, 4, and 12 months of age, and a 12-month catch-up program was established for children <2 years of age (11). The program was associated with a rapid decline in invasive pneumococcal disease (IPD) caused by PCV7 serotypes, and although some increase in IPD caused by non-PCV7 serotypes was observed, IPD decreased overall by 36% compared with pre-PCV7 levels through direct and indirect protection (12). During the first 4 years of the program, a 34% reduction in pneumococcal meningitis incidence was observed in children <5 years of age (13). However, this reduction was almost entirely offset by an increase in meningitis cases caused by non-PCV7 serotypes in older children and adults. After PCV7 introduction, pneumococcal meningitis was mainly caused by serotypes 1, 3, 7F, 19A, 22F, and 33F (14).

In April 2010, PCV7 was replaced with the 13-valent vaccine (PCV13), which led to a 32% reduction in overall IPD incidence compared with pre-PCV7 levels and a 56% reduction compared with pre-PCV13 levels (14). The effect of PCV13 on pneumococcal meningitis has not been assessed in the United Kingdom. Reports of the effects of PCV7 and PCV13 on pneumococcal meningitis in other countries with established pneumococcal

Author affiliations: Public Health England, London, UK (G. Oligbu, S. Collins, A. Djennad, C.L. Sheppard, N.K. Fry, N.J. Andrews, M.E. Ramsay, S.N. Ladhani); St. George's, University of London, London (G. Oligbu, S.N. Ladhani); Public Health England Manchester Royal Infirmary, Manchester, UK (R. Borrow)

DOI: <https://doi.org/10.3201/eid2509.180747>

immunization programs have been variable; in some countries, significant reductions were reported after PCV7 introduction, and in other countries, no change or a decline was reported only after PCV13 introduction (15–20). Here, we describe the epidemiology of pneumococcal meningitis in England and Wales over a 16-year period encompassing the introduction of PCV7 and PCV13 into the national immunization program.

Methods

Surveillance

Public Health England (PHE; London, England, UK) has legal permission under Regulation 3 of the Health Service (Control of Patient Information) Regulations 2002 (<http://www.legislation.gov.uk/ukxi/2002/1438/regulation/3/made>) to conduct national surveillance of communicable diseases. This regulation also provides PHE permission to access information required to monitor the safety and effectiveness of vaccines.

PHE conducts surveillance for IPD and provides a national reference service for serotyping pneumococcal isolates in England and Wales (12). Staff of the National Health Service laboratories electronically report invasive bacterial infections to PHE by using the Second Generation Surveillance System, which replaced LabBase2 in 2014, and routinely submit all invasive pneumococcal isolates to the PHE national reference laboratory for confirmation and serotyping (12). PHE staff actively follow up on reported cases when they do not receive an accompanying isolate. Case ascertainment has remained consistently high, especially for meningitis cases; >90% of invasive pneumococcal isolates are submitted to PHE for serotyping (12). Starting in September 2006, IPD surveillance was enhanced by the collection of 1-page surveillance questionnaires completed by the patient's general practitioner; questionnaires asked for information on patients' vaccination histories, underlying medical conditions, and outcomes.

Data Analysis

We exported anonymized (mainly descriptive) data to Stata v.11.0 (<https://www.stata.com>) for analysis. We included laboratory-confirmed cases of pneumococcal meningitis diagnosed during July 1, 2000–June 30, 2016 (16 epidemiologic years). We defined meningitis as identification of *S. pneumoniae* in cerebrospinal fluid or blood cultures of patients with a clinical diagnosis of meningitis, as designated on their electronic report or sample submission form sent to PHE. Excluding clinically diagnosed cases in which *S. pneumoniae* was not confirmed in the cerebrospinal fluid (25%–35% of all pneumococcal meningitis cases annually) reduced the total number of meningitis cases available for analysis without affecting the observed trends over time.

We identified fatal cases and dates of death through the patient demographic service and calculated the 30-day CFR.

We classified cases into 4 groups by serotype: PCV7 (serotypes 4, 6B, 9V, 14, 18C, 19F, 23F), additional PCV13 (serotypes 1, 3, 5, 6A, 7F, 19A), non-PCV13, and unknown (typically resulting from lack of referral or unsuccessful recovery from culture after sample transport). We analyzed cases as a whole and by patient age group (<5, 5–64, ≥65 years). We filled in missing age and serotype by assuming that age and serotype distribution were the same on reports with missing information as on reports for which these parameters were known. We obtained age-specific population denominators from the Office for National Statistics (www.statistics.gov.uk) and compared the adjusted annual incidence rates for pneumococcal meningitis in epidemiologic year 2015–16 with rates for the pre-PCV7 (July 1, 2000–June 30, 2006) and pre-PCV13 (July 1, 2008–June 30, 2010) periods by age and serotype group, assuming a Poisson distribution.

For cases diagnosed during the PCV13 period (July 1, 2011–June 30, 2016), we used multivariable logistic regression to calculate the odds of meningitis (vs. nonmeningitis) for individual serotypes (vs. all other serotypes) after adjusting for age group and surveillance year. We also used multivariable logistic regression to calculate the odds of death by clinical presentation (meningitis vs. nonmeningitis) after adjusting for age group and surveillance year. For meningitis cases, we used multivariable logistic regression to assess the odds of death by age group, serotype group, individual serotype (vs. all other serotypes), and surveillance year after adjusting for age group and surveillance year. Because of multiple comparisons, we considered $p < 0.01$ to be significant. We estimated the cases prevented according to age group by determining the difference between the expected (average corrected number of cases in absence of vaccination) and observed numbers of cases after the introduction of each vaccine.

Results

During the 16-year surveillance period, 84,473 laboratory-confirmed IPD cases occurred across all age groups; 4,160 (4.9%) cases were meningitis and 80,313 (95.1%) were nonmeningitis. Of the 4,108 meningitis cases with age reported, 1,611 (39.2%) were in children <5 years of age, 1,729 (42.1%) in persons 5–64 years of age, and 768 (18.7%) in adults ≥65 years of age. Of the 79,620 nonmeningitis cases with age reported, 8,324 (10.5%) were in children <5 years of age, 32,297 (40.6%) in persons 5–64 years of age, and 38,999 (48.9%) in adults ≥65 years of age.

Before PCV7 introduction, the mean annual incidence of pneumococcal meningitis was 0.55 cases/100,000 person-years (Table 1). The childhood PCV7 program had no effect on the overall annual incidence of pneumococcal

Table 1. Cases, incidence, and age-adjusted IRRs for pneumococcal meningitis and nonmeningitis cases by age group, serotype group, and period, England and Wales, July 1, 2000–June 30, 2016*

Case type, age group, and serotype group	July 1, 2015–June 30, 2016		Pre-PCV13 period, July 1, 2008–June 30, 2010			Pre-PCV7 period, July 1, 2000–June 30, 2006		
	No. corrected (raw) cases†	Incidence, cases/100,000 person-years	No. corrected (raw) cases†	Incidence, cases/100,000 person-years	IRR (95% CI) vs. 2015–16	No. corrected (raw) cases†	Incidence, cases/100,000 person-years	IRR (95% CI) vs. 2015–16
Meningitis								
<5 y								
All serotypes	41 (44)	1.22	105 (104)	3.10	0.39 (0.25–0.63)	138 (122)	4.08	0.30 (0.19–0.46)
PCV7	1 (1)	0.03	10 (10)	0.29	0.10 (0.01–1.84)	102 (76)	3.02	0.01 (0–0.16)
Additional PCV13	3 (3)	0.09	53 (51)	1.56	0.06 (0.01–0.29)	18 (14)	0.54	0.16 (0.03–0.85)
Non-PCV13	37 (38)	1.10	42 (41)	1.25	0.89 (0.51–1.56)	18 (13)	0.52	2.12 (1.22–3.75)
5–64 y								
All serotypes	96 (98)	0.22	155 (155)	0.36	0.62 (0.44–0.86)	117 (110)	0.27	0.82 (0.60–1.11)
PCV7	2 (2)	0.00	28 (27)	0.07	0.07 (0.01–0.56)	54 (39)	0.13	0.04 (0.01–0.29)
Additional PCV13	14 (13)	0.03	51 (47)	0.12	0.27 (0.11–0.62)	22 (16)	0.05	0.62 (0.26–1.39)
Non-PCV13	80 (77)	0.19	76 (71)	0.18	1.06 (0.71–1.58)	41 (29)	0.10	1.95 (1.31–2.86)
≥65 y								
All serotypes	24 (28)	0.27	52 (52)	0.59	0.46 (0.25–0.85)	53 (49)	0.60	0.45 (0.26–0.80)
PCV7	0 (0)	0	8 (8)	0.09	0 (0–0.52)	23 (17)	0.26	0 (0–0.17)
Additional PCV13	2 (2)	0.02	11 (10)	0.12	0.19 (0.02–1.57)	10 (7)	0.11	0.20 (0.02–1.55)
Non-PCV13	22 (22)	0.25	33 (32)	0.37	0.67 (0.33–1.34)	20 (15)	0.22	1.11 (0.56–2.18)
All ages								
All serotypes	162 (170)	0.29	311 (310)	0.56	0.51 (0.40–0.66)	301 (288)	0.55	0.52 (0.41–0.65)
PCV7	3 (3)	0.01	46 (44)	0.08	0.07 (0.01–0.35)	176 (133)	0.32	0.02 (0–0.09)
Additional PCV13	18 (18)	0.03	114 (108)	0.21	0.16 (0.08–0.32)	49 (38)	0.09	0.36 (0.18–0.72)
Non-PCV13	141 (137)	0.25	151 (143)	0.27	0.92 (0.69–1.25)	77 (58)	0.14	1.77 (1.33–2.36)
Nonmeningitis								
<5 y								
All serotypes	241 (257)	7.12	345 (341)	10.19	0.70 (0.57–0.86)	666 (592)	19.67	0.36 (0.30–0.44)
PCV7	5 (5)	0.15	25 (23)	0.74	0.21 (0.05–0.79)	479 (310)	14.17	0.01 (0–0.04)
Additional PCV13	30 (29)	0.89	217 (199)	6.40	0.14 (0.08–0.24)	112 (73)	3.30	0.27 (0.15–0.46)
Non-PCV13	206 (198)	6.08	103 (95)	3.05	2.00 (1.50–2.66)	75 (49)	2.20	2.76 (2.11–3.57)
5–64 y								
All serotypes	2,333 (2,387)	5.44	2,385 (2,377)	5.56	0.98 (0.91–1.05)	2,141 (2,028)	4.99	1.09 (1.01–1.16)
PCV7	57 (55)	0.13	313 (274)	0.73	0.18 (0.12–0.28)	865 (465)	2.02	0.07 (0.04–0.10)
Additional PCV13	375 (359)	0.87	1,163 (1,022)	2.71	0.32 (0.27–0.38)	651 (366)	1.52	0.57 (0.46–0.64)
Non-PCV13	1,901 (1,820)	4.43	909 (799)	2.12	2.09 (1.90–2.30)	625 (355)	1.46	3.04 (2.74–3.30)
≥65 y								
All serotypes	2,442 (2,818)	27.29	2,417 (2,391)	27.01	1.01 (0.94–1.08)	2,820 (2,601)	31.51	0.87 (0.82–0.92)
PCV7	49 (53)	0.55	402 (351)	4.49	0.12 (0.08–0.18)	1,466 (775)	16.39	0.03 (0.02–0.05)
Additional PCV13	422 (455)	4.71	913 (803)	10.20	0.46 (0.40–0.53)	574 (318)	6.42	0.73 (0.61–0.82)
Non-PCV13	1,971 (2,127)	22.03	1,103 (970)	12.32	1.79 (1.63–1.95)	779 (411)	8.70	2.53 (2.34–2.77)
All ages								
All serotypes	5,217 (5,467)	9.44	5,135 (5,116)	9.30	0.98 (0.93–1.02)	5,563 (5,321)	10.07	0.89 (0.85–0.93)
PCV7	115 (113)	0.21	735 (648)	1.33	0.15 (0.11–0.20)	2,813 (1,571)	5.09	0.04 (0.03–0.05)
Additional PCV13	862 (844)	1.56	2,290 (2,026)	4.15	0.36 (0.33–0.41)	1,311 (767)	2.37	0.60 (0.53–0.66)
Non-PCV13	4,239 (4,148)	7.67	2,109 (1,866)	3.82	1.92 (1.80–2.05)	1,439 (804)	2.61	2.75 (2.59–2.92)

*PCV7 refers to serotypes 4, 6B, 9V, 14, 18C, 19F, and 23F, and additional PCV13 refers to serotypes 1, 3, 5, 6A, 7F, and 19A. Non-PCV13 refers to all other serotypes. IRR, incident rate ratio; PCV7, 7-valent pneumococcal conjugate vaccine; PCV13, 13-valent pneumococcal conjugate vaccine.

†Raw numbers of cases for each year were corrected for missing serotype and age with the assumption that cases with missing data for age, serotype, or both had the same age and serotype distributions as those cases in which this information was known—the number of extra cases were then added to the raw numbers in each category; cases were also corrected for annual changes in population denominators in each age group (13).

meningitis (pre-PCV13 period 0.56 cases/100,000 person-years) because the decline in PCV7-type meningitis was offset by substantial increases in cases caused by other serotypes (Table 1; Figure 1). PCV7 replacement with PCV13 in April 2010, however, led to a 48% (95% CI 38%–62%) reduction in pneumococcal meningitis incidence by 2015–16. During the PCV13 period, meningitis cases caused by PCV7 and PCV13 serotypes continued to decline, and cases associated with non-PCV13 serotypes remained static. These findings are in contrast with those regarding non-meningitis IPD cases, in which reductions were observed across all age groups but were offset by increases in cases caused by nonvaccine serotypes after the introduction of PCV7 and PCV13 (Table 1). The serotypes responsible for meningitis varied among the pre-PCV7, pre-PCV13, and PCV13 periods (Figure 2).

Although meningitis cases were \approx 20 times less common than nonmeningitis cases during the 16-year period, the contribution of individual serotypes to these 2 clinical presentations was similar (Figure 3). During the PCV13 period, after adjusting for age and year of diagnosis, odds of causing meningitis were higher for only serotypes 10A, 22F, 23B, and 35B and lower for serotypes 1, 8, and 19A (Table 2).

Cases in Patients <5 Years of Age

Pneumococcal meningitis cases in children increased from birth and peaked at 5 months of age, before gradually declining (Figure 4). For patients <5 years of age, PCV7 serotypes contributed to 73.9% (102/138), additional PCV13 to 13.0% (18/138), and non-PCV13 to 13.0% (18/138) of pneumococcal meningitis cases during the pre-PCV7 period (Table 1). After PCV7 introduction, pneumococcal meningitis incidence fell from 4.08 cases/100,000 person-years to 3.10 cases/100,000 person-years in the pre-PCV13 period (Table 1). The rapid decline in PCV7-type meningitis (3.02 cases/100,000 person-years [pre-PCV7] to 0.29 cases/100,000 person-years [pre-PCV13]) was offset by an \approx 3-fold increase in PCV13-type disease incidence (0.54 cases/100,000 person-years to 1.56 cases/100,000 person-years), nearly all caused by serotypes 7F (4 cases/year to 26 cases/year), 19A (3 cases/year to 15 cases/year), and 1 (2 cases/year to 7 cases/year). In this age group, the incidence of non-PCV13 meningitis also increased from 0.52 cases/100,000 person-years to 1.25 cases/100,000 person-years in the pre-PCV13 period.

After PCV13 introduction, meningitis incidence declined to 1.22 cases/100,000 person-years by 2015–16, a reduction of 70% (95% CI 54%–81%) from the pre-PCV7 period (Table 1; Figure 1). This decline was caused by the continuing reduction in PCV7-type disease and a large reduction in the additional PCV13 serotypes (1.56 cases/100,000 person-years [pre-PCV13] to 0.09 cases/100,000 person-years [2015–16]) while meningitis incidence

caused by non-PCV13 serotypes remained static. Nearly all cases in 2015–16 were caused by non-PCV13 serotypes, and only 3 cases were caused by a PCV13 serotype (Table 1, Figure 5).

Cases in Patients 5–64 Years of Age

Among patients 5–64 years of age, PCV7 serotypes were responsible for 46.2% (54/117), additional PCV13 for 18.8% (22/117), and non-PCV13 for 35.0% (41/117) of pneumococcal meningitis cases during the pre-PCV7 period. In this age group, meningitis incidence increased after PCV7 introduction, peaking in 2008–09 before declining after PCV13 introduction (Figure 1). After PCV7 introduction, PCV7-type meningitis declined, and additional PCV13-type meningitis increased but then declined after PCV13 introduction. Meningitis caused by non-PCV13 serotypes increased after PCV7 introduction and then stabilized during the PCV13 period. During 2015–16, the additional PCV13, especially serotype 3 ($n = 5$), caused some meningitis cases, but the non-PCV13 serotypes 12F ($n = 10$) and 8 ($n = 9$) were the predominant causes of meningitis; other serotypes caused only 1–2 cases.

Cases in Patients \geq 65 Years of Age

Before PCV7 introduction, the serotype distribution among patients \geq 65 years of age was similar to that of patients 5–64 years of age, albeit with half the number of cases (Table 1). Meningitis incidence did not change after PCV7 introduction (0.60 cases/100,000 person-years [pre-PCV7] to 0.59 cases/100,000 person-years [pre-PCV13]) but declined substantially after PCV13 introduction to 0.27 cases/100,000 person-years by 2015–16, when serotypes 8 (25.0%, 6/24) and 23B (16.7%, 4/24) predominated. In 2015–16, only 2 cases were caused by PCV13 serotypes (3 and 19A).

Case-Fatality Rate

The overall CFR for pneumococcal meningitis was 17.5% (631/3,612; 95% CI 16.2%–18.7%) and pneumococcal nonmeningitis 19.9% (14,783/74,179; 95% CI 19.6%–20.2%). The CFR for pneumococcal meningitis was 10.7% (150/1,408; 95% CI 9.1%–12.4%) among patients <5 years of age, 17.3% (262/1,517; 95% CI 15.4%–19.3%) among patients 5–64 years of age, and 31.9% (219/686; 95% CI 31.8%–39.5%) among patients \geq 65 years of age. The CFR for pneumococcal nonmeningitis was 3.5% (254/7,163) among patients <5 years of age, 10.8% (3,235/30,090) among patients 5–64 years of age, and 30.6% (11,292/36,907) among patients \geq 65 years of age. The CFRs for patients with meningitis by serotype group were 14.2% (130/916) for PCV7 serotypes, 18.0% (143/793) for additional PCV13 serotypes, and 18.9% (290/1,534) for non-PCV13 serotypes.

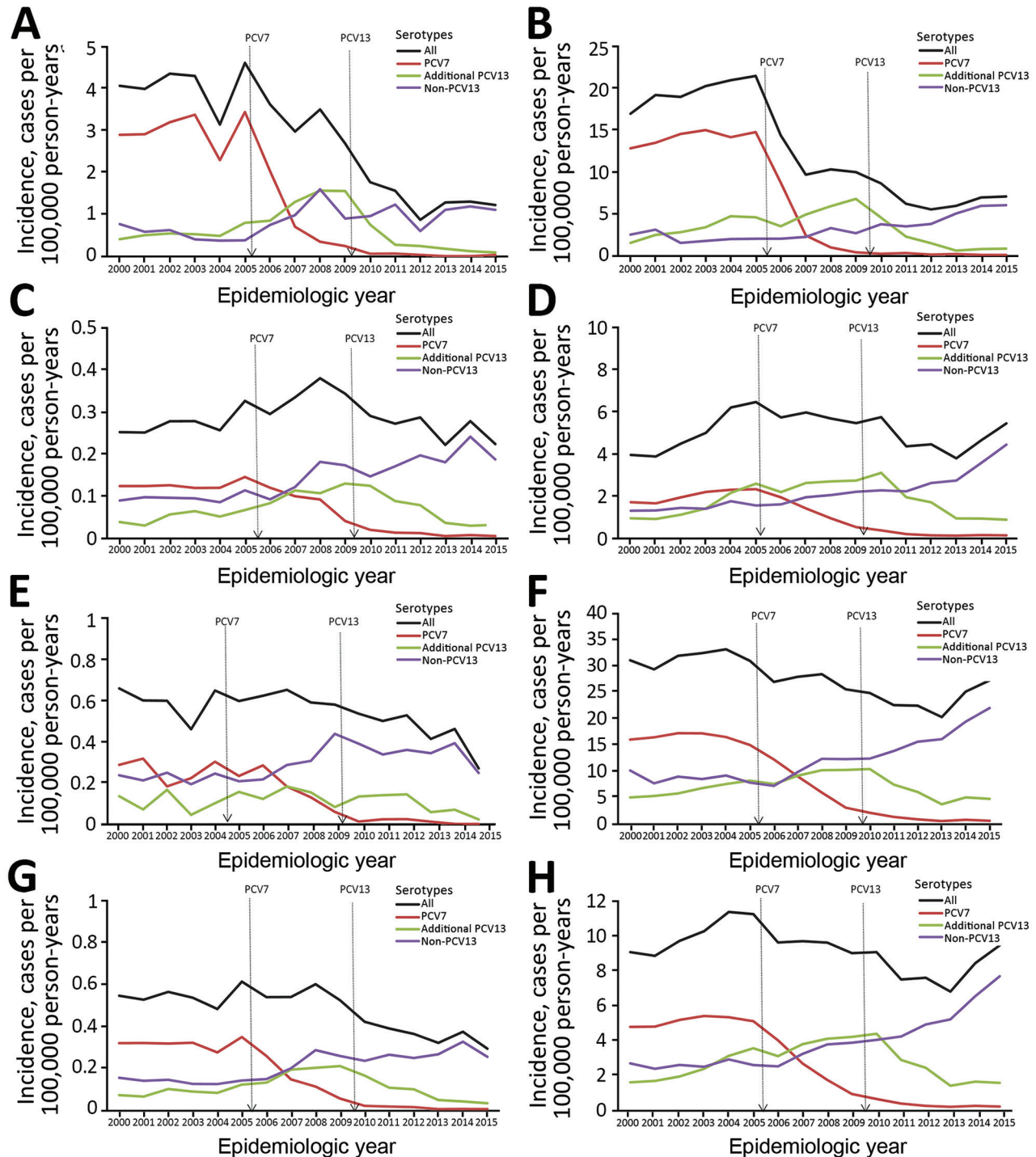


Figure 1. Corrected trends in incidence of pneumococcal meningitis and nonmeningitis cases by *Streptococcus pneumoniae* serotype, age group, and epidemiologic year, England and Wales, July 1, 2000–June 30, 2016. A–H) Meningitis (A, C, E, G) and nonmeningitis (B, D, F, H) cases in patients <5 years of age (A, B); patients 5–64 years of age (C, D); patients ≥65 years of age (E, F); and patients of all ages (G, H). The raw numbers of cases for each year were corrected for missing serotype and age with the assumption that cases with missing data for age, serotype, or both had the same age and serotype distribution as those cases for which this information was known; cases were also corrected for annual changes in population denominators in each age group (13). The vertical lines denote the introduction of PCV7 and PCV13 into the national childhood immunization program. PCV7 refers to serotypes 4, 6B, 9V, 14, 18C, 19F, and 23F, and additional PCV13 refers to serotypes 1, 3, 5, 6A, 7F, and 19A. Non-PCV13 refers to all other serotypes. PCV7, 7-valent pneumococcal conjugate vaccine; PCV13, 13-valent pneumococcal conjugate vaccine.

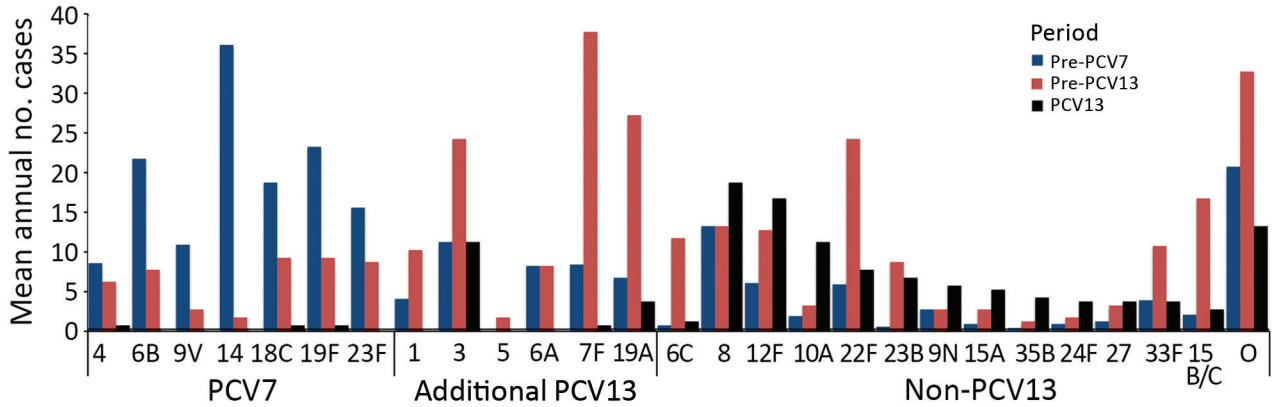


Figure 2. Mean annual number of pneumococcal meningitis cases among patients of all ages by *Streptococcus pneumoniae* serotype and period, England and Wales, July 1, 2000–June 30, 2016. The pre-PCV7 period refers to July 1, 2000–June 30, 2006, pre-PCV13 period July 1, 2008–June 30, 2010, and PCV13 period July 1, 2011–June 30, 2016. PCV7, 7-valent pneumococcal conjugate vaccine; PCV13, 13-valent pneumococcal conjugate vaccine. For cases diagnosed during the PCV13 period (July 1, 2011–June 30, 2016), we used multivariable logistic regression to calculate the odds of meningitis vs. nonmeningitis. O, other serotypes.

In a logistic regression model, meningitis was associated with death (adjusted odds ratio [aOR] 1.6, 95% CI 1.4–1.7), independent of age group, serotype group, or period. Among meningitis cases, only increasing age (5–64 years aOR 1.7 [95% CI 1.3–2.1] and ≥65 years aOR 3.9 [95% CI 3.1–5.0] vs. children <5 years of age; p<0.0001 for both) was independently associated with death but not serotype group or surveillance year. In a logistic regression model comparing the CFR of serotypes associated with meningitis during the PCV13 period, only serotype 8 (CFR 33.7% [33/98] vs. CFR other serotypes 15.7% [123/783]) was associated with an increased odds of death (aOR 2.9, 95% CI 1.8–4.7; p<0.0001).

Meningitis Cases Prevented

We estimated that 702 cases of meningitis were prevented during the 10 years since PCV7 introduction (2006–2016),

mainly occurring after PCV13 introduction and nearly all in children <5 years of age. In total, 1,471 fewer cases were caused by PCV7 serotypes, and 173 more cases were caused by additional PCV13 serotypes (207 additional cases before PCV13 introduction and 34 fewer cases after PCV13 introduction).

Discussion

In England and Wales, pneumococcal meningitis accounts for 5% of all IPD cases. Although large declines in IPD incidence were observed after PCV7 and PCV13 introduction, we observed a differential impact on pneumococcal meningitis and nonmeningitis. The annual incidence of pneumococcal meningitis remained unchanged after PCV7 introduction but declined by 48% after PCV13 replaced PCV7. The greatest decline in

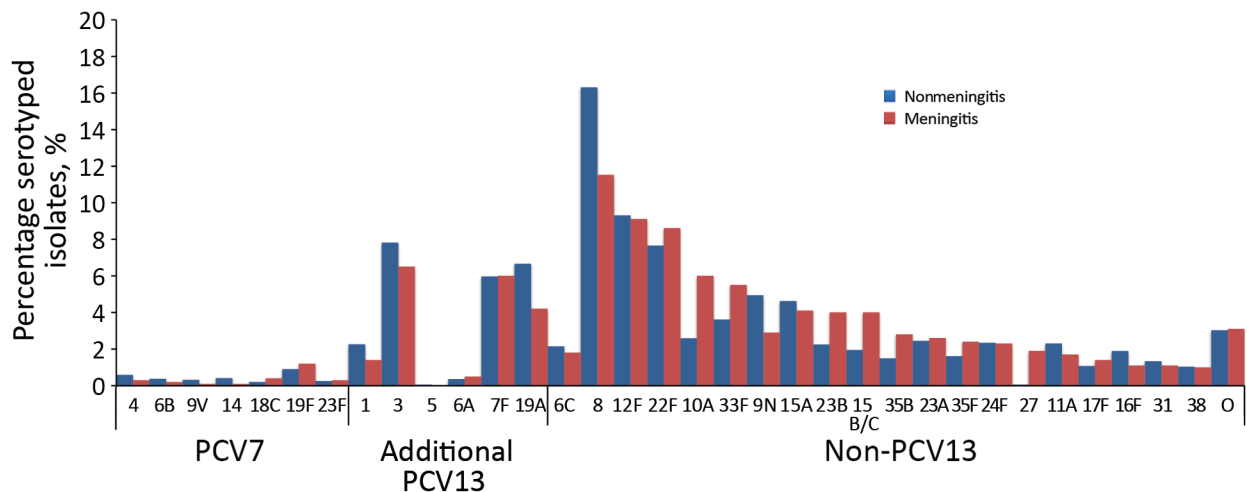


Figure 3. Contribution of individual *Streptococcus pneumoniae* serotypes to pneumococcal meningitis and nonmeningitis cases for all age groups after PCV13 introduction, England and Wales, July 1, 2011–June 30, 2016. We included the non-PCV13 serotypes that involved ≥10 cases. PCV7, 7-valent pneumococcal conjugate vaccine; PCV13, 13-valent pneumococcal conjugate vaccine. O, other serotypes.

Table 2. Association between *Streptococcus pneumoniae* serotype and meningitis (vs. nonmeningitis) by serotype ranking, England and Wales, July 1, 2011–June 30, 2016*

Serotype rank	Serotype	Total cases	Nonmeningitis cases, n = 20,800, no. (%)	Meningitis cases, n = 920, no. (%)	aOR (95% CI)	p value†
1‡	8	3,285	3,184 (15.3)	101 (11.0)	0.69 (0.56–0.86)	<0.001
2	12F	1,809	1,729 (8.3)	80 (8.7)	0.99 (0.78–1.27)	0.961
3§	22F	1,725	1,640 (7.9)	85 (9.2)	1.39 (1.1–1.76)	0.006
4	3	1,598	1,542 (7.4)	56 (6.1)	0.99 (0.74–1.31)	0.924
5	7F	1,542	1,482 (7.1)	60 (6.5)	0.73 (0.56–0.96)	0.026
6‡	19A	1,485	1,446 (7.0)	39 (4.2)	0.62 (0.45–0.86)	0.005
7	15A	1,024	986 (4.7)	38 (4.1)	1.09 (0.78–1.54)	0.603
8	9N	954	928 (4.5)	26 (2.8)	0.77 (0.51–1.15)	0.2
9	33F	827	774 (3.7)	53 (5.8)	1.34 (0.99–1.81)	0.057
10‡	1	602	588 (2.8)	14 (1.5)	0.33 (0.19–0.56)	<0.001
11§	10A	566	511 (2.5)	55 (6.0)	2.06 (1.52–2.79)	<0.001
12	23A	548	523 (2.5)	25 (2.7)	1.51 (1–2.29)	0.052
13	24F	548	528 (2.5)	20 (2.2)	0.73 (0.46–1.16)	0.187
14	6C	514	497 (2.4)	17 (1.8)	0.95 (0.58–1.57)	0.852
15	11A	512	498 (2.4)	14 (1.5)	0.71 (0.41–1.23)	0.221
16§	23B	499	462 (2.2)	37 (4.0)	1.73 (1.21–2.48)	0.003
17	15B/C	453	416 (2.0)	37 (4.0)	1.31 (0.91–1.89)	0.146
18	16F	418	408 (2.0)	10 (1.1)	0.77 (0.41–1.45)	0.415
19	35F	371	349 (1.7)	22 (2.4)	1.47 (0.93–2.32)	0.096
20§	35B	334	308 (1.5)	26 (2.8)	2.12 (1.38–3.25)	<0.001
21	31	282	273 (1.3)	9 (1.0)	1.14 (0.58–2.25)	0.703
22	20	240	235 (1.1)	5 (0.5)	0.46 (0.19–1.12)	0.086
23	38	239	229 (1.1)	10 (1.1)	0.79 (0.41–1.54)	0.49
24	17F	235	221 (1.1)	14 (1.5)	1.71 (0.98–2.98)	0.058
25	19F	183	171 (0.8)	12 (1.3)	1.24 (0.68–2.28)	0.483
26	4	135	132 (0.6)	3 (0.3)	0.4 (0.13–1.28)	0.123
27	14	94	93 (0.4)	1 (0.1)	0.26 (0.04–1.87)	0.18
28	6A	93	88 (0.4)	5 (0.5)	1.34 (0.52–3.45)	0.538
29	6B	90	88 (0.4)	2 (0.2)	0.54 (0.13–0.13)	0.397
30	9V	81	80 (0.4)	1 (0.1)	0.31 (0.04–2.25)	0.245
31	23F	60	57 (0.3)	3 (0.3)	1.24 (0.38–4.08)	0.722
32	18C	55	51 (0.2)	4 (0.4)	1.23 (0.43–3.52)	0.701
33	21	51	47 (0.2)	4 (0.4)	0.8 (0.28–2.3)	0.683

*Values were adjusted for age and year of diagnosis. Only serotypes responsible for ≥ 50 cases of invasive pneumococcal disease were included. aOR, adjusted odds ratio.

†Because of multiple comparisons, a p value of <0.01 was considered significant.

‡Serotype of decreased odds (decreased aOR with significant p value).

§Serotype of increased odds (increased aOR and significant p value).

pneumococcal meningitis incidence (70%) was observed among children <5 years of age. By 2015–16, PCV13-serotype meningitis was rare, and nearly all cases were caused by non-PCV13 serotypes. The CFR, however, remained high (17.5%) and increased with age, but we found evidence of a lower CFR after both PCV7 and PCV13 implementation.

The reduction in PCV7-type pneumococcal meningitis after PCV7 was introduced in 2006 was rapidly offset by an increase in cases caused by non-PCV7 serotypes, especially 7F and 19A (later included in PCV13) and especially among adults (21). The replacement of PCV7 by PCV13 in 2010, however, led to large declines in pneumococcal meningitis cases, mainly because of an 84% reduction in cases caused by the additional serotypes included in PCV13 without an increase in cases caused by non-PCV13 serotypes. Similar trends have been reported in Israel, where meningitis incidence declined only after PCV13 introduction (22). In France, PCV7 implementation led to a rebound in incidence of pneumococcal

meningitis, with a 2.2-fold increase among children, including a 6.5-fold increase among those <2 years of age (23), followed by a 44% decline after PCV13 introduction (16,24). In contrast, many countries with established PCV programs reported declines in pneumococcal meningitis after implementation of each vaccine (18,25–31). In the United States, PCV7 implementation was associated with declines in PCV7-type pneumococcal meningitis across all age groups, but the overall incidence of pneumococcal meningitis in adults did not change because disease with non-PCV7 serotypes increased (32). Possible explanations for the variable observations include differences in immunization doses and schedules, implementation of catch-up programs along with vaccine introduction, vaccine uptake rates, rapidity of increases in disease attributable to other serotypes after the introduction of each vaccine, and differences in the replacing serotypes' abilities to cause IPD and meningitis.

We observed shifts in serotypes causing meningitis over time. Before PCV7 implementation, serotype 14

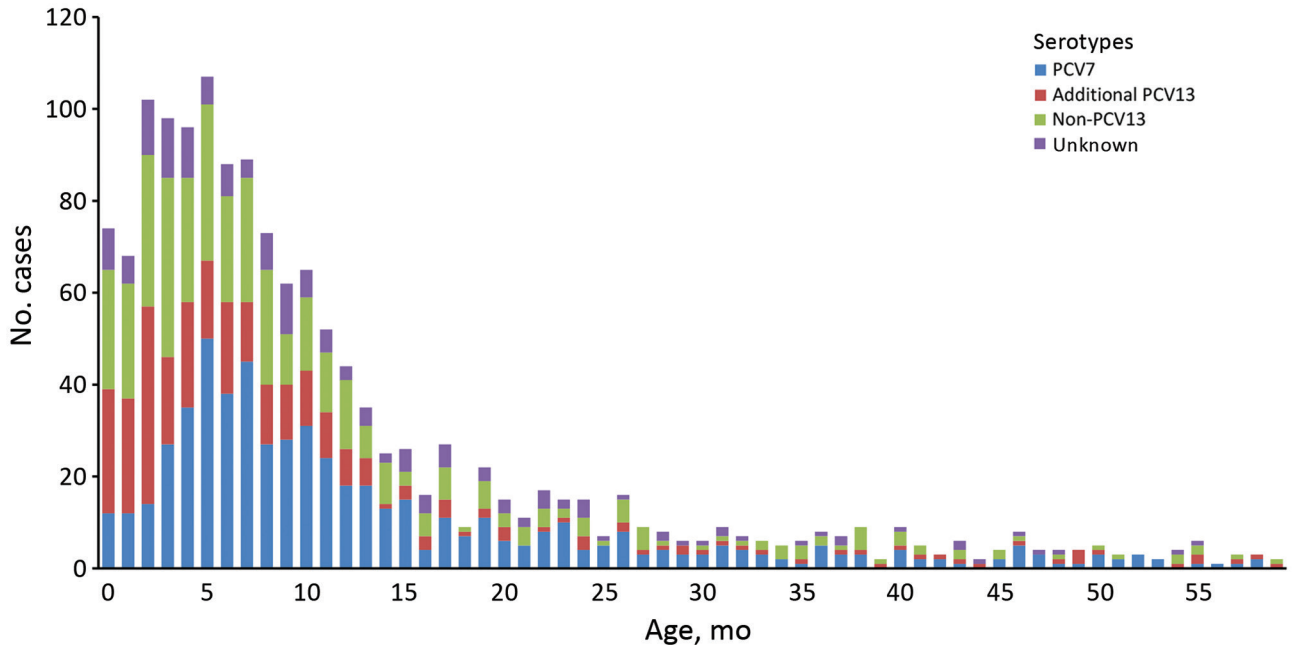


Figure 4. Distribution of pneumococcal meningitis cases in children <5 years of age, by month of age and *Streptococcus pneumoniae* serotype group, England and Wales, July 1, 2000–June 30, 2016. PCV7 refers to serotypes 4, 6B, 9V, 14, 18C, 19F, and 23F, and additional PCV13 refers to serotypes 1, 3, 5, 6A, 7F, and 19A. PCV7, 7-valent pneumococcal conjugate vaccine; PCV13, 13-valent pneumococcal conjugate vaccine.

caused most meningitis cases (10), consistent with findings in Germany, Belgium, and Brazil (33–35). During the PCV7 period, serotypes 7F and 19A (12), among others, emerged as the most common replacing serotypes causing meningitis in Europe and the United States, mainly through clonal expansion (36,37). In several countries, including France and the United States but not the United Kingdom, isolates of the emerging serotype 19A exhibited high rates of resistance to multiple antimicrobial drugs (38,39). Meningitis caused by serotype 7F has been associated with more severe disease (increased complications, higher CFR) in children than meningitis caused by other serotypes (40).

The replacement of PCV7 with PCV13, which covers serotypes 7F and 19A, led to a rapid reduction in IPD, including meningitis, caused by these serotypes across all age groups. Marked reductions in IPD caused by these 2 serotypes were observed especially among children <2 years of age, the age group in which incidence of pneumococcal meningitis is highest (12). By 2015–16, serotypes 8 and 12F were the main replacing serotypes causing meningitis across all age groups.

The predominance of serotype 8 appears to be unique to the England and Wales population (41). In Germany, serotypes 14 and 6B pre-PCV7 and serotype 7F post-PCV7 were the most common; whereas in England and Wales,

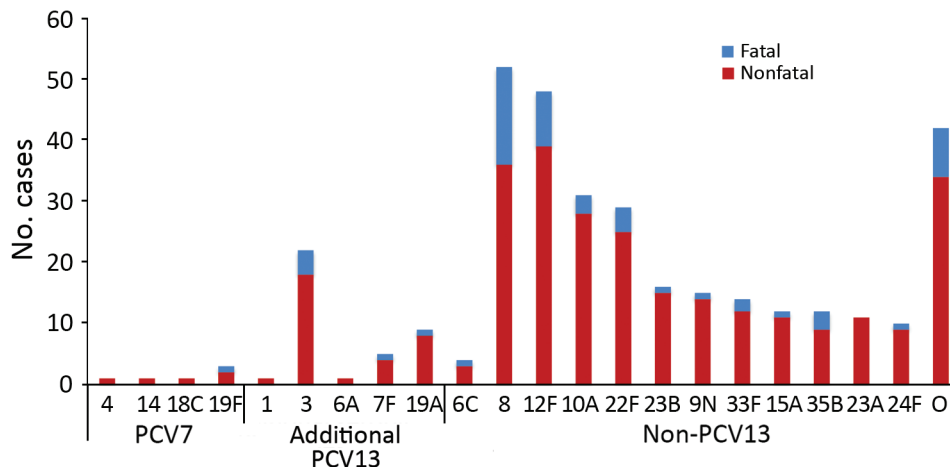


Figure 5. Pneumococcal meningitis cases, by *Streptococcus pneumoniae* serotype and severity, England and Wales, July 1, 2015–June 30, 2016. We included the non-PCV13 serotypes that involved ≥10 cases. O, other serotypes; PCV7, 7-valent pneumococcal conjugate vaccine; PCV13, 13-valent pneumococcal conjugate vaccine.

serotypes 12F, 8, and 10A caused nearly half of all pneumococcal meningitis cases in patients <5 years of age after PCV13 introduction (25). Of the most frequent serotypes isolated after PCV13 introduction in France (15B/C, 22F, 23B, 24F), only 24F had a high disease potential; 5 years after PCV13 introduction, no serotype predominated, and no significant increase in non-PCV13-type meningitis occurred (42). A common feature shared among countries with established PCV13 programs is the high proportion of cases (70%–80%) caused by non-PCV13 serotypes after PCV13 introduction (20,43).

In our cohort, the differences in disease trends among meningitis and nonmeningitis presentations after PCV7 and PCV13 implementation are probably a result of the different propensities of specific serotypes to cause meningitis, pneumonia, severe disease, and fatal outcomes. For example, before PCV7 introduction, some PCV7 (6B, 18C, 19F, 23F), additional PCV13 (3, 6A), and non-PCV13 (12F) serotypes were more likely to be associated with meningitis in the United Kingdom, while serotype 1 (additional PCV13) was less likely (10). Many of the serotypes that increased in incidence after PCV13 implementation did not exhibit a higher propensity for causing meningitis. Our findings (and those of others) highlight the importance of monitoring infectious diseases by their major clinical presentations. In the United States, after PCV7 introduction, the rates of meningitis and invasive pneumonia caused by non-PCV7 types increased for all age groups, whereas primary bacteremia rates did not change (32). In contrast, a study in Spain showed a shift in pneumococcal meningitis cases to persons in older age groups (18). In Canada, a higher proportion of IPD cases presented as meningitis after the introduction of PCV7 and PCV13 (44), and in Israel, disease caused by non-PCV13 serotypes increased by 256% for pneumococcal meningitis among children, 302% for pneumococcal bacteremic pneumonia, and 116% for other IPD presentations (15).

The CFR of our cohort (17.5%, 10.7% in children <5 years of age) was similar to that reported for the pre-PCV7 period (14.5%) but higher than that reported for children in Spain (5%) and the United States (8.3%–11.2%) (2,18,31). We have reported that nearly half of all children with IPD who died had meningitis (4) and that meningitis was an independent risk factor for death in children with IPD (45). Similar to our cohort, studies conducted in other countries have also indicated little change in CFR for pneumococcal meningitis after PCV introduction, despite significant reductions in disease incidence (18,31,46). Clinical follow-up of cases suggests that although the risk for pneumococcal meningitis was lowered after PCV introduction, once meningitis develops, the outcomes in terms of death or long-term sequelae are similar, irrespective of infecting serotype (20). Our finding of lower odds of meningitis but

higher risk for death with serotype 8 meningitis is novel (41) and needs to be verified for other populations.

The strengths of our study included established, long-term national surveillance along with a national reference laboratory for IPD covering a large population of 55 million persons across England and Wales. A study limitation was that bacterial meningitis cases caused by unknown species types, a substantial proportion of which were probably *S. pneumoniae*, would not have been captured in the surveillance, thus leading to an underestimation of the burden of pneumococcal meningitis. In addition, lumbar punctures are less likely to be performed on adults than children, and therefore, some IPD cases in adults were probably not reported as meningitis. Another limitation was that enhanced surveillance with questionnaires for vaccine-eligible children only began when PCV7 was introduced. This change could potentially have led to improved ascertainment of meningitis cases in the vaccine-eligible cohort after PCV7 introduction and, therefore, caused the effects of PCV7 to be underestimated. On the other hand, cases in and disease trends among older children and adults should not have been affected because enhanced surveillance was restricted to children ≤5 years of age. Overall, however, these differences were unlikely to affect the trends over time, effect of vaccination, or serotype distribution among meningitis and nonmeningitis cases. Finally, some pneumococcal serotypes exhibit cyclical trends, which could potentially explain some of the observed changes in serotype distribution; we did not evaluate changes in individual serotypes over time because of the relatively small numbers of meningitis cases caused by individual serotypes.

Comparisons of our findings with those found in studies of other populations should be made cautiously because of differences in the distribution of serotypes causing invasive disease in persons in different age groups, propensities of individual serotypes causing meningitis, replacement serotypes causing disease after PCV7 and PCV13 introduction, secular trends in non-PCV13 serotypes, vaccination schedules and coverage, antimicrobial use, emergence of resistant serotypes, clinical practices for investigating and treating patients with suspected meningitis, surveillance methods, case definitions, and completeness of case ascertainment. Of note, in the United Kingdom, antimicrobial resistance among invasive pneumococcal isolates remains low (47,48).

In conclusion, the childhood pneumococcal vaccination program has reduced the incidence of IPD, including pneumococcal meningitis, across all age groups through a combination of direct and herd protection. We estimated that >700 cases of pneumococcal meningitis were prevented during the first decade of the program, although CFRs across different age groups remain relatively unchanged.

By 2015–16, most cases of pneumococcal meningitis were caused by non-PCV13 serotypes. Further studies are needed to assess the risk factors, clinical course, and outcomes of pneumococcal meningitis associated with the replacing serotypes. Higher-valent vaccines are needed to target the emerging serotypes in the short term until serotype-independent vaccines become available.

About the Author

Dr. Oligbu is a consultant pediatrician with interest in pediatric infectious diseases, as well as a research fellow with St. George's, University of London (London, UK), and Public Health England, where he is involved with conducting enhanced national surveillance of invasive pneumococcal disease.

References

- Thigpen MC, Whitney CG, Messonnier NE, Zell ER, Lynfield R, Hadler JL, et al.; Emerging Infections Programs Network. Bacterial meningitis in the United States, 1998–2007. *N Engl J Med*. 2011;364:2016–25. <https://doi.org/10.1056/NEJMoa1005384>
- Johnson AP, Waight P, Andrews N, Pebody R, George RC, Miller E. Morbidity and mortality of pneumococcal meningitis and serotypes of causative strains prior to introduction of the 7-valent conjugate pneumococcal vaccine in England. *J Infect*. 2007;55:394–9. <https://doi.org/10.1016/j.jinf.2007.07.009>
- Stanek RJ, Mufson MA. A 20-year epidemiological study of pneumococcal meningitis. *Clin Infect Dis*. 1999;28:1265–72. <http://dx.doi.org/10.1086/514777>
- Oligbu G, Collins S, Sheppard CL, Fry NK, Slack M, Borrow R, et al. Childhood deaths attributable to invasive pneumococcal disease in England and Wales, 2006–2014. *Clin Infect Dis*. 2017;65:308–14. <https://doi.org/10.1093/cid/cix310>
- Neuman HB, Wald ER. Bacterial meningitis in childhood at the Children's Hospital of Pittsburgh: 1988–1998. *Clin Pediatr (Phila)*. 2001;40:595–600. <https://doi.org/10.1177/00092280104001102>
- Quagliarello V, Scheld WM. Bacterial meningitis: pathogenesis, pathophysiology, and progress. *N Engl J Med*. 1992;327:864–72. <https://doi.org/10.1056/NEJM199209173271208>
- Jit M. The risk of sequelae due to pneumococcal meningitis in high-income countries: a systematic review and meta-analysis. *J Infect*. 2010;61:114–24. <https://doi.org/10.1016/j.jinf.2010.04.008>
- Braun JS, Sublett JE, Freyer D, Mitchell TJ, Cleveland JL, Tuomanen EI, et al. Pneumococcal pneumolysin and H₂O₂ mediate brain cell apoptosis during meningitis. *J Clin Invest*. 2002;109:19–27. <https://doi.org/10.1172/JCI12035>
- Hoffmann O, Priller J, Prozorovski T, Schulze-Topphoff U, Baeva N, Lunemann JD, et al. TRAIL limits excessive host immune responses in bacterial meningitis. *J Clin Invest*. 2007;117:2004–13. <https://doi.org/10.1172/JCI30356>
- Trotter CL, Waight P, Andrews NJ, Slack M, Efstratiou A, George R, et al. Epidemiology of invasive pneumococcal disease in the pre-conjugate vaccine era: England and Wales, 1996–2006. *J Infect*. 2010;60:200–8. <https://doi.org/10.1016/j.jinf.2009.12.008>
- Salisbury D, Ramsay M, Noakes K, editors. Immunisation against infectious disease. The green book. Norwich, England: The Stationery Office; 2006 [cited 2018 May 3]. <https://webarchive.nationalarchives.gov.uk/20130104181824/https://www.wp.dh.gov.uk/immunisation/files/2012/09/Green-Book-updated-040113.pdf>
- Waight PA, Andrews NJ, Ladhani SN, Sheppard CL, Slack MPE, Miller E. Effect of the 13-valent pneumococcal conjugate vaccine on invasive pneumococcal disease in England and Wales 4 years after its introduction: an observational cohort study. *Lancet Infect Dis*. 2015;15:535–43. [https://doi.org/10.1016/S1473-3099\(15\)70044-7](https://doi.org/10.1016/S1473-3099(15)70044-7)
- Miller E, Andrews NJ, Waight PA, Slack MPE, George RC. Herd immunity and serotype replacement 4 years after seven-valent pneumococcal conjugate vaccination in England and Wales: an observational cohort study. *Lancet Infect Dis*. 2011;11:760–8. [https://doi.org/10.1016/S1473-3099\(11\)70090-1](https://doi.org/10.1016/S1473-3099(11)70090-1)
- Pichon B, Ladhani SN, Slack MPE, Segonds-Pichon A, Andrews NJ, Waight PA, et al. Changes in molecular epidemiology of *Streptococcus pneumoniae* causing meningitis following introduction of pneumococcal conjugate vaccination in England and Wales. *J Clin Microbiol*. 2013;51:820–7. <https://doi.org/10.1128/JCM.01917-12>
- Ben-Shimol S, Givon-Lavi N, Grisaru-Soen G, Megged O, Greenberg D, Dagan R; Israel Bacteremia and Meningitis Active Surveillance Group. Comparative incidence dynamics and serotypes of meningitis, bacteremic pneumonia and other-IPD in young children in the PCV era: insights from Israeli surveillance studies. *Vaccine*. 2018;36:5477–84. <https://doi.org/10.1016/j.vaccine.2017.05.059>
- Alari A, Chaussade H, Domenech De Cellès M, Le Foulher L, Varon E, Opatowski L, et al. Impact of pneumococcal conjugate vaccines on pneumococcal meningitis cases in France between 2001 and 2014: a time series analysis. *BMC Med*. 2016;14:211. <https://doi.org/10.1186/s12916-016-0755-7>
- Hsu HE, Shutt KA, Moore MR, Beall BW, Bennett NM, Craig AS, et al. Effect of pneumococcal conjugate vaccine on pneumococcal meningitis. *N Engl J Med*. 2009;360:244–56. <https://doi.org/10.1056/NEJMoa0800836>
- Ruiz-Contreras J, Picazo J, Casado-Flores J, Baquero-Artigao F, Hernández-Sampelayo T, Otheo E, et al.; Heracles Study Group. Impact of 13-valent pneumococcal conjugate vaccine on pneumococcal meningitis in children. *Vaccine*. 2017;35(35 Pt B):4646–51. <http://dx.doi.org/10.1016/j.vaccine.2017.06.070>
- Tsai CJ, Griffin MR, Nuorti JP, Grijalva CG. Changing epidemiology of pneumococcal meningitis after the introduction of pneumococcal conjugate vaccine in the United States. *Clin Infect Dis*. 2008;46:1664–72. <https://doi.org/10.1086/587897>
- Olarte L, Barson WJ, Barson RM, Lin PL, Romero JR, Tan TQ, et al. Impact of the 13-valent pneumococcal conjugate vaccine on pneumococcal meningitis in US children. *Clin Infect Dis*. 2015;61:767–75. <https://doi.org/10.1093/cid/civ368>
- Tsaban G, Ben-Shimol S. Indirect (herd) protection, following pneumococcal conjugated vaccines introduction: a systematic review of the literature. *Vaccine*. 2017;35:2882–91. <https://doi.org/10.1016/j.vaccine.2017.04.032>
- Ben-Shimol S, Greenberg D, Givon-Lavi N, Schlesinger Y, Miron D, Aviner S, et al.; Israel Bacteremia and Meningitis Active Surveillance Group. Impact of PCV7/PCV13 introduction on invasive pneumococcal disease (IPD) in young children: comparison between meningitis and non-meningitis IPD. *Vaccine*. 2016;34:4543–50. <https://doi.org/10.1016/j.vaccine.2016.07.038>
- Alexandre C, Dubos F, Courouble C, Pruvost I, Varon E, Martinot A; Hospital Network for Evaluating the Management of Common Childhood Diseases. Rebound in the incidence of pneumococcal meningitis in northern France: effect of serotype replacement. *Acta Paediatr*. 2010;99:1686–90. <https://doi.org/10.1111/j.1651-2227.2010.01914.x>
- Cohen R, Biscardi S, Levy C. The multifaceted impact of pneumococcal conjugate vaccine implementation in children in France between 2001 to 2014. *Hum Vaccin Immunother*. 2016;12:277–84. <https://doi.org/10.1080/21645515.2015.1116654>
- Imöhl M, Möller J, Reinert RR, Pernicario S, van der Linden M, Aktas O. Pneumococcal meningitis and vaccine effects in the era of conjugate vaccination: results of 20 years of nationwide

- surveillance in Germany. *BMC Infect Dis.* 2015;15:61. <https://doi.org/10.1186/s12879-015-0787-1>
26. Ricketson LJ, Wood ML, Vanderkooi OG, MacDonald JC, Martin IE, Demczuk WH, et al.; Calgary Streptococcus pneumoniae Epidemiology Research investigators. Trends in asymptomatic nasopharyngeal colonization with *Streptococcus pneumoniae* after introduction of the 13-valent pneumococcal conjugate vaccine in Calgary, Canada. *Pediatr Infect Dis J.* 2014;33:724–30. <https://doi.org/10.1097/INF.0000000000000267>
 27. Moreira M, Castro O, Palmieri M, Efklidou S, Castagna S, Hoet B. A reflection on invasive pneumococcal disease and pneumococcal conjugate vaccination coverage in children in southern Europe (2009–2016). *Hum Vaccin Immunother.* 2017;13:1242–53. <https://doi.org/10.1080/21645515.2016.1263409>
 28. de Oliveira LH, Camacho LA, Coutinho ES, Martinez-Silveira MS, Carvalho AF, Ruiz-Matus C, et al. Impact and effectiveness of 10 and 13-valent pneumococcal conjugate vaccines on hospitalization and mortality in children aged less than 5 years in Latin American countries: a systematic review. *PLoS One.* 2016;11:e0166736. <https://doi.org/10.1371/journal.pone.0166736>
 29. Polkowska A, Toropainen M, Ollgren J, Lyytikäinen O, Nuorti JP. Bacterial meningitis in Finland, 1995–2014: a population-based observational study. *BMJ Open.* 2017;7:e015080. <https://doi.org/10.1136/bmjopen-2016-015080>
 30. Shinjoh M, Yamaguchi Y, Iwata S. Pediatric bacterial meningitis in Japan, 2013–2015 – 3–5 years after the wide use of *Haemophilus influenzae* type b and *Streptococcus pneumoniae* conjugated vaccines. *J Infect Chemother.* 2017;23:427–38. <https://doi.org/10.1016/j.jiac.2017.02.014>
 31. Jacobs DM, Yung F, Hart E, Nguyen MNH, Shaver A. Trends in pneumococcal meningitis hospitalizations following the introduction of the 13-valent pneumococcal conjugate vaccine in the United States. *Vaccine.* 2017;35:6160–5. <https://doi.org/10.1016/j.vaccine.2017.09.050>
 32. Pilishvili T, Lexau C, Farley MM, Hadler J, Harrison LH, Bennett NM, et al.; Active Bacterial Core Surveillance/Emerging Infections Program Network. Sustained reductions in invasive pneumococcal disease in the era of conjugate vaccine. *J Infect Dis.* 2010;201:32–41. <https://doi.org/10.1086/648593>
 33. Verhaegen J, Vandecasteele SJ, Vandeven J, Verbiest N, Lagrou K, Peetermans WE. Antibiotic susceptibility and serotype distribution of 240 *Streptococcus pneumoniae* causing meningitis in Belgium 1997–2000. *Acta Clin Belg.* 2003;58:19–26. <https://doi.org/10.1179/acb.2003.58.1.003>
 34. Vieira AC, Gomes MC, Rolo Filho M, Eudes Filho J, Bello EJM, de Figueiredo RB. *Streptococcus pneumoniae*: a study of strains isolated from cerebrospinal fluid. *J Pediatr (Rio J).* 2007;83:71–8. <https://doi.org/10.2223/JPED.1580>
 35. Imöhl M, Reinert RR, van der Linden M. Regional differences in serotype distribution, pneumococcal vaccine coverage, and antimicrobial resistance of invasive pneumococcal disease among German federal states. *Int J Med Microbiol.* 2010;300:237–47. <https://doi.org/10.1016/j.ijmm.2009.05.005>
 36. Richter SS, Heilmann KP, Dohrn CL, Riahi F, Diekema DJ, Doern GV. Pneumococcal serotypes before and after introduction of conjugate vaccines, United States, 1999–2011. *Emerg Infect Dis.* 2013;19:1074–83. <https://doi.org/10.3201/eid1907.121830>
 37. Hanquet G, Kissling E, Fenoll A, George R, Lepoutre A, Lernout T, et al. Pediatric pneumococcal serotypes in 4 European countries. *Emerg Infect Dis.* 2010;16:1428–39. <https://doi.org/10.3201/eid1609.100102>
 38. Janoir C, Lepoutre A, Gutmann L, Varon E. Insight into resistance phenotypes of emergent non 13-valent pneumococcal conjugate vaccine type pneumococci isolated from invasive disease after 13-valent pneumococcal conjugate vaccine implementation in France. *Open Forum Infect Dis.* 2016;3:ofw020. <http://dx.doi.org/10.1093/ofid/ofw020>
 39. Mahjoub-Messai F, Doit C, Koeck JL, Billard T, Evrard B, Bidet P, et al. Population snapshot of *Streptococcus pneumoniae* serotype 19A isolates before and after introduction of seven-valent pneumococcal vaccination for French children. *J Clin Microbiol.* 2009;47:837–40. <https://doi.org/10.1128/JCM.01547-08>
 40. Rückinger S, von Kries R, Siedler A, van der Linden M. Association of serotype of *Streptococcus pneumoniae* with risk of severe and fatal outcome. *Pediatr Infect Dis J.* 2009;28:118–22. <https://doi.org/10.1097/INF.0b013e318187e215>
 41. Balsells E, Guillot L, Nair H, Kyaw MH. Serotype distribution of *Streptococcus pneumoniae* causing invasive disease in children in the post-PCV era: a systematic review and meta-analysis. *PLoS One.* 2017;12:e0177113. <https://doi.org/10.1371/journal.pone.0177113>
 42. Varon E, Cohen R, Béchet S, Doit C, Levy C. Invasive disease potential of pneumococci before and after the 13-valent pneumococcal conjugate vaccine implementation in children. *Vaccine.* 2015;33:6178–85. <https://doi.org/10.1016/j.vaccine.2015.10.015>
 43. Levy C, Varon E, Béchet S, Cohen R. Effect of the 13-valent pneumococcal conjugate vaccine on pneumococcal meningitis in children. *Clin Infect Dis.* 2016;62:131–2. <https://doi.org/10.1093/cid/civ692>
 44. Ricketson LJ, Conradi NG, Vanderkooi OG, Kellner JD. Changes in the nature and severity of invasive pneumococcal disease in children before and after the seven-valent and thirteen-valent pneumococcal conjugate vaccine programs in Calgary, Canada. *Pediatr Infect Dis J.* 2017;37:22–7. <https://doi.org/10.1097/INF.0000000000001709>
 45. Ladhani SN, Slack MPE, Andrews NJ, Waight PA, Borrow R, Miller E. Invasive pneumococcal disease after routine pneumococcal conjugate vaccination in children, England and Wales. *Emerg Infect Dis.* 2013;19:61–8. <https://doi.org/10.3201/eid1901.120741>
 46. Hirose TE, Maluf EM, Rodrigues CO. Pneumococcal meningitis: epidemiological profile pre- and post-introduction of the pneumococcal 10-valent conjugate vaccine. *J Pediatr (Rio J).* 2015;91:130–5. <https://doi.org/10.1016/j.jpmed.2014.07.002>
 47. Henderson KL, Muller-Pebody B, Ladhani S, Sharland M, Johnson AP. NICE on bacterial meningitis. Vancomycin may not be necessary. *BMJ.* 2010;341:c4704. <https://doi.org/10.1136/bmj.c4704>
 48. Henderson KL, Muller-Pebody B, Blackburn RM, Johnson AP. Reduction in erythromycin resistance in invasive pneumococci from young children in England and Wales. *J Antimicrob Chemother.* 2010;65:369–70. <https://doi.org/10.1093/jac/dkp442>

Address for correspondence: Shamez N. Ladhani, Public Health England, Immunization Department, 61 Colindale Ave, London NW9 5EQ, UK; email: shamez.ladhani@phe.gov.uk

Rickettsia japonica Infections in Humans, Xinyang, China, 2014–2017

Hao Li, Pan-He Zhang, Juan Du,
Zhen-Dong Yang, Ning Cui, Bo Xing,
Xiao-Ai Zhang, Wei Liu

During 2014–2017, we screened for *Rickettsia japonica* infection in Xinyang, China, and identified 20 cases. The major clinical manifestations of monoinfection were fever, asthenia, myalgia, rash, and anorexia; laboratory findings included thrombocytopenia and elevated hepatic aminotransferase concentrations. Physicians in China should consider *R. japonica* infection in at-risk patients.

Emerging and reemerging spotted fever group (SFG) rickettsioses are increasingly spreading and being recognized worldwide. Japanese spotted fever (JSF), caused by *Rickettsia japonica* and first reported in Japan in 1984 (1,2), is an SFG rickettsiosis characterized by fever, malaise, chills, headache, rash, and eschars (3,4). JSF cases have been increasingly reported, but mostly in Japan and the nearby countries of South Korea, the Philippines, and Thailand (4–7). *R. japonica* has been detected in 3 genera (*Haemaphysalis*, *Dermacentor*, *Ixodes*) and 8 species of ticks (8,9). Because of the wide spectrum of ticks in which this bacterium has been found, *R. japonica* is postulated to be distributed more widely throughout China. The identification of *R. japonica* in *H. flava* and *H. hystricis* ticks in Wuhan, China, further corroborated this hypothesis (10). Also, serologic responses to *R. japonica* were detected in patients in Hainan Province in southern China ≈3 decades ago (11). However, laboratory-confirmed JSF cases have been identified in only a few patients in China (12,13). In this study, we aimed to determine if more JSF cases were occurring in China by using hospital-based surveillance.

The Study

During March 2014–June 2017, we screened 2,236 febrile patients seeking treatment at The People's Liberation Army 990 Hospital in Xinyang, Henan Province, eastern central China (Appendix Figure, <https://wwwnc.cdc.gov/>

Author affiliations: Beijing Institute of Microbiology and Epidemiology, Beijing, China (H. Li, P.-H. Zhang, B. Xing, X.-A. Zhang, W. Liu); Peking University, Beijing (J. Du); People's Liberation Army 990 Hospital, Xinyang, China (Z.-D. Yang, N. Cui)

DOI: <https://doi.org/10.3201/eid2509.171421>

[EID/article/25/9/17-1421-App1.pdf](https://doi.org/10.3201/eid2509.171421)) with a history of tick bite or field activity within the previous month for infection with *R. japonica*. We extracted DNA from peripheral blood samples collected during the acute phase of illness and screened them by a nested PCR concurrently targeting the citrate synthase gene (*glTA*), 17-kDa antigen-encoding gene (*htrA*), and outer membrane protein A-encoding gene (*ompA*), as previously described (14). To minimize the risk for contamination, we performed template isolation and PCR setup in separate rooms with specified pipette sets, used certified DNAase- and RNase-free filter barrier tips to prevent aerosol contamination, and performed all PCR assays with appropriate controls. After amplification and sequencing, we found that 20 patients were infected with *R. japonica*.

The *glTA* gene sequence (456-bp) obtained from all 20 samples (GenBank accession no. MF693145) showed 100% similarity to the corresponding gene of *R. japonica* strain YH (GenBank accession no. AP017602). The *htrA* gene sequence (394-bp) obtained from 18 samples (GenBank accession no. MF693146) was identical to that of *R. japonica* YH, and the sequence in the remaining 2 samples (GenBank accession no. MF693147) differed by only 3 bp. The *ompA* gene sequence (311-bp) found in 16 samples (GenBank accession no. MF693148) was identical to that of *R. japonica* YH, and the remaining 4 samples each differed by just 1 bp (GenBank accession nos. MF693149–52) (Figure 1).

We also assessed other tickborne agents, including *Anaplasma phagocytophilum*, *Anaplasma capra*, *Ehrlichia chaffeensis*, *Borrelia burgdorferi* sensu lato, *Babesia microti*, and severe fever with thrombocytopenia syndrome virus, by PCR or reverse transcription PCR. Six of 20 patients were co-infected with severe fever with thrombocytopenia syndrome virus, so we excluded them from clinical analysis.

We tested the acute serum samples collected ≤7 days after illness onset and the convalescence serum samples collected ≥14 days after illness onset from the 14 patients with *R. japonica* monoinfection in parallel using an indirect immunofluorescence assay for *Rickettsia heilongjiangensis* IgG. We considered an IgG titer ≥1:64 a positive reaction. Using this definition, we found that 6 patients had a seroconversion, and the other 8 had a 4-fold increased IgG titer; thus, all patients had an acute infection with SFG rickettsiae.

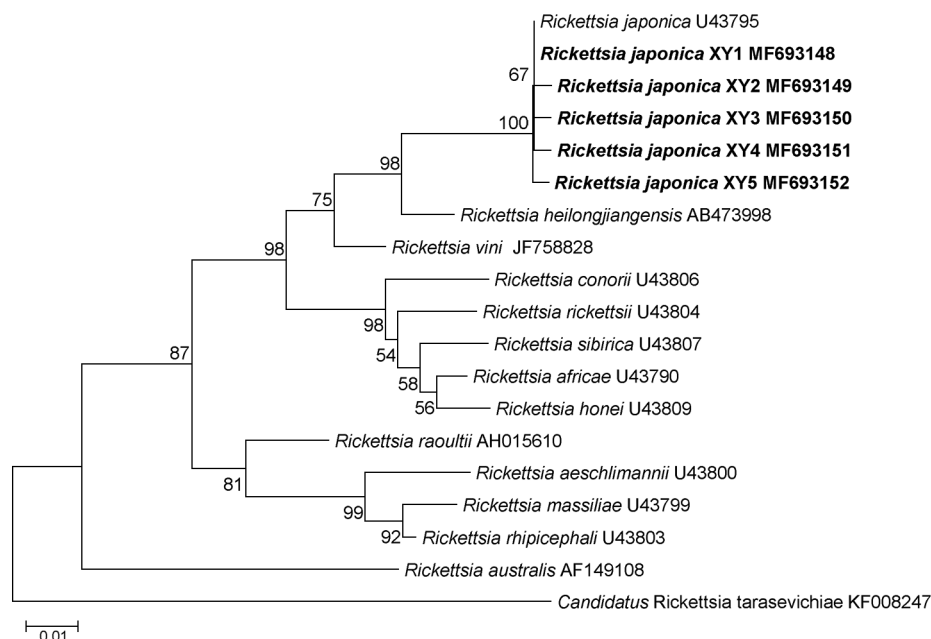


Figure 1. Phylogenetic analysis of *Rickettsia* species from febrile patients treated at The People's Liberation Army 990 Hospital for *Rickettsia japonica* infection, Xinyang, China, March 2014–June 2017 (bold), and reference species. Tree was constructed on the basis of the outer member protein A nucleotide (311-bp) gene sequence. We used the maximum-likelihood method with the best substitution model (Tamura 3-parameter plus gamma) and MEGA version 5.0 (<http://www.megasoftware.net>). We applied a bootstrap analysis of 1,000 replicates to assess the reliability of the reconstructed phylogenies. GenBank accession numbers are provided. Scale bar indicates estimated evolutionary distance.

All 14 patients had a history of field activity within the previous month, and 5 had a history of tick bite. Median patient age was 61.5 (range 44–77) years; 9 were men. The median time from tick bite to onset of illness was 4 (range 3–8) days and from onset of illness to physician visit 5 (range 2–7) days. The median duration of hospitalization was 6 (range 4–10) days.

Fever and asthenia were reported by all 14 patients. Other nonspecific symptoms included myalgia (10/14), lymphadenopathy (4/14), headache (3/14), dizziness (3/14), and chills (2/14). Gastrointestinal manifestations included anorexia (9/14), nausea (7/14), vomiting (3/14), and diarrhea (1/14). Three patients had cough and pneumonia, and we observed rash in 10 patients (Figure 2). The median time from onset of illness to rash was 4 (range 3–5) days, and the median duration of rash was 5.5 (range 4–8)

days. Only 3 patients had an eschar. Other signs included splenomegaly (2/14) and facial edema (1/14).

Urinalysis on admission revealed microscopic hematuria in 2 patients and a slight or moderate proteinuria in 8 patients. The most common findings on laboratory tests were thrombocytopenia, elevated hepatic aminotransferase concentrations, elevated serum lactate dehydrogenase, and hypoalbuminemia, followed by hyponatremia, anemia, hyperbilirubinemia, hypopotassemia, leukopenia, and elevated serum creatine kinase (Table). Mild multiple organ dysfunction developed in 3 patients.

Because of the appearance of typical rash, we suspected SFG rickettsioses in 10 patients and treated them with doxycycline (100 mg 2×/d) until their fevers dissipated and clinical disease improved (median 4 [range 3–5] days). The other 4 patients were treated with the antimicrobial drugs



Figure 2. Lesions on patients with *Rickettsia japonica* infection, Xinyang, China, March 2014–June 2017. A) Rash on ventrum; B) rash and eschar on back; C) eschar on femoribus internus; D) tick bite site on left armpit.

Table. Laboratory test results of samples from 14 patients with *Rickettsia japonica* infection at different time points, China, 2014–2017*

Result	No. patients		
	At admission	During hospitalization	At discharge from hospital
Anemia, $<3.5 \times 10^{12}$ erythrocytes/L	0	5	3
Leukopenia, $<4.0 \times 10^9$ leukocytes/L	3	3	0
Thrombocytopenia, $<150 \times 10^9$ platelets/L	9	11	0
Hyperbilirubinemia, albumin $>17.1 \mu\text{mol/L}$	4	5	2
Hypoalbuminemia, albumin $<35.0 \text{ g/L}$	3	9	7
Hyponatremia, sodium $<135.0 \text{ mmol/L}$	4	6	2
Hypopotassemia, potassium $<3.5 \text{ mmol/L}$	2	4	2
Increased ALT level, $>0.67 \mu\text{kat/L}$	8	10	5
Increased AST level, $>0.67 \mu\text{kat/L}$	10	12	5
Increased LDH level, $>4.1 \mu\text{kat/L}$	10	11	7
Increased CK level, $>4.1 \mu\text{kat/L}$	4	3	0

*ALT, alanine aminotransferase; AST, aspartate aminotransferase; CK, creatine kinase; LDH, lactate dehydrogenase.

cefminox or cefoperazone for a median of 6 (range 5–7) days. By the time patients were discharged from the hospital, their leukocyte and platelet counts had returned to reference range levels, but half of the patients still had laboratory test values outside of their respective reference ranges (Table). No patients reported clinically significant sequelae at their 2-week follow-up appointment.

Conclusions

The tick vectors of *R. japonica* (i.e., *H. flava*, *H. hystricis*, *H. cornigera*, *H. longicornis*, *I. ovatus*) are widely distributed throughout China (15), providing *R. japonica* ample opportunity to infect humans. By applying molecular screening techniques to simultaneously amplify 3 genes, we identified *R. japonica* infection in 14 patients.

The clinical signs and symptoms of *R. japonica* infection in our patient cohort differed from those reported in patients in Japan (3,4). We frequently observed fever, asthenia, and rash but not chills and headache. We also saw fewer eschars in our patient cohort, potentially because they were underreported during clinical examination; eschars are not always easy to identify. In addition, the patients we identified usually had myalgia and gastrointestinal symptoms.

These clinical findings expand the available knowledge of the disease spectrum of *R. japonica* infection. Compared with endemic rickettsiosis caused by *Candidatus Rickettsia tarasevichiae* infection (reference 16 in Appendix), rash is commonly seen, and hemorrhagic and neurologic signs and symptoms are rarely seen in patients with *R. japonica* infection. These distinctive features could be used to make a differential diagnosis.

We frequently observed in our patient cohort thrombocytopenia, hypoalbuminemia, elevated hepatic enzyme activity, and elevated lactate dehydrogenase levels, findings resembling those of patients with common SFG rickettsioses (reference 17 in Appendix). In general, disease is mild or moderate, and no deaths have been recorded, although mild multiple organ dysfunction developed in several patients.

In conclusion, we identified *R. japonica* as an emerging tickborne pathogen in China. Physicians in areas where *H. longicornis* and other competent vectors for *R. japonica* are endemic should be aware of the risk for infection in humans and prescribe doxycycline to patients in cases of ineffective therapy with other antimicrobial drugs. Surveillance needs to be extended to improve our understanding of the health burden of JSF.

This study was supported by the National Natural Science Foundation of China (81825019, 81722041, 81472005, and 81621005), the China Mega-Project for Infectious Diseases (2018ZX10713002-002), the National Key Research and Development Program of China (2016YFX1201905), and the New Star Plan of Science and Technology of Beijing (Z171100001117089).

About the Author

Dr. Li is a scientist in the State Key Laboratory of Pathogen and Biosecurity, Beijing Institute of Microbiology and Epidemiology, Beijing, China. His research interests include microbiology, epidemiology, and ecology of tickborne diseases.

References

- Mahara F, Koga K, Sawada S, Taniguchi T, Shigemi F, Suto T, et al. The first report of the rickettsial infections of spotted fever group in Japan: three clinical cases [in Japanese]. *Kansenshogaku Zasshi*. 1985;59:1165–72. <https://doi.org/10.11150/kansenshogakuzasshi1970.59.1165>
- Uchida T, Uchiyama T, Kumano K, Walker DH. *Rickettsia japonica* sp. nov., the etiological agent of spotted fever group rickettsiosis in Japan. *Int J Syst Bacteriol*. 1992;42:303–5. <https://doi.org/10.1099/00207713-42-2-303>
- Mahara F. Japanese spotted fever: report of 31 cases and review of the literature. *Emerg Infect Dis*. 1997;3:105–11. <https://doi.org/10.3201/eid0302.970203>
- Mahara F. Rickettsioses in Japan and the Far East. *Ann N Y Acad Sci*. 2006;1078:60–73. <https://doi.org/10.1196/annals.1374.007>
- Camer GA, Alejandria M, Amor M, Satoh H, Muramatsu Y, Ueno H, et al. Detection of antibodies against spotted fever group *Rickettsia* (SFGR), typhus group *Rickettsia* (TGR), and *Coxiella burnetii* in human febrile patients in the Philippines. *Jpn J Infect Dis*. 2003;56:26–8.

6. Chung MH, Lee SH, Kim MJ, Lee JH, Kim ES, Lee JS, et al. Japanese spotted fever, South Korea. *Emerg Infect Dis*. 2006;12:1122–4. <https://doi.org/10.3201/eid1207.051372>
7. Gaywee J, Sunyakumthorn P, Rodkvamtook W, Ruang-areerate T, Mason CJ, Sirisopana N. Human infection with *Rickettsia* sp. related to *R. japonica*, Thailand. *Emerg Infect Dis*. 2007;13:657–9. <https://doi.org/10.3201/eid1304.060585>
8. Ando S, Fujita H. Diversity between spotted fever group *Rickettsia* and ticks as vector. *Jap J Sanit Zool*. 2013;64:5–7. <https://doi.org/10.7601/mez.64.5>
9. Fournier PE, Fujita H, Takada N, Raoult D. Genetic identification of rickettsiae isolated from ticks in Japan. *J Clin Microbiol*. 2002;40:2176–81. <https://doi.org/10.1128/JCM.40.6.2176-2181.2002>
10. Lu M, Tian JH, Yu B, Guo WP, Holmes EC, Zhang YZ. Extensive diversity of rickettsiales bacteria in ticks from Wuhan, China. *Ticks Tick Borne Dis*. 2017;8:574–80. <https://doi.org/10.1016/j.ttbdis.2017.03.006>
11. Feng HM, Chen TS, Lin BH, Lin YZ, Wang PF, Su QH, et al. Serologic survey of spotted fever group rickettsiosis on Hainan Island of China. *Microbiol Immunol*. 1991;35:687–94. <https://doi.org/10.1111/j.1348-0421.1991.tb01602.x>
12. Li J, Hu W, Wu T, Li HB, Hu W, Sun Y, et al. Japanese spotted fever in eastern China, 2013. *Emerg Infect Dis*. 2018;24:2107–9. <https://doi.org/10.3201/eid2411.170264>
13. Lu Q, Yu J, Yu L, Zhang Y, Chen Y, Lin M, et al. *Rickettsia japonica* infections in humans, Zhejiang Province, China, 2015. *Emerg Infect Dis*. 2018;24:2077–9. <https://doi.org/10.3201/eid2411.170044>
14. Li H, Zhang PH, Huang Y, Du J, Cui N, Yang ZD, et al. Isolation and identification of *Rickettsia raoultii* and in human cases: a surveillance study in 3 medical centers in China. *Clin Infect Dis*. 2018;66:1109–15. <https://doi.org/10.1093/cid/cix917>
15. Chen Z, Yang X, Bu F, Yang X, Yang X, Liu J. Ticks (Acari: Ixodoidea: Argasidae, Ixodidae) of China. *Exp Appl Acarol*. 2010;51:393–404. <https://doi.org/10.1007/s10493-010-9335-2>

Address for correspondence: Hao Li and Wei Liu, Beijing Institute of Microbiology and Epidemiology, State Key Laboratory of Pathogen and Biosecurity, 20 Dong-Da St, Fengtai District, Beijing 100071, China; email: lihao_1986@126.com and liuwei@bmi.ac.cn

The Public Health Image Library (PHIL)



The Public Health Image Library (PHIL), Centers for Disease Control and Prevention, contains thousands of public health-related images, including high-resolution (print quality) photographs, illustrations, and videos.

PHIL collections illustrate current events and articles, supply visual content for health promotion brochures, document the effects of disease, and enhance instructional media.

PHIL images, accessible to PC and Macintosh users, are in the public domain and available without charge.

Visit PHIL at:
<http://phil.cdc.gov/phil>

Climate Classification System–Based Determination of Temperate Climate Detection of *Cryptococcus gattii* sensu lato

Emily S. Acheson, Eleni Galanis,
Karen Bartlett, Brian Klinkenberg

We compared 2 climate classification systems describing georeferenced environmental *Cryptococcus gattii* sensu lato isolations occurring during 1989–2016. Each system suggests the fungus was isolated in temperate climates before the 1999 outbreak on Vancouver Island, British Columbia, Canada. However, the Köppen-Geiger system is more precise and should be used to define climates where pathogens are detected.

A global systematic framework is needed to define climates where pathogens are detected. The 1999 cryptococcal outbreak of the fungal species complex *Cryptococcus gattii* sensu lato on Vancouver Island (1), British Columbia, Canada, was described as the first temperate climate emergence of the pathogen because, before this event, *C. gattii* s.l. was largely reported in areas described as tropical and subtropical (Appendix Figure, <https://wwwnc.cdc.gov/EID/article/25/9/18-1884-App1.pdf>). This assumption led to the belief that the Vancouver Island outbreak might be associated with a changing climate. The lack of precision and standardization of climate classification in the health literature makes comparing emergence areas around the world and determining why or how the organism emerged in that area difficult.

The lack of consensus might largely be rooted in the lack of a global systematic framework to define climates where pathogens are detected. Specifically, a standardized definition of tropical, subtropical, and temperate to compare pathogen isolation areas worldwide is unavailable. Here, we compare the 2 solar climate definitions and the Köppen-Geiger climate classification system to determine whether the 1999 Vancouver Island outbreak was the first-ever detection of *C. gattii* s.l. in a temperate environment and which system should be used for a global systematic climate classification framework.

Author affiliations: University of British Columbia, Vancouver, British Columbia, Canada (E.S. Acheson, E. Galanis, K. Bartlett, B. Klinkenberg); British Columbia Centre for Disease Control, Vancouver (E. Galanis)

DOI: <https://doi.org/10.3201/eid2509.181884>

The Study

We used environmental isolations of *C. gattii* s.l. (i.e., detections in plant and soil samples) to map global distribution. Geographically defined human and animal records of *C. gattii* infection are not always accessible because of privacy restrictions. In addition, the dates and locations of *C. gattii* s.l. exposures are often uncertain because of the mobility of animals and humans and *C. gattii*'s long, undetermined incubation and latency periods (2). We extended the data of a database of globally georeferenced environmental isolations of *C. gattii* s.l. from the peer-reviewed literature (3) through November 2018 (Appendix Table). We excluded studies in which only the country of sampling was specified because many countries extend through multiple climates. We recorded the earliest year of isolation or, if a sampling year was not specified, the year of study publication. In total, we used 83 geographically unique coordinates of *C. gattii* isolations occurring during 1989–2016.

According to the solar definition (the predominant definition used in the *C. gattii* literature to describe isolation climates), tropical, subtropical, and temperate regions are denoted by latitudinal boundaries (4). In contrast, the Köppen-Geiger system (5) uses precipitation, temperature, and vegetation traits to produce 5 main climate groups (tropical or equatorial, arid, temperate, continental, and polar) and subgroups and is the most widely used climate classification system by researchers, including medical geographers, worldwide (6). For the solar definition of climate, we set the latitudinal boundaries of the tropics at 23.4 degrees north and south of the equator, the area of the subtropics as the tropical extent to 35 or 40 degrees north and south of the equator, and the temperate area as the subtropical extent to 66.5 degrees north and south of the equator (4,7). For the Köppen-Geiger system, we used a map depicting the climate characteristics observed during 1976–2000 with a spatial resolution of 0.5 degrees (<http://koeppen-geiger.vu-wien.ac.at/shifts.htm>). Using ArcMap version 10.5.1 (ESRI 2017, <https://www.esri.com>), we overlaid the isolation coordinates of *C. gattii* on each map and extracted the corresponding climate classifications. If exact coordinates of the sample were not specified, we used ArcMap to estimate coordinates for the centroid of the park, city, or town where the sampling

occurred. We first compared the climates assigned to isolations by classification system and then determined which positive sampling years had ≥ 1 isolation in a temperate region and how many of these years preceded 1999.

The solar definition classified the 83 environmental *C. gattii* s.l. isolations as tropical, subtropical, or temperate (Figure 1). By comparison, the Köppen-Geiger system classified these same isolations into 11 different climate subgroups (Figure 1). Both systems identified ≥ 1 temperate-climate environmental *C. gattii* isolation (8) before 1999 (Figure 2).

Both variations of the solar definition and the Köppen-Geiger system classified the environmental samples of *C. gattii* s.l. isolated on Vancouver Island during the outbreak as temperate (Appendix Table). According to the Köppen-

Geiger system, the Vancouver Island outbreak areas have 2 different types of temperate climates: temperate oceanic and warm summer Mediterranean, that is, precipitation conditions that range from dry summers to fully humid year-round with warm summer temperatures (5). According to the more restrictive solar definition of temperate, the environmental *C. gattii* s.l. isolation coordinates from only 1 year before 1999 could be classified as temperate (Figure 2). By contrast, the Köppen-Geiger system classified the coordinates of environmental isolations from 7 different years before 1999 as temperate (Figure 2; Appendix Table). These isolation coordinates included areas in California (9,10) and southwestern and southeastern Australia (9,11). The solar definition of climate largely categorized these areas as tropical or subtropical (Appendix Table), but

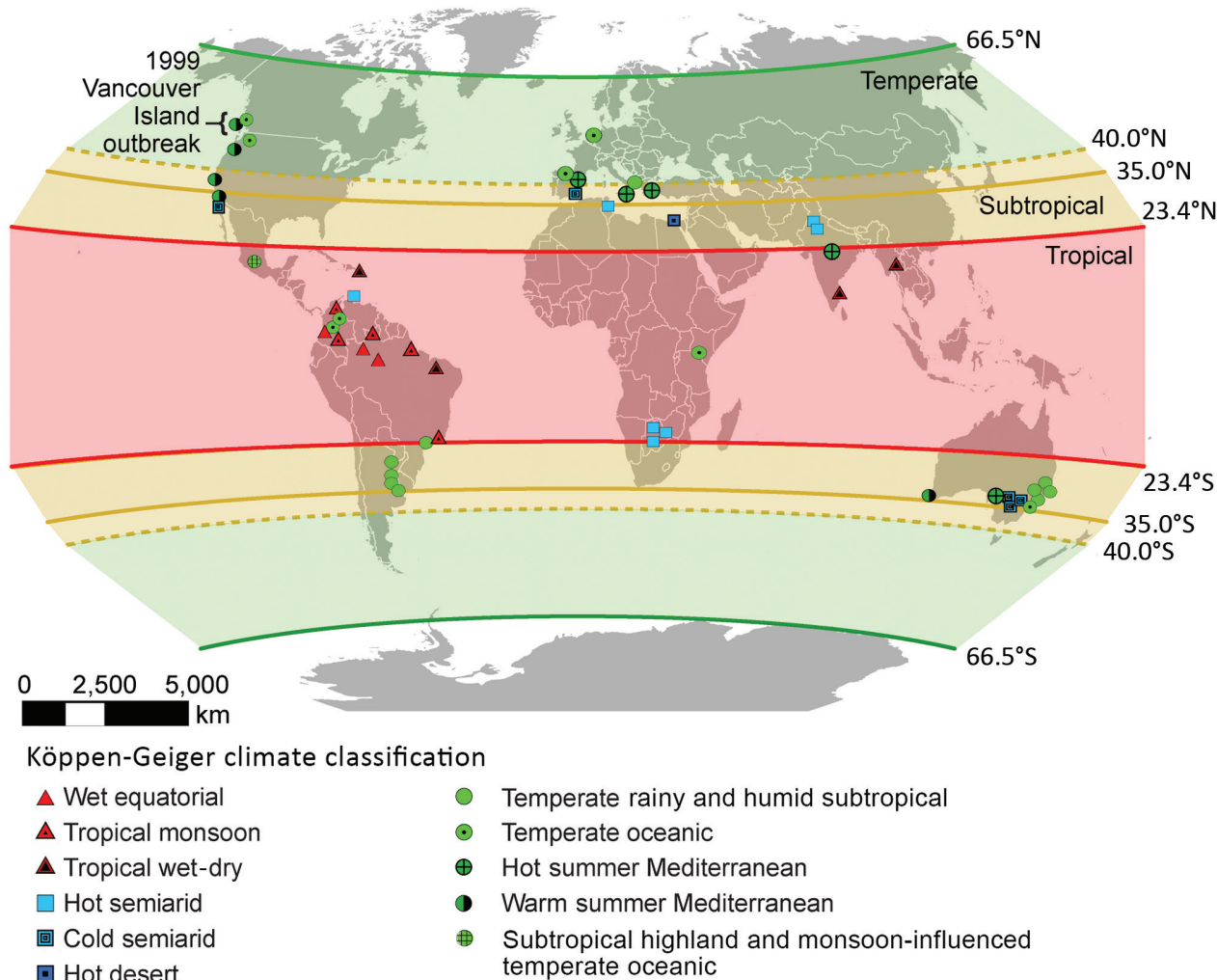


Figure 1. Global environmental isolations of *Cryptococcus gattii* sensu lato, 1989–2016. We mapped 83 unique geographic coordinates of *C. gattii* s.l. isolations and labeled them according to their Köppen-Geiger climate classification. Overlapping symbols of the same Köppen-Geiger climate classification (where isolations were 0–200 km apart) were removed for easier visualization. The solar definition of the tropics is shown as the semitransparent red area extending from the equator to 23.4 degrees north and south of the equator, the subtropics as the yellow area extending from the tropics to either 35 (solid line) or 40 (dashed line) degrees north and south of the equator, and the temperate zone as the green area extending from the subtropics to 66.5 degrees north and south of the equator.

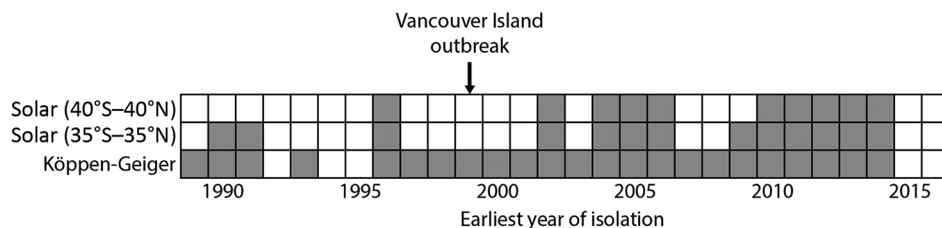


Figure 2. Timeline of environmental *Cryptococcus gattii* sensu lato isolations in temperate climates, by climate definition, 1989–2016. Gray squares indicate years in which ≥ 1 isolate from a temperate climate was obtained, and white squares indicate years in which no such isolate was obtained.

the Köppen-Geiger system labeled them as temperate oceanic and warm summer Mediterranean.

Conclusions

Both versions of the solar definition and the Köppen-Geiger system suggest that the Vancouver Island outbreak was not the first-ever temperate detection of *C. gattii* s.l. However, in terms of geographic scale, the solar definition of tropical, subtropical, and temperate are too coarse for the purposes of classifying or describing areas of local clinical, veterinary, or environmental isolations of *C. gattii* s.l. or any other environmentally contracted pathogen. Species, including pathogenic species, can live within geographically smaller refugia that maintain their climatic and biological needs across larger landscapes and solar boundaries, depending on topography, microclimates, and habitat fragmentation (12,13). Although the Köppen-Geiger system still generalizes across precipitation, temperature, and vegetation, the system accounts for more environmental variation and provides temperature and precipitation limits for each climate subtype. The Köppen-Geiger system is the most widely used climate classification system worldwide (5) and also provides projected maps for future climate shifts, making this system ideal as a global systematic framework for tracking the climates of pathogen detection. We, therefore, propose the use of the Köppen-Geiger system, as opposed to either of the overgeneralized solar definitions, for the sake of precision and consistency across global records when characterizing pathogen detection areas.

One limitation of our study was dependence on the reporting of environmental *C. gattii* samples in the English language peer-reviewed literature. As a result, our findings are an underrepresentation of the full global extent of *C. gattii* s.l. in the environment. Other evidence exists for the emergence of *C. gattii* s.l. in temperate climates before 1999. For example, in addition to the environmental isolations made in Busselton, Western Australia, Australia (9), in 1993, multiple *C. gattii* infections in animals were reported in southwestern Australia, including Perth, before 1999 (14). Both Busselton and Perth fall within a temperate Köppen-Geiger climate (5) (Figure 1). Another limitation was variability in the descriptions of pathogen detection areas. For example, some studies provided the

exact coordinates of *C. gattii* sampling, and others provided a park or city name. Providing the exact coordinates offers the greatest certainty of a detection location and better precision in climate classification.

By using *C. gattii* s.l. as an example for mapping georeferenced pathogen isolations worldwide, we demonstrated the opportunity to improve pathogen monitoring through the development of a standardized global climate classification framework. Using more spatially specific climate classification methods, such as the Köppen-Geiger system used by medical geographers, coupled with the continued reporting of pathogen isolation locations, will improve comparability of pathogen detection in new natural environments.

Acknowledgments

The authors thank Richard Malik, Mark Krockenberger, Peter Irwin, and Cristy Secombe for their expert input regarding *C. gattii* outbreaks and emergence in the environment in Australia. We also thank Mike Jerowsky, Peter Whitman, and José Aparicio for their help with the figures and edits to the manuscript.

Financial support for this project was provided by a Vanier Canada Graduate Scholarship for the Natural Sciences and Engineering Research Council of Canada, a University of British Columbia Four-Year Fellowship, and a Killam Doctoral Scholarship to E.S.A.

About the Author

Ms. Acheson is a doctoral candidate in the Geography Department at the University of British Columbia, Vancouver, British Columbia, Canada. Her primary research interests are in infectious disease emergence and disease vector ecology.

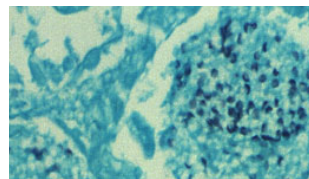
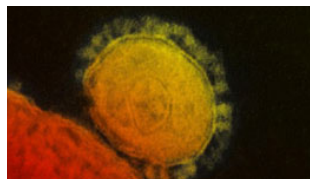
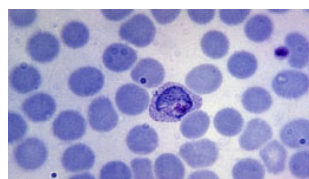
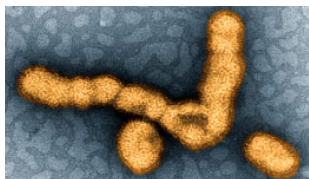
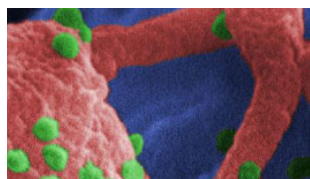
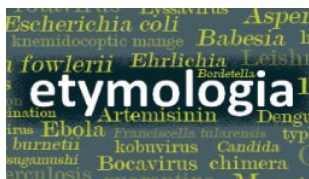
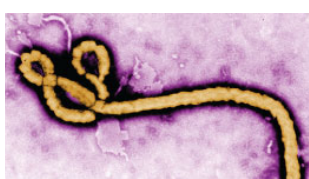
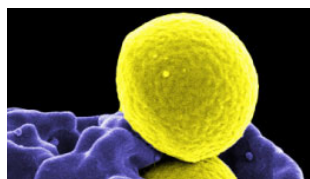
References

1. Stephen C, Lester S, Black W, Fyfe M, Raverty S. Multispecies outbreak of cryptococcosis on southern Vancouver Island, British Columbia. *Can Vet J.* 2002;43:792–4.
2. Hagen F, Colom MF, Swinne D, Tintelnat K, Iatta R, Montagna MT, et al. Autochthonous and dormant *Cryptococcus gattii* infections in Europe. *Emerg Infect Dis.* 2012;18:1618–24. <https://doi.org/10.3201/eid1810.120068>
3. Acheson ES, Galanis E, Bartlett K, Mak S, Klinkenberg B. Searching for clues for eighteen years: deciphering the ecological determinants of *Cryptococcus gattii* on Vancouver Island, British

- Columbia. *Med Mycol.* 2018;56:129–44. <https://doi.org/10.1093/mmy/myx037>
- Corlett RT. Where are the subtropics? *Biotropica.* 2013;45:273–5. <https://doi.org/10.1111/btp.12028>
 - Peel MC, Finlayson BL, McMahon TA. Updated world map of the Koppen-Geiger climate classification. *Hydrol Earth Syst Sci.* 2007;11:1633–44. <https://doi.org/10.5194/hess-11-1633-2007>
 - Polack S, Brooker S, Kuper H, Mariotti S, Mabey D, Foster A. Mapping the global distribution of trachoma. *Bull World Health Organ.* 2005;83:913–9.
 - Monson RK. Ecology of temperate forests. *Ecology and the environment.* New York: Springer New York; 2014. p. 273–96.
 - Montagna MT, Viviani MA, Pulito A, Aralla C, Tortorano AM, Fiore L, et al. *Cryptococcus neoformans* var. *gattii* in Italy. Note II. Environment investigation related to an autochthonous clinical case in Apulia. *J Mycol Med.* 1997;7:93–6.
 - Sorrell TC, Chen SCA, Ruma P, Meyer W, Pfeiffer TJ, Ellis DH, et al. Concordance of clinical and environmental isolates of *Cryptococcus neoformans* var. *gattii* by random amplification of polymorphic DNA analysis and PCR fingerprinting. *J Clin Microbiol.* 1996;34:1253–60.
 - Pfeiffer T, Ellis D. Environmental isolation of *Cryptococcus neoformans gattii* from California. *J Infect Dis.* 1991;163:929–30. <https://doi.org/10.1093/infdis/163.4.929>
 - Pfeiffer TJ, Ellis DH. Environmental isolation of *Cryptococcus neoformans* var. *gattii* from *Eucalyptus tereticornis*. *J Med Vet Mycol.* 1992;30:407–8. <https://doi.org/10.1080/02681219280000541>
 - Varner J, Dearing MD. The importance of biologically relevant microclimates in habitat suitability assessments. *PLoS One.* 2014;9:e104648. <https://doi.org/10.1371/journal.pone.0104648>
 - Jackson MM, Gergel SE, Martin K. Effects of climate change on habitat availability and configuration for an endemic coastal alpine bird [Erratum: *PLoS ONE.* 2015;11:e0146838]. *PLoS One.* 2015;10:e0142110. <https://doi.org/10.1371/journal.pone.0142110>
 - McGill S, Malik R, Saul N, Beetson S, Secombe C, Robertson I, et al. Cryptococcosis in domestic animals in Western Australia: a retrospective study from 1995–2006. *Med Mycol.* 2009;47:625–39. <https://doi.org/10.1080/13693780802512519>

Address for correspondence: Emily S. Acheson, University of British Columbia, Lab for Advanced Spatial Analysis, Department of Geography, 1984 West Mall, Rm 210J, Vancouver, British Columbia V6T 1Z2, Canada; email: emily.acheson@gmail.com

Emerging Infectious Diseases Spotlight Topics



Antimicrobial resistance • Ebola • Etymologia
Food safety • HIV-AIDS • Influenza
Lyme disease • Malaria • MERS • Pneumonia
Rabies • Tuberculosis • Ticks • Zika
<https://wwwnc.cdc.gov/eid/page/spotlight-topics>

EID's spotlight topics highlight the latest articles and information on emerging infectious disease topics in our global community.

Cluster of Nasal Rhinosporidiosis, Eastern Province, Rwanda

Annie I. Izimukwiye, Djibril Mbarushimana,
Marie C. Ndayisaba, Venerand Bigirimana,
Belson Rugwizangoga, Alvaro C. Laga

We report 4 recent cases of nasal rhinosporidiosis in Rwanda. All patients were boys or young men living in the same district (Gatsibo District, Eastern Province), suggesting a reservoir in the area. The recent reemergence of rhinosporidiosis in Rwanda might reflect increased availability of diagnostic services rather than emerging disease.

Rhinosporidiosis is a tropical disease of the mucous membranes (and, in rare cases, the skin or internal organs) caused by *Rhinosporidium seeberi*, an enigmatic microorganism of disputed taxonomy (1–3). *R. seeberi* has not been isolated from the environment and has no known natural host or reservoir; consequently, it has been difficult to classify. Originally considered to be a protozoan and subsequently a fungus, *R. seeberi* is currently classified as an aquatic mesomycetozoan (“between fungi and animals”), on the basis of phylogenetic analysis of 18S rDNA (1–3).

Originally described in Argentina in 1900 (4), rhinosporidiosis is most prevalent in India and Sri Lanka, followed by countries in South America and Africa (5). In Africa, rhinosporidiosis has been documented in Cameroon, Democratic Republic of the Congo, Côte d’Ivoire, Kenya, Malawi, South Africa, Tanzania, Uganda, and Zambia, predominantly as conjunctival disease (6–12). One previous report documented 3 cases of rhinosporidiosis in Rwanda: 2 in the nose (in a 60-year-old man in 1975 and in a 16-year-old young woman in 1977) and 1 in the conjunctiva (in a 3-year-old boy in 1986) (13). We report 4 recent cases of nasal rhinosporidiosis diagnosed by using histopathologic methods at the University Central Hospital of Kigali (CHUK) in Kigali, Rwanda.

The Study

We conducted a retrospective search for the period 2016–2013. We confirmed histopathologic diagnosis by

Author affiliations: University Central Hospital of Kigali, Kigali, Rwanda (A.I. Izimukwiye, D. Mbarushimana, M.C. Ndayisaba, V. Bigirimana, B. Rugwizangoga); Brigham and Women’s Hospital and Harvard Medical School, Boston, Massachusetts, USA (A.C. Laga)

DOI: <https://doi.org/10.3201/eid2509.190021>

identification of characteristic structures (e.g., sporangia containing endoconidia) on hematoxylin and eosin-stained sections. For 2 cases, we obtained periodic acid–Schiff and Grocott methenamine silver stains for further characterization. For each case, patient age, sex, place of residence, clinical signs and symptoms, and year of diagnosis were recorded.

We identified 4 cases of rhinosporidiosis (Table). The diagnosis was not suspected on clinical grounds. In keeping with previous studies, all patients were young boys and teenagers (7–15 years of age) who had nasal obstruction and a friable mass that bled on touch. Symptoms lasted from 2 months to 4 years (median 8.5 months) and consisted of epistaxis and sensation of mass but no discharge, pain, or pruritus. (8,10,11,13). All patients were treated by excisional biopsy, and the diagnosis was made by using histopathologic methods. All 4 patients received nonsteroidal antiinflammatory drugs for symptomatic relief before and after surgery but not antimicrobial therapy. After an early recurrence treated by reexcision (case 3 [Table]), all patients were free of disease at 36 months after excision. All patients lived in the same region (Eastern Province) of Rwanda, and 3 of them lived in the same village (in Gatsibo District). Two cases were diagnosed in 2014, 1 in 2015, and 1 in 2016. No additional cases have been documented since.

All biopsies showed numerous sporangia (juvenile, immature, and mature forms) and prominent lymphoplasmacytic inflammation with eosinophils, but no granulomas were detected (Figure, panel A). Juvenile sporangia measured 10–70 µm and contained a single nucleus with prominent nucleoli, granular cytoplasm, and well-defined cell walls (Figure, panel B). Immature (intermediate) sporangia measured 80–150 µm, contained several nuclei, and had granular cytoplasm and thicker cell walls. Mature sporangia measured up to 400 µm and contained hundreds of immature and mature endoconidia enveloped by thin cell walls (Figure, panel C). Some showed large pores (10–20 µm, best visualized on Grocott methenamine silver stain) in direct apposition with mature endoconidia (Figure, panel D).

The main histologic differential diagnosis for rhinosporidiosis is coccidioidomycosis, a fungal disease only found in the dry areas of the Americas (endemic in California and Arizona, USA; Mexico; and Central and South America). The spherules of *Coccidioides immitis* measure

Table. Clinical summary of 4 patients with rhinosporidiosis, Eastern Province, Rwanda, 2014–2016

Case no.	Patient age, y/sex	Signs and symptoms	District of residence	Method of diagnosis	Year of diagnosis	Treatment and outcome
1	7/M	Nasal bleeding and obstruction for 5 mo; reddish mass on right nasal cavity, adherent to lateral wall; bleeding on touch	Gatsibo	Punch biopsy	2014	Excision; no recurrence at last follow-up (4 y)
2	15/M	Nasal blockage with sensation of nasal mass for 2 mo; vascularized mass; bleeding on touch	Gatsibo	Excisional biopsy	2014	Excision; no recurrence at last follow-up (4 y)
3	13/M	Nasal blockage for 12 mo; mobile, expansile, nontender mass on right nostril; bleeding on touch	Gatsibo	Punch biopsy	2015	Excision; recurrence 3 mo after diagnosis; reexcision with no recurrence at last follow-up (3.5 y)
4	12/M	Progressive nasal blockage for 4 y; soft mass in left nostril attached to the septum; bleeding on touch	Kirehe	Excisional biopsy	2016	Excision; no recurrence at last follow-up (3 y)

30–60 μm and contain uniform endospores of similar size (Figure, panel C, inset). In contrast, the sporangia of *R. seeberi* are much larger (100–400 μm) and contain variably sized endospores, ranging from small, hyperchromic forms to larger forms (7 μm).

We have documented a small cluster of nasal rhinosporidiosis occurring during a 2-year period in Rwanda. Rhinosporidiosis was first documented in Rwanda in the nasal passages of wild birds from Butare (then Astrida) in 1951, including a goose and a duck (14). The first 3 human cases were reported from Rwanda by Gigase and Kestelyn in 1993 as part of a 13-patient case series (13). Two Rwanda patients in this case series were part of a cohort of 12 patients in whom nasal rhinosporidiosis was diagnosed in Antwerp, Belgium. These cases were identified in a collection of $\approx 25,000$ histologic specimens obtained from developing tropical countries during 1966–1988. The final case included in that study was diagnosed in 1986 in the Department of Ophthalmology at CHUK. That case was the only case diagnosed in 11 years among the $\approx 80,000$ outpatients with ophthalmologic signs and symptoms seen at CHUK during that period (13). The remaining 10 patients were from Burundi ($n = 2$), Tanzania ($n = 4$), Zaire (now

the Democratic Republic of the Congo) ($n = 3$), and Chad ($n = 1$). In contrast to larger case series identified in Africa (6–13), 2 of 3 previously reported cases (13) and all 4 of the more recent cases involved nasal rather than conjunctival disease. The contributing factors, if any, for onset of conjunctival versus nasal disease are not known and cannot be determined from our data.

Independent observations that rhinosporidiosis is epidemiologically associated with exposure to water, the placement of *R. seeberi* in a clade of aquatic parasites by molecular analysis, and the fact that watery substances facilitate the release of mature endoconidia from the sporangium (14) suggest that the natural niche of *R. seeberi* is water. Although the source of infection in the cohort we report cannot be determined from this study, the geographic clustering of cases suggests a possible reservoir of *R. seeberi* in the Eastern Province of Rwanda, given that all patients are native to that region and have no history of travel. Multiple water reservoirs and lakes exist in eastern Rwanda; Lake Muhazi is closest to Gatsibo District and Lake Cyambwe closest to Kirehe District, and the Kagera River runs nearby. In a previous study documenting 3 cases of rhinosporidiosis in Rwanda, the authors state that the

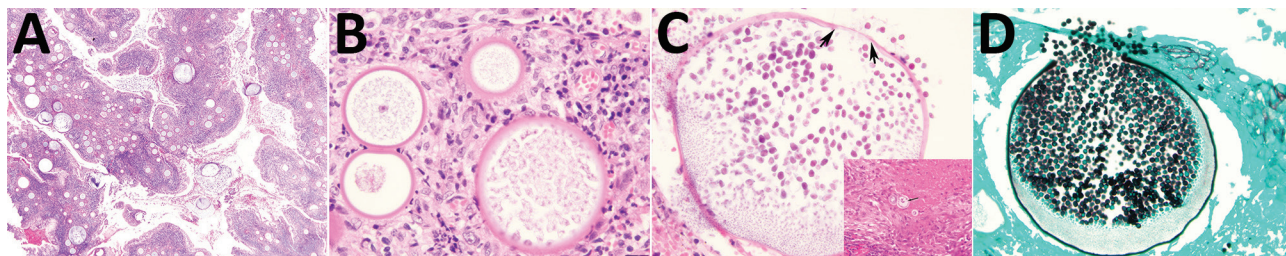


Figure. Histopathologic characteristics of rhinosporidiosis, Eastern Province, Rwanda, 2014–2016. A) At scanning magnification, multiple cystic structures (sporangia) of variable sizes are embedded in respiratory mucosa in a background of mononuclear inflammation (hematoxylin and eosin [H&E] stain; original magnification $\times 40$). B) *R. seeberi* early juvenile sporangium, with a well-delimited cell wall, granular cytoplasm, and reddish nucleus with prominent nucleolus, characteristic of this stage (H&E stain; original magnification $\times 400$). C) *R. seeberi* mature sporangium. Maturation of the endoconidia occurs from the periphery to the center of the cyst (H&E stain; original magnification $\times 600$). Inset shows the spherules of coccidioides are smaller (up to 80 μm) and contain endospores of similar size, which appear as clear vacuoles (arrow) on stained sections (H&E stain; original magnification $\times 600$). D) Both the cyst wall and endospores stain with the methenamine silver reaction, with discontinuity of the cyst wall at the upper pole, corresponding to the cyst pore zone (Grocott methenamine silver; original magnification $\times 400$).

cases “were native to the country, and as far as could be ascertained, native from places near the reference hospital” (13). However, no information about the place of origin or residence of those patients is available.

The somewhat contemporaneous appearance of the cases we describe probably reflects the availability of diagnostic services, rather than a newly emerging disease. Until recently, anatomic pathology services were scarce in Rwanda. In October 2013, the anatomic pathology laboratory at CHUK restarted operations after many years, which is probably a major factor in detecting these cases; no other diagnostic test for the disease exists. A study by Jones et al. (15) found high spatial reporting bias for emerging infectious diseases, reflective of increased surveillance and infectious disease research in developed countries of Europe, North America, Australia, and parts of Asia compared with developing regions, including tropical Africa, despite the greater risk for emerging infectious disease in hotspots attributable to zoonotic pathogens from wildlife and vector-borne pathogens (15).

Conclusions

We document a cluster of nasal rhinosporidiosis in eastern Rwanda. Clinicians and pathologists in Rwanda should be aware of this diagnosis because it might simulate a neoplasm and the disease is easily treatable. Although these findings might represent an emerging disease, the recent increase in availability of diagnostic pathology services probably played a major role in their identification.

About the Author

Dr. Izimukwiye is a pathologist at the Rwanda Military Hospital in Kigali, Rwanda. Her primary research interests include tropical and neglected infectious diseases.

References

- Herr RA, Ajello L, Taylor JW, Arseculeratne SN, Mendoza L, Mendoza L. Phylogenetic analysis of *Rhinosporidium seeberi*'s 18S small-subunit ribosomal DNA groups this pathogen among members of the protostistan Mesomycetozoa clade. *J Clin Microbiol*. 1999;37:2750–4.
- Fredricks DN, Jolley JA, Lepp PW, Kosek JC, Relman DA. *Rhinosporidium seeberi*: a human pathogen from a novel group of aquatic protistan parasites. *Emerg Infect Dis*. 2000;6:273–82. <http://dx.doi.org/10.3201/eid0603.000307>
- Vilela R, Mendoza L. The taxonomy and phylogenetics of the human and animal pathogen *Rhinosporidium seeberi*: a critical review. *Rev Iberoam Micol*. 2012;29:185–99. <http://dx.doi.org/10.1016/j.riam.2012.03.012>
- Seeber GR. A new sporozoan parasite of man. Two cases found in nasal polyps. Thesis presented to qualify for the degree of doctor of medicine [in Spanish]. Buenos Aires: Universidad de Buenos Aires, Facultad de Ciencias Médicas, Imprenta y Librería Boulosa; 1900.
- Almeida FA, Feitoza LM, Pinho JD, Mello GC, Lages JS, Silva FF, et al. Rhinosporidiosis: the largest case series in Brazil. *Rev Soc Bras Med Trop*. 2016;49:473–6. <http://dx.doi.org/10.1590/0037-8682-0193-2016>
- Salazar Campos MC, Surka J, Garcia Jardon M, Bustamante N. Ocular rhinosporidiosis. *S Afr Med J*. 2005;95:950–2, 952.
- Pe'er J, Gnessin H, Levinger S, Averbukh E, Levy Y, Polachek I. Conjunctival oculosporidiosis in east Africa caused by *Rhinosporidium seeberi*. *Arch Pathol Lab Med*. 1996;120:854–8.
- Venkataramaiah NR, van Raalte JA, Shabe JK. Rhinosporidiosis in Tanzania. *Trop Geogr Med*. 1981;33:185–7.
- Kaimbo KW, Parys-Van Ginderdeuren R. Conjunctival rhinosporidiosis: a case report from a Congolese patient. *Bull Soc Belge Ophtalmol*. 2008;309–310:19–22.
- Dago-Akribi A, Ette M, Diomande MI, Kioffi Y, Honde M, D'Ordock AF, et al. Clinico-pathologic aspects of rhinosporidiosis in the Ivory Coast. Report of 9 cases observed over 18 years [in French]. *Ann Pathol*. 1993;13:97–9.
- Naik KG, Shukla SM. Rhinosporidiosis in Zambia. *Med J Zambia*. 1980;14:78–80.
- Ravisse P, Le Gonidec G, Moliva B. Report on first 2 cases of rhinosporidiosis in Cameroon [in French]. *Bull Soc Pathol Exot Filiales*. 1976;69:222–4.
- Gigase P, Kestelyn P. Further African cases of rhinosporidiosis. *Ann Soc Belg Med Trop*. 1993;73:149–52.
- Mendoza L, Herr RA, Arseculeratne SN, Ajello L. In vitro studies on the mechanisms of endospore release by *Rhinosporidium seeberi*. *Mycopathologia*. 1999;148:9–15. <http://dx.doi.org/10.1023/A:1007108910025>
- Jones KE, Patel NG, Levy MA, Storeygard A, Balk D, Gittleman JL, et al. Global trends in emerging infectious diseases. *Nature*. 2008;451:990–3. <http://dx.doi.org/10.1038/nature06536>

Address for correspondence: Alvaro C. Laga, Brigham and Women's Hospital, Department of Pathology, Amory-3, 75 Francis St, Boston, MA 02115, USA; email: alagacanales@bwh.harvard.edu

Use of Human Intestinal Enteroids to Detect Human Norovirus Infectivity

Martin Chi-Wai Chan, Sarah K.C. Cheung,
Kirran N. Mohammad, Jenny C.M. Chan,
Mary K. Estes, Paul K.S. Chan

Tools to detect human norovirus infectivity have been lacking. Using human intestinal enteroid cultures inoculated with GII.Pe-GII.4 Sydney–infected fecal samples, we determined that a real-time reverse transcription PCR cycle threshold cutoff of 30 may indicate infectious norovirus. This finding could be used to help guide infection control.

Human norovirus accounts for 18% of acute gastroenteritis cases worldwide (1). Molecular nucleic acid tests, such as real-time reverse transcription PCR (rRT-PCR), are widely used for laboratory diagnosis of norovirus RNA in clinical samples (2). These molecular assays are virus specific and their analytical sensitivity is high, but they cannot distinguish between infectious and noninfectious viruses. To study the correlation between viral load measured by rRT-PCR and virus infectivity, we used a recently developed human intestinal enteroid (HIE) culture system (cultures that contain multiple intestinal epithelial cell types) for human norovirus. Ethics approval for this study was obtained from the Joint Chinese University of Hong Kong–New Territories East Cluster Clinical Research Ethics Committee (reference no. 2016.516).

The Study

We examined the infectivity of human pandemic norovirus genogroup II genotype 4 (GII.Pe-GII.4 Sydney) strains at different inoculating levels by using the adult stem cell–derived HIE line J2 as described previously (3). We seeded enteroid monolayers on 96-well cell culture plates at a density of $6\text{--}8 \times 10^4$ cells/well and maintained them in differentiation media for 5 days before being inoculated with norovirus. We used fecal samples from 3 norovirus-positive children and from adults in our norovirus surveillance program in Hong Kong (4). We prepared 1% fecal suspensions and filtered them once by

using 0.22- μm centrifugal filters, then prepared 3-fold serial dilutions of fecal filtrates in infection medium and stored them at -70°C in multiple aliquots for single use. These dilutions mimicked a broad range of cycle threshold (C_t) values of a widely used diagnostic rRT-PCR to represent high to very low norovirus levels (5). We used 33 μL of each dilution of fecal filtrate (brought to 100 μL in infection medium) for inoculation of each dilution and performed all virus inoculation steps and downstream cell cultures on enteroids with ≤ 20 passages in the presence of bile acid (glycochenodeoxycholic acid). We measured norovirus RNA levels in supernatant at 1, 24, and 72 h after inoculation by using rRT-PCR with a 10-fold serially diluted standard of in vitro–transcribed norovirus RNA. We considered a ≥ 10 -fold increase in RNA level at 72 h after inoculation from baseline (1 h after inoculation) to indicate productive viral replication and to confirm the presence of infectious virus. We also subjected fecal filtrate dilutions to norovirus antigen detection by use of the Food and Drug Administration–cleared commercial RIDASCREEN Norovirus 3rd Generation EIA (R-Biopharm AG, <https://clinical.r-biopharm.com>), according to the manufacturer’s instructions. We used the same amount of fecal filtrate for inoculation into HIE and EIA measurement and compared the analytical sensitivity of HIE and EIA.

We selected 3 strains of norovirus GII.Pe-GII.4 Sydney, and all replicated productively in HIE line J2; the maximum fold increase of norovirus RNA ranged from 120 ($2.1 \log_{10}$) to 45,793 ($4.7 \log_{10}$). Higher levels of replication were obtained from fecal samples from adults (Figure 1). We identified no virus replication when cells were inoculated with fecal filtrate dilutions with $C_t \geq 30$. The C_t values of the inoculating virus dilution that exhibited a transition from a positive-to-negative enteroid culture result (i.e., having a 10-fold RNA increase) were 27.7, 29.0, and 30.0 for each of the 3 strains. By using linear regression analysis on pooled data of the 3 strains, we estimated that a C_t cutoff of ≤ 30.1 in inoculating fecal filtrates would indicate the ability to generate productive norovirus GII.Pe-GII.4 Sydney replication (i.e., containing infectious norovirus) (Figure 2).

From 2014 through 2018, a total of 114 (6.5%) of 1,754 norovirus-positive fecal samples from patients admitted to the Prince of Wales Hospital, Sha Tin, Hong Kong, with

Author affiliations: The Chinese University of Hong Kong, Hong Kong, China (M.C.-W. Chan, S.K.C. Cheung, K.N. Mohammad, J.C.M. Chan, P.K.S. Chan); Baylor College of Medicine, Houston, Texas, USA (M.K. Estes)

DOI: <https://doi.org/10.3201/eid2509.190205>

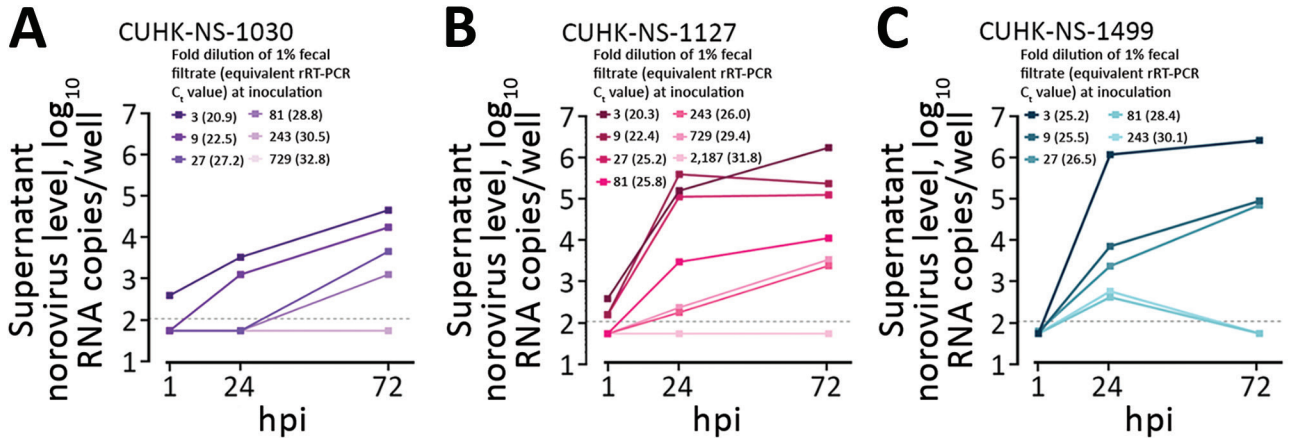


Figure 1. Performance of a human intestinal enteroid (HIE) line and an antigen-based enzyme immunoassay (EIA) to detect human norovirus in clinical fecal samples from 3 patients in Hong Kong. Replication kinetics of 3 human pandemic norovirus genogroup II genotype 4 (GII.Pe-GII.4 Sydney) strains (CUHK-NS-1030, from a 1-year-old boy; CUHK-NS-1127, from a 79-year-old man; CUHK-NS-1499, from a 46-year-old man) were tested in a monolayer culture of the adult stem cell–derived HIE line J2. We used 3-fold serial dilutions of norovirus-containing fecal filtrates to challenge J2 seeded on 96-well cell culture plates. Norovirus RNA levels in the culture supernatant at the indicated times were measured by rRT-PCR by using a 10-fold serially diluted standard of in vitro–transcribed norovirus RNA of genotype GII.Pe-GII.4 Sydney. Horizontal dotted lines denote the lower limit of detection of the rRT-PCR (13.8 RNA copies/reaction or 110 RNA copies/well) as determined by probit analysis. Samples with undetectable norovirus RNA were arbitrarily assigned a value equal to half of the lower limit of detection for calculation purpose. To convert the unit from RNA copies/well to RNA copies/mL, multiply the value by a factor of 10. hpi, hours postinoculation; rRT-PCR, real-time reverse transcription PCR.

acute gastroenteritis had C_t values >30 (C_t median 17.8; interquartile range 14.8–22.3; range 5.5–39.2). Among the 1,579 (90.0%) genotyped samples, the proportion of GII.4 was 49.1%; other GII, 44.8%; GI, 5.2%; and co-infections with >1 norovirus capsid genotype, 0.9%. Analytical sensitivity of virus replication in HIEs for measuring moderate norovirus shedding was higher than that of EIA by being able to detect infectious virus in fecal filtrate dilutions with C_t values of 25–30 (Table).

Conclusions

The limitations of highly sensitive molecular nucleic acid tests and the clinical value of proving virus infectivity were demonstrated in a recent study of Zika virus infection that found that the virus could be detected by culturing samples with high viral RNA levels only (6). For human norovirus, laboratory tools to detect its infectivity have been lacking. Recent technologic advancement in culturing human norovirus in HIE provides a chance to

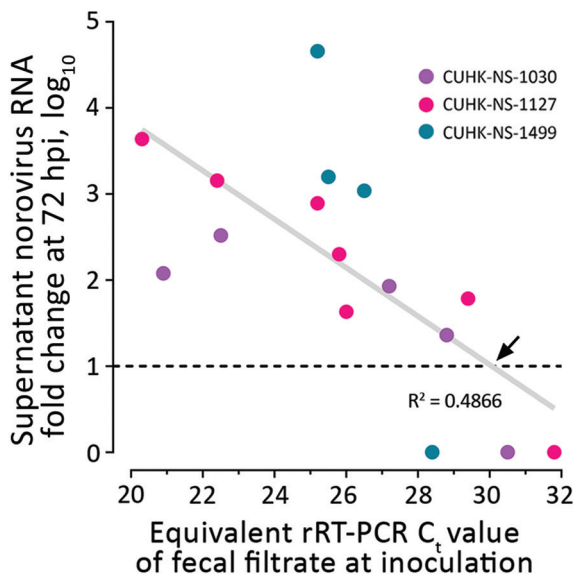


Figure 2. Estimation of a cutoff for rRT-PCR C_t value of inoculating fecal filtrate indicative of the ability to generate productive norovirus replication (i.e., containing infectious norovirus) in a human intestinal enteroid (HIE) line. We tested 3 strains of pandemic human norovirus genogroup II genotype 4 (GII.Pe-GII.4 Sydney) (CUHK-NS-1030, from a 1-year-old boy; CUHK-NS-1127, from a 79-year-old man; CUHK-NS-1499, from a 46-year-old man). We used 3-fold serial dilutions of norovirus-containing fecal filtrates to inoculate a monolayer culture of the adult stem cell–derived HIE line J2 seeded on 96-well cell culture plates. Productive norovirus replication was defined as having a supernatant viral RNA level increase of ≥ 10 -fold at 72 hpi from baseline (1 hpi) (horizontal dotted line). RNA fold change data were derived from those shown in Figure 1 and were arbitrarily defined as 1 for those with no observable viral RNA replication. For each strain, only the first dilution that resulted in undetectable viral RNA is shown and was included in downstream data analysis. The diagonal gray line denotes the best-fit line from linear regression, and the equation is $Y = -0.2818X + 9.47$, where Y represents RNA fold change and X represents C_t value. The black arrow specifies a C_t cutoff of 30.1 of inoculating fecal filtrate that yields productive norovirus replication as estimated from regression analysis. C_t , cycle threshold; CUHK, Chinese University of Hong Kong; hpi, hours postinoculation; rRT-PCR, real-time reverse transcription PCR.

Table. Comparison of rRT-PCR, HIE, and EIA used to detect human norovirus in samples from 3 patients in Hong Kong*

Isolate†	Fold dilution of 1% fecal filtrate	rRT-PCR C _t	HIE (fold change at 72 hpi)	EIA
CUHK-NS-1030	3	20.9	+ (120)	+
	9	22.5	+ (331)	+/-
	27	27.2	+ (85)	-
	81	28.8	+ (23)	-
	243	30.5	- (ND)	-
	729	32.8	- (ND)	-
CUHK-NS-1127	3	20.3	+ (4,362)	+
	9	22.4	+ (1,436)	+
	27	25.2	+ (781)	+
	81	25.8	+ (200)	-
	243	26.0	+ (43)	-
	729	29.4	+ (61)	-
	2,187	31.8	- (ND)	-
CUHK-NS-1499	3	25.2	+ (45,793)	+
	9	25.5	+ (1,587)	+
	27	26.5	+ (1,094)	-
	81	28.4	- (ND)	-
	243	30.1	- (ND)	-

*Results for HIE line J2 and the antigen-based RIDASCREEN Norovirus 3rd Generation EIA (R-Biopharm AG, <https://clinical.r-biopharm.com>) were compared with the rRT-PCR that had been widely used as a standard for clinical diagnostics of norovirus infections. The same amount of fecal filtrate was used in HIE line J2 inoculation and EIA measurement at the indicated dilutions. In HIE, numbers indicated fold changes of norovirus RNA level in culture supernatant at 72 hpi from baseline (1 hpi); an increase of ≥ 10 -fold was used to confirm the presence of infectious norovirus. C_t, cycle threshold; CUHK, Chinese University of Hong Kong; EIA, enzyme immunoassay; HIE, human intestinal enteroid; hpi, hours postinoculation; ND, not detectable; rRT-PCR, real-time reverse transcription PCR; +, positive as defined for each assay; -, negative as defined for each assay; +/-, equivocal as defined according to the manufacturer's instructions of the EIA.

†CUHK-NS-1030, from a 1-year-old boy; CUHK-NS-1127, from a 79-year-old man; CUHK-NS-1499, from a 46-year-old man.

examine norovirus infectivity in laboratory settings (3). Using pandemic norovirus GII.Pe-GII.4 Sydney strains, we showed that the most sensitive method for detecting human norovirus was rRT-PCR, followed by HIE infection; EIA was the least sensitive. We experimentally determined that norovirus inocula with C_t ≤ 30 can robustly yield productive virus replication in HIE, suggesting the presence of infectious virus. This value concurs with findings of a study that proposed an optimal C_t cutoff of 31 when attributing a disease to norovirus by comparing between symptomatic and asymptomatic cases (7). Our findings imply that a small proportion ($\approx 6.5\%$) of patients shedding low levels of norovirus RNA (C_t > 30) may not be infectious.

In an experimental human volunteer challenge study with norovirus GII.4, low levels of viral RNA shedding were found 10 days after challenge (8). HIE infection can now be used to reevaluate archived samples to better define parameters that would correlate with the infectious period of norovirus gastroenteritis to guide infection control. Of note, in a meta-analysis, the prevalence of norovirus RNA shedding from asymptomatic patients was estimated to be $\approx 9\%$ (9). Moreover, in a large-scale study of outbreak data from CaliciNet (<https://www.cdc.gov/norovirus/reporting/calicinet/index.html>), a national norovirus surveillance network in the United States, the median C_t value among asymptomatic patients was 28 (10). We hypothesize that a substantial proportion of asymptomatic patients are shedding infectious norovirus and that their role in spreading the virus merits our attention. We have shown that high levels of norovirus

replication can be achieved from fecal samples of adults, not just young children, in HIE cultures (11).

The use of a fixed C_t cutoff in clinical context needs to be interpreted with caution. First, neither a standardized protocol to perform rRT-PCRs nor a World Health Organization International Standard for norovirus is available to harmonize assay variability across laboratories worldwide. Differences in recovery among nucleic acid extraction methods may further complicate reproducible determination of C_t values. Second, virus culture systems in cell lines generally lack sensitivity (12), and that of HIE remains unknown. However, it is probably not optimal because input genome equivalents for norovirus to achieve replication are not extremely low (50% infectious dose 4.4×10^2 to 2.1×10^3 copies/well) (3,11). It is possible that samples with C_t > 30 might still contain infectious virus and that low amounts of replicating norovirus would only be detected with further serial propagation of the virus. Third, norovirus replication varies between samples and virus genotypes in HIE culture (11).

In summary, we demonstrate that a C_t cutoff of 30 for a widely used clinical diagnostic rRT-PCR can indicate the presence of infectious GII.Pe-GII.4 Sydney norovirus in an HIE culture model. Patients shedding low levels of norovirus RNA may not be infectious, which should be considered both for estimation of attributable norovirus burden and for clinical management of viral gastroenteritis.

This work was supported in part by the Hong Kong Research Grants Council (to M.C.-W.C.; reference no. 14162217), a seed fund for gut microbiota research by the Faculty of Medicine of

the Chinese University of Hong Kong (to P.K.S.C.), and a Public Health Service grant (to M.K.E.; reference no. PO1 AI057788).

M.K.E. is named as an inventor on patents related to cloning of the Norwalk virus genome and is a consultant to and has received support from Takeda Vaccines, Inc. Other authors have no conflict of interests to declare.

About the Author

Dr. M.C.-W. Chan is an assistant professor in the Department of Microbiology and Stanley Ho Centre for Emerging Infectious Diseases and a principal investigator in the Li Ka Shing Institute of Health Sciences of the Chinese University of Hong Kong. His research interest focuses on molecular epidemiology and pathogenesis of human noroviruses; other research interests include use of metagenomic next-generation sequencing in clinical diagnostics, gut virome, and food virology.

References

- Ahmed SM, Hall AJ, Robinson AE, Verhoef L, Premkumar P, Parashar UD, et al. Global prevalence of norovirus in cases of gastroenteritis: a systematic review and meta-analysis. *Lancet Infect Dis*. 2014;14:725–30. [https://doi.org/10.1016/S1473-3099\(14\)70767-4](https://doi.org/10.1016/S1473-3099(14)70767-4)
- Vinje J. Advances in laboratory methods for detection and typing of norovirus. *J Clin Microbiol*. 2015;53:373–81. <https://doi.org/10.1128/JCM.01535-14>
- Ettayebi K, Crawford SE, Murakami K, Broughman JR, Karandikar U, Tenge VR, et al. Replication of human noroviruses in stem cell-derived human enteroids. *Science*. 2016;353:1387–93. <https://doi.org/10.1126/science.aaf5211>
- Chan MC, Kwok K, Zhang LY, Mohammad KN, Lee N, Lui GCY, et al. Bimodal seasonality and alternating predominance of norovirus GII.4 and non-GII.4, Hong Kong, China, 2014–2017. *Emerg Infect Dis*. 2018;24:767–9. <https://doi.org/10.3201/eid2404.171791>
- Kageyama T, Kojima S, Shinohara M, Uchida K, Fukushi S, Hoshino FB, et al. Broadly reactive and highly sensitive assay for Norwalk-like viruses based on real-time quantitative reverse transcription-PCR. *J Clin Microbiol*. 2003;41:1548–57. <https://doi.org/10.1128/JCM.41.4.1548-1557.2003>
- Mead PS, Duggal NK, Hook SA, Delorey M, Fischer M, Olzenak McGuire D, et al. Zika virus shedding in semen of symptomatic infected men. *N Engl J Med*. 2018;378:1377–85. <https://doi.org/10.1056/NEJMoa1711038>
- Phillips G, Lopman B, Tam CC, Iturriza-Gomara M, Brown D, Gray J. Diagnosing norovirus-associated infectious intestinal disease using viral load. *BMC Infect Dis*. 2009;9:63. <https://doi.org/10.1186/1471-2334-9-63>
- Bernstein DI, Atmar RL, Lyon GM, Treanor JJ, Chen WH, Jiang X, et al. Norovirus vaccine against experimental human GII.4 virus illness: a challenge study in healthy adults. *J Infect Dis*. 2015;211:870–8. <https://doi.org/10.1093/infdis/jiu497>
- Qi R, Huang YT, Liu JW, Sun Y, Sun XF, Han HJ, et al. Global prevalence of asymptomatic norovirus infection: a meta-analysis. *EClinicalMedicine*. 2018;2-3:50–8. <https://doi.org/10.1016/j.eclinm.2018.09.001>
- Shioda K, Barclay L, Becker-Dreps S, Bucardo-Rivera F, Cooper PJ, Payne DC, et al. Can use of viral load improve norovirus clinical diagnosis and disease attribution? *Open Forum Infect Dis*. 2017;4:ofx131. <https://doi.org/10.1093/ofid/ofx131>
- Costantini V, Morantz EK, Browne H, Ettayebi K, Zeng XL, Atmar RL, et al. Human norovirus replication in human intestinal enteroids as model to evaluate virus inactivation. *Emerg Infect Dis*. 2018;24:1453–64. <https://doi.org/10.3201/eid2408.180126>
- Leland DS, Ginocchio CC. Role of cell culture for virus detection in the age of technology. *Clin Microbiol Rev*. 2007;20:49–78. <https://doi.org/10.1128/CMR.00002-06>

Address for correspondence: Martin C.-W. Chan, Prince of Wales Hospital, Department of Microbiology, 1/F, Lui Che Woo Clinical Sciences Bldg, Shatin, Hong Kong, China; email: martin.chan@cuhk.edu.hk

etymologia

Etymology is concerned with the origin of words, how they've evolved over time, and changed in form and meaning as they were translated from one language to another. Every month, *EID* publishes a feature highlighting the etymology of a word from medicine or public health.

featured monthly in **EMERGING
INFECTIOUS DISEASES[®]**

<http://wwwnc.cdc.gov/eid/articles/etymologia>

Vaccine Effectiveness against DS-1–Like Rotavirus Strains in Infants with Acute Gastroenteritis, Malawi, 2013–2015

Khuzwayo C. Jere, Naor Bar-Zeev, Adams Chande, Aisleen Bennett, Louisa Pollock, Pedro F. Sanchez-Lopez, Osamu Nakagomi, Jacqueline E. Tate, Umesh D. Parashar, Robert S. Heyderman, Neil French, Miren Iturriza-Gomara,¹ Nigel A. Cunliffe¹

Atypical DS-1–like G1P[8] rotaviruses emerged in 2013 in Malawi after rotavirus vaccine introduction. Vaccine effectiveness among infants hospitalized with acute DS-1–like G1P[8] rotavirus gastroenteritis was 85.6% (95% CI 34.4%–96.8%). These findings suggest that vaccine provides protection against these strains despite their emergence coinciding with vaccine introduction.

Rotavirus remains a major cause of severe dehydration, diarrhea, and death among children <5 years of age in many low-income countries. After the introduction of Rotarix (Glaxo SmithKline, <https://www.gsksource.com>) rotavirus vaccine into Malawi's immunization schedule in October 2012, enhanced surveillance combined with case-control studies have described the substantial population impact and effectiveness of Rotarix on hospitalized rotavirus disease and diarrheal deaths (1,2).

Both of the globally available rotavirus vaccines, Rotarix and RotaTeq (Merck & Co., <https://www.merckvaccines.com>), have been shown to protect against rotaviruses with a broad range of G and P types, as defined by the 2 viral outer-capsid proteins (3,4). A whole-

genome classification system describes rotavirus strains more completely by assigning genotypes to each of its 11 double-stranded RNA segments (5). Most rotavirus strains contain either a Wa (G1-P[8]-I1-R1-C1-M1-A1-N1-T1-E1-H1) or DS-1 (G2-P[4]-I2-R2-C2-M2-A2-N2-T2-E2-H2) genotype constellation (6). Typically, G1P[8] strains, including the Rotarix strain (RIX4414), possess a Wa-like genetic backbone, whereas G2P[4] strains generally have a DS-1–like genotype constellation (6). A switch in predominant rotavirus genotype from G1P[8] to G2P[4] after Rotarix introduction has been described in various settings (7,8), and higher vaccine effectiveness (VE) against G1P[8] strains has been described compared with G2P[4] in some settings (2,9). It is not known whether these changes in strain distribution and strain-specific differences in VE are related to differences in cross-protection afforded by the outer capsid proteins (G and P type) or to the distinct genetic backbones possessed by DS-1–like strains and the Wa-like Rotarix strain.

Previously, we demonstrated that all G1P[8] strains detected before Rotarix introduction in Malawi had a Wa-like genetic backbone (10). Shortly after Rotarix introduction, atypical DS-1–like G1P[8] rotavirus strains were detected, which provided an opportunity to examine whether emergence of DS-1–like G1P[8] strains could be the result of reduced protection afforded by the Wa-like G1P[8] Rotarix vaccine.

The Study

We used enzyme immunoassay (EIA) to detect rotaviruses in stool samples collected from children <5 years of age with acute gastroenteritis at Queen Elisabeth Central Hospital (QECH; Blantyre, Malawi) (2). We used reverse transcription PCR to assign G and P genotypes to rotavirus-positive samples (10,11). Samples with sufficient volume and containing G1 (n = 110), G2 (n = 64), or other (G4, G9, or G12, n = 42) rotavirus strains were selected at random during January 2013–December 2015.

We generated rotavirus whole-genome sequences (WGS) using the HiSeq 2000 platform (Illumina Inc., <https://www.illumina.com>) as described previously (10). We derived consensus sequences using Geneious (<https://www.geneious.com>) and genotyped them using RotaC (<http://rotac.regatools.be>). All complete nucleotide

¹These authors contributed equally to this article.

Author affiliations: University of Malawi, Blantyre, Malawi (K.C. Jere); Malawi-Liverpool-Wellcome Trust Clinical Research Programme, Blantyre (K.C. Jere, N. Bar-Zeev, A. Chande, A. Bennett, L. Pollock, R.S. Heyderman, N. French, M. Iturriza-Gomara); University of Liverpool, Liverpool, UK (K.C. Jere, N. Bar-Zeev, A. Bennett, L. Pollock, N. French, M. Iturriza-Gomara, N.A. Cunliffe); Johns Hopkins Bloomberg School of Public Health, Baltimore, Maryland, USA (N. Bar-Zeev); University of Murcia, Murcia, Spain (P.F. Sanchez-Lopez); Nagasaki University, Nagasaki, Japan (O. Nakagomi, J.E. Tate); Centers for Disease Control and Prevention, Atlanta, Georgia, USA (U.D. Parashar); University College London, London, UK (R.S. Heyderman)

DOI: <https://doi.org/10.3201/eid2509.190258>

sequences generated in this study were deposited into GenBank (12) (accession nos. MG181227–941).

We calculated rotavirus VE using logistic regression to compare 2-dose versus 0-dose vaccination status among hospitalized strain-specific rotavirus diarrhea case-patients and concurrently hospitalized control patients with non-rotavirus-caused diarrhea, matched by age at admission. We defined concurrency of controls for each endpoint (Table) as any patient hospitalized for diarrhea who tested negative for rotavirus occurring in the same date range (between the first and last hospitalized strain-specific case) in which cases of strain-specific rotavirus were detected. We limited VE analysis to infants <12 months of age because previous analysis did not demonstrate statistically significant protection in the second year of life (VE 31.7%, 95% CI –140.6% to 80.6%) (2). We obtained ethics approval from the National Health Sciences Research Committee, Malawi (867), and the Research Ethics Committee of the University of Liverpool, Liverpool, UK (000490).

Of 216 rotavirus strains sequenced, 114 (53%) had a Wa-like and 88 (44%) a DS-1-like genotype constellation. Among Wa-like strains, 72% were G1, <1% were G2, and 25% were G12. Of the DS-1-like strains, 31% were G1 and 69% were G2. Of the 110 G1 strains analyzed by WGS, 75% were Wa-like and 25% were DS-1-like. We detected atypical G1 rotaviruses with DS-1-like genotype constellation in Malawi in 2013; their circulation peaked in 2014 and subsequently decreased in 2015 (<1%, 1/72) (Figure).

In logistic regression analysis adjusted for year of presentation, Rotarix effectiveness against DS-1-like G1P[8] rotavirus was 85.6% (95% CI 34.4%–96.8%; $p = 0.01$). Effectiveness estimates against Wa-like G1 (VE 76.7%, 95% CI –153.8% to 97.9%) and DS-1-like G2 (VE 48.5%, 95% CI –154.3% to 89.6%) rotaviruses included wide bounds and the null value (Table).

Conclusions

Atypical DS-1-like G1 rotavirus strains emerged in Malawi shortly after Rotarix vaccine introduction (10). Although strain oscillation and emergence of novel types have been reported globally in the absence of vaccination, the mechanisms driving this phenomenon are not well

understood. It is possible that the emergence of these DS-1-like G1P[8] strains was coincidental with vaccine introduction. The high VE strongly suggests that escape from vaccine-induced immunity is not the driver for emergence. The swift decline in prevalence of these strains is in contrast with more sustained changes in strain circulation described in other settings in the context of high VE (13). The decline could have been precipitated by the observed high VE or may represent a natural phenomenon related to viral fitness and associated periodic nature of the circulation of the DS-1-like strains, which has been observed historically and globally in the absence of vaccine. These findings support continued use of rotavirus vaccine in this population as an intervention to reduce severe diarrhea caused by rotavirus strains possessing either Wa-like or DS-1-like genetic backbones. The observed decline in rotavirus hospitalizations in children after vaccine introduction (2), together with reduction in infant diarrhea deaths in Malawi (14), are public health benefits that could be sustained through rotavirus vaccination in this region, which has one of the highest burdens of rotavirus disease.

The VE against DS-1-like G1P[8] strains in this study resembles our previous findings of VE of 82% (95% CI 42%–95%) against all G1P[8] strains 3 years after vaccine introduction (2013–2015) (2). In contrast, we were unable to demonstrate statistically significant VE against DS-1-like G2 rotaviruses despite a comparable number of such strains, consistent with our earlier study (VE 45.9%, 95% CI –47.0% to 80.1%; $p = 0.228$) (2). The apparently lower VE against rotavirus disease caused by DS-1-like strains associated with G2, but not with G1P[8], lends support to the proposed dominant role of the outer capsid proteins VP7 and VP4 as drivers of homotypic protection. Although increasing evidence suggests that Rotarix vaccine does not provide the same degree of protection against G2 strains as G1 strains, this difference in protection appears to have little effect on total VE among populations in which vaccination performs optimally and high VE is maintained. However, the difference in protection between the strains may exacerbate underperformance of rotavirus vaccines in low-resource settings such as Malawi, where overall VE is generally lower for reasons that remain poorly understood (2,15).

Table. Point estimates of vaccine effectiveness by rotavirus genotype constellation based on the complete genetic composition of rotavirus strains, Blantyre, Malawi*

Rotavirus strain type	Sequenced strains from test-positive case-patients†			Rotavirus test-negative controls			Adjusted logistic regression for year of presentation	
	No. tested positive	No. known vaccine status	No. (%) 2-dose vaccine	No. controls	No. known vaccine status	No. (%) 2-dose vaccine	Rotarix vaccine effectiveness, % (95% CI)	p value
DS-1-like G1P[8]	13	13	10 (76.9)	426	410	365 (89)	85.6 (34.4–96.8)	0.01
DS-1-like G2	30	28	24 (85.7)	481	465	411 (88.4)	48.5 (–154.3 to 89.6)	0.42
Wa-like G1	38	38	34 (89.5)	440	424	376 (88.7)	76.7 (–153.8 to 97.9)	0.23

*Rotavirus strains detected at Queen Elisabeth Central Hospital during January 2013–December 2015. Case-patients were fully vaccinated infants <12 mo of age.

†Complete whole-genome sequences were generated.

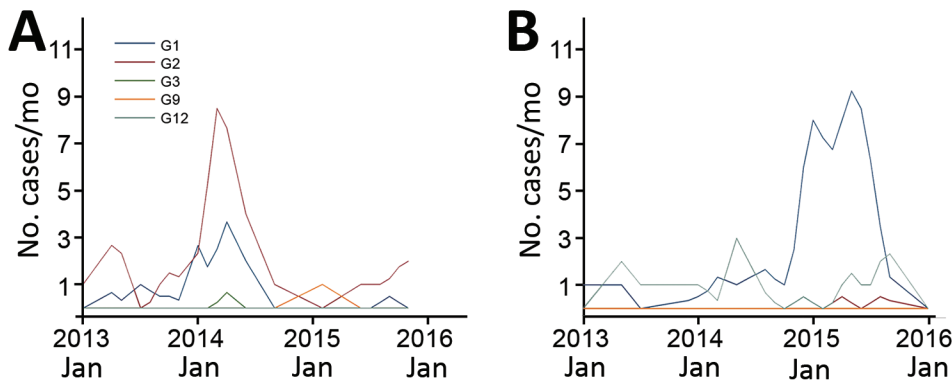


Figure. Monthly number of rotavirus cases at Queen Elisabeth Central Hospital, Blantyre, Malawi. Numbers are based on the presence of either DS-1–like (A) or Wa-like (B) constellation of rotavirus strains.

We could not demonstrate statistically significant effectiveness against Wa-like G1P[8] rotaviruses ($p = 0.23$). Wa-like G1P[8] cases became dominant and replaced DS-1–like G1P[8] once vaccine coverage had reached high and stable levels (Figure). At high population vaccine coverage, case–control analysis of VE became challenging and difficult to power sufficiently.

Our data demonstrate that Rotarix provides a high degree of protection against severe disease caused by homotypic G1P[8] rotaviruses in Malawi regardless of genomic backbone. VE for patients <1 year of age is comparable to that seen in middle-income countries. The lower VE against heterotypic G2P[4] strains previously described (15) suggests that more detailed immune response studies, clarification of the correlates of protection for rotavirus disease, and strain surveillance are needed to monitor the impact of sustained, high vaccine coverage on rotavirus strain distribution.

Acknowledgments

We thank the laboratory staff at the Malawi-Liverpool-Wellcome Trust Clinical Research Programme and the sequencing and informatics teams at the Centre for Genomic Research (CGR), University of Liverpool, UK.

This work was supported by an investigator-initiated research grant from GlaxoSmithKline Biologicals SA (eTrack no. 207219) and by the Wellcome Trust (Programme grant no. 091909/Z/10/Z and the MLW Programme Core Award). K.C.J. is a Wellcome Trust Training Fellow (grant no. 201945/Z/16/Z). M.I.-G. is partly supported by the NIHR HPRU in Gastrointestinal Infections.

Author contributions: K.C.J., N.B.-Z., N.A.C., and M.I.-G. conceived and designed the study. K.C.J. and N.B.-Z. collected clinical data and stool samples. K.C.J. performed the laboratory work. K.C.J. and N.B.-Z. carried out the statistical analyses. K.C.J. drafted the manuscript, with major input from N.A.C. and M.I.-G. All authors contributed to interpretation of the data and commented on the manuscript. All authors have read and approved the final manuscript.

Disclaimer: The funders had no role in the study design, data collection and interpretation, or the decision to submit the work for publication. GlaxoSmithKline Biologicals SA was provided the opportunity to review a preliminary version of this manuscript for factual accuracy, but the authors are solely responsible for final content and interpretation. The authors received no financial support or other form of compensation related to the development of the manuscript.

M. I.-G. is affiliated with the National Institute for Health Research Health Protection Research Unit in Gastrointestinal Infections at University of Liverpool in partnership with Public Health England, in collaboration with University of East Anglia, University of Oxford, and the Quadram Institute. The views expressed are those of the author(s) and not necessarily those of the NHS, the NIHR, the Department of Health, or Public Health England.

Potential conflicts of interest: K.C.J., N.B.-Z. and N.F. have received investigator-initiated research grant support from the GSK group of companies. M.I.-G. has received investigator-initiated research grant support from the GSK group of companies and Sanofi Pasteur Merck Sharpe & Dohme and Merck. O.N. has received research grant support and honoraria from Japan Vaccine and MSD for delivering lectures on rotavirus vaccines. N.A.C. has received research grant support and honoraria for participation in rotavirus vaccine data safety monitoring committee meetings from the GSK group of companies. All other authors report no potential conflicts.

About the Author

Dr. Jere is a Wellcome International Training Fellow who conducted this research as part of his postdoctoral studies. His research interests are in enteric viral pathogens.

References

1. Tate JE, Burton AH, Boschi-Pinto C, Parashar UD, World Health Organization–Coordinated Global Rotavirus Surveillance Network. Global, regional, and national estimates of rotavirus mortality in children <5 years of age, 2000–2013. *Clin Infect Dis.* 2016;62 (Suppl 2):S96–105. <https://doi.org/10.1093/cid/civ1013>

2. Bar-Zeev N, Jere KC, Bennett A, Pollock L, Tate JE, Nakagomi O, et al.; Vaccine Effectiveness and Disease Surveillance Programme, Malawi (VACSURV) Consortium. Population impact and effectiveness of monovalent rotavirus vaccination in urban Malawian children 3 years after vaccine introduction: ecological and case-control analyses. *Clin Infect Dis*. 2016;62(Suppl 2): S213–9. <https://doi.org/10.1093/cid/civ1183>
3. Vesikari T, Karvonen A, Prymula R, Schuster V, Tejedor JC, Cohen R, et al. Efficacy of human rotavirus vaccine against rotavirus gastroenteritis during the first 2 years of life in European infants: randomised, double-blind controlled study. *Lancet*. 2007;370:1757–63. [https://doi.org/10.1016/S0140-6736\(07\)61744-9](https://doi.org/10.1016/S0140-6736(07)61744-9)
4. Zaman K, Anh DD, Victor JC, Shin S, Yunus M, Dallas MJ, et al. Efficacy of pentavalent rotavirus vaccine against severe rotavirus gastroenteritis in infants in developing countries in Asia: a randomised, double-blind, placebo-controlled trial. *Lancet*. 2010;376:615–23. [https://doi.org/10.1016/S0140-6736\(10\)60755-6](https://doi.org/10.1016/S0140-6736(10)60755-6)
5. Matthijnssens J, Ciarlet M, McDonald SM, Attoui H, Bányai K, McDonald SM, et al. Full genome-based classification of rotaviruses reveals a common origin between human Wa-like and porcine rotavirus strains and human DS-1–like and bovine rotavirus strains. *J Virol*. 2008;82:3204–19. <https://doi.org/10.1128/JVI.02257-07>
6. Matthijnssens J, Ciarlet M, McDonald SM, Attoui H, Bányai K, Brister JR, et al. Uniformity of rotavirus strain nomenclature proposed by the Rotavirus Classification Working Group (RCWG). *Arch Virol*. 2011;156:1397–413. <https://doi.org/10.1007/s00705-011-1006-z>
7. Zeller M, Rahman M, Heylen E, De Coster S, De Vos S, Arijis I, et al. Rotavirus incidence and genotype distribution before and after national rotavirus vaccine introduction in Belgium. *Vaccine*. 2010;28:7507–13. <https://doi.org/10.1016/j.vaccine.2010.09.004>
8. Kirkwood CD, Boniface K, Barnes GL, Bishop RF. Distribution of rotavirus genotypes after introduction of rotavirus vaccines, Rotarix and RotaTeq, into the National Immunization Program of Australia. *Pediatr Infect Dis J*. 2011;30(Suppl):S48–53. <https://doi.org/10.1097/INF.0b013e3181fed90>
9. Braeckman T, Van Herck K, Meyer N, Pirçon JY, Soriano-Gabarró M, Heylen E, et al.; RotaBel Study Group. Effectiveness of rotavirus vaccination in prevention of hospital admissions for rotavirus gastroenteritis among young children in Belgium: case-control study. *BMJ*. 2012;345(aug08 1):e4752. <https://doi.org/10.1136/bmj.e4752>
10. Jere KC, Chaguzo C, Bar-Zeev N, Lowe J, Peno C, Kumwenda B, et al. Emergence of double- and triple-gene reassortant G1P[8] rotaviruses possessing a DS-1–like backbone after rotavirus vaccine introduction in Malawi. *J Virol*. 2018;92:e01246–17. <https://doi.org/10.1128/JVI.01246-17>
11. Cunliffe NA, Ngwira BM, Dove W, Thindwa BD, Turner AM, Broadhead RL, et al. Epidemiology of rotavirus infection in children in Blantyre, Malawi, 1997–2007. *J Infect Dis*. 2010;202(Suppl):S168–74. <https://doi.org/10.1086/653577>
12. Benson DA, Karsch-Mizrachi I, Lipman DJ, Ostell J, Rapp BA, Wheeler DL. GenBank. *Nucleic Acids Res*. 2002;30:17–20. <https://doi.org/10.1093/nar/30.1.17>
13. Hungerford D, Allen DJ, Nawaz S, Collins S, Ladhani S, Vivancos R, et al. Impact of rotavirus vaccination on rotavirus genotype distribution and diversity in England, September 2006 to August 2016. *Euro Surveill*. 2019;24. <https://doi.org/10.2807/1560-7917.ES.2019.24.6.1700774>
14. Bar-Zeev N, King C, Phiri T, Beard J, Mvula H, Crampin AC, et al.; VacSurv Consortium. Impact of monovalent rotavirus vaccine on diarrhea-associated post-neonatal infant mortality in rural communities in Malawi: a population-based birth cohort study. *Lancet Glob Health*. 2018;6:e1036–44. [https://doi.org/10.1016/S2214-109X\(18\)30314-0](https://doi.org/10.1016/S2214-109X(18)30314-0)
15. Bar-Zeev N, Kapanda L, Tate JE, Jere KC, Ituriza-Gomara M, Nakagomi O, et al.; VacSurv Consortium. Effectiveness of a monovalent rotavirus vaccine in infants in Malawi after programmatic roll-out: an observational and case-control study. *Lancet Infect Dis*. 2015;15:422–8. [https://doi.org/10.1016/S1473-3099\(14\)71060-6](https://doi.org/10.1016/S1473-3099(14)71060-6)

Address for correspondence: Khuzwayo C. Jere, University of Liverpool, Institute of Infection and Global Health, Ronald Ross Bldg, 8 West Derby St, Liverpool, L69 7BE, UK; email: Khuzwayo.Jere@liverpool.ac.uk

PubMed Central

PubMed



Find *Emerging Infectious Diseases* content in the digital archives of the National Library of Medicine

www.pubmedcentral.nih.gov

Rodent Host Abundance and Climate Variability as Predictors of Tickborne Disease Risk 1 Year in Advance

Emil Tkadlec, Tomáš Václavík, Pavel Šíroký

Using long-term data on incidences of Lyme disease and tickborne encephalitis, we showed that the dynamics of both diseases in central Europe are predictable from rodent host densities and climate indices. Our approach offers a simple and effective tool to predict a tickborne disease risk 1 year in advance.

In Europe, the generalist tick *Ixodes ricinus* is the principal vector transmitting tickborne pathogens to humans. It has 3 blood-feeding stages, depending on small rodents, such as voles and mice, as the chief reservoir hosts for larval ticks (1). The development from larva to nymph is a key aspect in pathogen transmission because the exposure to pathogens is most likely to happen at this stage and therefore directly influences the density of infected nymphs (2). Vole population densities change dramatically over time in intervals of 3–5 years (3), known as population cycles (4). As a result, the chances for questing larvae to encounter a host are expected to vary considerably over time, along with vole population numbers. Investigations of direct relationships between abundance of ticks, disease incidence, and host populations are rare, usually targeting large mammals that provide a blood meal for female adult ticks (5). Little is known about the effect of rodent population dynamics on abundance of nymphal ticks (6), and studies of the direct effects on disease risk are even rarer (7,8).

We studied interannual variation in incidences of 2 tickborne diseases (TBDs), Lyme disease (LD) and tick-borne encephalitis (TBE). We aimed to determine if, as suggested by a previous work in North America (8), disease risk is related to rodent abundance during

the previous year. We also tested the hypothesis that population outbreaks in the common vole (*Microtus arvalis*), along with favorable weather conditions, increase survival of larval ticks and the abundance of nymphal ticks in the following year, thereby resulting in higher disease incidence.

The Study

We analyzed periods of 17–18 years to assess TBD incidences in 7 countries in central Europe (Figure 1; Appendix Figure 1, <https://wwwnc.cdc.gov/EID/article/25/9/19-0684-App1.pdf>). First, we computed the cross-correlations between disease incidences, vole densities from the Czech Republic, and climate variables to examine the degree of synchrony among their dynamics. Second, we applied autoregressive linear models of order 0–2 to test whether the predictive abilities of vole abundance in year $t - 1$ are supported by data (Appendix). Finally, we tested the influence of climate indices that are known to affect tick ecology (9). We used Akaike information criterion for small samples to compare models. The effect included in the model was considered to be strongly supported by data if the model Akaike information criterion was reduced by >2 . We obtained data on annual TBD incidences, vole abundance (autumn counts of burrow entrances per hectare), and climate variability (North Atlantic oscillation [NAO] indices) from public databases (Appendix).

LD incidences for 3 countries in central Europe fluctuated over time (Figure 2). Cross-correlation analysis revealed strong positive correlations between incidences in the Czech Republic in year t and vole densities in $t - 1$ and negative correlations between the annual NAO index in $t - 1$ (Appendix Figures 2–4). By fitting autoregressive linear models, we found strong evidence that vole abundance in year $t - 1$ and the annual NAO index in $t - 1$ are key to predicting LD incidences during year t in the Czech Republic (Table 1); the final model predicted observed incidence with reasonable accuracy (Appendix Figure 5). LD incidence increased with vole densities and decreased with the annual NAO index (Appendix Figure 6).

TBE incidence from 7 countries fluctuated greatly from year to year (Figure 2). Cross-correlations showed that TBE incidence was strongly positively correlated with

Author affiliations: Palacký University Olomouc, Olomouc, Czech Republic (E. Tkadlec, T. Václavík); Institute of Vertebrate Biology, Brno, Czech Republic (E. Tkadlec), UFZ–Helmholtz Centre for Environmental Research, Leipzig, Germany (T. Václavík); University of Veterinary and Pharmaceutical Sciences Brno, Brno (P. Šíroký); Central European Institute of Technology, Brno (P. Šíroký)

DOI: <https://doi.org/10.3201/eid2509.190684>



Figure 1. Countries in central Europe where Lyme disease and tickborne encephalitis incidence were analyzed relative to the common vole abundance from the Czech Republic and climate indices, 2000–2017, and where we found evidence for these external predictors. LD, Lyme disease; TBE, tickborne encephalitis.

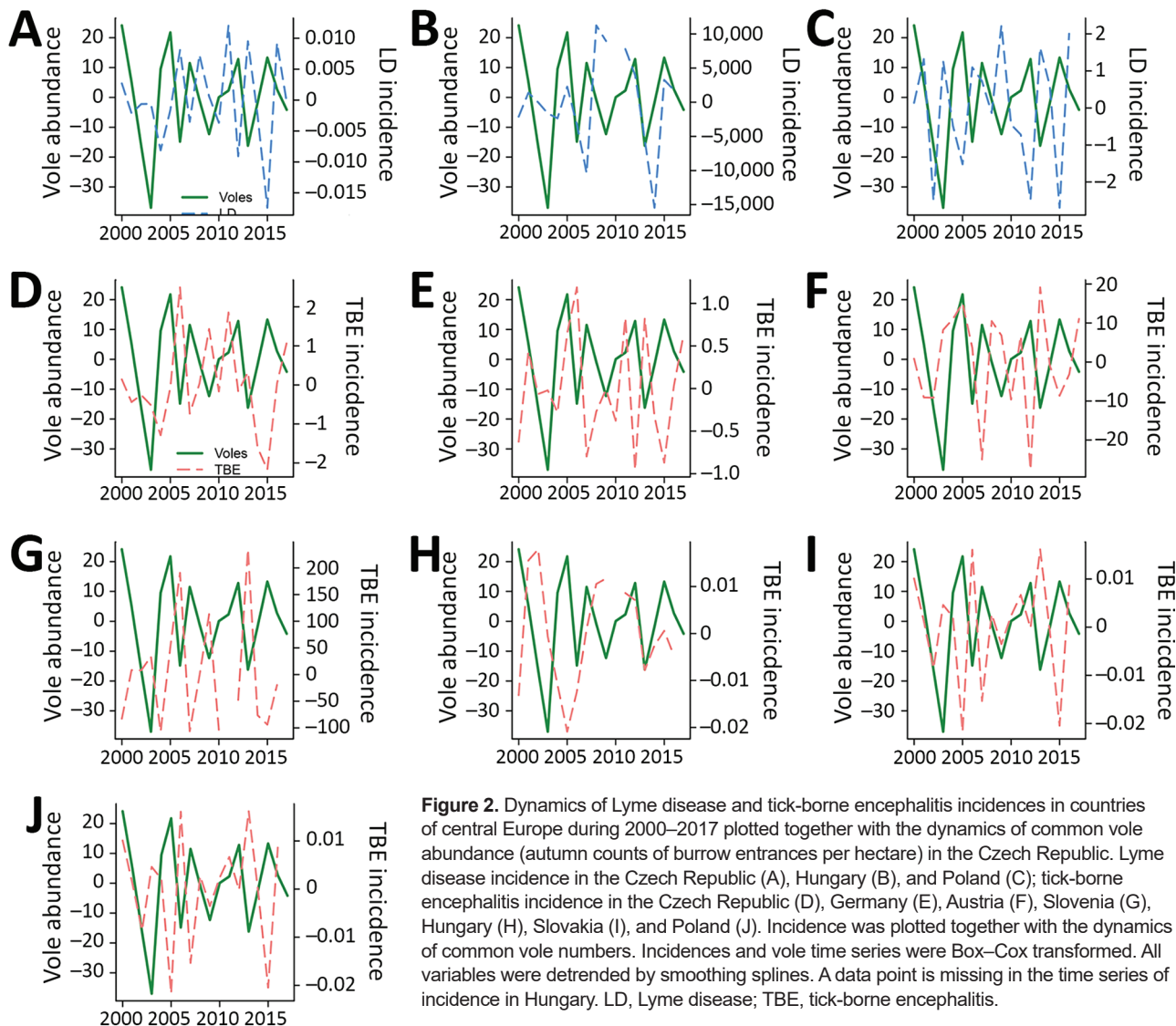
vole density with a lag of 1 year for the Czech Republic, Germany, and Slovenia (Appendix Figure 7). A lag of 1 year for the effect of the annual NAO index was negatively correlated with TBE incidence in the Czech Republic and Germany, whereas a 2-year lag was positively correlated with TBE incidence in Germany and Austria (Appendix Figure 8). Autoregressive linear models showed that including vole abundance from year $t - 1$ improved fit for the Czech Republic, Germany, and Slovenia (Table 2). Adding the effect of the annual NAO index in $t - 1$ to the model improved the fit in the Czech Republic and Germany. The effect of the annual NAO index in $t - 2$ produced better predictive power for Austria. As a result, the best models for TBE incidence in all 4 countries (Czech Republic, Germany, Slovenia, and Austria) included both host abundance and climate effect. Incidence of both diseases fluctuated over time in close synchrony, as revealed for the Czech Republic (correlation coefficient 0.71) and Poland (correlation coefficient 0.70) (Appendix Figure 9).

Conclusions

For 4 of the 7 countries in Europe we studied, our results show support for the hypothesis that incidence of 2 TBDs should lag 1 year behind the rodent host density because of the beneficial effect on survival of *I. ricinus* larvae (10). Our results agree with evidence from North America that the number of *I. scapularis* nymphs can be predicted by small rodent density from the preceding year (7,8). In addition, acorn abundance was demonstrated to predict the nymph densities equally well 2 years ahead (7,8). Hence,

results from North America indicated a complete causal mechanism for variation in LD incidences over time, starting with abundant acorns in year $t - 2$, which increased the population of rodents in year $t - 1$. High rodent density then led to the increased number of nymphs in year t , resulting in a greater disease incidence in humans. Our data support this mechanism and suggest that the LD system in North America based on *I. scapularis* and that in Europe based on *I. ricinus* might be functionally quite similar, differing primarily in the species involved, and that this mechanism also applies to other tickborne diseases, such as TBE.

Unlike bank voles (*Myodes glareolus*) and *Apodemus* mice (2), the common vole occupying open farmland habitats has never been regarded as the chief host for *Ixodes* larvae in central Europe, though it is well-known as a competent host for pathogens and larval ticks (11,12). We suggest 2 explanations for the role of this rodent in disease transmission. First, common voles can be encountered frequently in forests or wetlands in peak years (13), when their densities often exceed 2,000 voles/hectare. Thus, the common vole can act as an amplifying host and contribute substantially to the whole population of suitable hosts for larval ticks. The voles' irruptive population dynamics can readily explain the upsurge in TBE disease prevalence observed in the Czech Republic in 2006, which occurred after a massive population outbreak of voles during 2004–2005 (14). Second, population fluctuations of most rodent species are spatially synchronized across large geographic areas (15). Therefore, common vole abundance is a correlative measure for bank voles or mice.



Our observation that the annual NAO index in $t - 1$ was able to improve model fit is in agreement with known tick ecology. A negative annual NAO index is generally associated with cold, snowy winters and moderate summers that are wetter, which can help larval ticks conserve body water and thus increase their survival to the nymphal stage (9). The positive effect of the annual NAO index in $t - 2$ might signify a generally warmer year that can be related to mast seeding of trees, triggering the growth of rodent populations.

Some countries in central Europe, such as the Czech Republic, Germany, and Poland, have built programs to monitor common vole densities. These data are stored in public electronic databases and thus can be used readily for predicting TBDs, using the methods we describe.

Acknowledgments

We thank Whalen W. Dillon and Monica A. Dorning for helpful comments that greatly improved the manuscript, the National Institute of Public Health for providing us with the data on TBD incidences, and the Central Institute for Supervising and Testing in Agriculture for the data on common vole abundance.

The work was supported by the Ministry of Health of the Czech Republic (grant no. AZV 16-33934A) and Palacký University Olomouc (grant no. IGA_PrF_2019_021).

Author contributions: E.T. and T.V. conceived the ideas; E.T. analyzed the data; and E.T., T.V., and P.Š. wrote the paper.

Table 1. Differences in AIC from the best model for Lyme disease incidences as modeled by AR linear models of order 0–2 with vole abundance and annual NAO index as external predictors, 3 countries in central Europe, 2000–2017*

Country and model structure	Order of AR model		
	0	1	2
Czech Republic			
Pure AR model	4.1	3.2	5.0
Voles _{t-1}	2.9	2.6	4.9
NAO annual index _{t-1}	2.8	3.2	3.7
Voles _{t-1} + NAO annual index _{t-1}	0.0	1.3	2.2
Hungary			
Pure AR model	0.0	3.2	4.6
Voles _{t-1}	0.0	2.1	5.6
NAO annual index _{t-1}	3.3	7.2	6.5
Voles _{t-1} + NAO annual index _{t-1}	4.1	7.0	12.0
Poland			
Pure AR model	0.4	0.0	1.6
Voles _{t-1}	3.1	3.5	4.8
NAO annual index _{t-2}	0.3	0.1	2.3
Voles _{t-1} + NAO annual index _{t-2}	3.9	4.5	6.5

*AIC, Akaike information criterion; AR, autoregressive; NAO, North Atlantic oscillation.

Table 2. Differences in AIC from the best model for tick-borne encephalitis as modeled by AR linear models of order 0–2 with vole abundance and annual NAO index as external predictors, 7 countries in central Europe, 2000–2017*

Country and model structure	Order of AR model		
	0	1	2
Czech Republic			
Pure AR model	4.5	7.4	10.6
Voles _{t-1}	2.8	6.0	10.1
NAO annual index _{t-1}	3.4	6.8	8.1
Voles _{t-1} + NAO annual index _{t-1}	0.0	3.5	7.5
Germany			
Pure AR model	6.0	7.2	9.2
Voles _{t-1}	3.6	6.4	10.1
NAO annual index _{t-1}	4.8	7.6	9.7
Voles _{t-1} + NAO annual index _{t-1}	0.0	3.8	7.1
Austria			
Pure AR model	5.3	6.5	9.1
Voles _{t-2}	5.8	7.3	9.3
NAO annual index _{t-2}	5.8	4.1	7.0
Voles _{t-2} + NAO annual index _{t-2}	0.0	3.5	5.7
Slovenia			
Pure AR model	3.8	5.2	5.7
Voles _{t-1}	0.2	3.3	5.8
NAO annual index _{t-1}	5.2	5.9	3.7
Voles _{t-1} + NAO annual index _{t-1}	0.0	3.2	4.2
Hungary			
Pure AR model	0.0	3.2	4.6
Voles _{t-2}	0.0	2.1	5.6
NAO annual index _{t-1}	3.3	7.2	6.5
Voles _{t-2} + NAO annual index _{t-1}	4.1	7.0	12.0
Slovakia			
Pure AR model	1.2	0.0	3.0
Voles _{t-1}	3.5	3.4	7.1
NAO annual index _{t-1}	3.3	1.3	3.0
Voles _{t-1} + NAO annual index _{t-1}	6.1	5.4	8.1
Poland			
Pure AR model	0.0	1.7	2.0
Voles _{t-1}	2.8	4.2	5.8
NAO annual index _{t-2}	2.3	4.2	6.3
Voles _{t-1} + NAO annual index _{t-2}	5.2	6.7	8.2

*AIC, Akaike information criterion; AR, autoregressive; NAO, North Atlantic oscillation.

About the Author

Dr. Tkadlec is a professor of ecology in the Department of Ecology and Environmental Sciences at Palacký University Olomouc, Czech Republic. His research interests include population ecology of vertebrates.

References

- Han BA, Schmidt JP, Bowden SE, Drake JM. Rodent reservoirs of future zoonotic diseases. *Proc Natl Acad Sci U S A*. 2015;112:7039–44. <http://dx.doi.org/10.1073/pnas.1501598112>
- van Duijvendijk G, Sprong H, Takken W. Multi-trophic interactions driving the transmission cycle of *Borrelia afzelii* between *Ixodes ricinus* and rodents: a review. *Parasit Vectors*. 2015;8:643. <http://dx.doi.org/10.1186/s13071-015-1257-8>
- Tkadlec E, Stenseth NC. A new geographical gradient in vole population dynamics. *Proc Biol Sci*. 2001;268:1547–52. <http://dx.doi.org/10.1098/rspb.2001.1694>
- Krebs CJ. Population fluctuations in rodents. Chicago: University of Chicago Press; 2013.
- Gilbert L, Maffey GL, Ramsay SL, Hester AJ. The effect of deer management on the abundance of *Ixodes ricinus* in Scotland. *Ecol Appl*. 2012;22:658–67. <http://dx.doi.org/10.1890/11-0458.1>
- Cayol C, Koskela E, Mappes T, Siukkola A, Kallio ER. Temporal dynamics of the tick *Ixodes ricinus* in northern Europe: epidemiological implications. *Parasit Vectors*. 2017;10:166. <http://dx.doi.org/10.1186/s13071-017-2112-x>
- Ostfeld RS, Schaubert EM, Canham CD, Keesing F, Jones CG, Wolff JO. Effects of acorn production and mouse abundance on abundance and *Borrelia burgdorferi* infection prevalence of nymphal *Ixodes scapularis* ticks. *Vector Borne Zoonotic Dis*. 2001;1:55–63. <http://dx.doi.org/10.1089/153036601750137688>
- Ostfeld RS, Levi T, Keesing F, Oggenfuss K, Canham CD. Tick-borne disease risk in a forest food web. *Ecology*. 2018;99:1562–73. <http://dx.doi.org/10.1002/ecy.2386>
- Sonenshine DE, Mather TN, editors. Ecological dynamics of tick-borne diseases. Oxford: Oxford University Press; 1994.
- Keesing F, Brunner J, Duerr S, Killilea M, Logiudice K, Schmidt K, et al. Hosts as ecological traps for the vector of Lyme disease. *Proc Biol Sci*. 2009;276:3911–9. <http://dx.doi.org/10.1098/rspb.2009.1159>
- Šumilo D, Bormane A, Asokliene L, Vasilenko V, Golovljova I, Avsic-Zupanc T, et al. Socio-economic factors in the differential upsurge of tick-borne encephalitis in Central and Eastern Europe. *Rev Med Virol*. 2008;18:81–95. <http://dx.doi.org/10.1002/rmv.566>
- Blaškovič D. The public health importance of tick-borne encephalitis in Europe. *Bull World Health Organ*. 1967;36(Suppl):5–13.
- Pelikan J. Stanoviště, sídliště a etologie. In: Kratochvíl J, Balát F, Folk Č, Grulich I, Havlín J, Holířová V, et al., editors. Hraňoš polní, *Microtus arvalis*. Prague: Nakladatelství ČSAV; 1959. p. 80–100.
- Daniel M, Kříž B, Danielová V, Beneš Č. Sudden increase in the tick-borne encephalitis cases in the Czech Republic, 2006. *Int J Med Microbiol*. 2008;298(S1):81–7. <http://dx.doi.org/10.1016/j.ijmm.2008.02.006>
- Carlslake D, Cornulier T, Inchausti P, Bretagnolle V. Spatio-temporal covariation in abundance between the cyclic common vole *Microtus arvalis* and other small mammal prey species. *Ecography*. 2011;34:327–35. <http://dx.doi.org/10.1111/j.1600-0587.2010.06334.x>

Address for correspondence: Emil Tkadlec, Palacký University Olomouc, Department of Ecology and Environmental Sciences, Faculty of Science, Šlechtitelů 27, 783 71 Olomouc, Czech Republic; e-mail: emil.tkadlec@upol.cz

Delays in Coccidioidomycosis Diagnosis and Relationship to Healthcare Utilization, Phoenix, Arizona, USA¹

Rachel Ginn, Ralph Mohty, Kerilyn Bollmann,
Jessica Goodsell, Guillermo Mendez,
Barrie Bradley, John N. Galgiani

We developed an electronic records methodology to programmatically estimate the date of first appearance of coccidioidomycosis symptoms in patients. We compared the diagnostic delay with overall healthcare utilization charges. Many patients (46%) had delays in diagnosis of >1 month. Billed healthcare charges before diagnosis increased with length of delay.

Coccidioidomycosis (also known as Valley fever) is an endemic fungal infection (1,2). In Arizona, USA, it is responsible for one quarter of all community-acquired pneumonia (CAP) (3,4). Although accurate diagnosis requires specific laboratory tests (5), such testing was only ordered in ≤13% of patients with CAP in Phoenix, Arizona (6), raising the possibility that delays in accurate diagnosis might be extensive. We report a retrospective analysis from the coccidioidomycosis-endemic region of Phoenix to estimate diagnostic delays and healthcare utilization before and after a coccidioidal diagnosis was confirmed.

The Study

This study focused on cases recorded at clinics operated by Banner Health in the Phoenix area, using programmatic use of data from NextGen (<https://www.nextgen.com>). This electronic medical record system was used during the study period by most of Banner Health's clinics but not its hospitals. We programmatically searched the system for all patients ≥18 years of age who were seen from January 1, 2011, through December 31, 2014, whose records showed codes from the International Classification of Diseases, 9th Revision (ICD-9), that indicated

coccidioidomycosis (114.*). The earliest diagnosis of coccidioidomycosis served as the diagnosis date for each patient. We excluded patients with a coccidioidomycosis diagnosis in 2011 who also had a coccidioidomycosis diagnosis in the prior 12 months. We corroborated all diagnoses by a programmatic identification of any positive coccidioidal serologic test result (5) <30 days before or >60 days after the date of diagnosis.

To estimate the date when patients first sought medical attention for their illness, we used a set of ICD-9 codes that represented an expansion of codes previously associated with early coccidioidal illnesses that were used in a Phase I independent chart review of 37 patients performed by 2 physicians in training and an internist (7). For our study, an internist and a medical student independently reviewed all ICD-9 codes occurring 6 months before the coccidioidomycosis diagnosis and included only those that they both judged to be similar to the original set from the previous Phase I study. An infectious disease specialist settled cases of nonconcordance. We removed 3 Phase I symptoms that were deemed erroneous. This process resulted in a total of 121 ICD-9 codes (Appendix Table, <https://wwwnc.cdc.gov/EID/article/25/8/19-0019-App1.pdf>). We defined the date of first presentation (i.e., the date signs and symptoms were first clinically noted) as the earliest record in which ≥1 of the expanded ICD-9 codes were recorded, within 6 months before the diagnosis date. We calculated the delay in diagnosis as the difference between the date of first presentation and the diagnosis date.

Healthcare charges represented total healthcare utilization. Billing data were available for ambulatory care from NextGen and for Banner Health's hospitalizations from MedSeries4 (Siemens Medical Solutions USA, Inc., <https://www.siemens.com>). We defined healthcare utilization as the total charges, for any cause, from the date of first visit to 6 months after the diagnosis date. We distinguished total charges from actual reimbursement amount because the total is only 1 aspect of a complicated financial billing system.

We used the SAS Enterprise Guide Software Suite version 7.13 (SAS Institute Inc., <https://www.sas.com>) for

¹Preliminary results from this study were presented in part at the 62nd Annual Coccidioidomycosis Study Group Meeting, April 14, 2018, Flagstaff, Arizona, USA.

Author affiliations: Banner Health Corporation, Phoenix, Arizona, USA (R. Ginn, J. Goodsell, G. Mendez, B. Bradley); University of Arizona College of Medicine—Phoenix, Phoenix (R. Mohty, K. Bollmann, J.N. Galgiani); Banner University Medical Center—Phoenix, Phoenix (K.L. Bollmann, J.N. Galgiani); University of Arizona College of Medicine—Tucson, Tucson, Arizona, USA (J.N. Galgiani)

DOI: <https://doi.org/10.3201/eid2509.190019>

data retrieval and analysis. The Banner Health Institutional Review Board approved this study.

We identified newly diagnosed coccidioidal infections in 139 patients. The mean patient age was 49.2 years (SD ± 15.3 years) (Appendix Figure 1), and 52% of patients were female.

The 3 most frequently occurring coccidioidal ICD-9 codes were unspecified (114.9, 47%), primary pulmonary (114.0, 37%), and pulmonary unspecified (114.5, 8%) (Appendix Figure 2). Confirmatory serologic tests were recorded within 15 days before or after the date of diagnosis in 81% of patients (Appendix Figure 3).

The expanded set of ICD-9 codes failed to identify an initial presentation date for 20 patients. Of the 119 patients with an identified presentation date, 16 (13%) received a diagnosis on the day of presentation, 24% within 1 week of first presentation, 46% within 1 month, and 54% from 30 days to 6 months after presentation (Figure).

We queried total charges for all 139 patients from the date of first visit (the coccidioidomycosis diagnosis date, if no initial presentation date was available) until 6 months after the diagnosis date. By cross-referencing patient identifiers, we found 66 (47%) patients to have hospitalization billings, which were included in the total healthcare cost. Median healthcare charges seemed to increase as diagnosis delays increased (Table). When we compared diagnosis delay to the log-normal of total charges, we found a significant, positive, linear relationship for overall charges ($R^2 = 0.07$, $p = 0.003$), attributable to those occurring before ($R^2 = 0.16$, $p \leq 0.0001$) but not to those on or after the diagnosis date ($R^2 = 0.01$, $p = 0.2748$). Although we saw issues with data normality because of our small sample size, we assumed normality for linear regression analysis (Appendix Figures 4–6).

Conclusions

For this retrospective study, we developed a set of ICD-9 codes to use as a surrogate indicator for the date coccidioidomycosis patients were first seen within Banner Health clinics for signs or symptoms of their infection. This list expanded on an initial set of codes discovered through a manual chart review (7). Many of the codes are common and are unlikely themselves to be predictive of diagnosis. Previous studies have been unable

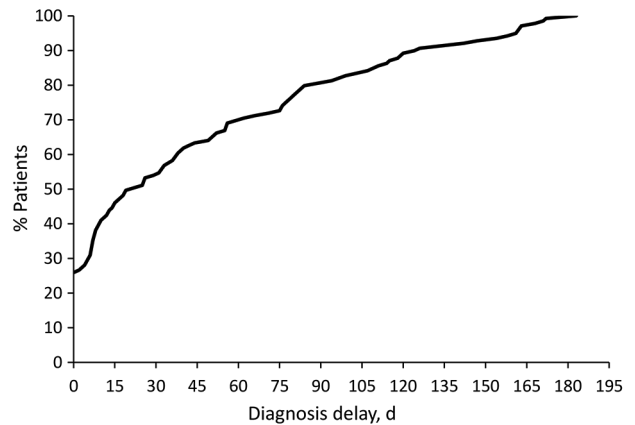


Figure. Cumulative distribution of coccidioidomycosis patient population in relation to diagnosis delay for cohort of patients in Phoenix, Arizona, USA. At 30 days of delay, ≈55% of the population had received a diagnosis.

to meaningfully distinguish presenting syndromes of coccidioidomycosis in patients from other overlapping etiologies (3,4,8). However, this code set was useful to computationally establish the date of first healthcare contact for these patients. If this analytic method is validated and perhaps improved in future studies, it could allow for automated monitoring of diagnostic delay as a metric of quality assessment, without the need for expert chart review.

Of the 139 patients analyzed in this study, 20 did not have an eligible ICD-9 code, and 16 others had their initial presentation code recorded on the same day as their coccidioidomycosis diagnosis. Factors leading to these problems might include failure of a clinician to record sufficient diagnostic information or use of codes that are not sufficiently comprehensive. Future studies could manually examine the full patient records to further expand the code set. It is also possible that patients entered the Banner Health electronic system with a diagnosis of coccidioidomycosis from elsewhere or that the coccidioidal infection was truly without symptoms.

This investigation identified a prolonged diagnosis delay for much of the population; 46% had a delay >1 month (Figure). With increased delays, total healthcare charges increased substantially. However, this study was

Table. Median charges by monthly range of diagnostic delays before and after the date of coccidioidomycosis diagnosis for cohort of patients in Phoenix, Arizona, USA*

Time from presentation to diagnosis, mo	No. patients	Before diagnosis		After diagnosis		Combined	
		Median	Total	Median	Total	Median	Total
<1	55	\$373	\$30,081	\$637	\$239,681	\$749	\$269,762
1–3	37	\$791	\$217,662	\$2,707	\$436,233	\$2,492	\$653,895
4–6	27	\$915	\$338,810	\$1,199	\$710,911	\$2,680	\$1,049,720
No recorded symptoms	20	NA	NA	\$4,172	\$854,597	\$4,172	\$854,597
Overall	139	\$637	\$586,553	\$875	\$2,241,422	\$1,231	\$2,827,974

*NA, not applicable.

not limited to coccidioidomycosis-related charges; any diagnosis delay could result in increased healthcare utilization, regardless of relationship to coccidioidomycosis. In addition, data gaps may have occurred because of difficulty in cross-referencing identifiers or visits by patients to a non-Banner facility. However, our findings are consistent with the simple concept that diagnostic delays in a protracted coccidioidal illness would result in additional testing, visits, and possible use of empiric antibacterial treatments until a precise diagnosis is achieved.

Our study investigates only patients with confirmed coccidioidomycosis and not patients who never received a correct diagnosis. Previous studies indicate that appropriate testing for coccidioidomycosis is often not done in Phoenix and Tucson (6,9,10). Thus, the costs of delayed coccidioidal diagnosis probably underestimates the situation for this clinical practice within a coccidioidomycosis-endemic region. A recent study of coccidioidomycosis diagnosed outside endemic regions also showed substantial delays (11), making our research relevant to those with a recent travel history to endemic regions.

Acknowledgments

We thank Sweta Narasimhan, Natalie Crawford, Nadav Fields, and Siamac Yazdchi for their assistance with the preliminary chart review.

R.M. submitted part of this study to satisfy graduation requirements for his medical degree at the University of Arizona College of Medicine—Phoenix.

About the Author

Ms. Ginn is a data science analyst at Banner Health's Centralized Analytics team. Her interests include data visualization, hierarchical data modeling, and infectious diseases.

References

- Hector RF, Rutherford GW, Tsang CA, Erhart LM, McCotter O, Anderson SM, et al. The public health impact of coccidioidomycosis in Arizona and California. *Int J Environ Res Public Health*. 2011;8:1150–73. <http://dx.doi.org/10.3390/ijerph8041150>
- Litvintseva AP, Marsden-Haug N, Hurst S, Hill H, Gade L, Driebe EM, et al. Valley fever: finding new places for an old disease: *Coccidioides immitis* found in Washington State soil associated with recent human infection. *Clin Infect Dis*. 2015;60:e1–3. <http://dx.doi.org/10.1093/cid/ciu681>
- Valdivia L, Nix D, Wright M, Lindberg E, Fagan T, Lieberman D, et al. Coccidioidomycosis as a common cause of community-acquired pneumonia. *Emerg Infect Dis*. 2006;12:958–62. <http://dx.doi.org/10.3201/eid1206.060028>
- Kim MM, Blair JE, Carey EJ, Wu Q, Smilack JD. Coccidioidal pneumonia, Phoenix, Arizona, USA, 2000–2004. *Emerg Infect Dis*. 2009;15:397–401. <http://dx.doi.org/10.3201/eid1563.081007>
- Galgiani JN, Ampel NM, Blair JE, Catanzaro A, Geertsma F, Hoover SE, et al. 2016 Infectious Diseases Society of America (IDSA) clinical practice guideline for the treatment of coccidioidomycosis. *Clin Infect Dis*. 2016;63:e112–46. <http://dx.doi.org/10.1093/cid/ciw360>
- Chang DC, Anderson S, Wannemuehler K, Engelthaler DM, Erhart L, Sunenshine RH, et al. Testing for coccidioidomycosis among patients with community-acquired pneumonia. *Emerg Infect Dis*. 2008;14:1053–9. <http://dx.doi.org/10.3201/eid1407.070832>
- Bollmann K, Narasimhan S, Crawford N, Fields N, Yazdchi D, Goodsell J, et al. Rapidity of coccidioidomycosis diagnosis and its effect on healthcare utilization [poster presentation]. In: American College of Physicians Arizona Chapter 2015 Annual Meeting; November 13–15, 2015; Tucson, Arizona, USA [cited 2019 Jun 17]. https://www.acponline.org/system/files/documents/about_acp/chapters/az/salud_15.pdf
- Yozwiak ML, Lundergan LL, Kerrick SS, Galgiani JN. Symptoms and routine laboratory abnormalities associated with coccidioidomycosis. *West J Med*. 1988;149:419–21.
- Campion JM, Gardner M, Galgiani JN. Coccidioidomycosis (Valley fever) in older adults: an increasing problem. *Ariz Geriatr Soc J*. 2003;8:3–12.
- Stern NG, Galgiani JN. Coccidioidomycosis among scholarship athletes and other college students, Arizona, USA. *Emerg Infect Dis*. 2010;16:321–3. <http://dx.doi.org/10.3201/eid1602.090918>
- Benedict K, Ireland M, Weinberg MP, Gruninger RJ, Weigand J, Chen L, et al. Enhanced surveillance for coccidioidomycosis, 14 US states, 2016. *Emerg Infect Dis*. 2018;24:1444–52. <http://dx.doi.org/10.3201/eid2408.171595>

Address for correspondence: John N. Galgiani, University of Arizona—Valley Fever Center for Excellence, PO Box 245215, Tucson, AZ 85724, USA; email: spherule@u.arizona.edu; Rachel Ginn, Banner Health Corporation, 2901 N Central Ave, Phoenix, AZ 85012, USA; email: rachel.ginn@bannerhealth.com

Delays in Coccidioidomycosis Diagnosis and Associated Healthcare Utilization, Tucson, Arizona, USA

Fariba M. Donovan, Patrick Wightman, Yue Zong, Luke Gabe, Aneela Majeed, Tiffany Ynosencio, Edward J. Bedrick, John N. Galgiani

Tucson, Arizona, USA, is a highly coccidioidomycosis-endemic area. We conducted a retrospective review of 815 patients in Tucson over 2.7 years. Of 276 patients with coccidioidomycosis, 246 had a delay in diagnosis; median delay was 23 days. Diagnosis delay was associated with coccidioidomycosis-related costs totaling \$589,053 and included extensive antibacterial drug use.

Coccidioidomycosis, also known as Valley fever, is a fungal infection endemic to the southwestern United States and Mexico (1); it typically manifests as a respiratory syndrome (2). Without specific laboratory confirmation, coccidioidomycosis cannot be distinguished from community-acquired pneumonia (3,4). However, the necessary tests are conducted for <13% of patients with community-acquired pneumonia in urban Arizona ambulatory clinics (5) and 2.8% of patients in emergency departments (6). Until coccidioidomycosis is correctly diagnosed, patients are likely to receive unnecessary antibacterial drugs, laboratory tests, imaging, and invasive procedures, all of which could contribute to unnecessary costs and additional adverse health consequences. The extent to which there is a delay in coccidioidomycosis diagnosis and how much healthcare utilization occurs with that delay is uncertain.

We report a retrospective study within metropolitan Tucson, Arizona, USA, an area in which coccidioidomycosis is highly endemic, to determine the delay for patients from the date when they first sought care to the date they received a laboratory-confirmed coccidioidomycosis diagnosis. We also analyzed healthcare costs, efforts, and antibacterial drug use within that period.

Author affiliations: University of Arizona, Tucson, Arizona, USA (F.M. Donovan, P. Wightman, L. Gabe, A. Majeed, T. Ynosencio, E.J. Bedrick, J.N. Galgiani); Valley Fever Center for Excellence, Tucson (F.M. Donovan, Y. Zong, J.N. Galgiani)

DOI: <https://doi.org/10.3201/eid2509.190023>

The Study

We conducted a retrospective review of medical charts from January 1, 2015, through September 18, 2017, for patients at Banner University Medical Center in Tucson (BUMC-T). During this time, BUMC-T used the Epic electronic medical record system (7). The University of Arizona Health Sciences Clinical Data Warehouse (CDW; <https://cb2.uahs.arizona.edu/clinical-data-warehouse>) provided the information. Two physicians, an infectious disease fellow (A.M.) and pulmonology clinical fellows (L.G., T.Y.), independently reviewed charts with codes 114.*/B38.* from the International Classification of Diseases, 9th Revision (ICD-9) or 10th Revision (ICD-10). We divided records into 2 cohorts and, when combined, sampled the entire study period. Two different reviewers were assigned to each cohort. We excluded records if coccidioidomycosis was diagnosed before the study, if the ICD-9/10 coding was in error, if patient age was <18 years, or if diagnosis was not confirmed by laboratory testing (2). For the remaining records, we determined initial presentation date (i.e., the date signs and symptoms were first clinically noted). We categorized presenting syndromes by type: acute symptomatic pulmonary infection or immunologic response (rash, arthralgia, fatigue), fibrocavitary chronic pulmonary infection, asymptomatic pulmonary nodule, and extrapulmonary disseminated infection. The specimen collection date leading to laboratory confirmation was designated as the diagnosis date and the time between initial evaluation and diagnosis date as the diagnosis delay. Agreement between reviewers for delay was 98% and 96.5% in the 2 cohorts; the lead investigator (F.M.D.) resolved discrepancies.

Within the range for diagnostic delay, we queried the CDW for Healthcare Common Procedure Coding System/Current Procedural Terminology (HCPCS/CPT) codes to estimate total effort (i.e., all CPTs associated with each encounter). We used publicly available Medicare fee schedules assigning values to codes associated with charges. These included the Physician Fee Schedule, Clinical Laboratory Fee Schedule (Arizona-specific), Payment Allowance for Medicare Part B Drugs, and the Durable Medical Equipment, Prosthetics/Orthotics, and Supplies (DME-POS) Fee Schedule. We used 2016 schedules to correspond

with the last full year that Banner used Epic software and to impose a uniform price scheme. We manually reviewed each CPT code and tabulated costs related to coccidioidomycosis diagnosis; costs are presented in US dollars. The University of Arizona institutional review board approved this study.

We summarized categorical variables using counts and percentages and summarized time to events and costs using medians and interquartile ranges (Figures 1, 2). We showed total costs by disease category. We compared the distributions of time to diagnosis and costs across coccidioidomycosis presentation categories using nonparametric Kruskal-Wallis tests. We based pairwise comparisons of groups on nonparametric Wilcoxon-Mann-Whitney tests and CIs for differences in medians. We used a χ^2 test to compare percentages between groups. We conducted statistical analyses in R version 3.1 (<https://www.r-statistics.com/2014/11/r-3-1>) and defined statistical significance as $p < 0.05$.

We reviewed a total of 815 electronic charts in 2 cohorts and excluded 539 (66%) of them (Appendix 1 Table 1, <https://wwwnc.cdc.gov/EID/article/25/9/19-0023-App1.pdf>). Exclusions were for prior coccidioidomycosis (57%), mistaken coding (11%), age < 18 years (10%), and unconfirmed diagnosis (22%). Of 276 remaining cases, 126 (46%) were in female patients; average patient age was 55.5 years (SD ± 18.4), and median age was 53.3 years. Disease category distribution was acute symptomatic pulmonary (63%), chronic pulmonary (8%), asymptomatic pulmonary nodule (17%), and disseminated infection (12%). We found no significant difference ($p = 0.38$) between excluded and included cases in the 2 cohorts.

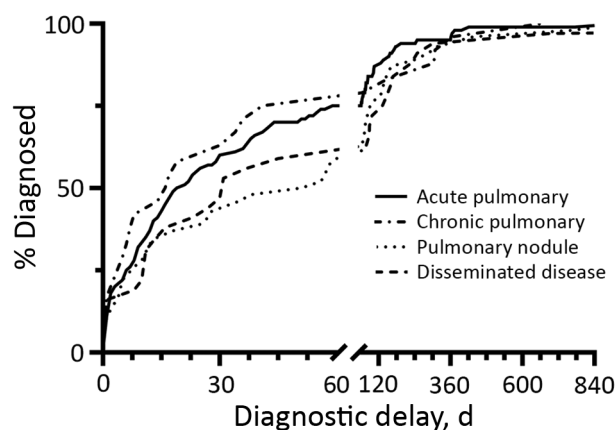


Figure 1. Cumulative distribution for time to diagnosis of coccidioidomycosis for 4 disease categories among patients in Tucson, Arizona, USA, January 1, 2015–September 18, 2017. Time points related to patients with very extended delay period (909 days in acute pulmonary disease, 928 days in pulmonary nodule, and 3,315 days in disseminated disease) are not shown in the graph. Timeline truncated for readability.

We compiled cumulative distribution functions for time to diagnosis (Figure 1). Differences in delay among disease categories were not statistically significant ($p = 0.14$). Median delay was 23 days (95% CI 17–34), and 43% of patients (95% CI 38–50) had a delay ≥ 1 month.

Of 276 patients, 30 (11%) received a coccidioidomycosis diagnosis at presentation (zero delay) and 12 of the 30 during hospital admission. Because hospitalization of these 12 either was not required for diagnosis or was required for disease complication management, we excluded coccidioidomycosis-associated costs from the analysis. Of the remaining 264 patients, 246 had delayed diagnosis of ≥ 1 day, with coccidioidomycosis-associated costs of \$589,053 (82%) of the \$718,401 total. Coccidioidomycosis-related costs for patients with diagnostic delay were significantly greater ($p = 0.0004$) than for the 18 patients without delay (Figure 2; Appendix Table 2).

Not all CPT codes are associated with charges or reflected in patients' bills, so we assessed total effort by analyzing the frequency of CPT codes and determining whether codes were related to coccidioidomycosis infection (Appendix 2, <https://wwwnc.cdc.gov/EID/article/25/9/19-0023-App2.xls>). Coccidioidomycosis-related charges for CPT code-related effort was higher in patients with delays in diagnosis compared with charges for patients without delays (Appendix 1 Figure 1).

Outpatient and inpatient prescriptions for a total of 1,103 antibacterial medication orders submitted before coccidioidomycosis diagnosis are an approximate measure of antibacterial use. Vancomycin and daptomycin comprised 22% of antimicrobial drugs ordered (Appendix 1 Figure 2).

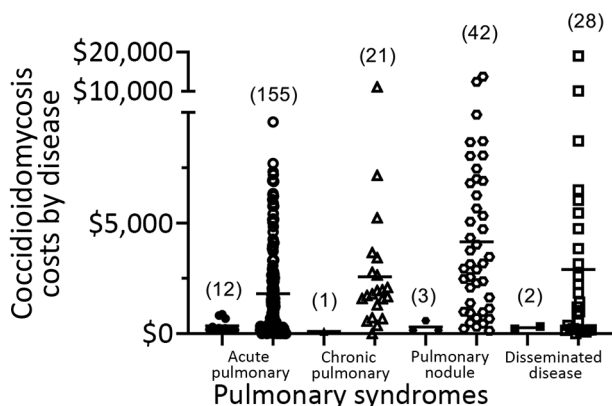


Figure 2. Coccidioidomycosis costs by disease category for 264 case-patients in Tucson, Arizona, USA, January 1, 2015–September 18, 2017. Costs are shown in 2 columns for each category: the left column for diagnosis at initial presentation and the right column for delayed diagnosis. Each symbol represents 1 case. Numbers in parentheses indicate the number of cases in each category. Cost axis truncated for readability.

Conclusions

Our findings demonstrate significant delays in accurate coccidioidomycosis diagnosis and substantial costs associated with these delays. Median delays for different disease categories ranged from 17 to 54 days; 43% of patients with coccidioidomycosis had a diagnosis delay >1 month. The 23-day median delay we presented (interquartile range 7–74 days) corresponds with a recently reported 23-day delay in Arizona (8) and in a 2010 study (9). In our cohort, these delays were associated with \$589,053 in coccidioidomycosis-related costs, as determined from Medicare fee schedules. Although median coccidioidomycosis-related costs were lowest for acute coccidioidal pneumonia, the total was greatest for this group because it accounted for >63% of patients. If our findings were extrapolated across institutions in coccidioidomycosis-endemic regions, diagnostic delays and excess healthcare utilization would probably represent millions of dollars.

Overall healthcare effort as indicated by CPT code frequencies, irrespective of whether or not they resulted in billed charges, showed similar delay-associated excesses. Of additional concern is unnecessary use of antibacterial drugs, such as broad-spectrum medications like vancomycin, in coccidioidomycosis patients before an accurate diagnosis (Appendix 1 Figure 2). If coccidioidomycosis diagnostic delays were shortened, unnecessary antibacterial treatments could be reduced greatly.

This study extends earlier reports of the economic burden associated with coccidioidomycosis (9). It is certainly an underestimate of costs, because we did not include in our cohort an unknown number of patients with coccidioidomycosis who were misdiagnosed. Our results suggest earlier diagnosis will lower costs and provide secondary benefits including patient reassurance, decreased antibacterial drug use, and improved antibiotic stewardship. This study reinforces the ongoing challenge to increase coccidioidomycosis awareness for healthcare providers and the urgent need to improve the ease, rapidity, and reliability of coccidioidomycosis testing.

This work was supported by the Centers for Disease Control and Prevention (contract no. 200-2017-95513).

About the Author

Dr. Donovan is an assistant professor with the Valley Fever Center for Excellence in the University of Arizona Department of Medicine. Her primary research interest is medical mycology, with an emphasis on fungus–host interactions.

References

1. Nguyen C, Barker BM, Hoover S, Nix DE, Ampel NM, Frelinger JA, et al. Recent advances in our understanding of the environmental, epidemiological, immunological, and clinical dimensions of coccidioidomycosis. *Clin Microbiol Rev.* 2013;26:505–25. <https://doi.org/10.1128/CMR.00005-13>
2. Galgiani JN, Ampel NM, Blair JE, Catanzaro A, Geertsma F, Hoover SE, et al. 2016 Infectious Diseases Society of America (IDSA) clinical practice guideline for the treatment of coccidioidomycosis. *Clin Infect Dis.* 2016;63:e112–46. <https://doi.org/10.1093/cid/ciw360>
3. Valdivia L, Nix D, Wright M, Lindberg E, Fagan T, Lieberman D, et al. Coccidioidomycosis as a common cause of community-acquired pneumonia. *Emerg Infect Dis.* 2006;12:958–62. <https://doi.org/10.3201/eid1206.060028>
4. Kim MM, Blair JE, Carey EJ, Wu Q, Smilack JD. Coccidioidal pneumonia, Phoenix, Arizona, USA, 2000–2004. *Emerg Infect Dis.* 2009;15:397–401. <https://doi.org/10.3201/eid1563.081007>
5. Chang DC, Anderson S, Wannemuehler K, Engelthaler DM, Erhart L, Sunenshine RH, et al. Testing for coccidioidomycosis among patients with community-acquired pneumonia. *Emerg Infect Dis.* 2008;14:1053–9. <https://doi.org/10.3201/eid1407.070832>
6. Jones JM, Koski L, Khan M, Brady S, Sunenshine R, Komatsu KK. Coccidioidomycosis: An underreported cause of death—Arizona, 2008–2013. *Med Mycol.* 2018;56:172–9. <https://doi.org/10.1093/mmy/myx041>
7. Eisen M. Epic systems: epic tale. *Isthmus.* 2008 Jun 20 [cited 2019 Jun 10]. <https://isthmus.com/news/cover-story/epic-systems-epic-tale>
8. Benedict K, Ireland M, Weinberg MP, Gruninger RJ, Weigand J, Chen L, et al. Enhanced surveillance for coccidioidomycosis, 14 US states, 2016. *Emerg Infect Dis.* 2018;24:1444–52. <https://doi.org/10.3201/eid2408.171595>
9. Tsang CA, Anderson SM, Imholte SB, Erhart LM, Chen S, Park BJ, et al. Enhanced surveillance of coccidioidomycosis, Arizona, USA, 2007–2008. *Emerg Infect Dis.* 2010;16:1738–44. <https://doi.org/10.3201/eid1611.100475>

Address for correspondence: Fariba M. Donovan or John N. Galgiani, University of Arizona—Valley Fever Center for Excellence, PO Box 245215, Tucson, AZ 85724, USA; email: faribadonovan@deptofmed.arizona.edu or spherule@u.arizona.edu

Soft Tissue Infection with *Diaporthe phaseolorum* in Heart Transplant Recipient with End-Stage Renal Failure

Julia C. Howard,¹ Kevin Chen,²
Anja Werno, Sarah Metcalf

Author affiliations: Canterbury Health Laboratories, Christchurch, New Zealand (J.C. Howard, A. Werno); Christchurch Hospital, Christchurch (K. Chen, S. Metcalf)

DOI: <https://doi.org/10.3201/eid2509.190768>

Diaporthe phaseolorum is a fungal plant parasite that has rarely been described as causing invasive human disease. We report a case of human soft tissue infection with *Diaporthe phaseolorum* in a heart transplant patient with end-stage renal failure in New Zealand.

Diaporthe phaseolorum is a fungal plant parasite found in soil, salt and fresh water, and sewage (1). There are few case reports of human infection with *Diaporthe* species, and most have been described in highly immunosuppressed persons, especially solid organ transplantation recipients (2–6). One case of *Diaporthe* spp. soft tissue infection was reported in a heart transplant patient in the United States (5), but the patient did not have end-stage renal failure (ESRF), making the choice of antifungal therapy less complex. We report a case of human infection with *D. phaseolorum* in a heart transplant patient with end-stage renal failure.

The patient was a 46-year-old man from Samoa, resident in New Zealand, who had had a heart transplant 10 years earlier for dilated cardiomyopathy. We obtained signed consent from the patient for publication of the details of his condition. He had a 1-year history of a slowly enlarging, nontender lump in the pretibial area of his left leg. He noticed the lesion after sustaining a minor abrasion while playing a game of touch rugby. He had not been back to Samoa for 17 years. He was receiving peritoneal dialysis for ESRF secondary to tacrolimus toxicity. At the time of presentation, he was taking mycophenolate (500 mg 2×/d), tacrolimus (5 mg 2×/d; daily trough level 6.6 µg/L), and prednisone (2.5 mg 1×/d).

Magnetic resonance imaging of the leg showed a 37 × 23 × 43 mm complex subcutaneous cystic lesion over the proximal medial tibia with thin septations and no evidence of bony invasion. An aspirate of the lesion

was used for microbiological analysis and culture. Histologic examination showed reactive fibroblastic proliferation and numerous fungal hyphae by periodic acid–Schiff staining (Figure).

Microscopy showed numerous fungal hyphae with no identifiable distinctive features by direct microscopic examination. After 3 days of culture, there was growth of small, white, woolly colonies on only chocolate agar and no bacterial growth.

We extracted DNA by using the UCP Pathogen Kit (QIAGEN, <https://www.qiagen.com>) and sequenced the internal transcribed spacer 2 region. A BLAST query (<http://www.ncbi.nih.gov>) showed 100% identity and 100% query coverage with *D. phaseolorum* (GenBank accession nos. KX498068.1, KX355829.1, JQ514150.1, and AY577815.1) and *Phomopsis* sp. (GenBank accession nos. GU066693.1 and GQ352481.1, isolates from India and Malaysia).

These findings raised the question of genus assignment. Previously, *Phomopsis* was considered to be the asexual morphotype of *Diaporthe* species. Thus, it is possible that these deposits in GenBank were the same genus and perhaps even the same species. However, without further information about GenBank cultures or morphologic description of our isolate, we can only conclude that our isolate was probably *D. phaseolorum*.

The patient was given voriconazole, and domperidone was replaced with metoclopramide. Severe tremor then developed, so he was given itraconazole before surgical excision of the lesion. Tissue samples grew *D. phaseolorum*.

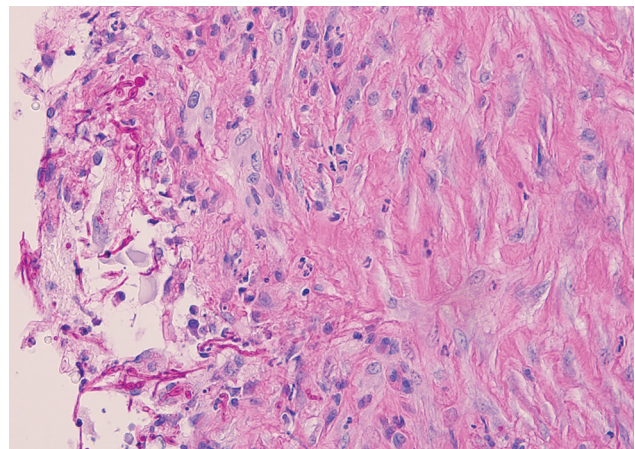


Figure. Soft tissue infection with *Diaporthe phaseolorum* in a 46-year-old man from Samoa, resident in New Zealand, who was a heart transplant recipient with end-stage renal failure. Histologic examination of a cystic lesion over the proximal medial tibia showed reactive fibroblastic proliferation and numerous long-branching fungal septate hyphae of uneven widths. Periodic acid–Schiff staining; original magnification ×40. Photograph provided by Frederica Loghides, Department of Anatomic Pathology, Canterbury Health Laboratories. A color version of this figure is available online (<http://wwwnc.cdc.gov/EID/article/25/9/19-0768-F1.htm>).

¹Current affiliation: Waikato District Health Board, Hamilton, New Zealand.

²Current affiliation: Pathlab Bay of Plenty, Tauranga, New Zealand.

However, drug susceptibility testing could not be performed because of inadequate growth. The patient received itraconazole for 7 months and the infection resolved, with no evidence to date of recurrence.

Infection with *D. phaseolorum* usually occurs after inoculation from direct trauma (1). In this patient, the history of a minor leg abrasion during touch rugby was only suggestive of direct inoculation. Previous publications have reported different suspected sources of infection, such as a prick from a plant thorn or spine (7,8), walking barefoot (8), or eye surgery (9). Activities that have been implicated in acquisition of infection include gardening (5,7), farming (6,8), and hunting (5). Another possibility suggested in a case series (10) is that the patient might have had a penetrating injury with a wood fragment many years earlier. Marty et al. (10) reported 3 cases of cutaneous, invasive fungal disease in which patients had received penetrating soft-tissue injuries with wood fragments months to years (10 months–13 years) before their transplant, suggesting the fungus persisted at the site of injury over a long period.

In the past, diagnosis of this type of unusual fungal infection would be reliant on macroscopic and microscopic morphology and growth characteristics. For this patient, the fungus did not grow on subculture. However, advances in molecular microbiology now enable clinical microbiologists to identify unusual fungal pathogens by sequencing of 18S rDNA or internal transcribed spacer 2 region.

This case was challenging because human infection with this pathogen is rare. Therapeutic options are based on experience detailed in a limited number of case reports. Treatment with itraconazole (4,6,8), posaconazole (5), and voriconazole (3,4) has been successful. However, treatment failure has been reported with voriconazole (despite a low MIC) and terbinafine (2). Most case-patients needed surgical resection for infection resolution. Keratitis has been successfully treated with topical amphotericin B and voriconazole (topical and oral) (7) and topical natamycin and fluconazole (topical and oral) (9).

This case highlights the difficulties faced by clinicians trying to use appropriate directed antifungal therapy when a patient is receiving multiple immunosuppressing drugs. Clinicians and clinical microbiologists should be aware of the possibility of invasive fungal infection with unusual pathogens, even if the patient is seen many years after a transplant.

About the Author

At the time of this study, Dr. Howard was a microbiology registrar at the Canterbury Health Laboratories, Christchurch, New Zealand. She is currently a clinical microbiologist at the Waikato District Health Board, Hamilton, New Zealand. Her research interests include antimicrobial resistance, infections in immunocompromised persons, and public health microbiology.

References

1. Sutton DA. Coelomycetous fungi in human disease. a review: clinical entities, pathogenesis, identification and therapy. *Rev Iberoam Micol.* 1999;16:171–9.
2. Garcia-Reyne A, López-Medrano F, Morales JM, García Esteban C, Martín I, Eraña I, et al. Cutaneous infection by *Phomopsis longicolla* in a renal transplant recipient from Guinea: first report of human infection by this fungus. *Transpl Infect Dis.* 2011;13:204–7. <https://doi.org/10.1111/j.1399-3062.2010.00570.x>
3. Cariello PF, Wickes BL, Sutton DA, Castlebury LA, Levitz SM, Finberg RW, et al. *Phomopsis bougainvilleicola* prepatellar bursitis in a renal transplant recipient. *J Clin Microbiol.* 2013;51:692–5. <https://doi.org/10.1128/JCM.02674-12>
4. Guégan S, Garcia-Hermoso D, Sitbon K, Ahmed S, Moguelet P, Dromer F, et al.; French Mycosis Study Group. Ten-year experience of cutaneous and/or subcutaneous infections due to Coelomycetes in France. *Open Forum Infect Dis.* 2016;3:ofw106. <https://doi.org/10.1093/ofid/ofw106>
5. Rakita RM, O'Brien KD, Bourassa L. *Diaporthe* soft tissue infection in a heart transplant patient. *Transpl Infect Dis.* 2017;19:e12680. <https://doi.org/10.1111/tid.12680>
6. Mattei AS, Severo CB, Guazzelli LS, Oliveira FM, Gené J, Guarro J, et al. Cutaneous infection by *Diaporthe phaseolorum* in Brazil. *Med Mycol Case Rep.* 2013;2:85–7. <https://doi.org/10.1016/j.mmcr.2013.03.001>
7. Mandell KJ, Colby KA. Penetrating keratoplasty for invasive fungal keratitis resulting from a thorn injury involving *Phomopsis* species. *Cornea.* 2009;28:1167–9. <https://doi.org/10.1097/ICO.0b013e31819839e6>
8. Iriart X, Binois R, Fior A, Blanchet D, Berry A, Cassaing S, et al. Eumycetoma caused by *Diaporthe phaseolorum* (*Phomopsis phaseoli*): a case report and a mini-review of *Diaporthe/Phomopsis* spp. invasive infections in humans. *Clin Microbiol Infect.* 2011;17:1492–4. <https://doi.org/10.1111/j.1469-0691.2011.03568.x>
9. Gajjar DU, Pal AK, Parmar TJ, Arora AI, Ganatra DA, Kayastha FB, et al. Fungal scleral keratitis caused by *Phomopsis phoenicicola*. *J Clin Microbiol.* 2011;49:2365–8. <https://doi.org/10.1128/JCM.02449-10>
10. Marty FM, Petschnigg EM, Hammond SP, Ready JE, Ho VT, Soiffer RJ, et al. Invasive fungal disease after remote inoculation in transplant recipients. *Clin Infect Dis.* 2011;52:e7–10. <https://doi.org/10.1093/cid/ciq040>

Address for correspondence: Julia C. Howard, Microbiology Department, Waikato Hospital, Pembroke St, Hamilton 3204, New Zealand; email: julia.howard@waikatodhb.health.nz

Disseminated Emergomycosis in a Person with HIV Infection, Uganda

Isabelle Rooms, Peter Mugisha, Thilo Gambichler, Eva Hadaschik, Stefan Esser, Peter-Michael Rath, Gerhard Haase, Dunja Wilmes, Ilka McCormick-Smith, Volker Rickerts

Author affiliations: University Duisburg-Essen, Essen, Germany (I. Rooms, E. Hadaschik, S. Esser); Mbarara Referral Hospital, Mbarara, Uganda (P. Mugisha); St. Joseph Hospital Bochum, Bochum, Germany (T. Gambichler); University Hospital Essen, Essen (P.-M. Rath); RWTH Aachen University Hospital, Aachen, Germany (G. Haase); Robert Koch Institute, Berlin, Germany (D. Wilmes, I. McCormick-Smith, V. Rickerts)

DOI: <https://doi.org/10.3201/eid2509.181234>

We describe emergomycosis in a patient in Uganda with HIV infection. We tested a formalin-fixed, paraffin-embedded skin biopsy to identify *Emergomyces pasteurianus* or a closely related pathogen by sequencing broad-range fungal PCR amplicons. Results suggest that emergomycosis is more widespread and genetically diverse than previously documented. PCR on tissue blocks may help clarify emergomycosis epidemiology.

Emergomycosis is a fungal infection caused by fungi of the newly described genus *Emergomyces*, of the order Onygenales, which includes obligate fungal pathogens, such as *Histoplasma*, *Blastomyces*, and *Paracoccidioides* (1). Emergomycosis manifests after dissemination to the lungs and skin; it is associated with 50% mortality. Most cases of emergomycosis have been reported in persons with HIV from South Africa infected with *E. africanus*, the DNA of which has been amplified from soil there (2). Emergomycosis from *E. orientalis* or *E. canadensis* infection has been identified in limited geographic areas.

In contrast, *E. pasteurianus* infections have been widely documented in Asia, Europe, and South Africa (Appendix Table 2) (2). *E. pasteurianus* infections were first described in 1998 in a patient in Italy with HIV infection and skin lesions (3). The isolate was initially placed in the genus *Emmonsia* because of the similarity of the ribosomal large subunit genes. The new genus *Emergomyces* was suggested by Dukik et al. to distinguish fungi that produce small yeasts in host tissues, comparable to *Histoplasma* instead of the adiaspores found in *Emmonsia* (4). We report a case of *E. pasteurianus* infection in a patient in Uganda with HIV infection.

A 38-year-old woman from Rwanda sought treatment in Uganda for a 3-month history of disseminated skin lesions, nodules, papules, and ulcers (Figure). A chest radiograph revealed no signs of disease. The woman was living in southwestern Uganda, working as a trader. She reported no travel except for a short visit to Dubai 5 years earlier. She had also been diagnosed with HIV 5 years earlier. She was treated for HIV with zidovudine, lamivudine, and nevirapine. CD4 lymphocyte count was 140 cells/ μ L. HIV viral load testing was not performed.

A skin biopsy was taken, but fungal isolation was not performed because laboratorians lacked the necessary equipment. As therapy for emergomycosis, experts suggest amphotericin B, which was not available for the patient, followed by oral triazoles (2). The patient was started on fluconazole (400 mg 1 \times /d) for suspected cutaneous cryptococcosis. Histopathology showed narrow budding yeast cells (2–4 μ m) (Figure). Because skin lesions increased during 6 weeks of fluconazole and antiretroviral treatments, treatment was changed to itraconazole (400 mg 2 \times /d). Lesions decreased markedly within 8 weeks, which we considered the key finding suggesting treatment response. No follow-up data are available beyond this point. As reported by Dukik et al., in vitro resistance testing of *Emergomyces* documents activity of itraconazole, voriconazole, and posaconazole, but not fluconazole (5).

In Germany, DNA was extracted from the formalin-fixed, paraffin-embedded (FFPE) skin biopsy as previously described (6). Fungal DNA was amplified by 2 broad-range

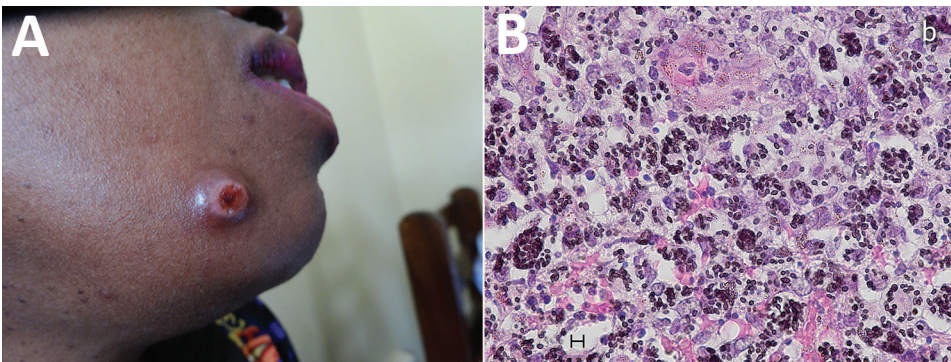


Figure. Imaging from investigation of emergomycosis in a 38-year-old woman from Rwanda with HIV infection living in Uganda. A) Skin lesion on face. B) Histopathology of skin biopsy specimen (Grocott stain) showing multiple budding yeast cells (2–3 μ m), mostly in clusters. Scale bar indicates 5 μ m.

PCR assays targeting a region of the 28S and the internal transcribed spacer (ITS) 2 regions of the fungal ribosomal RNA genes. Sanger sequencing of the PCR amplicons revealed 365-bp and 273-bp sequences (Appendix, <https://wwwnc.cdc.gov/EID/article/25/9/18-1234-App1.pdf>). A BLAST search (<https://blast.ncbi.nlm.nih.gov/Blast.cgi>) revealed *Paracoccidioides lutzii* (98.6% pairwise identity) and *E. pasteurianus* (98.9% pairwise identity) to be the closest matches for the 28S and ITS2 amplicons. Because no generally accepted pairwise identity break points for fungal species identification are available and sequence data for the region amplified by the 28S assay are lacking for many fungi, we sequenced the amplicons of the 2 broad-range PCR assays from fungi of the family *Ajellomycetaceae* and of the species *Coccidioides immitis* (Appendix Table 2). Phylogenetic analysis of the concatenated sequences of both broad-range PCR assays suggested that the patient was infected with *E. pasteurianus* or a closely related species (Appendix Figure).

Identification of fungi from pathology blocks may be used to investigate the etiology of mycosis and define endemic regions of fungal pathogens. However, species identification by histopathology is limited and the optimal molecular identification strategy remains to be defined. Amplification of fungal DNA from FFPE tissue is restricted by amplicon length, PCR inhibition, an excess of host DNA, and contaminating fungal DNA (7). The broad-range assays we used were introduced to amplify fungal DNA from an excess of host DNA. They have been successfully applied on FFPE tissue before (6,8).

The ITS2 assay targets a diverse, noncoding region well represented in public databases. However, variable amplicon length (200–300 bp) suggests that detection limits may vary for different fungi and phylogenetic analysis may be impaired. In contrast, the 28S assay amplifies a more conserved coding region (330–350 bp). Whereas identification of a genus may be achieved, species resolution within a genus may not be possible and sequences of this region are underrepresented in public databases (4,6).

Our results suggest that emergomycosis is more widespread and genetically diverse than previously documented. This case suggests that using broad-range fungal PCR assays with specific PCR assays to target prevalent pathogens may

be a successful approach for identifying fungal etiology from pathology blocks and defining the epidemiology of emergomycosis and related infections.

About the Author

Dr. Rooms is a fifth-year resident in dermatology and venereology at the University Hospital of Essen, Germany; she has volunteered as a dermatologist and HIV specialist in Mbarara, Uganda. Her primary interests are tropical dermatological diseases and skin lesions in immunosuppressed patients.

References

- Jiang Y, Dukik K, Munoz JF, Sigler L, Schwartz I, Govender N, et al. Phylogeny, ecology and taxonomy of systemic pathogens and their relatives in Ajellomycetaceae (Onygenales): *Blastomyces*, *Emergomyces*, *Emmonsia*, *Emmonsiiopsis*. *Fungal Divers*. 2018;90:245–91. <https://doi.org/10.1007/s13225-018-0403-y>
- Schwartz IS, Maphanga TG, Govender NP. Emergomyces: a new genus of dimorphic fungal pathogens causing disseminated disease among immunocompromised persons globally. *Curr Fungal Infect Rep*. 2018;12:44–50. <https://doi.org/10.1007/s12281-018-0308-y>
- Gori S, Drouhet E, Gueho E, Huerre M, Lofaro A, Parenti M, et al. Cutaneous disseminated mycosis in a patient with AIDS due to a new dimorphic fungus. *J Mycol Med*. 1998;8:57–63.
- Dukik K, Muñoz JF, Jiang Y, Feng P, Sigler L, Stielow JB, et al. Novel taxa of thermally dimorphic systemic pathogens in the *Ajellomycetaceae* (Onygenales). *Mycoses*. 2017;60:296–309. <https://doi.org/10.1111/myc.12601>
- Dukik K, Al-Hatmi AMS, Curfs-Breuker I, Faro D, de Hoog S, Meis JF. Antifungal susceptibility of emerging dimorphic pathogens in the family *Ajellomycetaceae*. *Antimicrob Agents Chemother*. 2017;62:e01886–17. <https://doi.org/10.1128/AAC.01886-17>
- Rickerts V, Khot PD, Myerson D, Ko DL, Lambrecht E, Fredricks DN. Comparison of quantitative real time PCR with sequencing and ribosomal RNA-FISH for the identification of fungi in formalin fixed, paraffin-embedded tissue specimens. *BMC Infect Dis*. 2011;11:202. <https://doi.org/10.1186/1471-2334-11-202>
- Rickerts V. Identification of fungal pathogens in formalin-fixed, paraffin-embedded tissue samples by molecular methods. *Fungal Biol*. 2016;120:279–87. <https://doi.org/10.1016/j.funbio.2015.07.002>
- Springer J, McCormick Smith I, Hartmann S, Winkelmann R, Wilmes D, Cornely O, et al. Identification of *Aspergillus* and *Mucorales* in formalin-fixed, paraffin-embedded tissue samples: comparison of specific and broad-range fungal qPCR assays. *Med Mycol*. 2019;57:308–13. <https://doi.org/10.1093/mmy/myy041>

Address for correspondence: Volker Rickerts, Robert Koch Institute, Seestr. 10, Berlin 13353, Germany; email: RickertsV@RKI.de

Bourbon Virus in Wild and Domestic Animals, Missouri, USA, 2012–2013

Katelin C. Jackson,¹ Thomas Gidlewski, J. Jeffrey Root, Angela M. Bosco-Lauth, R. Ryan Lash, Jessica R. Harmon, Aaron C. Brault, Nicholas A. Panella, William L. Nicholson, Nicholas Komar

Author affiliations: Centers for Disease Control and Prevention, Fort Collins, Colorado, USA (K.C. Jackson, A.C. Brault, N.A. Panella, N. Komar); US Department of Agriculture, Fort Collins (T. Gidlewski, J.J. Root); Colorado State University, Fort Collins (A.M. Bosco-Lauth); Centers for Disease Control and Prevention, Atlanta, Georgia, USA (R.R. Lash, J.R. Harmon, W.L. Nicholson)

DOI: <https://doi.org/10.32301/eid2510.181902>

Since its recent discovery, Bourbon virus has been isolated from a human and ticks. To assess exposure of potential vertebrate reservoirs, we assayed banked serum and plasma samples from wildlife and domestic animals in Missouri, USA, for Bourbon virus–neutralizing antibodies. We detected high seroprevalence in raccoons (50%) and white-tailed deer (86%).

Bourbon virus (BRBV) was first isolated from a febrile patient with a history of tick bites in Bourbon County, Kansas, USA; the patient later died from severe illness in 2014 (1). Several additional human BRBV infections were reported subsequently from the midwestern and southern United States (2). BRBV belongs to the family *Orthomyxoviridae*, genus *Thogotovirus*, which is distributed worldwide and includes Araguari, Aransas Bay, Dhori, Jos, Thogoto, and Upolu viruses (1,3). Thogoto and Dhori viruses have been associated with human disease (4–6). Viruses within the genus *Thogotovirus* have been associated with hard or soft ticks (7). Recent studies suggest that the lone star tick (*Amblyomma americanum*) is involved with BRBV transmission (2,3,8). These ticks feed primarily on mammals, which might play a role in BRBV ecology.

We evaluated banked animal serum and plasma for evidence of BRBV infection by using the plaque-reduction neutralization test (PRNT) to detect BRBV-reactive antibodies. We tested specimens of white-tailed deer (*Odocoileus virginianus*), raccoon (*Procyon lotor*), Virginia opossum (*Didelphis virginiana*), and various other mammals and birds from northwest Missouri, USA, for neutralizing antibodies against BRBV to identify naturally exposed host species and to implicate potential zoonotic amplifiers.

¹Current affiliation: Washington State University, Pullman, Washington, USA.

We collected specimens from wild and domestic vertebrates as described (9). We performed PRNTs on serum and plasma samples by using Vero cell culture as described (9). In brief, we initially screened samples by diluting them 1:5 and mixing them with an equal amount of BRBV suspension containing ≈ 100 PFUs/0.1 mL. Samples that showed $\geq 70\%$ reduction of plaques were confirmed by serial 2-fold titration in duplicate from serum dilutions of 1:10–1:320. We considered 70% PRNT titers ≥ 10 as positive.

We screened serum and plasma samples from 301 birds and mammals for BRBV-neutralizing antibodies. A total of 48 (30.8%) of 156 mammalian serum samples were positive at the 70% neutralization level (Table). Mammals with evidence of past infection included domestic dogs, eastern cottontail, horse, raccoon, and white-tailed deer. None of 26 avian species were seropositive (Appendix Table, <https://wwwnc.cdc.gov/EID/article/25/9/18-1902-App1.pdf>).

BRBV is probably transmitted to humans and other vertebrates by the lone star tick, an abundant arthropod in the south-central United States (8). This virus was cultured from these ticks in northwestern Missouri in 2013 and eastern Kansas in 2015 (2,8). Our results indicated that mammals are frequently exposed to BRBV. This finding was expected because lone star ticks feed primarily on mammals, and rarely on birds. Our study corroborates that birds are not involved in BRBV transmission, and our data establish that the vertebrate host range for infection now includes ≥ 5 mammalian species, 2 of which are domestic animals (dogs and horses). Of the wildlife species, the seropositivity rate for white-tailed deer was high (86%), whereas Virginia opossums, despite a moderate sample size ($n = 28$), showed no evidence of virus exposure. Deer and raccoons (seroprevalence 50%) could be useful wildlife sentinels for tracking the geographic distribution of BRBV. Dogs (seroprevalence 15%) and horses (seroprevalence 4%) merit further consideration among domestic animals for use as sentinels for either tracking virus activity or as an early warning system for mitigation of human risk. Because of limited sampling, we observed no statistically significant difference in seroprevalence between these 2 species.

A limitation of our study was small sample sizes, which reduces the accuracy of the seroprevalence measurements. Furthermore, serologic data provide indirect evidence of virus infection, rather than the detection of the virus itself or its parts (i.e., antigen or nucleic acid). However, a closely related congener could exist and generate cross-reactive antibodies to BRBV, causing false-positive results in our assay. Nevertheless, the PRNT is generally considered the standard for serologic assays.

In conclusion, we have demonstrated that nonhuman vertebrates are exposed to BRBV. These findings are useful for future public health efforts and to better understand the ecology of BRBV. Specifically, we identified 2 candidate wildlife sentinels and potential domestic sentinels for tracking

Table. PRNT₇₀ results for mammals tested for Bourbon virus–neutralizing antibodies, Missouri, USA, 2012–2013*

Common name	Species name	No. positive/no. tested	Titer	Proportion positive (95% CI)
Domestic cat	<i>Felis catus</i>	0/2	<10	0 (0–0.66)
Domestic dog	<i>Canis lupus familiaris</i>	2/13	10–≥320	0.15 (0.04–0.42)
Eastern cottontail	<i>Sylvilagus floridanus</i>	2/9	≥320	0.22 (0.06–0.55)
Fox squirrel	<i>Sciurus niger</i>	0/4	<10	0 (0.0–0.49)
Horse	<i>Equus caballus</i>	1/24	20	0.04 (0.007–0.20)
Raccoon	<i>Procyon lotor</i>	31/62	10–≥320	0.50 (0.38–0.62)
Virginia opossum	<i>Didelphis virginiana</i>	0/28	<10	0 (0.0–0.12)
White-tailed deer	<i>Odocoileus virginianus</i>	12/14	10–≥320	0.86 (0.60–0.96)

*PRNT₇₀, 70% plaque reduction neutralization titer.

and possible early warning of BRBV transmission risk. However, whether any of these mammalian species are competent amplifier hosts for BRBV remains to be determined.

Acknowledgments

We thank the property owners who granted access to their properties; the Missouri Departments of Health and Senior Services and Conservation, the Andrew County Health Department and participating veterinary clinics for providing assistance; David Ashley for providing laboratory space for specimen processing at Missouri Western State University; Luke Miller, Nathan Hubbard, and Sonja Weiss for assisting with mammal trapping; and Jason Velez for preparing Vero cell cultures for the neutralization assays performed.

About the Author

During this study, Ms. Jackson was an intern at the Division of Vector-Borne Diseases, National Center for Emerging and Zoonotic Infectious Diseases, Centers for Disease Control and Prevention, Fort Collins CO. She is currently a doctoral candidate at Washington State University, Pullman, WA. Her research interests include a One Health approach to zoonotic infectious diseases.

References

- Kosoy OI, Lambert AJ, Hawkinson DJ, Pastula DM, Goldsmith CS, Hunt DC, et al. Novel thogotovirus associated with febrile illness and death, United States, 2014. *Emerg Infect Dis*. 2015;21:760–4. <https://doi.org/10.3201/eid2105.150150>
- Savage HM, Burkhalter KL, Godsey MS Jr, Panella NA, Ashley DC, Nicholson WL, et al. Bourbon virus in field-collected ticks, Missouri, USA. *Emerg Infect Dis*. 2017;23:2017–22. <https://doi.org/10.3201/eid2312.170532>
- Lambert AJ, Velez JO, Brault AC, Calvert AE, Bell-Sakyi L, Bosco-Lauth AM, et al. Molecular, serological and *in vitro* culture-based characterization of Bourbon virus, a newly described human pathogen of the genus *Thogotovirus*. *J Clin Virol*. 2015;73:127–32. <https://doi.org/10.1016/j.jcv.2015.10.021>
- Butenko AM, Leshchinskaja EV, Semashko IV, Donets MA, Mart'ianova LI. Dhori virus—a causative agent of human disease: 5 cases of laboratory infection [in Russian]. *Vopr Virusol*. 1987;32:724–9.
- Filipe AR, Calisher CH, Lazuick J. Antibodies to Congo-Crimean haemorrhagic fever, Dhori, Thogoto and Bhanja viruses in southern Portugal. *Acta Virol*. 1985;29:324–8.
- Frese M, Kochs G, Meier-Dieter U, Siebler J, Haller O. Human MxA protein inhibits tick-borne Thogoto virus but not Dhori virus. *J Virol*. 1995;69:3904–9.
- Hubálek Z, Rudolf I. Tick-borne viruses in Europe. *Parasitol Res*. 2012;111:9–36. <https://doi.org/10.1007/s00436-012-2910-1>
- Savage HM, Godsey MS Jr, Tatman J, Burkhalter KL, Hamm A, Panella NA, et al. Surveillance for Heartland and Bourbon viruses in eastern Kansas, June 2016. *J Med Entomol*. 2018;55:1613–6. <https://doi.org/10.1093/jme/tjy103>
- Bosco-Lauth AM, Panella NA, Root JJ, Gidlewski T, Lash RR, Harmon JR, et al. Serological investigation of Heartland virus (Bunyaviridae: Phlebovirus) exposure in wild and domestic animals adjacent to human case sites in Missouri 2012–2013. *Am J Trop Med Hyg*. 2015;92:1163–7. <https://doi.org/10.4269/ajtmh.14-0702>

Address for correspondence: Nicholas Komar, Centers for Disease Control and Prevention, 3156 Rampart Rd, Fort Collins, CO 80521, USA; email: nck6@cdc.gov

Fatal Case of Lassa Fever, Bangolo District, Côte d'Ivoire, 2015

Mathieu Mateo, Caroline Picard, Yahaya Sylla, Emilie Kamo, Danielle Odegue, Alexandra Journeaux, Stéphane Kouassi Kan, Marcelle Money, David N'Golo Coulibaly, Eugène Koffi, Souleymane Meite, Véronique Akran, Hervé Kadjo, Edgard Adjogoua, Solange N'Gazoa Kakou, Sylvain Baize, Mireille Dosso

Author affiliations: Institut Pasteur, Lyon, France (M. Mateo, C. Picard, A. Journeaux, S. Baize); Centre International de Recherche en Infectiologie, Lyon (M. Mateo, C. Picard, A. Journeaux, S. Baize); Institut Pasteur de Côte d'Ivoire, Abidjan, Côte d'Ivoire (Y. Sylla, E. Kamo, D. Odegue, S.K. Kan, M. Money, D. N'Golo Coulibaly, E. Koffi, S. Meite, V. Akran, H. Kadjo, E. Adjogoua, S. N'Gazoa Kakou, S. Baize, M. Dosso)

DOI: <https://doi.org/10.3201/eid2509.190239>

Lassa fever has not been reported in Côte d'Ivoire. We performed a retrospective analysis of human serum samples collected in Côte d'Ivoire in the dry seasons (January–April) during 2015–2018. We identified a fatal human case of Lassa fever in the Bangolo District of western Côte d'Ivoire during 2015.

Lassa fever is endemic to western Africa. Nigeria, Guinea, Sierra Leone, and Liberia regularly have outbreaks of Lassa fever, mostly during the first few months of the year, corresponding to the dry season (January–May), when the *Mastomys natalensis* rodent reservoir of Lassa fever virus (LASV) has more contact with the human population in rural areas to access food. The epidemic zone of Lassa fever has recently been extended into Benin, and sporadic cases have been documented in Burkina Faso, Mali, Ghana, and Togo.

Côte d'Ivoire appears to be an exception; no Lassa fever cases have been reported in this country. A tourist from Germany traveling through Côte d'Ivoire, Burkina, and Ghana died from Lassa fever upon her return to Germany but it was not possible to determine in which country she contracted the disease (1). In 2013, LASV RNA was identified in *M. natalensis* rodents captured in northern Côte d'Ivoire, near Korhogo (2). Virus RNA corresponded to the same AV strain of LASV as that isolated from the tourist, suggesting that she might have been infected in Côte d'Ivoire. Seroprevalence among forest workers in western Côte d'Ivoire also suggests that LASV might currently circulate in this country (3).

We performed a retrospective analysis of 268 human serum samples received at the National Reference Center for Yellow Fever (Institut Pasteur de Côte d'Ivoire, Abidjan, Côte d'Ivoire) for diagnosis of arbovirus infection. We selected yellow fever–negative samples from the western region of Côte d'Ivoire (Biankouma, Danané, Duékoué, Guiglo, Man, Odienné, Touba, Toulépleu, and Zouan Hounien Districts), near the borders with Liberia and Guinea collected during January–April 2015–2018.

We inactivated serum samples by using AVL buffer (QIAGEN, <https://www.qiagen.com>) and ethanol and isolated RNA by using the QIAamp Viral RNA Extraction Kit (QIAGEN). We analyzed RNA by using a reverse transcription PCR (RT-PCR) and pan–Old World arenavirus primers specific for the large RNA segment (OW RT-PCR).

We identified 1 positive serum sample (001/15) by OW RT-PCR; we then determined that this sample was LASV positive by using a LASV-specific RT-PCR specific for the glycoprotein complex (GPC) gene (Figure, panel A). We sequenced amplicons for the GPC and L genes and aligned partial sequences of this new strain, Bangolo-CIV-2015, with the corresponding regions of a set of representative published LASV strains (4).

We generated phylogenetic trees by using a general time reversible plus gamma plus proportion of invariable sites model and parallel maximum-likelihood with Phy-ML Smart Model Selection (5). The GPC (MK978784) and large RNA (MK978785) fragments of the Bangolo-CIV-2015 strain (Figure, panel B) were genetically similar to strain BA-366 isolated from an *M. natalensis* rodent captured in the Bantou District of central Guinea during 2003 (6). On the basis of these phylogenetic trees, we concluded that Bangolo-CIV-2015 belongs to the IV clade, along with the highly pathogenic LASV strain Josiah, and diverges from the clade V AV strain of LASV (Figure, panel B) found in rodents and a patient from Germany (1,2).

The LASV-positive serum sample originated from a 30-year-old man from the Bangolo District of Côte d'Ivoire who was admitted to Duékoué Hospital in January 2015 because of fever, asthenia, and gingivorrhagia. His health rapidly deteriorated after admission; he had hypotension and a consciousness disorder and died 4 days later. The sample was collected at the time of death. Further investigations by doctors at Institut Pasteur de Côte d'Ivoire were unable to obtain more information about this patient. Without the travel history of the patient during the 3 weeks preceding his hospital admission, we could not determine whether this case of Lassa fever was endemic or imported. Exported cases are common (7) because many workers travel to Côte d'Ivoire from Guinea and Sierra Leone.

Next-generation sequencing in an outbreak setting, combined with phylogenetic analyses, has recently showed that many strains of LASV have been responsible for cases of Lassa fever in Nigeria, suggesting independent transmission events from the reservoir, rather than the emergence of an epidemic strain (8). The case we report remains isolated because no other suspected cases were reported during this period. None of the healthcare workers who had been in contact with the patient showed any signs of Lassa fever. An additional set of 35 human serum samples collected during October 2014–April 2015 in the Biankouma, Duékoué, Guiglo, Issia, Man, Minignan, Odienné, Soubre, and Tengrela Districts were LASV negative by RT-PCR.

In 2015, Kouadio et al. highlighted possible underreporting of Lassa fever cases in Côte d'Ivoire because of lack of diagnoses (2). We provide evidence of a fatal case of human Lassa fever in the Bangolo District of western Côte d'Ivoire. Thus, measures should be taken to reinforce the diagnosis of Lassa fever and arenavirus surveillance in general in this country. Human serologic surveys should help in identifying the area of LASV circulation in Côte d'Ivoire. RNA from novel arenaviruses has recently been identified in rodents captured in Côte d'Ivoire, but their pathogenic potential for humans remains unknown (9).

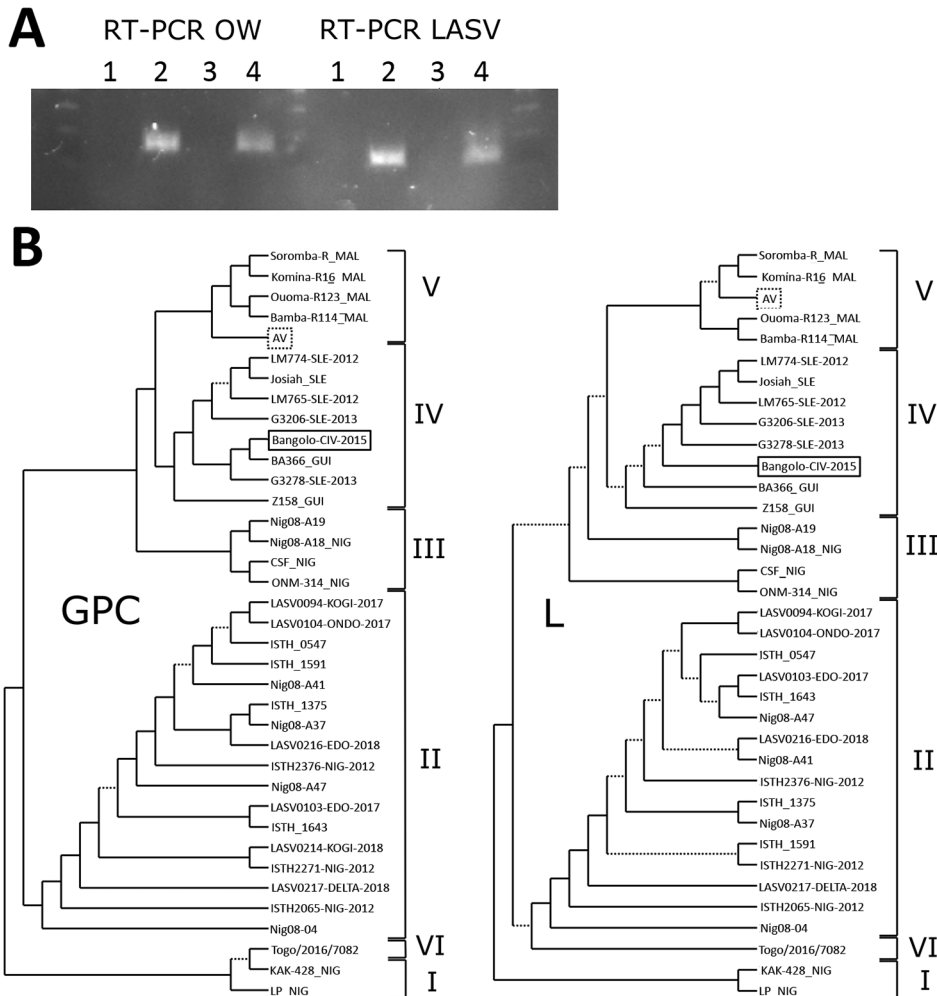


Figure. Analysis of LASV strains, Bangolo District, Côte d'Ivoire, 2015. A) RT-PCR analysis of human serum samples 132/16 and 001/15 by using OW and LASV RT-PCRs. Lane 1, negative control; lane 2, positive control; lane 3, 132/16; lane 4, 001/15. B) Phylogenetic analysis of LASV strains. Trees were inferred by using the PhyML Smart Model Selection (5) general time-reversible plus gamma plus proportion of invariable sites model with 200 bootstrap replicates. Poorly supported branches with bootstrap values <0.50 are indicated by dotted lines. Lassa virus lineages are indicated by the Roman numerals on the right. The Bangolo-CIV-2015 strain (solid box), which was isolated in this study, appears to be related to clade IV, and the AV strain (dotted box) is related to clade V. GPC, glycoprotein complex gene; L, large RNA segment; LASV, Lassa virus; OW, Old World; RT-PCR, reverse transcription PCR.

Acknowledgments

We thank the Ministère de la Santé et de l'Hygiène Publique de Côte d'Ivoire and personnel from Duékoué Hospital for providing information about the patient; all members of Département des Virus Epidémiques, Plateforme de Biologie Moléculaire, and Département Technique et Technologie at IPCI and West African Biobank for assistance and support during the visit of M.M. to the IPCI; Ghislain Tiemoko Gueu for technical assistance in managing human samples; N'cho Sonan for helpful discussions; Marc Jouan and Marianne Lucas-Hourani for administrative and logistical assistance; and Frédéric Lemoine for assistance with phylogenetic analyses.

This study was supported by the Institut Pasteur (grant Y-SU16001-13 to M.M.).

About the Author

Dr. Mateo is a research scientist in the Unit of Biology of Emerging Viral Infections, Institut Pasteur, Lyon, France. His primary research interest is viral hemorrhagic fevers.

References

- Günther S, Emmerich P, Laue T, Kühle O, Asper M, Jung A, et al. Imported lassa fever in Germany: molecular characterization of a new Lassa virus strain. *Emerg Infect Dis.* 2000;6:466–76. <https://doi.org/10.3201/eid0605.000504>
- Kouadio L, Nowak K, Akoua-Koffi C, Weiss S, Allali BK, Witkowski PT, et al. Lassa virus in multimammate rats, Côte d'Ivoire, 2013. *Emerg Infect Dis.* 2015;21:1481–3. <https://doi.org/10.3201/eid2108.150312>
- Akoua-Koffi C, Ter Meulen J, Legros D, Akran V, Aidara M, Nahounou N, et al. Detection of anti-Lassa antibodies in the Western Forest area of the Ivory Coast [in French]. *Med Trop (Mars).* 2006;66:465–8.
- Andersen KG, Shapiro BJ, Matranga CB, Sealfon R, Lin AE, Moses LM, et al.; Viral Hemorrhagic Fever Consortium. Clinical sequencing uncovers origins and evolution of Lassa virus. *Cell.* 2015;162:738–50. <https://doi.org/10.1016/j.cell.2015.07.020>
- Lefort V, Longueville JE, Gascuel O. SMS: smart model selection in PhyML. *Mol Biol Evol.* 2017;34:2422–4. <https://doi.org/10.1093/molbev/msx149>
- Lecompte E, Fichet-Calvet E, Daffis S, Koulémou K, Sylla O, Kourouma F, et al. *Mastomys natalensis* and Lassa fever, West Africa. *Emerg Infect Dis.* 2006;12:1971–4. <https://doi.org/10.3201/eid1212.060812>

7. Kofman A, Choi MJ, Rollin PE. Lassa fever in travelers from West Africa, 1969–2016. *Emerg Infect Dis*. 2019;25:245–8. <https://doi.org/10.3201/eid2502.180836>
8. Kafetzopoulou LE, Pullan ST, Lemey P, Suchard MA, Ehichioya DU, Pahlmann M, et al. Metagenomic sequencing at the epicenter of the Nigeria 2018 Lassa fever outbreak. *Science*. 2019;363:74–7. <https://doi.org/10.1126/science.aau9343>
9. Coulibaly-N'Golo D, Allali B, Kouassi SK, Fichet-Calvet E, Becker-Ziaja B, Rieger T, et al. Novel arenavirus sequences in *Hylomyscus* sp. and *Mus (Nannomys) setulosus* from Côte d'Ivoire: implications for evolution of arenaviruses in Africa. *PLoS One*. 2011;6:e20893. <https://doi.org/10.1371/journal.pone.0020893>

Address for correspondence: Mathieu Mateo, Unit of Biology of Emerging Viral Infections, Institut Pasteur, 21 Ave Tony Garnier, Lyon 69007, France; email: mathieu.mateo@pasteur.fr

Household Transmission of Human Adenovirus Type 55 in Case of Fatal Acute Respiratory Disease

Shuping Jing,¹ Jing Zhang,¹ Mengchan Cao, Minhong Liu, Yuqian Yan, Shan Zhao, Na Cao, Junxian Ou, Kui Ma, Xiangran Cai, Jianguo Wu, Ya-Fang Mei, Qiwei Zhang

Author affiliations: Southern Medical University, Guangzhou, China (S. Jing, J. Zhang, Y. Yan, S. Zhao, N. Cao, J. Ou, Q. Zhang); Guangdong Provincial Key Laboratory of Tropical Disease Research, Guangzhou (S. Jing, J. Zhang, Y. Yan, S. Zhao, N. Cao, J. Ou, Q. Zhang); Anqing Center for Disease Control and Prevention, Anhui, China (M. Cao, M. Liu); Jinan University, Guangzhou, China (K. Ma, X. Cai, J. Wu, Q. Zhang); Umeå University, Umeå, Sweden (Y.-F. Mei)

DOI: <https://doi.org/10.3201/eid2509.181937>

We identified a case of fatal acute respiratory disease from household transmission of human adenovirus type 55 (HAdV-55) in Anhui Province, China. Computed tomography showed severe pneumonia. Comparative genomic analysis of HAdV-55 indicated the virus possibly originated in Shanxi Province, China. More attention should be paid to highly contagious HAdV-55.

¹These authors contributed equally to this article.

Human adenoviruses are associated with mild and acute respiratory infections, depending on the virus type and host immunity. Human adenovirus type 55 (HAdV-55) (1), formerly known as HAdV-11a (2), is a reemergent respiratory pathogen that has caused severe pneumonia outbreaks in military and civilian populations in Europe and Asia (2–7). However, household transmission of HAdV-55 is rarely reported. We report a case of household transmission of HAdV-55 involving 3 confirmed adult cases with 1 death. Epidemiologic, clinical, and laboratory investigations, along with whole-genome sequencing, elucidate the disease progression and the pathogen origin.

During April 1–May 5, 2012, 7 household members (5 males and 2 females; 3 children and 4 adults) in Anhui Province, China, sequentially experienced influenza-like symptoms, including fever, productive cough, fatigue, pharyngalgia, dyspnea, and other symptoms. The youngest patient was 4 months of age, the oldest, whom we refer to as AQ-1, was a 55-year-old man. The family lived together near a farm in a house with poor sanitary and ventilation conditions.

The first onset of acute respiratory disease (ARD) occurred on April 1, when the index case, a 4-year-old granddaughter of AQ-1, had a febrile respiratory infection with cough. Three days later, AQ-1's grandson, 1 year of age, displayed similar symptoms. On April 9 and 11, AQ-1's daughter, 28 years of age, and another grandson, 4 months of age, both had influenza-like symptoms. On April 14, AQ-1 had a fever, chills, and lumbago. He was admitted to the hospital on April 14 where clinicians diagnosed pneumonia. AQ-1 had close contact with his sick grandsons and granddaughter and had not been out of the house during the month he cared for them.

While hospitalized, AQ-1 had bilateral pneumonia seen on chest computed tomography (CT), a temperature of 41.0°C, and low total leukocyte ($3.63 \times 10^9/L$) and platelet ($42 \times 10^9/L$) counts. AQ-1 sustained high fever and yellow phlegm despite antiinflammatory and antiviral treatment, including levofloxacin, piperacillin sodium, tazobactam sodium, and ribavirin.

On April 24, AQ-1 had indications of severe pneumonia, including respiratory failure, hypoxemia, double lung rales, and a mass of shadows visible on chest CT. In addition, he had indications of liver damage and multi-organ failure. Transverse chest CT images demonstrated increased areas of patchy shadows and consolidation in both lungs compared to CT images from April 22, indicative of disease progression (Appendix Figure 1, <http://wwwnc.cdc.gov/EID/article/25/9/18-1937-App1.pdf>).

AQ-1 died on April 27, 3 days after onset of respiratory failure, and 13 days after his illness began. On the same day, his 20-year-old son, AQ-2, and 31-year-old nephew, AQ-3, who had taken care of AQ-1 for 5 days, also exhibited

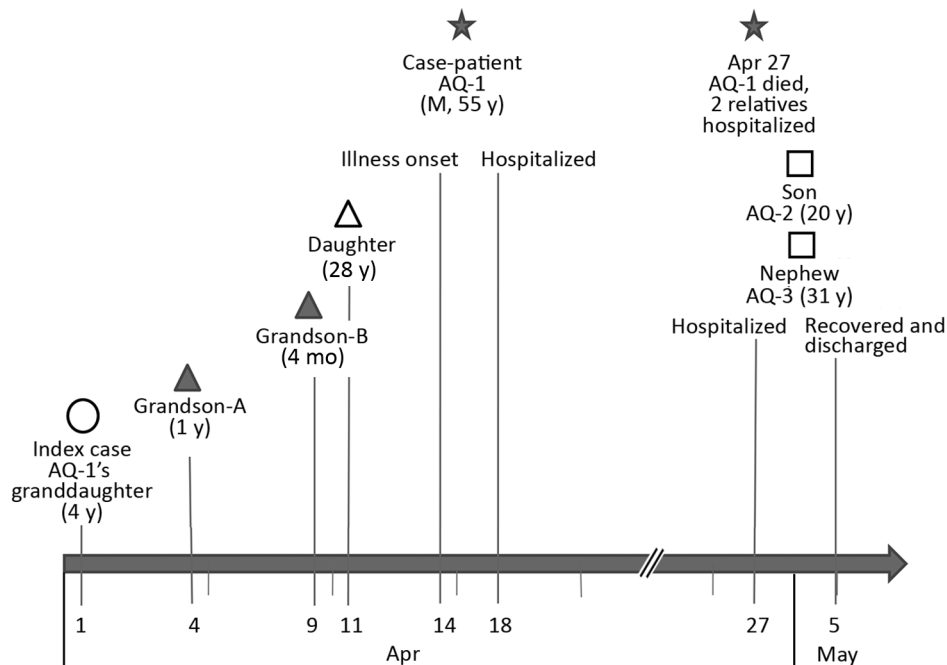


Figure. Timeline of patients' illness onset in a household cluster of acute respiratory disease from human adenovirus 55, Anhui Province, China, 2012. The star indicates AQ-1, the case described in this study. Case relationships to AQ-1 are indicated along with their ages at the date of their illness onset.

symptoms of influenza-like illness. Both were hospitalized and had normal chest CT scans, but AQ-2's leukocyte count was $5.4 \times 10^9/L$ and AQ-3's was $6.7 \times 10^9/L$. After anti-inflammatory and antiviral treatment, including vitamin C, sulbactam, amoxicillin, amikacin, cefoperazone, ribavirin, and oseltamivir, they recovered and were discharged on May 5 (Figure).

We tested endotracheal aspirates from AQ-1 and throat swabs from AQ-2 and AQ-3 for influenza A and B viruses, severe acute respiratory syndrome coronavirus, human metapneumovirus, rhinoviruses, parainfluenza viruses 1–4, and HAdVs by real-time PCR. Only adenovirus was strongly positive for all 3 patients. Testing for antibodies against *Mycoplasma pneumoniae*, *Mycobacterium tuberculosis*, *Treponema pallidum*, hepatitis B and C viruses, and HIV were all negative. After treatment, samples from AQ-2 and AQ-3, were negative for adenovirus by PCR.

We isolated AQ-1's adenovirus in culture and sequenced the genome (GenBank accession no. KP279748). Sequences for the hexon, penton base, and fiber genes were identical to those previously reported for HAdV-55. Phylogenetic analysis showed that the 3 isolates clustered closely with other strains from China (Appendix Figure 2). The genome of AQ-1's strain had the highest nucleotide identity (99.951%) with QZ01_2011, an isolate from a military trainee in Shanxi Province, China. The second highest identity (99.948%) was with QS-DLL_2006, which caused a fatal ARD outbreak in a senior high school in Shaanxi Province, China (1,8) (Appendix Table). We hypothesize the strain infecting AQ-1 and his family originated from Shanxi Province.

In this household transmission of ARD, the index case was a probable case because no specimens were collected to confirm virologic identification. From the timeline of illness onset in this household cluster of ARD cases (Figure), we suspect that the pathogen spread rapidly among the children and further circulated in adults who had close contact with infected children and one another.

HAdV-55 contains a 97.4% genome of HAdV-14 and a hexon from HAdV-11 (1). Since 2006, HAdV-14 has caused severe ARD in America, Europe, and Asia (8,9), with high hospitalization (38%) and case-fatality (5%) rates (10). Because the risk for infection among the close contacts may rise, more attention should be paid to these highly contagious pathogens.

This study was approved by the institutional review board of Anqing Center for Disease Control and Prevention and was supported by the National Natural Science Foundation of China (grant nos. 31570155, 31370199, 81730061, 81471942) and Guangzhou Healthcare Collaborative Innovation Major Project (grant nos. 201803040004, 201803040007).

About the Author

Ms. Jing was a graduate student at Southern Medical University and works at Zhuhai Center for Disease Control and Prevention, Guangdong Province, China. Her research interest is the epidemiology of human adenoviruses. Jing Zhang is a PhD candidate at Southern Medical University, Guangzhou, China, whose primary research interests are genomics and evolution of human adenoviruses.

References

- Walsh MP, Seto J, Jones MS, Chodosh J, Xu W, Seto D. Computational analysis identifies human adenovirus type 55 as a re-emergent acute respiratory disease pathogen. *J Clin Microbiol*. 2010;48:991–3. <http://dx.doi.org/10.1128/JCM.01694-09>
- Kajon AE, Dickson LM, Metzgar D, Houg HS, Lee V, Tan BH. Outbreak of febrile respiratory illness associated with adenovirus 11a infection in a Singapore military training camp. *J Clin Microbiol*. 2010;48:1438–41. <http://dx.doi.org/10.1128/JCM.01928-09>
- Cao B, Huang GH, Pu ZH, Qu JX, Yu XM, Zhu Z, et al. Emergence of community-acquired adenovirus type 55 as a cause of community-onset pneumonia. *Chest*. 2014;145:79–86. <http://dx.doi.org/10.1378/chest.13-1186>
- Salama M, Amitai Z, Amir N, Gottesman-Yekutieli T, Sherbany H, Drori Y, et al. Outbreak of adenovirus type 55 infection in Israel. *J Clin Virol*. 2016;78:31–5. <http://dx.doi.org/10.1016/j.jcv.2016.03.002>
- Lafolie J, Mirand A, Salmona M, Lautrette A, Archimbaud C, Brebion A, et al. Severe pneumonia associated with adenovirus type 55 infection, France, 2014. *Emerg Infect Dis*. 2016;22:2012–4. <http://dx.doi.org/10.3201/eid2211.160728>
- Heo JY, Noh JY, Jeong HW, Choe KW, Song JY, Kim WJ, et al. Molecular epidemiology of human adenovirus-associated febrile respiratory illness in soldiers, South Korea. *Emerg Infect Dis*. 2018;24:1221–7. <http://dx.doi.org/10.3201/eid2407.171222>
- Zhu Z, Zhang Y, Xu S, Yu P, Tian X, Wang L, et al. Outbreak of acute respiratory disease in China caused by B2 species of adenovirus type 11. *J Clin Microbiol*. 2009;47:697–703. <http://dx.doi.org/10.1128/JCM.01769-08>
- Carr MJ, Kajon AE, Lu X, Dunford L, O'Reilly P, Holder P, et al. Deaths associated with human adenovirus-14p1 infections, Europe, 2009–2010. *Emerg Infect Dis*. 2011;17:1402–8. <http://dx.doi.org/10.3201/1708.101760>
- Huang G, Yu D, Zhu Z, Zhao H, Wang P, Gray GC, et al. Outbreak of febrile respiratory illness associated with human adenovirus type 14p1 in Gansu Province, China. *Influenza Other Respi Viruses*. 2013;7:1048–54. <http://dx.doi.org/10.1111/irv.12118>
- Centers for Disease Control and Prevention. Acute respiratory disease associated with adenovirus serotype 14—four states, 2006–2007. *MMWR Morb Mortal Wkly Rep*. 2007; 56:1181–4.

Address for correspondence: Qiwei Zhang, Southern Medical University, School of Public Health, 1838 N Guangzhou Ave, Guangzhou, Guangdong 510515, China; email: zhangqw@smu.edu.cn.

Worldwide Reduction in MERS Cases and Deaths since 2016

Christl A. Donnelly, Mamun R. Malik, Amgad Elkholy, Simon Cauchemez, Maria D. Van Kerkhove

Author affiliations: University of Oxford, Oxford, UK (C.A. Donnelly); Imperial College London, London, UK (C.A. Donnelly); World Health Organization Regional Office for the Eastern Mediterranean, Cairo, Egypt (M.R. Malik, A. Elkholy); Institut Pasteur, Paris, France (S. Cauchemez); World Health Organization, Geneva, Switzerland (M.D. Van Kerkhove)

DOI: <https://doi.org/10.3201/eid2509.190143>

Since 2012, Middle East respiratory syndrome (MERS) coronavirus has infected 2,442 persons worldwide. Case-based data analysis suggests that since 2016, as many as 1,465 cases and 293–520 deaths might have been averted. Efforts to reduce the global MERS threat are working, but countries must maintain vigilance to prevent further infections.

From 2012 through May 31, 2019, Middle East respiratory syndrome coronavirus (MERS-CoV) has infected 2,442 persons and killed 842 worldwide (1). MERS-CoV is currently circulating in dromedary camels in Africa, the Middle East, and southern Asia; however, most cases of human infection have been reported in the Arabian Peninsula (2). Large hospital outbreaks in 2014 and 2015 (3,4) (Appendix Figure 1, <https://wwwnc.cdc.gov/EID/article/25/9/19-0143-F1.htm>) motivated affected countries to substantially invest in prevention and control activities.

To estimate the potential number of MERS cases and deaths that might have been averted since 2016 had the risk levels of 2014–2015 continued, we analyzed case-based data on laboratory-confirmed human cases of MERS-CoV infections reported to the World Health Organization (5). We categorized cases as either secondary (human-to-human transmission) or community-acquired (presumed camel-to-human transmission). In addition, we used case-based data on date of onset (for symptomatic infections) or report (for asymptomatic infections), outcome (died/recovered), and dates and sizes of reported clusters of human-to-human–transmission cases (3,4,6–8).

We compared incidence of camel-to-human–transmission cases (i.e., community-acquired cases, assuming all of those not positively attributed to human-to-human transmission were in this category) during 2016, 2017, and 2018 (through September only) with incidence during 2014–2015, assuming that case numbers were Poisson distributed

(yielding a 2-sided *p* value). Furthermore, we obtained the expected total number of cases in 2016, 2017, and through September 2018, conditional on the incidence of community-acquired cases, by simulating 10,000 times from the distribution of human-to-human transmission cluster sizes observed during 2014–2015. Thus, the observed incidence rates in these years could be compared with simulations to test the null hypothesis that human-to-human transmission levels remained constant since 2014–2015 (yielding a 2-sided *p* value). The intervals reported are the 2.5th and 97.5th percentiles of the simulations (95% CIs). We examined a range of mortality rates from healthcare-associated outbreaks in South Korea and Saudi Arabia (3,5) and the case-fatality ratio (CFR) from all reported cases globally (35.5%, 800 fatalities/2,254 cases) (9). When numbers of cases averted were not statistically significant, we truncated the lower bound of the 95% CI to 0 cases averted.

Of the 2,254 laboratory-confirmed cases reported to the World Health Organization from 2012 through October 1, 2018 (Appendix Figure 1), 1,087 were classified as human-to-human transmission cases and the remaining 1,167 as community-acquired cases. During this same period, clusters/outbreaks were reported each year (range 2–255 cases).

Although 739 cases were reported in 2014 and 768 cases in 2015, only 244 cases were reported in 2016, another 244 in 2017, and 113 through September 2018. We assessed potential components of this reduction (i.e., reduction of community-acquired cases, human-to-human transmission cases, or both). The incidence of community-acquired cases was 177 in 2016, 151 in 2017, and 86 through September 2018 (Appendix Table). These rates were each significantly ($p < 0.001$) lower than expected compared with the incidence in 2014–2015 (334 for 2016, 334 for 2017, and 251 through September 2018). Conditional on the number of community-acquired cases, we observed no significant reduction in the risk for secondary cases from 2014–2015 to 2016, 2017, and through September 2018, although we did find nonsignificant trends. We estimated that 154 secondary cases (95% CI 0–495) were averted from the 177 community-acquired cases in 2016,

96 (95% CI 0–419) from the 151 community-acquired cases in 2017, and 80 (95% CI 0–338) from the 86 community-acquired cases through September 2018, totaling 330 (95% CI 0–819) from the 414 community-acquired cases during 2016–September 2018 (Table). Assuming a 20% CFR (3,10), these 330 (95% CI 0–819) cases averted correspond to 66 (95% CI 0–164) expected deaths averted; assuming a 35.5% CFR (9), they correspond to 117 (95% CI 0–291) expected deaths averted.

The total number of cases averted, when simultaneously taking into account reduced camel-to-human and human-to-human transmission, was estimated at 507 (95% CI 189–967) in 2016, 507 (95% CI 189–967) in 2017, and 451 (95% CI 191–855) through September 2018, totaling 1,465 (95% CI 895–2,165) cases averted and 293 (95% CI 179–433) expected deaths averted (under the assumption of a 20% CFR) from 2016 through September 2018. Assuming a 35.5% CFR, this estimate corresponds to 520 (95% CI 318–769) expected deaths averted.

We believe that affected countries are reducing the global threat of MERS by addressing knowledge gaps with regard to transmission, enhancing surveillance, and strengthening the ability to detect cases early and contain outbreaks through improved infection prevention and control measures in hospitals. Critical for preventing international spread and sustained transmission have been improved prevention and control measures in hospitals, restriction of camel movement in affected areas, stronger and more comprehensive investigations of cases and clusters, and improved communication.

Although global efforts seem to have prevented hundreds of infections and deaths, vigilance must be maintained by all countries. More needs to be done to limit spillover infections from dromedaries, which requires stronger surveillance of dromedary populations and persons in direct contact with infected herds and accelerated development of a vaccine for dromedaries (2). The international community and affected countries have a collective and shared responsibility to curtail a major health security threat such as MERS in the Middle East and beyond.

Table. Estimated Middle East respiratory syndrome cases and deaths averted because of reduced human-to-human transmission and camel-to-human transmission*

Year	Estimated cases and deaths averted because of reduced human-to-human transmission†				Estimated cases and deaths averted because of reduced camel-to-human and human-to-human transmission			
	Cases averted‡	2-sided <i>p</i> value	Deaths averted		Cases averted‡	2-sided <i>p</i> value	Deaths averted	
			Assuming 20% CFR‡	Assuming 35.5% CFR‡			Assuming 20% CFR‡	Assuming 35.5% CFR‡
2016	154 (0–495)	0.2714	31 (0–99)	55 (0–176)	507 (189–967)	<0.0001	101 (38–193)	180 (67–343)
2017	96 (0–419)	0.5810	19 (0–84)	34 (0–149)	507 (189–967)	<0.0001	101 (38–193)	180 (67–343)
2018§	80 (0–338)	0.4316	16 (0–68)	29 (0–120)	451 (191–855)	<0.0001	90 (38–171)	160 (68–304)
2016–2018§	330 (0–819)	0.0896	66 (0–164)	117 (0–291)	1,465 (895–2,165)	<0.0001	293 (179–433)	520 (318–769)

*Values are estimated no. (95% range) except as indicated. CFR, case-fatality ratio.

†Conditional on reported community-acquired cases.

‡The 95% intervals reported are the 2.5th and 97.5th percentiles of the simulations. When cases averted were not statistically significant, we truncated the lower bound of the 95% CI to 0 cases averted.

§Through September 2018.

Acknowledgments

We thank the many ministry and government officials working to detect and respond to MERS cases and clusters.

C.A.D. thanks the UK Medical Research Council for center funding (MR/R015600/1) and the National Institute for Health Research for funding the NIHR Health Protection Research Unit in Modelling Methodology and the Vaccine Efficacy Evaluation for Priority Emerging Diseases Epidemic Modelling Consortium (EPIDZO34). S.C. acknowledges financial support from the Investissement d'Avenir program, the Laboratoire d'Excellence Integrative Biology of Emerging Infectious Diseases program (grant ANR-10-LABX-62-IBEID), the Models of Infectious Disease Agent Study of the National Institute of General Medical Sciences, and the AXA Research Fund.

About the Author

Dr. Donnelly is a professor of applied statistics at the University of Oxford and a professor of statistical epidemiology at Imperial College London. As a statistician and epidemiologist, her research interest is the spread and control of infectious diseases, with a particular focus on outbreaks.

References

- World Health Organization. Middle East respiratory syndrome coronavirus (MERS-CoV) [cited 2019 June 4]. <http://www.who.int/emergencies/mers-cov>
- FAO-OIE-WHO MERS Technical Working Group. MERS: progress on the global response, remaining challenges and the way forward. *Antiviral Res.* 2018;159:35–44. <https://doi.org/10.1016/j.antiviral.2018.09.002>
- Ki M. 2015 MERS outbreak in Korea: hospital-to-hospital transmission. *Epidemiol Health.* 2015;37:e2015033. <https://doi.org/10.4178/epih/e2015033>
- Oboho IK, Tomczyk SM, Al-Asmari AM, Banjar AA, Al-Mugti H, Aloraini MS, et al. 2014 MERS-CoV outbreak in Jeddah—a link to health care facilities. *N Engl J Med.* 2015;372:846–54. <https://doi.org/10.1056/NEJMoa1408636>
- World Health Organization. 2017 Middle East respiratory syndrome coronavirus: case definition for reporting to WHO [cited 2019 Jun 4]. https://www.who.int/csr/disease/coronavirus_infections/case_definition
- Balkhy HH, Alenazi TH, Alshamrani MM, Baffoe-Bonnie H, Al-Abdely HM, El-Saed A, et al. Notes from the field: nosocomial outbreak of Middle East respiratory syndrome in a large tertiary care hospital—Riyadh, Saudi Arabia, 2015. *MMWR Morb Mortal Wkly Rep.* 2016;65:163–4. <https://doi.org/10.15585/mmwr.mm6506a5>
- Assiri A, McGeer A, Perl TM, Price CS, Al Rabeeah AA, Cummings DA, et al.; KSA MERS-CoV Investigation Team. Hospital outbreak of Middle East respiratory syndrome coronavirus. *N Engl J Med.* 2013;369:407–16. <https://doi.org/10.1056/NEJMoa1306742>
- Bernard-Stoecklin S, Nikolay B, Assiri A, Aziz Bin Saeed AA, Karim Ben Embarek P, El Bushra H, et al. Comparative analysis of eleven healthcare-associated outbreaks of MERS-CoV from 2015–2017. *Sci Rep.* 2019;9:7385. <https://doi.org/10.1038/s41598-019-43586-9>
- World Health Organization. Middle East respiratory syndrome coronavirus (MERS-CoV) [cited 2019 Jun 4]. <http://www.who.int/emergencies/mers-cov>
- World Health Organization. Middle East respiratory syndrome coronavirus (MERS-CoV) infection—Republic of Korea [cited 2019 Jun 4]. <http://www.who.int/csr/don/12-september-2018-mers-republic-of-korea>

Address for correspondence: Maria D. Van Kerkhove, World Health Organization, High Threat Pathogens, Global Infectious Hazards Management, Health Emergencies Program, Geneva, Switzerland; email: vankerkhovem@who.int

Limited Scope of Shorter Drug Regimen for MDR TB Caused by High Resistance to Fluoroquinolone

Pravin K. Singh, Amita Jain

Author affiliation: King George Medical University, Lucknow, India

DOI: <https://doi.org/10.3201/eid2509.190105>

Resistance to second-line tuberculosis drugs for patients with multidrug-resistant tuberculosis has emerged globally and is a potential risk factor for unfavorable outcomes of shorter duration drug regimens. We assessed the proportion of patients eligible for a shorter drug regimen in Uttar Pradesh, India, which had the highest rate of multidrug-resistant tuberculosis in India.

India has the largest burden of multidrug-resistant (MDR) tuberculosis (TB) worldwide (1). The success rate for MDR TB treatment is low (47%), largely caused by death, suboptimal adherence of patients to long treatment courses, and frequent drug-related adverse events (2).

In 2016, the World Health Organization recommended a shorter drug regimen (9–12 months) for patients with MDR TB or rifampin-resistant TB who had not received second-line drugs (SLDs) and in whom resistance to fluoroquinolones and injectable SLDs is considered highly unlikely (3). A shorter regimen is a promising step toward high treatment success rates. Recently, this regimen was instituted in Uttar Pradesh, which has ≈20% of the total

MDR TB and rifampin-resistant TB burden in India (2). We assessed the proportion of rifampin-resistant TB patients in Uttar Pradesh who would be eligible for a shorter regimen under a programmatic setting.

Under the Revised National Tuberculosis Control Program for India, all TB patients are tested for drug susceptibility for at least rifampin by the GeneXpert MTB/RIF assay (<http://www.cephheid.com>), which is available in every district laboratory. Two samples per patient are usually collected, and if rifampin-resistant TB is confirmed, the second sample is transported to the state laboratory for susceptibility testing of SLDs by line-probe assay (LPA) (LPA-SLD Genotype MTBDRsl; Bruker, <https://www.hain-lifescience.de>). Because it might take ≈ 1 week to obtain an LPA-SLD result, a shorter treatment regimen is initiated without delay for all patients with rifampin-resistant TB, except for patients who have received SLDs, those with extrapulmonary TB, and those who are pregnant (4). If resistance to SLD is detected, patients are given an appropriate, longer treatment regimen.

Over a 2-month period (July–August 2018), sputum samples from 708 patients with rifampin-resistant TB (1 sample/patient) were collected before treatment with any SLDs and submitted to our reference laboratory for LPA-SLD. Smears from each sputum sample were examined for acid-fast bacilli (AFB). AFB-positive samples were subjected directly to LPA, AFB-negative samples were cultured in *Mycobacterium* growth indicator tube liquid medium, and LPA was performed indirectly for culture isolates, if recovered. LPA testing on smear-positive sputum samples with inconclusive results (*Mycobacterium tuberculosis* not detected/indeterminate resistance/invalid) was

repeated by using the indirect method. Resistance patterns for fluoroquinolones and injectable SLD (as determined by LPA-SLD) were analyzed.

Of 708 samples, drug susceptibilities were determined for 541 (498 by direct LPA and 43 by indirect LPA). For the remaining 167 samples (AFB negative, 112; AFB scanty, 52), results were inconclusive because of no growth or contamination (Figure). Plausible reasons for lower rate of culture recovery include testing of only AFB-negative/scanty samples, expected low culture yield if patients have a history of tuberculosis treatment or if a sample was of suboptimal quality (5), and a harsh decontamination process used for the sample. This last reason is unlikely because the culture contamination rate was not lower than standard range.

In our study, a high proportion (21.4%) of patients were smear negative, although they were given a diagnosis of rifampin-resistant TB by GeneXpert. Low analytical sensitivity for smear microscopy (compared with that for GeneXpert) could be a potential reason. This observation highlights the need of submitting 2 quality samples for LPA.

Of 541 conclusive LPA-SLD results, the proportion of strains resistant to only fluoroquinolone was 50.1%, to injectable SLD 1.5%, and to fluoroquinolone and injectable SLD 8.3%. Fluoroquinolone resistance (with or without injectable SLD resistance) was high, indicating that 58.4% of patients were ineligible for a shorter regimen. This estimate raises concern because, in an earlier trial of a shorter regimen, fluoroquinolone resistance was a key risk factor for a bacteriologically unfavorable outcome (6).

Our estimate might not be a true representation for fluoroquinolone resistance burden because we included only

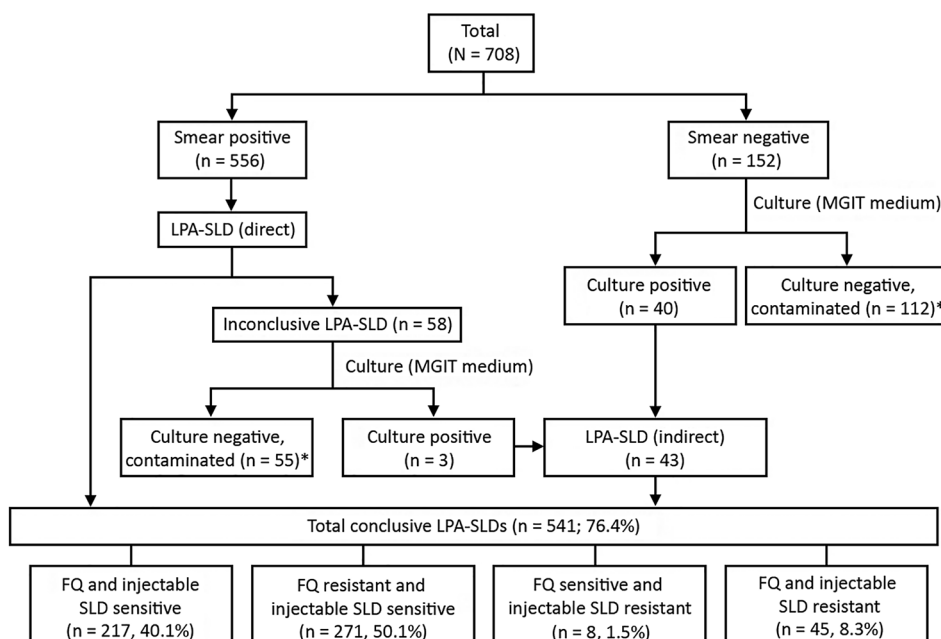


Figure. Flow diagram of participants and testing results in study of limitation of shorter treatment regimen for multidrug-resistant tuberculosis by high resistance to fluoroquinolone, Uttar Pradesh, India. *Inconclusive LPA-SLD (n = 167; 23.6% of total samples received). LPA-SLD, line-probe assay for second-line drugs; FQ, fluoroquinolones; MGIT, *Mycobacterium* growth indicator tube.

rifampin-resistant TB patients in our study, not patients with rifampin-susceptible but fluoroquinolone-resistant TB. Nevertheless, our estimate might be extrapolated for a programmatic setting in Uttar Pradesh because the number of patients in the study was $\approx 7.0\%$ of MDR TB and rifampin-resistant TB patients reported in Uttar Pradesh during 2017 (1).

In India, a high incidence of fluoroquinolone-resistant TB has been reported (7,8). It is believed that widespread and indiscriminate use of fluoroquinolones was a key contributor. However, primary resistance caused by transmission of fluoroquinolone-resistant strains might be a potential reason for such a high rate of fluoroquinolone resistance. This hypothesis is well supported by increasing evidence for countries with high burdens of TB where MDR TB is increasing in patients who have not received TB treatment (9,10). In our study, we could not stratify our data into new and previously treated patients because of the observational design and limited access to patient information.

Considering high levels of fluoroquinolone resistance and possible intolerance/resistance to certain drugs in a regimen, only $\approx 40.0\%$ of rifampin-resistant TB patients would be eligible for a shorter drug regimen in our setting. Thus, a shorter regimen should not be an obvious choice for empiric treatment of MDR TB or rifampin-resistant TB patients in this region.

Acknowledgment

We thank the Central TB Division (New Delhi), State TB Cell (Lucknow) for providing kits and consumables for MDR TB diagnostic services at our reference laboratory and the laboratory staff at King George Medical University, Lucknow, India, for their contributions to this study.

About the Authors

Dr. Singh is a microbiologist at the Intermediate Reference Laboratory, Department of Microbiology, King George Medical University, Lucknow, Uttar Pradesh, India. His research interests are diagnosis and epidemiology of infectious diseases.

Dr. Jain is a professor and head of the Department of Microbiology, King George Medical University, Lucknow, Uttar Pradesh, India. Her research interests are tuberculosis, virology, and clinical microbiology.

References

1. World Health Organization. Global tuberculosis report 2018 [cited 2019 Jun 24]. https://www.who.int/tb/publications/global_report
2. India TB. Report 2018—Revised National Tuberculosis Control Program Annual Status Report 2018: Central TB Division, Directorate General of Health Services, Government of India; 2018 [cited 2019 Jun 24]. <https://tbcindia.gov.in>
3. World Health Organization. Treatment guidelines for drug-resistant tuberculosis, 2016 update [cited 2019 Jun 24]. <https://apps.who.int/medicinedocs/en/m/abstract/Js23097en>
4. Programmatic Management of Drug Resistance, 2017. Guidelines on programmatic management of drug resistant tuberculosis in India 2017: Central TB Division, Directorate General of Health Services, Government of India; 2018 [cited 2019 Jun 24]. <https://tbcindia.gov.in/index1.php?lang=1&level=2&sublinkid=4780&lid=3306>
5. Shi J, Dong W, Ma Y, Liang Q, Shang Y, Wang F, et al. GeneXpert MTB/RIF outperforms Mycobacterial culture in detecting *Mycobacterium tuberculosis* from salivary sputum. *BioMed Res Int*. 2018;2018:1514381. <https://doi.org/10.1155/2018/1514381>
6. Aung KJ, Van Deun A, Declercq E, Sarker MR, Das PK, Hossain MA, et al. Successful '9-month Bangladesh regimen' for multidrug-resistant tuberculosis among over 500 consecutive patients. *Int J Tuberc Lung Dis*. 2014;18:1180–7. <https://doi.org/10.5588/ijtld.14.0100>
7. Agrawal D, Udawadia ZF, Rodriguez C, Mehta A. Increasing incidence of fluoroquinolone-resistant *Mycobacterium tuberculosis* in Mumbai, India. *Int J Tuberc Lung Dis*. 2009;13:79–83.
8. Jain A, Dixit P, Prasad R. Pre-XDR and XDR in MDR and ofloxacin and kanamycin resistance in non-MDR *Mycobacterium tuberculosis* isolates. *Tuberculosis (Edinb)*. 2012;92:404–6. <https://doi.org/10.1016/j.tube.2012.05.010>
9. Zhao M, Li X, Xu P, Shen X, Gui X, Wang L, et al. Transmission of MDR and XDR tuberculosis in Shanghai, China. *PLoS One*. 2009;4:e4370. <https://doi.org/10.1371/journal.pone.0004370>
10. Shah NS, Auld SC, Brust JC, Mathema B, Ismail N, Moodley P, et al. Transmission of extensively drug-resistant tuberculosis in South Africa. *N Engl J Med*. 2017;376:243–53. <https://doi.org/10.1056/NEJMoa1604544>

Address for correspondence: Amita Jain, Department of Microbiology, King George Medical University, Lucknow, Uttar Pradesh, India; email: amita602002@yahoo.com

***Candida auris* in Germany and Previous Exposure to Foreign Healthcare**

Axel Hamprecht, Amelia E. Barber, Sibylle C. Mellinghoff, Philipp Thelen, Grit Walther, Yanying Yu, Priya Neurgaonkar, Thomas Dandekar, Oliver A. Cornely, Ronny Martin, Oliver Kurzai, on behalf of the German *Candida auris* Study Group¹

Author affiliations: German Centre for Infection Research, Cologne, Germany (A. Hamprecht, S.C. Mellinghoff, O.A. Cornely); University of Cologne, Cologne (A. Hamprecht, O.A. Cornely); Leibniz Institute for Natural Product Research and Infection Biology–Hans-Knoell-Institute, Jena, Germany (A.E. Barber, G. Walther, O. Kurzai); University Hospital Cologne, Cologne (S.C. Mellinghoff, P. Thelen); University of Würzburg, Würzburg, Germany (Y. Yu, P. Neurgaonkar, T. Dandekar, R. Martin, O. Kurzai)

DOI: <https://doi.org/10.3201/eid2509.190262>

The emerging yeast *Candida auris* has disseminated worldwide. We report on 7 cases identified in Germany during 2015–2017. In 6 of these cases, *C. auris* was isolated from patients previously hospitalized abroad. Whole-genome sequencing and epidemiologic analyses revealed that all patients in Germany were infected with different strains.

Candida auris is an emerging yeast that was initially described in 2009 after a case of otitis externa in Japan (1). Since then, healthcare-associated infections have been reported worldwide (2). *C. auris* has caused outbreaks in hospitals in Asia, Africa, and Latin America (2–4). In Europe, 620 *C. auris* cases were observed during 2013–2017 (24% infections, 76% colonizations), including 7 cases in Germany (5). Most *C. auris* isolates exhibit resistance to fluconazole, and susceptibility to other azoles, amphotericin B, and echinocandins varies among isolates. Some strains show resistance to all 3 classes of antifungal drugs (6).

We report on the occurrence of *C. auris* in Germany and its link to prior healthcare exposure in the Middle East, Asia, Africa, or the United States. *C. auris* was isolated from 7 patients (4 male, 3 female, all in different, unrelated hospitals) during November 2015–December 2017 (Appendix Table, <http://wwwnc.cdc.gov/EID/article/25/9/19-0262-App1.pdf>). Six of the patients had previously been treated in healthcare centers outside Germany and were transferred to Germany for further treatment. No further suspicious cases or isolates were reported to the National

Reference Centre for Fungal Infections (Jena, Germany); however, reporting is not mandatory, and the possibility of missed cases cannot be excluded.

Of the 7 patients, 3 had been in isolation before detection of *C. auris* as a result of known colonization with carbapenemase-producing *Enterobacteriaceae*. No secondary *C. auris* cases were detected in any of the hospitals until March 2019. However, because no contact screening was performed, transmission resulting in asymptomatic carriage cannot be excluded.

Isolates from 6 patients were available for further testing. Biochemical identification of isolates by API ID 32C resulted in misidentification as *C. sake* (5 of 6) or *C. intermedia* (1 of 6). In contrast to previous versions, Vitek 2 version 08.01 (bioMérieux, <https://www.biomerieux-diagnostics.com>) identified all isolates as *C. auris* with 93%–99% likelihood. With VitekMS (bioMérieux) matrix-assisted laser desorption ionization time-of-flight (MALDI-TOF) mass spectrometry, no identification was achieved. However, a recent database update for VitekMS (version 3.2), which was not available at the time of our testing, corrected the identification failure in the VitekMS (data not shown). The Bruker Biotyper system (<https://www.bruker.com>) correctly identified all strains, albeit some with a low score (1.6–1.99). Whereas Bruker recommends that a score of 2.0 be used for species identification, a score >1.7 has been shown to be sufficient for reliable species identification (7). At the time of testing, Bruker's research-use-only library did not include a *C. auris* strain of the South Asian clade, which most of the German isolates belong to. Because *C. auris* exhibits considerable heterogeneity of mass spectra between geographic clusters, this missing clade likely explains the low scores (8).

Molecular identification using internal transcribed spacer technology identified all *C. auris* strains with 100% identity to the reference strain DSM 21092/CBS 10913. For available isolates, we performed whole-genome sequencing and aligned reads to the B8441 v2 reference genome (Figure; Appendix). A phylogenetic tree generated from whole-genome single-nucleotide polymorphism (SNP) data indicated that the isolates NRZ-2015-214, NRZ-2017-288, NRZ-2017-367, NRZ-2017-394/1-2, and NRZ-2017-505 belong to the South Asian clade, whereas NRZ-2018-545 was related to the African clade (Figure). In line with previous studies, the genetic differences observed between isolates of the same clade were small (30–800 SNPs), whereas differences between clades were large (36,000–147,000 SNPs) (4,9). Whole-genome data show that all cases identified in Germany harbor unique isolates, thus excluding transmission between these patients (Figure). As a control, the clonality of serial isolates NRZ-2017-394/1 and NRZ-2017-394/2, taken from the same patient on 2 different occasions, was confirmed; the 2 isolates were separated by only a single SNP (Figure).

¹Group members are listed at end of this article.

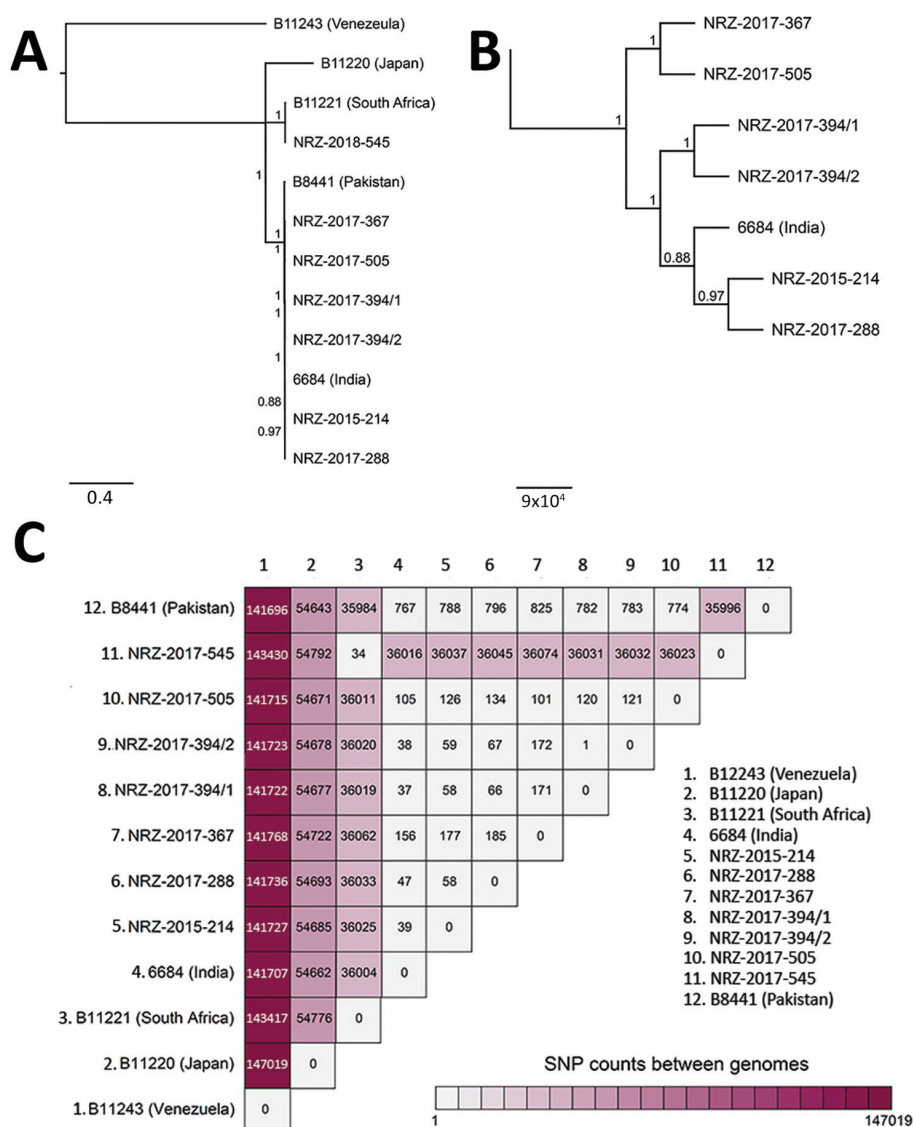


Figure. Genetic relationships of *Candida auris* isolates based on whole-genome sequencing SNP analysis. A) Maximum-likelihood phylogeny of *C. auris* isolates from Germany (indicated by NRZ prefix) inferred to reveal a possible geographic origin. The isolates were contrasted against strains representing the 4 different clades of *C. auris*: South American (strain B11243 from Venezuela), East Asian (B11220 from Japan), South African (B11221 from South Africa), and South Asian (B8441 from Pakistan and 6684 from India). B) Higher resolution of the tree shown in panel A to better visualize the relationship between the isolates belonging to the South Asian clade. Scale bars in panels A and B indicate nucleotide substitutions per site. C) SNP counts between the genomes of the isolates from Germany and the representative strains from the different clades. SNP, single-nucleotide polymorphism.

MICs of fluconazole were high for all isolates (>64 mg/L), whereas the MICs for other antifungals were variable (Appendix Table). With the exception of NRZ-2017-545, all isolates carried either the Y132F or the K143R mutations in the *ERG11* gene. However, although these mutations are linked to azole resistance, they did not result in elevated MICs for all azoles in these isolates (Appendix Table) (10). We identified a S639Y mutation in the *FKSI* hotspot 1 of isolate NRZ-2017-505, which was highly resistant to anidulafungin (MIC 16 mg/L).

In conclusion, *C. auris* has so far been isolated from individual cases in Germany. Most of these cases (6 of 7) occurred in patients who had previously been hospitalized abroad and were admitted to hospitals in Germany for continuation of medical treatment. No information on contact or environmental screening was

available; such screening was likely not performed in most institutions. Thus, silent transmission and resulting carriage may have occurred unnoticed. However, no secondary cases were detected in any of the 7 hospitals affected.

Members of the German *Candida auris* Study Group: Gerhard Haase (Labordiagnostisches Zentrum, Universitätsklinikum RWTH Aachen, Aachen, Germany); Jette Jung (Max von Pettenkofer-Institut, Munich, Germany); Heike Freidank (Städtisches Klinikum München GmbH, Munich); Michaela Simon (Institut für Med. Mikrobiologie und Hygiene, Regensburg, Germany); Jörg Steinmann (Institut für Klinikhygiene, Medizinische Mikrobiologie und Klinische Infektiologie, Universitätsinstitut der Paracelsus Medizinischen Privatuniversität, Nuremberg, Germany).

Acknowledgments

We thank Shneh Sethi for helpful advice and Sabrina Mündlein, Grit Mrotzek, and Ahmad Saleh for excellent technical assistance.

The German National Reference Center NRZMyk is funded by the Robert Koch Institute from funds provided by the German Ministry of Health (grant no. 1369-240). Calculations were performed on the Freiburg Galaxy server using computing services provided by the Center of Genetic Epidemiology (Danish Technical University, Lyngby, Denmark). The Freiburg Galaxy project is supported by the Collaborative Research Centre 992 Medical Epigenetics (DFG grant no. SFB 992/1 2012) and German Federal Ministry of Education and Research (BMBF grant no. 031 A538A). T.D. acknowledges support by the Deutsche Forschungsgemeinschaft (project no. 210879364–TRR 124/B1).

About the Author

Dr. Hamprecht is a clinical microbiologist at the Institute for Medical Microbiology, Immunology and Hygiene and professor for antibiotic resistance of gram-negative pathogens at the University of Cologne, Germany, and the German Centre for Infection Research (DZIF), also in Cologne. His research interests include multidrug-resistant organisms (mainly Enterobacterales and fungi), their resistance mechanisms, and the improvement of diagnostic methods.

References

- Satoh K, Makimura K, Hasumi Y, Nishiyama Y, Uchida K, Yamaguchi H. *Candida auris* sp. nov., a novel ascomycetous yeast isolated from the external ear canal of an inpatient in a Japanese hospital. *Microbiol Immunol*. 2009;53:41–4. <http://dx.doi.org/10.1111/j.1348-0421.2008.00083.x>
- Chowdhary A, Voss A, Meis JF. Multidrug-resistant *Candida auris*: “new kid on the block” in hospital-associated infections? *J Hosp Infect*. 2016;94:209–12. <http://dx.doi.org/10.1016/j.jhin.2016.08.004>
- Schelenz S, Hagen F, Rhodes JL, Abdolrasouli A, Chowdhary A, Hall A, et al. First hospital outbreak of the globally emerging *Candida auris* in a European hospital. *Antimicrob Resist Infect Control*. 2016;5:35. <http://dx.doi.org/10.1186/s13756-016-0132-5>
- Lockhart SR, Etienne KA, Vallabhaneni S, Farooqi J, Chowdhary A, Govender NP, et al. Simultaneous emergence of multidrug-resistant *Candida auris* on 3 continents confirmed by whole-genome sequencing and epidemiological analyses. *Clin Infect Dis*. 2017;64:134–40. <http://dx.doi.org/10.1093/cid/ciw691>
- Kohlenberg A, Struelens MJ, Monnet DL, Plachouras D; The *Candida auris* Survey Collaborative Group. *Candida auris*: epidemiological situation, laboratory capacity and preparedness in European Union and European Economic Area countries, 2013 to 2017. *Euro Surveill*. 2018;23:18-00136. <http://dx.doi.org/10.2807/1560-7917.ES.2018.23.13.18-00136>
- Jeffery-Smith A, Taori SK, Schelenz S, Jeffery K, Johnson EM, Borman A, et al.; *Candida auris* Incident Management Team. *Candida auris*: a review of the literature. *Clin Microbiol Rev*. 2017;31:e00029-17. <http://dx.doi.org/10.1128/CMR.00029-17>
- Hamprecht A, Christ S, Oestreicher T, Plum G, Kempf VA, Göttig S. Performance of two MALDI-TOF MS systems for the identification of yeasts isolated from bloodstream infections and cerebrospinal fluids using a time-saving direct transfer protocol. *Med Microbiol Immunol (Berl)*. 2014;203:93–9. <http://dx.doi.org/10.1007/s00430-013-0319-9>
- Prakash A, Sharma C, Singh A, Kumar Singh P, Kumar A, Hagen F, et al. Evidence of genotypic diversity among *Candida auris* isolates by multilocus sequence typing, matrix-assisted laser desorption/ionization time-of-flight mass spectrometry and amplified fragment length polymorphism. *Clin Microbiol Infect*. 2016;22:277e1–9. <http://dx.doi.org/10.1016/j.cmi.2015.10.022>
- Magobo RE, Corcoran C, Seetharam S, Govender NP. *Candida auris*-associated candidemia, South Africa. *Emerg Infect Dis*. 2014;20:1250–1. <http://dx.doi.org/10.3201/eid2007.131765>
- Chowdhary A, Prakash A, Sharma C, Kordalewska M, Kumar A, Sarma S, et al. A multicentre study of antifungal susceptibility patterns among 350 *Candida auris* isolates (2009–17) in India: role of the ERG11 and FKS1 genes in azole and echinocandin resistance. *J Antimicrob Chemother*. 2018;73:891–9. <http://dx.doi.org/10.1093/jac/dkx480>

Address for correspondence: Oliver Kurzai, University of Würzburg Institute for Hygiene and Microbiology, Josef-Schneider-Straße 2 / E1, Würzburg 97080, Germany; email: okurzai@hygiene.uni-wuerzburg.de

Characterization of Clinical Isolates of *Talaromyces marneffe* and Related Species, California, USA

Linlin Li, Katelyn Chen, Nirmala Dhungana, Yvonne Jang, Vishnu Chaturvedi,¹ Ed Desmond²

Author affiliation: California Department of Public Health, Richmond, California, USA

DOI: <https://doi.org/10.3201/eid2509.190380>

Talaromyces marneffe and other *Talaromyces* species can cause opportunistic invasive fungal infections. We characterized clinical *Talaromyces* isolates from patients in California, USA, a non-*Talaromyces*-endemic area, by a multiphasic approach, including multigene phylogeny, matrix-assisted laser desorption/ionization time-of-flight mass spectrometry, and phenotypic methods. We identified 10 potentially pathogenic *Talaromyces* isolates, 2 *T. marneffe*.

¹Current affiliation: New York State Department of Health, Albany, New York, USA.

²Current affiliation: Hawaii State Department of Health, Pearl City, Hawaii, USA.

Talaromyces marneffei is a dimorphic fungal pathogen that causes focal or systemic infection in immunocompromised persons, primarily HIV-infected patients (1). Many cases have been reported in travelers returning from areas of Southeast Asia, southern China, and eastern India to which it is endemic. Other *Talaromyces* species also have been reported to cause invasive fungal infections, including *T. amestolkiae* (2), *T. purpurogenus* (3,4), and *T. piceus* (5,6). *Talaromyces* species are common in air, soil, and human habitats. Clinical laboratories in areas to which this fungus is not endemic often do not perform identification of *T. marneffei* and other *Talaromyces* species (2). Therefore, we devised a multiphasic approach for identifying *T. marneffei* and other potentially pathogenic *Talaromyces* species.

We conducted this study during 2018. *Talaromyces* isolates from 10 human specimens were submitted to the Microbial Diseases Laboratory (MDL), California Department of Public Health (Richmond, CA, USA), to rule out *T. marneffei* (Appendix, <https://wwwnc.cdc.gov/EID/article/25/9/19-0380-App1.pdf>). Temperature and pH are known to influence pigment production and colony morphology of *Talaromyces* species; therefore, growth characteristics were observed using 2 different culture media (Sabouraud dextrose agar, pH 5.6; and Sabouraud dextrose agar, Emmons, pH 6.9), incubated at 25°C and 30°C. Fungal DNA was extracted using a previously reported method (7). *Talaromyces* isolates were identified to species level using the internal transcribed spacer (ITS) region, partial β -tubulin gene (BenA), and partial RNA polymerase II largest subunit gene (RPB1) (8). The ITS and partial BenA and RPB1 sequences were used to search for homologies in GenBank and CBS databases (<http://www.westerdijk-institute.nl/collections>). Multigene phylogenetic analysis was conducted on the concatenated ITS–BenA–RPB1 nucleotide sequence alignment (Appendix). A blastn search (<https://blast.ncbi.nlm.nih.gov/blast>) through the GenBank database, pairwise comparison alignment through the CBS database, or both showed 99%–100% homology for ITS, 97%–100% for BenA, and 91%–100% for RPB1 sequences with the best-matched sequences of known *Talaromyces* species isolates.

Phylogenetic analysis of the *Talaromyces* isolates showed 7 genetic clades, consistent with previous descriptions of the *Talaromyces* genera (9) (Figure). Species identification using a comparison of the ITS, BenA, and RPB1 sequences with existing sequences and multigene phylogenetic analysis identified *T. marneffei* (isolates MDL17022 and MDL18026), *T. atrovirens* (MDL17026, MDL17144, MDL17164, and MDL18070), *T. islandicus* (MDL18167), *T. stollii* (MDL18054), *T. coalescens* (MDL18102), and *T. australis* (MDL18159). The 2 *T. marneffei* isolates produced diffuse red pigment early, by 3 days of growth, on

both medium types and at both incubation temperatures. *T. australis* and *T. stollii* isolates also produced red pigment by 3 days but with variations based on media or temperature. At 7 days of growth, the 4 *T. atrovirens* isolates also showed variable red pigment production (abundant, weak, and absent) (Appendix). Microscopically, most isolates showed biverticillate conidiophores and globose to fusiform conidia in unbranched chains. Both *T. marneffei* isolates were from HIV-positive patients. MDL17022 was from a blood sample of a 37-year-old man with a travel history to Southeast Asia; MDL18026 was from skin tissue of a 36-year-old man with no available travel history.

Using matrix-assisted laser desorption/ionization-time-of-flight (MALDI-TOF) mass spectrometry, we generated main spectrum profiles (MSP) of *Talaromyces* species following Bruker's custom MSP and library creation standard operating procedure (<https://www.bruker.com>). We extracted proteins of *Talaromyces* isolates using the previously published National Institutes of Health (NIH) protocol (10). We analyzed *Talaromyces* spectra with MALDI Biotyper 4.1 software against combined databases of the Filamentous Fungi Library 2.0 (Bruker) and the NIH Mold Library (10), with and without inclusion of newly created MSPs of *Talaromyces* species (Appendix). The threshold for species identification was >1.9 ; for genus identification, ≥ 1.7 .

Using the combined databases of Filamentous Fungi Library 2.0 (Bruker) and NIH Mold Library, we identified none of the isolates to species level; results showed either no identification or genus-level identification. However, when we expanded the combined database with the MDL Mold Library, we correctly identified all *Talaromyces* isolates to the species level with the best score ≥ 1.9 . There were no ambiguous identification results; that is, the second-best matched species also had a high confidence score ≥ 1.9 .

T. marneffei can be readily differentiated from other red pigment-producing *Talaromyces* species by yeast-like colony conversion at 37°C. However, many clinical laboratories no longer conduct yeast conversions. For those laboratories, yellow-green colonies producing red soluble pigment at ≈ 3 days on common fungal culture media at 25°C–30°C might indicate the need to further confirm *T. marneffei*. It is difficult to distinguish *Talaromyces* species only by macroscopic and microscopic examination. Multilocus sequencing, although confirmatory, might be too time-consuming and expensive for routine use. Therefore, we identified all *Talaromyces* isolates to species level by MALDI-TOF mass spectrometry by using an expanded database with well-characterized *Talaromyces* strains.

In conclusion, our results show that MALDI-TOF mass spectrometry is a good choice for rapid, less expensive primary identification of *Talaromyces* species and other medically important fungal pathogens. Species-level

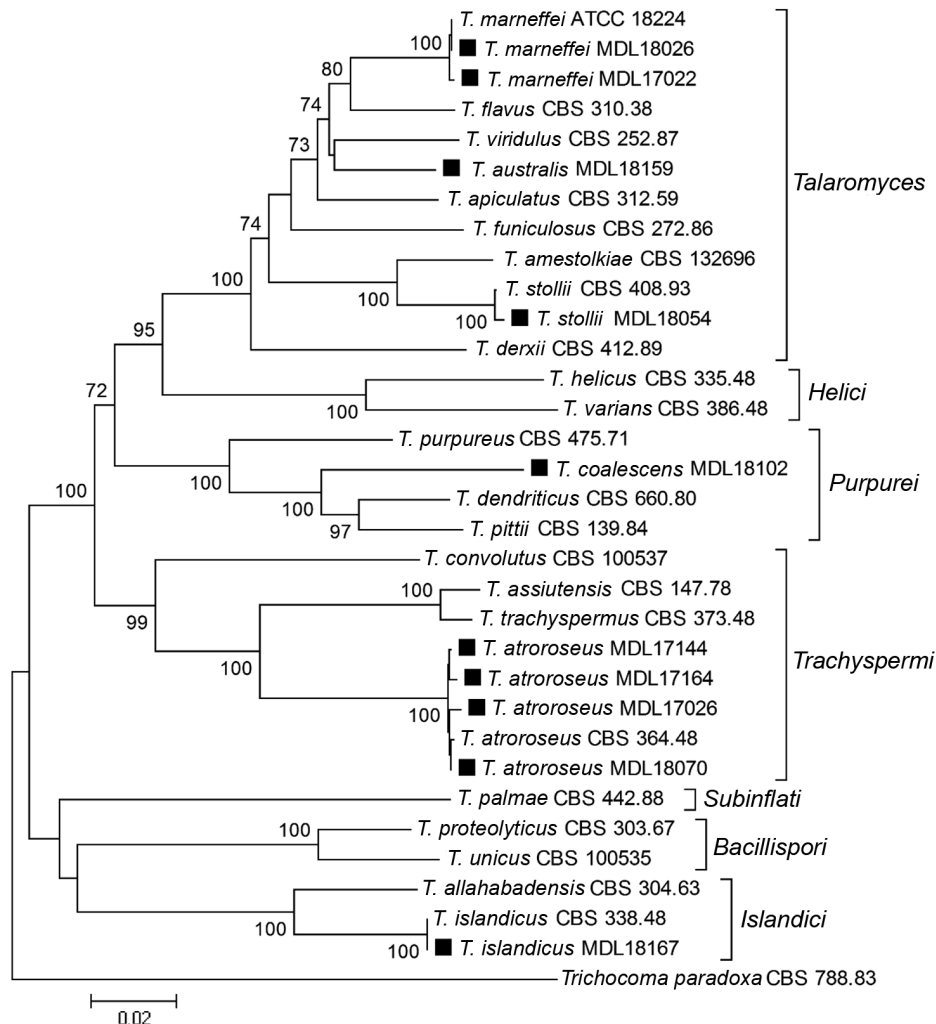


Figure. Phylogenetic analysis of *Talaromyces* species based on concatenated nucleotide alignments of internal transcribed spacer, partial β -tubulin gene, and partial RNA polymerase II largest subunit gene regions, showing the relationship among clinical isolates from patients in California, USA (black squares), and reference *Talaromyces* species. The tree was constructed by the neighbor-joining method with 1,000 bootstrap replicates by using MEGA software (<https://www.megasoftware.net>). Bootstrap support values >70% are presented at the nodes. The tree was rooted with *Trichocoma paradoxa* CBS 788.83. GenBank accession numbers for newly generated sequences are MK601832–41 for the internal transcribed spacer, MK626499–508 for the β -tubulin gene, and MK626509–518 for the RNA polymerase II largest subunit gene. CBS, Westerdijk Fungal Biodiversity Institute; MDL, Microbial Diseases Laboratory, California Department of Public Health. Scale bar indicates estimated phylogenetic divergence.

identification of *Talaromyces* isolates is clinically useful for treatment of patients with underlying conditions, such as immunodeficiency, cancer, advanced age, and immunosuppressive therapy.

Acknowledgments

We thank Zenda Berrada for her support and helpful suggestions on this study.

The Microbial Diseases Laboratory at the California Department of Public Health provided funding for this study.

About the Author

Dr. Li is a research scientist and a certified public health microbiologist at the Microbial Diseases Laboratory, California Department of Public Health. Her primary research interests include molecular diagnosis of mycotic diseases, Valley fever, candidemia, antifungal susceptibility testing, mycobacteriology, metagenomics, and next-generation sequencing.

References

1. Ustianowski AP, Sieu TP, Day JN. *Penicillium marneffeii* infection in HIV. *Curr Opin Infect Dis.* 2008;21:31–6. <http://dx.doi.org/10.1097/QCO.0b013e3282f406ae>
2. Villanueva-Lozano H, Treviño-Rangel RJ, Renpenning-Carrasco EW, González GM. Successful treatment of *Talaromyces amestolkiae* pulmonary infection with voriconazole in an acute lymphoblastic leukemia patient. *J Infect Chemother.* 2017;23:400–2. <http://dx.doi.org/10.1016/j.jiac.2016.12.017>
3. Atalay A, Koc AN, Akyol G, Cakir N, Kaynar L, Ulu-Kilic A. Pulmonary infection caused by *Talaromyces purpurogenus* in a patient with multiple myeloma. *Infesz Med.* 2016;24:153–7.
4. Lyratzopoulos G, Ellis M, Nerringer R, Denning DW. Invasive infection due to *Penicillium* species other than *P. marneffeii*. *J Infect.* 2002;45:184–95. <http://dx.doi.org/10.1053/jinf.2002.1056>
5. Santos PE, Piontelli E, Shea YR, Galluzzo ML, Holland SM, Zelazko ME, et al. *Penicillium piceum* infection: diagnosis and successful treatment in chronic granulomatous disease. *Med Mycol.* 2006;44:749–53. <http://dx.doi.org/10.1080/13693780600967089>
6. Horré R, Gilges S, Breig P, Kupfer B, de Hoog GS, Hoekstra E, et al. Case report. Fungaemia due to *Penicillium piceum*, a member of the *Penicillium marneffeii* complex. *Mycoses.* 2001;44:502–4. <http://dx.doi.org/10.1046/j.1439-0507.2001.00710.x>

7. Romanelli AM, Fu J, Herrera ML, Wickes BL. A universal DNA extraction and PCR amplification method for fungal rDNA sequence-based identification. *Mycoses*. 2014;57:612–22. <http://dx.doi.org/10.1111/myc.12208>
8. Samson RA, Yilmaz N, Houbraken J, Spierenburg H, Seifert KA, Peterson SW, et al. Phylogeny and nomenclature of the genus *Talaromyces* and taxa accommodated in *Penicillium* subgenus *Biverticillium*. *Stud Mycol*. 2011;70:159–83. <http://dx.doi.org/10.3114/sim.2011.70.04>
9. Yilmaz N, Visagie CM, Houbraken J, Frisvad JC, Samson RA. Polyphasic taxonomy of the genus *Talaromyces*. *Stud Mycol*. 2014;78:175–341. <http://dx.doi.org/10.1016/j.simyco.2014.08.001>
10. Lau AF, Drake SK, Calhoun LB, Henderson CM, Zelazny AM. Development of a clinically comprehensive database and a simple procedure for identification of molds from solid media by matrix-assisted laser desorption ionization-time of flight mass spectrometry. *J Clin Microbiol*. 2013;51:828–34. <http://dx.doi.org/10.1128/JCM.02852-12>

Address for correspondence: Ed Desmond, State Laboratories Division, Hawaii State Department of Health, 2725 Waimano Home Rd, Pearl City, HI 96782, USA; email: edward.desmond@doh.hawaii.gov

***Parathyridaria percutanea* and Subcutaneous Phaeohyphomycosis**

Shivaprakash M. Rudramurthy,¹ Megha Sharma,¹ Nandini Sethuraman, Pinaki Dutta, Bansidhar Tarai, Jayanthi Savio, Amanjit Bal, Usha Kalawat, Arunaloke Chakrabarti

Author affiliations: Postgraduate Institute of Medical Education and Research, Chandigarh, India (S.M. Rudramurthy, M. Sharma, N. Sethuraman, P. Dutta, A. Bal, A. Chakrabarti); Apollo Hospitals, Chennai, India (N. Sethuraman); Max Super Speciality Hospitals, New Delhi, India (B. Tarai); St. Johns Medical College and Research Institute, Bengaluru, India (J. Savio); Sri Venkateshwara Institute of Medical Sciences, Tirupati, India (U. Kalawat)

DOI: <https://doi.org/10.3201/eid2509.190383>

Parathyridaria percutanea is an emerging fungus causing subcutaneous phaeohyphomycoses in renal transplant recipients in India. We identified *P. percutanea* from a patient with subcutaneous phaeohyphomycosis. From our culture collection, we identified the same fungus from 4 similar patients. We found 5 cases previously described in literature.

¹These first authors contributed equally to this article.

Parathyridaria percutanea, earlier known as *Roussoella percutanea* in the order *Pleosporales*, has been reported to cause subcutaneous phaeohyphomycoses (1,2). *P. percutanea* belongs to coelomycetes, a group of fungi in which the conidia or asexual propagules lie within a cavity. *Parathyridaria* spp. generally exist as plant saprobes; *P. percutanea* is the only species reported as an opportunistic pathogen.

We recently observed a case of subcutaneous phaeohyphomycosis caused by *P. percutanea*. The patient was a 33-year-old man who had ACTH-dependent Cushing's disease with 2 cutaneous lesions, one under the left axilla and the other on the ulnar aspect of the left forearm, that had progressed slowly over 3 years (Appendix Figure 1, panel A, <https://wwwnc.cdc.gov/EID/article/25/9/19-0383-App1.pdf>). Direct microscopy of a biopsy sample taken from the left forearm lesion revealed dematiaceous septate hyphae with irregular hyphal swellings (Appendix Figure 1, panel B). Colonies on Sabouraud's dextrose agar at 25°C were flat, spreading with sparse aerial hyphae after 1 week, and later turned to cottony greenish-black growth (Appendix Figure 1, panel C). Lactophenol cotton blue mount revealed nonsporulating dematiaceous hyphae with chlamydospores (Appendix Figure 1, panel D). Several attempts to induce sporulation (on oatmeal agar and malt extract agar) failed. Histopathologic examination (Appendix Figure 1, panels E–G) showed neutrophilic infiltration with fungal hyphae, nodular swellings on Giemsa stain, and black hyphae on Grocott-Gomori's methamine silver stain.

We identified the fungus as *Roussoella percutanea* of the order *Pleosporales*, later renamed *P. percutanea*, by PCR sequencing of the internal transcribed spacer (ITS) and 28S regions of ribosomal DNA, as described previously (3). ITS sequencing of our strain NCCPF104001 (GenBank accession nos. MG708109 [by ITS] and MG708116 [by 28S]) had 99.8% identity with CBS128203 (type strain, GenBank accession no. KF322117) and CBS868.95 (GenBank accession no. KF322118), whereas 28S sequences had 100% identity with CBS128203 (GenBank accession no. KF366448) and CBS868.95 (GenBank accession no. KF366449) (Appendix Figure 2, panels A, B). The patient refused further treatment in the hospital and left against medical advice.

We screened all the isolates deposited in our National Culture Collection of Pathogenic Fungi (NCCPF, Chandigarh) and characterized them phenotypically as *Pleosporales*. Of 7 such isolates, we identified 4 as *P. percutanea* by sequencing (Table, <https://wwwnc.cdc.gov/EID/article/25/9/19-0383-T1.htm>). We further subjected these isolates to phylogenetic analysis of ITS and large ribosomal subunit (28S) of the rDNA using MEGA software version 6 (<https://megasoftware.net>) (3). The strains identified as *P. percutanea* clustered together with the ITS and 28S sequences of CBS12608 and CBS868.95 strains, the other 2 *P. percutanea*

isolates reported with gene sequences (2). Phylogenetically, *Parathyridaria* is now a distinct genus and clearly separated from closely related genera such as *Rousoella* and *Thyridaria* (Appendix Figure 2, panels A, B).

We searched published literature on Medline and PubMed for subcutaneous phaeohyphomycoses caused by *P. percutanea* or *R. percutanea* and identified 5 cases (Table). All 5 patients originated from tropical countries including the Caribbean islands (5), Republic of the Congo (6), Somalia (7), and India (2,8). Including these 5 with the case-patients we identified from culture and our study patient, 7 of 10 total cases originated in India. The patients had lesions in the extremities; we expect that the fungus is present in our environment and gains access from traumatic inoculation of patients working in the field or walking barefoot. The clinical description of all 10 patients is presented in the Table. Male patients outnumbered female patients. In 2 patients, underlying muscle tendon (2) and joint bursa (7) were involved. No discharging sinus or granuloma formation was seen in any of the 10 patients.

P. percutanea infection occurred in immunosuppressed patients; 9/10 patients were either renal transplant recipients (7 patients) or on steroid therapy (2 patients). The disease manifested 1–3 years posttransplant. Incidence of subcutaneous phaeohyphomycoses is reported in $\leq 3.6\%$ of renal transplant recipients (10). The tenth patient had diabetes, and the infection of *P. percutanea* occurred at a tattoo site, manifesting 2 years after tattooing. The fungus may remain dormant in subcutaneous tissue after traumatic inoculation and multiply slowly at the opportune time when host immunity is depressed because of immunosuppression or diabetes.

The outcome of *P. percutanea* infection was known in 5/10 patients, and they responded to surgical resection of the lesion followed by voriconazole therapy. The joint guidelines of the European Society of Clinical Microbiology and Infectious Diseases Fungal Infection Study Group and the European Confederation of Medical Mycology on the management of subcutaneous phaeohyphomycosis (9) recommended surgical resection (recommendation AII) along with oral azoles in immunosuppressed patients to prevent dissemination of disease (recommendation BIII). In vitro susceptibility testing, conducted for 3 isolates by Ahmed et al. (2) and Almagro-Molto et al. (7), revealed that *P. percutanea* exhibited low MIC to itraconazole, voriconazole, and posaconazole (Table). Therefore, itraconazole and posaconazole can be used in patients receiving other liver-metabolized drug therapies.

Especially in renal transplant patients in India, *P. percutanea* could be a possible etiologic agent of subcutaneous phaeohyphomycosis. Sequencing of ITS and 28S regions of ribosomal DNA confirms diagnosis. Effective treatment could include surgical excision of lesions and voriconazole or posaconazole therapy.

About the Author

Dr. Rudramurthy is a professor at the tertiary care hospital at the Postgraduate Institute of Medical Education and Research, which hosts a World Health Organization collaborating center for reference and research on fungi of medical importance and the National Culture of Pathogenic Fungi, Chandigarh, India. His research interests include antifungal resistance, molecular techniques for diagnosis of fungal infections, and identification and typing of fungi.

References

1. Tanaka K, Hirayama K, Yonezawa H, Sato G, Toriyabe A, Kudo H, et al. Revision of the *Massarineae* (Pleosporales, Dothideomycetes). *Stud Mycol*. 2015;82:75–136. <http://dx.doi.org/10.1016/j.simyco.2015.10.002>
2. Ahmed SA, Stevens DA, van de Sande WWJ, Meis JF, de Hoog GS. *Rousoella percutanea*, a novel opportunistic pathogen causing subcutaneous mycoses. *Med Mycol*. 2014;52:689–98. <http://dx.doi.org/10.1093/mmy/myu035>
3. Shivaprakash MR, Appannanavar SB, Dhaliwal M, Gupta A, Gupta S, Gupta A, et al. *Colletotrichum truncatum*: an unusual pathogen causing mycotic keratitis and endophthalmitis. *J Clin Microbiol*. 2011;49:2894–8. <http://dx.doi.org/10.1128/JCM.00151-11>
4. Galipothu S, Kalawat U, Ram R, Kishore C, Sridhar AV, Chaudhury A, et al. Cutaneous fungal infection in a renal transplant patient due to a rare fungus belonging to order Pleosporales. *Indian J Med Microbiol*. 2015;33:165–7. <http://dx.doi.org/10.4103/0255-0857.148435>
5. Meis JFGM, Schouten RA, Verweij PE, Dolmans W, Wetzels JFM. Atypical presentation of *Madurella mycetomatis* mycetoma in a renal transplant patient. *Transpl Infect Dis*. 2000;2:96–8. <http://dx.doi.org/10.1034/j.139-3062.2000.020208.x>
6. El Khalfi A, Biau D, Audard V, Heisse C, Paugam A. Phaeohyphomycosis in *Rousoella percutanea* [in French]. *J Mycol Med*. 2016;26:e30 <http://dx.doi.org/10.1016/j.mycmed.2016.04.065>
7. Almagro-Molto M, Haas A, Melcher C, Nam-Apostolopoulos YC, Schubert S. First case of *Rousoella percutanea* bursitis. *Diagn Microbiol Infect Dis*. 2017;87:172–4. <http://dx.doi.org/10.1016/j.diagmicrobio.2016.10.021>
8. Vasant JA, Maggiani F, Borman AM. Subcutaneous mycotic cyst caused by *Rousoella percutanea* in a UK renal transplant patient. *Mycopathologia*. 2017;182:721–5. <http://dx.doi.org/10.1007/s11046-017-0121-0>
9. Chowdhary A, Meis JF, Guarro J, de Hoog GS, Kathuria S, Arendrup MC, et al.; European Society of Clinical Microbiology and Infectious Diseases Fungal Infection Study Group; European Confederation of Medical Mycology. ESCMID and ECMM joint clinical guidelines for the diagnosis and management of systemic phaeohyphomycosis: diseases caused by black fungi. *Clin Microbiol Infect*. 2014;20(Suppl 3):47–75. <http://dx.doi.org/10.1111/1469-0691.12515>
10. Schieffelin JS, Garcia-Diaz JB, Loss GE Jr, Beckman EN, Keller RA, Staffeld-Coit C, et al. Phaeohyphomycosis fungal infections in solid organ transplant recipients: clinical presentation, pathology, and treatment. *Transpl Infect Dis*. 2014;16:270–8. <http://dx.doi.org/10.1111/tid.12197>

Address for correspondence: Arunaloke Chakrabarti, Postgraduate Institute of Medical Education and Research, Department of Medical Microbiology, Sector 12, Chandigarh, Union Territory, 160012, India; email: arunaloke@hotmail.com

Disease Exposure and Antifungal Bacteria on Skin of Invasive Cane Toads, Australia

Chava L. Weitzman, Mirjam Kaestli, Karen Gibb, Gregory P. Brown, Richard Shine, Keith Christian

Author affiliations: Virginia Polytechnic Institute and State University, Blacksburg, Virginia, USA (C.L. Weitzman); Charles Darwin University, Casuarina, Northern Territory, Australia (M. Kaestli, K. Gibb, K. Christian); University of Sydney, Sydney, New South Wales, Australia (G.P. Brown, R. Shine); Macquarie University, Sydney (G.P. Brown, R. Shine)

DOI: <https://doi.org/10.3201/eid2509.190386>

Cane toads, an invasive species in Australia, are resistant to fungal pathogens affecting frogs worldwide (*Batrachochytrium dendrobatidis*). From toad skin swabs, we detected higher proportions of bacteria with antifungal properties in Queensland, where toad and pathogen distributions overlap, than in other sites. This finding suggests that site-specific pathogen pressures help shape skin microbial communities.

The westward and southward spread of invasive cane toads (*Rhinella marina*) in Australia since their introduction to Queensland in 1935 threatens many native species. In addition to their skin-secreted bufotoxins affecting predators, toads are resistant to the fungal pathogen *Batrachochytrium dendrobatidis* associated with global frog die-offs, but their capacity to spread the pathogen to other frog species remains unclear (1,2).

As a skin pathogen, *B. dendrobatidis* interacts not only with the host's immune system, but also with other community members in the skin microbiome (3). Many bacteria on frog skin have antifungal properties that can help the host fight *B. dendrobatidis* (4), and the presence of bacteria with anti-*B. dendrobatidis* capacity may increase a host's pathogen resistance. In a previous study about gene expression in experimentally infected cane toads, their strong resistance to *B. dendrobatidis* was not attributed to strong immune function (1). Thus, the skin environment, including microbes inhabiting it, alongside an immediate, localized immune response, might play a large role in fighting the pathogen and resisting disease (1).

Invading species are predicted to invest in less costly immune defenses while decreasing their investment in costly inflammatory immune responses (5). With the assumption that skin bacteria are relatively inexpensive for the host to maintain, we used skin swab samples collected in 2017 to test whether cane toads have increased

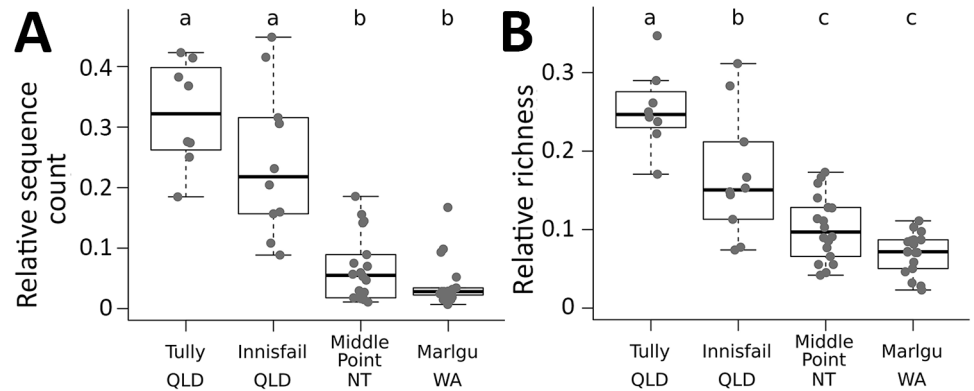
proportions of putative *B. dendrobatidis*-inhibiting bacteria at the invasion front in Australia, consistent with a previously reported increased investment into low-cost innate immune functions (6). Alternatively, we predicted that patterns of *B. dendrobatidis*-inhibitory bacteria on toad skin might depend on the current distribution of, and thus likely exposure to, *B. dendrobatidis*. Our 4 sampling locations (8–18 per site; Appendix Figure 1, <https://wwwnc.cdc.gov/EID/article/25/9/19-0386-App1.pdf>) comprised 2 sites overlapping the current *B. dendrobatidis* distribution (Queensland) and 2 sites outside the area of threat of chytridiomycosis (Northern Territory and Western Australia). These 4 sites also represent the toad's westward expansion; Western Australian toads were sampled near the invasion front. Sampling was in accordance with Charles Darwin University Animal Ethics permit A14012.

We compared bacterial amplicon sequence variants (sequences available on FigShare, <https://doi.org/10.6084/m9.figshare.7855670>) against a database of known anti-*B. dendrobatidis* isolates from the skin of frog species around the world (4). We detected 63 bacterial types with previously described anti-*B. dendrobatidis* function in the wild toad samples in our study. The 4 sampling sites differed in the proportion of total sequences and bacterial types represented by putative *B. dendrobatidis*-inhibitory bacteria, and toads from Queensland sites had proportionately more of these sequences and taxa than did toads from other sites (Figure). Some of the *B. dendrobatidis*-inhibitory bacteria were extremely common among our samples (particularly at the Tully site in Queensland [Appendix]).

Our results indicate that the skin bacterial communities on toads from sites overlapping the *B. dendrobatidis* distribution contain more putative *B. dendrobatidis*-inhibitory bacteria than is the case for toads from sites not yet invaded by the pathogen. Rather than following predictions regarding immunocompetence at the invasion front, this pattern suggests that *B. dendrobatidis*-inhibitory bacteria are selected for where the disease is present, in concordance with the adaptive microbiome hypothesis presented by Jin Song et al. (7). Outside of the *B. dendrobatidis* range, selection for anti-*B. dendrobatidis* microbes is relaxed; inhibitory microbes represent less of the community, and some disappear.

In cane toads, juvenile life stages succumb to *B. dendrobatidis*, although they have higher survival rates and better ability to clear an infection than other amphibians (e.g., 1). The prevalence of bacteria with *B. dendrobatidis*-inhibitory capacity on adult cane toads in Queensland suggests that the skin microbiome might confer some of the resistance to disease in this host species. Although amphibian skin microbiome communities change across ontogeny, host species is a strong predictor of skin communities

Figure. Proportions of sequences (A) and richness (B) represented by *Batrachochytrium dendrobatidis*-inhibitory bacteria detected on the skin of invasive cane toads (*Rhinella marina*) at 4 sites in Australia, 2017. Points indicate values for individual toads. Box plots indicate the median (thick line), interquartile range (box), reasonable range of the data (dashed lines to the whiskers), and outliers. Letters above plots indicate significant differences from Tukey's post hoc tests with $p < 0.05$. QLD, Queensland; NT, Northern Territory; WA, Western Australia.



across life stages (8). Thus, the communities found on these adult toads may predict those found on juvenile toads.

Our results could be affected by larger differences in bacterial community composition that can occur among sampling sites in cane toads (9) and other frog species (8). These differences could be due to diverse environmental microbiota supported by climatic and other abiotic and biotic conditions that change across the landscape.

The detection of *B. dendrobatidis*-inhibitory microbes at *B. dendrobatidis*-naïve sites might be misleading. The presence of a functional gene does not necessarily imply gene activity (10). Thus, the approach of ascribing *B. dendrobatidis*-inhibitory roles based on presence might be too simplistic in the absence of direct evidence of *B. dendrobatidis*-inhibitory action, which was outside the scope of this study. Some of these bacteria may be commonly found on cane toad skin, regardless of an active function to inhibit *B. dendrobatidis*. Nonetheless, the higher frequency of these bacteria in *B. dendrobatidis*-exposed locations suggests that the microbiome on the skin of cane toads is shaped, at least partly, by natural selection in response to geographic variation in the degree of threat posed by specific diseases.

Acknowledgments

We thank 2 anonymous reviewers for their comments to improve the quality of this paper and Alea Rose for technical assistance in the laboratory.

Financial support was provided from the Faculty of Engineering, Health, Science and the Environment of Charles Darwin University and the Australian Research Council (ARC-LP120200110).

About the Author

Dr. Weitzman is a postdoctoral associate at Virginia Polytechnic Institute and State University. Her research focuses on disease ecology and herpetology.

References

- Poorten TJ, Rosenblum EB. Comparative study of host response to chytridiomycosis in a susceptible and a resistant toad species. *Mol Ecol*. 2016;25:5663–79. <https://doi.org/10.1111/mec.13871>
- Brannelly LA, Martin G, Llewelyn J, Skerratt LF, Berger L. Age- and size-dependent resistance to chytridiomycosis in the invasive cane toad *Rhinella marina*. *Dis Aquat Organ*. 2018;131:107–20. <https://doi.org/10.3354/dao03278>
- Jani AJ, Briggs CJ. The pathogen *Batrachochytrium dendrobatidis* disturbs the frog skin microbiome during a natural epidemic and experimental infection. *Proc Natl Acad Sci U S A*. 2014;111:E5049–58. <https://doi.org/10.1073/pnas.1412752111>
- Woodhams DC, Alford RA, Antwis RE, Archer H, Becker MH, Belden LK, et al. Antifungal isolates database of amphibian skin-associated bacteria and function against emerging fungal pathogens. *Ecology*. 2015;96:595–595. <https://doi.org/10.1890/14-1837.1>
- Lee KA, Klasing KC. A role for immunology in invasion biology. *Trends Ecol Evol*. 2004;19:523–9. <https://doi.org/10.1016/j.tree.2004.07.012>
- Brown GP, Phillips BL, Dubey S, Shine R. Invader immunology: invasion history alters immune system function in cane toads (*Rhinella marina*) in tropical Australia. *Ecol Lett*. 2015;18:57–65. <https://doi.org/10.1111/ele.12390>
- Jin Song S, Woodhams DC, Martino C, Allaband C, Mu A, Javorschi-Miller-Montgomery S, et al. Engineering the microbiome for animal health and conservation. *Exp Biol Med* (Maywood). 2019;244:494–504. <https://doi.org/10.1177/1535370219830075>
- Kueneman JG, Parfrey LW, Woodhams DC, Archer HM, Knight R, McKenzie VJ. The amphibian skin-associated microbiome across species, space and life history stages. *Mol Ecol*. 2014;23:1238–50. <https://doi.org/10.1111/mec.12510>
- Christian K, Weitzman C, Rose A, Kaestli M, Gibb K. Ecological patterns in the skin microbiota of frogs from tropical Australia. *Ecol Evol*. 2018;8:10510–9. <https://doi.org/10.1002/ece3.4518>
- Wang Y, Zhang R, He Z, Van Nostrand JD, Zheng Q, Zhou J, et al. Functional gene diversity and metabolic potential of the microbial community in an estuary-shelf environment. *Front Microbiol*. 2017;8:1153. <https://doi.org/10.3389/fmicb.2017.01153>

Address for correspondence: Chava L. Weitzman, Department of Biological Sciences, Virginia Tech, 4020A Derring Hall (MC 0406), Blacksburg, VA 24061, USA; email: weitzman.chava@gmail.com

Case of *Plasmodium knowlesi* Malaria in Poland Linked to Travel in Southeast Asia

Szymon P. Nowak, Paweł Zmora, Łukasz Pielok, Łukasz Kuszel, Ryszard Kierzek, Jerzy Stefaniak, Małgorzata Paul

Author affiliations: Poznań University of Medical Sciences, Poznań, Poland (S.P. Nowak, Ł. Pielok, Ł. Kuszel, J. Stefaniak, M. Paul); Institute of Bioorganic Chemistry, Polish Academy of Sciences, Poznań (P. Zmora, R. Kierzek)

DOI: <https://doi.org/10.3201/eid2509.190445>

We report a case of *Plasmodium knowlesi* malaria imported to central Europe from Southeast Asia. Laboratory suspicion of *P. knowlesi* infection was based on the presence of atypical developmental forms of the parasite in Giemsa-stained microscopic smears. We confirmed and documented the clinical diagnosis by molecular biology techniques.

The simian malaria parasite, *Plasmodium knowlesi*, is an emergent public health threat for persons traveling to Southeast Asia (1). We report a case of *P. knowlesi* malaria imported to central Europe from Southeast Asia.

On June 25, 2018, a 27-year-old woman returned to Poland after an 8-month tourist stay in Southeast Asia (Appendix Figure 1, <http://wwwnc.cdc.gov/EID/article/25/9/19-0445-App1.pdf>). The patient did not use malarial chemoprophylaxis during her travels. While in Sumatra, Indonesia, she experienced 2 episodes of subfebrile body temperature of $\leq 38^{\circ}\text{C}$. After returning to Poland, she reported having general malaise, weakness, chills, and a low-grade fever. She consulted a family physician, who diagnosed pharyngitis and recommended empiric antimicrobial drug therapy, cephalosporin combined with a fluoroquinolone, which provided no clinical improvement. After another episode of fever (temperature 39°C), she sought treatment at the regional hospital in Racibórz, Poland. Basic laboratory tests revealed leucopenia, thrombocytopenia, and elevated levels of C-reactive protein and procalcitonin. The patient did not have any chronic diseases or drug allergies. She was not pregnant, and her family history was unremarkable.

On July 5, 2018, the patient was transferred to the Department of Tropical and Parasitic Diseases, Poznań University of Medical Sciences, Poznań, Poland, because of high fever. At admission, on day 5 of her illness, she was conscious and responded logically. Her clinical status was stable. She was febrile (temperature 40°C) and experiencing hypotension (91/68 mm Hg), chills, headache, weakness,

malaise, and tachycardia (110 bpm) but did not have signs of multiorgan failure. Laboratory analyses showed mild normocytic anemia (hemoglobin 10.3 g/dL, hematocrit 29.0%, and erythrocyte count 3.34×10^{12} cells/L); low levels of platelets ($22 \times 10^9/\text{L}$), leukocytes ($2.13 \times 10^3/\mu\text{L}$), neutrophils ($0.76 \times 10^3/\mu\text{L}$), and lymphocytes ($1.01 \times 10^3/\mu\text{L}$); marked elevation of inflammatory markers C-reactive protein (66.3 mg/L) and procalcitonin (0.67 ng/mL); a high concentration of D-dimers (6.48×10^3 mg/mL); slightly prolonged prothrombin time (12.9 s); and elevated lactate dehydrogenase level (249 U/L).

Staff examining the first thick and thin blood films during screening in the emergency department reported an “atypical mixed infection with *P. vivax* and *P. malariae* with a strange morphology of the parasites” and a low parasitemia of 0.3%. A reference microscopic analysis performed at the Department of Tropical and Parasitic Diseases, Poznań University of Medical Sciences, showed infected erythrocytes of normal size and shape with a lack of Schuffner stippling and Maurer’s cleft. We observed multiple young trophozoites in the erythrocytes, with a delicate, thin ring of cytoplasm. Some also had narrow band shapes. In addition, we saw mature schizonts with <16 merozoites, large round gametocytes, and notable amounts of hemozoin pigment (Appendix Figure 2). ELISA revealed a high level of *Plasmodium* sp. IgM/IgG (52 U/mL), but we could not identify the *Plasmodium* species from these features. We later used PCR to confirm *P. knowlesi* infection from peripheral blood collected in EDTA tubes and frozen at -20°C . In brief, we extracted DNA from a 1.2-mL venous blood sample by using an automated nucleic acid extractor, MagCore HF16 Plus, with a MagCore genomic DNA large volume whole blood kit (RBC Bioscience Corp., <https://www.rbcbioscience.com>), according to standard protocol. To identify the *Plasmodium* species, we used nested PCR according to Komaki-Yasuda et al. (2). In patients with previously described *P. falciparum* malaria, we have observed a specific band for the parasite. We did not observe this band in the case-patient’s sample, suggesting infection with another *Plasmodium* species. The *P. vivax* primers did not yield amplification, but the *P. knowlesi* oligos resulted in clear bands, indicating that this patient was infected with *P. knowlesi* (Figure). In addition, the *P. knowlesi* band diminished after malarial therapy, demonstrating treatment efficacy.

On the basis of the patient’s travel history, clinical signs and symptoms, test results, and World Health Organization guidelines (3), we diagnosed uncomplicated *P. knowlesi* infection. The patient received oral artemether and lumefantrine combined with intravenous doxycycline and the parasites cleared in microscopic smears within 4 days. The patient’s fever subsided, her blood morphology

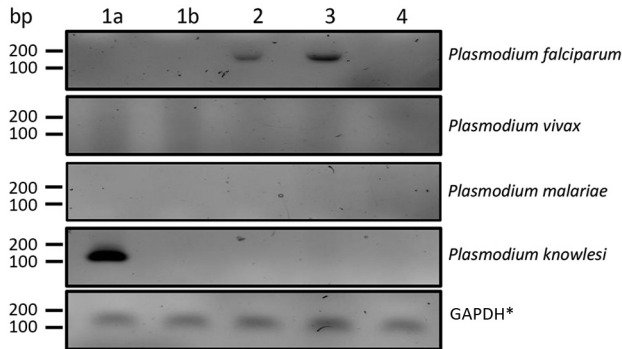


Figure. Nested PCR of *Plasmodium knowlesi* DNA isolated from a patient in Poland with recent travel to Southeast Asia. Lane 1a, patient sample from day of admission; lane 1b, patient sample taken 11 days after implementing malarial treatment; lanes 2 and 3, samples taken from patients previously diagnosed with *Plasmodium falciparum* malaria; lane 4, sample from an afebrile person from Poland with no history of travel to tropical countries. *GAPDH, glyceraldehyde 3-phosphate dehydrogenase.

and biochemistry parameters improved, and her levels of inflammatory and coagulation system markers decreased. In addition, PCR was negative for *P. knowlesi* DNA in peripheral blood after treatment. During a 3-month follow-up period, morphological and biochemical laboratory parameters all normalized, and the level of *Plasmodium*-specific antibodies diminished to <28 U/mL.

In conclusion, we describe a rare case of *P. knowlesi* infection imported to Poland in a traveler returning from Southeast Asia. Previous research studies report imported cases of *P. knowlesi* malaria in travelers returning to other countries in western and northern Europe, including Spain, Italy, France, Germany, and Sweden (4–10). Travelers from Poland increasingly choose Southeast Asia as a common and popular destination. With that in mind, parasitology laboratories in Poland could diagnose *P. knowlesi* more often as an etiologic agent of tropical malaria. The ambiguous morphology and low number of parasites seen in microscopy make diagnosing *P. knowlesi* difficult. Proper diagnosis relies on thorough epidemiology, including travel history, augmented with molecular biology techniques.

Acknowledgments

The authors thank Matylda Kłudkowska and Krystyna Frąckowiak for technical assistance in microscopy.

About the Author

Dr. Nowak is a physician and research fellow at the Department and Clinic of Tropical and Parasitic Diseases, Poznań University of Medical Sciences, Poznań, Poland. His research interest is in imported tropical diseases.

References

1. Singh B, Kim Sung L, Matusop A, Radhakrishnan A, Shamsul SS, Cox-Singh J, et al. A large focus of naturally acquired *Plasmodium knowlesi* infections in human beings. *Lancet*. 2004;363:1017–24. [https://doi.org/10.1016/S0140-6736\(04\)15836-4](https://doi.org/10.1016/S0140-6736(04)15836-4)
2. Komaki-Yasuda K, Vincent JP, Nakatsu M, Kato Y, Ohmagari N, Kano S. A novel PCR-based system for the detection of four species of human malaria parasites and *Plasmodium knowlesi*. *PLoS One*. 2018;13:e0191886. <https://doi.org/10.1371/journal.pone.0191886>
3. World Health Organization. Guidelines for the treatment of malaria. 3rd ed. Geneva: The Organization; 2015.
4. Ta TT, Salas A, Ali-Tammam M, Martínez MC, Lanza M, Arroyo E, et al. First case of detection of *Plasmodium knowlesi* in Spain by real time PCR in a traveller from Southeast Asia. *Malar J*. 2010;9:219. <https://doi.org/10.1186/1475-2875-9-219>
5. De Canale E, Sgarabotto D, Marini G, Menegotto N, Masiero S, Akkouche W, et al. *Plasmodium knowlesi* malaria in a traveller returning from the Philippines to Italy, 2016. *New Microbiol*. 2017;40:291–4.6. Berry A, Iriart X, Wilhelm N, Valentin A, Cassaing S, Witkowski B, et al. Imported *Plasmodium knowlesi* malaria in a French tourist returning from Thailand. *Am J Trop Med Hyg*. 2011;84:535–8. <https://doi.org/10.4269/ajtmh.2011.10-0622>
7. Froeschl G, Beissner M, Huber K, Bretzel G, Hoelscher M, Rothe C. *Plasmodium knowlesi* infection in a returning German traveler from Thailand: a case report on an emerging malaria pathogen in a popular low-risk travel destination. *BMC Infect Dis*. 2018;18:148. PubMed <https://doi.org/10.1186/s12879-018-3059-z>
8. Bronner U, Divis PC, Färnert A, Singh B. Swedish traveller with *Plasmodium knowlesi* malaria after visiting Malaysian Borneo. *Malar J*. 2009;8:15. <https://doi.org/10.1186/1475-2875-8-15>
9. Seilmaier M, Hartmann W, Beissner M, Fenzl T, Haller C, Guggemos W, et al. Severe *Plasmodium knowlesi* infection with multi-organ failure imported to Germany from Thailand/Myanmar. *Malar J*. 2014;13:422. <https://doi.org/10.1186/1475-2875-13-422>
10. Froeschl G, Nothdurft HD, von Sonnenburg F, Bretzel G, Polanetz R, Kroidl I, et al. Retrospective clinical case series study in 2017 identifies *Plasmodium knowlesi* as most frequent *Plasmodium* species in returning travellers from Thailand to Germany. *Euro Surveill*. 2018;23. <https://doi.org/10.2807/1560-7917.ES.2018.23.29.1700619>

Address for correspondence: Szymon P. Nowak, Poznań University of Medical Sciences, Department and Clinic of Tropical and Parasitic Diseases, 49 Przybyszewskiego St, 60-355 Poznań, Poland; email: snowak@ump.edu.pl

Bombali Virus in *Mops condylurus* Bats, Guinea

Lyudmila S. Karan, Marat T. Makenov, Mikhail G. Korneev, Noumany Sacko, Sanaba Boumbaly, Sergey A. Yakovlev, Kerfalla Kourouma, Roman B. Bayandin, Anastasiya V. Gladysheva, Andrey V. Shipovalov, Irina A. Yurganova, Yana E. Grigorieva, Marina V. Fedorova, Svetlana A. Scherbakova, Vladimir V. Kutryev, Alexander P. Agafonov, Renat A. Maksyutov, German A. Shipulin, Viktor V. Maleev, Mamadou Boiro, Vasiliy G. Akimkin, Anna Y. Popova

Author affiliations: Central Research Institute of Epidemiology, Moscow, Russia (L.S. Karan, M.T. Makenov, Y.A. Grigorieva, M.V. Fedorova, V.V. Maleev, V.G. Akimkin); Russian Research Anti-Plague Institute, Saratov, Russia (M.G. Korneev, S.A. Yakovlev, S.A. Scherbakova, V.V. Kutryev); International Center for Research of Tropical Infections in Guinea, N'Zerekore, Guinea (N. Sacko, S. Boumbaly); Research Institute of Applied Biology of Guinea, Kindia, Guinea (N. Sacko, S. Boumbaly, K. Kourouma, M. Boiro); State Research Center of Virology and Biotechnology VECTOR, Kol'tsovo, Russia (R.B. Bayandin, A.V. Gladysheva, A.V. Shipovalov, I.A. Yurganova, A.P. Agafonov, R.A. Maksyutov); Center of Strategical Planning and Biomedical Health Risks Management, Moscow (G.A. Shipulin); Federal Service for Surveillance on Consumer Rights Protection and Human Wellbeing, Moscow (A.Y. Popova)

DOI: <https://doi.org/10.3201/eid2509.190581>

In 2018, a previously unknown Ebola virus, Bombali virus, was discovered in Sierra Leone. We describe detection of Bombali virus in Guinea. We found viral RNA in internal organs of 3 Angolan free-tailed bats (*Mops condylurus*) trapped in the city of N'Zerekore and in a near-by village.

In 2018, a new species of the genus *Ebolavirus* (family *Filoviridae*), Bombali virus (BOMV), was discovered in Sierra Leone (1). The virus was detected in oral and rectal swab specimens from 2 free-tailed bat species, *Chaerephon pumilus* (little free-tailed bat) and *Mops condylurus* (Angolan free-tailed bat). Both bat species are widespread in Africa, and their ranges include countries where human Ebola virus disease (EVD) outbreaks have occurred. Forbes et al. (2) detected BOMV RNA in mouth swabs and internal parenchymal organs, except kidneys, of *M. condylurus* bats in Kenya in May 2018.

Most known outbreaks of EVD among humans were Zaire Ebola virus, including the large epidemic in West Africa during 2013–2016 (3). The reservoir hosts of Ebola virus (EBOV) remain unclear, but bats commonly are suspected. Viral RNA and EBOV antibodies have been detected in a few species of fruit bats (4,5). The discovery of BOMV supports the hypothesis regarding the role of bats as hosts of EBOVs, but further study is required to determine the bat species involved in viral transmission, prevalence of the virus in bat populations, and geographic distribution of the virus.

We detected BOMV RNA in free-tailed bats in N'Zerekore Prefecture, Guinea. We trapped bats in Guinea and Liberia during 2018–2019 (Table; Appendix, <https://wwwnc.cdc.gov/EID/article/25/9/19-0581-App1.pdf>) and detected BOMV RNA by reverse transcription PCR in 2 pools of kidney and lung samples from 2 *M. condylurus* bats captured in Yalenzou village in May 2018 (cycle threshold [C_t] 17.4 and 19.6) and in a pool of liver and spleen tissues (C_t 28.2) of an *M. condylurus* bat from a school in the city of N'Zerekore in March 2019 (Table). Blood, intestine, and brain samples were negative for viral RNA. Sequencing of the 483-bp fragment of the large gene (GenBank accession no. MK543447) demonstrated 99.3% identity with BOMV RNA from Sierra Leone (accession no. NC039345) and 98.3% identity with BOMV RNA from Kenya (accession no. MK340750).

Marí Saéz et al. (5) suggested that the Angolan free-tailed bat was the most plausible zoonotic source of the EVD

Table. Locations where free-tailed bats were trapped and tested for Bombali virus, Guinea and Liberia*

Location	Date	Total trapped	Species, no. tested (no. positive)		
			<i>Mops condylurus</i>	<i>Chaerephon pumilus</i>	<i>Chaerephon cf. major</i>
Yalenzou	2018 May 4	26	26 (2)	0	0
Gbao	2018 May 2	1	0	1	0
Yalenzou	2019 Mar 2	30	30	0	0
Bololowee†	2019 Mar 3	11	11	0	0
N'Zerekore, school	2019 Mar 5	47	27 (1)	0	20
N'Zerekore, house	2019 Mar 6	23	1	0	22
N'Zerekore, gazebo	2019 Mar 7	5	0	0	5
Dar Salam‡	2019 Mar 17	22	14	8	0
Total		165	109 (3)	9	47

*All bats were collected in N'Zerekore Prefecture, Guinea, except as indicated, and were tested by reverse transcription PCR for Bombali virus.

†Liberia.

‡Madina Oula Prefecture, Guinea.

epidemic in West Africa. In addition, EBOV nucleotide sequences previously have been found in *Hypsignathus monstrosus*, *Epomops franqueti*, and *Myonycteris torquata* bats in Gabon (6). He et al. (7) detected filovirus RNA in brown fruit bats (*Rousettus leschenaultii*) in China, and another study showed that 3 distinct groups of unclassified filoviruses are circulating in *Eonycteris spelaea* and *Rousettus* spp. fruit bats in China (8). These studies demonstrate that bats are promising targets for identifying emerging filoviruses, and additional Chiroptera species, both insectivorous and fruit bats, should be examined for EBOVs.

EBOV IgG was detected in the human population of Sierra Leone in 2006, 8 years before the EVD outbreak began in that country (9). Seroprevalence to EBOVs was also found in the medical staff of hospitals that were not involved in treating EVD-positive patients and in community contacts that worked with villages where EVD was not detected (10). The highest seroprevalence to EBOVs was found in the inhabitants of villages with the lowest number of documented EVD cases during the 2013–2016 outbreak in Sierra Leone (10). Cross-reactivity or nonspecific binding could be responsible for artifacts of immunoassay. However, other plausible explanations for the presence of antibodies against EBOV among persons with no symptoms of EVD exist, including subclinical EBOV infection in humans and antibody reactions to previously undiscovered, nonpathogenic filoviruses. The newly discovered BOMV could be a causative agent of these types of asymptomatic infections that produce antibodies with cross-reactivity to other EBOVs. Other undiscovered filoviruses also could be circulating in the region. Further surveillance with family-level primers is needed for insectivorous bats, as well as fruit bats and patients with acute infections.

Although BOMV had been detected in the northern part of Sierra Leone (1) and in the Taita Hills area of Kenya (2), we isolated it from bats in Guinea, far from these sites. Our finding provides additional evidence that BOMV is more widely distributed than previously suspected. Consequently, we advise screening of free-tailed bats for BOMV across their range. The high concentration of BOMV RNA we found in the internal organs of *M. condylurus* bats provides additional confirmation that BOMV could amplify in these bats and that this species is a reservoir host of this virus.

About the Author

Mrs. Karan is the head of the research group of Vector-borne and Zoonotic Diseases at Central Research Institute of Epidemiology, Moscow, Russia. Her research interests include tickborne and mosquito-borne diseases and related molecular diagnostics.

References

1. Goldstein T, Anthony SJ, Gbakima A, Bird BH, Bangura J, Tremeau-Bravard A, et al. The discovery of Bombali virus adds further support for bats as hosts of ebolaviruses. *Nat Microbiol*. 2018;3:1084–9. <https://doi.org/10.1038/s41564-018-0227-2>
2. Forbes KM, Webala PW, Jääskeläinen AJ, Abdurahman S, Ogola J, Masika MM, et al. Bombali virus in *Mops condylurus* bat, Kenya. *Emerg Infect Dis*. 2019;25:955–7. <https://doi.org/10.3201/eid2505.181666>
3. Baize S, Pannetier D, Oestereich L, Rieger T, Koivogui L, Magassouba N, et al. Emergence of Zaire Ebola virus disease in Guinea. *N Engl J Med*. 2014;371:1418–25. <https://doi.org/10.1056/NEJMoa1404505>
4. Pourrut X, Délicat A, Rollin PE, Ksiazek TG, Gonzalez JP, Leroy EM. Spatial and temporal patterns of Zaire ebolavirus antibody prevalence in the possible reservoir bat species. *J Infect Dis*. 2007;196(Suppl 2):S176–83. <https://doi.org/10.1086/520541>
5. Marí Saéz A, Weiss S, Nowak K, Lapeyre V, Zimmermann F, Dux A, et al. Investigating the zoonotic origin of the West African Ebola epidemic. *EMBO Mol Med*. 2015;7:17–23. <https://doi.org/10.15252/emmm.201404792>
6. Leroy EM, Kumulungui B, Pourrut X, Rouquet P, Hassanin A, Yaba P, et al. Fruit bats as reservoirs of Ebola virus. *Nature*. 2005;438:575–6. PubMed <https://doi.org/10.1038/438575a>
7. He B, Feng Y, Zhang H, Xu L, Yang W, Zhang Y, et al. Filovirus RNA in Fruit Bats, China. *Emerg Infect Dis*. 2015;21:1675–7. <https://doi.org/10.3201/eid2109.150260>
8. Yang XL, Zhang YZ, Jiang RD, Guo H, Zhang W, Li B, et al. Genetically diverse filoviruses in *Rousettus* and *Eonycteris* spp. bats, China, 2009 and 2015. *Emerg Infect Dis*. 2017;23:482–6. <https://doi.org/10.3201/eid2303.161119>
9. Richardson ET, Kelly JD, Barrie MB, Mesman AW, Karku S, Quiwa K, et al. Minimally symptomatic infection in an Ebola ‘hotspot’: A cross-sectional serosurvey. *PLoS Negl Trop Dis*. 2016;10:e0005087. <https://doi.org/10.1371/journal.pntd.0005087>
10. Mafopa NG, Russo G, Wadoum REG, Iwerima E, Batwala V, Giovanetti M, et al. Seroprevalence of Ebola virus infection in Bombali District, Sierra Leone. *J Public Health Africa*. 2017;8:732. <https://doi.org/10.4081/jphia.2017.732>

Address for correspondence: Marat T. Makenov, Research Group of Vector-Borne and Zoonotic Diseases, 3-A Novogireevskaya St. 415, Moscow 111123, Russia; email: mmakenov@gmail.com

Blastomycosis Misdiagnosed as Tuberculosis, India

Anil Kumar, Akhilesh Kunoor, Malini Eapen, Pradeep Kumar Singh, Anuradha Chowdhary

Author affiliations: Amrita Institute of Medical Sciences and Research Centre, Kochi, India (A. Kumar, A. Kunoor, M. Eapen); Vallabhbhai Patel Chest Institute, Delhi, India (P.K. Singh, A. Chowdhary)

DOI: <https://doi.org/10.3201/eid2509.190587>

Chronic pulmonary blastomycosis is often misdiagnosed and treated as tuberculosis in disease-endemic and non-disease-endemic areas. We report the case of a 32-year-old man who, after visiting Chicago, Illinois, USA, returned to India and received treatment for tuberculosis for 12 months before receiving the correct diagnosis of blastomycosis.

Blastomyces dermatitidis is a dimorphic fungus that is rarely reported from India; no well-defined area of endemicity in that part of the world has been recorded (1). However, it is endemic to the Ohio and Mississippi River valleys of North America and the states bordering the Great Lakes (2). Acute pulmonary infection is caused by inhalation of aerosolized *B. dermatitidis* conidia, which convert to yeast forms within the lungs (3). In the acute stage, blastomycosis may be misdiagnosed as bacterial pneumonia and sometimes as another illness. Most cases of blastomycosis are usually diagnosed after the infection has become chronic. Severe pulmonary disease can occur in apparently immunocompetent, as well as immunocompromised, persons (3). Persons from non-disease-endemic areas usually acquire this disease during travel to disease-endemic areas (1).

In November 2014, a 32-year-old man, native to the state of Kerala, India, sought care for multiple discharging sinuses on his anterior chest wall (Figure, panel A). He weighed 75 kg and had been receiving first-line anti-tuberculosis (anti-TB) therapy for 12 months for nonresolving left upper lung lobe consolidation. Skin on his legs and forearms showed patchy hair loss without erythema,

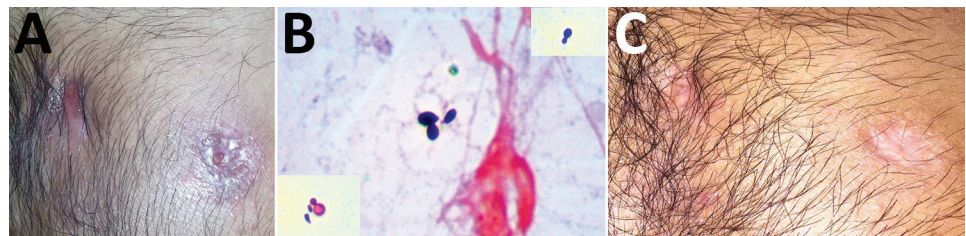
nodularity, or scarring. Past records showed that sputum, bronchoalveolar lavage fluid, and pus from a cold abscess were negative for *Mycobacterium tuberculosis* by smear, culture (BACTEC MGIT 960; Becton Dickinson, <https://www.bd.com>), and PCR (Cepheid Xpert MTB-RIF, <http://www.cepheid.com>). A fine-needle aspirate, obtained from the left upper lung lobe with computed tomography guidance, showed suppurative granulomas. Results of Mantoux, anti-cyclic citrullinated peptide, antinuclear antibody testing, and serologic testing for HIV were negative. In the absence of a definitive diagnosis, first-line anti-TB therapy was empirically initiated and continued for another 12 months without any clinical improvement.

High-resolution computed tomography of the chest showed consolidation with air space opacities, and multiple subcutaneous pockets of pus with discharging sinuses above the sternum were noted. Detailed travel history revealed that before the illness, the patient had worked on a 9-month project in Chicago, Illinois, USA, during which time he resided in Lisle, Illinois. He did not indulge in outdoor activities that may increase the possibility of inhaling spores of this fungus, such as river rafting or hiking.

At the Department of Microbiology, Amrita Institute of Medical Sciences and Research Centre, Kochi, India, Gram and calcofluor white staining of the pus collected from the discharging sinus showed budding yeast cells (Figure, panel B). Examination of a pus smear revealed no acid-fast bacilli. Pus was cultured on Sabouraud dextrose agar and 5% sheep blood agar. Biopsy samples from lesions on the forearm, stained with periodic acid-Schiff and Grocott-Gomori methenamine silver, were negative for fungal elements.

Because of strong suspicion of a fungal infection, probably blastomycosis, and considering the patient's stay in Chicago, anti-TB therapy was replaced with itraconazole at a dose of 200 mg 2×/d. Cultures on Sabouraud dextrose agar grew a dimorphic fungus identified microscopically as *B. dermatitidis* and confirmed by sequencing (GenBank accession no. KT443881). Antifungal susceptibility (according to the Clinical and Laboratory Standards Institute, <https://clsi.org>) showed low MICs for itraconazole (0.06 µg/mL), voriconazole (0.25 µg/mL), amphotericin B (0.5

Figure. Patient with blastomycosis, India, 2014. A) Photograph of chest showing actively discharging sinuses before treatment with antifungal medication. B) Slide of Gram-stained pus discharge, showing broad-based budding yeast cells. The insets show Gram staining of the same organism, with narrow and broad-based budding in different fields. Original magnification ×100. C) Photograph of chest showing closed sinuses and disappearance of sinus line after treatment with antifungal medication.



µg/mL), micafungin (0.125 µg/mL), anidulafungin (0.06 µg/mL), and caspofungin (0.25 µg/mL). After 12 months of antifungal therapy, the chest wall sinuses closed and the sinus lines disappeared (Figure, panel C). High-resolution computed tomography showed complete healing of left upper lobe lesions, which had resulted in focal fibrosis and cystic and tubular traction bronchiectasis. At this time, antifungal therapy was discontinued.

Chronic pulmonary blastomycosis results in chronic cough, weight loss, and hemoptysis, often masquerading as TB or malignancy (4). The patient described here exemplifies the challenges of diagnosing pulmonary blastomycosis in a non-blastomycosis-endemic area where TB is prevalent. Most patients receive multiple courses of anti-TB treatment, which can delay blastomycosis diagnosis by >1 month (5). Chronic pulmonary blastomycosis has been misdiagnosed and treated as TB in disease-endemic and non-disease-endemic areas (1,4). Even in blastomycosis-endemic areas such as Illinois, the median time from onset to diagnosis is 128 days (range 12–489 days) (6). The presence of skin lesions increases the recognition of blastomycosis (2). The patient reported here had worked for 9 months in an area where *B. dermatitidis* is highly endemic (6). Presence of skin lesions, negative mycobacterial cultures and Xpert MTB/RIF assay results, and the absence of response to anti-TB treatment should have raised the suspicion of blastomycosis for this patient.

Definitive diagnosis of blastomycosis can be made only by culture, which often takes weeks. Direct potassium hydroxide smears and cytopathology are inexpensive, produce rapid results, and can demonstrate characteristic broad-based budding yeasts in samples (1). Although the sensitivity of urinary antigen test for blastomycosis is high, that test lacks specificity because of cross-reactions with *Histoplasma* spp. (7).

Blastomycosis is rarely reported in India; a review by Kumar et al. (1) reported only 6 definitively diagnosed cases, of which 2 were associated with travel to disease-endemic areas in the United States (8,9). The choice of antifungal medication for blastomycosis depends on disease severity. For severe disease, the recommended treatment is initial amphotericin B therapy for 1–2 weeks followed by oral itraconazole; for mild and moderate disease, the recommended treatment is oral itraconazole. A minimum of 6 months of treatment is required for all patients with pulmonary blastomycosis (8).

A high index of suspicion is needed to detect blastomycosis in non-disease-endemic areas where TB is prevalent. Clinicians should elicit a thorough travel history from patients with illness that does not respond to anti-TB treatment.

About the Author

Dr. Kumar is a clinical microbiologist and professor at Amrita Institute of Medical Sciences and Research Centre, Kochi, Kerala, India. His research interests include emerging fungal infections, antifungal resistance, antimicrobial drug stewardship, and epidemiology of neglected tropical infectious diseases.

References

1. Kumar A, Sreehari S, Velayudhan K, Biswas L, Babu R, Ahmed S, et al. Autochthonous blastomycosis of the adrenal: first case report from Asia. *Am J Trop Med Hyg.* 2014;90:735–9. <https://doi.org/10.4269/ajtmh.13-0444>
2. Saccante M, Woods GL. Clinical and laboratory update on blastomycosis. *Clin Microbiol Rev.* 2010;23:367–81. <https://doi.org/10.1128/CMR.00056-09>
3. Castillo CG, Kauffman CA, Miceli MH. Blastomycosis. *Infect Dis Clin North Am.* 2016;30:247–64. <https://doi.org/10.1016/j.idc.2015.10.002>
4. Koroscil MT, Skabelund A. Chronic pulmonary blastomycosis mimicking pulmonary tuberculosis. *Mil Med.* 2018;183:e332–e333.
5. Alpern JD, Bahr NC, Vazquez-Benitez G, Boulware DR, Sellman JS, Sarosi GA. Diagnostic delay and antibiotic overuse in acute pulmonary blastomycosis. *Open Forum Infect Dis.* 2016;3:ofw078. <https://doi.org/10.1093/ofid/ofw078>
6. Dworkin MS, Duckro AN, Proia L, Semel JD, Huhn G. The epidemiology of blastomycosis in Illinois and factors associated with death. *Clin Infect Dis.* 2005;41:e107–11. <https://doi.org/10.1086/498152>
7. Chapman SW, Dismukes WE, Proia LA, Bradsher RW, Pappas PG, Threlkeld MG, et al.; Infectious Diseases Society of America. Clinical practice guidelines for the management of blastomycosis: 2008 update by the Infectious Diseases Society of America. *Clin Infect Dis.* 2008;46:1801–12. <https://doi.org/10.1086/588300>
8. Randhawa HS, Chowdhary A, Kathuria S, Roy P, Misra DS, Jain S, et al. Blastomycosis in India: report of an imported case and current status. *Med Mycol.* 2013;51:185–92. <https://doi.org/10.3109/13693786.2012.685960>
9. Savio J, Muralidharan S, Macaden RS, D'Souza G, Mysore S, Ramachandran P, et al. Blastomycosis in a South Indian patient after visiting an endemic area in USA. *Med Mycol.* 2006;44:523–9. <https://doi.org/10.1080/13693780500406865>

Address for correspondence: Anil Kumar, Amrita Institute of Medical Sciences and Research Centre, Amrita Vishwa Vidyapeetham, Ponekkara, Kochi, Kerala, India; email: vanilkumar@aims.amrita.edu

Invasive Fungal Disease, Isavuconazole Treatment Failure, and Death in Acute Myeloid Leukemia Patients

Anne-Pauline Bellanger, Ana Berceanu, Emeline Scherer, Yohan Desbrosses, Etienne Daguindau, Steffi Rocchi, Laurence Millon

Author affiliations: University Hospital, Besançon, France (A.-P. Bellanger, E. Scherer, S. Rocchi, L. Millon); Franche-Comté University, Besançon (A.-P. Bellanger, E. Scherer, L. Millon); Besançon University Hospital, Besançon (A. Berceanu, Y. Desbrosses, E. Daguindau)

DOI: <https://doi.org/10.3201/eid2509.190598>

We present 2 fatal cases of invasive fungal disease with isavuconazole treatment failure in immunocompromised patients: one with a TR34-L98H azole-resistant *Aspergillus fumigatus* isolate and the other a *Rhizomucor–A. fumigatus* co-infection. Such patients probably require surveillance by galactomannan antigen detection and quantitative PCRs for *A. fumigatus* and Mucorales fungi.

Isavuconazole, an antifungal azole used to treat invasive fungal diseases (IFDs), is approved as a first-line treatment for invasive aspergillosis and can be used as an alternative treatment for mucormycosis (1). We present 2 cases of IFD and isavuconazole treatment failure in acute myeloid leukemia (AML) patients with prolonged neutropenia after hematopoietic stem-cell transplantation (SCT).

Patient 1, a 52-year-old truck driver with AML (diagnosed in 2017), received a haplo-identical SCT (day 0) 4 months after the diagnosis. The patient had incomplete hematologic reconstitution and experienced graft-versus-host disease of the digestive tract (day 0), which we treated with corticosteroids and ruxolitinib. We gave the patient oral posaconazole (300 mg/day, starting day 1) for

IFD prophylaxis, as recommended by the 4th European Conference on Infections in Leukaemia (2). On about day 65, we diagnosed probable invasive aspergillosis according to the criteria of the European Organisation for Research and Treatment of Cancer Mycoses Study Group (3,4); the patient had fever, neutropenia, and a discrete pulmonary lesion on chest computed tomography (CT), and serum samples were repeatedly positive by an in-house *A. fumigatus* quantitative PCR (qPCR) but negative for galactomannan antigen (Figure) (1,4). On the same day, we switched treatment to oral isavuconazole (200 mg/day). On day 126, chest CT showed the persistence of pulmonary lesions, and we switched patient treatment to liposomal amphotericin B (5 mg/day by injection). Thereafter, serum samples became repeatedly positive for galactomannan antigen and *A. fumigatus* DNA. At day 158, we found TR34-L98H azole-resistant *A. fumigatus* fungus in his bronchial aspirate. The French National Reference Center for Invasive Mycoses and Antifungals (Paris, France) performed MIC testing using European Committee on Antibiotic Susceptibility Testing methods (<https://www.pasteur.fr/fr/sante-publique/CNR/les-cnr/mycoses-invasives-antifongiques>). The following MICs were obtained: amphotericin B 0.25 mg/L (susceptibility unknown, no breakpoint available), itraconazole >8 mg/L (resistant), isavuconazole 4 mg/L (resistant), and voriconazole 2 mg/L (susceptible). The patient died 182 days after the SCT.

Patient 2, a 61-year-old businessman with AML (diagnosed in 2013), received his first allogenic hematopoietic SCT 4 months after the diagnosis. He experienced a relapse 3 years after the first transplantation, and a second allogenic hematopoietic SCT was performed (day 0), which was followed by severe sepsis with *Escherichia coli*. An excavated nodule was visible on chest CT (day 4), and the *A. fumigatus* biomarker was repeatedly positive, suggesting probable invasive aspergillosis according to European Organisation for Research and Treatment of Cancer criteria (3). On day 5, treatment with isavuconazole (200 mg/day orally) was initiated. Graft-versus-host disease of the digestive tract also developed (day 12) in this patient, which

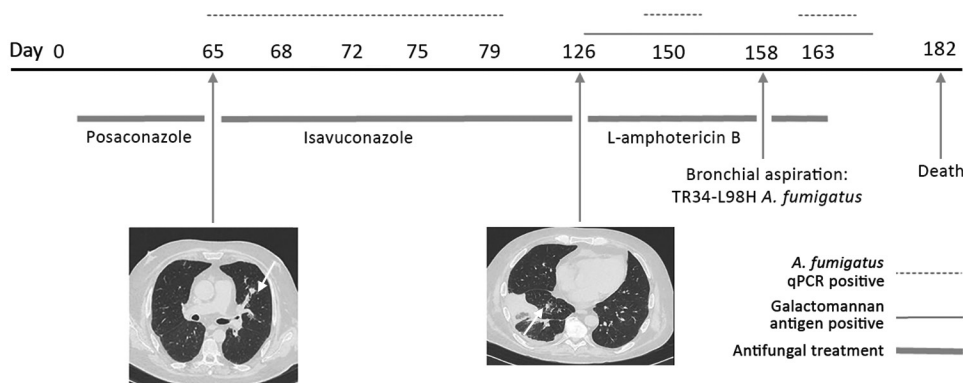


Figure. Evolution of fungal biomarkers, computed tomography chest scans, and antifungal treatments for immunocompromised patient 1 with invasive *Aspergillus fumigatus* infection, France, 2018. Arrows indicate lesions. qPCR, quantitative PCR.

we treated with ruxolitinib, tacrolimus, and prednisolone. On day 92, the patient had asthenia, fever, and thoracic pain, and chest CT showed multiple micronodules. On days 95–116, systematic fungal surveillance testing of serum samples showed 1 test positive for galactomannan antigen, 4 positive for *A. fumigatus* DNA, and 3 positive for *Rhizomucor* DNA. Two cultured pulmonary samples collected on days 114 and 116 were positive for *A. fumigatus*. We performed ETESTs (bioMérieux, <https://www.biomerieux-diagnostics.com>), which indicated the following MICs: amphotericin B 0.023 mg/L (susceptibility unknown), isavuconazole 0.25 mg/L (susceptible), and voriconazole 0.38 mg/L (susceptible). We switched patient treatment to liposomal amphotericin B (5 mg/kg by injection) on day 117, but the patient died on day 129.

These 2 cases had in common AML treated by SCT, followed by severe digestive graft-versus-host disease, IFD resistant to isavuconazole diagnosed >100 days after SCT, use of combined fungal biomarkers to detect IFD, and death despite rapid prescription of amphotericin B. Severe digestive graft-versus-host disease might have affected the levels of isavuconazole absorbed by the patient because the drug was administered orally in both cases. Intravenous isavuconazole is not recommended for treating IFD and was not available at the treatment facility (University Hospital, Besançon, France). However, these cases suggest that isavuconazole levels should be checked in patients with severe digestive graft-versus-host disease. For patient 1, a change in class of antifungal drugs could have been made as early as day 65, and earlier treatment with amphotericin B could have had a positive effect on his prognosis. The long duration between the initial positive qPCR and galactomannan antigen test result suggests patient 1 might have been infected with multiple *A. fumigatus* isolates, with 1 being resistant. For patient 2, the systematic use of Mucorales qPCR enabled early detection of a mixed *Aspergillus*-Mucorales fungal infection (5). These types of mixed mold infection were reported to have a prevalence of 25% in studies including Mucorales qPCR (6). The diagnosis of *Rhizomucor* infection was based on 3 successive samples being positive by *Rhizomucor* qPCR. A Mucorales qPCR of the patient's bronchoalveolar lavage fluid (validated assay with satisfying sensitivity) was surprisingly negative (6).

In summary, these cases demonstrate that systematic surveillance is needed for severely immunocompromised patients treated for IFD. Galactomannan antigen detection and qPCRs targeting *Aspergillus fumigatus* and Mucorales fungi might be the optimal surveillance strategy.

Acknowledgments

We thank Pamela Albert for her editorial assistance.

About the Author

Dr. Bellanger is a microbiologist involved in the diagnosis of invasive fungal infections at University Hospital, Besançon, France. Her research focus is on invasive aspergillosis and mucormycosis.

References

1. Cresemba® (isavuconazium sulfate) [package insert]. Northbrook (IL): Astellas Pharma US, Inc.;2015.
2. Groll AH, Castagnola E, Cesaro S, Dalle JH, Engelhard D, Hope W, et al.; Fourth European Conference on Infections in Leukaemia; Infectious Diseases Working Party of the European Group for Blood Marrow Transplantation; Infectious Diseases Group of the European Organisation for Research and Treatment of Cancer; International Immunocompromised Host Society; European Leukaemia Net. Fourth European Conference on Infections in Leukaemia (ECIL-4): guidelines for diagnosis, prevention, and treatment of invasive fungal diseases in paediatric patients with cancer or allogeneic haemopoietic stem-cell transplantation. *Lancet Oncol*. 2014;15:e327–40. [https://doi.org/10.1016/S1470-2045\(14\)70017-8](https://doi.org/10.1016/S1470-2045(14)70017-8)
3. De Pauw B, Walsh TJ, Donnelly JP, Stevens DA, Edwards JE, Calandra T, et al.; European Organization for Research and Treatment of Cancer/Invasive Fungal Infections Cooperative Group; National Institute of Allergy and Infectious Diseases Mycoses Study Group Consensus Group. Revised definitions of invasive fungal disease from the European Organization for Research and Treatment of Cancer/Invasive Fungal Infections Cooperative Group and the National Institute of Allergy and Infectious Diseases Mycoses Study Group (EORTC/MSG) Consensus Group. *Clin Infect Dis*. 2008;46:1813–21. <https://doi.org/10.1086/588660>
4. Ullmann AJ, Aguado JM, Arikan-Akdagli S, Denning DW, Groll AH, Lagrou K, et al. Diagnosis and management of *Aspergillus* diseases: executive summary of the 2017 ESCMID-ECMM-ERS guideline. *Clin Microbiol Infect*. 2018;24 (Suppl 1):e1–38. <https://doi.org/10.1016/j.cmi.2018.01.002>
5. Millon L, Scherer E, Rocchi S, Bellanger AP. Molecular strategies to diagnose mucormycosis. *J Fungi (Basel)*. 2019;5:24. <https://doi.org/10.3390/jof5010024>
6. Scherer E, Iriart X, Bellanger AP, Dupont D, Guitard J, Gabriel F, et al. Quantitative PCR (qPCR) detection of Mucorales DNA in bronchoalveolar lavage fluid to diagnose pulmonary mucormycosis. *J Clin Microbiol*. 2018;56:e00289-18. <https://doi.org/10.1128/JCM.00289-18>

Address for correspondence: Anne-Pauline Bellanger, Department of Parasitology-Mycology, Besançon University Hospital Jean Minjot, 2 Blvd Fleming, 25030 Besançon CEDEX, France; email: apbellanger@chu-besancon.fr

and within the South American clade, isolates from cases in Colombia, the United States, and Venezuela clustered together (Figure).

The *C. auris* isolate from Iran appears to represent a fifth major clade. Although this case was reported in 2018, additional cases of *C. auris* infections and colonization are thought to exist in Iran, given that challenges in diagnostic capacity in the country have probably limited the identification of more *C. auris* cases. The patient in this case was reported to have never traveled outside Iran (8), suggesting that this population structure might not be a result of a recent *C. auris* introduction into the country and that it might have emerged in Iran some time ago. Determining whether additional *C. auris* cases exist in Iran and whether such strains are related will help shed light on how *C. auris* emerged in Iran.

The isolate from Iran was susceptible to the 3 major classes of antifungal drugs and was cultured from ear swab specimens from the patient (8). *C. auris* of the East Asian clade is thought to have a propensity for the ear that is uncharacteristic of the other major clades (9). A recent study showed that, of 61 *C. auris* isolates obtained from 13 hospitals across South Korea during a 20-year period, 57 (93%) came from ear cultures (10). Although a systematic analysis has not been conducted, there are limited reports of ear infections or colonization caused by *C. auris* of the South Asian, African, or South American clades, so it is of interest that the isolate from Iran was most closely related to isolates of the East Asian clade, albeit with a difference of hundreds of thousands of single nucleotide polymorphisms. Ultimately, our discovery is a reminder that much about *C. auris* remains to be learned and underscores the need for vigilance in areas where *C. auris* has not yet emerged.

Acknowledgments

We thank the Canisius-Wilhelmina Hospital for providing the research funds for the molecular analysis in this study.

Authors' contributions: N.A.C. and J.F.M. designed the study; T.dG., H.B., and M.A. were involved in laboratory investigations; N.A.C. and T.M.C. performed the bioinformatics; N.A.C. drafted the manuscript; and all authors read, revised, and approved the final manuscript.

About the Author

Dr. Chow is a molecular epidemiologist in the Mycotic Diseases Branch of the Division of Foodborne, Waterborne, and Environmental Diseases, National Center for Emerging

and Zoonotic Infectious Diseases, Centers for Disease Control and Prevention. Her primary research interests include application of whole-genome sequencing and metagenomics for outbreak investigations as well as integrating and visualizing epidemiologic and laboratory data sources.

References

1. Chowdhary A, Sharma C, Meis JF. *Candida auris*: a rapidly emerging cause of hospital-acquired multidrug-resistant fungal infections globally. *PLoS Pathog*. 2017;13:e1006290. <https://doi.org/10.1371/journal.ppat.1006290>
2. Saris K, Meis JF, Voss A. *Candida auris*. *Curr Opin Infect Dis*. 2018;31:334–40.
3. Welsh RM, Bentz ML, Shams A, Houston H, Lyons A, Rose LJ, et al. Survival, persistence, and isolation of the emerging multidrug-resistant pathogenic yeast *Candida auris* on a plastic healthcare surface. *J Clin Microbiol*. 2017;55:2996–3005. <https://doi.org/10.1128/JCM.00921-17>
4. Lockhart SR, Etienne KA, Vallabhaneni S, Farooqi J, Chowdhary A, Govender NP, et al. Simultaneous emergence of multidrug-resistant *Candida auris* on 3 continents confirmed by whole-genome sequencing and epidemiological analyses. *Clin Infect Dis*. 2017;64:134–40. <https://doi.org/10.1093/cid/ciw691>
5. Chow NA, Gade L, Tsay SV, Forsberg K, Greenko JA, Southwick KL, et al.; US *Candida auris* Investigation Team. Multiple introductions and subsequent transmission of multidrug-resistant *Candida auris* in the USA: a molecular epidemiological survey. *Lancet Infect Dis*. 2018;18:1377–84. [https://doi.org/10.1016/S1473-3099\(18\)30597-8](https://doi.org/10.1016/S1473-3099(18)30597-8)
6. Escandón P, Chow NA, Caceres DH, Gade L, Berkow EL, Armstrong P, et al. Molecular epidemiology of *Candida auris* in Colombia reveals a highly related, countrywide colonization with regional patterns in amphotericin B resistance. *Clin Infect Dis*. 2019;68:15–21.
7. Rhodes J, Abdolrasouli A, Farrer RA, Cuomo CA, Aanensen DM, Armstrong-James D, et al. Genomic epidemiology of the UK outbreak of the emerging human fungal pathogen *Candida auris*. *Emerg Microbes Infect*. 2018;7:43. <https://doi.org/10.1038/s41426-018-0045-x>
8. Abastabar M, Haghani I, Ahangarkani F, Rezaei MS, Taghizadeh Armaki M, Roodgari S, et al. *Candida auris* otomycosis in Iran and review of recent literature. *Mycoses*. 2019; 62:101–5. <https://doi.org/10.1111/myc.12886>
9. Welsh RM, Sexton DJ, Forsberg K, Vallabhaneni S, Litvintseva A. Insights into the unique nature of the East Asian clade of the emerging pathogenic yeast *Candida auris*. *J Clin Microbiol*. 2019;57:e00007–19. <https://doi.org/10.1128/JCM.00007-19>
10. Kwon YJ, Shin JH, Byun SA, Choi MJ, Won EJ, Lee D, et al. *Candida auris* clinical isolates from South Korea: Identification, antifungal susceptibility, and genotyping. *J Clin Microbiol*. 2019;57:e01624–18. <https://doi.org/10.1128/JCM.01624-18>

Address for correspondence: Jacques F. Meis, Department of Medical Microbiology and Infectious Diseases, Canisius Wilhelmina Hospital, Weg door Jonkerbos 100, 6500GS Nijmegen, The Netherlands; email: j.meis@cwz.nl

Dengue Virus Type 1 Infection in Traveler Returning from Tanzania to Japan, 2019

Kazuma Okada, Ryo Morita, Kazutaka Egawa, Yuki Hirai, Atsushi Kaida, Michinori Shirano, Hideyuki Kubo, Tetsushi Goto, Seiji P. Yamamoto

Author affiliations: Osaka Institute of Public Health, Osaka, Japan (K. Okada, K. Egawa, Y. Hirai, A. Kaida, H. Kubo, S.P. Yamamoto); Osaka City General Hospital, Osaka (R. Morita, M. Shirano, T. Goto)

DOI: <https://doi.org/10.3201/eid2509.190814>

The largest outbreak of dengue fever in Tanzania is ongoing. Dengue virus type 1 was diagnosed in a traveler who returned from Tanzania to Japan. In phylogenetic analysis, the detected strain was close to the Singapore 2015 strain, providing a valuable clue for investigating the dengue outbreak in Tanzania.

Dengue fever is a febrile illness and a major public health problem caused by dengue virus (DENV), which infects almost 400 million persons worldwide every year (1). DENV has 4 serotypes (DENV-1–4), which are antigenically distinct. Although many countries in Africa are listed as being at a risk of DENV transmission, the molecular characterization of circulating DENV strains in these countries is poor.

In Tanzania, the number of patients with dengue fever increased sharply during April–May 2019, when >3,000 new suspected dengue cases were reported, including 2 deaths. Of these cases, 71.4% were confirmed by rapid diagnostic tests according to the World Health Organization; this total exceeded the previous worst dengue outbreak in 2014, which had 2,129 suspected and 1,018 confirmed cases (2). DENV-2 was reported as the causative agent of the 2014 outbreak in Tanzania (3,4), whereas DENV-3 exported from Tanzania was also documented (5). We describe the case of a traveler from Japan who was infected with DENV-1 in Tanzania amid the country's largest dengue outbreak in 2019.

In early May 2019, a 32-year-old man who returned to Japan from Tanzania was admitted to Osaka City General Hospital in Osaka, Japan, after receiving a diagnosis of dengue fever at the Kansai International Airport quarantine station. He had been vaccinated against yellow fever before travel; additional test results were negative for chikungunya virus, Zika virus, and malaria. During his 10-day stay in Tanzania, the patient arrived at the airport in Dar es Salaam and stayed there during days 1–2 (specific locations in the

Appendix Figure, <http://wwwnc.cdc.gov/EID/article/25/9/19-0814-App1.pdf>). On day 3, the patient flew to Kigoma, located in northwestern Tanzania; he reported being bitten by mosquitoes several times during the day there. On day 4, he visited Mahale Mountains National Park; the visit lasted for 3 days. On day 7, the patient returned to Kigoma and noticed fever and headache (disease onset). He traveled to Dar es Salaam on day 8 and stayed there for 2 days but was sick in bed at the hotel the entire time. He left Tanzania on day 10 to return to Japan and subsequently reported that he had been bitten by mosquitoes only in Kigoma.

We detected DENV-1 in the patient's blood sample, collected 4 days after disease onset, using real-time reverse transcription PCR (RT-PCR) (6). We amplified a region of the envelope gene (1,485 nt) by RT-PCR using DENV-1-specific primers (7) and determined the sequence by direct sequencing (deposited in the DNA Data Bank of Japan as DV1/TZA/19RM-Osaka under accession no. LC485151). Through phylogenetic analysis based on a recent report (8), we classified the DV1/TZA/19RM-Osaka strain as genotype V and closely related to a 22125 strain in Singapore in 2015 with 98.6% nucleotide identity (Figure). The DV1/TZA/19RM-Osaka strain was distinct from other genotype V strains detected in Africa, suggesting that the DENV-1 strain in Tanzania might have been introduced from outside Africa.

Dengue outbreaks occurred in 2010, 2012, 2013, and 2014 in Dar es Salaam, with the largest in 2014 (3). Recent studies have reported DENV-2 as the cause of the 2014 outbreak; the high similarity of the virus to DENV-2 strains from China, India, East Timor, and Singapore indicates that it might have been introduced by travelers from Asia (4). Another study indicated that DENV-3 was introduced or reintroduced in Tanzania from other countries in Africa or from the Middle East (5). In this study, we showed that the transmission of DENV-1, the genome of which was phylogenetically related to the strain derived in Singapore, has occurred in Tanzania.

Dar es Salaam has been the epicenter of the 2019 dengue outbreak and past outbreaks. From this patient's mosquito bite history, we concluded that the patient was most likely infected with DENV-1 in Kigoma, but we cannot deny the possibility of unrecognized mosquito bites in Dar es Salaam. A recent study showed that 1% of dengue cases in the 2014 outbreak were reported from regions outside Dar es Salaam, including Kigoma, and model prediction suggested that Kigoma could have the possibility of occurrence of dengue concurrently with the dengue outbreak in Dar es Salaam (9). However, the disease was not detected on a large scale because of a lack of proper diagnosis (9), which suggests several unrecognized dengue cases in Kigoma even in the ongoing 2019 outbreak. Taken together, the DV1/TZA/19RM-Osaka strain may have originated from the outbreak strain in Dar es Salaam in 2019.

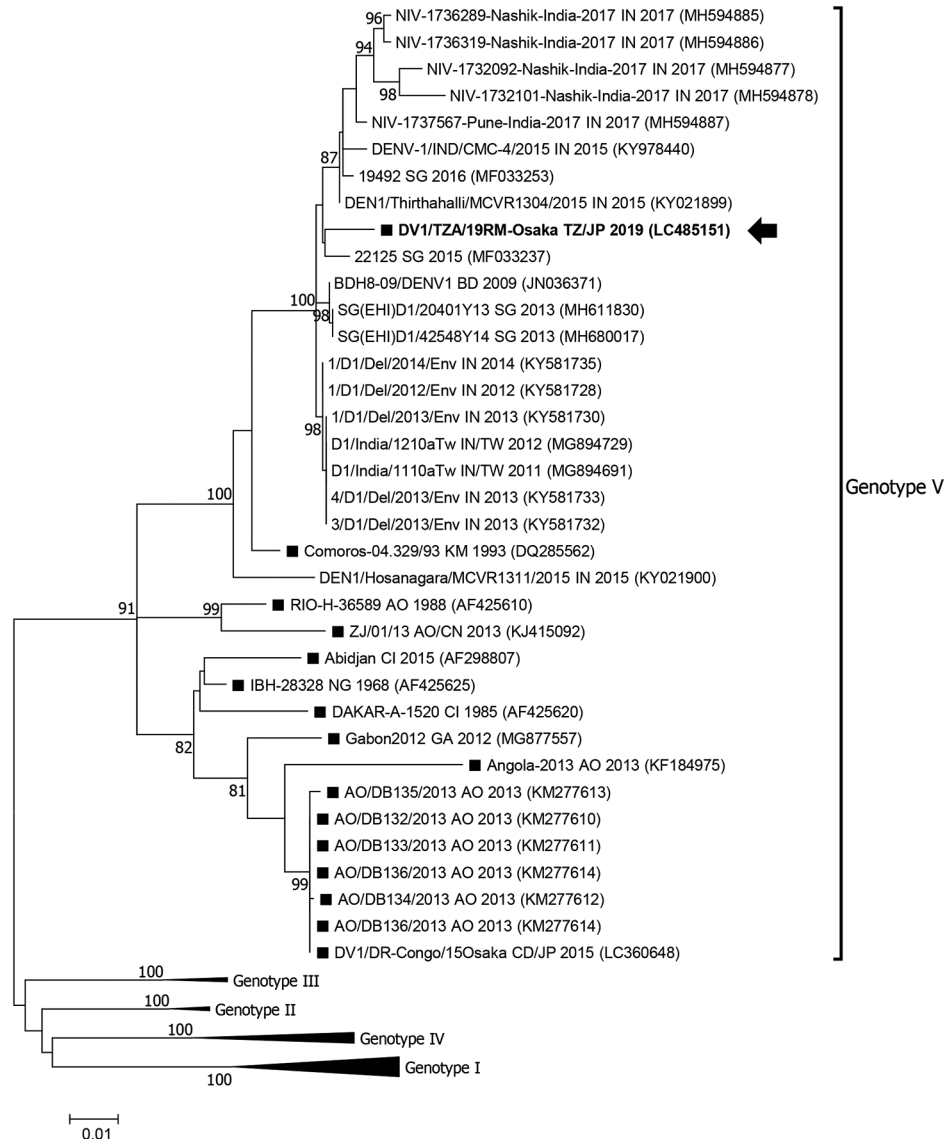


Figure. Maximum-likelihood phylogram of the envelope gene (1,485 nt) of dengue virus type 1 strains detected in Osaka, Japan, 2019 (arrow), Africa (black squares), and reference strains. Based on Bayesian information criteria, the Tamura-Nei plus gamma model was used to construct the phylogram. Numbers at the nodes indicate the bootstrap support values, which are expressed as a percentage of 1,000 replicates (values <80% are omitted). Each strain is identified by strain name, 2-letter country name abbreviation (country exported from/to, in the case of travelers), and detection year; accession numbers are shown in parentheses. Genotype I–IV branches are condensed for space. Scale bar indicates genetic distance (nucleotide substitutions per site). AO, Angola; BD, Bangladesh; CD, Democratic Republic of the Congo; CI, Côte d'Ivoire; GA, Gabon; IN, India; JP, Japan; KM, Comoros; NG, Nigeria; SG, Singapore; TW, Taiwan; TZ, Tanzania.

The phylogenetic relationships among DENV strains detected at different locations during the same epidemic in Tanzania are yet to be studied. Our data contribute to a better understanding of the epidemiology of DENV infections in Tanzania. Additional studies of dengue fever in Tanzania, not only in Dar es Salaam but also in other regions, would further clarify the epidemiology of this serious public health concern in this country.

Acknowledgments

We thank members of the Microbiology Section, Division of Microbiology, Osaka Institute of Public Health, Osaka, Japan, for supporting our work. We are also grateful to members of Osaka City Health Centers for their support in a virus surveillance in Osaka City.

This study was approved by the ethics committee of the Osaka Institute of Public Health (no. 1709-08-03) and was supported by

the Japan Society for the Promotion of Science, Grant-in-Aid for Scientific Research, grant no. 16K21709.

About the Author

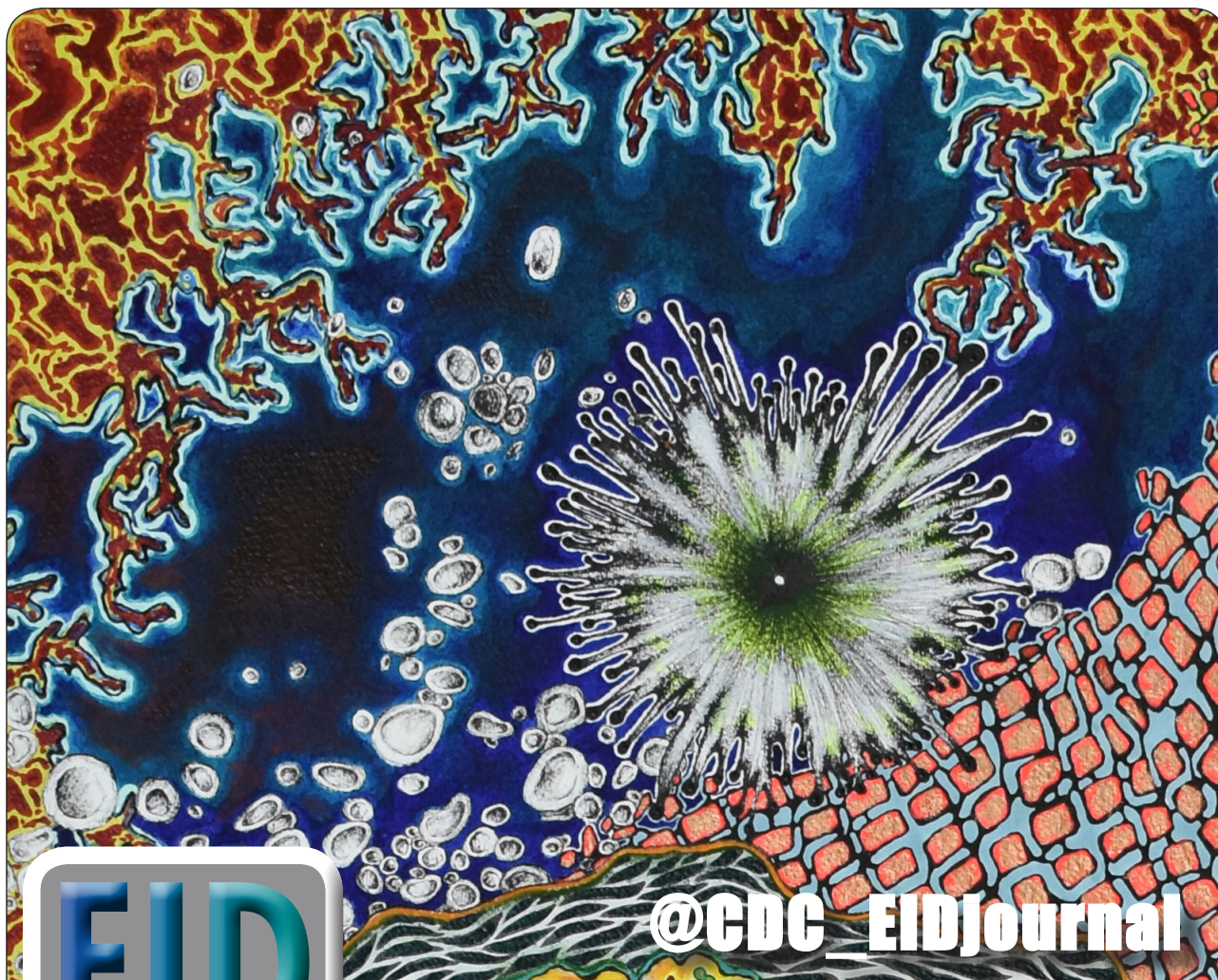
Dr. Okada is a researcher at Osaka Institute of Public Health in Osaka, Japan. His research interests include dengue and chikungunya viruses.

References

- Bhatt S, Gething PW, Brady OJ, Messina JP, Farlow AW, Moyes CL, et al. The global distribution and burden of dengue. *Nature*. 2013;496:504–7. <https://doi.org/10.1038/nature12060>
- Ward T, Samuel M, Maoz D, Runge-Ranzinger S, Boyce R, Toledo J, et al. Dengue data and surveillance in Tanzania: a systematic literature review. *Trop Med Int Health*. 2017;22:960–70. <https://doi.org/10.1111/tmi.12903>

3. Mboera LE, Mweya CN, Rumisha SF, Tungu PK, Stanley G, Makange MR, et al. The risk of dengue virus transmission in Dar es Salaam, Tanzania during an epidemic period of 2014. *PLoS Negl Trop Dis*. 2016;10:e0004313. <https://doi.org/10.1371/journal.pntd.0004313>
4. Vairo F, Mboera LE, De Nardo P, Oriyo NM, Meschi S, Rumisha SF, et al. Clinical, virologic, and epidemiologic characteristics of dengue outbreak, Dar es Salaam, Tanzania, 2014. *Emerg Infect Dis*. 2016;22:895–9. <https://doi.org/10.3201/eid2205.151462>
5. Moi ML, Takasaki T, Kotaki A, Tajima S, Lim CK, Sakamoto M, et al. Importation of dengue virus type 3 to Japan from Tanzania and Côte d'Ivoire. *Emerg Infect Dis*. 2010;16:1770–2. <https://doi.org/10.3201/eid1611.101061>
6. Ito M, Takasaki T, Yamada K, Nerome R, Tajima S, Kurane I. Development and evaluation of fluorogenic TaqMan reverse transcriptase PCR assays for detection of dengue virus types 1 to 4. *J Clin Microbiol*. 2004;42:5935–7. <https://doi.org/10.1128/JCM.42.12.5935-5937.2004>
7. Warrilow D, Northill JA, Pyke AT. Sources of dengue viruses imported into Queensland, Australia, 2002–2010. *Emerg Infect Dis*. 2012;18:1850–7. <https://doi.org/10.3201/eid1811.120014>
8. de Bruycker-Nogueira F, Mir D, Dos Santos FB, Bello G. Evolutionary history and spatiotemporal dynamics of DENV-1 genotype V in the Americas. *Infect Genet Evol*. 2016;45:454–60. <https://doi.org/10.1016/j.meegid.2016.09.025>
9. Mweya CN, Kimera SI, Stanley G, Misinz G, Mboera LE. Climate change influences potential distribution of infected *Aedes aegypti* co-occurrence with dengue epidemics risk areas in Tanzania. *PLoS One*. 2016;11:e0162649. <https://doi.org/10.1371/journal.pone.0162649>

Address for correspondence: Seiji P. Yamamoto, Osaka Institute of Public Health, 8-34 Tojo-cho, Tennoji-ku, Osaka 543-0026, Japan; email: yamamotosei@iph.osaka.jp



@CDC_EIDJournal

Want to stay updated on the latest news in *Emerging Infectious Diseases*? Let us connect you to the world of global health. Discover groundbreaking research studies, pictures, podcasts, and more by following us on Twitter at @CDC_EIDJournal.

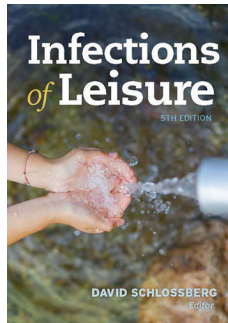
Infections of Leisure, Fifth Edition

David Schlossberg, editor; ASM Press, Washington, DC, USA, 2016; ISBN-10: 1555819222; ISBN-13: 978-1555819224; e-ISBN: 978-1555819231; Pages: 411; Price: \$80

The fifth edition of *Infections of Leisure* is a comprehensive, detailed survey of infectious hazards associated with a number of activities we may do in our leisure time, such as eating exotic cuisines, challenging ourselves at high altitude, owning pets, playing at the seashore or in a pool, getting tattoos or body piercings, and traveling abroad. This edition has been updated to "... incorporate new and changing pathogens that can compromise our leisure activities" (1).

As in previous editions, this edition covers infections associated with just about any type of leisure activity one can imagine and contains good doses of history alongside clinical, microbiological, and epidemiologic information. I was fascinated by the history of humankind's attempts to eradicate rats (Chapter 9: Diseases Transmitted by Man's Worst Friend: The Rat), a notable failed effort; the anecdote about the Duke of Richmond, the Governor General of British North America (now Canada) in 1817, who died from rabies after a fox bite that occurred while he was trying to separate his hunting dogs from a fox (Chapter 11: The Ancient Curse: Rabies); and the history of tattooing, dating back to the Egyptians (Chapter 15: Infections from Body Piercing and Tattoos). The chapters covering zoonoses from domestic pets (dogs, cats, birds, and other less common house pets) are comprehensive, covering bacterial zoonoses that are topical, such as campylobacteriosis associated with exposure to puppies (2), as well as quantifying the number of ferret-owning households in the United States (334,000).

Of note, the next edition could expand a bit on harmful algal bloom-associated illnesses, which were only briefly mentioned in the fifth edition as cyanobacterium infections in the chapter on fresh water. These illnesses have been reported in conjunction with untreated recreational water and drinking water and can encompass more than cyanobacterial toxins (3). *Shigella*, a bacterium that causes travelers' diarrhea and foodborne gastrointestinal disease, is more frequently being reported in association



with sexual activity among men who have sex with men and could potentially be included in the chapter on sexually transmitted diseases, as could other enteric infections that are transmitted person-to-person through the fecal-oral route (4).

The index proves most useful for locating information that might be associated with multiple leisure activities; leptospirosis, for example, in addition to being discussed at length in the section on rat-associated infections, is also discussed in the chapters on garden-associated infections, dog-associated infections, international travel-associated infections, and infections at high altitude. The breadth of infections covered in this book is extensive, from amnesiac shellfish poisoning to Carrion disease (causative agent *Bartonella bacilliformis*), monkeypox, and weeverfish envenomation.

This book is readable, topical, and a useful resource for those who want to balance the relaxation or excitement they may derive from their chosen leisure pursuits with an in-depth knowledge of all the things that could go wrong. Of note, a section in each chapter focuses on prevention measures that can be taken. This book is appropriate for undergraduate students; professionals; and clinical, microbiology, and public health practitioners.

Katie Fullerton

Author affiliation: Centers for Disease Control and Prevention, Atlanta, Georgia, USA

DOI: <https://doi.org/10.3201/eid2509.190634>

References

1. Editor Schlossberg D. *Infections of leisure*. 5th edition. Washington: ASM Press; 2016. p. xv–411.
2. Centers for Disease Control and Prevention. Multistate outbreak of multidrug-resistant *Campylobacter* infections linked to contact with pet store puppies. 2018 Jan 30 [cited 2018 Jul 12]. <https://www.cdc.gov/campylobacter/outbreaks/puppies-9-17/index.html>
3. Figgatt M, Hyde J, Dziewulski D, Wiegert E, Kishbaugh S, Zelin G, et al. Harmful algal bloom-associated illnesses in humans and dogs identified through a pilot surveillance system—New York, 2015. *MMWR Morb Mortal Wkly Rep*. 2017;66:1182–4. <https://doi.org/10.15585/mmwr.mm6643a5>
4. Bowen A, Grass J, Bicknese A, Campbell D, Hurd J, Kirkcaldy RD. Elevated risk for antimicrobial drug-resistant *Shigella* infection among men who have sex with men, United States, 2011–2015. *Emerg Infect Dis*. 2016;22:1613–6. <https://doi.org/10.3201/eid2209.160624>

Address for correspondence: Katie Fullerton, Centers for Disease Control and Prevention, 1600 Clifton Rd NE, Mailstop H24-9, Atlanta, GA 30329-4027, USA; email: kfullerton@cdc.gov



Helen Beatrix Potter (1866–1943), *Agaricus augustus* (c. 1892–1895) (detail). Watercolor on paper, 9 in × 7 in/23 cm × 18 cm, Perth Museum and Art Gallery, Perth and Kinross Council, Scotland.

Beatrix Potter, Author, Naturalist, Mycologist

Byron Breedlove

Baroque artists often featured mushrooms in still life paintings; medieval artists used toadstools (the name ascribed to poisonous mushrooms) to symbolize evil; and Victorian illustrators often populated fantasy scenes with fungi and fairies. Clearly, fungi have long been a staple of artists and illustrators.¹

Among those was Beatrix Potter. She completed 350 paintings of the various mushrooms and lichen that flourished in the moist green Scottish countryside and English Lake district, locales Potter visited with her family. Before she introduced her anthropomorphic animals such as Jemima Puddleduck, Squirrel Nutkin, and Peter Rabbit in her 23 colorful children's books that she wrote and illustrated, Potter was an accomplished artist and a naturalist. Biographer Linda Lear writes Potter “never saw art and science as mutually exclusive activities, but recorded what she saw in nature primarily to evoke an aesthetic response.” Potter’s

experiences in those lush settings influenced her later interest in land conservation and preservation.

By the early 1890s, notes Lear, Potter’s “interests as an artist and a naturalist had converged on fungi” and she “was drawn to fungi first by their ephemeral fairy qualities and then by the variety of their shape and colour and the challenge they posed to watercolour techniques.” Potter painted her first known watercolors of mushrooms when she was 20 years old.

During 1892, she befriended Charlie McIntosh, a shy Scottish mail carrier known as the Perthshire naturalist “who used his miles of postal delivery route as a great outdoor laboratory,” according to Marta McDowell, author of *Beatrix Potter’s Gardening Life*. McIntosh, a self-educated naturalist, carefully observed local flora and fauna and encouraged Potter to make her paintings more precise. He sent her specimens, advised her on scientific classification and nomenclature, and instructed her on microscope techniques. As Lear notes, McIntosh “not only provided just

Author affiliation: Centers for Disease Control and Prevention, Atlanta, Georgia, USA

DOI: <https://doi.org/10.3201/eid2509.AC2509>

¹The North American Mycological Association has a Registry of Mushrooms in Works of Art.

the right level of expertise and objectivity to allow Beatrix to advance her skills, but he also gave her the professional validation she longed for.”

Appearing on this month’s cover is Potter’s sketch showing different stages in the life cycle of *Agaricus augustus* mushrooms. Swedish botanist and mycologist Elias Magnus Fries first identified and named this mushroom in 1838. Considered among the finest of edible fungi, its admirers dubbed it the “Prince of Mushrooms” for its appearance and flavor.

The Perth Museum and Art Gallery, which houses 25 of Potter’s paintings, describes this watercolor: “The principal image shows it at maturity, where the convex cap evident in the second sketch has flattened out and begun to split round the edges. Similarly, the younger gills appear light in colour but turn a chocolate brown at maturity. . . . At the rear is a large fungus with a broad, shallow, upturned cap. The cap is a creamy white with splits around the edge and dark brown gills beneath. It has a white stem, which is largely straight, curving slightly to the right at the base. In front of it is a smaller fungus of similar shape and colour, except that the cap is not inverted, there are no splits visible at its edges, and the gills are a much lighter shade of brown.” A closer look reveals the outline of another fungus to the left.

Potter pursued mycology largely on her own and was invited to study fungi at the Royal Botanical Gardens in Kew, London. As Lear discusses, Potter also made microscopic drawings of fungus spores and developed a theory of their germination. In 1897, she submitted a research paper to the Linnean Society of London but was prevented from attending the proceedings or reading her paper because she was a woman. However, Lear writes, “there is no evidence that she had any ambition to be recognized by the scientific community as a mycologist, or that she wished for a life devoted to scientific enquiry,” although Potter’s “watercolours are considered so accurate that modern mycologists refer to them still to identify fungi.”

The fungi that intrigued Potter include molds, mushrooms, and yeasts. Its members exist in air, water, and soil; experience a range of life cycles; and exhibit an array of morphologic forms. Fungi are integral for decomposition within many ecosystems, have forged symbiotic relationships with other organisms, provide industrial enzymes and metabolites with antimicrobial properties, and serve as experimental organisms. Estimates regarding the biodiversity within the kingdom Fungi suggest that it contains between 2.2 to 3.8 million species.

Some fungi are dangerous and can cause severe health problems, including disability and death. Fortunately, according to researchers Köhler, Casadevall, and Perfect “few among the millions of fungal species fulfill four basic conditions necessary to infect humans: high

temperature tolerance, ability to invade the human host, lysis and absorption of human tissue, and resistance to the human immune system.” Fungi that meet those criteria can cause infections on the skin, in the lungs, in the bloodstream; those infections are often challenging to treat, and antifungal resistance is a growing public health concern. An estimated 150 million people have serious fungal diseases, and more than a billion have fungal infections of their hair, nails, or skin.

Diseases caused by fungal pathogens include blastomycosis, coccidioidomycosis, histoplasmosis, *Pneumocystis* pneumonia, and sporotrichosis. Recent studies estimate that fungal infections, especially those caused by *Candida*, *Cryptococcus*, and *Aspergillus* species, kill more than one million people annually. The concurrent appearance of drug-resistant *Candida auris* on three continents is the first example of a new pathogenic fungi disease emerging from climate change. The urgency underscoring public health efforts to enable earlier detection of fungal infections, apply novel prevention measures, and develop low-toxicity therapies is well founded.

Bibliography

1. Bongomin F, Gago S, Oladele RO, Denning DW. Global and multi-national prevalence of fungal diseases—estimate and precision. *J Fungi* (Basel). 2017;3:57. <https://doi.org/10.3390/jof3040057>
2. Casadevall A, Kontoyiannis DP, Robert V. On the emergence of *Candida auris*: climate change, azoles, swamps, and birds. *MBio*. 2019;10:e01397–19. <https://doi.org/10.1128/mBio.01397-19>
3. Centers for Disease Control and Prevention. Fungal diseases [cited 2019 Jul 14]. <https://www.cdc.gov/fungal/index.html>
4. Culture Perth & Kinross. Potter—Helen Beatrix Potter (1866–1943). Studies of Perthshire fungi by the creator of the Tale of Peter Rabbit [cited 2019 Jul 1]. <https://www.culturepk.org.uk/museums-galleries/collections/galleries-collections/fine-applied-art/potter-helen-beatrix-potter-1866-1943>
5. First Nature. *Agaricus augustus* Fr—The Prince [cited 2019 Jul 14] <https://www.first-nature.com/fungi/agaricus-augustus.php>
6. Hawksworth DL, Lücking R. Fungal diversity revisited: 2.2 to 3.8 million species. *Microbiol Spectr*. 2017;5.
7. Köhler JR, Casadevall A, Perfect J. The spectrum of fungi that infects humans. *Cold Spring Harb Perspect Med*. 2014;5:a019273. <https://doi.org/10.1101/cshperspect.a019273>
8. Lear L. Beatrix Potter, a life in nature. New York: St. Martin’s Griffin; 2007. p. 76–103, 124–127.
9. McDowell M. Beatrix Potter’s gardening life: the plants and places that inspired the classic children’s tales. Portland (OR): Timber Press, Inc; 2013. p. 47–55.
10. Norman Rockwell Museum. Illustration history. Beatrix Potter [cited 2019 Jul 19]. <https://www.illustrationhistory.org/artists/beatrix-potter>
11. Perth Museum and Art Gallery—collections database. FA107/79.12. *Agaricus augustus* [cited 2019 Jul 1]. <http://collectionsearch.pkc.gov.uk/detail.aspx=>

Address for correspondence: Byron Breedlove, EID Journal, Centers for Disease Control and Prevention, 1600 Clifton Rd NE, Mailstop H16-2, Atlanta, GA 30329-4027, USA; email: wbb1@cdc.gov

EMERGING INFECTIOUS DISEASES®

Upcoming Issue

- Global Epidemiology of Diphtheria, 2000–2017
- Localized Outbreaks of Epidemic Polyarthrits among Military Personnel Caused by Different Sublineages of Ross River Virus, Northeast Australia, 2016–2017
- Emergence and Containment of Canine Influenza Virus H3N2, Ontario, Canada, 2017–2018
- Economic Burden of West Nile Virus Disease, Quebec, Canada, 2012–2013
- Invasive Group A *Streptococcus*, Group B *Streptococcus*, and *S. pneumoniae* Infection among Adults Experiencing Homelessness, Alaska, 2002–2015
- Early Diagnosis of Tularemia with Flow Cytometry, Czech Republic, 2003–2015
- Risk Factors for Carbapenem-Resistant *Pseudomonas aeruginosa*, Zhejiang Province, China
- Sensitive and Specific Detection of Low-Level Antibody Responses in Middle East Respiratory Syndrome Coronavirus Infections
- Comparison of Serologic Assays for Middle East Respiratory Syndrome Coronavirus
- Susceptibility of Influenza A, B, C, and D Viruses to Baloxavir
- Powassan Virus, Increasingly Recognized Cause of Encephalitis in Northern United States
- Melioidosis after Hurricanes Irma and Maria, St. Thomas/St. John District, US Virgin Islands, October 2017
- Characterization of Highly Pathogenic Avian Influenza Virus H5N6 and H5N5 Clade 2.3.4.4b Reassortants, Germany, 2017–18
- *Borrelia miyamotoi* Meningitis, Sweden
- Bidirectional Human–Swine Transmission of Seasonal Influenza A(H1N1)pdm09 Virus in Pig Herd, France, 2018
- Estimated Incubation Period and Serial Interval for Human-to-Human Influenza A(H7N9) Virus Transmission
- Emergence of Influenza A(H7N4) Virus, Cambodia
- Genomic Characterization of Rift Valley Fever Virus, South Africa, 2018
- Geospatial Variation in Rotavirus Vaccination Coverage in Infants, United States, 2010–2017

Complete list of articles in the October issue at
<http://www.cdc.gov/eid/upcoming.htm>

Upcoming Infectious Disease Activities

October 2–6, 2019

ID Week

Washington, DC, USA

<https://idweek.org/>

November 20–24, 2019

ASTMH

American Society of Tropical

Medicine and Hygiene

68th Annual Meeting

National Harbor, MD, USA

<https://www.astmh.org/>

February 20–23, 2020

International Society for

Infectious Diseases

Kuala Lumpur, Malaysia

<https://www.isid.org/>

March 26–30, 2020

6th Decennial International Conference

on Healthcare Associated Infections

Atlanta, GA, USA

<https://decennial2020.org/>

Announcements

Email announcements to eideditor@cdc.gov. Include the event's date, location, sponsoring organization, and a website. Some events may appear only on EID's website, depending on their dates.

Another Dimension

Emerging Infectious Diseases accepts thoughtful essays, short stories, or poems on philosophical issues related to science, medical practice, and human health. Topics may include science and the human condition, the unanticipated side of epidemic investigations, or how people perceive and cope with infection and illness. This section is intended to evoke compassion for human suffering and to expand the science reader's literary scope. Manuscripts are selected for publication as much for their content (the experiences they describe) as for their literary merit.

Earning CME Credit

To obtain credit, you should first read the journal article. After reading the article, you should be able to answer the following, related, multiple-choice questions. To complete the questions (with a minimum 75% passing score) and earn continuing medical education (CME) credit, please go to <http://www.medscape.org/journal/eid>. Credit cannot be obtained for tests completed on paper, although you may use the worksheet below to keep a record of your answers.

You must be a registered user on <http://www.medscape.org>. If you are not registered on <http://www.medscape.org>, please click on the “Register” link on the right hand side of the website.

Only one answer is correct for each question. Once you successfully answer all post-test questions, you will be able to view and/or print your certificate. For questions regarding this activity, contact the accredited provider, CME@medscape.net. For technical assistance, contact CME@medscape.net. American Medical Association’s Physician’s Recognition Award (AMA PRA) credits are accepted in the US as evidence of participation in CME activities. For further information on this award, please go to <https://www.ama-assn.org>. The AMA has determined that physicians not licensed in the US who participate in this CME activity are eligible for AMA PRA Category 1 Credits™. Through agreements that the AMA has made with agencies in some countries, AMA PRA credit may be acceptable as evidence of participation in CME activities. If you are not licensed in the US, please complete the questions online, print the AMA PRA CME credit certificate, and present it to your national medical association for review.

Article Title

Classification of Trauma-Associated Invasive Fungal Infections to Support Wound Treatment Decisions

CME Questions

1. You are seeing a 20-year-old male soldier who was severely injured in an explosion 12 days ago. He has a 10-cm leg wound that appears infected, and you are concerned about the possibility of a fungal infection. What should you consider regarding the classifications of wounds established in the current study by Ganesan and colleagues?

- A. Wounds that had been surgically debrided could not be classified as invasive fungal infection (IFI)
- B. A positive fungal culture defined proven IFI
- C. Spontaneous wound dehiscence was a criterion defining IFI
- D. Wounds meeting criteria for deep skin and soft tissue infection that had been treated with antifungals were classified as high-suspicion wounds

2. You review the patient’s chart. Which of the following clinical characteristics was most associated with IFI vs high- or low-suspicion wounds?

- A. History of blast injury
- B. Higher injury severity score
- C. Higher requirement for blood transfusions within 24 hours of injury
- D. Traumatic amputation

3. You note that the patient has a positive wound fungal culture. Which of the following statements regarding the wound microbiology findings of the current study is most accurate?

- A. *Mucorales* species accounted for <5% of positive cultures overall
- B. IFI was associated with the highest rate of growth of “other” fungi
- C. *Fusarium* species were more likely to be isolated from low-suspicion wounds compared with IFI wounds
- D. *Mucorales* species were more likely to be isolated from IFI wounds compared with low-suspicion wounds

4. The patient meets criteria for IFI, and he wants to know his prognosis. Which of the following statements regarding the outcomes of patients in the current study was most accurate?

- A. Patients with IFI had a higher risk for mortality compared with patients with high- and low-suspicion wounds
- B. Patients with IFI had a higher risk for mortality compared with patients with low-suspicion wounds only
- C. Patients with IFI had a higher risk for surgical amputation compared with patients with high- and low-suspicion wounds
- D. The number of debridements was similar regardless of wound status

Earning CME Credit

To obtain credit, you should first read the journal article. After reading the article, you should be able to answer the following, related, multiple-choice questions. To complete the questions (with a minimum 75% passing score) and earn continuing medical education (CME) credit, please go to <http://www.medscape.org/journal/eid>. Credit cannot be obtained for tests completed on paper, although you may use the worksheet below to keep a record of your answers.

You must be a registered user on <http://www.medscape.org>. If you are not registered on <http://www.medscape.org>, please click on the "Register" link on the right hand side of the website.

Only one answer is correct for each question. Once you successfully answer all post-test questions, you will be able to view and/or print your certificate. For questions regarding this activity, contact the accredited provider, CME@medscape.net. For technical assistance, contact CME@medscape.net. American Medical Association's Physician's Recognition Award (AMA PRA) credits are accepted in the US as evidence of participation in CME activities. For further information on this award, please go to <https://www.ama-assn.org>. The AMA has determined that physicians not licensed in the US who participate in this CME activity are eligible for AMA PRA Category 1 Credits™. Through agreements that the AMA has made with agencies in some countries, AMA PRA credit may be acceptable as evidence of participation in CME activities. If you are not licensed in the US, please complete the questions online, print the AMA PRA CME credit certificate, and present it to your national medical association for review.

Article Title

Risk for *Clostridioides difficile* Infection among Older Adults with Cancer

CME Questions

1. You are advising a large hospital regarding *Clostridioides difficile* infection (CDI) prevention among older adults. According to the retrospective cohort study using population-based Surveillance, Epidemiology, and End Result Medicare data for 2011 by Kamboj and colleagues, which of the following statements about findings of cohort analysis regarding risk for CDI in older adults is correct?

- A. Among the 93,566 Medicare beneficiaries in the cohort, 3.7% overall had CDI during the study period
- B. The proportion of CDI was 2.8% among patients with cancer and 2.4% in patients without cancer in unadjusted analyses
- C. Men had a higher proportion of CDI than did women
- D. Region of residence did not affect CDI incidence

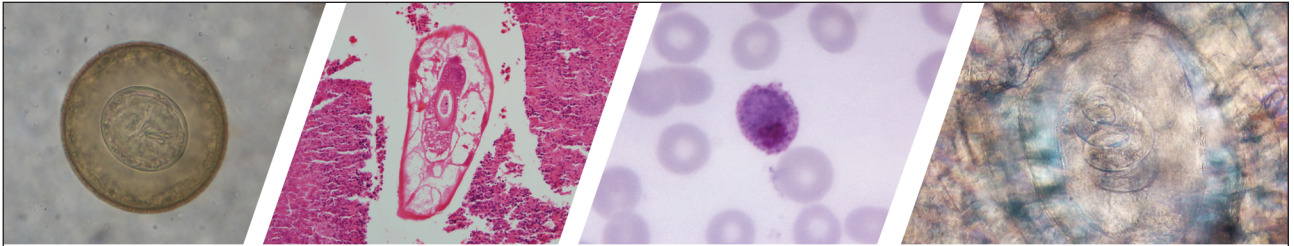
2. According to the nested case–control analysis among 2,421 case-patients with CDI and 12,105 control participants matched on age and sex, which of the following statements about factors affecting risk for CDI in older adults is correct?

- A. Risk for CDI was significantly increased for all solid tumors, regardless of time of diagnosis and presence or absence of metastasis

- B. Patients with cancer vs. patients without cancer did not have significantly higher odds for CDI
- C. Regardless of having a cancer diagnosis, ≥ 2 prior hospitalizations and a prior skilled nursing facility stay were each associated with increased odds for CDI occurrence
- D. Race distribution was significantly different in CDI cases than in controls

3. According to the retrospective cohort study with a nested case–control analysis by Kamboj and colleagues, which of the following statements about clinical implications of risk for CDI in older adults with cancer is correct?

- A. The study proves that excessive antibiotic use associated with cancer treatment increases risk for CDI
- B. This study showed that the burden of CDI in older adults is greater among persons with underlying cancer, which can inform targets for prevention
- C. Symptoms and complications of CDI in elderly patients are similar to those in younger patients
- D. CDI during cancer treatment does not significantly affect management



Diagnostic Assistance and Training in Laboratory Identification of Parasites

A free service of CDC available to laboratorians, pathologists, and other health professionals in the United States and abroad



Diagnosis from photographs of worms, histological sections, fecal, blood, and other specimen types



Expert diagnostic review



Formal diagnostic laboratory report



Submission of samples via secure file share

Visit the DPDx website for information on laboratory diagnosis, geographic distribution, clinical features, parasite life cycles, and training via Monthly Case Studies of parasitic diseases.

www.cdc.gov/dpdx
dpdx@cdc.gov

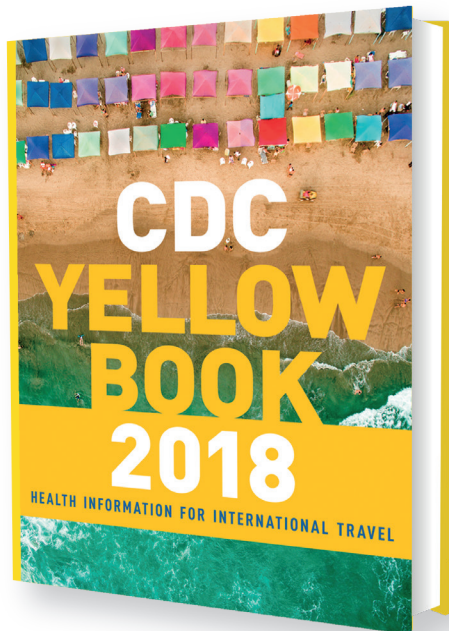


**U.S. Department of
Health and Human Services**
Centers for Disease
Control and Prevention

CDC YELLOW BOOK

HEALTH INFORMATION FOR INTERNATIONAL TRAVEL

2018



The fully revised and updated *CDC Yellow Book 2018: Health Information for International Travel* codifies the U.S. government's most current health guidelines and information for clinicians advising international travelers, including pretravel vaccine recommendations, destination-specific health advice, and easy-to-reference maps, tables, and charts.

ISBN: 9780190628611 | \$49.95 | May 2017 | Paperback | 704 pages

The 2018 Yellow Book includes important travel medicine updates:

- The latest information about emerging infectious disease threats such as Zika, Ebola, and sarcocystosis
- New cholera vaccine recommendations
- Updated guidance on the use of antibiotics in the treatment of travelers' diarrhea
- Special considerations for unique types of travel such as wilderness expeditions, work-related travel, and study abroad

IDSA members: log in via www.idsociety.org before purchasing this title to receive your **20% discount**

OXFORD
UNIVERSITY PRESS

Order your copy at:

www.oup.com/academic

Emerging Infectious Diseases is a peer-reviewed journal established expressly to promote the recognition of new and reemerging infectious diseases around the world and improve the understanding of factors involved in disease emergence, prevention, and elimination.

The journal is intended for professionals in infectious diseases and related sciences. We welcome contributions from infectious disease specialists in academia, industry, clinical practice, and public health, as well as from specialists in economics, social sciences, and other disciplines. Manuscripts in all categories should explain the contents in public health terms. For information on manuscript categories and suitability of proposed articles, see below and visit <http://wwwnc.cdc.gov/eid/pages/author-resource-center.htm>.

Summary of Authors' Instructions

Authors' Instructions. For a complete list of EID's manuscript guidelines, see the author resource page: <http://wwwnc.cdc.gov/eid/page/author-resource-center>.

Manuscript Submission. To submit a manuscript, access Manuscript Central from the Emerging Infectious Diseases web page (www.cdc.gov/eid). Include a cover letter indicating the proposed category of the article (e.g., Research, Dispatch), verifying the word and reference counts, and confirming that the final manuscript has been seen and approved by all authors. Complete provided Authors Checklist.

Manuscript Preparation. For word processing, use MS Word. Set the document to show continuous line numbers. List the following information in this order: title page, article summary line, keywords, abstract, text, acknowledgments, biographical sketch, references, tables, and figure legends. Appendix materials and figures should be in separate files.

Title Page. Give complete information about each author (i.e., full name, graduate degree(s), affiliation, and the name of the institution in which the work was done). Clearly identify the corresponding author and provide that author's mailing address (include phone number, fax number, and email address). Include separate word counts for abstract and text.

Keywords. Use terms as listed in the National Library of Medicine Medical Subject Headings index (www.ncbi.nlm.nih.gov/mesh).

Text. Double-space everything, including the title page, abstract, references, tables, and figure legends. Indent paragraphs; leave no extra space between paragraphs. After a period, leave only one space before beginning the next sentence. Use 12-point Times New Roman font and format with ragged right margins (left align). Italicize (rather than underline) scientific names when needed.

Biographical Sketch. Include a short biographical sketch of the first author—both authors if only two. Include affiliations and the author's primary research interests.

References. Follow Uniform Requirements (www.icmje.org/index.html). Do not use endnotes for references. Place reference numbers in parentheses, not superscripts. Number citations in order of appearance (including in text, figures, and tables). Cite personal communications, unpublished data, and manuscripts in preparation or submitted for publication in parentheses in text. Consult List of Journals Indexed in Index Medicus for accepted journal abbreviations; if a journal is not listed, spell out the journal title. List the first six authors followed by "et al." Do not cite references in the abstract.

Tables. Provide tables within the manuscript file, not as separate files. Use the MS Word table tool, no columns, tabs, spaces, or other programs. Footnote any use of bold-face. Tables should be no wider than 17 cm. Condense or divide larger tables. Extensive tables may be made available online only.

Figures. Submit editable figures as separate files (e.g., Microsoft Excel, PowerPoint). Photographs should be submitted as high-resolution (600 dpi) .tif or .jpg files. Do not embed figures in the manuscript file. Use Arial 10 pt. or 12 pt. font for lettering so that figures, symbols, lettering, and numbering can remain legible when reduced to print size. Place figure keys within the figure. Figure legends should be placed at the end of the manuscript file.

Videos. Submit as AVI, MOV, MPG, MPEG, or WMV. Videos should not exceed 5 minutes and should include an audio description and complete captioning. If audio is not available, provide a description of the action in the video as a separate Word file. Published or copyrighted material (e.g., music) is discouraged and must be accompanied by written release. If video is part of a manuscript, files must be uploaded with manuscript submission. When uploading, choose "Video" file. Include a brief video legend in the manuscript file.

Types of Articles

Perspectives. Articles should not exceed 3,500 words and 50 references. Use of subheadings in the main body of the text is recommended. Photographs and illustrations are encouraged. Provide a short abstract (150 words), 1-sentence summary, and biographical sketch. Articles should provide insightful analysis and commentary about new and reemerging infectious diseases and related issues. Perspectives may address factors known to influence the emergence of diseases, including microbial adaptation and change, human demographics and behavior, technology and industry, economic development and land use, international travel and commerce, and the breakdown of public health measures.

Synopses. Articles should not exceed 3,500 words in the main body of the text or include more than 50 references. Use of subheadings in the main body of the text is recommended. Photographs and illustrations are encouraged. Provide a short abstract (not to exceed 150 words), a 1-line summary of the conclusions, and a brief

biographical sketch of first author or of both authors if only 2 authors. This section comprises case series papers and concise reviews of infectious diseases or closely related topics. Preference is given to reviews of new and emerging diseases; however, timely updates of other diseases or topics are also welcome. If detailed methods are included, a separate section on experimental procedures should immediately follow the body of the text.

Research. Articles should not exceed 3,500 words and 50 references. Use of subheadings in the main body of the text is recommended. Photographs and illustrations are encouraged. Provide a short abstract (150 words), 1-sentence summary, and biographical sketch. Report laboratory and epidemiologic results within a public health perspective. Explain the value of the research in public health terms and place the findings in a larger perspective (i.e., "Here is what we found, and here is what the findings mean").

Policy and Historical Reviews. Articles should not exceed 3,500 words and 50 references. Use of subheadings in the main body of the text is recommended. Photographs and illustrations are encouraged. Provide a short abstract (150 words), 1-sentence summary, and biographical sketch. Articles in this section include public health policy or historical reports that are based on research and analysis of emerging disease issues.

Dispatches. Articles should be no more than 1,200 words and need not be divided into sections. If subheadings are used, they should be general, e.g., "The Study" and "Conclusions." Provide a brief abstract (50 words); references (not to exceed 15); figures or illustrations (not to exceed 2); tables (not to exceed 2); and biographical sketch. Dispatches are updates on infectious disease trends and research that include descriptions of new methods for detecting, characterizing, or subtyping new or reemerging pathogens. Developments in antimicrobial drugs, vaccines, or infectious disease prevention or elimination programs are appropriate. Case reports are also welcome.

Research Letters Reporting Cases, Outbreaks, or Original Research. EID publishes letters that report cases, outbreaks, or original research as Research Letters. Authors should provide a short abstract (50-word maximum), references (not to exceed 10), and a short biographical sketch. These letters should not exceed 800 words in the main body of the text and may include either 1 figure or 1 table. Do not divide Research Letters into sections.

Letters Commenting on Articles. Letters commenting on articles should contain a maximum of 300 words and 5 references; they are more likely to be published if submitted within 4 weeks of the original article's publication.

Commentaries. Thoughtful discussions (500–1,000 words) of current topics. Commentaries may contain references (not to exceed 15) but no abstract, figures, or tables. Include biographical sketch.

Another Dimension. Thoughtful essays, short stories, or poems on philosophical issues related to science, medical practice, and human health. Topics may include science and the human condition, the unanticipated side of epidemic investigations, or how people perceive and cope with infection and illness. This section is intended to evoke compassion for human suffering and to expand the science reader's literary scope. Manuscripts are selected for publication as much for their content (the experiences they describe) as for their literary merit. Include biographical sketch.

Books, Other Media. Reviews (250–500 words) of new books or other media on emerging disease issues are welcome. Title, author(s), publisher, number of pages, and other pertinent details should be included.

Conference Summaries. Summaries of emerging infectious disease conference activities (500–1,000 words) are published online only. They should be submitted no later than 6 months after the conference and focus on content rather than process. Provide illustrations, references, and links to full reports of conference activities.

Online Reports. Reports on consensus group meetings, workshops, and other activities in which suggestions for diagnostic, treatment, or reporting methods related to infectious disease topics are formulated may be published online only. These should not exceed 3,500 words and should be authored by the group. We do not publish official guidelines or policy recommendations.

Photo Quiz. The photo quiz (1,200 words) highlights a person who made notable contributions to public health and medicine. Provide a photo of the subject, a brief clue to the person's identity, and five possible answers, followed by an essay describing the person's life and his or her significance to public health, science, and infectious disease.

Etymology. Etymologia (100 words, 5 references). We welcome thoroughly researched derivations of emerging disease terms. Historical and other context could be included.

Announcements. We welcome brief announcements of timely events of interest to our readers. Announcements may be posted online only, depending on the event date. Email to eideditor@cdc.gov.

In This Issue

Synopses

Genotyping Approach for Potential Common Source of <i>Enterocytozoon bieneusi</i> Infection in Hematology Unit.....	1625
Epidemiology of Carbapenemase-Producing <i>Klebsiella pneumoniae</i> in a Hospital, Portugal	1632
Classification of Trauma-Associated Invasive Fungal Infections to Support Wound Treatment Decisions	1639
Clinical Characteristics and Treatment Outcomes for Patients Infected with <i>Mycobacterium haemophilum</i>	1648

Research

<i>Theileria orientalis</i> Ikeda Genotype in Cattle, Virginia, USA	1653
Genetic Characterization and Enhanced Surveillance of Ceftriaxone-Resistant <i>Neisseria gonorrhoeae</i> Strain, Alberta, Canada, 2018	1660
Clonality of Fluconazole-Nonsusceptible <i>Candida tropicalis</i> Bloodstream Infections, Taiwan, 2011–2017	1668
Association of Enterovirus D68 with Acute Flaccid Myelitis, Philadelphia, Pennsylvania, USA, 2009–2018	1676
Risk for <i>Clostridiodes difficile</i> Infection among Older Adults with Cancer	1683
Whole-Genome Sequencing of <i>Salmonella</i> Mississippi and Typhimurium Definitive Type 160, Australia and New Zealand	1690
Epidemiologic Shift in Candidemia Driven by <i>Candida auris</i> , South Africa, 2016–2017	1698
Effect of Pneumococcal Conjugate Vaccines on Pneumococcal Meningitis, England and Wales, July 1, 2000–June 30, 2016	1708

Dispatches

<i>Rickettsia japonica</i> Infections in Humans, Xinyang, China, 2014–2017.....	1719
Climate Classification System–Based Determination of Temperate Climate Detection of <i>Cryptococcus gattii sensu lato</i>	1723
Cluster of Nasal Rhinosporidiosis, Eastern Province, Rwanda.....	1727
Use of Human Intestinal Enteroids to Detect Human Norovirus Infectivity.....	1730
Vaccine Effectiveness Against DS-1–like Rotavirus Strains in Infants with Acute Gastroenteritis, Malawi, 2013–2015	1734
Rodent Host Abundance and Climate Variability as Predictors of Tickborne Disease Risk 1 Year in Advance.....	1738
Delays in Coccidioidomycosis Diagnosis and Relationship to Healthcare Utilization, Phoenix, Arizona, USA	1742
Delays in Coccidioidomycosis Diagnosis and Associated Healthcare Utilization, Tucson, Arizona, USA.....	1745